Les isotopes du lithium: exemples d'applications en géochimie

Romain Millot

Mémoire présenté en vue de l'obtention de l'Habilitation à Diriger des Recherches

Dr. Romain MILLOT

BRGM – Direction des Laboratoires

Institut des Sciences de la Terre d'Orléans

UMR 7327 BRGM-ISTO

Les isotopes du lithium: exemples d'applications en géochimie

Soutenue le 27 novembre 2013
devant le jury composé de :

Pr. Francis ALBAREDE (École Normale Supérieure, Lyon) - rapporteur
Dr. Marc CHAUSSIDON (CRPG, Nancy) - rapporteur
Pr. Eric MARCOUX (Université d'Orléans) - examinateur
Dr. Philippe NEGREL (BRGM, Orléans) - examinateur
Dr. Bruno SCAILLET (ISTO, Orléans) - directeur du laboratoire d'accueil
Pr. Avner VENGOSH (Duke University, USA) - rapporteur
Dr. Pierpaolo ZUDDAS (Université Pierre et Marie Curie, Paris) - examinateur

à Chloé, Célia et Lilian

Préambule

Ce mémoire constitue la synthèse des travaux de Recherches menés au BRGM au cours de ces 10 dernières années.

Après une introduction qui précise le contexte et les objectifs de ce travail, ce manuscrit présente tout d'abord les grands principes de la géochimie isotopique du lithium.

Puis, dans un second temps, nous décrivons en détails le protocole de mesure des isotopes du lithium dans des matrices liquides et solides.

Ensuite, et cette partie constitue le cœur de ce manuscrit, nous illustrons au travers de différents exemples ciblés l'application de cet outil isotopique à la compréhension des systèmes et des milieux comme les eaux de pluies et les fleuves ainsi que dans les interactions eau/roche à basse et haute température, au travers des eaux thermo-minérales et des eaux géothermales et enfin des systèmes expérimentaux. Les eaux thermales ou thermominérales du Massif Central ont été séparées des eaux géothermales (Antilles et N^{elle} Zélande qui se trouvent en contexte volcanique insulaire).

La dernière partie de ce manuscrit est consacrée à la synthèse des activités de recherches en terme de publications (articles, congrès, rapports) et d'encadrement scientifique d'étudiants. Nous présentons aussi une synthèse des activités de recherches dans le cadre de projets de R&D. Enfin, en annexe, une sélection d'articles scientifiques illustre ces travaux par thématique. Ces exemples ont été sélectionnés dans le but de garder un fil conducteur dans ce manuscrit. Il a donc fallu faire des choix pour illustrer au mieux les différentes applications.

Le lecteur est averti ici que les illustrations sont en anglais, ces figures sont directement reproduites de publications scientifiques internationales rassemblées en annexe.

Sommaire

Liste des illustrations

1. Introduction

La matière est constituée d'éléments chimiques tous bâtis sur le même modèle : l'atome est constitué d'un noyau composé de protons (chargés positivement) et de neutrons (électriquement neutres). Autour de ce noyau gravitent des électrons, particules chargées négativement.

Chaque atome se distingue donc par son nombre de protons (ou d'électrons), également appelé numéro atomique Z, le nombre de neutrons N et le nombre de nucléons (protons + neutrons) A.

$$\mathbf{{}^{A}_{Z}E}$$

E : élément chimique

A : masse atomique (protons + neutrons)

Z : numéro atomique (nombre de protons)

Le nombre de protons est égal au nombre d'électrons, ce qui assure la neutralité de l'atome. L'ensemble des atomes dont le noyau possède le même couple (Z, A) est appelé un nucléide; un élément chimique correspond à l'ensemble des atomes de même numéro atomique Z.

Le mot **isotope**, composé du grec isos "égal, le même" et topos "lieu, place", proprement "qui occupe la même place", fait référence à la classification de Mendeleïev (Figure 1) car pour un même élément chimique, il peut exister différents noyaux. En effet, si le nombre de protons est toujours égal à Z, le nombre de neutrons peut varier et on parle alors d'isotopes de l'élément chimique. Les isotopes sont caractérisés par le nombre de nucléons (protons + neutrons) A. On différencie les isotopes d'un élément E par la notation ^{A}E avec par exemple, le noyau de l'atome d'hydrogène qui est constitué d'un proton pouvant à l'état naturel être accompagné de zéro, un ou deux neutron(s). L'hydrogène existe donc sous trois formes isotopiques ^{1}H, ^{2}H (appelé deutérium, noté D) et ^{3}H (appelé tritium, noté T). Les propriétés chimiques des isotopes d'un même élément sont identiques car ces isotopes ont le même nombre d'électrons.

La **géochimie isotopique** a connu ces dernières années un développement sans précédent en ce qui concerne les applications concernant le traçage des éléments dans l'environnement. Cet essor est le résultat des développements instrumentaux dans le domaine de l'analyse isotopique. En effet, l'outil de spectrométrie de masse à source plasma et multi-collection (MC-ICP-MS : Multi Collector Inductively Coupled Plasma Mass Spectrometer) a permis la mesure juste et précise à de très faibles teneurs de systèmes isotopiques non traditionnels, notamment certains métaux, métalloïdes et non-métaux.

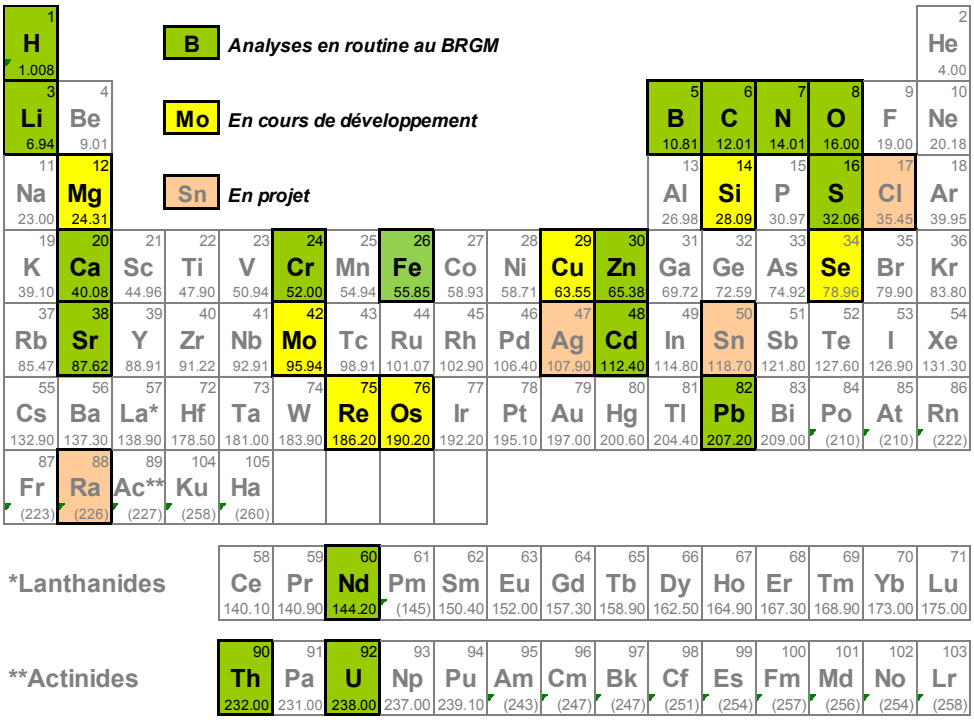

Figure 1 - Classification des éléments chimiques dans le tableau de Mendeleïev. Les couleurs identifient les différentes systématiques isotopiques appliquées, en développement et en projet au BRGM à la date de ce document.

L'élément chimique lithium (Z=3) est constitué de deux isotopes de masse 6 et 7, voir la figure 2, ci-dessous. Le lithium 7 (^{7}Li) est l'un des rares nuclides ayant été formé lors de la nucléosynthèse primordiale (Big Bang), alors que très peu de ^{6}Li a été généré durant cet évènement. De nos jours, les atomes de Li sont principalement produits lors de réactions de spallations, c'est-à-dire lors de la destruction d'atomes plus lourds de carbone et d'oxygène sous l'effet de rayonnements cosmiques. La cosmochimie du lithium revêt une importance particulière car les rapports isotopiques ^{7}Li/^{6}Li permettent à la fois d'aborder des problèmes cosmologiques, c'est-à-dire touchant au Big-Bang et à l'origine de l'Univers, et d'étudier l'évolution de la composition chimique et isotopique de la galaxie (Chaussidon et Robert, 1998 ; Beck et al., 2004).

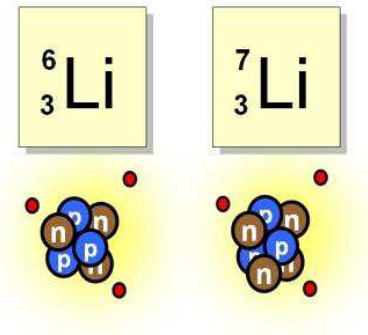

Figure 2 - Représentation schématique des isotopes de masse 6 et 7 du lithium avec respectivement 3 et 4 neutrons.

Le développement technologique instrumental des cers dernières années a généré de nombreux programmes de recherches appliquées concernant l'étude de l'origine, du transfert et du devenir de ces éléments dans les systèmes géologiques de surface et de sub-surface.

La mise en évidence de variations des signatures isotopiques pour ces éléments dans les différents réservoirs géochimiques permet non seulement d'étudier les processus ou mécanismes de transfert de ces éléments entre ces réservoirs, mais aussi de quantifier les flux et de caractériser les réactions physico-chimiques à l'origine de ces fractionnements isotopiques (Faure, 1986 ; 1998 ; Allègre 2005).

Ainsi, la géochimie isotopique utilise les contrastes hérités de l'histoire de la Terre (différenciation des réservoirs géochimiques terrestres) pour étudier les transferts géochimiques actuels des éléments entre les différents réservoirs terrestres superficiels et profonds (Allègre, 1987 ; Wasserburg, 1987).

L'analogie intéressante qui peut être faite ici pour expliquer le niveau d'information supplémentaire obtenu par l'analyse isotopique par rapport à l'analyse élémentaire est décrite ci-après (Figure 3). En faisant le parallèle entre une étude géochimique et une étude démographique, l'analyse élémentaire (mesure de la concentration d'un élément) s'apparente à compter le nombre d'individus dans une population. Alors que la mesure isotopique consiste à faire le rapport des individus selon leur sexe (rapport isotopique) ou selon leur âge (datation en géochronologie).

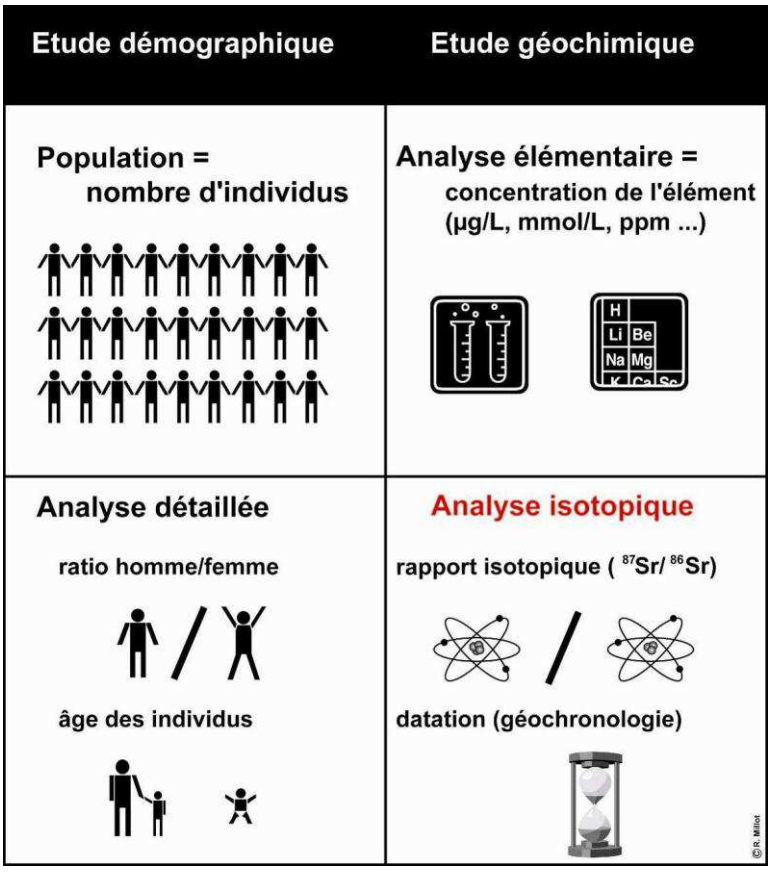

Figure 3 - Analogie entre une étude démographique et une étude géochimique.

D'une manière générale, les compositions isotopiques mesurées dans les éléments chimiques peuvent selon les cas, soit caractériser les sources (origine de l'élément) ou soit être des marqueurs des processus physico-chimiques conduisant à un fractionnement entre isotopes et par là-même à une modification de la composition isotopique. Il est évident que les deux phénomènes peuvent très bien se surimposer.

En ce qui concerne **le traçage des sources** (origine et quantification des flux), l'exemple le plus connu est probablement celui des isotopes du plomb. En effet, l'utilisation des différents rapports isotopiques du plomb ($^{206}Pb/^{204}Pb$, $^{207}Pb/^{204}Pb$ et $^{208}Pb/^{204}Pb$) permet généralement de mettre en évidence la présence d'une ou plusieurs sources de plomb dans l'environnement (citons ici les travaux pionniers dans le domaine de Clair Patterson et son équipe dès les années 1960 : Tatsumoto et Patterson 1963 ; Murozimi et al., 1969).

La gamme de variation de la composition isotopique en Pb dans les matériaux terrestres est tellement importante que l'empreinte isotopique laissée par l'histoire géologique du Pb (différenciation des réservoirs et évolution dans le temps) est intégrée à la source de pollution. Ainsi, la composition isotopique du plomb varie en fonction du rapport chimique initial U/Pb (rapport dit père/fils) et de l'âge de son gisement d'extraction. De ce fait, le plomb anthropique par exemple dispersé dans l'atmosphère par différents processus (incinération, combustion...) conserve la signature isotopique de son minerai d'origine, lequel diffère très généralement du plomb endogène local. Et donc, on utilise la composition isotopique du plomb à la manière d'une empreinte digitale pour discriminer différentes sources naturelles ou anthropiques.

En ce qui concerne **les processus**, les principaux mécanismes de fractionnements isotopiques résultent principalement des réactions physico-chimiques comme les transformations d'oxydoréduction, de la dissolution ou de la précipitation de minéraux et/ou de phases néoformées (oxy-hydroxydes) lors de l'altération, mais aussi des mécanismes d'adsorption et de désorption sur des surfaces. A cela peuvent s'ajouter les effets liés aux micro-organismes (bactéries) qui pour leur développement peuvent intégrer certains métaux dans leur métabolisme et être à l'origine de fractionnements isotopiques dans leurs milieux de croissance.

2. Géochimie isotopique du lithium

2.1. Variations isotopiques du lithium dans les matériaux géologiques

Le lithium est un métal alcalin et comme les autres éléments de son groupe, le Li possède un seul électron de valence qui est facilement perdu pour former le cation Li^+, ce qui explique sa faible électronégativité. Le Li est le 3ème élément de la classification périodique de Mendeleïev, il se place en colonne 1A juste au-dessus du sodium, un élément aux propriétés chimiques très proches. Comme souvent dans le tableau périodique, le Li peut être relié à l'élément voisin selon une diagonale: le magnésium. En effet, le rayon ionique du Li est 0.163 nm c'est à dire très proche de celui du Mg 0.168 nm et permet donc une substitution de ces deux éléments. Toutefois le lithium, contrairement au Mg, reste un élément incompatible lors des processus de fusion et de la cristallisation. D'après la classification de Goldschmidt, le Li est dit lithophile, modérément incompatible et se trouve donc en abondance dans les roches silicatées de notre planète (lithium vient de « lithos » : la roche).

Le lithium est un élément chimique qui possède deux isotopes de masse 6 et 7, dont les abondances naturelles sont respectivement de 7.5% et 92.5% (Figure 4).

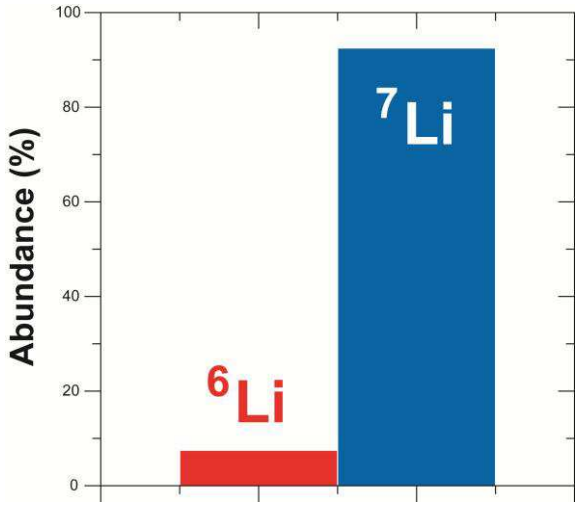

Figure 4 - Abondances en % des deux isotopes du lithium.

Le lithium présente donc un caractère lithophile et très fortement soluble. La différence de masse relative entre les deux isotopes est considérable (17%, Figure 5) et engendre des fractionnements de masse importants lors des processus géochimiques. Coplen et al., (2002) ont montré que la gamme de variation des compositions isotopiques du lithium est de plus de 60‰ dans les matériaux géologiques.

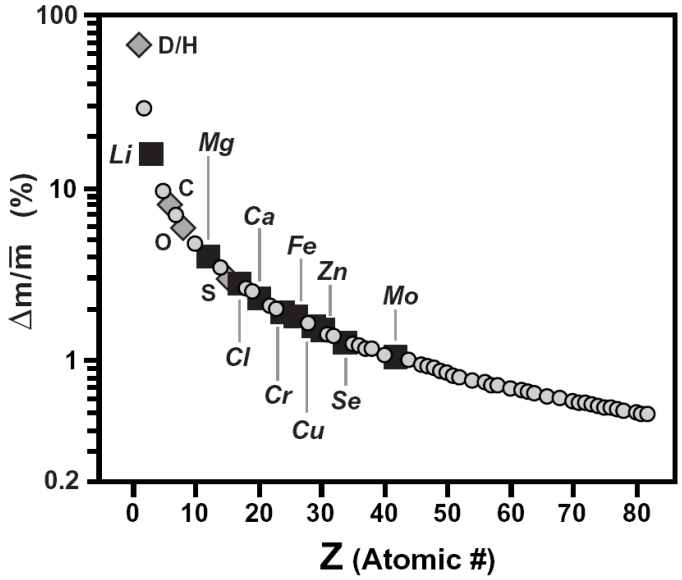

Figure 5 - Graphique représentant l'écart de masse relatif (Δm/m) en fonction du numéro atomique Z (Johnson et al., 2004).

La composition isotopique du lithium d'un échantillon (« sample ») se note en déviation relative (en ‰) par rapport à la valeur d'un standard:

$$\delta^7 Li\ (‰) = \left(\frac{\left(\frac{^7Li}{^6Li} \right)_{sample}}{\left(\frac{^7Li}{^6Li} \right)_{L-SVEC}} - 1 \right) \times 10^3$$

Le standard de référence est un carbonate de lithium (L-SVEC, NIST RM8545) dont la valeur du δ^7Li est de 0‰ par définition (^{7}Li/^{6}Li = 12.02 ± 0.03, Flesch et al., 1973).

Dans son article de synthèse, Tomascak (2004) a compilé l'amplitude des variations isotopiques des différents réservoirs terrestres. De plus, Teng et al., (2004) ont également reporté les compositions isotopiques de différents types de roches (shales, loess et granites) dans le but d'estimer la composition isotopique du lithium de la croûte continentale supérieure.

Ainsi, les granites présentent des compositions isotopiques en lithium comprises généralement entre -2 et +2‰, quant aux basaltes (de type MORB, OIB et basaltes d'arc) leurs δ^7Li varient de +2 à +6‰.

L'eau de mer actuelle possède une composition isotopique en lithium très homogène d'environ +31‰, les eaux de rivières ont des compositions intermédiaires entre +6 et +37‰ et les eaux thermo-minérales ont des compositions isotopiques qui varient entre -20 et +10‰ (Figure 6).

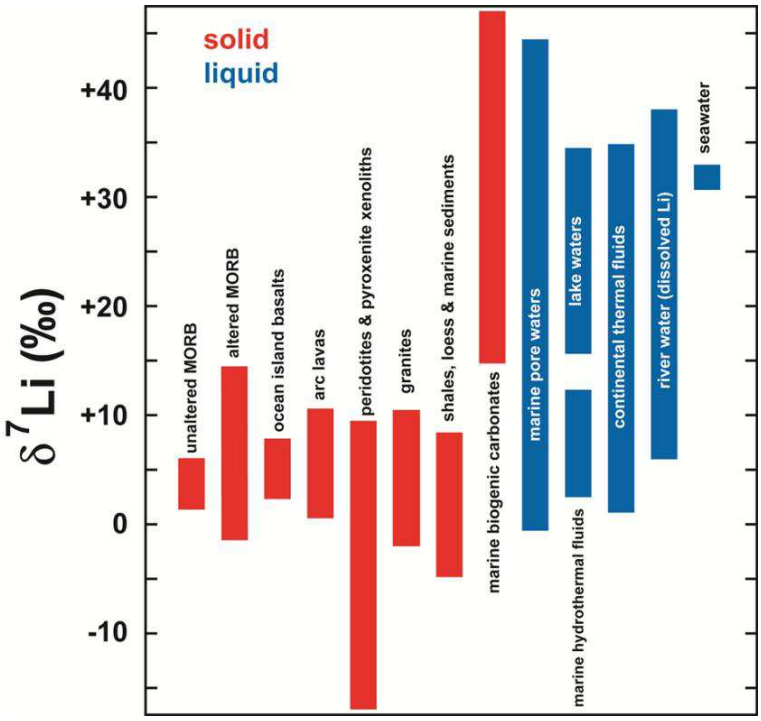

Figure 6 - Variations des compositions isotopiques du Li dans les matériaux terrestres. Modifié d'après Tomascak (2004).

D'une manière générale, les concentrations en lithium des eaux ne sont contrôlées que par les processus d'interactions eux-mêmes (intensité d'interaction, température et assemblage minéralogique), par la formation de minéraux secondaire d'altération ainsi que par les processus d'adsorption/désorption lors d'échange entre le lithium en solution et les surfaces minérales. D'autre part, il a été montré que les réactions d'oxydo-réduction, de complexation organique ou de spéciation n'ont aucun effet de contrôle vis-à-vis des concentrations de lithium dans les eaux.

2.2. Fractionnement isotopique du lithium et paramètres de contrôle

Deux grands types de fractionnement des isotopes stables sont aujourd'hui connus :

1- **le fractionnement d'équilibre** se produit lors des réactions chimiques ou physiques faisant intervenir une réaction d'équilibre. L'importance de ce type de fractionnement est directement proportionnelle à la différence de masse entre les deux isotopes et l'amplitude du fractionnement est inversement proportionnelle à la température. En effet, lorsque la température de la réaction augmente, le fractionnement isotopique d'équilibre tend à devenir nul.

2- **lors d'un fractionnement cinétique**, les isotopes les plus légers sont systématiquement avantagés par leur vitesse lors des réactions chimiques ou lors des processus de transport. Ce mode de fractionnement est théoriquement insensible à la température.

En ce qui concerne l'amplitude des fractionnements isotopiques du Li lors des interactions eau/roche et les facteurs qui les contrôlent, des études menées dans des contextes d'altération de basse/moyenne température ont montré que le fractionnement isotopique associé aux interactions eau/roche favorise l'enrichissement de la solution en isotope lourd (^{7}Li). Ce résultat vient du fait que l'isotope léger (^{6}Li) est préférentiellement retenu dans les phases solides en particulier dans les minéraux secondaires d'altération (c.f. Tomascak, 2004).

Lors de l'altération des roches par les eaux à la surface de la Terre, les isotopes du lithium sont fortement fractionnés (α[1] peut varier de 0.970 à 0.990 entre les phases dissoutes et particulaires transportées par les rivières ; Huh et al., 1998 ; 2001). A l'échelle d'un bassin versant, la signature isotopique du lithium des eaux n'est pas un traceur des lithologies, mais il a été montré que l'amplitude du fractionnement isotopique (Δ) est à mettre en relation avec l'intensité de l'altération (Huh et al., 2001 ; Millot et al., 2010a).

En ce qui concerne le fractionnement isotopique à plus haute température, notamment lors des processus d'altération sous-marine de la croûte océanique, Chan et al., (1992) ont montré qu'il existait un fractionnement de α = 0.981 pour une température de 150°C ($\alpha_{\text{minéral-fluide}}$), alors qu'il est de 0.993 à 0.997 à 350°C environ (Chan et al., 1993). Enfin, l'analyse isotopique du lithium de différentes laves d'une série de différentiation magmatique a clairement montré l'absence de fractionnement isotopique à partir de 1050°C (Tomascak et al., 1999a). De plus, une loi expérimentale qui relie le fractionnement isotopique (entre une solution et la phase solide) et la température a été établie par Millot et al., (2010b) et s'exprime de la façon suivante avec la température en Kelvin :

$$\Delta_{\text{solution – solide}} = 7847 / T - 8.093$$

La plupart des fractionnements isotopiques du lithium se produisent à la surface de la Terre. La faible charge ionique, le rayon relativement petit et le fort degré de covalence dans ses liaisons donnent au lithium des propriétés qui vont faire qu'il sera présent dans de nombreux environnements géochimiques (eaux, roches, sols, sédiments...). Le lithium possède en solution une coordination tétraédrique hydratée par des molécules d'eau. Dans les solides, le lithium occupe des sites de coordination soit tétraédrique, soit octaédrique.

Le fractionnement isotopique associé à la cristallisation/recristallisation, dans laquelle le gain en énergie se produit par l'incorporation préférentielle d'un isotope par rapport à l'autre dans un site cristallographique, est un mécanisme important à la surface de la Terre. Les calculs thermodynamiques (Yamaji et al., 2001) montrent que l'échange de lithium vers des sites cristallographiques octaédriques à partir d'une solution favorise l'incorporation préférentielle de l'isotope ^{6}Li dans le solide. Ce fractionnement isotopique a été mis en évidence dans de nombreux environnements naturels, et l'effet de fractionnement semble être dépendant à la fois de la température de réaction et du rapport eau/roche dans une moindre mesure (Wunder et al., 2006 ; Millot et al., 2010b).

Les lois thermodynamiques de fractionnement isotopique du lithium lors de la dissolution de minéraux primaires (fractionnement d'équilibre) tiennent compte des faibles différences

[1] α est le facteur de fractionnement entre les phases A et B, tel que : 10^3 x ln $\alpha_{A\text{-}B} \approx \delta^7Li_A - \delta^7Li_B \equiv \Delta_{A\text{-}B}$

d'énergies de liaison entre les ions des différentes masses (O'Neil, 1986). Ainsi la rupture de la liaison du ^{6}Li (haute énergie) est favorable du point de vu énergétique, de telle sorte que le fractionnement isotopique d'équilibre va favoriser l'enrichissement relatif de la solution en isotope ^{6}Li. D'autre part, lors d'expériences de dissolution de verres basaltiques, Verney-Carron et al. (2010) ont montré que des lessivages partiels peuvent également produire des solutions enrichies en ^{6}Li du fait de l'enrichissement par diffusion de cet isotope léger dans les couches externes des verres basaltiques. Toutefois, il a été aussi montré (Pistiner et Henderson, 2003) par des expériences de dissolution de roches en laboratoire que la dissolution minérale congruente ne semble pas être à l'origine d'un fractionnement isotopique significatif (c'est à dire mesurable dans la limite des performances analytiques actuelles, au mieux ± 0.5‰).

Quoiqu'il en soit, la dissolution en tant que mécanisme de fractionnement isotopique n'est pas forcément le processus dominant dans les environnements de basse température, où ses effets sont généralement masqués par des processus postérieurs, comme lors l'altération continentale et la néoformation de minéraux d'altération (Huh et al., 2001 ; Millot et al., 2010a ; Lemarchand et al, 2010).

L'adsorption sur les surfaces minérales est un des mécanismes majeurs du fractionnement isotopique du lithium dans l'hydrosphère. A la température de la surface de la Terre, l'adsorption du lithium sur des phases minérales à partir d'une solution a été mise en évidence (Taylor et Urey, 1938 ; Anderson et al., 1989), bien que les lois d'adsorption prédisent que le lithium doit être adsorbé en faible proportion en comparaison des autres éléments de la famille des alcalins. La sorption et la rétention des ions en solution dépend fortement de la chimie des surfaces minérales et de la composition de la solution.

D'autre part, il a été montré expérimentalement que l'amplitude du fractionnement de masse à la désorption est équivalente à celle liée à l'adsorption (Taylor et Urey, 1938), alors que des analyses d'échantillons naturels ont montré que ce fractionnement n'était pas réversible (James et Palmer, 2000). L'irréversibilité de ce processus peut être attribuée au fait que du lithium soit incorporé dans des sites cristallographiques structuraux plutôt que dans des sites échangeables à la surface, suggérant que l'amplitude de ce fractionnement peut être très différente selon les surfaces minérales considérées.

Le comportement du lithium dissous lors de la sorption d'une eau de mer sur des minéraux argileux et des sédiments a été étudié par Zhang et al., (1998). Ces auteurs ont observé un fractionnement isotopique similaire pour la vermiculite, la kaolinite et des sédiments du fleuve Mississippi ($\alpha \sim 0.978$). Pistiner et Henderson (2003) ont également réalisé des expériences sur l'effet isotopique lors de la sorption du lithium sur différents minéraux. Leurs résultats montrent que les réactions de sorption dans lesquelles le lithium n'est pas incorporé de manière structurale ne produit pas de fractionnement isotopique. Alors que leurs expériences montrent que lorsque le lithium est incorporé par des liaisons plus fortes, un fractionnement isotopique est observé et dépend de la structure chimique des minéraux, en accord avec les données acquises par Anghel et al. (2002). Le fractionnement le plus important est mesuré pour la gibbsite avec $\alpha \sim 0.986$, ce résultat est en accord avec ceux de Millot et Girard (2007).

3. Mesure des rapports isotopiques du lithium

3.1. Spectrométrie de masse

Les rapports isotopiques d'un élément sont mesurés par un spectromètre de masse, où un faisceau d'ions est produit dans une source sous vide à partir d'un échantillon. Les différents ions sont séparés selon leur rapport masse/charge par une combinaison de champs électromagnétiques incluant une accélération/focalisation par un champ électrique et une séparation en masse par un champ magnétique. Ils sont enfin détectés et exprimés en fonction de leur abondance relative.

Dans la spectrométrie de masse appliquée aux isotopes du lithium deux grands types sont utilisés :

1- les spectromètres de masse à source « solide » (**TIMS** pour Thermo-Ionisation Mass Spectrometer)

2- les spectromètres de masse à source plasma à couplage inductif et multi-collection **MC-ICP-MS**.

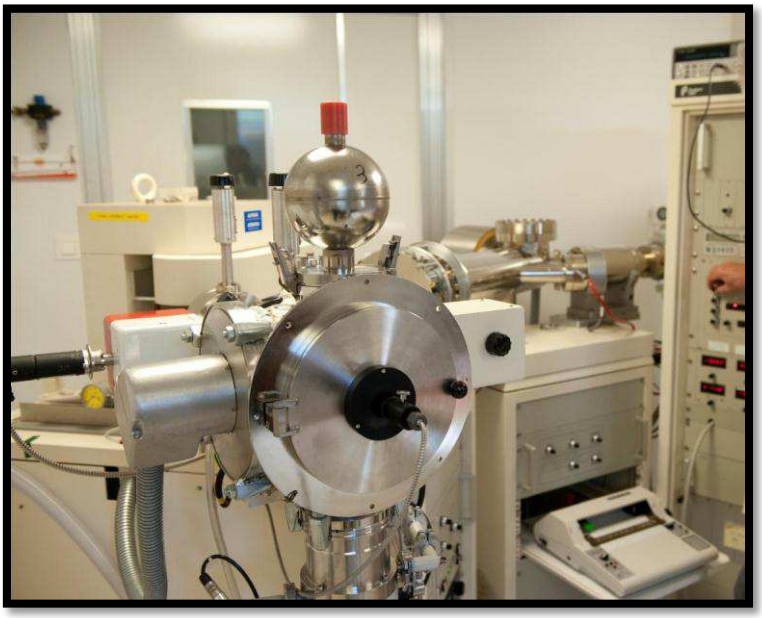

Figure 7 - Spectromètre de masse à source solide (TIMS) modèle MAT 262 du brgm. La partie en premier plan correspond à la source, ensuite nous pouvons apercevoir l'aimant au second plan à gauche et enfin le tube et la partie « collection/détection » à l'arrière plan à droite.

La technique TIMS (Thermo-ionisation Mass Spectrometry, Figure 7), met en jeu la thermo-ionisation d'un élément dans une source dite « solide » sous vide à des températures supérieures à 1000°C. L'échantillon est déposé sous forme de très fines gouttes sur des filaments d'un métal réfractaire (rhénium, tungstène ou tantale); l'évaporation de la solution

laisse un sel sur le filament. Ce filament est chauffé jusqu'à une température suffisante pour que le sel soit évaporé et que l'élément soit ionisé.

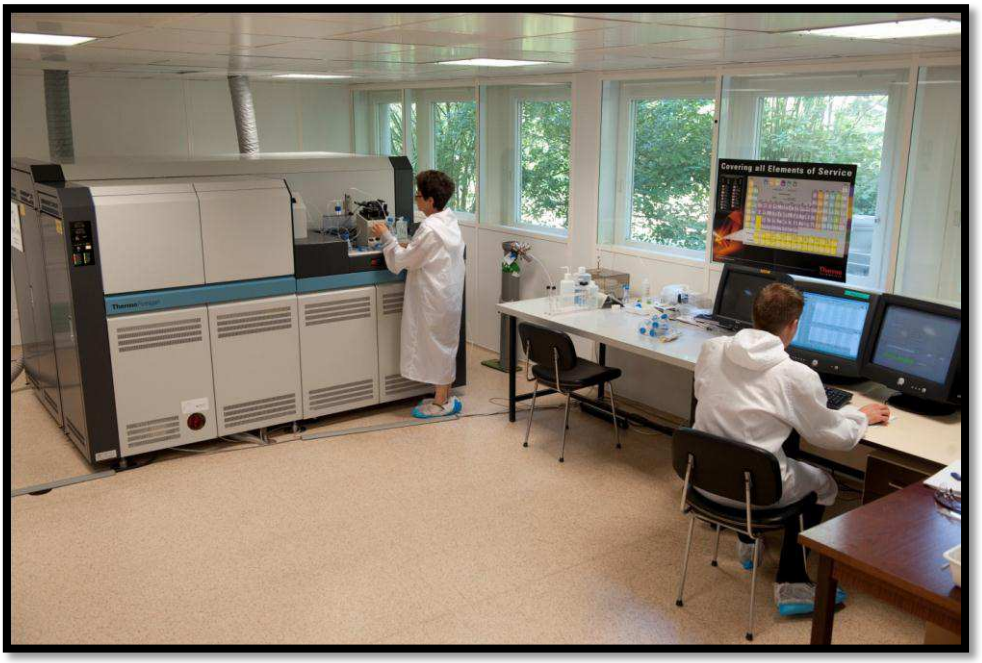

Figure 8 - Neptune MC-ICP-MS en service au brgm.

Les MC-ICP-MS (Figure 8) utilisent la méthode dite à source plasma des ICP-MS pour la vaporisation et l'ionisation des échantillons couplée avec la technique de spectrométrie de masse pour la séparation des isotopes et la mesure des rapports isotopiques. L'échantillon liquide est introduit dans la source du spectromètre sous la forme d'un aérosol où il est vaporisé et ionisé par un plasma, gaz partiellement ionisé sous l'influence d'une forte différence de potentiel. Cette méthode, par rapport à la technique TIMS, présente l'avantage de créer un très bon taux d'ionisation pour un grand nombre d'éléments.

Au préalable à cette mesure isotopique par TIMS ou MC-ICP-MS, l'échantillon subit une étape de préparation : l'élément dont on souhaite mesurer la composition isotopique doit être purifié, c'est à dire séparé du reste de la matrice. Cette étape de préparation des échantillons, nécessaire pour isoler l'élément dont on veut analyser les isotopes, se déroule dans des salles blanches en surpression, avec des réactifs purifiés permettant une contamination négligeable.

Les premières mesures isotopiques du lithium ont été réalisées par spectrométrie de masse à thermo-ionisation (TIMS) dans les années 80, à des niveaux de précision proche de 1 à 2‰ et pour une quantité de lithium de 100 ng à 1000 ng (Chan, 1987 ; Xiao et Beary, 1989). Mais ce n'est que très récemment, avec le développement technologique des dernières générations de spectromètres de masse à source plasma et multi-collection (MC-ICP-MS), que la mesure isotopique a été rendue possible pour des quantités beaucoup plus faibles (20 à 50 ng) avec une précision meilleure (0.5 à 1‰ ; Tomascak et al., 1999b ; Nishio et Nakai, 2002 ; Bryant et al., 2003 ; Millot et al., 2004). A l'heure actuelle, la mesure par MC-ICP-MS combine de très nombreux avantages, notamment en ce qui concerne la sensibilité, la reproductibilité mais également la rapidité d'analyse.

Le lien qui existe entre les développements des méthodes instrumentales et le nombre de publications dans la thématique du lithium dans les Sciences de la Terre est représenté graphiquement dans la Figure 9, où sont reportées les publications par année avec en bas les différentes évolutions dans les techniques de mesures. Cette compilation bibliographique, bien que datant de 2010, illustre l'augmentation significative des publications dans le domaine en relation avec les dernières évolutions de MC-ICP-MS au début des années 2000.

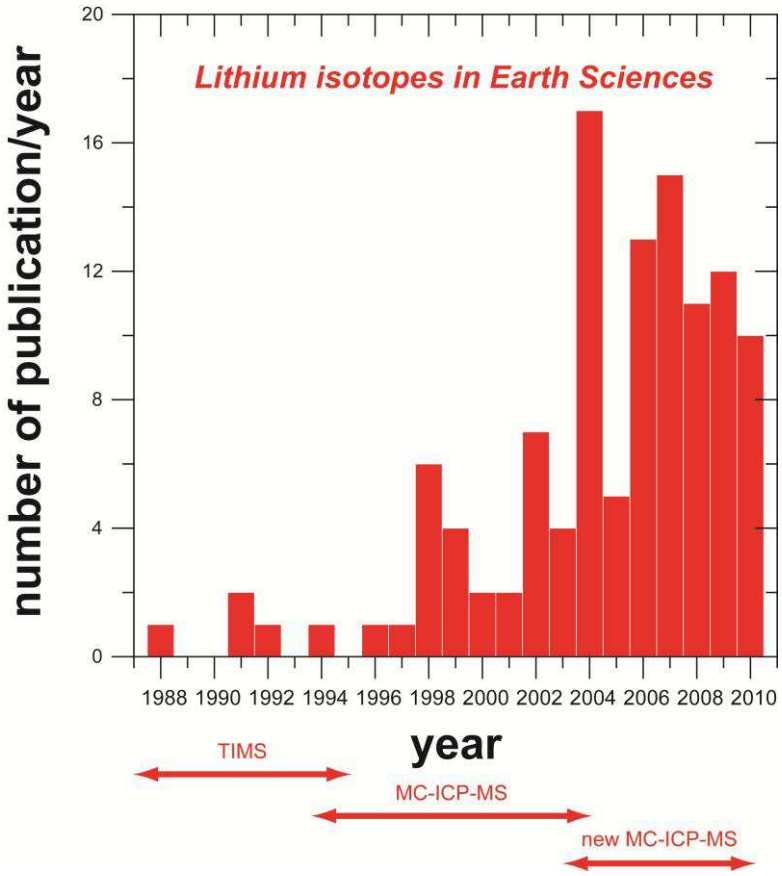

Figure 9 - Nombre de publications scientifiques par année dans la thématique des isotopes du lithium dans les Sciences de la Terre (étude bibiographique réalisée en 2010).

3.2. Protocole de purification du lithium

Comme déjà dit précédemment, avant la mesure isotopique, nous procédons à une préparation chimique de l'échantillon de façon à obtenir une quantité purifiée de lithium de 60 ng. Pour les échantillons solides (roches, sédiments, minéraux) une autre étape préalable à la purification est nécessaire et consiste en la mise en solution de l'échantillon par attaque acide à chaud (HF, HNO_3 $HClO_4$, HCl).

Un fois en solution, le lithium est donc séparé de sa matrice par chromatographie ionique sur résine échangeuse d'ions dans une salle blanche sous hotte à flux laminaire (Figure 10).

Figure 10 - Colonnes en Téflon contenant de la résine cationique, ces colonnes se trouvent dans une hotte à flux laminaire, elle-même située dans une salle blanche.

L'étape de purification par chromatographie ionique consiste à séparer les éléments chimiques contenus dans une matrice. Le principe repose sur les équilibres successifs lors de l'élution d'une solution dans une colonne contenant de la résine, ces équilibres sont régis par les coefficients de partage des différents éléments entre la résine et la phase d'élution. La figure 11 illustre le principe de séparation des deux éléments. Les résultats de la calibration en ce qui concerne les éléments Li et Na sont reportés dans la figure 12 pour une matrice d'eau de mer. L'exemple de la purification du lithium de l'eau de mer a été choisi d'une part parce que le rapport Na/Li de l'eau de mer est très important et d'autre part parce que les éléments Li et Na possèdent des coefficients de partage relativement proches pour ce type de résines (les autres cations majeurs Mg^{2+}, K^{+}, Ca^{2+} sont retenus en milieu acide HCl 0.2N dans la résine). La séparation quantitative du Li et du Na de l'eau de mer constitue donc un vrai challenge analytique.

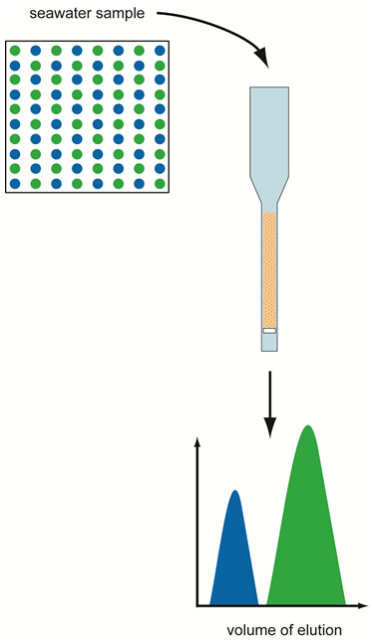

Figure 11 - Schéma de principe de séparation de deux éléments par chromatographie ionique.

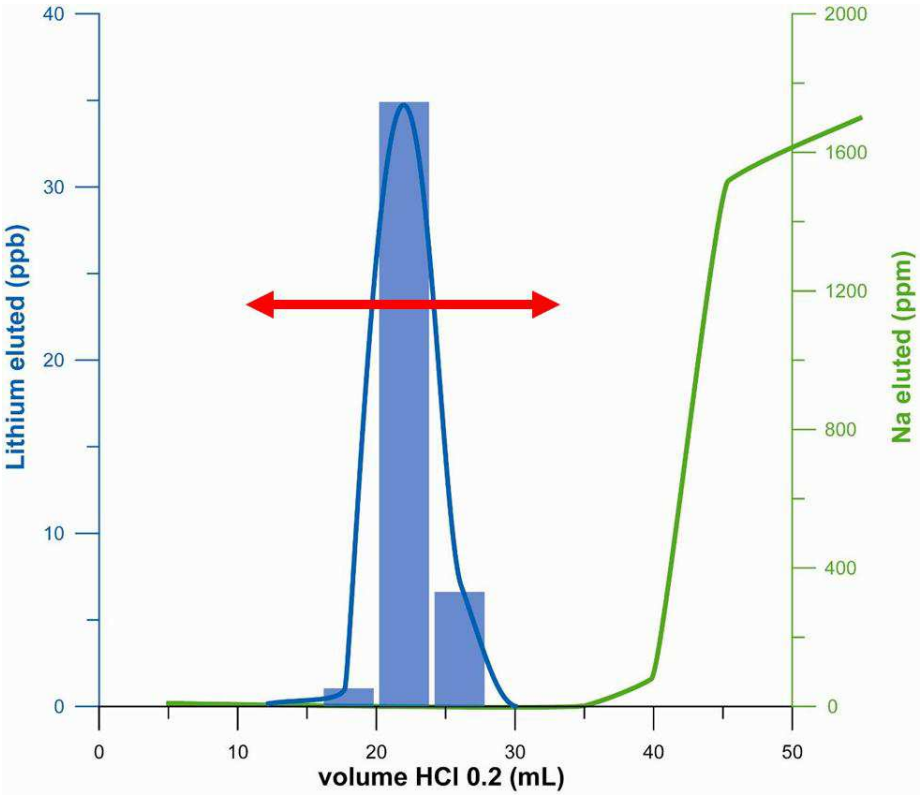

Figure 12 - Courbes d'élution du lithium et du sodium en milieu acide HCl 0.2N pour une matrice eau de mer. Seule la fraction comprise entre 10 et 35 mL est collectée (flèche rouge) et contient uniquement le lithium. A noter la différence d'échelle significative entre le lithium et le sodium.

Lors de cette étape de purification, il a été montré que les deux isotopes de masse 6 et 7 du lithium peuvent être fractionnés si le rendement de purification n'est pas exactement de

100%. Dans la figure 13, le rapport isotopique $^{7}Li/^{6}Li$ est reporté en fonction du pourcentage de Li élué. Ce graphique illustre bien la différence qui existe au cours de l'élution : le ^{6}Li et le ^{7}Li présentent un comportement légèrement différent (le ^{6}Li est fixé de manière plus efficace du fait de la différence de masse).

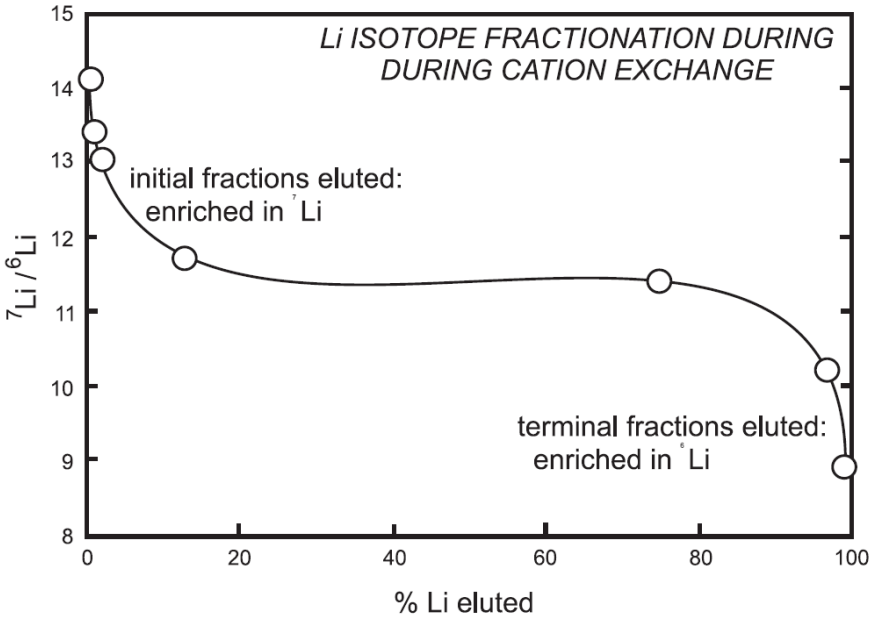

Figure 13 - Evolution de la composition isotopique du lithium au cours de l'élution sur résine échangeuse d'ions (d'après Tomascak, 2004).

Au cours des développements analytiques que nous avons réalisés, nous avons testé l'absence de fractionnement lors de l'analyse répétée de solutions de référence de Li (après purification). De plus, nous avons également évalué notre reproductibilité totale externe par la mesure répétée du standard d'eau de mer IRMM BCR-403 après purification chimique ($\delta^{7}Li$ = +31.0 ± 0.5‰, 2σ, n = 31, Millot et al., 2004). La figure 14 montre les données compilées dans la littérature pour l'eau de mer actuelle, sachant que la composition isotopique du lithium de l'océan est homogène (Huh et al., 1998). La reproductibilité que nous obtenons est de ± 0.5‰ (2σ).

Le standard de roche JB-2 a également été analysé après la mise en solution de ce basalte par attaque acide et la purification du lithium de sa matrice. Nous obtenons la valeur moyenne de $\delta^{7}Li$ = +4.9‰ ± 0.6 (2 σ, n = 17), qui est en très bon accord avec les données publiées dans la littérature (voir une compilation des données dans Tomascak 2004).

D'autre part, dans le cadre d'une collaboration avec le Centre de Recherches Pétrographiques et Géochimiques de Nancy (CRPG) qui a synthétisé 3 solutions standards (Li6-N, LiCl-N et Li7-N) qui couvre une très large gamme de variations isotopiques du lithium (de -10 à +30‰), nous avons pu tester la justesse de notre mesure (Carignan et al., 2007 ; Figure 15) sur deux instruments différents : respectivement l'ISOPROBE à Nancy et le NEPTUNE à Orléans.

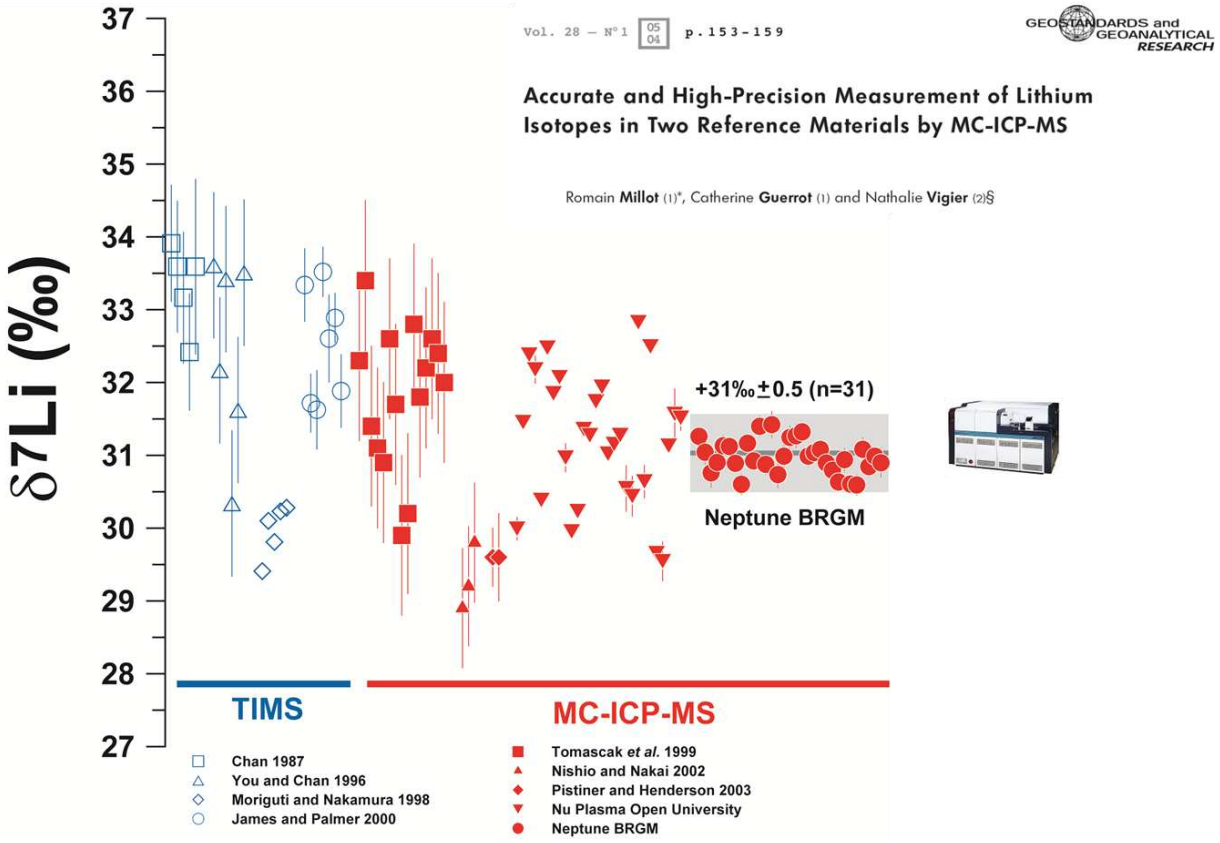

Figure 14 - Compilation des mesures de la composition isotopique de l'eau de mer par TIMS (en bleu) et MC-ICP-MS (en rouge). Nos valeurs sont reportées à droite de la figure (Millot et al., 2004).

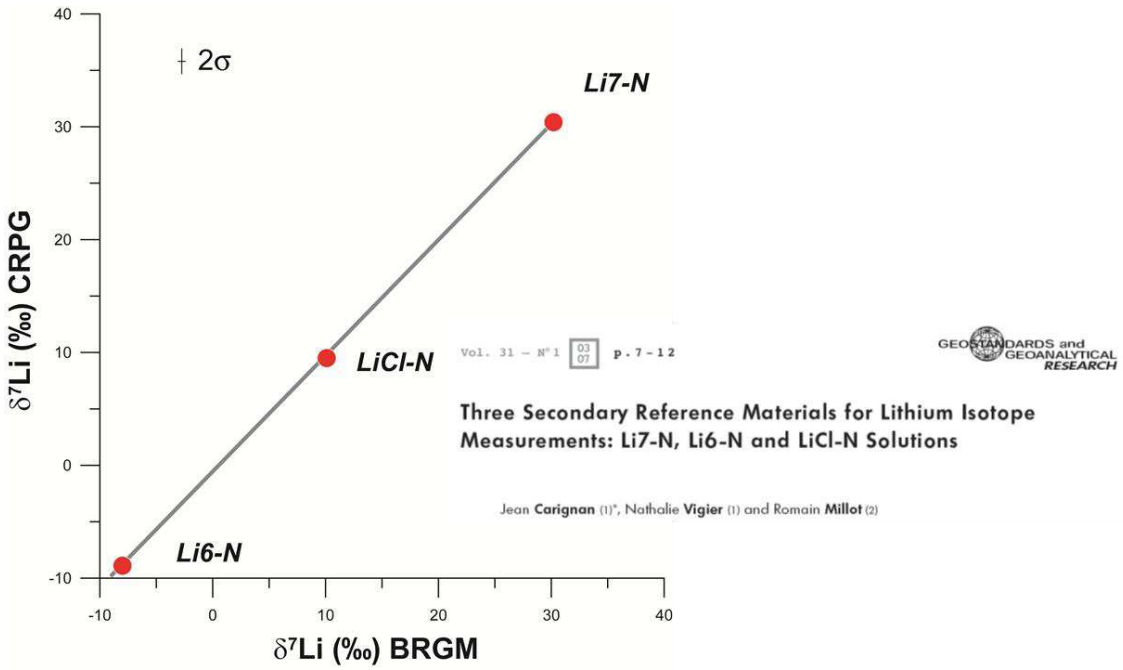

Figure 15 - Comparaison entre les valeurs obtenues à Nancy (axe des Y) et au BRGM (axe des X) lors de la mesure de 3 solutions standards Li6-N, LiCl-N et Li7-N (Carignan et al., 2007). A noter les erreurs différentes reportées en haut à gauche pour deux MC-ICP-MS différents.

3.3. Acquisition de données et corrections

Le biais de masse instrumental qui se produit dans la source plasma de l'instrument résulte de l'extraction et de la transmission préférentielle des ions les plus lourds dans la source ICP (Figure 16).

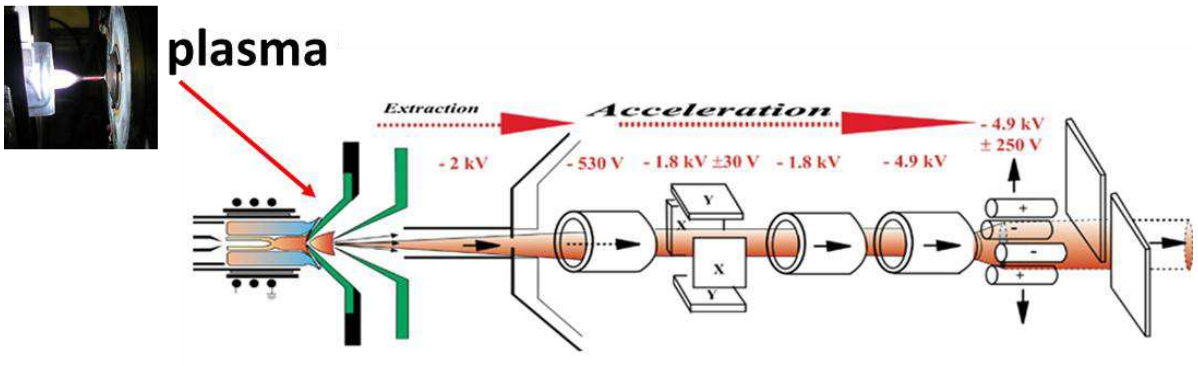

Figure 16 - Schéma et photographie de la source ICP du Neptune. Successivement de gauche à droite : le lithium est tout d'abord ionisé dans le plasma, les ions sont ensuite extraits par une différence de potentiels de 2000 V, puis ce faisceau est accélerré (5000 V) et focalisé à la fois dans les 3 dimensions de l'espace (X-Y-Z) mais aussi en énergie par un filtre électrostatique.

Afin de corriger de ce biais de masse instrumental et de sa dérive au cours du temps, la mesure de la composition isotopique se fait selon la méthode dite de « standard-bracketing » en normalisant au standard L-SVEC (NIST, RM8545). Chaque mesure isotopique (échantillon et standard L-SVEC) est également corrigée du « blanc » qui correspond au milieu d'introduction contenant l'échantillon (HNO_3 3%) et au bruit de fond instrumental. Le principe est décrit dans la figure 17, où l'on alterne successivement un standard, un échantillon, un standard etc.

La mesure des isotopes du lithium se fait en mode « plasma chaud » (1200W) et le système d'introduction utilisé est le SIS (Stable Introduction Système) qui est constitué d'une double chambre de nébulisation (cyclonique + type Scott) associée à un micro-nébuliseur en Téflon PFA (Figure 18).

Une fois l'échantillon liquide introduit dans la source sous la forme d'un aérosol, le lithium est ionisé dans le plasma (partie **ICP** : Inductively Coupled Plasma, Figure 19). Le faisceau d'ions ainsi créé est accéléré puis focalisé par un système composé de lentilles et de plaques de focalisation.

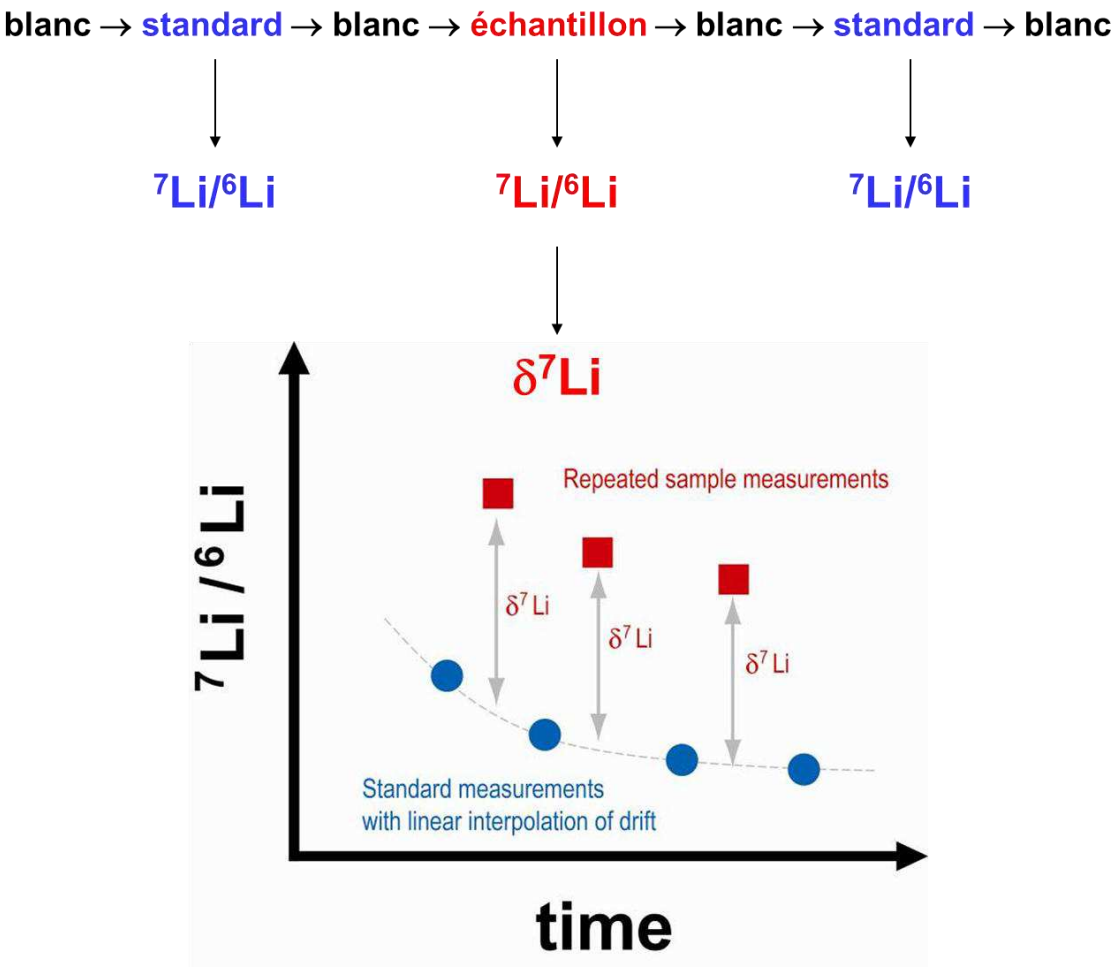

Figure 17 - Principe du standard-bracketing et de la correction des blancs. Le schéma du bas montre l'évolution au cours du temps du rapport isotopique pour le standard et l'échantillon ainsi que le principe d'interpolation pour le calcul du delta.

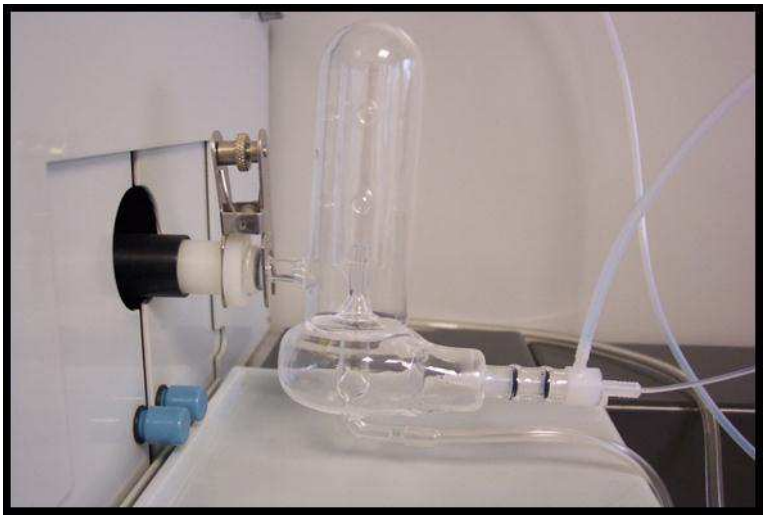

Figure 18 - Système SIS d'introduction de l'échantillon liquide dans le plasma.

La partie principale du spectromètre de masse est l'aimant (partie **MS** : Mass Spectrometry, Figure 18). En effet, c'est dans cette partie que les trajectoires des particules chargées vont être séparées en fonction de leur masse.

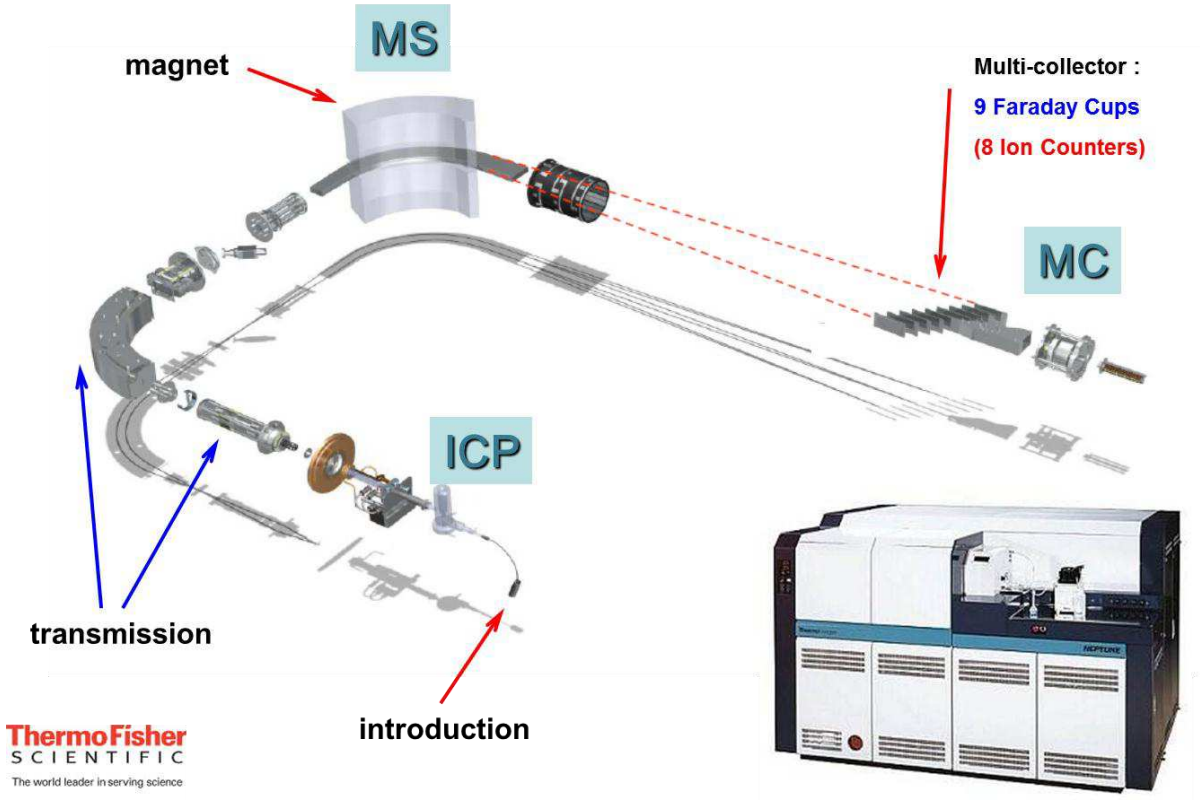

Figure 19 - Schéma de fonctionnement du MC-ICP-MS Neptune.

Enfin, dans la partie **MC** (Multi Collection) les faisceaux d'ions pour les isotopes 6 et 7 du lithium sont mesurés en multi-collection statique sur les cages de Faraday les plus éloignées (L4 et H4, Figue 20) après amplification du signal.

La mesure se fait lors de l'acquisition des signaux sur les masses 6 et 7 pendant 15 scans de 16 secondes de temps d'intégration. La mesure au total dure donc 4 minutes, auxquels il faut ajouter 1 minute 30 « d'uptake » pour permettre à la solution d'arriver et au signal de se stabiliser. Avec la configuration telle que décrite précédemment, nous obtenons des signaux proches de 2V et 0.1V respectivement pour les masses 7 et 6 du lithium (Figure 20). La statistique de mesure nous donne une erreur interne de l'ordre de 0.1 à 0.2‰ ($2\sigma_m$). Lors de la mesure, environ 500 µL d'une solution à 30 ng/mL sont consommés, ce qui correspond à une quantité totale de 15 ng du lithium.

Enfin, le blanc (milieu d'introduction de l'échantillon) est faible, de l'ordre de quelques mV sur la masse 7 du lithium, ce qui correspond à moins de 0.2% du signal de l'échantillon. Un rinçage en milieu HNO_3 3% pendant 5 minutes entre chaque mesure est suffisant pour un retour à la ligne de base et une correction juste de ce blanc lors de la mesure.

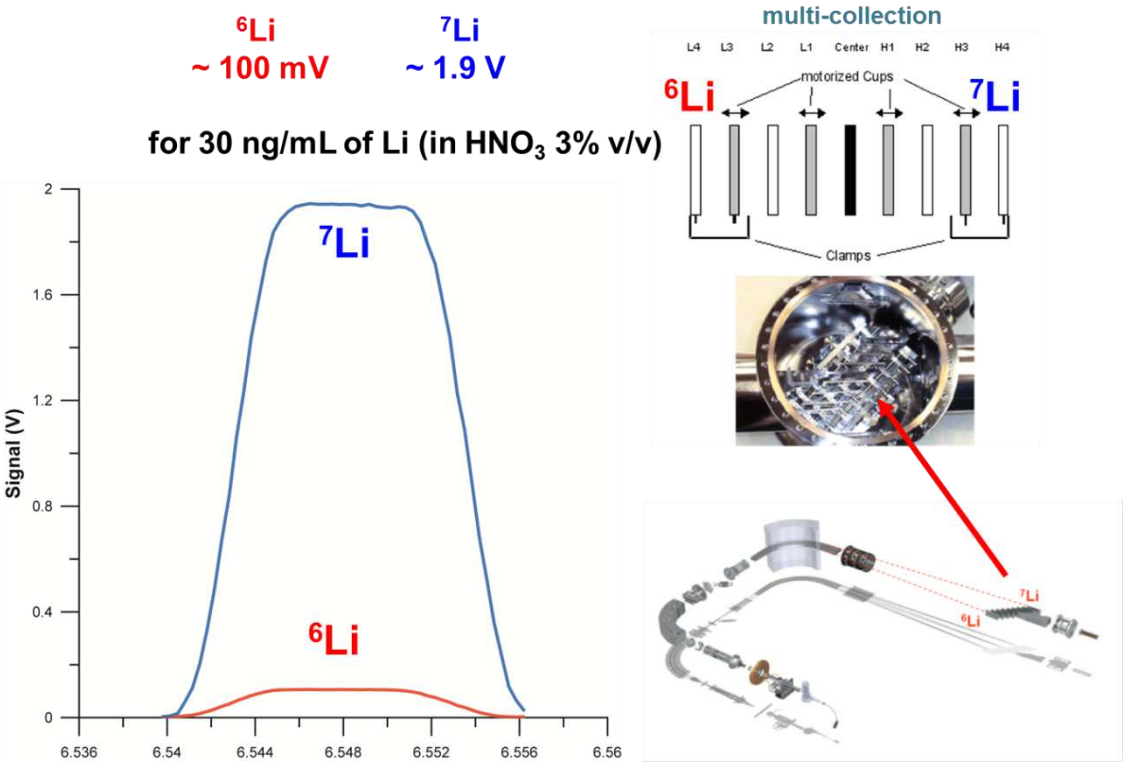

Figure 20 - Configuration pour la mesure des isotopes du lithium sur les cages L4 et H4. Les spectres de masse pour les masses 6 et 7 sont donnés pour la mesure d'une solution standard de 30 ng/mL de lithium.

Pour conclure en ce qui concerne la mesure des isotopes du lithium par MC-ICP-MS, nous retiendrons que :

- **La méthode de mesure des isotopes du lithium sur Neptune MC-ICP-MS est relativement rapide et très sensible : 15 ng de lithium suffisent pour la mesure de la composition isotopique. Cette mesure requiert des réglages fins de l'instrument et une bonne validation de l'ensemble de la chaine analytique.**

- **Au préalable à la mesure, une étape de purification du lithium est nécessaire. Lors de cette étape, il faut s'assurer du rendement de 100%, de l'absence de fractionnement et de l'absence de contamination soit par les réactifs soit par l'opérateur. Au cours de la préparation de l'échantillon, l'apport en lithium lié aux réactifs utilisés et à la manipulation est totalement négligeable. Aucune correction de blanc de chimie n'est donc apportée. Toutefois des mesures de blancs de chimie et des réactifs sont réalisées périodiquement pour contrôler leurs niveaux et leurs reproductibilités.**

- **Le protocole a été validé par la mesure répétée sur le long terme de différentes solutions standards et de matériaux de référence. Il est important de souligner que la reproductibilité externe de notre protocole pour la mesure isotopique du lithium**

d'échantillons naturels après purification est de ± 0.5‰ (2σ, 2 standard déviation) (Millot et al., 2004). Dès lors, l'incertitude analytique attribuée à chaque détermination de δ^7Li est donc de ± 0.5‰ (2σ), elle correspond à la reproductibilité totale externe du protocole.

4. Exemples d'applications : synthèse des principaux résultats

4.1. Eaux météoriques (Millot et al., 2010[2])

Dans cette étude, nous reportons pour la première fois la composition isotopique d'eaux de pluies. Nous avons réalisé le suivi mensuel de 4 sites en France tout au long d'une année à la fois pour des stations proches de l'océan (Brest, Dax) et des stations plus continentales (Orléans, Clermont-Ferrand ; Figure 21).

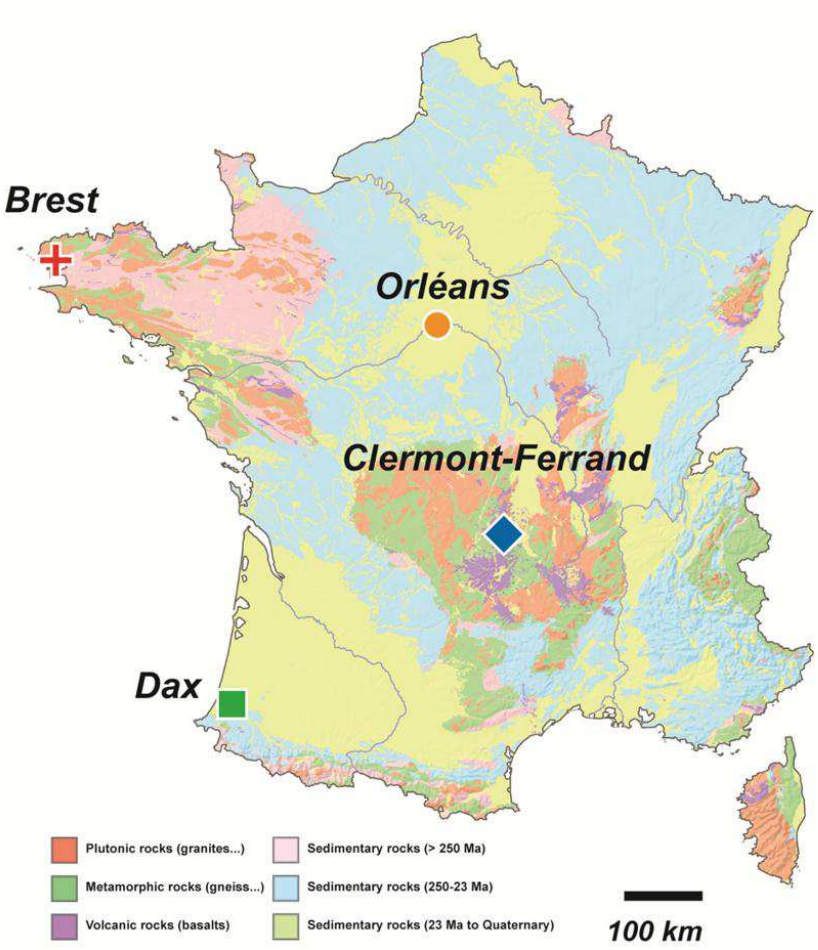

Figure 21 - Carte de localisation des sites de suivi des eaux de pluies sur fond de carte géologique (Millot et al., 2010c).

L'objectif de ce travail était de contraindre l'origine du lithium dans les eaux de pluie par une approche isotopique en étudiant les variations spatio-temporelles des eaux météoriques à l'échelle de la France au cours d'un suivi annuel. Un autre objectif de ce travail visait également à contraindre l'apport des eaux météoriques aux eaux de surface en terme de

[2] Millot R., Petelet-Giraud E., Guerrot C., Négrel Ph. (2010) Multi-isotopic composition (δ^7Li-δ^{11}B-δD-δ^{18}O) of rainwaters in France: origin and spatio-temporal characterization. Applied Geochemistry, 25: 1510-1524.

signature isotopique moyenne. Cet apport serait intégré par la suite dans les modèles de mélange pour les eaux de surface (rivières, fleuves) et les eaux de subsurface (eaux souterraines).

Avant cette étude des isotopes du lithium dans les pluies, l'hypothèse qui était faite dans la littérature consistait à considérer que le lithium de la pluie était uniquement d'origine marine et donc que sa composition isotopique était celle de l'océan actuel (δ^7Li = +31‰).

Le premier résultat majeur de cette étude est graphiquement représenté dans la figure 22, où les compositions isotopiques du lithium sont reportées sous la forme d'un histogramme pour les 4 sites d'étude : nous pouvons voir très clairement que les eaux de pluie n'ont pas la signature isotopique de l'eau de mer (δ^7Li = +31‰).

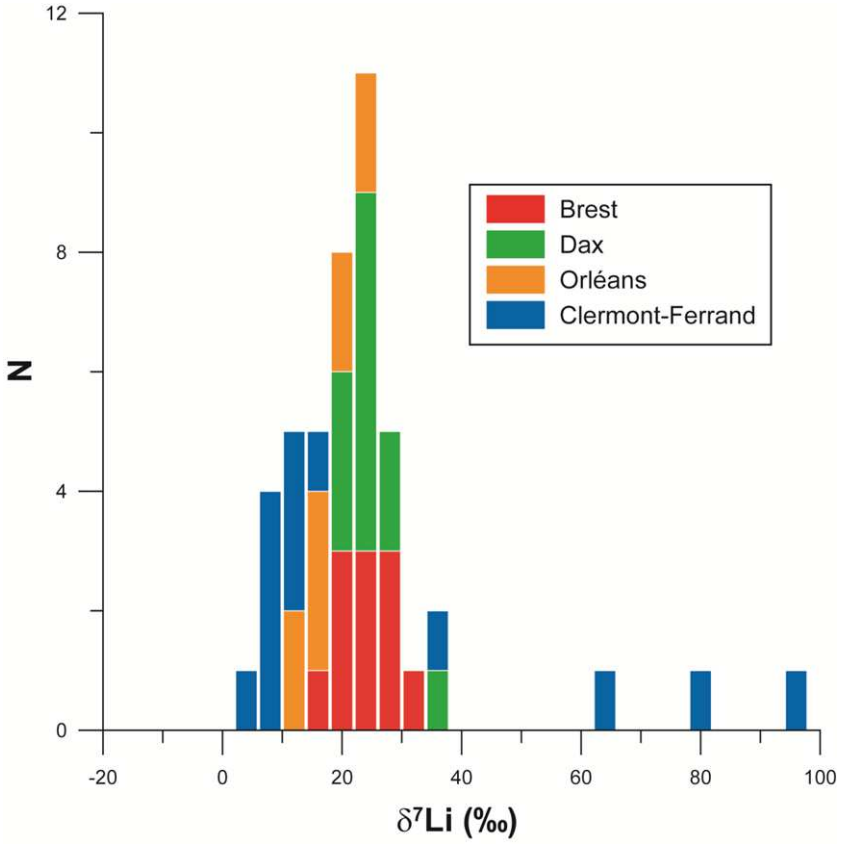

Figure 22 - Histogramme des compositions isotopiques du lithium des eaux de pluies pour les 4 sites d'étude (Millot et al., 2010c).

Si nous regardons les données plus en détail, nous pouvons noter que les eaux de pluies présentent une signature isotopique en lithium qui est extrêmement variable puisque comprise entre +3.2 et +95.6‰. Les moyennes (± σ) sont respectivement de +22.5‰ ± 4.3, +22.8‰ ± 4.3, +16.1‰ ± 4.8 et +26.2‰ ± 29.7 pour Brest, Dax, Orléans et Clermont-Ferrand. Nous pouvons également remarquer que les pluies de Clermont-Ferrand présentent la plus grande variabilité. Nous reviendrons sur ce point par la suite, notamment sur les valeurs très élevées en ^{7}Li pour certaines pluies de Clermont-Ferrand.

Il apparait donc que le lithium n'est pas uniquement d'origine marine dans les eaux de pluies. Avant de caractériser les autres sources de lithium dans les pluies, nous pouvons

quantifier cet apport marin en considérant que le sodium est uniquement marin, nous pouvons écrire que :

$$Li_{marin} = Na_{pluie} \times (Li/Na)_{marin}$$

L'origine de cet apport marin peut être visualisé géographiquement par la représentation des roses des vents pour les stations étudiées (Figure 23). Nous pouvons voir que l'origine des vents est globalement sud-ouest pour Dax et Orléans, et est très légèrement différente (sud-ouest et sud) pour Brest et Clermont-Ferrand.

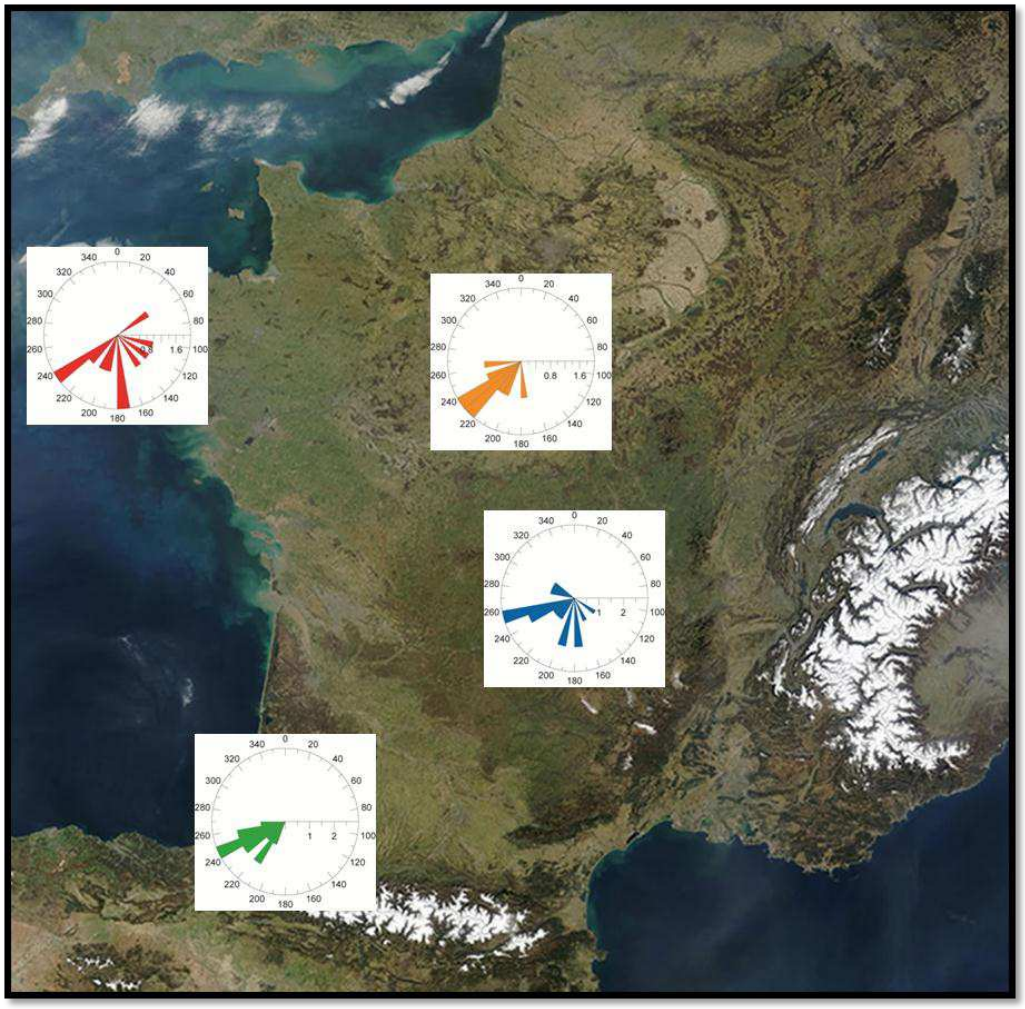

Figure 23 - Roses des vents pour les 4 sites d'étude (Millot et al., 2010c).

La figure 24 présente graphiquement la contribution marine (%Li sea salt) en fonction de la composition isotopique du lithium (δ^7Li). La lecture de cette figure montre de manière évidente que la contribution marine reste faible (< 20%, excepté pour certaines pluies de Brest).

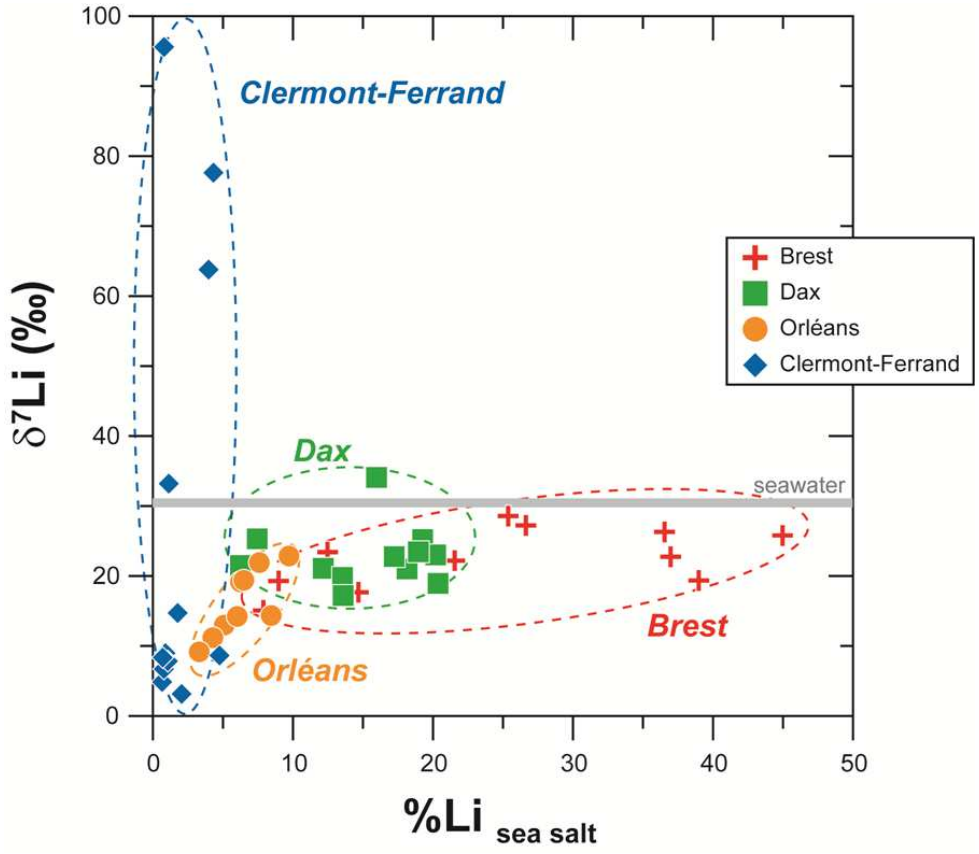

Figure 24 - Composition isotopique du lithium en fonction de la contribution marine du lithium (Millot et al., 2010c).

D'autre part, nous pouvons souligner que pour les pluies d'Orléans, Dax et Brest : plus la contribution marine du Li est importante, plus la signature δ^7Li se rapproche de celle de l'eau de mer. Ce schéma n'est absolument pas respecté pour les pluies de Clermont-Ferrand, où la contribution marine est très faible (entre 0 et 5%) et le δ^7Li varie beaucoup et de manière indépendante.

Pour expliquer la distribution du lithium et de ses isotopes dans les pluies de Brest, Dax, Orléans et Clermont-Ferrand, nous avons reporté dans la figure 25, la composition isotopique du lithium en fonction du rapport Na/Li.

Les roches continentales silicatées ont des compositions isotopiques en lithium qui peuvent varier entre -4 et +8‰ (Teng et al., 2004 ; Millot et al., 2010a), les carbonates ont des compositions qui varient de +6 à > +25‰ (Hoefs and Sywall, 1997; Hall et al. 2005; Hathorne and James, 2006; Vigier et al., 2007). Ces lithologies peuvent contribuer à la signature des pluies si l'on tient compte de l'interaction de particules continentales et des molécules d'eau dans l'atmosphère.

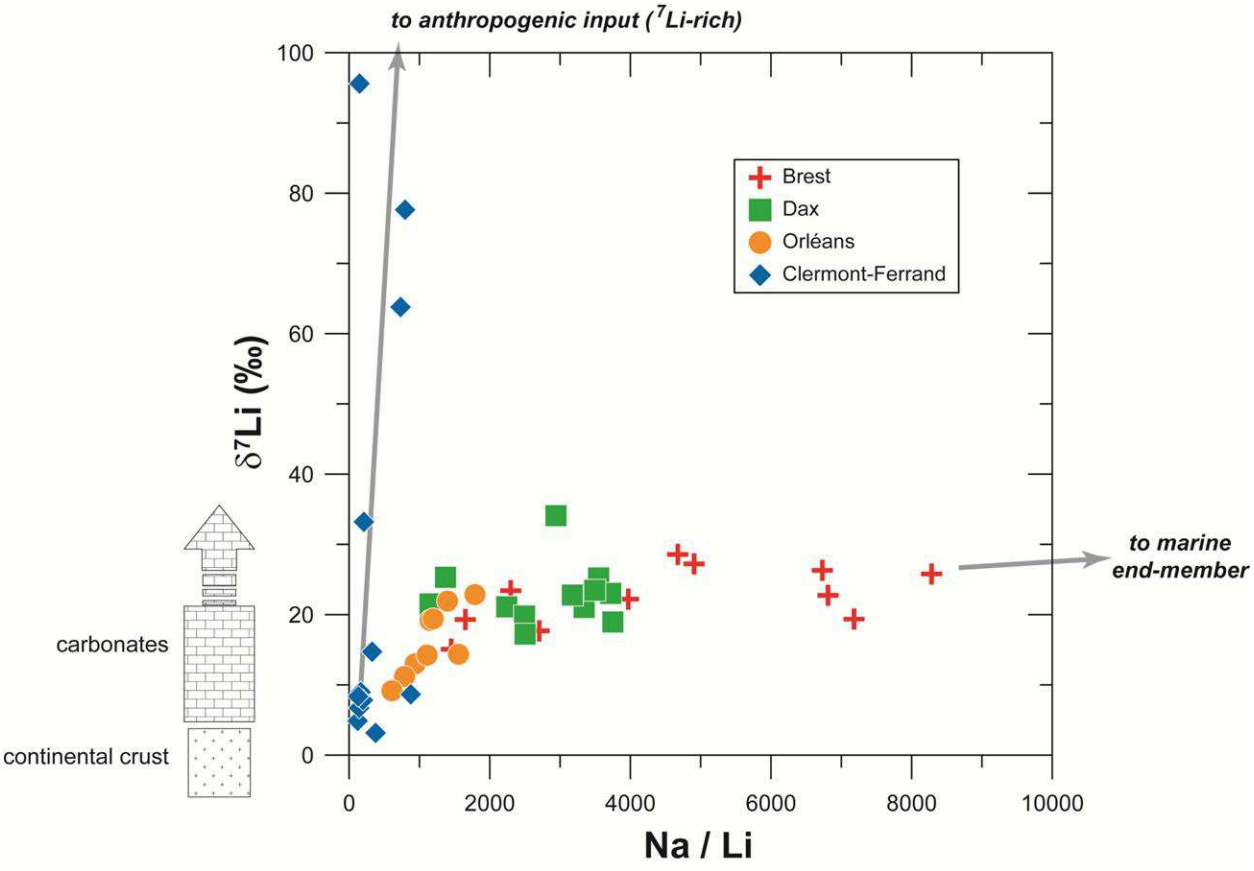

Figure 25 - Composition isotopique du lithium en fonction du rapport molaire Na/Li (Millot et al., 2010c).

Les 3 pluies de Clermont-Ferrand qui présentent une signature très enrichie en ^{7}Li (> +60‰) ont des compositions isotopiques plus élevées que celle de l'eau de mer. D'autre part, pour ces mêmes eaux de pluies, Négrel et Roy (1998) et Roy et Négrel (2001) ont montré l'existence d'une contamination anthropique liée aux engrais par le traçage isotopique du plomb et du strontium dans ces pluies. Ces valeurs élevées en ^{7}Li pourraient donc s'expliquer par une contribution locale provenant des engrais et/ou des amendements de sols utilisés par les agriculteurs dans cette zone. Ce résultat est aussi en accord avec ceux de Négrel et al. (2010) en ce qui concerne la caractérisation isotopique du lithium d'une tourbière située près du site d'échantillonnage des pluies (site de la Sauvetat). La signature enrichie en ^{7}Li des eaux de surface de la tourbière s'explique par la dissolution des engrais et des amendements qui possèdent des δ^7Li dont certaines valeurs peuvent atteindre +215‰ (Négrel et al., 2010). Ce composant extrêmement riche en ^{7}Li est attribué à la présence de lithium ajouté aux engrais et/ou amendements de sol, ce lithium proviendrait d'un stock enrichi en ^{7}Li comme cela a été proposé par Qi et al. (1997). Ce lithium très enrichi en ^{7}Li est commercialisé dans la filière industrielle du lithium et provient principalement de résidus de l'industrie nucléaire qui utilise uniquement du lithium ^{6}Li (pour ses propriétés de capture de neutrons) ainsi le lithium résiduel qui provient de cette filière est par conséquent très enrichi en ^{7}Li (Coplen et al., 2002).

Lorsque les isotopes du Li sont reportés en fonction du rapport Na/Li (Figure 25), les pluies de Clermont-Ferrand semble indiquer un mélange entre un composant crustal (silicates et/ou carbonates) et un composant anthropique (enrichi en ^{7}Li). D'autre part, les pluies de

Brest, Dax et Orléans montrent un mélange entre un composant crustal (complexe en raison de la contribution relative des différentes lithologies) et un composant marin.

Pour conclure en ce qui concerne le lithium dans les eaux de pluies, nous retiendrons que :

- **La distribution du lithium et de ses isotopes dans les pluies est très variable au niveau spatio-temporel. Les teneurs sont relativement faibles (de 0.004 à 0.292 µmol/L) et les compositions isotopiques varient de +3.2 à +95.6‰.**

- **L'effet de saisonnalité (quantité de pluie) n'est pas le facteur dominant de contrôle mais l'effet de continentalité (distance par rapport à l'océan) est très important puisqu'il détermine la contribution marine de la pluie.**

- **L'un des principaux résultats de cette étude est que majoritairement le lithium des pluies n'a pas une origine marine. Les autres sources doivent donc être prise en compte, qu'il s'agisse de particules continentales ayant interagit avec les molécules d'eau dans l'atmosphère, ou bien, comme nous l'avons vu pour le site de Clermont-Ferrand, d'un apport anthropique lié aux activités agricoles.**

4.2. Eaux de rivières (Millot et al., 2010[3] ; Lemarchand et al., 2010[4])

Dans cette partie, nous faisons la synthèse de deux articles :

1- le premier concerne un grand bassin versant aux lithologies très contrastées : **le bassin du fleuve Mackenzie au Canada** (Millot et al., 2010a)

2- le second concerne un petit bassin versant monolithologique sur granite : le **bassin du Strengbach dans les Vosges** (Lemarchand et al., 2010)

Cette approche multi-échelle nous permet de contraindre les paramètres de contrôle du fractionnement isotopique du lithium lors de l'altération par les fleuves.

4.2.1. Le bassin du fleuve Mackenzie

Le bassin du fleuve Mackenzie se situe au nord-ouest du Canada. Ce bassin est majoritairement composé de roches sédimentaires et est soumis à un climat subarctique. Les différentes zones morphologiques du bassin sont très contrastées à la fois en terme de lithologies mais aussi en terme de régime/contexte d'altération (relief, température, influence de la matière organique). La géochimie des eaux et des sédiments de ce fleuve et de ses principaux affluents a été étudiée en détails au cours de ces dernières années (Millot et al., 2002 ; 2003 ; Gaillardet et al., 2003).

L'objectif de ce travail a consisté à évaluer le potentiel des isotopes du lithium en tant que traceur des processus d'altération à l'échelle d'un grand bassin versant par l'étude des eaux et des matières en suspension.

Dans la figure 26, nous avons reporté sur la carte les points d'échantillonnage ainsi que les différentes zones morphologiques d'ouest en est : la Cordillère, les montagnes Rocheuses, la plateforme et le bouclier.

Cette zonation géographique est clairement conservée lorsque l'on regarde les compositions isotopiques du lithium des eaux en fonction de la concentration (Figure 27). Les concentrations varient de 0.05 à 1.29 µmol/L alors que les compositions isotopiques sont comprises entre +9.3 et +29.0‰.

D'autre part, il existe un très fort contraste isotopique entre les phases liquides et solides, c'est à dire entre les eaux d'une part, et les sédiments (matières en suspension) et les roches d'autre part (Figure 28). Les eaux du bassin du Mackenzie présentent des δ^7Li systématiquement plus élevés que les matières en suspension et les roches du bassin.

[3] Millot R., Vigier N., Gaillardet J. (2010) Behaviour of lithium and its isotopes during weathering in the Mackenzie Basin, Canada. Geochimica et Cosmochimica Acta, 74: 3897-3912.

[4] Lemarchand E., Chabaux F., Vigier N., Millot R., Pierret M.C. (2010) Lithium isotope systematics in a forested granitic catchment (Strengbach, Vosges Mountains, France). Geochimica et Cosmochimica Acta, 74: 4612-4628.

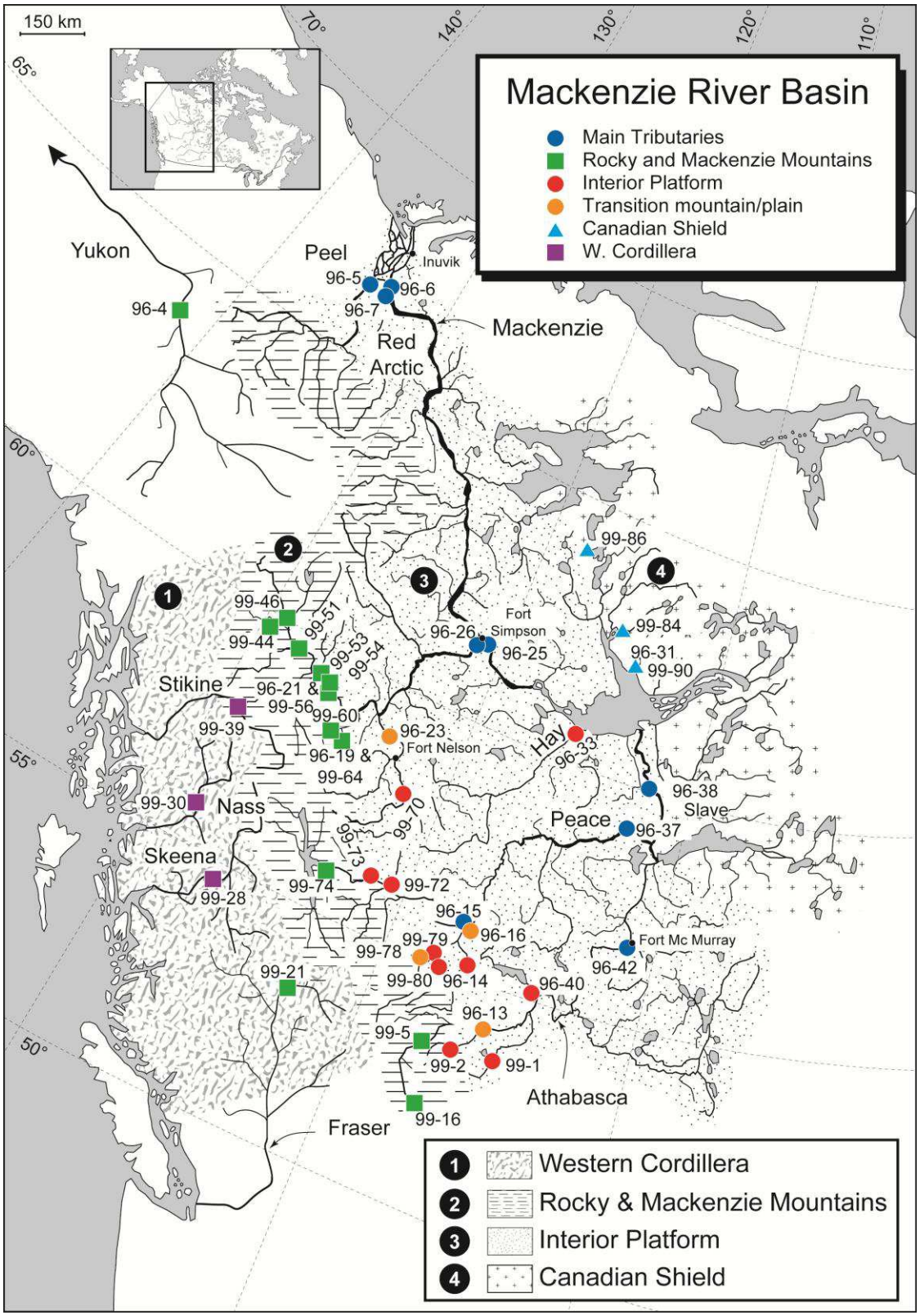

Figure 26 - Carte du bassin du fleuve Mackenzie avec les points d'échantillonage et les zones morphotectoniques (Millot et al., 2010a).

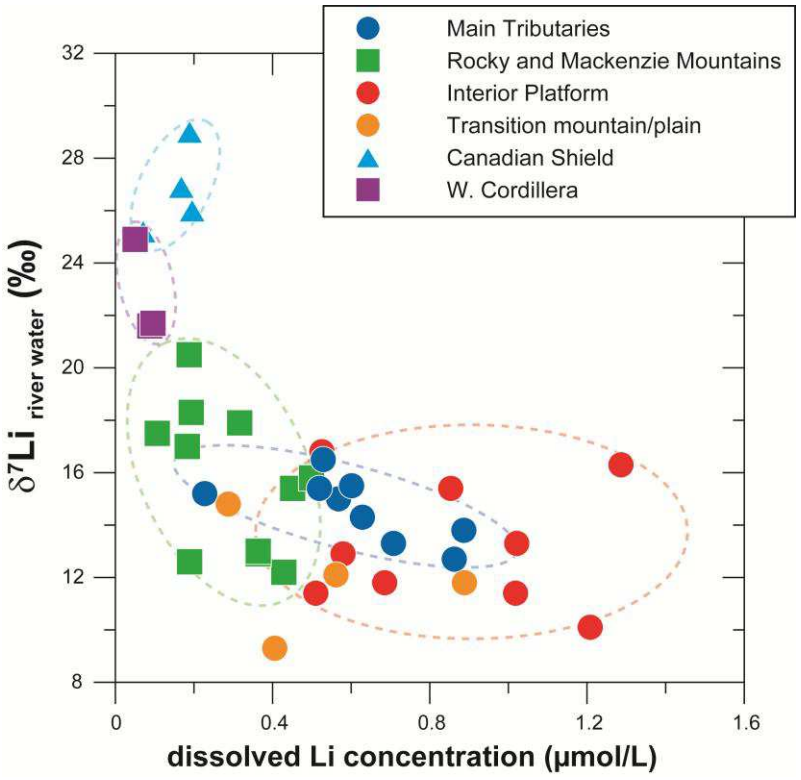

Figure 27 - Compositions isotopiques du lithium en fonction de la teneur en lithium dans les eaux du bassin du fleuve Mackenzie (Millot et al., 2010a).

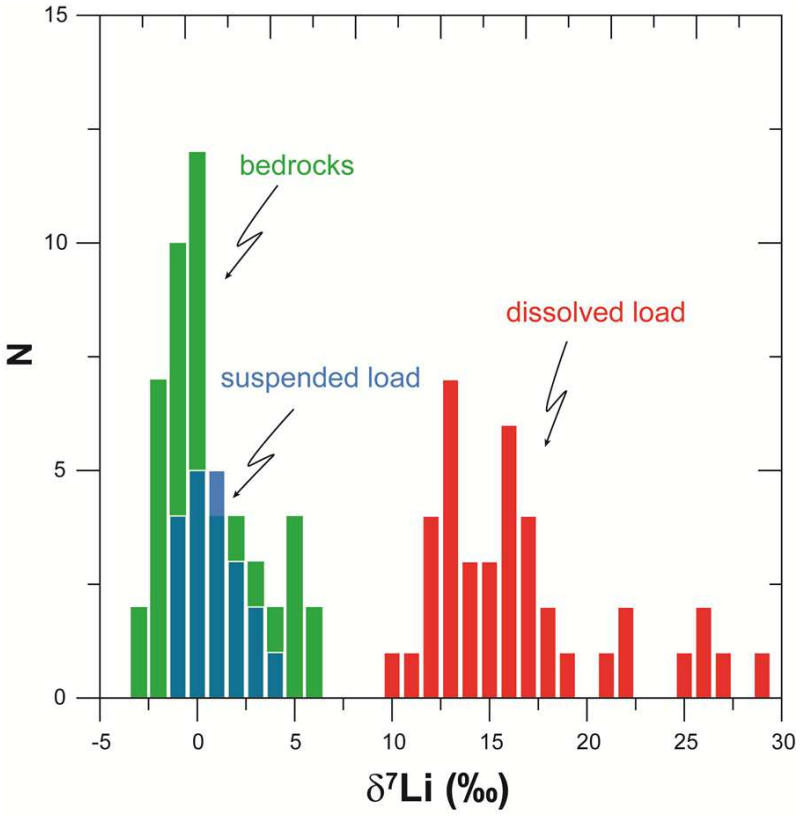

Figure 28 - Compositions isotopiques du lithium des eaux (rouge), des matières en suspension (bleu) et des roches (vert) dans le bassin du fleuve Mackenzie (Millot et al., 2010a).

Le lithium dans les eaux du bassin du Mackenzie provient quasi exclusivement de l'altération des roches silicatées (Millot et al., 2003 ; 2010a). D'autre part, l'examen attentif des signatures isotopiques des eaux en fonction de la charge dissoute provenant de l'altération de ces silicates (Figure 29) montre que les enrichissements en ^{7}Li les plus importants se produisent dans un régime d'altération relativement faible pour les fleuves des Rocheuses, de la Cordillère et du bouclier canadien (« weathering regime #1 », Figure 29 et 30).

D'un autre côté, pour les principaux affluents, les fleuves de la plateforme et de la zone de transition (« weathering regime #2 »), le régime d'altération est d'une part plus intense et d'autre part les signatures isotopiques du lithium sont relativement homogènes (notons toutefois que les δ^{7}Li sont toujours supérieurs à ceux des roches).

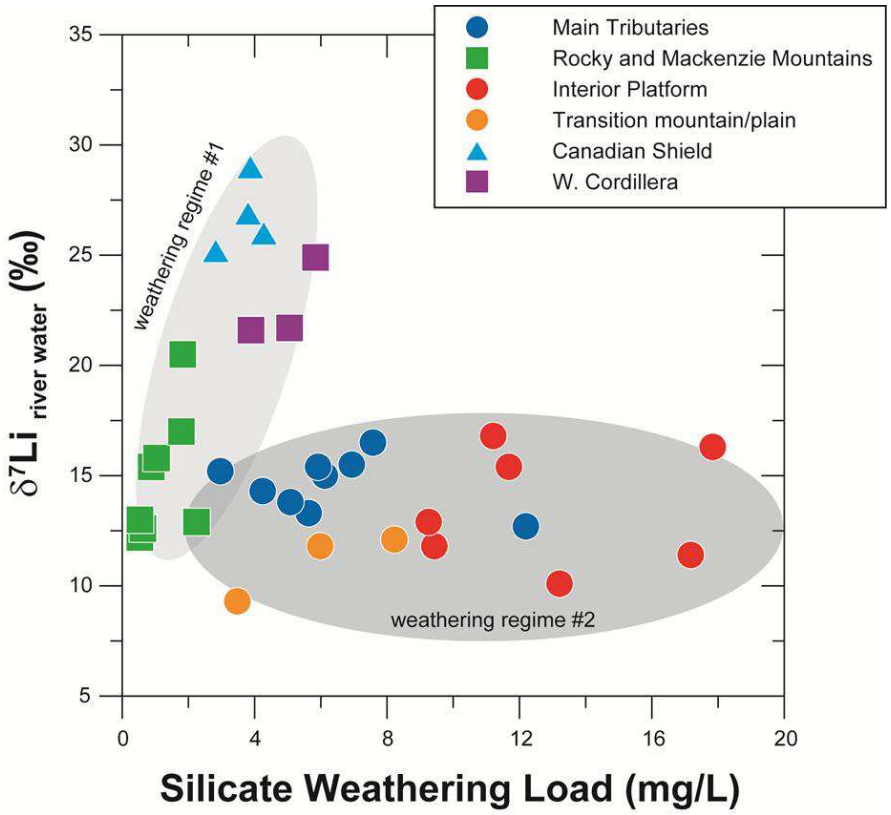

Figure 29 - Compositions isotopiques du lithium des eaux en fonction de la charge dissoute provenant de l'altération des roches silicatées (Millot et al., 2010a).

Si l'on raisonne maintenant en terme de mécanismes de contrôle (Figure 30) et pour expliquer ces variations, nous proposons l'interprétation suivante : dans le cas n°1, l'altération faible a pour résultat un très net enrichissement des eaux en ^{7}Li (Rocheuses, Cordillère et bouclier) qui ne résulte pas d'un lessivage préférentiel de cet isotope, mais de l'incorporation préférentielle du ^{6}Li lors de la précipitation d'oxy- hydroxyde de fer, seule phase d'altération susceptible de se former dans ces environnements et ces contextes d'altération très superficielle. Ce mécanisme a également été proposé pour expliquer les signatures d'autres rivières en zones périglaciaires comme en Islande ou au Groenland.

En ce qui concerne le cas n°2 pour les grands fleuves situés dans la plateforme intérieure, les eaux ont des δ^{7}Li plus bas (mais toujours plus élevés comparés aux matières en suspension

et aux roches). Dans ces zones où l'altération est nettement plus intense, un équilibre entre eaux et minéraux d'altération (des argiles dans ce cas) est le mécanisme principal de contrôle des δ^7Li. De plus, la contribution d'eaux souterraines et des temps de résidence relativement longs sont aussi des paramètres qui favorisent à la fois une altération plus importante et un équilibre entre dissolution et formation de minéraux secondaires d'altération.

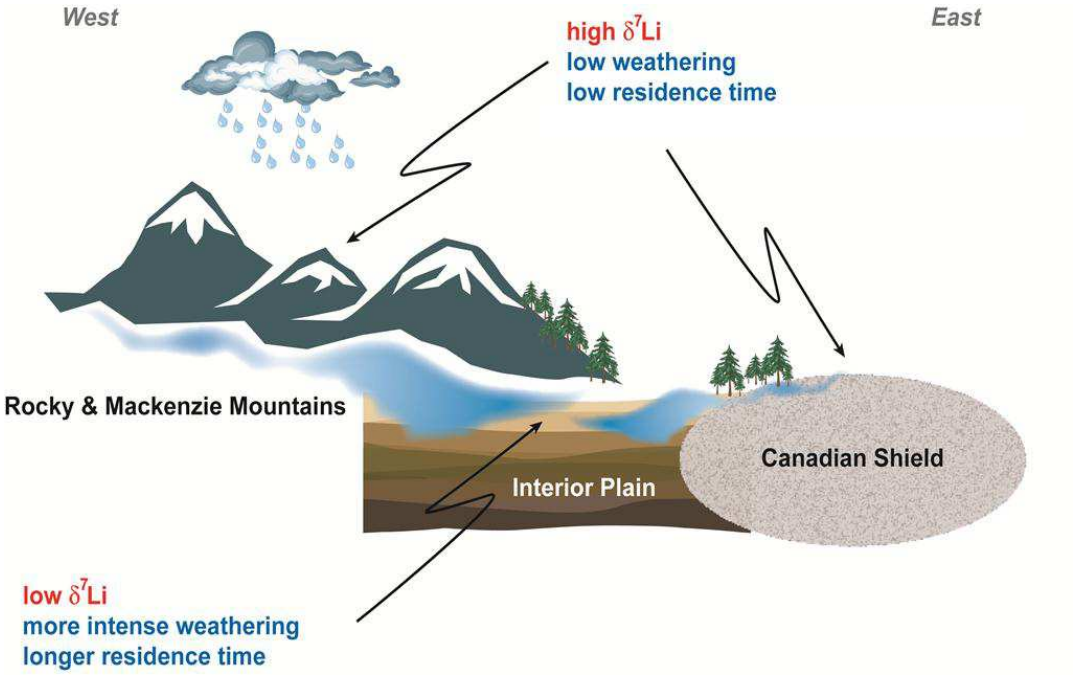

Figure 30 - Schéma conceptuel de contôle des compositions isotopiques du lithim dans le bassin du fleuve Mackenzie entre les différentes zones morphotectoniques et les régimes d'altération (Millot et al., 2010a).

4.2.2. Le bassin du Strengbach

Dans le bassin versant du Strengbach, situé dans les Vosges et d'une superficie de 80 ha, Lemarchand et al. (2010) ont étudié les eaux et les sols qui se développent sur une roche mère granitique.

Alors qu'il n'existe que très peu de variation de la composition isotopique du lithium du sol (valeurs proches de 0‰ quel que soit la profondeur, Figure 31), les eaux porales présentent des δ^7Li très variables : les eaux superficielles ont des compositions basses (de -17 à -5‰) alors que plus en profondeur les eaux ont des compositions plus élevées (jusqu'à +30‰). Dans les eaux porales, ces variations sont attribuées à des processus de dissolution et de précipitation. En profondeur, la formation de minéraux secondaires d'altération qui incorporent préférentiellement du ^{6}Li a pour effet d'augmenter le δ^7Li de l'eau vers des valeurs élevées. Au contraire, pour les eaux porales plus proches de la surface, les données ont tendance à montrer que les minéraux secondaires et les minéraux primaires résiduels se dissolvent ce qui engendre des valeurs de δ^7Li plus basses dans les eaux.

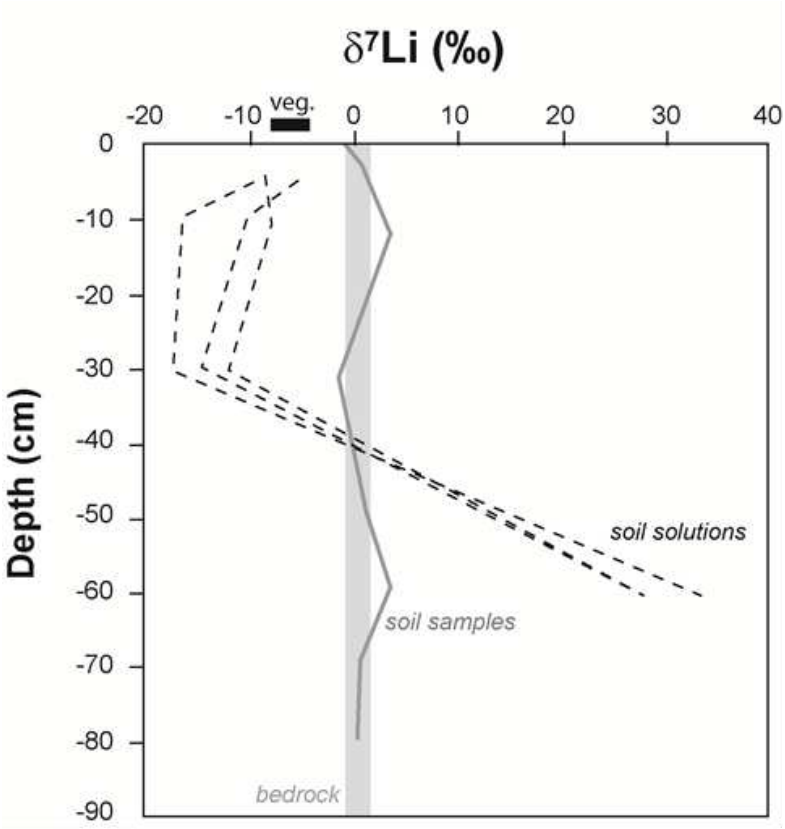

Figure 31 - Compositions isotopiques du Li mesurées dans le bassin versant du Strengbach. L'échantillon de roche mère (bedrock) correspond à la roche affleurant dans le milieu du bassin versant du Strengbach (Lemarchand et al., 2010).

Pour conclure en ce qui concerne le lithium dans les eaux des rivières, nous retiendrons que :

- **La distribution du lithium et de ses isotopes dans les fleuves est très variable. Le lithium dans les eaux de rivières provient quasi exclusivement de l'altération des roches silicatées.**

- **La composition isotopique des eaux est systématiquement plus élevée (enrichie en ^{7}Li) que celle des roches mères et des matières en suspension.**

- **Les compositions isotopiques du lithium dans les eaux des rivières sont donc un bon traceur du régime d'altération qui est contrôlé par la balance entre la dissolution des minéraux primaires et la précipitation des minéraux secondaires qui fractionnent les rapports isotopiques en incorporant préférentiellement du ^{6}Li.**

4.3. Eaux thermominérales (Millot et al., 2007[5] ; Millot et Négrel, 2007[6])

Dans cette partie, nous faisons la synthèse de deux articles :

1- le premier concerne les **eaux thermominérales du Massif Central** et une caractérisation multi-isotopique Li-B-Sr-Nd de l'origine de ces eaux (Millot et al., 2007)

2- le second article porte sur un ensemble d'eaux thermominérales en France et une **approche couplée isotopique et géothermométrie** (Millot et Négrel, 2007).

4.3.1. Caractérisation multi-isotopique Li-B-Sr-Nd d'eaux thermominérales du Massif Central

Dans cette étude (Millot et al., 2007) nous avons réalisé une caractérisation multi isotopique d'eaux thermominérales de la zone de la faille d'Aigueperse du bassin de la Limagne dans le Massif Central (Figure 32). Les rapports isotopiques du lithium (δ^7Li), du bore (δ^{11}B), du strontium (^{87}Sr/^{86}Sr) et du néodyme (^{143}Nd/^{144}Nd) ont été déterminés dans les eaux et les roches afin de contraindre l'origine de ces fluides d'un point de vu de la nature du réservoir.

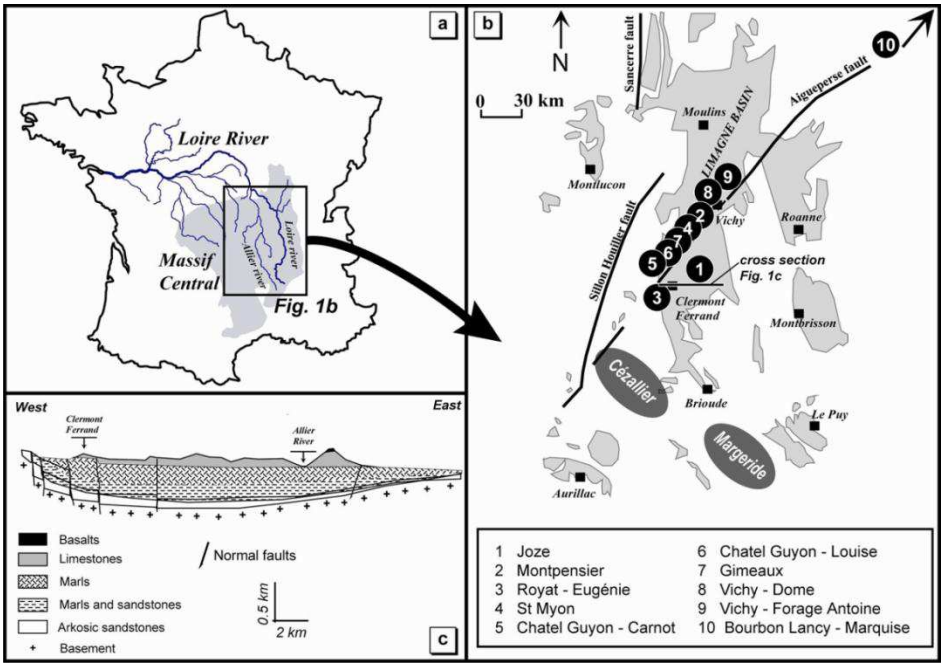

Figure 32 - (a) carte de localisation du Massif Central, (b) carte du bassin de la Limagne avec la localisation des dix sites de prélèvement, (c) coupe géologique synthétique et séquence lithostratigraphique (Millot et al., 2007).

[5] Millot R., Négrel Ph., Petelet-Giraud E. (2007) Multi-isotopic (Li, B, Sr, Nd) approach for geothermal reservoir characterization in the Limagne Basin (Massif Central, France). Applied Geochemistry, 22: 2307-2325.

[6] Millot R., Négrel Ph. (2007) Multi-isotopic tracing (δ^7Li- δ^{11}B, ^{87}Sr/^{86}Sr) and chemical geothermometry: evidence from hydro-geothermal systems in France. Chemical Geology, 244: 664-678.

Les systématiques isotopiques Sr et Nd montrent que la plupart de ces eaux proviennent d'un réservoir de type granitique (socle) à l'exception de quelques eaux dont la signature isotopique Sr-Nd montre également une contribution de roche volcanique (basalte, Chatel Guyon). Dans cette étude, nous avons également déterminé les compositions isotopiques du lithium et du bore, dans la mesure où ces systématiques isotopiques peuvent être de bons traceurs des processus et mécanismes mis en jeu lors des interactions eau/roche.

D'une manière générale, les caractéristiques isotopiques Sr-Nd-Li-B sont très variables à l'échelle de la zone d'étude de la faille d'Aigueperse (Figure 33), ces différences traduisent des origines variables mais aussi des intensités d'interaction eau/roche contrastées (profondeur, température).

Dans ce contexte, l'étude couplée des isotopes Li-B-Sr-Nd illustre la complexité quant à la caractérisation des réservoirs d'eaux thermominérales dans la mesure où l'utilisation d'un seul outil peut mener à des informations incomplètes en ce qui concerne l'origine de l'eau. L'approche nouvelle par les isotopes du lithium sera approfondie par une étude systématique d'eau thermales et thermominérales en France (Millot et Négrel, 2007) dans le but de contraindre notamment la thermo-dépendance de la signature isotopique du lithium avec une approche couplée isotopique et géothermométrie.

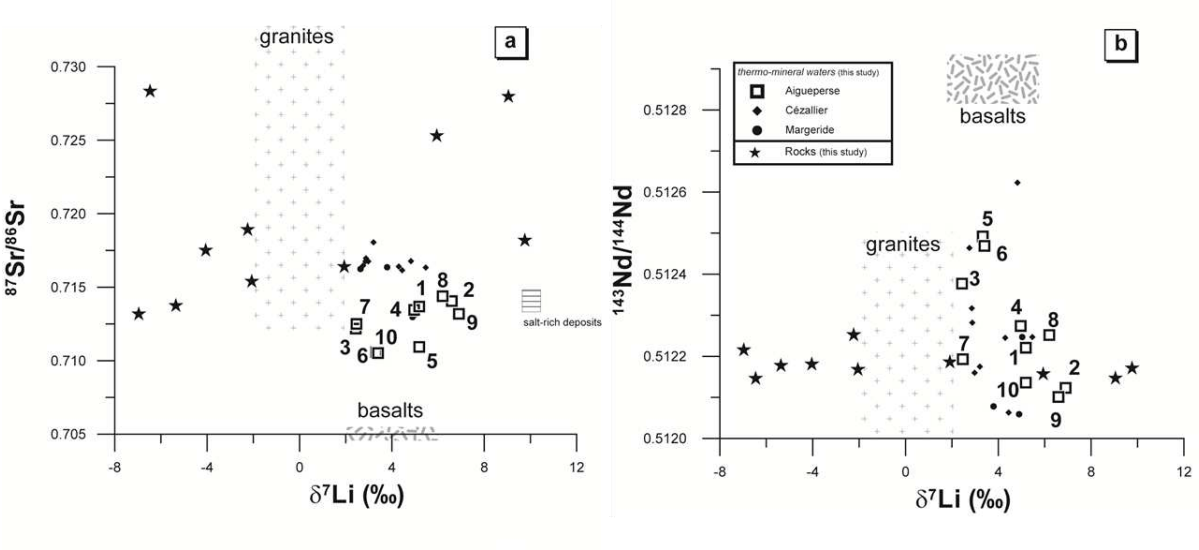

Figure 33 - Compositions isotopiques du Sr et du Nd reportées en fonction de celle du Li pour les eaux et les roches de la zone de la faille d'Aigueperse. Les numéros correspondent aux eaux suivantes : [1] Joze, [2] Montpensier, [3] Royat - Eugénie, [4] St Myon, [5] Chatel Guyon - Carnot, [6] Chatel Guyon - Louise, [7] Gimeaux, [8] Vichy - Dôme, [9] Vichy - forage Antoine and [10] Bourbon Lancy - Marquise. (Millot et al., 2007).

4.3.2. Approche couplée isotopique et géothermométrie

Dans le but d'étendre nos investigations en ce qui concerne le potentiel des isotopes du lithium en tant que traceur des interactions eau/roche, nous avons analysé un certain nombre d'eaux thermales (eaux chaudes) et d'eaux thermominérales (eaux chaudes et salées) en France. Cette base de données a été réalisée pour les isotopes du lithium mais aussi pour les isotopes du Sr et du B. L'objectif de ce travail (Millot et Négrel, 2007) consistait

à croiser les signatures isotopiques du lithium avec les données de géothermométrie qui traduisent la température du réservoir en profondeur et donc l'intensité de l'interaction eau/roche.

La base de données est constituée de 36 eaux thermales (Figure 34) qui ont été sélectionnées afin de couvrir une très large gamme de variation à la fois en terme de contexte lithologique mais aussi de température du réservoir en profondeur.

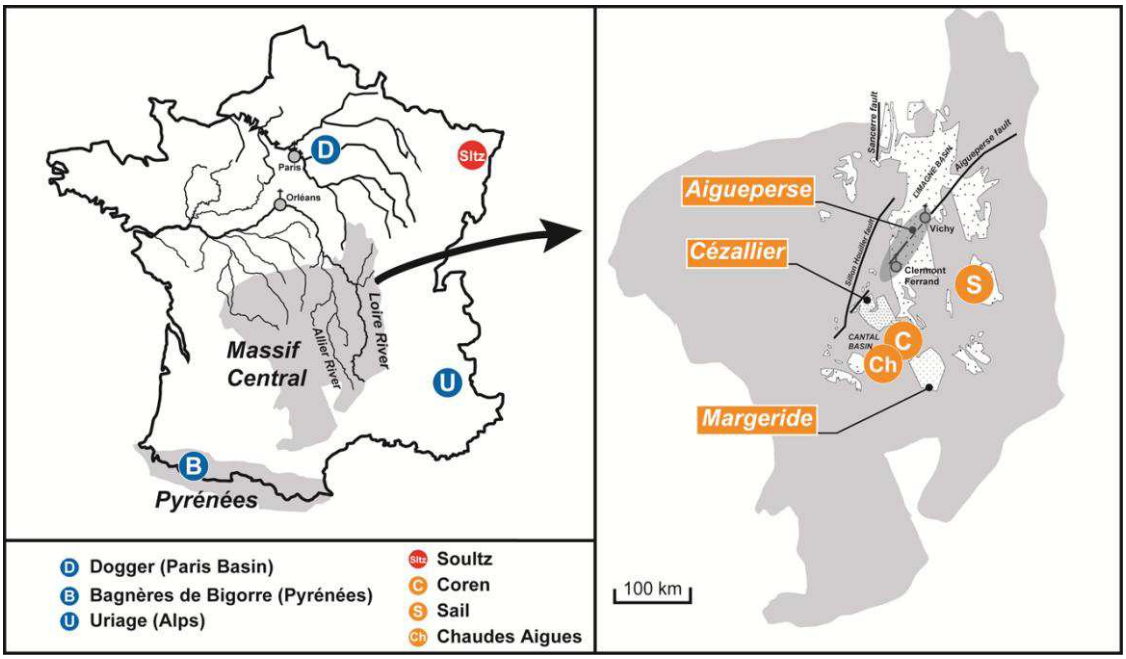

Figure 34 - Carte de localisation des eaux thermales étudiées avec à droite un zoom sur les eaux thermominérales du Massif Central (Millot et Négrel, 2007).

Nous observons que les variations isotopiques du strontium (le rapport $^{87}Sr/^{86}Sr$ est compris entre 0.70755 et 0.72187) sont contrôlées par les variations lithologiques : les plus hautes valeurs (>0.714) sont typiques des interactions avec des granites et/ou des gneiss (Vichy, Cézallier, Chaudes-Aigues, Uriage), alors que les valeurs les plus basses sont observées en contexte sédimentaire (<0.712, Dogger et Bagnères de Bigorre). Les compositions isotopiques du bore ($\delta^{11}B$) sont très variables et sont comprises entre -8.3 et +21.6‰. Nous n'observons pas de relation directe pour l'ensemble de la base de données entre d'une part les compositions isotopiques du strontium ou du bore et d'autre part la température du réservoir calculée en profondeur par géothermométrie[7].

[7] Nous pouvons rappeler ici que la concentration de certains éléments chimiques dissous dans les eaux géothermales dépend à la fois de la température d'interaction et de l'assemblage minéralogique de la roche (White, 1965; Ellis, 1970; Truesdell, 1976; Arnórsson et al., 1983; Fouillac, 1983). Ainsi, comme les concentrations des éléments sont contrôlées par des réactions qui dépendent de la température, ces concentrations peuvent être théoriquement utilisées pour déterminer la température de l'eau en profondeur. Cependant, et comme l'ont souligné Fournier et Truesdell (1974), Michard (1979) et Giggenbach (1981) il faut que: 1- les réactions qui dépendent de la température se produisent en profondeur, 2- les concentrations en éléments soient suffisamment abondantes (la quantité de l'élément ne doit pas être un facteur limitant), 3- l'équilibre eau/roche se produise à la température du réservoir, 4- qu'il n'existe pas ou peu de ré-équilibration ou d'échange lors de la remontée de l'eau vers la surface, 5- que les eaux chaudes profondes ne soient pas diluées par des eaux plus froides en surface et 6- qu'il n'y ait pas de réactions d'échanges avec des minéraux argileux en ce qui concerne spécifiquement Na et K (Weissberg et Wilson, 1977).

Les équations traditionnelles de la géothermométrie (White, 1965; Fournier et Rowe, 1966; Ellis, 1970; Fournier, 1973; 1977; 1979; Fournier et Truesdell, 1973; Fournier et Potter, 1979; Truesdell, 1976; Giggenbach et al., 1983; Giggenbach, 1988) sont basées :

- sur la silice (quartz, calcédoine, cristobalite α et β, silice amorphe),
- le géothermomètre Na/K (contrôlé par l'équilibre plagioclase/feldspath K)
- et un géothermomètre Na-K-Ca (dans le cas des eaux riches en Ca et qui peut inclure une correction en Mg également).

D'autres géothermomètres ont été développés, notamment ceux basés sur le lithium (Fouillac and Michard, 1979 ; 1981; Kharaka et al., 1982; Michard, 1990). Au contraire du géothermomètre Na/K basé sur un équilibre thermodynamique, les relations thermométriques basées sur le lithium ne sont liées à aucun équilibre entre l'eau et un minéral porteur du lithium. Il s'agit de relations qui ont été calibrées soit dans des contextes sédimentaires (Kharaka et al., 1982; 1985 ; Kharaka et Mariner, 1989) ou cristallins (Fouillac and Michard, 1979 ; 1981; Michard, 1990).

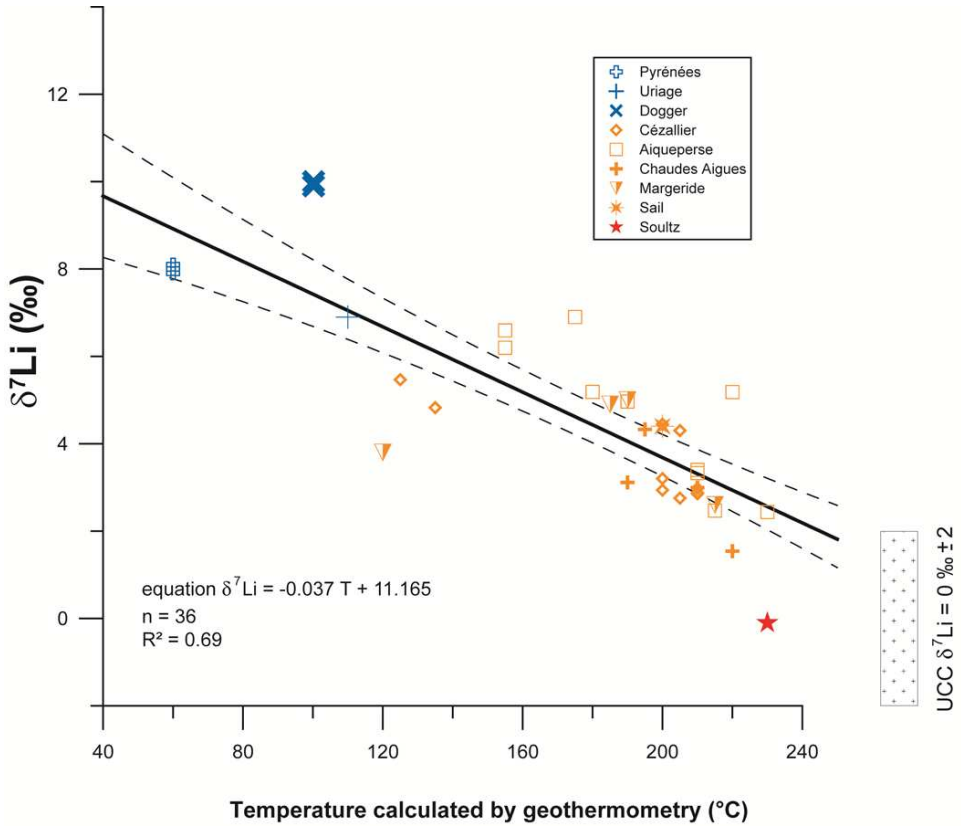

Figure 35 - Composition isotopique du lithium représentée en fonction de la température du réservoir calculée par géothermométrie (Millot et Négrel, 2007).

Les températures des réservoirs des différents systèmes étudiés sont reportés dans la figure 35 avec les compositions isotopiques du lithium. Différents géothermomètres ont été utilisés, et la température reportée sur l'axe des X correspond à la valeur vers laquelle les équations convergent. Cette valeur est aussi en accord avec les données de la littérature reportées pour chaque site par Millot et Négrel (2007).

Nous pouvons remarquer dans la figure 35 qu'il existe une bonne relation entre la composition isotopique du lithium et la température. Pour une température qui varie de 60 à 230°C, le δ^7Li décroit de +10.0 à 0.1‰. Cette relation peut s'écrire comme suit avec la température en °C :

$$\delta^7\text{Li (‰)} = -0.043 \pm 0.003\ T\ (°C) + 11.9 \pm 0.5$$

Au premier ordre, il semble donc que la composition isotopique du lithium soit un bon traceur de la température d'interaction. En réalité, c'est l'inverse, puisque c'est la température d'interaction qui est en fait préservée dans la signature isotopique du lithium de l'eau.

Comme tous les systèmes isotopiques stables, l'amplitude du fractionnement dépend de la température, avec des plus grands fractionnements à basse température. Et donc la relation observée dans la figure 35 est interprétée comme le résultats d'un fractionnement plus important entre l'eau et la roche à plus basse température, alors que les δ^7Li des fluides à plus haute température se rapprochent de celui de la roche mère (qui est représentée graphiquement sur la figure 35 par la valeur moyenne de la croûte continentale supérieure d'après Teng et al., 2004 avec δ^7Li = 0‰ ± 2 ; UCC : Upper Continental Crust). La dispersion observée autour de la relation moyenne peut être due soit à de faibles variations des signatures des roches mères soit éventuellement à des phénomènes de mélange/dilution en surface, dont l'ampleur reste faible.

Un des résultats majeurs de ce travail a permis de montrer la pertinence de cet outil pour l'étude des eaux thermominérales. Nous verrons par la suite, dans l'étude des eaux géothermales, qu'il est essentiel de tenir compte de la signature de la roche et donc de considérer la différence entre l'eau et la roche ($\Delta_{\text{eau - roche}}$) en ce qui concerne la thermo-dépendance du fractionnement isotopique.

Pour conclure en ce qui concerne le lithium dans les eaux thermominérales, nous retiendrons que :

- **Les compositions isotopiques du lithium dans les eaux thermominérales sont très variables.**
- **La composition isotopique du lithium d'une eau (δ^7Li) est inversement corrélée à la température profonde du réservoir.**
- **La thermo-dépendance du fractionnement isotopique du lithium doit être considérée entre l'eau et la roche à fois pour des systèmes naturels et expérimentaux afin de contraindre les paramètres de contrôle. Ces objectifs sont ceux des deux prochaines parties de ce manuscrit.**

4.4. Eaux géothermales (Millot et al., 2012[8] ; 2010[9])

Dans cette partie, nous faisons la synthèse de deux articles qui concernent des eaux géothermales en contexte d'ile volcanique :

1- le premier concerne les **eaux géothermales de la zone du volcan Taupo en Nouvelle Zélande** (Millot et al., 2012)

2- le second article concerne les **eaux géothermales des Antilles : Guadeloupe et Martinique** (Millot et al., 2010b).

4.4.1. Eaux géothermales de N^{elle} Zélande

Les eaux géothermales que nous avons étudiées (Millot et al., 2012) se situent dans la zone volcanique de Taupo en N^{elle} Zélande (Figure 36).

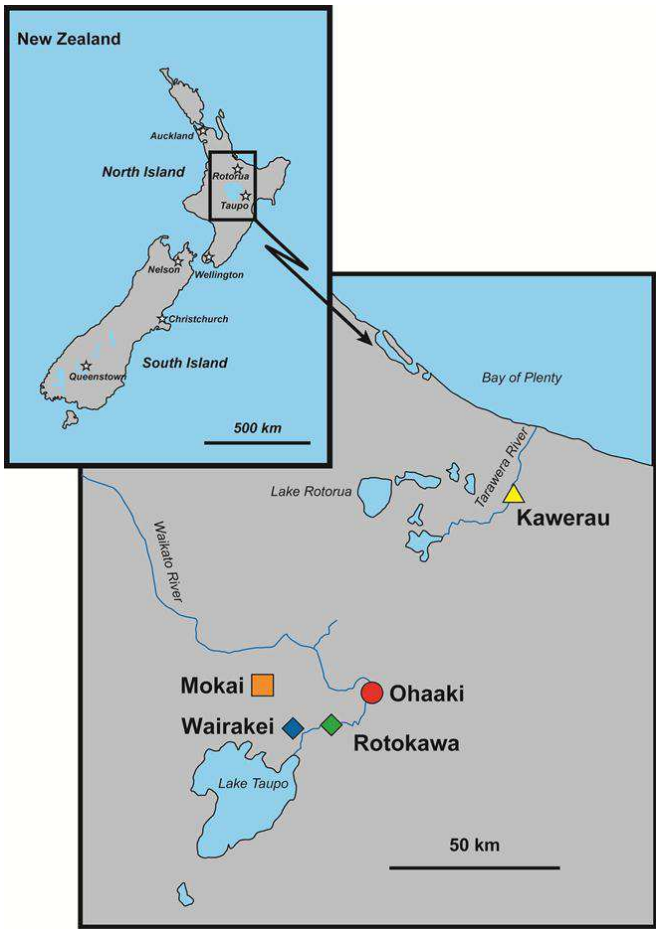

Figure 36 - Carte des champs géothermaux étudiés en N^{elle} Zélande (Millot et al., 2012).

[8] Millot R., Hegan A., Négrel Ph. (2012) Geothermal waters from the Taupo Volcanic Zone, New Zealand: Li, B and Sr isotopes characterization. Applied Geochemistry, 27: 677-688.

[9] Millot R., Scaillet B., Sanjuan B. (2010) Lithium isotopes in island arc geothermal systems: Guadeloupe, Martinique (French West Indies) and experimental approach. Geochimica et Cosmochimica Acta, 74: 1852-1871.

Cette zone (TVZ : Taupo Volcanic Zone) est connue pour son activité volcanique et géothermale avec des réservoirs dont la température se situe entre 250° et 320°C.

L'objectif de cette étude consistait à caractériser le ou les réservoirs de cette TVZ par la mesure des isotopes du lithium dans les eaux géothermales des champs géothermaux de Kawerau, Mokai, Ohaaki, Wairakei et Rotokawa.

La figure 37 présente les résultats de la composition isotopique du lithium (δ^7Li) en fonction de la teneur en lithium.

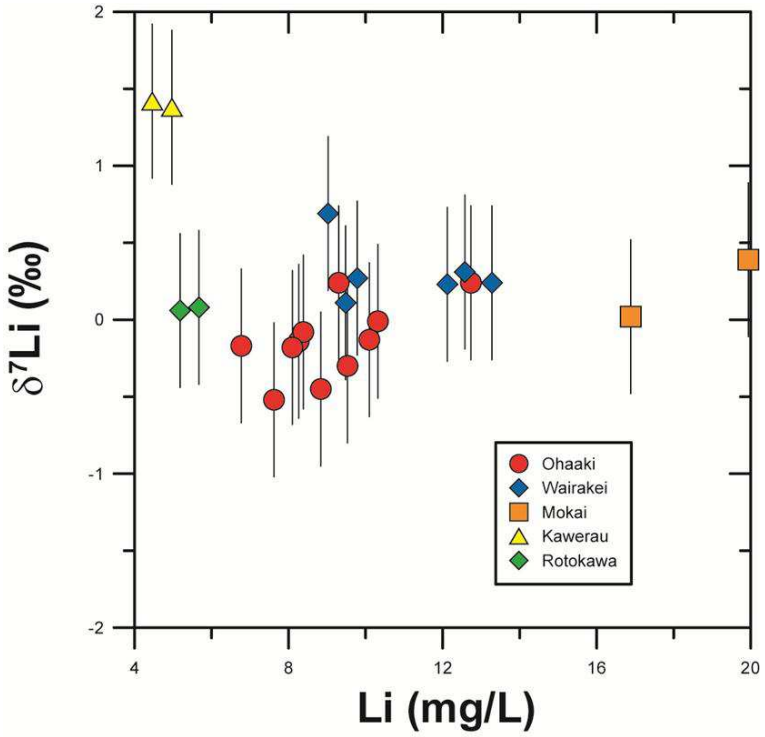

Figure 37 - Compositions isotopiques du lithium en fonction de la teneur en lithium dans les eaux géothermales de la Taupo Volcanic Zone en N^{elle} Zélande (Millot et al., 2012).

L'examen de cette figure montre bien que les δ^7Li sont très homogènes, ils varient de -0.5 à +1.4‰. D'autre part, pour ces eaux, nous n'observons pas de relation directe entre le δ^7Li et la température du réservoir. Cette homogénéité des signatures isotopiques du lithium montre que les fluides sont bien « mélangés » pour le lithium et que l'interaction entre une eau météorique (pas d'influence marine ; Millot et al., 2012) et la roche magmatique en profondeur est le principal facteur de contrôle dans la composition isotopique du lithium.

4.4.2. Eaux géothermales des Antilles : Guadeloupe et Martinique

Les eaux géothermales que nous avons étudiées (Millot et al., 2010b) se situent au niveau de l'arc volcanique des Antilles françaises. Dans ce manuscrit, nous nous focaliserons sur les résultats obtenus sur les champs géothermaux de Bouillante en Guadeloupe et du Lamentin en Martinique (Figure 38). Ces deux champs possèdent des température assez contrastées avec respectivement 90°-120°C pour le Lamentin et 250°-260°C pour Bouillante.

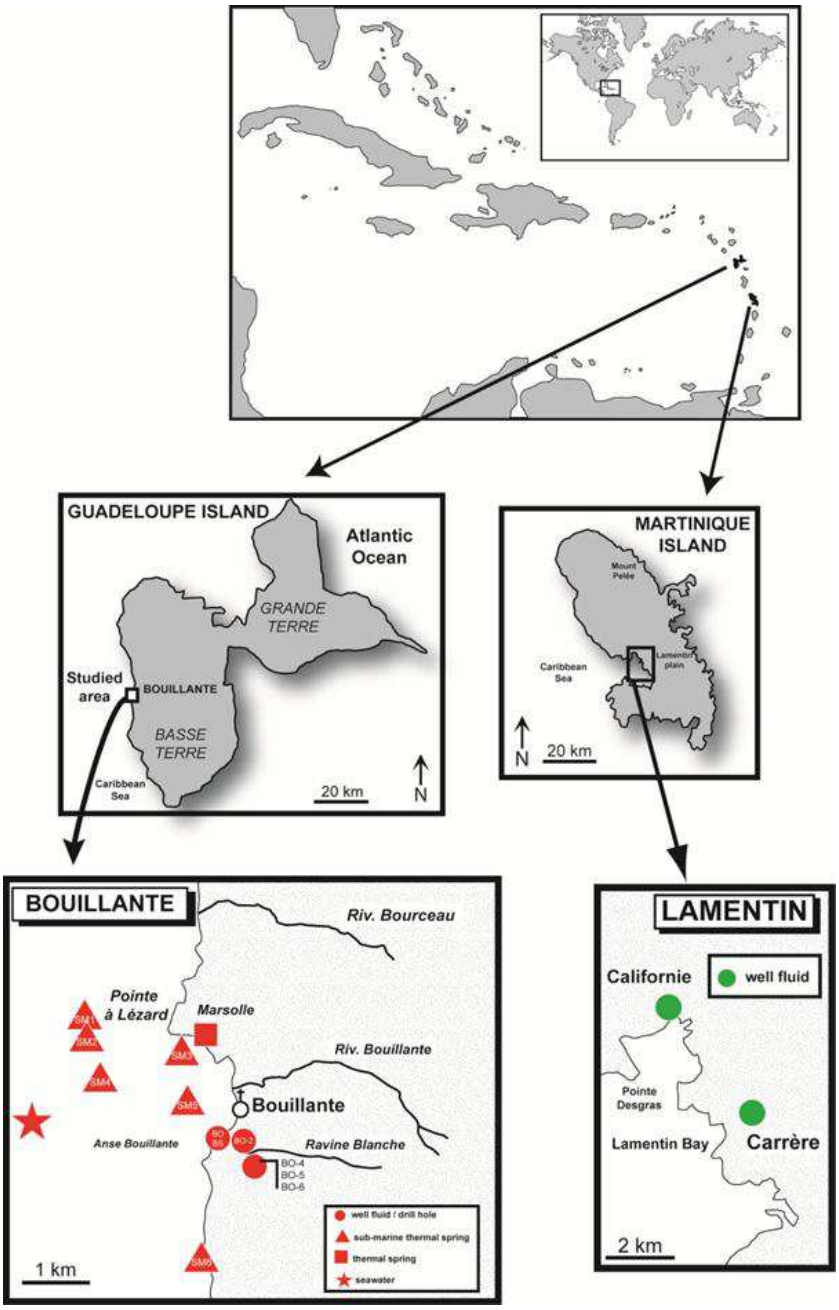

Figure 38 - Carte de localisation des champs géothermaux étudiés en Guadeloupe et en Martinique (Millot et al., 2010b).

Dans la figure 39, la composition isotopique du lithium est reportée en fonction du rapport Li/Cl. Cette représentation permet une meilleure vision des eaux les plus riches en lithium (ces eaux se situeront sur la partie droite du diagramme) et ces eaux riches en lithium sont également les plus chaudes, il s'agit donc bien des échantillons d'intérêt en géothermie.

Nous pouvons remarquer que les eaux qui définissent le réservoir profond de Bouillante et du Lamentin sont bien situées à droite du diagramme (haut rapport Li/Cl) : ces réservoirs sont définis par les eaux des forages profonds à Bouillante (BO-4, BO-5 et BO-6) et ceux des forages Californie et Carrère au Lamentin. Ces deux réservoirs sont différents à la fois pour les rapports isotopiques (δ^7Li) mais aussi pour les rapports chimiques Li/Cl.

D'autre part, il est intéressant de confirmer, par les isotopes du lithium, le mélange qu'il existe entre d'une part le réservoir profond et d'autre part l'eau de mer pour les différentes sources thermales sous-marines de Bouillante (Figure 39).

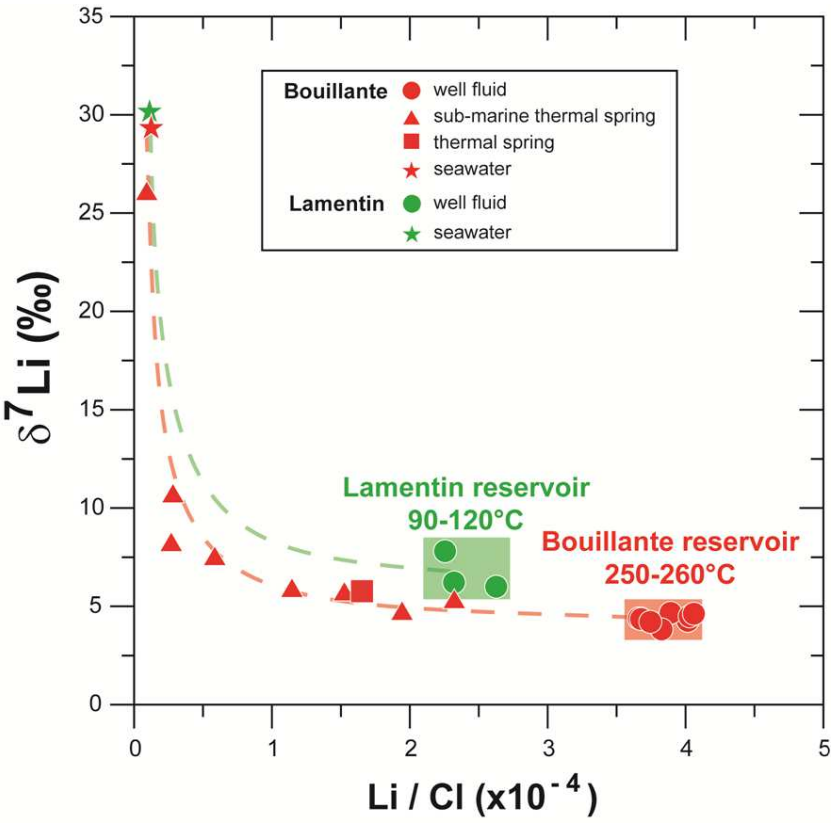

Figure 39 - Composition isotopique du lithium en fonction du rapport Li/Cl pour les eaux du Lamentin et de Bouillante (Millot et al., 2010b).

Enfin, lorsque l'on compare les réservoirs profonds du Lamentin et de Bouillante, plus la température est élevée, plus le δ^7Li est bas et plus le rapport Li/CL est important.

Pour contraindre les mécanismes d'interaction eau/roche en contexte volcanique (eau de mer/basalte) et quantifier le fractionnement isotopique en fonction de la température, nous avons réalisé une série d'expériences en laboratoire que nous détaillerons dans une dernière partie.

Pour conclure en ce qui concerne le lithium dans les eaux géothermales de N^{elle} Zélande et des Antilles, nous retiendrons que :

- **Les compositions isotopiques du lithium dans les eaux géothermales de N^{elle} Zélande sont très homogènes à l'échelle de la zone d'étude de la TVZ.**

- **Le δ^7Li et les teneurs en lithium d'une eau géothermale sont donc homogènes pour un réservoir donné mais peuvent varier significativement en fonction du contexte (assemblage minéralogique, profondeur mais également température).**

- **C'est cette thermo-dépendance du fractionnement isotopique du lithium entre l'eau et la roche ainsi que les mécanismes associés qui représentent les objectifs d'étude de la partie expérimentale.**

4.5. Approche expérimentale (Millot et al., 2010[10])

Dans cette partie, nous faisons la synthèse de l'article qui concerne les Antilles (Millot et al., 2010b) en nous focalisant sur les résultats des expériences de laboratoire.

Dans le but de déterminer l'amplitude du fractionnement isotopique du lithium pendant une interaction eau/roche et la variation en fonction de la température, nous avons réalisé une série d'expériences en laboratoire. Ces expériences consistent à mesurer le fractionnement isotopique du lithium entre une eau de mer et un basalte à différentes températures (25°, 75°, 200° et 250°C).

La roche choisie pour réaliser ces expériences est un basalte tholéitique du JGS (Japan Geological Survey) : le basalte JB-2 dont la composition et la concentration en lithium sont respectivement de δ^7Li = +4.9‰ et 7.78 µg/g (voir une compilation des données dans Carignan et al., 2007). L'eau de mer choisie est le matériau de référence de l'IRMM (Institute for Reference Materials and Measurements) : le BCR-403 (δ^7Li = +31.0‰ ± 0.5, Li = 0.18 mg/L, Millot et al., 2004).

Les expériences ont été menées avec un rapport eau/roche de 10 et une eau de mer diluée à 60% (avec de l'eau ultrapure H_2O Milli-Q) dans le but de reproduire les conditions naturelles qui prévalent dans le champ géothermal de Bouillante.

La durée de ces expériences est très variable (Millot et al., 2010b), de quelques jours jusqu'à plusieurs mois en fonction de la cinétique de réaction. La variation de la concentration et de la composition isotopique du lithium ont donc été mesurées au cours du temps dans des aliquotes d'une solution d'eau de mer ayant interagit avec un basalte à différentes températures (25°, 75°, 200° et 250°C).

Deux types de dispositifs expérimentaux ont été utilisés :

1- pour les expériences à 25°, 75° et 200°C, nous avons utilisé des volumes importants : 5 à 10 mL de solution et 0.5 à 1 g de roche ont été placés dans des béchers fermés dans une armoire thermo-statée et une étuve au BRGM (Figure 40)

2- pour les expériences à plus hautes températures (200° et 250°C), un très faible volume de solution (300 µL) et 30 mg de roche sont placés dans des capsules en or qui seront ensuite chauffées et mises sous pression dans un autoclave dans les laboratoires de l'ISTO (Figure 41).

[10] Millot R., Scaillet B., Sanjuan B. (2010) Lithium isotopes in island arc geothermal systems: Guadeloupe, Martinique (French West Indies) and experimental approach. Geochimica et Cosmochimica Acta, 74: 1852-1871..

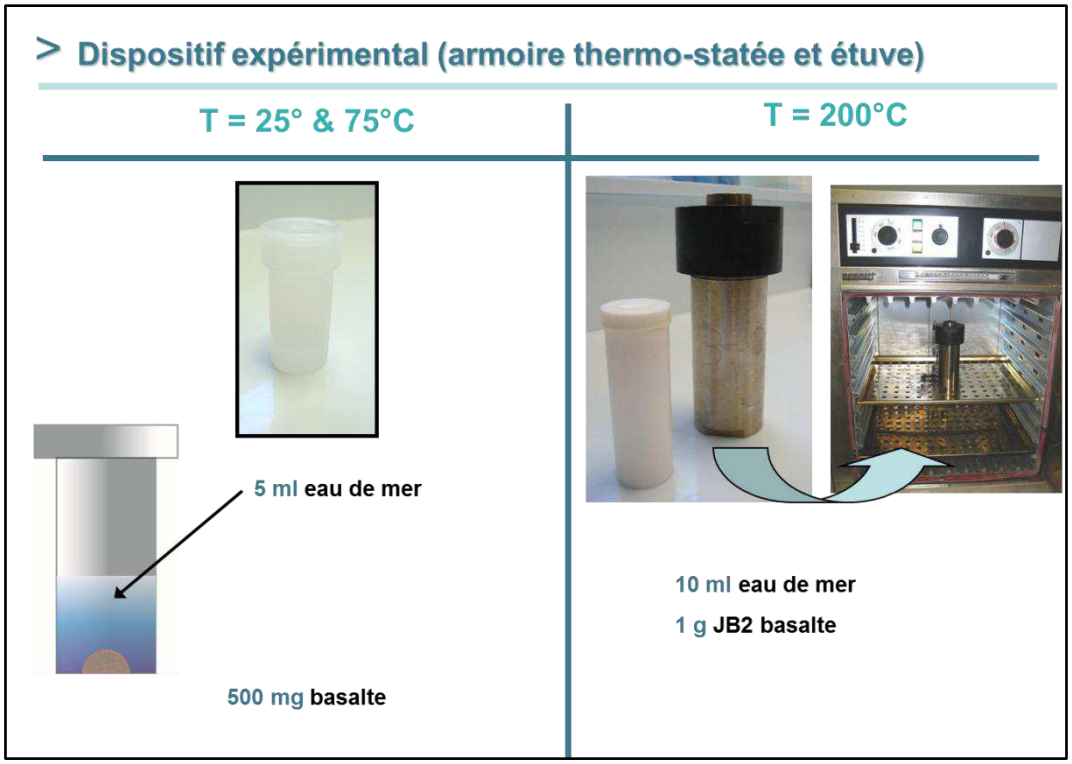

Figure 40 - Dispositif expérimental pour les interactions à 25°, 75° et 200°C (BRGM).

Figure 41 - Dispositif expérimental pour les interactions à 200° et 250°C (ISTO).

A la fin de chacune des expériences (25°, 75°, 200° et 250°C), la composition isotopique du lithium est également mesurée dans la phase solide résiduelle, elle sera comparée à la valeur obtenue dans l'eau également en fin d'expérience (après l'atteinte de l'équilibre) pour déterminer le fractionnement entre l'eau et la roche : $\Delta_{eau\text{ - }roche} = \delta^7Li_{eau} - \delta^7Li_{roche}$. La variation du Δ avec la température correspond donc à la thermo-dépendance du fractionnement isotopique du lithium.

La variation au cours du temps de la composition isotopique et de la concentration du lithium est reportée graphiquement dans la figure 42 avec les différentes températures d'interaction.

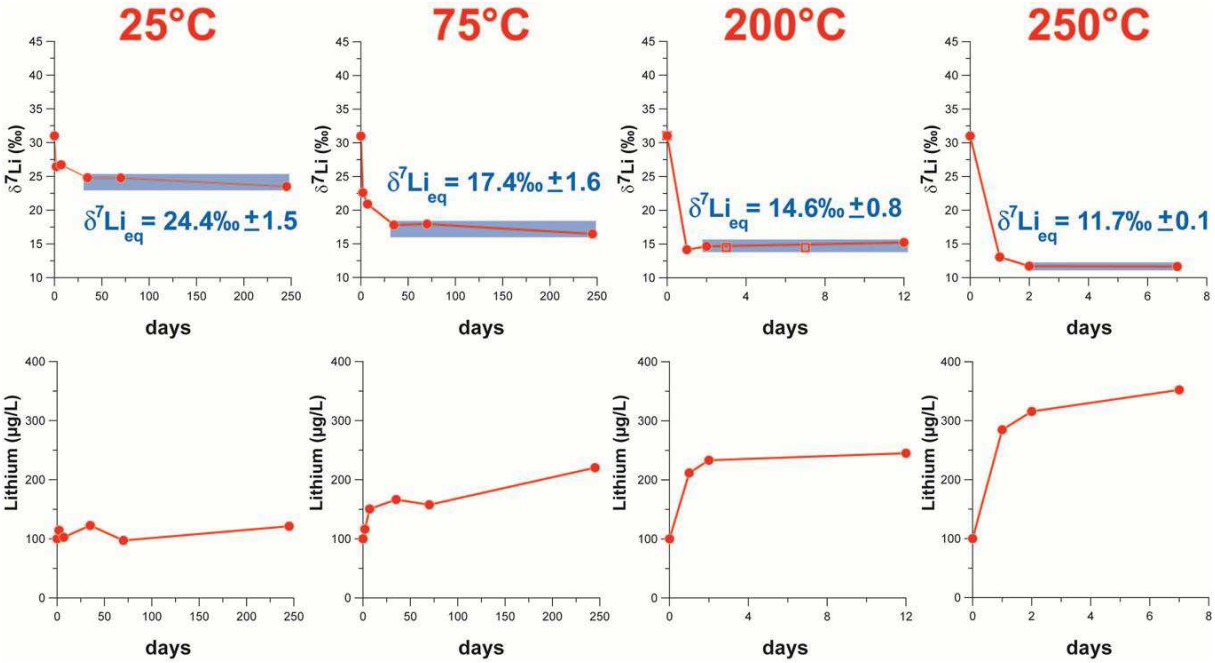

Figure 42 - Evolution temporelle de la composition isotopique et de la concentration en lithium dans la solution à différentes températures (Millot et al., 2010b).

L'évolution temporelle de la composition isotopique et de la concentration en lithium dans la solution à différentes températures (Figure 42) est riche d'enseignement à plusieurs titres :

- tout d'abord, en ce qui concerne les teneurs en lithium de l'eau, nous voyons clairement qu'à partir d'une solution initiale à 100 µg/L, plus la réaction avance dans le temps et plus la teneur augmente (ceci est vrai quelle que soit la température).
- cette augmentation de la teneur en lithium dans l'eau est également vraie lorsque la température augmente, ainsi la concentration atteint plus de 300 µg/L en fin d'expérience à 250°C.
- le résultat le plus important concerne l'évolution de la composition isotopique du lithium, notamment le fait qu'à partir d'une valeur initiale de +31‰ (eau de mer), le δ^7Li diminue très significativement au cours du temps.
- pour chacune des expériences, nous pouvons aussi noter que le δ^7Li diminue pour atteindre une valeur plateau qui est d'autant plus basse que la température est élevée.

- pour chacune des expériences, nous pouvons définir une valeur d'équilibre (δ^7Li_{eq}) qui correspond à la valeur dans l'eau en fin d'expérience, lorsque l'équilibre isotopique a été atteint.

Ces variations dans le temps de la composition isotopique et de la concentration du lithium sont interprétées dans le schéma de la figure 43.

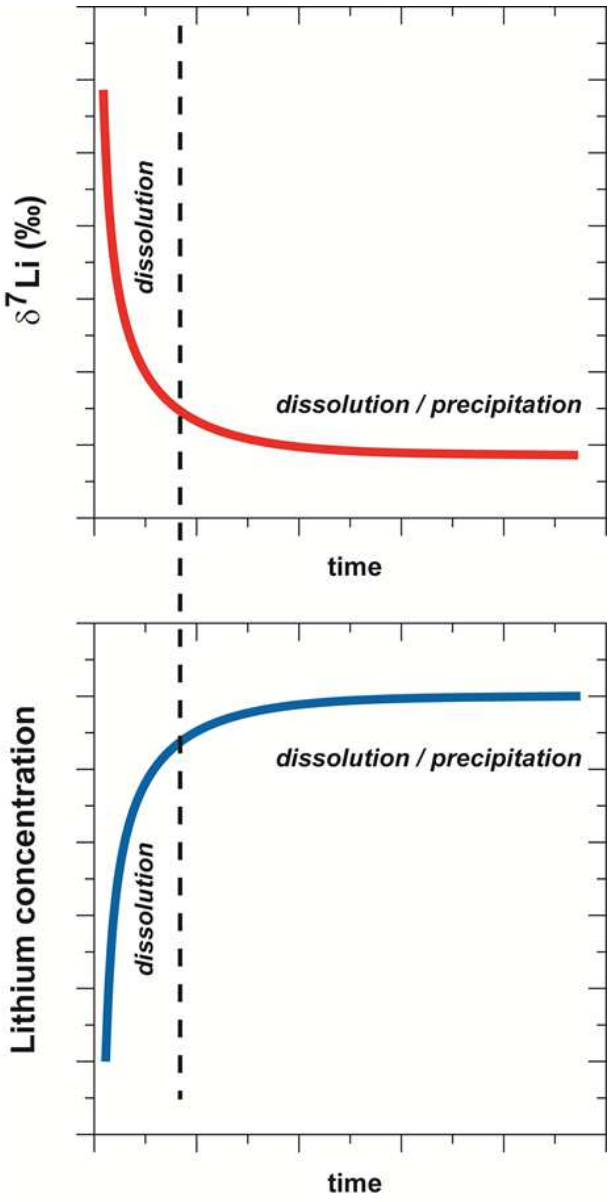

Figure 43 - Schéma interprétatif de l'évolution temporelle de la composition isotopique et de la concentration en lithium (Millot et al., 2010b).

Au cours de l'interaction eau/roche deux étapes successives peuvent être identifiées :

1- lors de la première étape, il y a tout d'abord dissolution de la roche, ce qui entraine à la fois une augmentation de la teneur en Li dans la solution mais aussi une diminution du δ^7Li de la solution, puisque, rappelons-le, le δ^7Li du basalte est plus bas (+4.9‰)

que celui de l'eau de mer (+31‰). Cette première étape est plus ou moins courte en fonction de la température de l'expérience.

2- Lors d'une seconde étape, des minéraux d'altération commencent à se former. Ainsi le lithium et ses isotopes sont contrôlés par l'équilibre qui existe entre dissolution de la roche et précipitation de minéraux secondaires d'altération.

Ces minéraux secondaires d'altération ont été caractérisés pour chacune des expériences (pour chacune des températures) à la fois par TEM (microscope électronique à transmission), par FTIR (infra rouge à transformée de Fourier) et par XRD (diffraction des rayons X). Cette caractérisation minérale montre deux choses : tout d'abord, plus la température est élevée et plus les minéraux d'altération sont importants (en quantité) ; d'autre part, ces minéraux secondaires sont de type argileux et sont aussi différents selon la température de l'expérience.

Lorsque l'on reporte la différence entre la solution (δ^7Li_{eq}) et la roche résiduelle (δ^7Li_{roche}) à la fin de l'expérience ($\Delta_{eau\ -\ roche} = \delta^7Li_{eau} - \delta^7Li_{roche}$), en fonction de l'inverse de la température (1/T, Kelvin), nous obtenons la corrélation de la figure 44 qui illustre bien la thermo-dépendance du fractionnement isotopique du lithium.

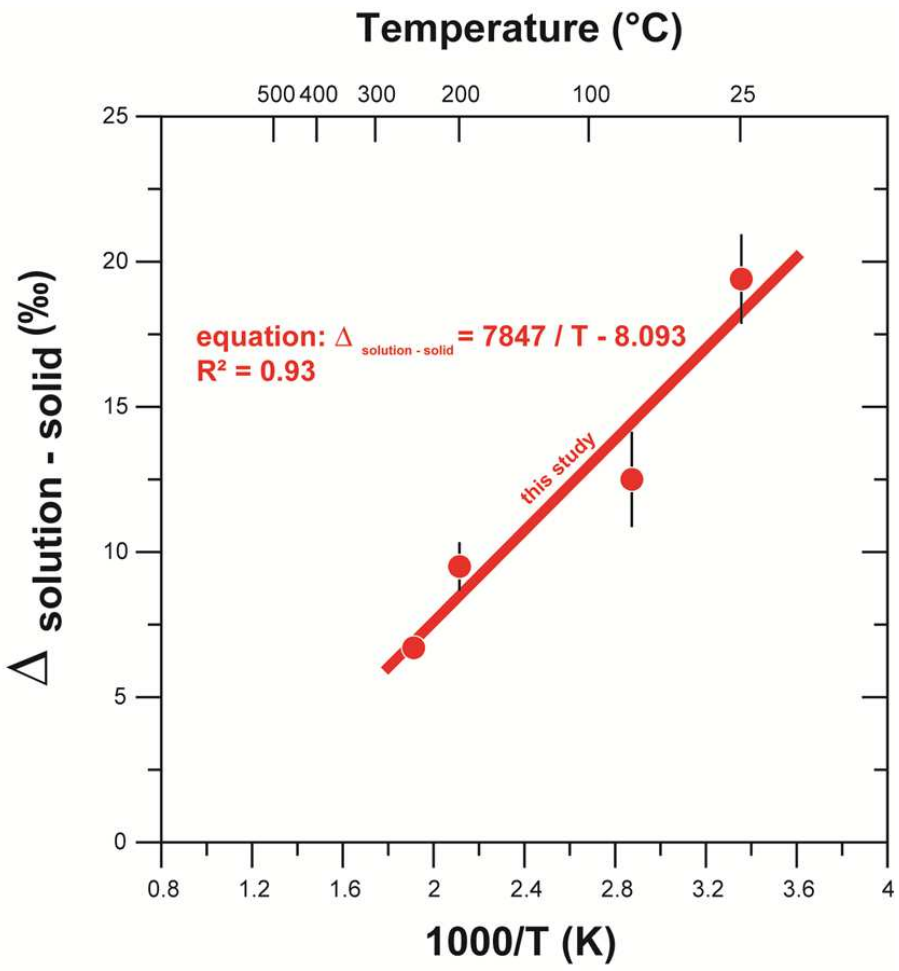

Figure 44 - Fractionnement isotopique du lithium entre l'eau et la roche en fonction de l'inverse de la température (Millot et al., 2010b).

Pour conclure en ce qui concerne l'approche expérimentale, nous retiendrons que :

- **Les expériences d'interaction basalte/eau de mer ont permis d'établir une loi de thermo-dépendance pour le fractionnement isotopique du lithium entre l'eau et la roche, qui peut s'écrire avec l'équation suivante :**

$$\Delta_{\text{solution – solide}} = 7847 / T – 8.093$$

- **Les fractionnements eau/roche diminuent de +20‰ à +7‰ lorsque la température augmente de 25° à 250°C.**

- **Les mécanismes mis en jeu et qui contrôlent ce fractionnement sont des équilibres entre dissolution de minéraux primaires et formation de minéraux secondaires.**

- **Ces minéraux secondaires dépendent des conditions de formation, notamment en terme de température.**

5. Conclusions et perspectives

Avant de conclure, nous pouvons rappeler l'objectif principal de ce manuscrit qui est résumé dans la figure ci-dessous : à la suite de développements analytiques, l'objectif de ce manuscrit était d'illustrer l'utilisation des isotopes du lithium en géochimie au travers d'exemples applicatifs dans le domaine des interactions eau/roche à basse et haute température.

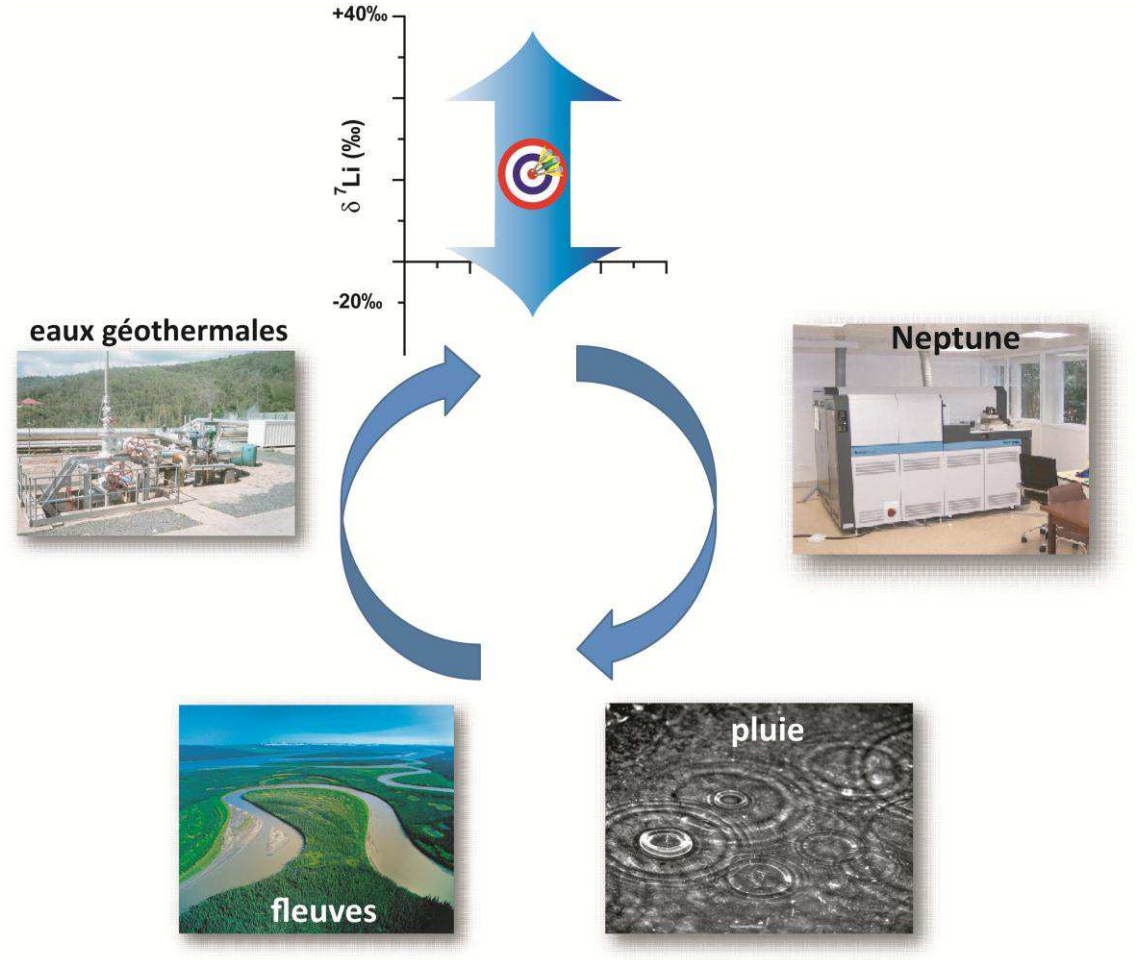

Figure 45 - Schéma qui rappelle les objectifs de ce travail.

Les principales conclusions de ce travail sont les suivantes :

- La méthode de mesure des isotopes du lithium avec le Neptune MC-ICP-MS est relativement rapide et très sensible. Cette mesure requiert une bonne validation de l'ensemble de la chaine analytique. Au préalable à la mesure, une étape de purification du lithium est nécessaire. Lors de cette étape, il faut s'assurer du rendement de 100%, de l'absence de fractionnement et de l'absence de contamination éventuelle.

Le protocole a été validé par la mesure répétée sur le long terme de différentes solutions standards et de matériaux de référence. Il est important de souligner que la reproductibilité externe de notre protocole pour la mesure isotopique du lithium d'échantillons naturels après purification est de ± 0.5‰ (2σ).

- La distribution du lithium et de ses isotopes dans les eaux de pluies est très variable au niveau spatio-temporel. L'effet de saisonnalité (quantité de pluie) n'est pas le facteur dominant de contrôle mais l'effet de continentalité (distance par rapport à l'océan) est très important puisqu'il détermine la contribution marine de la pluie. L'un des résultats importants de cette étude est que majoritairement le lithium des pluies n'a pas une origine marine. Les autres sources doivent donc être prises en compte, qu'il s'agisse de particules continentales ayant interagit avec les molécules d'eau dans l'atmosphère ou bien les apports anthropiques liés aux activités agricoles.

- La distribution du lithium et de ses isotopes dans les fleuves est également très variable. Le lithium dans les eaux de rivières provient quasi exclusivement de l'altération des roches silicatées. La composition isotopique des eaux est systématiquement plus élevée (enrichie en ^{7}Li) que celle des roches mères et des matières en suspension.
  Les compositions isotopiques du lithium dans les eaux des rivières sont donc un bon traceur du régime d'altération qui est contrôlé par la balance entre la dissolution des minéraux primaires et la précipitation des minéraux secondaires qui fractionnent les rapports isotopiques des eaux en incorporant préférentiellement du ^{6}Li.

- Les compositions isotopiques du lithium dans les eaux thermominérales présentent aussi de grandes variations et le δ^{7}Li d'une eau est inversement corrélé à la température profonde du réservoir en première approximation. Toutefois, la thermo-dépendance du fractionnement isotopique du lithium doit être considérée entre l'eau et la roche, à fois pour des systèmes naturels et expérimentaux. Ainsi, les expériences d'interaction basalte/eau de mer ont permis d'établir une loi de thermo-dépendance pour le fractionnement isotopique du lithium entre l'eau et la roche, qui peut s'écrire avec l'équation suivante :

$$\Delta_{\text{solution – solide}} = 7847 / T – 8.093$$

Les mécanismes qui contrôlent ce fractionnement sont des équilibres entre dissolution de minéraux primaires et formation de minéraux secondaires. Ces minéraux secondaires dépendent des conditions de formation à différentes températures.

Le fractionnement des isotopes du lithium dans les hydrosystèmes dépend donc de l'intensité des interactions eau/roche à la fois en terme de température dans les systèmes géothermaux et du régime d'altération pour les eaux de surface. Le mécanisme commun de contrôle est l'équilibre entre dissolution de minéraux primaires et formation de minéraux secondaires.

A ce jour, trois directions principales sont envisagées en ce qui concerne les perspectives de recherches à court et moyen terme. Ces trois directions de recherches sont à la fois complémentaires et permettent d'appréhender les processus, les milieux et les systèmes géochimiques à différentes échelles.

1- Le premier axe concerne les isotopes du lithium mais à l'échelle micrométrique par l'analyse in situ. En effet, dans la cadre d'un projet de développement du BRGM, nous avons pu brièvement tester la faisabilité d'un couplage entre l'ablation laser (213 nm) et la mesure par MC-ICP-MS Neptune.
   Il est évident que cette perspective ouvre un champ important de recherche sur la compréhension fine des processus de contrôle des fractionnements des isotopes du lithium à l'échelle du minéral (résolution de 100 µm avec l'ablation laser).
   Cet outil peut être essentiel dans la compréhension des systèmes géothermaux notamment en ce qui concerne la distribution du lithium entre le fluide et les minéraux secondaires d'altération. Mais c'est aussi un outil à fort potentiel dans l'aide à la gestion des ressources minérales, notamment en ce qui concerne la caractérisation des roches et des dépôts sédimentaires porteurs de métaux rares comme le lithium.

2- Le second axe de recherche concerne également les isotopes du lithium mais l'objectif viserait à identifier les différentes sources anthropiques du lithium dans l'environnement à l'aide du traçage isotopique.
   En effet, nous avons pu voir dans ce manuscrit que les apports agricoles liés aux engrais pouvaient être identifiés dans les eaux de pluies par leurs signatures isotopiques. Nous proposons ici d'identifier les autres sources potentielles de pollution en lithium dans l'environnement. Il s'agit par exemple du lithium qui pourrait provenir des décharges de matériel informatique ou de téléphonie mobile (les batteries au lithium en particulier) ou bien encore du lithium provenant des médicaments. En effet, il a été montré très récemment que l'utilisation du lithium dans certains traitements thérapeutiques était en nette augmentation. Ce lithium prescrit dans le traitement de troubles bipolaires est du carbonate de lithium, et du fait de sa forte solubilité, le lithium se retrouve dans les effluents des usines de traitement des eaux usées.

3- Enfin, le troisième axe de recherche consisterait en une mise œuvre de plusieurs systématiques isotopiques pour l'étude et la compréhension des éléments métalliques dans l'environnement. En effet, pour puissant qu'il soit, le traçage isotopique d'un élément unique n'apporte des informations que sur les sources et/ou les processus affectant ou ayant affecté cet élément. A l'inverse, l'approche multi-isotopique intégrant l'analyse conjointe de plusieurs systèmes isotopiques sur un objet géochimique porte un potentiel beaucoup plus important, notamment pour les études dont l'objectif est de caractériser l'origine et le transfert de ces éléments entre les différents réservoirs géochimiques.
   Alors que certains éléments sont d'excellents traceurs de source (isotopes du Sr, du Pb, du Nd), d'autres éléments sont des traceurs de processus chimiques (isotopes du Li, du B, du Ca), des réactions d'oxydo-réduction (isotopes du Cr, du Se) ou encore

des géo-chronomètres (datations U/Pb, U/Th). Il apparait donc essentiel de croiser ces outils pour une meilleure approche des objets que l'on souhaite étudier. C'est dans le domaine des ressources minérales métalliques et du transfert des métaux dans l'environnement que ce couplage de méthodes isotopiques serait à même d'apporter des réponses quant à l'origine des métaux (gitologie, genèse des minéralisations) puis le transfert dans l'environnement (origine géogénique ou anthropique, facteurs de contrôle).

6. Références bibliographiques

Allègre C.J. (1987) Isotope Geodynamics. Earth Planet. Sci. Lett., 86: 175-203.

Allègre C.J. (2005) Géologie isotopique. Belin, 495p.

Anderson M.A., Bertsch P.M., Miller W.P. (1989) Exchange and apparent fixation of lithium in selected soils and clay minerals. Soil Science, 148: 46-52.

Anghel I., Turin H.J., Reimus P.W. (2002) Lithium sorption to Yucca Mountains tuffs. Applied Geochemistry, 17: 819-824.

Arnórsson S., Gunnlaugsson E., Svavarsson H. (1983) The geochemistry of geothermal waters in Iceland. III. Chemical geothermometry in geothermal investigations. Geochim. Cosmochim. Acta, 47: 567-577.

Beck P., Barrat J.A., Chaussidon M., Gillet Ph. , Bohn M. (2004) Li isotopic variations in single pyroxenes from the Northwest Africa 480 shergottite (NWA 480): a record of degassing of Martian magmas? Geochimica et Cosmochimica Acta, 68 : 2925-2933.

Bryant C.J., McCulloch M.T., Bennett V.C. (2003) Impact of matrix effects on the accurate measurement of Li isotope ratios by inductively coupled mass spectrometry (MC-ICP-MS) under "cold" plasma conditions. J.Anal. Atom. Spectrom. 18: 734-737.

Carignan J., Vigier N., Millot R. (2007) Three secondary reference materials for Li isotope measurements: Li7-N, Li6-N and LiCl-N., Geostandards and Geoanalytical Research, 31: 7-12.

Chan L.H. (1987) Lithium isotope analysis by thermal ionization mass spectrometry of lithium tetraborate. Anal. Chem. 59: 2662-2665.

Chan L.H., Edmond J.M., Thompson G., Gillis K. (1992) Lithium isotopic composition of submarine basalts : implications for the lithium cycle in the oceans. Earth and Planetary Science Letters, 108, pp. 151-160.

Chan L.H., Edmond J.M., Thompson G. (1993) A lithium isotope study of hot springs and metabasalts from mid-ocean ridge hydrothermal systems. Journal of Geophysical Research, vol. 98, pp. 9653-9659.

Chaussidon M., Robert F. (1998) $^{7}Li/^{6}Li$ and $^{11}B/^{10}B$ variations in chondrules from the Semarkona unequilibrated chondrite. Earth Planet. Sci. Lett. 164: 577–589.

Coplen T.B., Hopple J.A., Böhlke J.K., Peiser H.S., Rieder S.E., Krouse H.R., Rosman K.J.R., Ding T., Vocke R.D.Jr., Révész K.M., Lamberty A., Taylor P. and De Bièvre P. (2002) Compilation of minimum and maximum isotope ratios of selected elements in naturally occurring terrestrial materials and reagents. U.S. Geological Survey, Water-Resources Investigations, Report 01-4222.

Ellis A.J. (1970) Quantitative interpretations of chemical characteristics of hydrothermal systems. Geothermics Special Issue, 2: 516-528.

Faure G. (1986) Principles of Isotope Geology, Second Edition, John Wiley & Sons, 589 p.

Faure G. (1998) Principles and Applications of Geochemistry, Second Edition, Prentice Hall, 600 p.

Flesch G.D., Anderson A.R. and Svec H.J. (1973) A secondary isotopic standard for $^{6}Li/^{7}Li$ determinations. International Journal of Mass Spectrometry and Ion Physics, 12: 265-272.

Fouillac C. (1983) Chemical geothermometry in CO_2-rich thermal waters. Example of the French Massif central. Geothermics, 12: 149-160.

Fouillac C., Michard G. (1979) Estimation des températures des réservoirs alimentant les sources thermales de la Limagne. C. R. Acad. Sc., 289: 289-292.

Fouillac C., Michard G. (1981) Sodium/Lithium ratio in water applied to geothermometry of geothermal reservoirs. Geothermics, 10: 55-70.

Fournier R.O. (1973) Silica in thermal water: Laboratory and field investigations. In: Proceedings of the International Symposium on Hydrogeochemistry and Biogeochemistry, Japan, 1970: Vol. 1, Washington, DC, The Clark Company, 122-139.

Fournier R.O. (1977) Chemical geothermometers and mixing models for geothermal systems. Geothermics, 5: 41-50.

Fournier R.O. (1979) A revised equation for the Na/K geothermometer. Geotherm. Res. Counc. Trans., 3: 221-224.

Fournier R.O., Potter II R.W. (1979) A magnesium correction to the Na-K-Ca chemical geothermometer. Geochim. Cosmochim. Acta, 43: 1543-1550.

Fournier R.O., Truesdell A.H. (1973) An empirical Na-K-Ca geothermometer for natural waters. Geochim. Cosmochim. Acta, 37: 1255-1275.

Fournier R.O., Truesdell A.H. (1974) Geochemical indicators of subsurface temperature– Part 2, Estimation of temperature and fraction

Fournier R.O., Rowe J.J. (1966) Estimation of underground temperatures from the silica content of water from hot springs and wet-steam wells. American Journal of Science, 264: 685-697.

Gaillardet J., Millot R., Dupré B. (2003) Chemical denudation rates of the western Canadian orogenic belt: the Stikine terrane. Chemical Geology, 201: 257-279.

Giggenbach W.F. (1981) Geothermal mineral equilibria. Geochimica et Cosmochimica Acta, 45: 393-410.

Giggenbach W.F. (1988) Geothermal solute equilibria. Derivation of Na-K-Mg-Ca geoindicators. Geochim. Cosmochim Acta, 52: 2749-2765.

Giggenbach W.F., Gonfiantini R., Jangi B.L., Truesdell A.H. (1983) Isotopic and chemical compositions of Parbati Valley geothermal discharges, Northwest Himalaya, India. Geothermics, 12: 199-222.

Hall J.M., Chan L.H., McDonough W.F., Turekian K.K. (2005) Determination of the lithium isotopic composition of planktic foraminifera and its application as a paleo-seawater proxy. Marine Geology, 217: 255-265.

Hathorne E.C., James, R.H. (2006) Temporal record of lithium in seawater: A tracer for silicate weathering? Earth and Planetary Science Letters, 246: 393-406.

Hoefs J., Sywall M. (1997) Lithium isotope composition of Quaternary biogene carbonates and a global lithium isotope balance. Geochimica et Cosmochimica Acta, 61: 2679-2690.

Huh Y., Chan L.C., Zhang L., Edmond J.M. (1998) Lithium and its isotopes in major world rivers: implications for weathering and the oceanic budget. Geochimica et Cosmochimica Acta, 62: 2039-2051.

Huh Y., Chan L.C., Edmond J.M. (2001) Lithium isotopes as a probe of weathering processes: Orinoco River. Earth and Planetary Science Letters, 194: 189-199.

James R.H., Palmer M.R. (2000) The lithium isotope composition of international rock standards. Chemical Geology, 166: 319-326.

Johnson C.M., Beard B.L., Albarède F. (2004) Overview and general concepts. In Reviews in Mineralogy & Geochemistry, 55: 1-24.

Kharaka Y.K., Lico M.S., Law-Leroy M. (1982) Chemical geothermometers applied to formation waters, Gulf of Mexico and California basins. AAPG Bulletin, 66, 5, 588.

Lemarchand E., Chabaux F., Vigier N., Millot R., Pierret M.C. (2010) Lithium isotope systematics in a forested granitic catchment (Strengbach, Vosges Mountains, France). Geochimica et Cosmochimica Acta, 74: 4612-4628.

Michard G. (1979) Géothermomètres chimiques. Bull. du BRGM ($2^{ème}$ série), Section III, n°2 : 183-189.

Michard G. (1990) Behaviour of major elements and some trace elements (Li, Rb, Cs, Sr, Fe, Mn, W, F) in deep hot waters from granitic areas. Chem. Geol., 89: 117-134.

Millot R., Gaillardet J., Dupré B., Allègre C.J. (2002) The global control of silicate weathering rates and the coupling with physical erosion: new insights from the Canadian Shield. Earth and Planetary Science Letters, 196: 83-98.

Millot R., Gaillardet J., Dupré B., Allègre C.J. (2003) Northern latitude chemical weathering rates: clues from the Mackenzie River Basin, Canada. Geochimica et Cosmochimica Acta, 67: 1305-1329.

Millot R., Guerrot C., Vigier N. (2004) Accurate and high precision measurement of lithium isotopes in two reference materials by MC-ICP-MS. Geostandards and Geoanalytical Research, 28: 53-159.

Millot R, Girard J.P. (2007) Lithium isotope fractionation during adsorption onto mineral surfaces. Proceedings of the 3rd International Meeting on "Clay in natural & engineered barriers for radioactive waste confinement", Lille, France, September 2007.

Millot R., Vigier N., Gaillardet J. (2010a) Behaviour of lithium and its isotopes during weathering in the Mackenzie Basin, Canada. Geochimica et Cosmochimica Acta, 74: 3897-3912.

Millot R., Scaillet B., Sanjuan B. (2010b) Lithium isotopes in island arc geothermal systems: Guadeloupe, Martinique (French West Indies) and experimental approach. Geochimica et Cosmochimica Acta, 74: 1852-1871.

Millot R., Petelet-Giraud E., Guerrot C., Négrel Ph. (2010c) Multi-isotopic composition (δ^7Li δ^{11}B- δD- δ^{18}O) of rainwaters in France: origin and spatio-temporal characterization. Applied Geochemistry, 25: 1510-1524.

Murosimi M., Chow T.J., Patterson C. (1969) Chemical concentrations of pollutant lead aerosols, terrestrial dusts and sea salts in Greenland and Antarctic snow strata. Geochimica et Cosmochimica Acta, 33: 1247-1294.

Négrel Ph., Roy S. (1998) Chemistry of rainwater in the Massif Central (France) A Strontium isotope and major element study. Applied Geochemistry, 13: 941-952.

Négrel Ph., Millot R., Brenot A., Bertin C. (2010) Tracing groundwater circulation in a peatland using lithium isotopes. Chemical Geology, 15: 1345-1367.

Nishio Y., Nakai S. (2002) Accurate and precise lithium isotopic determinations of igneous rock samples using multi-collector inductively coupled plasma mass spectrometry. Anal. Chim. Acta 456, 271-281.l J.R. (1986) Theoretical and experimental aspects of isotopic fractionation. Rev. Mineral, 16:, 1-40.

Pistiner J.S., Henderson G.M. (2003) Lithium isotope fractionation during continental weathering processes. Earth and Planetary Science Letters, 214: 327-339.

Qi H.P., Coplen T.B., Wang Q.Z., Wang Y.H. (1997) Unnatural isotopic composition of lithium reagents. Analytical Chemistry, 69: 4076-4078.

Roy S., Négrel Ph. (2001) A Pb isotope and trace element study of rainwater from the Massif Central (France). Science of the Total Environment, 277: 225-239.

Tatsumoto M., Patterson C. (1963) Concentrations of common lead in some Atlantic and Mediterranean waters and snow. Nature, 199: 350-356.

Taylor T.I., Urey H.C. (1938) Fractionation of the lithium and potassium isotopes by chemical exchange with zeolites. J. Chem. Phys., 6: 429-438.

Teng F.Z., McDonough W.F., Rudnick R.L., Dalpé C., Tomascak P.B., Chappell B.W., Gao S. (2004) Lithium isotopic composition and concentration of the upper continental crust. Geochimica et Cosmochimica Acta, 68: 4167-4178.

Tomascak P.B., Tera F., Helz R.T., Walker R.J. (1999) The absence of lithium isotope fractionation during basalt differentiation : new measurements by multicollector sector ICP-MS. Geochimica et Cosmochimica Acta, 63: 907-910.

Tomascak P.B., Carlson R.W., Shirey S.B. (1999b). Accurate and precise determination of Li isotopic compositions by multi-collector ICP-MS. Chemical Geology, 158: 145-154.

Tomascak P.B. (2004) Developments in the Understanding and Application of Lithium Isotopes in the Earth and Planetary Sciences. In Reviews in Mineralogy & Geochemistry, 55: 153-195.

Truesdell A.H. (1976) Geochemical techniques in exploration, summary of section III. Proc. Sec. United Nations Symp. Develop. Use Geotherm. Res., San Francisco, 53-79.

Verney-Carron A., Vigier N., Millot R. (2011) Experimental determination of the role of diffusion on Li isotope fractionation during basaltic glass weathering. Geochimica et Cosmochimica Acta, 75: 3452-3468.

Vigier N., Rollion-Bard C., Spezzaferri S., Brunet F. (2007) In-situ measurements of Li isotopes in foraminifera. G^3: Geochemistry, Geophysics, Geosystems: Q01003.

Wasserburg G.J. (1987) Isotopic abundances: inferences on solar system and planetary evolution. Earth Planet. Sci. Lett., 86; 129-173.

Weissberg B.G., Wilson P.T. (1977) Montmorillonite and the Na/K geothermometer. In Geochemistry 77, N.Z. Dept. Sci. Indust. Res. Bull., 218: 31-35.

White D.E. (1965) Saline waters of sedimentary rocks. Fluids in Subsurface Environments - A Symposium. Am. Ass. Petrol. Geol. Mem., 4: 342-366.

Wunder B., Meixner A., Romer R.L. and Heinrich W. (2006) Temperature-dependent isotopic fractionation of lithium between clinopyroxene and high-pressure hydrous fluids. Contrib. Mineral Petrol., 151: 112-120.

Xiao Y.K., Beary E.S. (1989) High-precision isotopic measurement of lithium by thermal ionization mass spectrometry. Int. J. Mass Spectrom. Ion Proc. 94: 101-114.

Yamaji K., Makita Y., Watanabe H., Sonoda A., Kanoh H., Hirotsu T., Ooi K. (2001) Theoretical estimation of lithium isotopic reduced partition function ratio for lithium ions in aqueous solution. J. Phys. Chem., 105: 602-613.

Zhang L., Chan L.H., Gieskes J.M. (1998) Lithium isotope geochemistry in pore waters from Ocean Drilling Program Sites 918 and 919, Irminger Basin. Geochim. Cosmochim. Acta, 62: 2437-2450.

7. Curriculum Vitae

MILLOT Romain

Géochimiste Isotopiste, Ingénieur de Recherche

BRGM

Direction des Laboratoires – Unité Géochimie Isotopique

BRGM, ISTO, UMR 7327

3, avenue Claude Guillemin BP 36009 45060 Orléans Cedex 2 France

Mail : r.millot@brgm.fr Tél : 02 38 64 48 32

EXPÉRIENCE ET FORMATION

2004-Poste Actuel:	Ingénieur-Chercheur, Chef de Projet Sénior Responsable du Plateau Analytique MC-ICP-MS Neptune BRGM - Direction des Laboratoires - Unité Géochimie Isotopique Traçage multi-isotopique dans le domaine des interactions eau/roche à basse et haute température, assure le pilotage de la thématique traceurs isotopiques nouveaux au BRGM Management de projets nationaux et internationaux
2003-2004:	Post-doctorat : BRGM, Service Métrologie, Monitoring, Analyse Développement de la mesure des isotopes du lithium par MC-ICP-MS et TIMS
1998-2002:	Thèse de Doctorat de l'Université Paris 7 Denis Diderot, Institut de Physique du Globe de Paris IPGP Sujet: "Étude chimique et isotopique des produits d'érosion des grands fleuves canadiens : Impact des rivières arctiques dans les bilans globaux d'altération". Directeurs de Thèse: J. Gaillardet et C.J. Allègre. Thèmes de recherche: Quantification des processus d'érosion et modélisation des transferts d'éléments par l'altération. Analyses chimiques et isotopiques (Sr et Pb).
1997-1998:	DEA de Géochimie Fondamentale et Appliquée, Université Paris 7, IPGP
1996-1997:	Maîtrise de Sciences Physiques de la Terre, spécialité Géochimie, Université Paris 7

1995-1996: Licence de Sciences Physiques de la Terre, Université Paris 7

1993-1995: DEUG B (Biologie - Sciences de la Terre) Université Paris 7

Divers : membre de l'European Association of Geochemistry (EAGC), de l'International Association of Geochemistry (IAGC), de l'European Association of Geosciences (EGU) et de l'American Geophysical Union (AGU).

COMPÉTENCES TECHNIQUES

- Spectrométrie de Masse à Source Plasma et Multi-Collection MC-ICP-MS (Neptune, Nu Plasma 1700) mesures isotopiques Li, Se, Cr et Pb
- Spectrométrie de Masse à Thermo-Ionisation TIMS (MAT 261, 262, Triton, VG 354) mesure des isotopes Li, Sr, Nd et Pb
- Purification chimique par méthodes chromatographiques en salle blanche (Li, Sr, Nd, Pb, Cr)
- Mesure des éléments majeurs et traces (HPLC et ICP-MS Quad)
- Couplage Laser (213 nm) / MC-ICP-MS
- Prélèvements et mesures physico-chimiques sur site (eaux de surface, souterraines, géothermales)

LABORATOIRES DE RECHERCHE

- Direction des Laboratoires (anciennement Service Métrologie, Monitoring, Analyse) BRGM, Orléans, France (depuis 2003)
- Laboratoire de Géochimie et Cosmochimie, IPGP, Paris 7 (1998-2002)
- Earth Science Department, Open University, Milton Keynes, Angleterre (1 semaine, 2002)
- Earth Science Department, Oxford University, Oxford, Angleterre (1 semaine, 2000)
- Muséum d'Histoire Naturelle, Département de Minéralogie, Paris (6 mois, 1998)

COLLABORATIONS SCIENTIFIQUES EXTERNES (PAR ORDRE ALPHABÉTIQUE)

Tiziano Boschetti (Université de Parme, Italie), Tom Bullen (USGS, USA), François Chabaux (Université de Strasbourg), Laurent Charlet (Université de Grenoble), Jiubin Chen (Institut de Géochimie, Académie des Sciences, Guiyang, Chine), Geerke Floor (Institute for Reference Materials and Measurements, Belgique), Jérôme Gaillardet (IPGP, Paris), Tom Johnson (Université de l'Illinois, USA), Ed Mroczek (GNS Science, Nelle Zélande), Dave Polya (Université de Manchester, Angleterre), Tom Powell (Mighty River Power Limited, Nelle Zélande), Gabriela Roman-Ross (Université de Girone, Espagne), Roberta Rudnick (Université du Maryland, USA), Bruno Scaillet (ISTO, Orléans), Nathalie Vigier (CRPG, Nancy), David Widory (Géotop/UQAM, Canada)

ACTIVITÉS D'ENCADREMENT

Encadrement d'un post-doctorat: Dr. Julie Gattacceca - Développement analytique de la mesure isotopique du cuivre et de l'étain pour des applications environnementales. Cofinancement Région Centre : novembre 2012 – octobre 2013.

Co-encadrement thèse de Doctorat: Naresh Kumar - Metallic particles for the remediation of groundwater contaminated with arsenic oxyanions: interaction between microbiology and (geo)chemistry. Co-encadrement de thèse avec le CEREGE et VITO (Belgique) dans le cadre du projet européen AquaTRAIN : 6 mois sur la période 2008 – 2012.

Co-encadrement thèse de Doctorat: Aimee Hegan - The Occurrence and Mobility of Arsenic in Soils and Sediments: Assessing Environmental Controls. Co-encadrement de thèse avec l'Université de Manchester (Angleterre) dans le cadre du projet européen AquaTRAIN : 6 mois sur la période 2007 – 2011.

Co-encadrement thèse de Doctorat: Geerke Floor - Selenium cycling in volcanic environments: the role of soils as reactive interfaces. Co-encadrement de thèse avec l'Université de Girone (Espagne) dans la cadre du projet européen AquaTRAIN : 1 an sur la période 2007 – 2011

Membre du Jury de Thèse de Ségolène Saulnier, Université de Lorraine – CRPG, titre : « Exploration des compositions isotopiques en magnésium dans les carbonates marins comme traceurs paléoenvironnementaux », thèse soutenue le 12/11/12.

Membre du Comité de Thèse de Mathieu Dellinger 2009-2013 Thèse en co-tutelle Institut de Physique du Globe de Paris – Géotop Université du Québec à Montréal, titre : « Etude des liens entre composition de la croute, recyclage sédimentaire et altération chimique : exemple du fleuve Mackenzie (Canada) et géochimie isotopique du lithium dans les sédiments de fleuves », soutenance prévue au printemps 2013.

Co-encadrement d'un Master M2 : Guillaume Morin - Lixiviation de verre basaltique en conditions contrôlées. Influence de la composition du fluide sur la signature isotopique du lithium. Stage de Master 2ème année Recherche, Géosciences et Ressources Minérales, Métallogénie et Géochimie des ressources, CRPG de Nancy et Ecole Nationale Supérieure de Géologie de Nancy (ENSG) : 1 semaine en mai 2010.

Co-encadrement d'un Master M2 : Pascal Krezel - Calcul des incertitudes liées à l'analyse isotopique par la méthode de Double-Spike: l'exemple du Chrome. Stage de Master 2ème année ICMS (Instrumentation Contrôle et Management des Systèmes) Université d'Orléans / CNAM ; 4 mois entre décembre 2005 – mars 2006.

BILAN SYNTHÉTIQUE DES ACTIVITÉS DE RECHERCHE

Romain Millot a obtenu un doctorat de Géochimie fondamentale et appliquée en 2002 à l'Institut de Physique du Globe de Paris IPGP et à l'Université Paris 7 Denis Diderot. Après un post-doctorat au BRGM dans le Service Analyse où il a développé la mesure isotopique du lithium par Spectrométrie de Masse à Multi-Collection et Source Plasma (MC-ICP-MS), Romain Millot est actuellement Ingénieur de Recherche dans la Direction des Laboratoires du BRGM au sein de l'unité de Géochimie isotopique.

Romain Millot est chef de projet Senior et assure le montage, la conduite, la réalisation et la gestion de projets R&D nationaux et internationaux sur des thématiques diverses (ressources en eau, géothermie, processus géologiques, interactions eau/roche, traçage de polluants métalliques, développement analytique) en collaboration avec les autres directions du BRGM et avec des partenariats extérieurs variés.

Depuis 2010, Romain Millot assure la fonction de coordinateur du plateau analytique Neptune ISOTOPE, il a en charge le planning, les devis, l'organisation, la validation des résultats et la gestion de ce laboratoire (4 ingénieurs chercheurs et un budget annuel de 400 k€), il encadre également les ingénieurs, post-docs, thésards, stagiaires et techniciens qui interviennent dans le cadre des activités du plateau analytique. Il coordonne la production, la maintenance et le reporting et il gère et négocie les ressources correspondantes (investissements, consommables et maintenance).

Romain Millot assure également le pilotage de la thématique « traceurs isotopiques nouveaux » au BRGM, à travers une veille technologique et des développements techniques et méthodologiques en géochimie isotopique avec un large éventail de champs d'applications. Il assure la qualité des développements analytiques innovateurs en Métrologie de l'Environnement au travers de nouvelles systématiques isotopiques dans le cadre du Système du Management de la Qualité du BRGM certifié ISO 9001 et 14001.

Dans le cadre de ses activités de recherche, Romain Millot assure la valorisation et la capitalisation de ses travaux de R&D par des canaux de communication diversifiés en s'adressant à des publics hétérogènes (communauté scientifique, décideurs, grand public) et à différentes échelles (régionale à internationale). Il organise également des sessions scientifiques dans le domaine de la Géochimie dans des congrès internationaux (Applied Isotope Geochemistry Conference : AIG et American Geophysical Union : AGU).

Romain Millot a publié 36 articles scientifiques (dont 12 en premier auteur) son H-index est de 13 (Source Web of Science, février 2013). Ses publications portent sur les thématiques suivantes : le traçage isotopique lors des interactions eau/roche à basse et haute température, l'altération par les grands fleuves, les bilans de masse lors de l'érosion, la caractérisation des eaux thermo-minérales, des eaux géothermales, l'identification des sources de pollution et le développement de méthodes d'analyses en géochimie isotopique.

Romain Millot a présenté ses travaux scientifiques lors de 75 congrès nationaux et internationaux au cours de ces dernières années (31 présentations en 1er auteur). Au cours des conférences AGU en 2011 et 2012 (American Geophysical Union Fall meeting à San Francisco) mais aussi lors de la dernière Goldschmidt Conférence à Montréal en juin 2012, Romain Millot assurait la fonction de juge pour les présentations orales et posters d'étudiants dans le but d'attribuer un prix récompensant la meilleure présentation scientifique.

Romain Millot est le relecteur régulier de manuscrits soumis pour publication dans des revues internationales (Applied Geochemistry, Chemical Geology, Geochimica et Cosmochimica Acta, Journal of Hydrology, Earth and Planetary Science Letters). Il est également le relecteur de projets soumis à l'ANR (Agence Nationale de le Recherche) et à la NSF (National Science Foundation) mais aussi le relecteur de chapitres d'ouvrage (tels que « Handbook of Environmental Isotope Geochemistry » ou « the Treatise on Geochemistry »).

En 2010, dans la cadre du projet européen AquaTRAIN (Marie Curie Research Training Network), Romain Millot a eu la charge d'organiser la conférence finale du projet pour plus de 120 personnes sur une période de 3 jours (programme scientifique, conférenciers invités et activités sociales en marge du congrès). Il est également membre du comité d'organisation de la prochaine conférence AIG-10 (10th Applied Isotope Geochemistry Conference) qui se tiendra à Budapest en septembre 2013.

Depuis son arrivée au BRGM en 2003, Romain Millot a travaillé dans de nombreux projets nationaux et internationaux où il s'est efforcé de développer et de mettre en application des outils innovants de la géochimie isotopique dans des thématiques diverses et variées des Sciences de la Terre. Il a directement collaboré ou a eu la charge de chef de projets cofinancés par l'ANR, l'ADEME, l'ANDRA, la Région Centre, ou l'INSU. Romain Millot a été fortement impliqué dans des projets européens du 6ème PCRD : AquaTerra, Hiti, et AquaTRAIN dont il a été le chef de projet au BRGM sur la période 2007-2010. Il est aussi depuis 2008 le chef d'un projet de R&D interne au BRGM (TRISEAUP : Traçage Isotopique des Eaux et des Polluants) dont le but est de mettre en application sur des cas de démonstration certains développements méthodologiques dans le domaine de la géochimie isotopique.

Depuis 2012, Romain Millot est également le chef d'un projet cofinancé par l'Agence de l'Eau Loire Bretagne (AELB) dont le but est l'identification des sources de pollution métallique (Pb-Zn-Cd-Hg) dans les eaux et les sédiments du bassin de la Loire à l'aide d'une approche multi-isotopique couplée de ces métaux. Plus récemment, Romain Millot fait partie du groupe de travail « Fluides » de l'Unité Mixte de Recherche (UMR ISTO/BRGM).

Enfin, dans le cadre de ses activités de recherche, Romain Millot encadre actuellement un post-doctorat (cofinancement Région Centre), mais il a aussi co-encadré 3 étudiants en thèse (projet AquaTRAIN) et deux étudiants en Master 2 ces dernières années.

8. Liste détaillée des publications et de l'activité de recherche

H-index 13 (Source Web of Science, Février 2013)

ARTICLES SCIENTIFIQUES EN 1ER AUTEUR (12)

Millot R., Négrel Ph. (2013) Lead isotope systematics of groundwaters: implications for source tracing in various aquifer types. Applied Geochemistry, en révision.

Millot R., Hegan A., Négrel Ph. (2012) Geothermal waters from the Taupo Volcanic Zone, New Zealand: Li, B and Sr isotopes characterization. Applied Geochemistry, 27: 677-688.

Millot R., Guerrot C., Innocent C., Négrel Ph., Sanjuan B. (2011) Chemical, multi-isotopic (Li-B-Sr-U-H-O) and thermal characterization of Triassic formation waters from the Paris Basin. Chemical Geology, 283: 226-241.

Millot R., Charlet L., Polya D. (2011) Un fléau mondial : la contamination de l'eau par l'arsenic. Pour La Science, n° 408, Octobre 2011: 76-82.

Millot R., Scaillet B., Sanjuan B. (2010) Lithium isotopes in island arc geothermal systems: Guadeloupe, Martinique (French West Indies) and experimental approach. Geochimica et Cosmochimica Acta, 74: 1852-1871.

Millot R., Vigier N., Gaillardet J. (2010) Behaviour of lithium and its isotopes during weathering in the Mackenzie Basin, Canada. Geochimica et Cosmochimica Acta, 74: 3897-3912.

Millot R., Petelet-Giraud E., Guerrot C., Négrel Ph. (2010) Multi-isotopic composition (δ^7Li- δ^{11}B- δD- δ^{18}O) of rainwaters in France: origin and spatio-temporal characterization. Applied Geochemistry, 25: 1510-1524.

Millot R., Négrel Ph. (2007) Multi-isotopic tracing (δ^7Li- δ^{11}B, ^{87}Sr/^{86}Sr) and chemical geothermometry: evidence from hydro-geothermal systems in France. Chemical Geology, 244: 664-678.

Millot R., Négrel Ph., Petelet-Giraud E. (2007) Multi-isotopic (Li, B, Sr, Nd) approach for geothermal reservoir characterization in the Limagne Basin (Massif Central, France). Applied Geochemistry, 22: 2307-2325.

Millot R., Guerrot C., Vigier N. (2004) Accurate and high precision measurement of lithium isotopes in two reference materials by MC-ICP-MS. Geostandards and Geoanalytical Research, 28: 53-159.

Millot R., Allègre C.J., Roy S., Gaillardet J. (2004) Lead isotopic systematics of major river sediments: a new estimate of the Pb isotopic composition of the Upper Continental Crust. Chemical Geology, 203: 75-90.

Millot R., Gaillardet J., Dupré B., Allègre C.J. (2003) Northern latitude chemical weathering rates: clues from the Mackenzie River Basin, Canada. Geochimica et Cosmochimica Acta, 67: 1305-1329.

Millot R., Gaillardet J., Dupré B., Allègre C.J. (2002) The global control of silicate weathering rates and the coupling with physical erosion: new insights from rivers of the Canadian Shield. Earth and Planetary Science Letters, 196: 83-98.

AUTRES ARTICLES SCIENTIFIQUES (24 EN CO-AUTEUR)

Boschetti T., Etiope G., Pennisi M., **Millot R.**, Toscani L. (2013) Boron, lithium and methane isotope composition of hyperalkaline waters (Northern Apennines, Italy): Terrestrial serpentinization or mixing with brine ? Applied Geochemsitry, 32: 17-25.

Négrel Ph., Blessing M., **Millot R.**, Petelet-Giraud E., Innocent C. (2012) Isotopic methods give clues about the origins of trace metals and organic pollutants in the environment. Trends in Analytical Chemistry, 38: 143-153.

Schmitt A.D., Vigier N., Lemarchand D., **Millot R.**, Stille P., Chabaux F. (2012) Processes controlling the stable isotope compositions of Li, B, Mg and Ca in plants, soils and waters: A review. Comptes Rendus Geoscience, 344: 704-722.

Négrel Ph., **Millot R.**, Guerrot C., Petelet-Giraud E., A. Brenot, E. Malcuit (2012) Heterogeneities and interconnections in groundwaters: Coupled B, Li and stable-isotope variations in a large aquifer system (Eocene Sand aquifer, Southwestern France. Chemical Geology, 296-297: 83-95.

Kumar N., **Millot R.**, Battaglia-Brunet F., Négrel Ph., Diels L., Rose J., Bastiaens L. (2012) Sulfur and oxygen isotope tracing in zero valent iron based In situ remediation system for metal contaminants, 90: 1366-1371.

Verney-Carron A., Vigier N., **Millot R.** (2011) Experimental determination of the role of diffusion on Li isotope fractionation during basaltic glass weathering. Geochimica et Cosmochimica Acta, 75: 3452-3468.

Floor G.H., **Millot R.**, Iglesias M., Négrel Ph. (2011) Influence of methane addition on selenium isotope sensitivity and their spectral interferences. Journal of Mass Spectrometry, 46: 182-188.

Rowland H.A.L., Omoregie E.O., **Millot R.**, Jimenez C., Mertens J., Baciu C., Hug S.J., Berg M. (2011) Geochemistry and arsenic behaviour in groundwater resources of the Pannonian Basin (Hungary and Romania). Applied Geochemistry, 26: 1-17.

Guerrot C., **Millot R.**, Robert M., Négrel Ph. (2011) Accurate and High-Precision Determination of Boron Isotopic Ratios at Low Concentration by MC-ICP-MS (Neptune). Geostandards and Geoanalytical Research, 35: 275-284.

Lemarchand E., Chabaux F., Vigier N., **Millot R.**, Pierret M.C. (2010) Lithium isotope systematics in a forested granitic catchment (Strengbach, Vosges Mountains, France). Geochimica et Cosmochimica Acta, 74: 4612-4628.

Négrel Ph., **Millot R.**, Brenot A., Bertin C. (2010) Tracing groundwater circulation in a peatland using lithium isotopes. Chemical Geology, 15: 1345-1367.

Négrel Ph., **Millot R.**, Roy S., Guerrot C., Pauwels H. (2010) Lead isotopes in groundwater as an indicator of water–rock interaction (Masheshwaram catchment, Andhra Pradesh, India). Chemical Geology, 274: 136-148.

Sanjuan B., **Millot R.**, Dezayes C., Brach M. (2010) Main characteristics of the deep geothermal brine (5 km) at Soultz-sous-Forêts (France) determined using geochemical and tracer test date. Comptes rendus Géoscience, 342: 546-559.

Kloppmann W., Chikurel H., Picot G., Pettenati M., Guttman Y., Aharoni A., Guerrot C., **Millot R.**, Gaus I., Wintgens T., (2009) B and Li isotopes as intrinsic tracers for injection tests in aquifer storage and recovery systems, Applied Geochemistry, 24: 1214-1223.

Vigier N., Gislasson S.R., Burton K.W., **Millot R.**, Mokadem F. (2009) The relationship between riverine lithium isotope composition and silicate weathering rates in Iceland., Earth and Planetary Science Letters, 287: 434-441.

Kloppmann W., Vengosh A., Guerrot C., **Millot R.**, Pankratov I. (2008) Isotope and ion selectivity in reverse osmosis desalination: Geochemical tracers for man-made freshwater, Environmental Science and Technology, 42: 4723-4731.

Kloppmann W., Van Houtte E., Gaus I., Picot G., Vandenbohede A., Lebbe L., Guerrot C., **Millot R.**, Wintgens T. (2008) Monitoring reverse osmosis treated wastewater recharge into a coastal aquifer by environmental isotopes (B, Li, O, H), Environmental Science and Technology, 42: 8759-8765.

Vigier N., Decarreau A., **Millot R.**, Carignan J., Petit S., France Lanord C. (2008) Quantifying Li isotope fractionation during smectite formation and implications for the Li cycle., Geochimica et Cosmochimica Acta, 72: 780-792.

Carignan J., Vigier N., **Millot R.** (2007) Three secondary reference materials for Li isotope measurements: Li7-N, Li6-N and LiCl-N., Geostandards and Geoanalytical Research, 31: 7-12.

Négrel Ph., Guerrot C., **Millot R.** (2007) Chemical and strontium isotope characterization of rainwater in France: influence of sources and hydrogeochemical implications., Isotopes in Environmental and Health Studies, 43: 179-196.

Négrel Ph., Roy S., Petelet-Giraud E., **Millot R.**, Brenot A.(2007) Long term fluxes of dissolved and suspended matter in the Ebro River Basin (Spain). Journal of Hydrology, 342: 249-260.

Fouillac A.M., Cocherie A., Girard J.P., Guerrot C., Innocent C., **Millot R.**, Motelica-Heino M., Sanjuan B., Widory D. (2005) Traceurs isotopiques : sources et processus. Oil & Gas Science and Technology, 60: 923-935.

Dupré B., Dessert C., Oliva P., Goddéris Y., Viers J., François L., **Millot R.**, Gaillardet J. (2003) Rivers, chemical weathering and Earth's climate. Comptes rendus Geoscience, 335: 1141-1160.

Gaillardet J., **Millot R.**, Dupré B. (2003) Chemical denudation rates of the western Canadian orogenic belt: the Stikine terrane. Chemical Geology, 201: 257-279.

RAPPORTS SCIENTIFIQUES (19 DONT 3 EN PREMIER AUTEUR)

Deguilhem A., **Millot R.**, Rocher P., Leconte S. (2012) BRGM/RP-59862-FR - Projet PRESCRIRE - Préserver et protéger les ressources en eau souterraine - Le site du Breuil-Sur-Couze (63). Rapport final, 79 p.

Genna A., Deguilhem A., **Millot R.**, Vigouroux P. (2012) BRGM/RP-60286-FR - Projet PRESCRIRE - Préserver et protéger la ressource - Le site d'Evaux-Les-Bains (23) Rapport final, 62 p.

Millot R., Innocent C., Blanc Ph., Guerrot C., Gaucher E., Négrel Ph. (2011) BRGM/RP-59480-FR - Apport de la géochimie isotopique B-U-Li-Th appliquée aux eaux des formations de l'Oxfordien et du Dogger. Rapport final, 80 p.

Millot R., Hegan A., Négrel Ph. (2011) BRGM/RP-59688-FR - Multi isotopic characterization (Li-B-Sr) of geothermal waters from New Zealand. Final Report, 48 p.

Prognon F., Deguilhem A., **Millot R.**, Leconte S. (2011) BRGM/RP-59878-FR - Projet PRESCRIRE - Préserver et protéger les ressources en eau souterraine - Le site de Châteldon (63) Rapport final, 66 p.

Ladouche B., **Millot R.**, Guerrot C., Lamotte C. (2011) BRGM/RP-59922-FR - Caractérisation géochimique des eaux de l'hydrosystème de la presqu'ile de Balaruc-Les-Bains lors d'un épisode d'inversac. Rapport final, 93 p.

Négrel Ph., Petelet-Giraud E., Blessing M., Innocent C., **Millot R.** (2010) Méthodes isotopiques d'identification de l'origine des polluants métalliques et organiques dans les milieux : état de l'art et approche critique d'application, Etude RECORD n° 09-0138/1A, 115 p.

Millot R., Innocent C. Guerrot C., Gaucher E., Négrel Ph. (2009) BRGM/RP-57316-FR - Apport de la géochimie isotopique B-U-Li-Th appliquée aux eaux des formations de l'Oxfordien et du Dogger. Rapport d'avancement, 46 p.

Sanjuan B., **Millot R.** (2009) BRGM/RP-57346-FR - Bibliographical review about the Na/Li geothermometer and lithium isotopes applied on the world geothermal waters, 58 p.

Brenot A., **Millot R.**, Bertin C., Négrel Ph. (2008) BRGM/RP-56282-FR - Caractérisation isotopique et hydrogéologique du site des Narces de la Sauvetat (Haute-Loire) : programme de recherche préliminaire à l'aménagement du site. Rapport final, 99 p.

Négrel Ph., Innocent I., **Millot R.**, Brenot A., Petelet-Giraud E. (2008) BRGM/RP-56291-FR - Caractérisation isotopique et géochimique des masses d'eau dans le bassin Adour-Garonne : interconnections et hétérogénéités : CARISMEAU, Rapport Final, 192 p.

Lopez S., **Millot R.**, Brach M., Hervé J.Y., Innocent C., Négrel Ph., Sanjuan B. (2008) BRGM/RP-56630-FR - Problématique de réinjection des fluides géothermiques dans un réservoir argilo-gréseux : retour d'expériences et apport de l'étude des fluides du Trias du Bassin de Paris. Rapport final, 197 p.

Bouchot V., Desayes C., Lopez S., **Millot R.**, Bialkowski A., Calcagno P., Sanjuan B., Jorand C., Ossi A., Courrioux G., Genter A., Garibaldi C., Bonte D., Guillou-Frottier L., Thinon I., Tourliere B., Brach M. Hervé J.Y., Innocent C., Négrel Ph., Delobelle G., Baujard C., Kohlt T. (2008) BRGM/RP-56626-FR - Projet CLASTIQ : CLAyed sandSTone In Question. Rapport final, 68 p.

Négrel Ph., Colin A., Petelet-Giraud E., Brenot A., Roy S., **Millot R.** (2006) BRGM/RP-55069-FR - CARISMEAU : Caractérisation isotopique et géochimique des masses d'eau dans le bassin Adour Garonne : interconnections et hétérogénéités. Rapport de phase 1, 128 p.

Girard J.P., Guerrot C., **Millot R.**, Casanova J., Blanc P, Gaucher E. (2006) – Apport des isotopes du B, Li et Fe à la compréhension des interactions et transferts dans les argilites du Callovo-Oxfordien. Rapport final. BRGM/RP-55216-FR. 129 p.

Casanova J., Guerrot C., **Millot R.**, Girard J.P. (2004) Projet ISOBLiFe : Caractérisation isotopique des eaux des forages scientifiques du site de Meuse/Haute Marne : résultats préliminaires B et Li. Rapport BRGM/RP-53384-FR, Rapport d'avancement, 38 p.

Casanova J., Brach M., **Millot R.**, Négrel Ph., Petelet-Giraud E. (2004) BRGM/RP-52880-FR - Projet PALEOHYD II. Paléo-hydrogéologie et géoprospective : modèles conceptuels et processus d'acquisition de la chimie des eaux dans les massifs granitiques. Rapport d'avancement, 66 p.

Casanova J., Négrel Ph., Petelet-Giraud E., Brach M., Bourguignon A., **Millot R.** (2004) BRGM/RP-53469-FR - Projet PALEOHYD II. Paléohydrogéologie et géoprospective : modèles conceptuels et processus d'acquisition de la chimie des eaux dans les massifs granitiques. Rapport final, 124 p.

Négrel Ph., Petelet-Giraud E., Serra H., **Millot R.**, Kloppmann W. (2004) BRGM/RP-53597-FR - Caractéristiques hydrogéochimiques et isotopiques d'eaux thermo-minérales du Massif-Central. Inventaire du potentiel géothermique de la Limagne (projet COPGEN). Rapport final, 165 p.

CONFÉRENCES INVITÉS (5)

Millot R., Guerrot C., Petelet-Giraud E., Brenot A. , Négrel Ph. (2012) Hydrogeochemistry of the surface waters of the Ebro River Basin (Spain): a view through Li-B-Sr isotopes. Invited Talk AGU Fall meeting (American Geophysical Union), San Francisco, USA, 03 au 07 décembre 2012.

Millot R. (2012) Lithium isotopes : analytical developments and applications in hydrosystems. Mai 2012. State Key Laboratory of Environmental Geochemistry Institute of Geochemistry, Chinese Academy of Sciences, Guiyang, Chine.

Millot R., Négrel Ph. (2011) Fluxes in rivers and their labels: 'non-traditional' isotope systematics in river basins. 2nd Water Research Horizon Conference "New Concepts in Model Development and Data Integration for Understanding Water, Matter and Energy Fluxes at Management Scale". Berlin, Allemagne, 08 au 09 juin 2011.

Millot R., Cocherie A., Robert M. (2011) Laser Ablation MC-ICP-MS and applications in geochronology. Working Group on Inorganic Analysis (IAWG), Workshop on new or specialised measurement techniques. BIPM, Bureau International des Poids et Mesures, Sèvres, 11 au 12 avril 2011.

Millot R. (2008) Exchanging best practices in isotopes measurements. AquaTRAIN Workshop, Université de Barcelone, Juillet 2008.

CONFÉRENCES EN 1ER AUTEUR (34)

Millot R., Négrel Ph. (2013) Chemical weathering of granitic rocks: experimental approach and Pb-Li isotopes tracing. WRI 14, 14th Water Rock Interaction Conference, Avignon, France, 09 au 14 juin 2013.

Millot R., Négrel Ph. Desaulty A.M., Brenot A. (2013) Lithium isotopes in surficial waters: examples from rivers and peatlands. 23ème Goldschmidt Conference. Florence, Italie, 25 au 30 août 2013.

Millot R., Desaulty A.M., Widory D., Guerrot C., Innocent C., Bourrain X., Bartov G., Johnson T.M. (2013) Pb-Zn-Cd-Hg multi isotopic characterization of the Loire River Basin, France. AIG-10, 10th International Symposium on Applied Isotope Geochemistry, Budapest, Hongrie, 22 au 27 septembre 2013.

Millot R., Négrel Ph., Widory D., Desaulty A.M., Gattacceca J., Innocent C., Guerrot C., Bourrain X., Johnson T.M. (2013) Multi isotope characterization (Pb-Zn-Cd-Hg) of the suspended sediments from the Loire River Basin, France. SedNet Conference 2013, 8th International SedNet conference, 6 au 9 novembre, Lisbonne, Portugal.

Millot R., Widory D., Innocent C., Guerrot C., Bourrain X., Johnson T.M. (2012) Pb-Zn-Cd-Hg multi isotopic characterization of the Loire River Basin, France. AGU Fall meeting (American Geophysical Union), San Francisco, USA, 03 au 07 décembre 2012.

Millot R., Guerrot C., Petelet-Giraud E., Brenot A. , Négrel PH. (2012) Hydrogeochemistry of the surface waters of the Ebro River Basin (Spain): a view through Li-B-Sr isotopes. Invited Talk AGU Fall meeting (American Geophysical Union), San Francisco, USA, 03 au 07 décembre 2012.

Millot R., Négrel Ph., Sanjuan B. (2012) Lithium isotopes systematics in Geothermal systems. 22ème Goldschmidt Conference. Montréal, Canada, 25 au 29 juin 2012.

Millot R., Guerrot C., Petelet-Giraud E., Brenot A., Négrel Ph. (2012) Hydrogeochemistry of the surface waters of the Ebro River Basin (Spain): a multi-isotopic characterization (H-O-Li-B-Sr isotopes. EUG 12 European Geosciences Union General Assembly, Vienne, Autriche, 22 au 29 Avril 2012.

Millot R., Gaillardet J., Vigier N., Sanjuan B., Négrel Ph. (2011) Lithium isotopes in low and high temperature hydrosystems. AIG-9, 9th International Symposium on Applied Isotope Geochemistry, Tarragona, Espagne, 19 au 23 septembre 2011.

Millot R., Hegan A., Négrel Ph. (2011) Geothermal waters from the Taupo Volcanic Zone: a view through Li, B and Sr isotopes. AIG-9, 9th International Symposium on Applied Isotope Geochemistry, Tarragona, Espagne, 19 au 23 septembre 2011.

Millot R., Négrel Ph. (2011) Wine and Champagne: evidence from lithium isotopes. AIG-9, 9th International Symposium on Applied Isotope Geochemistry, Tarragona, Espagne, 19 au 23 septembre 2011.

Millot R., Négrel Ph. (2011) Water/rock interactions: clues from experiments and Pb-Li isotopes tracing. EUG 11 European Geosciences Union General Assembly, Vienne, Autriche, 03 au 08 Avril 2011.

Millot R., Négrel Ph. (2011) Chemical weathering of granitic rock: experiments and Pb-Li isotopes tracing. AGU Fall meeting (American Geophysical Union), San Francisco, USA, 05 au 09 décembre 2011.

Millot R., Petelet-Giraud E., Guerrot C., Négrel Ph. (2010) Lithium and Boron isotopic compositions of rainwaters in France: origin and spatio-temporal characterization. EUG 10 European Geosciences Union General Assembly, Vienne, Autriche, 02 au 07 Mai 2010.

Millot R., Gaillardet J., Vigier N., Sanjuan B., Négrel Ph. (2010) Lithium isotopes and water/rock interactions: Clues from low and high temperature hydrosystems. AGU 2010 Fall Meeting, San Francisco, USA, December 13-17.

Millot R., Négrel Ph. (2010) Wine and Champagne: evidence from Lithium isotopes. Fourth FIRMS (Forensic Isotope Ratio Mass Spectrometry) Network, Washington, USA, April 12-14 2010.

Millot R., Asmundsson R., Négrel Ph., Sanjuan B., Bullen T.D. (2009) Multi-isotopic (H, O, C, S, Li, B, Si, Sr, Nd) approach for geothermal fluid characterization in Iceland. Goldschmidt Conference 2009, Davos, Suisse, 22 au 26 juin 2009.

Millot R., Négrel Ph. (2008) Wine and Champagne: a view through lithium isotopes., JESIUM 2008 - Joint European Stable Isotope User Meeting - Presqu'ile de Giens - France - 31/08-05/09/2008.

Millot R., Asmundsson R., Sanjuan B. (2008) Lithium isotopes in geothermal fluids form Iceland., AGU 2008 Fall Meeting - San Francisco - Californie - Etats-Unis - 15-19/12/2008.

Millot R., Girard J.P. (2007) Lithium isotope fractionation during adsorption onto mineral surfaces., Clay in natural & engineered barriers for radioactive waste confinement - 3rd International Meeting - Lille - France - 17-20/09/2007.

Millot R., Négrel Ph., Sanjuan B. (2007) Lithium isotopes in geothermal systems., Goldschmidt Conference 2007 - Cologne - Germany - 19-24/08/2007.

Millot R., Sanjuan B. (2007) Mesure isotopique du lithium par MC-ICP-MS et exemple d'application en Géothermie., Spectr'Atom 2007 3ème édition - Palais Beaumont - PAU - France - 21-24/05/2007.

Millot R., Innocent C., Krezel P. (2006) Mesure isotopique du chrome et calcul des incertitudes par la méthode double spike. Atelier ISOTRACE, Université de Strasbourg, septembre 2006.

Millot R., Guerrot C., Motelica Heino M., Casanova J., Girard J.P. (2005) Etude des isotopes du B, Li et Fe dans les eaux porales du Callovo-Oxfordien et de ses épontes carbonatées. 2ème Journée du Partenariat R&D BRGM-ANDRA - Orléans - France - 20/01/2005.

Millot R., Cocherie A., Innocent C., Motelica Heino M., Robert M., Wiederin D. (2005) Test du système d'introduction APEX pour la mesure isotopique du Li, Fe, Cd, Pb, Th et U par MC-ICP-MS Neptune. Spectr'Atom 2005 - Pau - France - 06-08/04/2005.

Millot R., Sanjuan B. (2005) Lithium isotopes in geothermal systems: clues from the Guadeloupe and Martinique islands., AIG-6 - 6th International Symposium on Applied Isotope Geochemistry - Prague - Czech Republic - 12-15/09/2005.

Millot R., Guerrot C., Bullen T.D. (2004) Precise measurement of Li isotopes by MC-ICP-MS and comparison with TIMS analyses., Winter Conference on Plasma Spectrochemistry - Fort Lauderdale - Floride - USA - 07-13/01/2004.

Millot R., Guerrot C., Bullen T.D. (2004) Analyse isotopique du lithium par MC-ICP-MS et intercomparaison TIMS., 3ème Réunion de la Société Française des Isotopes Stables - Paris - France - 09-10/09/2004.

Millot R., Guerrot C., Girard J.P. (2003) Analyse des isotopes du lithium par ICP-MS-MC., Spectr'Atom 2003 - Pau - France - 09-11/04/2003.

Millot R., Gaillardet J., Dupré B., Allègre C.J. (2001) New insights on the global control of silicate weathering rate inferred from River study of the Canadian Shield. European Union of Geosciences (EUG 11), April 8-12, Strasbourg, France.

Millot R., Gaillardet J., Dupré B., Allègre C.J. (2000) Silicate Weathering rates inferred from Sr isotopes systematics in the Mackenzie River Basin. Goldschmidt 2000, September 3-8, Oxford, UK.

Millot R., Gaillardet J., Dupré B., Allègre C.J. (2000) Flux d'altération chimique, bassins monolithologiques du Bouclier Canadien, 18ème Réunion des Sciences de la Terre, April 17-20, Paris, France.

Millot R., Gaillardet J., Dupré B., Allègre C.J. (1999) Silicate weathering rates in the Mackenzie River basin, North-West Territories, Canada, 5th International Symposium on Geochemistry of the Earth's Surface, August 16-20, Reykjavik, Iceland.

Millot R., Gaillardet J., Dupré B., Allègre C.J. (1999) Global silicate weathering rates in the Mackenzie River Basin, North-West Territories, Canada. Influence of dissolved organic matter ? European Union of Geosciences (EUG 10), March 28- April 1, Strasbourg, France.

AUTRES CONFÉRENCES (44)

Négrel Ph., Guerrot C., **Millot R.**, Petelet-Giraud E., Bullen T.D. (2013) $^{44}/^{40}$Ca and ^{87}Sr/^{86}Sr isotopes as tracers of silicate weathering in small catchments of the Massif Central, France. EUG 13 European Geosciences Union General Assembly, Vienne, Autriche, 08 au 12 Avril 2013.

Négrel Ph., **Millot R.**, Petelet-Giraud E., Guerrot C. (2012) Pb isotope systematics in volcanic river system: Constraints about weathering processes. AGU Fall meeting (American Geophysical Union), San Francisco, USA, 03 au 07 décembre 2012.

Guerrot C., Négrel Ph., **Millot R.**, Petelet-Giraud E., Brenot A. (2012) Ca isotopes in the Ebro River Basin: mixing and lithological tracer. AGU Fall meeting (American Geophysical Union), San Francisco, USA, 03 au 07 décembre 2012.

Widory D., **Millot R.** (2012) Can Li isotopes help to detect leakage in future CCS sites? The example of a natural analogue in France. 22ème Goldschmidt Conference. Montréal, Canada, 25 au 29 juin 2012.

Sanjuan B., Asmundsson R., **Millot R.**, Brach M. (2012) Use of two new Na/Li thermometric relationships for geothermal fluids in volcanic environments. 22ème Goldschmidt Conference. Montréal, Canada, 25 au 29 juin 2012.

Schmitt A.D., Vigier N., Lemarchand D., **Millot R.**, Stille P., Chabaux F. (2012) Contribution of non-traditional stable isotopes (B,Ca,Li, Mg) to the quantification of soil-water-plant exchanges. Symposium Ebelmen, Colloque de l'Académie des Sciences, 26-27 Mars 2012.

Ladouche B., **Millot R.**, Guerrot C., Lamotte C. (2012) Caractérisation géochimique de l'aquifère hydrothermal de Balaruc-les-Bains lors d'un épisode d'inversac. Dix-huitièmes journées techniques du Comité Français d'Hydrogéologie de l'Association Internationale des Hydrogéologues. « Ressources et gestion des aquifères littoraux. Cassis 2012. »

Sanjuan B., **Millot R.**, Brach M., Lasne E. (2011) Comparison of the fluid geochemical signatures between the hydrothermal systems of Bouillante and Soufrière (Guadeloupe, French West Indies). 19ème Conference Géologique Caraïbe, Le Gosier, Guadeloupe, France, 21 au 24 mars 2011.

Verney-Carron A., Vigier A., **Millot R.** (2011) Modelling Li isotope signatures of waters altering a basaltic glass in under-saturated conditions. 21ème Goldschmidt Conference. Prague, République Tchèque, août 2011.

Négrel Ph., Brenot A., **Millot R.**, Bertin C. (2011) Li isotopes: a new tracer of groundwater circulation in a peat land. EUG 11 European Geosciences Union General Assembly, Vienne, Autriche, 03 au 08 Avril 2011.

Négrel Ph., Petelet-Giraud E., **Millot R.**, Malcuit E. (2011) Source and mobility of Rare Earth Elements in a sedimentary aquifer system: Aquitaine basin (Southern France). AGU Fall meeting (American Geophysical Union), San Francisco, USA, 05 au 09 décembre 2011.

Kumar N., **Millot R.**, Rose J., Négrel Ph. Battaglia-Brunet F., Diels L. (2010) Biogeochemical dynamics of pollutants in Insitu groundwater remediation systems. AGU 2010 Fall Meeting, San Francisco, USA, December 13-17.

Négrel Ph., **Millot R.**, Guerrot C., Petelet-Giraud E., Brenot A., Malcuit E. (2010) Heterogeneities and interconnections in groundwater: Coupled B, and Li isotope variations in a large aquifer system (Eocene sand aquifer, south western France). AGU 2010 Fall Meeting, San Francisco, USA, December 13-17.

Guerrot C., **Millot R.**, Innocent C., Négrel Ph., Sanjuan B. (2010) Chemical, multi-isotopic (Li-B-Sr-U-H-O) and thermal characterization of Triassic formation waters from the Paris Basin (France). AGU 2010 Fall Meeting, San Francisco, USA, December 13-17.

Petelet-Giraud E., Négrel Ph., **Millot R.**, Guerrot C., Brenot A., Malcuit E. (2010) Large sedimentary aquifer systems functioning. Constraints by classical isotopic and chemical tools, and REE in the Eocene sand aquifer, SW France. AGU 2010 Fall Meeting, San Francisco, USA, December 13-17.

Kumar N., Battaglia-Brunet F., Vanbroekhoven C., Bastians L., Diels L, Négrel Ph., **Millot R.** (2010) Performance of Zero Valent Iron based groundwater treatment systems for arsenic and heavy metal removal: A column study. AquaTRAIN International Conference on Geogenic Chemicals in Groundwaters and Soils, BRGM, Orléans, France, July 8 - 9th, 2010.

Kumar N., Battaglia-Brunet F., Négrel Ph., **Millot R**. (2010) Stable isotope fractionation in Zero Valent Iron induced Insitu groundwater remediation systems. AquaTRAIN International Conference on Geogenic Chemicals in Groundwaters and Soils, BRGM, Orléans, France, July 8 - 9th, 2010.

Hegan A., **Millot R.**, Négrel Ph., Polya D. (2010) Occurrence of Arsenic in River Sediments: The use of isotopic analysis as a possible tracer of the mineralogical source. AquaTRAIN International Conference on Geogenic Chemicals in Groundwaters and Soils, BRGM, Orléans, France, July 8 - 9th, 2010.

Floor G., **Millot R.**, Négrel Ph. Johnson T.M., Bullen T.D., Iglesias M. (2010) Analytical improvements for selenium isotope measurements by Hydride Generation Multi-Collector ICP-MS. AquaTRAIN International Conference on Geogenic Chemicals in Groundwaters and Soils, BRGM, Orléans, France, July 8 - 9th, 2010.

Floor G., Arbelo C., **Millot R.**, Négrel Ph., Rodriguez A., Roman-Ross G., Pardini G. (2010) Weathering and geogenic elements on a volcanic islands: a case study from Tenerife. AquaTRAIN International Conference on Geogenic Chemicals in Groundwaters and Soils, BRGM, Orléans, France, July 8 - 9th, 2010.

Sanjuan B., **Millot R.**, Brach M., Asmundsson R., Giroud N. (2010) Use of a new Na/Li geothermometric relationship for High Temperature (HT) dilute geothermal fluids from Iceland. World Geothermal Congress, Bali, Indonesia, 25-29 April 2010.

Kumar N., Bastians L., Vanbroekhoven C., **Millot R.**, Battaglia-Brunet F., Diels L. (2010) Synergistic use of ZVI and SRB in groundwater remediation: Impact on metal removal and stability. Goldschmidt Conference, Knoxville, USA, 13 au 18 Juin 2010.

Verney-Carron A., Vigier N., **Millot R.**, Hardarson B.S. (2010) Lithium isotope signatures of hydrothermally altered basalts (Hengill, Iceland). Goldschmidt Conference, Knoxville, USA, 13 au 18 Juin 2010.

Widory D., **Millot R.**, Minet J.J., Barbe Le Borgne M. (2010) Multi-Collector ICP-MS: A New Direction for Isotopically Characterising Explosives? Fourth FIRMS (Forensic Isotope Ratio Mass Spectrometry) Network, Washington, USA, April 12-14 2010.

Vigier N., Decarreau A., **Millot R.**, Petit S. (2010) Quantifying lithium isotope fractionation during clay formation at low temperatures. EUG 10 European Geosciences Union General Assembly, Vienne, Autriche, 02 au 07 Mai 2010.

Kumar N., Bastians L., Vanbroekhoven C., **Millot R.**, Battaglia-Brunet F., Diels L. (2010) Metallic particles to stimulate sulfate reduction: A new approach for Bioremediation in low pH streams. EUG 10 European Geosciences Union General Assembly, Vienne, Autriche, 02 au 07 Mai 2010.

Petelet-Giraud E., **Millot R.**, Guerrot C., Négrel Ph. (2010) Map of rainwater stable isotopic composition (O and D) over the French territory: signature of aquifer recharge. EUG 10 European Geosciences Union General Assembly, Vienne, Autriche, 02 au 07 Mai 2010.

Négrel Ph., Pauwels H., **Millot R.**, Roy S., Guerrot C. (2010) Dual isotopic approach for determining groundwater origin and water-rock interactions in over exploited watershed in India. EUG 10 European Geosciences Union General Assembly, Vienne, Autriche, 02 au 07 Mai 2010.

Innocent C., Casanova J., Guerrot C., **Millot R.**, Buschaert S. (2010) $^{234}U/^{238}U$-$\delta^{7}Li$-$\delta^{11}B$ isotope systematics on aquifer groundwaters from deep scientific boreholes from the Meuse-Haute Marne site. Preliminary results. Clay in natural & engineered barriers for radioactive waste confinement – 4th International Meeting - Nantes - France – septembre 2010.

Négrel Ph., **Millot R.**, Roy S., Guerrot C., Pauwels H. (2009) Lead isotopes in groundwater as indicator of water-rock interaction (Masheshwaram catchment, India). Goldschmidt Conference 2009, Davos, Suisse, 22 au 26 juin 2009.

Négrel Ph, **Millot R.**, Brenot A. (2008) Lithium isotopes as a probe of groundwater circulation in a peat land. AIG-8, 8th International Symposium on Applied Isotope Geochemistry, La Malbaie, Canada, septembre 2008.

Gaillardet J., **Millot R.**, Lemarchand D., Vigier N. (2009) Boron and Lithium isotopic signatures in rivers as proxies of silicate weathering regimes : the example of the Mackenzie river system, Canada. AGU 2009 Fall Meeting - San Francisco - Californie - Etats-Unis – décembre 2009.

Gaillardet J., Calmels D., France-Lanord C., Lemarchand D., **Millot R.**, Vigier N. (2008) The river geochemical toolbox : application to the Mackenzie River Basin, Canada. EUG European Geosciences Union General Assembly, Vienne, Autriche, Avril 2008.

Lemarchand E., Chabaux F., Vigier N., **Millot R.**, Pierret M.C. (2007) Lithium isotopes systematic in the Strengbach catchment (Vosges, France) EUG European Geosciences Union General Assembly, Vienne, Autriche, Avril 2007.

Négrel Ph., **Millot R.**, Robert M., Cocherie A. (2006) Traçage isotopique du plomb dans les eaux: Mesure directe par MC-ICP-MS et exemple d'application. 4ème Réunion de la Société Française des Isotopes Stables - Nantes - France - 11-14/09/2006.

Vigier N., Decarreau A., **Millot R.**, Carignan J., Petit S., France-Lanord C. (2006) Quantifying the isotopic fractionation of lithium during clay formation at various temperatures. Goldschmidt Conference, Melbourne Australie, juin 2006.

Casanova J., Girard J.P., Guerrot C., Innocent C., **Millot R.**, Motelica M., Buschaert S. (2006) Isotopic characterisation (B, Li, Fe, U, Th) and WRI processes from two confined aquifers in the eastern part of the Paris basin. Congrès AIH journées techniques du Comité Français d'Hydrogéologie de l'Association Internationale des Hydrogéologues, Dijon, France.

Vigier N., Decarreau A., Carignan J., **Millot R.**, Petit S., France-Lanord C. (2005) Quantifying the isotopic fractionation of lithium during clay formation at various temperatures. EUG European Geosciences Union General Assembly, Vienne, Autriche, Avril 2005

Carignan J., Vigier N., **Millot R.**, Brenot A. (2005) Li isotopic measurements : preparation and characterisation of secondary reference materials and applications to hydrochemistry and weathering. EUG European Geosciences Union General Assembly, Vienne, Autriche, Avril 2005

Girard J.P., Guerrot G., **Millot R.**, Casanova J. (2005) Investigation of B and Li isotopes in Callovo-Oxfordian porewater at Bure, Eastern Paris Basin: objective and preliminary results. Clay in natural & engineered barriers for radioactive waste confinement – 2nd International Meeting - Tours - France – 14-18/03/2005.

Casanova J., Négrel Ph., Petelet-Giraud E., Bourguignon A., Brach M., **Millot R.**, Buschaert S. (2005) Variabilité hydrogéochimique des massifs granitiques en fonction des contextes géodynamiques et hydroclimatiques. 2ème Journée du Partenariat R&D BRGM-ANDRA - Orléans - France - 20/01/2005.

Girard J.P., Fléhoc C., Guerrot C., **Millot R.,** Huiban Y., Prinzhofer A., Buschaert S. (2005) A multi stable isotope investigation of porewater in the Callovo-Oxfordian argillites of Bure, eastern Paris Basin : new approaches. AIG-6 - 6th International Symposium on Applied Isotope Geochemistry - Prague - Czech Republic - 12-15/09/2005.

Carignan J., Vigier N., Brenot A., **Millot R.** (2005) Li concentration and isotopic composition of river waters in NE France. AGU 2005 Fall Meeting - San Francisco - Californie - Etats-Unis – décembre 2005.

Guerrot C., Robert M., **Millot R.** (2003) Analyse isotopique du bore par MC-ICP-MS. Spectr'Atom 2003 - Pau - France - 09-11/04/2003.

ACTIVITÉS ET PROGRAMMES DE RECHERCHES (DEPUIS 2003)

- **Post-doctorat** 2003/2004 : BRGM, Service Métrologie, Monitoring, Analyse : Développement de la mesure des isotopes du lithium par MC-ICP-MS et TIMS

- Projet **GHEDOM** : Géothermie Haute Enthalpie dans les DOM – 2003/2009 - co-financement ADEME. Etude du champ géothermique de Bouillante, application des isotopes du lithium aux eaux géothermales en contexte volcanique. Projet GEO3BOU depuis 2010. Chef de projet: B. Sanjuan (BRGM).

- Projet **COPGEN** : Compilation du Potentiel Géothermique de la Limagne - 2003/2004 - co-financement ADEME. Caractéristiques hydrogéochimiques et isotopiques (Li, B, Sr, Nd) d'eaux thermo-minérales du Massif Central. Chef de projet : A. Genter (BRGM).

- Projet **ISOBLiFe** : Composition isotopique B-Li de l'eau porale des argilites du Callovo-Oxfordien – 2004/2006 - cofinancé par l'ANDRA. Chef de projet : J.P. Girard (BRGM).

- Projet **BULiTh** : Apport de la géochimie isotopique B-U-Li-Th appliquée aux eaux des formations de l'Oxfordien et du Dogger - 2007/2011 - cofinancé par l'ANDRA. Chef de projet : R. Millot (BRGM).

- Projet **Hiti** : High Temperature Instruments for Supercritical Geothermal Reservoir Characterization and Exploration – 2006/2009 - Projet Européen FP6 coordonné par R. Ásmundsson (ISOR, Iceland Geosurvey). Applications des isotopes du lithium aux eaux géothermales islandaises : caractérisation multi-isotopique des fluides haute température (H-O-S-Sr-Li-B-Si). Chef de projet BRGM et coordinateur d'un Work Package : B. Sanjuan.

- Projet **CLASTIQ** : CLAyed sandSTone In Question – 2006/2008 - cofinancé par l'ADEME. Problématique de réinjection des fluides géothermiques dans un réservoir argilo-gréseux : retour d'expériences et apport de l'étude des fluides du Trias du Bassin de Paris. Chef de projet : V. Bouchot (BRGM).

- Projet **CARISMEAU** : Caractérisation isotopique et géochimique des masses d'eau dans le bassin Adour-Garonne: interconnections et hétérogénéités – 2006/2008 - co-financement Agence de l'Eau Adour Garonne. Chef de projet : Ph. Négrel (BRGM).

- Projet **AquaTerra** : Integrated Modelling of the river-sediment-soil-groundwater system; advanced tools for the management of catchment areas and river basins in the context of global change – 2006/2009 - Projet Européen FP6 coordonné par J. Barth (Université de Erlangen, Allemagne) Etudes géochimique et multi-isotopique (Li, B, Sr, Ca, SO_4) des bassins versants de l'Ebre et du Danube. Chef de projet BRGM et coordinateur d'un Work Package : Ph. Négrel.

- Projet **Reliefs de la Terre** 2007/2009 financement INSU (Programme national). Quantification de l'érosion chimique des silicates par l'étude des isotopes stables légers (Li, B, Mg). Collaboration avec le CRPG de Nancy. Chef de projet N. Vigier (CRPG).

- Projet **ISOSIL** 2007/2009 financement ANR Jeune Chercheur. Etude du rôle du climat et de la végétation sur l'érosion chimique des silicates avec les isotopes stables non conventionnels. Collaboration avec le CRPG de Nancy, l'Hydrasa de Poitiers et l'INRA de Nancy. Chef de projet N. Vigier (CRPG).

- Projet **SAUVETAT** : Caractérisation isotopique et hydrogéologique du site des Narces de la Sauvetat (Haute-Loire) – 2008/2009 - cofinancement Conseil Général de la Haute Loire Chef de projet : Ph. Négrel (BRGM).

- Projet **AquaTRAIN** : Geogenic chemicals in groundwaters and soils: a research training network) - 2007/2010 - Projet Européen Marie Curie Research Training Network FP7 coordonné par D. Polya (Université de Manchester) Co-encadrement de 3 thèses de Doctorat et organisation du congrès final du projet (3 jours/120 personnes) Chef de projet BRGM : R. Millot.

- Projet **BALARUC** : Caractérisation géochimique des eaux de l'hydrosystème de la presqu'ile de Balaruc-Les-Bains lors d'un épisode d'inversac- cofinancement Conseil Général de l'Hérault et fond FEDER de l'Union Européenne - 2010/2011 - Chef de projet BRGM : B. Ladouche.

- Projet **TRISEAUP** : Traçage Isotopique des Eaux et des Polluants - depuis 2008 - projet interne BRGM de R&D - différentes actions scientifiques ces dernières années - Chef de projet : R. Millot (BRGM)
  - Pb-eaux-Inde : mesure de la composition isotopique en Pb dans les aquifères d'alimentation en eau potable du bassin de Masheshwaram en Inde, expériences de laboratoire pour contraindre les paramètres de contrôle.
  - N^{elle} Zélande : collaboration avec Ed Mroczek (GNS Science) et Tom Powell (Mighty River Power Limited) caractérisation multi-isotopique des eaux géothermales de la zone volcanique de Taupo en N^{elle} Zélande (Li-B-Sr isotopes).
  - ISOTRIAS : caractérisation multi-isotopique des eaux du Trias du Bassin de Paris et de la zone de recharge à l'Est dans les Vosges (Li-B-Sr-Nd-U/Th).

- Projet **ORIGAMI** (Outils innovants pour la suRveillance des eaux souterraIne : échantillonnaGe pAssif couplé à la Mesure Isotopique) 2012/2014 financement ANR Développement d'outils innovants de caractérisation des eaux basés sur le couplage échantillonneurs passifs et mesures isotopiques pour le suivi des métaux (Pb, Zn et Cd) et des nitrates dans l'environnement. Chef de projet : C. Berho (BRGM). Responsable de tâche : R. Millot.

- Projet **ISOP** (Recherche méthodologique pour l'Identification des SOurces de Polluants métalliques sur le bassin Loire- Bretagne) 2011/2013 co-financement Agence de L'Eau Loire Bretagne (AELB). Identification des sources de pollution pour les métaux Zn-Cd-Pb-Hg dans les eaux et les sédiments du bassin de la Loire par une approche multi-isotopique. Chef de projet depuis 2012 : R. Millot (BRGM).

9. Remerciements

Arrivé au terme de la rédaction de ce manuscrit, je tiens à remercier toutes les personnes qui ont contribué à ce travail.

En premier lieu, je me souviens que c'est Christian Fouillac qui m'a proposé comme sujet post-doctoral le développement analytique des isotopes du lithium. Et c'est ensuite sous la direction de Jean-Pierre Girard et d'Anne-Marie Fouillac que j'ai effectué ce travail. Merci aussi à Nathalie Vigier et Kevin Burton pour leur accueil et l'accès à leur Nu plasma à l'Open University en Angleterre, où j'ai pu « faire mes premiers pas » dans la mesure des isotopes du lithium.

Je tiens également à remercier tout particulièrement Philippe Négrel et Bernard Sanjuan avec qui je travaille depuis 10 ans maintenant et qui ont su voir très tôt de multiples applications pour les isotopes du lithium dans le cadre de leurs thématiques et leurs projets.

Bien évidemment, ce travail doit beaucoup à la Direction de la Recherche du BRGM qui a financé tous les projets de Recherche dans lesquels j'ai pu intervenir. Je tiens aussi à mentionner le financement lié à la labélisation Carnot du BRGM qui m'a permis de rédiger ce manuscrit d'HDR. Je remercie aussi l'ADEME pour le financement des projets liés aux eaux géothermales.

Je remercie tous les techniciens, les ingénieurs, les chercheurs et les étudiants avec qui j'ai travaillé au sein du Service ANA. Ce service a porté par la suite le nom de MMA (Métrologie, Monitoring, Analyse) et s'appelle désormais : Direction des Laboratoires.

Si je parle beaucoup d'interactions eau/roche dans ce manuscrit, les interactions « homme/machine » (et « femme/machine » !) sont essentielles dans le domaine de la métrologie ; je remercie donc tout particulièrement les personnes suivantes pour leur travail efficace et leur disponibilité : Catherine Guerrot, Michèle Robert et Thibauld Conte.

Je remercie aussi mes co-auteurs pour les échanges scientifiques et les interactions intellectuelles, soit *de visu*, soit par mél, soit par téléphone, ou bien encore par Skype.

Merci aux membres du jury pour avoir accepté de juger ce travail.

Enfin, merci à Bruno Scaillet qui m'a encouragé pour la rédaction de ce mémoire.

10. Annexes : Sélection de publications

1- Mesure isotopique du lithium

Millot R., Guerrot C., Vigier N. (2004) Accurate and high precision measurement of lithium isotopes in two reference materials by MC-ICP-MS. Geostandards and Geoanalytical Research, 28: 53-159.

2- Eaux de surface (pluies, rivières)

Millot R., Petelet-Giraud E., Guerrot C., Négrel Ph. (2010) Multi-isotopic composition (δ^7Li-δ^{11}B-δD-δ^{18}O) of rainwaters in France: origin and spatio-temporal characterization. Applied Geochemistry, 25: 1510-1524.

Millot R., Vigier N., Gaillardet J. (2010) Behaviour of lithium and its isotopes during weathering in the Mackenzie Basin, Canada. Geochimica et Cosmochimica Acta, 74: 3897-3912.

Lemarchand E., Chabaux F., Vigier N., Millot R., Pierret M.C. (2010) Lithium isotope systematics in a forested granitic catchment (Strengbach, Vosges Mountains, France). Geochimica et Cosmochimica Acta, 74: 4612-4628.

3- Eaux thermominérales et géothermales

Millot R., Négrel Ph., Petelet-Giraud E. (2007) Multi-isotopic (Li, B, Sr, Nd) approach for geothermal reservoir characterization in the Limagne Basin (Massif Central, France). Applied Geochemistry, 22: 2307-2325.

Millot R., Négrel Ph. (2007) Multi-isotopic tracing (δ^7Li- δ^{11}B, ^{87}Sr/^{86}Sr) and chemical geothermometry: evidence from hydro-geothermal systems in France. Chemical Geology, 244: 664-678.

Millot R., Hegan A., Négrel Ph. (2012) Geothermal waters from the Taupo Volcanic Zone, New Zealand: Li, B and Sr isotopes characterization. Applied Geochemistry, 27: 677-688.

4- Approche expérimentale

Millot R., Scaillet B., Sanjuan B. (2010) Lithium isotopes in island arc geothermal systems: Guadeloupe, Martinique (French West Indies) and experimental approach. Geochimica et Cosmochimica Acta, 74: 1852-1871.

Vol. 28 — N° 1 05 04 p. 153–159

GEOSTANDARDS and GEOANALYTICAL RESEARCH

Accurate and High-Precision Measurement of Lithium Isotopes in Two Reference Materials by MC-ICP-MS

Romain **Millot** (1)*, Catherine **Guerrot** (1) and Nathalie **Vigier** (2)§

(1) BRGM Analysis and Mineral Characterisation Department, 3 avenue C. Guillemin, BP 6009, 45060 Orléans Cedex 2, France
(2) Department of Earth Sciences, The Open University, Walton Hall, Milton Keynes MK7 6AA, UK
§ Present address: CRPG, CNRS, 15 rue Notre Dame des Pauvres, BP 20, 54501 Vandoeuvre-lès-Nancy, France
* Corresponding author. e-mail: r.millot@brgm.fr

We report here a newly developed method for measurement of Li isotopes by use of multi-collector ICP-MS (Neptune) allowing rapid and high precision determination of Li isotope ratios at low levels of lithium (15-20 ng). The lithium reference sample solution IRMM-016 was analysed over a period of ten months with an external reproducibility of 0.24‰ (2*s*, n = 52). Chemical separation of Li from matrix was performed on the seawater sample IRMM BCR-403, for which a mean δ^7Li value of + 31.0 ± 0.1‰ (2*s*/√n, n = 31) was obtained. This mean value is in good agreement with those previously published for other seawater samples. BCR-403 seawater being readily available, we propose that this seawater sample be used as a reference sample for Li isotope measurements.

Keywords: lithium isotopes, standard solution, MC-ICP-MS, IRMM-016, seawater, IRMM BCR-403.

Nous présentons ici une nouvelle méthode pour la mesure des isotopes du lithium par ICP-MS à multi-collection (Neptune) permettant l'analyse rapide et très précise des rapports isotopiques du Li à faible teneur (15-20 ng). La solution échantillon de référence IRMM-016 en lithium a été analysée sur une période de 10 mois avec une reproductibilité externe de 0.24‰ (2s, n = 52). La séparation chimique du Li de sa matrice a été réalisée pour un échantillon d'eau de mer (IRMM, BCR-403), pour lequel nous obtenons une valeur moyenne de δ^7Li = + 31.0 ± 0.1‰ (2s/√n, n = 31). Cette valeur moyenne est en bon accord avec celles publiées dans la littérature pour d'autres échantillons d'eau de mer. L'eau de mer BCR-403 étant facilement disponible, nous proposons que cet échantillon d'eau de mer soit utilisé comme un échantillon de référence pour la mesure des isotopes du lithium.

Mots-clés : isotopes lithium, solution échantillon de référence, MC-ICP-MS, IRMM-016, eau de mer, IRMM BCR-403.

In a similar manner to other low atomic number ("light") elements, the isotopic composition of lithium is usually expressed as delta units calculated from isotopic ratios relative to the composition of a specified reference sample. Over the last few decades, authors have frequently reported δ^6Li values based on ^{6}Li/^{7}Li ratios. However, δ^7Li values have been also reported in the literature and it has been recently agreed by the isotope geoscience community that the δ^7Li notation would be preferentially reported (Coplen 1996, Carignan *et al.* 2004). δ^7Li is defined as the deviation in parts per thousand relative to the L-SVEC certified reference material as follows:

$$\delta^7\text{Li}\ (‰) = \left(\frac{\left(\frac{^7\text{Li}}{^6\text{Li}}\right)_{\text{sample}}}{\left(\frac{^7\text{Li}}{^6\text{Li}}\right)_{\text{L-SVEC}}} - 1 \right) \times 10^3 \qquad (1)$$

The L-SVEC reference material (Flesch *et al.* 1973) is a pure lithium carbonate originally prepared by NIST as a fine powder (SRM 8545), with an assigned δ^7Li value of 0‰. The IRMM-016 lithium carbonate is also available as a fine powder from the Institute of Reference Materials and Measurements (Geel, Belgium) and is isotopically identical to L-SVEC within

Received 10 Dec 03 — Accepted 01 Mar 04

analytical uncertainty (Lamberty *et al.* 1987, Grégoire *et al.* 1996, Qi *et al.* 1997). Aside from L-SVEC and IRMM-016 (both with δ^7Li = 0‰), no other reference samples for Li isotopes are available to date, although a strong need exists for reference materials with δ^7Li values away from 0‰ in order to validate analytical methods. Seawater (δ^7Li ~ + 31‰) has been considered by many authors as a natural secondary standard and the Li isotope composition of seawater has been frequently reported in the literature (see James and Palmer 2000, Nishio and Nakai 2002 for data compilations). However, no single seawater sample has been adopted throughout the Li isotope community as a reference sample.

Accurate measurement of Li isotopic compositions in geological materials is of great interest in the Earth Sciences. Because of their large mass difference, the two naturally occurring isotopes of lithium (^{6}Li ~ 7.5% and ^{7}Li ~ 92.5%) have the potential to fractionate significantly during natural processes. This is illustrated by the wide range of Li isotopic compositions for geological materials covering 60‰ delta units (see data compilation by Coplen *et al.* 2002). Over the last decades, lithium isotope compositions have been measured with a variable degree of accuracy and precision by different techniques. The first precise Li isotope measurements were performed in the late 1980s by thermal ionisation mass spectrometry (TIMS) at the microgram level (Chan 1987, Xiao and Beary 1989) using the Li tetraborate form for ionisation. Later, phosphoric acid was used as an activator, requiring smaller quantities of Li (100 ng to 1 μg) and yielding an external reproducibility of between 0.7 and 1.5‰ (2*s*) for highly purified samples (You and Chan 1996, Moriguti and Nakamura 1998, James and Palmer 2000).

The use of ICP-MS techniques represents a good alternative to TIMS. The high sensitivity of the quadrupole ICP-MS allows measurement of Li isotopes with an external reproducibility of 1.5-2.0‰ (2*s*) on quantities as low as 5 to 10 ng Li (Grégoire *et al.* 1996, Kosler *et al.* 2001). Recently, the use of multi-collector ICP-MS was shown to provide the most rapid and precise measurements of Li isotopes (about 0.5-1‰ at 2*s*; Tomascak *et al.* 1999, Nishio and Nakai 2002, Bryant *et al.* 2003). To date, the MC-ICP-MS approach combines advantages that no other technique can match in terms of accuracy, reproducibility, sensitivity and analysis throughput. This paper focuses on a newly developed methodology for high precision measurement of lithium isotope composition by use of the Neptune MC-ICP-MS.

All uncertainties reported in this paper, either derived from data acquired in this study or from literature data are given at the 2*s* level, where *s* represents the standard deviation. External reproducibility is given by the mean ± 2*s* and the number of analyses (n) used in the calculations of the standard deviation of the mean ($2s_m = 2s/\sqrt{n}$) is systematically specified (Goldstein *et al.* 2003).

Instrument operating conditions

Measurement of lithium isotopes was performed at the Isotope Geochemistry Unit of the BRGM using the double focusing MC-ICP-MS manufactured by ThermoElectron (formerly ThermoFinnigan). The Neptune is an MC-ICP-MS of the third generation allowing simultaneous measurement of ^{6}Li$^+$ and ^{7}Li$^+$ by use of the movable low mass and high mass Faraday cups. Indeed, the maximum adjustable distance between the outermost cup positions corresponds to a relative mass range of 17% (16.7% is needed for ^{6}Li and ^{7}Li). The Neptune provided excellent short-term and long-term stability of both signal intensity and mass bias. Measurements were performed under "hot" plasma conditions, with the plasma torch operating typically at 1200 W. Sensitivity varies for different sample introduction systems as outlined by Bouman *et al.* (2002). In our study, the ThermoElectron stable introduction system (SIS) was used. It consisted of a quartz dual spray chamber with a low-flow PFA microconcentric nebuliser. With this introduction system (wet plasma) and using the "X" cones (a recent development in the geometry of the skimmer cone), a mean ^{7}Li signal of about 50-60 V per μg g^{-1} was routinely obtained. This sensitivity is 5-10 times better than those reported for Micromass-IsoProbe (Nishio and Nakai 2002) and VG Plasma 54-30 (Tomascak *et al.* 1999) instruments using dry plasma conditions, but is similar to the sensitivity obtained with a Nu-Instruments MC-ICP-MS used in conjunction with a Cetac Aridus desolvating nebuliser system (dry plasma conditions) at the Open University. In addition, the sensitivity obtained with the Neptune MC-ICP-MS at the BRGM is significantly better than the sensitivity reported by Bryant *et al.* (2003), using a Neptune MC-ICP-MS under variable plasma conditions.

At the beginning of each analytical session, a pure Li standard solution was run to determine the most efficient instrumental settings. Once adjusted, settings were kept throughout the session. Gas flow rates, torch position, ion lens settings and electrostatic sector parameters (ESA) were adjusted to optimise signal intensity

and stability, and peak shape for both isotopes. In order to minimise drift of instrumental mass bias and to improve beam stability, a 4-5 hours warm-up period was allowed for the plasma to stabilise, during which a blank solution (3% v/v HNO_3) was run through the nebuliser.

Lithium isotope measurement

Analyses were performed on 3% v/v HNO_3 solutions with Li concentrations of 30 ng ml^{-1} typically yielding a current intensity of 1.5 to 2 x 10^{-11} A for the ^7Li ion (using 10^{11} Ω resistors). Total duration of data acquisition did not exceed 5-6 min, including sample uptake and peak centring. The analytical protocol involved the acquisition of 15 ratios with 16 s integration time per ratio, and yielded in-run precisions of better than 0.2‰ ($2s_m$). The sample introduction rate was about 80-100 µl min^{-1} and the total volume of sample used for each measurement was less than 500-600 µl, corresponding to about 15-20 ng of Li (for a sample solution at 30 ng ml^{-1}).

Instrumental mass fractionation produced by the plasma source is large, especially for low relative atomic mass ions (about 25% for lithium isotopes), but can be precisely corrected for by reference sample bracketing. The following analysis sequence was used: Blank1, L-SVEC1, Blank2, Sample1, Blank3, L-SVEC2, etc... For n samples, there were n+1 measurements on L-SVEC reference solutions (Tomascak *et al.* 1999). In this way, samples were bracketed by L-SVEC reference analyses in order to correct isotopic compositions for instrumental mass fractionation. The measured $^7Li/^6Li$ ratio of a sample was normalised to the mean $^7Li/^6Li$ ratio of the two L-SVEC reference samples run immediately before and after the sample. Over the duration of a typical analysis sequence (about 20 hours), variation in mass bias remained small (~ 2-4‰ total range). On the short-term (i.e. 30 min, which is a more relevant timing considering we used the reference sample bracketing approach), mass bias stability was better than 0.1‰ and represents a significant improvement relative to other MC-ICP-MS instruments.

In addition, during a sequence of analyses, blanks were measured before and after each unknown and reference sample for background correction (including the contribution from the introduction medium, 3% v/v HNO_3). Blank values were low, typically 3-4 mV for the ^7Li (i.e. 0.2%), and 5 minutes wash time was enough to reach a stable background value. Because blanks were very stable and with no memory effect recorded at all throughout an analysis sequence, the background correction applied to unknown and reference samples was done using the average value of the two bracketing blanks.

Accuracy and long-term reproducibility

Accuracy and long-term reproducibility were tested by repeated measurements of the pure Li reference material solution IRMM-016 and the IRMM BCR-403 seawater sample (after chemical separation of Li from the matrix).

IRMM-016

A total of fifty-two analyses (Figure 1) of the IRMM-016 reference material solution were performed over a period of 10 months, yielding a mean δ^7Li value of + 0.20‰ with an external reproducibility of 0.24‰ (2*s*, n = 52). This mean δ^7Li value is consistent with values reported in the literature, i.e. + 0.1 ± 0.4‰ (2*s*, n = 60, McDonough *et al.* 2002) and + 0.15 ± 1.0‰ (2s, n =

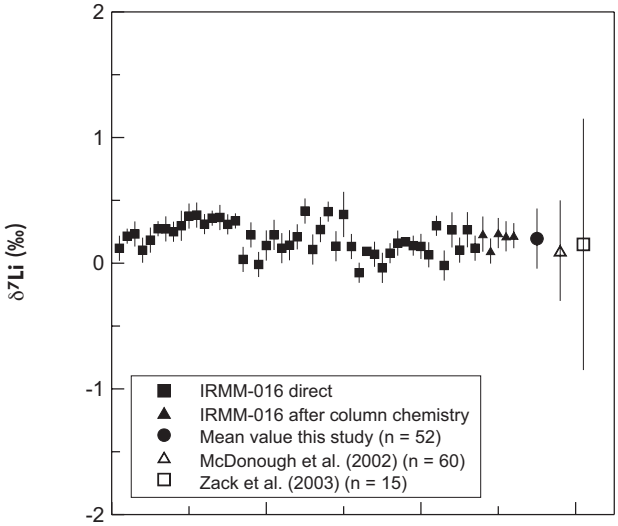

Figure 1. Long-term IRMM-016 analysis performed by Neptune MC-ICP-MS (black symbols). Black squares correspond to direct analyses (n = 47) and black triangles to analyses after processing through cation exchange resin (n = 5). These data show that our protocol yielded no isotope fractionation. Black circle corresponds to the mean of our analyses i.e. + 0.20 ± 0.24‰ (2*s*, n = 52). Two others mean values are shown for comparison, respectively from McDonough *et al.* (2002) (open triangle, n = 60) and from Zack *et al.* (2003) (open square, n = 15).

15, Zack *et al.* 2003). This result also demonstrates that, within analytical uncertainty, the IRMM-016 reference sample is indeed isotopically identical to the L-SVEC reference used for normalisation, as indicated by Lamberty *et al.* (1987), Grégoire *et al.* (1996) and Qi *et al.* (1997).

Seawater BCR-403

The accuracy and reproducibility of the analytical method were also tested through long-term repeated measurements of seawater. The Li isotope composition of seawater has been reported in a number of studies (see above) and the choice of seawater as a natural Li isotopic reference sample can be explained by summarising several advantages: (1) the seawater sample is readily available to everyone, (2) lithium is a conservative element in seawater (Stoffyn-Egli and Mackenzie 1984), the residence time of Li in seawater is about 1 Ma and it is assumed that the ocean is isotopically homogeneous (Chan and Edmond 1988), (3) many geochemical studies dealing with seawater/basalt interactions are available in which many Li isotope analyses of seawater are reported, (4) the seawater Li isotope composition is very different from that of the L-SVEC reference sample (~ + 31‰) and has been frequently used to validate analytical methods, (5) Li concentration in seawater being relatively high (~ 185 μg l^{-1}), there is no need to process large volumes of sample even if using low sensitivity techniques, (6) Li in seawater is present in a dissolved form (Li^+), so there is no requirement for preliminary sample preparation before Li purification, in contrast with sediments and rocks (which require sample dissolution).

However, it is important to point out that using seawater as a natural reference material also presents one major disadvantage. As already mentioned, MC-ICP-MS and TIMS analyses of seawater require purification of Li. It has been shown that achieving a 100% recovery yield of Li during the purification protocol is very critical because significant isotopic fractionation occurs during the cation exchange process (Moriguti and Nakamura 1998, Kosler *et al.* 2001, Chan *et al.* 2002, Pistiner and Henderson 2003, Nishio *et al.* 2004). Consequently, when comparing Li isotope compositions of seawater measured with different techniques or by different laboratories, not only the accuracy of the analytical technique is evaluated but also the quality of the purification method in terms of reproducibility and recovery yield.

We decided to perform repeated analyses of a commercially available seawater sample, i.e., IRMM BCR-403. The Li isotope composition was determined after Li purification from the matrix for a set of thirty-one individual aliquots of BCR-403 (i.e. thirty-one purifications of individual samples) according to a method modified from that of James and Palmer (2000). Results are given in Table 1. BCR-403 seawater yielded a mean δ^7Li value of + 31.0 ± 0.1‰ ($2s/\sqrt{n}$, n = 31) for 30 ng g^{-1} Li aliquots measured at the BRGM, corresponding to an external reproducibility of 0.5‰ ($2s$). Another seawater sample was analysed at the Open University with a Nu-Instruments MC-ICP-MS, and aliquots of 5-30 ng g^{-1} level yielded a mean value of + 31.2 ± 0.3‰ ($2s/\sqrt{n}$, n = 28). The external reproducibility was 1.8‰ ($2s$), similar to the reproducibility found by Tomascak *et al.* (1999), but significantly higher than the external reproducibility obtained with

Table 1.
Reproducibility of Li isotope composition of IRMM BCR-403 seawater

Seawater	δ^7Li (‰)	$2s_m$
	+ 31.3	0.1
	+ 31.0	0.2
	+ 30.8	0.2
	+ 30.9	0.2
	+ 31.1	0.1
	+ 31.1	0.1
	+ 30.9	0.1
	+ 30.6	0.1
	+ 31.2	0.1
	+ 30.9	0.1
	+ 31.4	0.1
	+ 30.9	0.1
	+ 31.4	0.2
	+ 30.7	0.2
	+ 31.0	0.2
	+ 31.2	0.2
	+ 31.3	0.2
	+ 31.3	0.1
	+ 31.0	0.1
	+ 31.0	0.1
	+ 31.1	0.1
	+ 30.9	0.1
	+ 30.8	0.1
	+ 30.6	0.1
	+ 30.9	0.2
	+ 30.6	0.1
	+ 30.6	0.1
	+ 31.1	0.2
	+ 30.8	0.1
	+ 31.0	0.1
	+ 30.9	0.2
Mean	+ 31.0	± 0.1

Analytical uncertainty for each determination is given by $2s_m$ and standard deviation of the mean is given by $2s/\sqrt{n}$, n = 31.

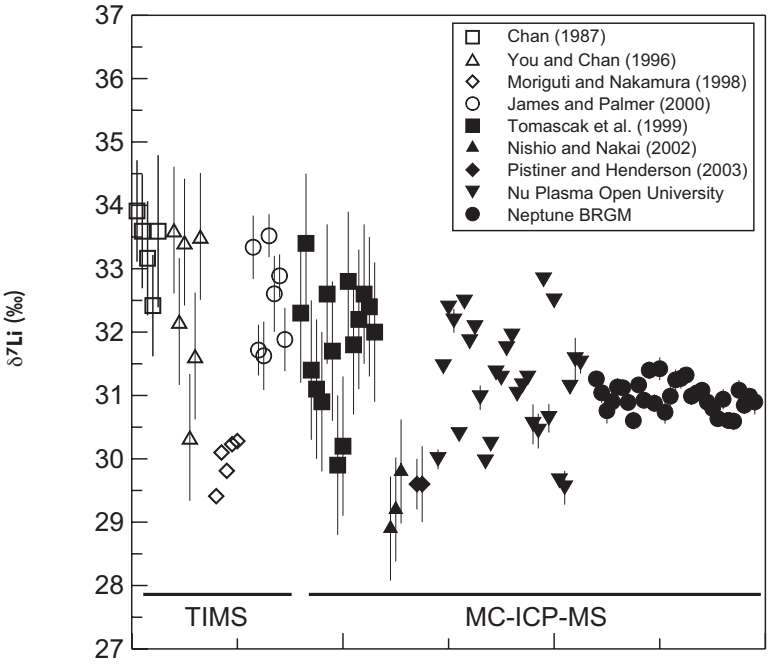

Figure 2. Comparison of δ^7Li values for seawater. In-run errors correspond to 2*s* external reproducibility for data reported by Tomascak *et al.* (1999) and Nishio and Nakai (2002). Error bars for measurements of Moriguti and Nakamura (1998) are equivalent to symbol size. δ^7Li values for Chan (1987), You and Chan (1996) and James and Palmer (2000) were converted from published δ^6Li data. Data from Bryant *et al.* (2003) are not shown because they do not report individual measurements but only mean values (see Table 2).

the Neptune. This difference is not explained by the chemical purification step used before analyses, because the same protocol was used in both laboratories, but rather comes from the mass analysis itself. The two mass spectrometers used at the Open University and BRGM present different levels of instrumental mass bias stability during data acquisition, perhaps due to the use (for sensitivity purposes at low levels) of a Cetac Aridus desolvating nebuliser with the Nu-Instruments ICP-MS at the Open University. Mass bias stability was about 0.6‰ hr^{-1} for the Nu Plasma during a typical analysis sequence, whereas it was usually less than 0.2‰ hr^{-1} for the Neptune. It is obvious that instabilities in instrumental mass bias, even if small, can produce worse reproducibility in lithium isotopic measurements. For example, Tomascak *et al.* (1999) report that ^{7}Li/^{6}Li ratio of the reference samples varies over time up to 60‰ over 12 hours (5‰ hr^{-1}). The reproducibility for seawater analyses was about 1.9‰ (2*s*) in this study. Mass bias stability of the instrument is clearly a key parameter for achieving very low reproducibilities (< 0.5‰ at 2*s*).

The mean δ^7Li value of seawater obtained here is in good agreement with data previously reported (Figure 2). The external reproducibility determined on the thirty-one replicates was 0.5‰ at the 2*s* level for the Neptune MC-ICP-MS and is consistent with that of Bryant *et al.* (2003) who report a similar reproducibility. This represents a significant improvement compared to reproducibilities reported by other MC-ICP-MS and TIMS laboratories (Table 2). Considering all data plotted in Figure 2, we observe that δ^7Li values for seawater range from + 28.9 to + 33.9‰, covering 5 delta units, with a mean value of + 31.3 ± 0.6‰ (2*s*/√n, n = 102). No systematic discrepancy is observed as a function of technique (TIMS or MC-ICP-MS, Table 2). This wide range in δ^7Li values of seawater (Figure 2) may be attributed to (1) poor reproducibility of analytical procedures for Li purification, or (2) isotopic heterogeneity of the seawater and/or the L-SVEC reference sample. In agreement with Tomascak (2003) and Nishio *et al.* (2004), our own tests (Millot *et al.* 2004) indicate that improper separation of Li from the geochemical matrix generates very significant fractionation of Li isotopes and, hence, poor reproducibility. To some extent, this is illustrated in the data reported here, as the 2*s* external reproducibility for seawater samples is twice as great as the reproducibility of pure Li reference sample solutions. Therefore, it is clear that quality of Li purification prior to analysis is a critical factor in obtaining good reproducibility (i.e. below 0.5‰, 2*s*). Isotopic heterogeneity of the L-SVEC reference sample is unlikely because, to our knowledge, informal checks conducted to date tend to point towards a good isotopic homogeneity of all L-SVEC aliquots. Regarding seawater, it is generally considered that ocean water would not display isotopic heterogeneity greater than about 0.5‰ world-wide. However, the isotopic homogeneity of ocean water samples used by

Table 2.
Comparison of δ^7Li values for seawater obtained by different techniques in different laboratories

Reference	Analytical method	Li amount required	δ^7Li (‰)	2*s*	n	2*s*/√n
Chan (1987)	TIMS / $Li_2B_4O_7$	3.5 µg	+ 33.3	1.2	5	0.5
You and Chan (1996)	TIMS / Li_3PO_4	100 ng	+ 32.4	2.6	6	1.1
Moriguti and Nakamura (1998)	TIMS / Li_3PO_4	100 ng	+ 30.0	0.7	5	0.3
James and Palmer (2000)	TIMS / Li_3PO_4	100 ng	+ 32.5	1.6	7	0.6
Tomascak *et al.* (1999)	MC-ICP-MS / Plasma 54	40 ng	+ 31.8	1.9	15	0.5
Nishio and Nakai (2002)	MC-ICP-MS / IsoProbe	45 ng	+ 29.3	0.9	3	0.5
Pistiner and Henderson (2003)	MC-ICP-MS / Nu Plasma	15 ng	+ 29.6	0.4-0.9	2	0.3-0.6
Bryant *et al.* (2003)	MC-ICP-MS / Neptune 1200W	40 ng	+ 32.0	0.2	3	0.1
Bryant *et al.* (2003)	MC-ICP-MS / Neptune 800 W	30-35 g	+ 30.4	0.9	11	0.3
Bryant *et al.* (2003)	MC-ICP-MS / Neptune 680 W	25 ng	+ 30.7	0.4	4	0.2
this study (Open University)	MC-ICP-MS / Nu Plasma	3-15 ng	+ 31.2	1.8	28	0.3
this study (BRGM)	MC-ICP-MS / Neptune 1200W	15-20 ng	+ 31.0	0.5	31	0.1

Mean values are reported with external reproducibilities in 2*s* (standard deviation) and the number of measurements (n). 2*s* uncertainty for data from Pistiner and Henderson (2003) corresponds to external reproducibility based on repeated measurements of Li reference samples. Data from Bryant *et al.* (2003) include measurements performed under "hot" (1200 W) and cooler (800 and 680 W) plasma conditions.

different groups has not been demonstrated and requires further work. Based on present work, we therefore propose that IRMM BCR-403 be used as the natural seawater reference sample of preference for lithium isotope measurements, in order that systematic comparisons between laboratories are based on use of the same sample. We propose a mean δ^7Li value of + 31.0 ± 0.1‰ (2*s*/√n, n = 31) for this reference seawater.

Conclusions

We carried out long-term measurements of lithium isotopes on a Neptune MC-ICP-MS for two reference materials, the Li carbonate IRMM-016 and the seawater IRMM BCR- 403, in order to evaluate the accuracy and reproducibility of our analytical method. The pure Li reference sample solution IRMM-016 yielded a mean δ^7Li value of + 0.20‰ with an external reproducibility of 0.24‰ (2*s*, n = 52) over a period of 10 months. The IRMM BCR-403 reference seawater gave a mean δ^7Li value of + 31.0 ± 0.1‰ (2*s*/√n, n = 31) corresponding to an external reproducibility of 0.5‰ (2*s*). We propose that the IRMM BCR-403 seawater be adopted by the Li isotope research community as a natural Li reference sample, following appropriate purification of Li by ion exchange separation techniques. The need for additional reference materials with Li isotopic compositions significantly different from 0% and not requiring Li purification still remains an important priority.

Acknowledgements

This work was supported by the Research Division of BRGM as a part of a post-doctoral fellowship to RM. Financial support from the Région Centre for the acquisition of scientific equipment (including Neptune MC-ICP-MS) is acknowledged. We would like to express special thanks to M. Robert for analytical assistance in the laboratory. The authors are grateful to K. Burton for providing access to the Li laboratory at the Open University and R. James for help and advice about the Li purification procedure. C. Bouman is thanked for comments of an early version of the manuscript. A. Cocherie, J.P. Girard and C. Innocent are acknowledged for fruitful discussions and helpful comments. We thank two anonymous reviewers for critical comments. J. Carignan is also acknowledged for editorial work allowing the quick preparation of this special section on stable isotope reference materials. This is BRGM contribution No. 02313.

References

Bouman C., Vroon P.Z., Elliott T.R., Schwieters J.B. and Hamester M. (2002)
Determination of lithium isotope compositions by MC-ICP-MS (Thermo Finnigan MAT Neptune). Goldschmidt Conference Abstracts, Davos, Switzerland.

Bryant C.J., McCulloch M.T. and Bennett V.C. (2003)
Impact of matrix effects on the accurate measurement of Li isotope ratios by inductively coupled mass spectrometry (MC-ICP-MS) under "cold" plasma conditions. Journal of Analytical Atomic Spectrometry, 18, 734-737.

references

Carignan J., Cardinal D., Eisenhauer A., Galy A., Rehkämper M., Wombacher F. and Vigier N. (2004)
A reflection on Mg, Cd, Ca, Li and Si isotopic measurements and related reference materials. Geostandards and Geoanalytical Research, 28, 139-148 (this issue).

Chan L.H. (1987)
Lithium isotope analysis by thermal ionisation mass spectrometry of lithium tetraborate. Analytical Chemistry, 59, 2662-2665.

Chan L.H. and Edmond J.M. (1988)
Variations of lithium isotope composition in the marine environment: A preliminary report. Geochimica et Cosmochimica Acta, 52, 1711-1717.

Chan L.H., Leeman W.P. and You C.F. (2002)
Lithium isotopic composition of Central American volcanic arc lavas: Implications for modification of sub-arc mantle by slab-derived fluids: Correction. Chemical Geology, 182, 293-300.

Coplen T.B. (1996)
Weights of the elements 1995. Pure and Applied Chemistry, 68, 2339-2359.

Coplen T.B., Hopple J.A., Böhlke J.K., Peiser H.S., Rieder S.E., Krouse H.R., Rosman K.J.R., Ding T., Vocke Jr. R.D., Révész K.M., Lamberty A., Taylor P. and De Bièvre P. (2002)
Compilation of minimum and maximum isotope ratios of selected elements in naturally occurring terrestrial materials and reagents. U.S. Geological Survey, Water- Resources Investigations, Report 01-4222.

Flesch G.D., Anderson A.R. and Svec H.J. (1973)
A secondary isotopic standard for $^{6}Li/^{7}Li$ determinations. International Journal of Mass Spectrometry and Ion Physics, 12, 265-272.

Goldstein S.L., Deines P., Oelkers E.H., Rudnick R.L. and Walter L.M. (2003)
Standards for publication of isotope ratio and chemical data in Chemical Geology. Chemical Geology, 202, 1-4.

Grégoire D.C., Acheson B.M. and Taylor R.P. (1996)
Measurement of lithium isotope ratios by inductively coupled plasma-mass spectrometry: Application to geological materials. Journal of Analytical Atomic Spectrometry, 11, 765-772.

James R.H. and Palmer M.R. (2000)
The lithium isotope composition of international rock standards. Chemical Geology, 166, 319-326.

Kosler J., Kucera M. and Sylvester P. (2001)
Precise measurement of Li isotopes in planktonic foraminiferal tests by quadrupole ICP-MS. Chemical Geology, 181, 169-179.

Lamberty A., Michiels E. and De Bièvre P. (1987)
On the atomic weight of lithium. International Journal of Mass Spectrometry and Ion Processes, 79, 311-313.

McDonough W., Teng F.T., Rudnick R., Dalpe C. and Tomascak P.B. (2002)
Lithium isotopic measurements: MS technique and results for reference materials. 3rd International Conference on High Resolution Sector Field ICP-MS, Atlanta, USA.

Millot R., Guerrot C. and Bullen T.D. (2004)
Precise measurement of Li isotopes by MC-ICP-MS and comparison with TIMS analyses. Winter Conference on Plasma Spectrochemistry, Fort Lauderdale, USA.

Moriguti T. and Nakamura E. (1998)
High-yield lithium separation and the precise isotopic analysis for natural rock and aqueous sample. Chemical Geology, 145, 91-104.

Nishio Y. and Nakai S. (2002)
Accurate and precise lithium isotopic determinations of igneous rock samples using multi-collector inductively coupled plasma-mass spectrometry. Analytica Chimica Acta, 456, 271-281.

Nishio Y., Nakai S., Yamamoto J., Sumino H., Matsumoto T., Prikhod'ko S. and Arai S. (2004)
Lithium isotopic systematics of the mantle-derived ultramafic xenoliths: Implications for EM1 origin. Earth and Planetary Science Letters, 214, 245-261.

Pistiner J.S. and Henderson G.M. (2003)
Lithium isotope fractionation during continental weathering processes. Earth and Planetary Science Letters, 214, 327-339.

Qi H.P., Taylor P.D.P., Berglund M. and De Bièvre P. (1997)
Calibrated measurements of the isotopic composition and atomic weight of the natural Li isotopic reference material IRMM-016. International Journal of Mass Spectrometry and Ion Processes, 171, 263-268.

Stoffyn-Egli P. and Mackenzie F.T. (1984)
Mass balance of dissolved lithium in the oceans. Geochimica et Cosmochimica Acta, 48, 859-872.

Tomascak P.B., Carlson R.W. and Shirey S.B. (1999)
Accurate and precise determination of Li isotopic compositions by multi-collector ICP-MS. Chemical Geology, 158, 145-154.

Tomascak P.B. (2003)
Lithium isotopes in the solid Earth. Goldschmidt Conference Abstracts, Kurashiki, Japan.

Xiao Y.K. and Beary E.S. (1989)
High-precision isotopic measurement of lithium by thermal ionisation mass spectrometry. International Journal of Mass Spectrometry and Ion Processes, 94, 101-114.

You C.F. and Chan L.H. (1996)
Precise determination of lithium isotopic composition in low concentration natural samples. Geochimica et Cosmochimica Acta, 60, 909-915.

Zack T., Tomascak P.B., Rudnick R.L., Dalpe C. and McDonough W.F. (2003)
Extremely light Li in orogenic eclogites: The role of isotope fractionation during dehydration in subducted oceanic crust. Earth and Planetary Science Letters, 208, 279-290.

Applied Geochemistry 25 (2010) 1510–1524

Contents lists available at ScienceDirect

Applied Geochemistry

journal homepage: www.elsevier.com/locate/apgeochem

Multi-isotopic composition (δ^7Li–δ^{11}B–δD–δ^{18}O) of rainwaters in France: Origin and spatio-temporal characterization

Romain Millot [a,*], Emmanuelle Petelet-Giraud [b], Catherine Guerrot [a], Philippe Négrel [a]

[a] BRGM, Metrology Monitoring Analysis Department, Orléans, France
[b] BRGM, Water Department, Orléans, France

ARTICLE INFO

Article history:
Received 20 January 2010
Accepted 2 August 2010
Available online 9 August 2010
Editorial handling by L. Aquilina

ABSTRACT

In the present work, the first results are reported for both Li and B isotope ratios in rainwater samples collected over a long time period (i.e. monthly rainfall events over 1 a) at a national scale (from coastal and inland locations). In addition, the stable isotopes of the water molecule (δD and δ^{18}O) are also reported here for the same locations so that the Li and B isotope data can be discussed in the same context. The range of Li and B isotopic variations in these rainwaters were measured to enable the determination of the origin of these elements in rainwaters and the characterization of both the seasonal and spatio-temporal effects for δ^7Li and δ^{11}B signatures in rainwaters. Lithium and B concentrations are low in rainwater samples, ranging from 0.004 to 0.292 μmol/L and from 0.029 to 6.184 μmol/L, respectively. δ^7Li and δ^{11}B values in rainwaters also show a great range of variation between +3.2‰ and +95.6‰ and between −3.3‰ and +40.6‰ over a period of 1 a, respectively, clearly different from the signature of seawater. Seasonal effects (i.e. rainfall amount and month) are not the main factors controlling element concentrations and isotopic variations. δ^7Li and δ^{11}B values in rainwaters are clearly different from one site to another, indicating the variable contribution of sea salts in the rainwater depending on the sampling site (coastal vs. inland: also called the distance-from-the-coast-effect). This is well illustrated when wind direction data (origin of air masses) is included. It was found that seawater is not the main supplier of dissolved atmospheric Li and B, and non-sea-salt sources (i.e. crustal, anthropogenic, biogenic) should also be taken into account when Li and B isotopes are considered in hydrogeochemistry as an input to surface waters and groundwater bodies as recharge. In parallel, the isotopic variations of the water molecule, vector of the dissolved B and Li, are also investigated and reported as a contour map for δ^{18}O values based on compiled data including more than 400 δ^{18}O values from throughout France. This δ^{18}O map could be used as a reference for future studies dealing with δ^{18}O recharge signature in relation to the characterization of surface waters and/or groundwater bodies.

1. Introduction

Atmospheric aerosols including sea salts, crustal dusts, biogenic materials and anthropogenic emissions are the main sources of chemical elements in rainwaters (Junge, 1963). The determination of the chemical composition of rainwater provides an understanding of the source types that contribute to rainwater chemistry and enhances understanding of the dispersion of elements, whether pollutants or not, and their potential impact on hydrosystems through precipitation and wet deposition processes (Berner and Berner, 1987).

In this study the first results are presented for both Li and B isotope ratios in rainwater samples collected over a long time period (i.e. monthly rainfall events over 1 a, Négrel et al., 2007) at a national scale in France (Brest, Dax, Orléans and Clermont-Ferrand, Fig. 1). In addition, the stable isotopes of the water molecule (δD and δ^{18}O) are also reported here for the same locations (Brest, Dax and Orléans) so that the Li and B isotope can be discussed in the same context and to provide a framework for the main processes affecting the isotope signatures of the rainwater.

The main processes controlling the δ^{18}O and δD isotopic signatures in precipitations were summarized by Rozanski et al. (1993): i.e. the rainfall amount, continental and altitude effects and the origins of air masses. The morphology of France is complex with the Massif Central in the centre, the Alps to the East and the Pyrénées to the South, together with the influences of both the Atlantic Ocean and the Mediterranean Sea, which have very different characteristics, as evidenced by Celle-Jeanton et al. (2001) and Ladouche et al. (2009). It is, therefore, of primary importance to constrain the signature of the atmospheric signal in different geographical and geomorphological contexts by means of a rainfall-monitoring network. Since rainwater is the main input in hydrogeological systems, monitoring the H–O–Li–B isotopic

* Corresponding author. Tel.: +33 2 38 64 48 32; fax: +33 2 38 64 37 11.
E-mail address: r.millot@brgm.fr (R. Millot).

0883-2927/$ - see front matter © 2010 Elsevier Ltd. All rights reserved.
doi:10.1016/j.apgeochem.2010.08.002

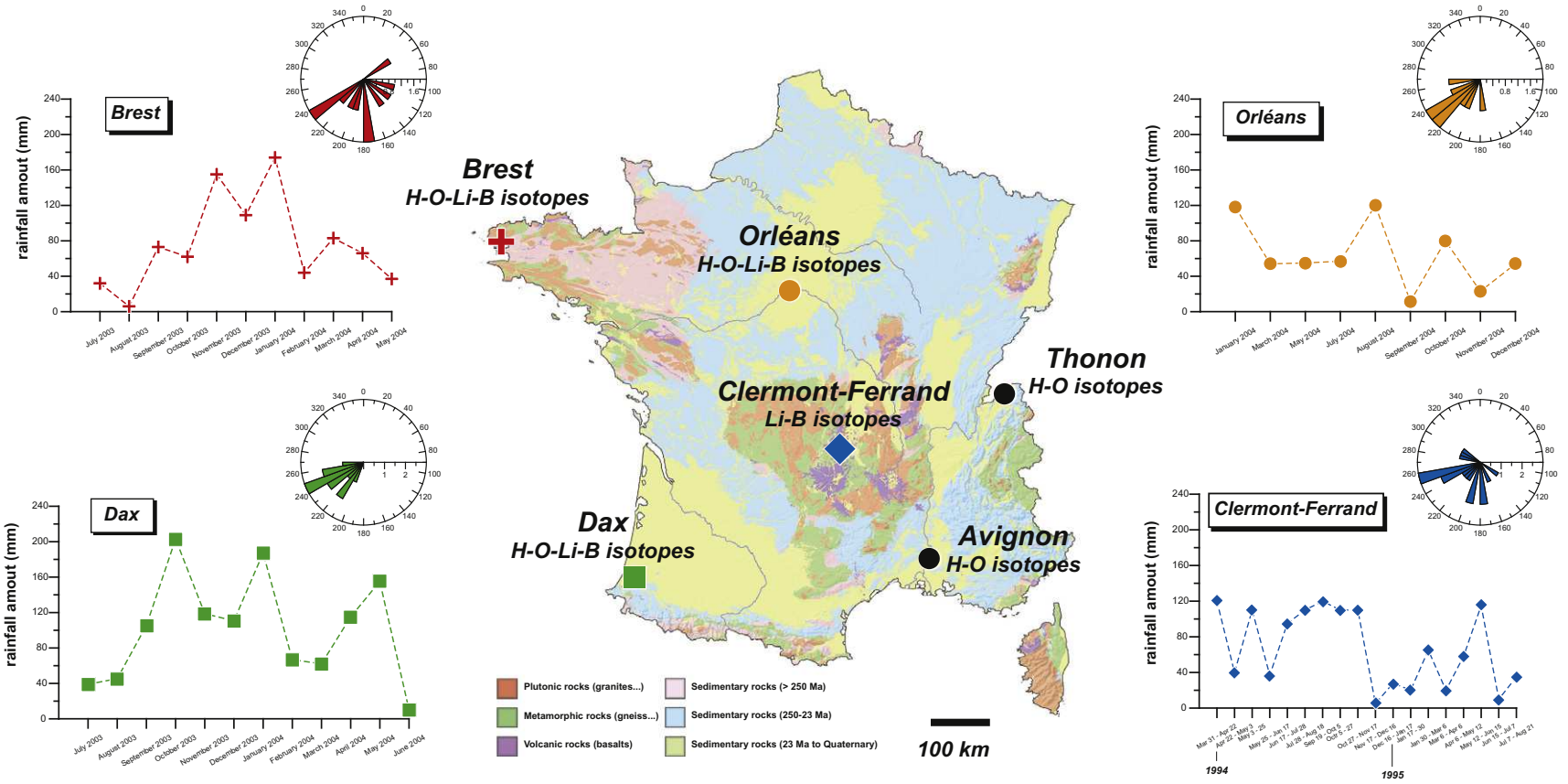

Fig. 1. Map of the rainwater sampling sites for Li and B isotopes (Brest, Dax, Orléans and Clermont-Ferrand). Graphs show the monthly mean rainfall amount (mm) at each site (modified from Négrel et al. (2007)). Long-term monitoring stations for H and O isotopes of the water molecule, at Thonon and Avignon, are also shown on this map. Windroses are also reported in this figure for the Brest, Orléans, Dax and Clermont-Ferrand sampling stations. Within the map different symbols are used for the stations used in the different samplings (five stations in total for water isotopes, four stations for δ^{7}Li and δ^{11}B, though three stations in common). Isotopes monitored at each site are given below the name of the station.

compositions of rainwater at the national scale should enable compilation of a reference system of meteoric isotopic signatures for all of France, as an addition to the Sr isotope data previously reported by Négrel et al. (2007).

The recent development of new isotopic techniques (e.g. for δ^7Li, δ^{11}B) to investigate aquifer systems has highlighted the gap in knowledge of the atmospheric inputs that are the major contributor to groundwater recharge (Widory et al., 2005; Millot et al., 2007). In this context, knowledge of the spatial and temporal variability of the isotopic compositions of rainwater appears to be essential for hydrogeological investigations and also for sustainable water management.

This paper presents, firstly, the H and O isotope data from the French Isotopic Data Base (BDISO, 2007), in the form of a contour map linked to data from neighbouring countries and, secondly, B and Li isotopic data on selected samples from this French monitoring network, part of the international database of the Global Network of Isotopes in Precipitation (GNIP, 2007) managed by the International Agency of the Atomic Energy (IAEA).

The characterization of δ^7Li and δ^{11}B signatures in rainwaters is of major importance to increase knowledge of the external cycles of these elements and, more specifically in the field of hydrogeochemistry, to characterize the Li and B isotope signatures of the rainwater input to surface waters and/or groundwater bodies as a recharge. To date, one measurement of δ^7Li (+14.3 ± 0.7‰) has been reported in the literature for a rainwater event collected in Hawaii (Pistiner and Henderson, 2003) and another (+33.3‰), slightly higher than the seawater signature, for a snow sample collected in Iceland (Pogge von Strandmann et al., 2006).

On the other hand, δ^{11}B signatures of rainwaters have been better studied (Miyata et al., 2000; Chetelat et al., 2005, 2009; Rose-Koga et al., 2006). Indeed, previous work on the characterization of δ^{11}B signatures in rainwaters have shown that seawater may be a major supplier of atmospheric B, and that B isotopic fractionation during evaporation from seawater and removal from the atmosphere may account for the large variations of δ^{11}B signatures observed in the atmosphere and in rainwater (Miyata et al., 2000). In addition, it has been shown that B isotopes in rainwater are potentially good tracers of biomass burning (Chetelat et al., 2005) and anthropogenic sources in the atmosphere in a polluted environment (Chetelat et al., 2009).

A better understanding of the H–O–Li–B isotope signatures in rainwaters is needed for a better knowledge of the origin of these elements in the atmosphere and also to constrain the isotopic signatures of the rainwater input to surface waters and/or groundwater bodies as recharge. Indeed, it is difficult to estimate recharge using conventional water balance methods and it has been shown that environmental isotopes in groundwater combined with chemistry can produce a more reliable conceptual model of a groundwater system on both local and regional scales.

The present study aims, therefore, at: 1 – investigating Li and B isotope signatures in the rainfall input, which should be identified in either surface water or groundwater since the sources of both Li and B are atmospheric, the dissolution of Li- and B-bearing minerals, biogenic and/or anthropogenic. This study also aims to more accurately define the input of Li and B to either surface water or groundwater and place constraints on the δ^7Li and δ^{11}B values, which should be corrected for atmospheric input, in order to characterize the anthropogenic signature and/or the signature derived from water–rock interaction; 2 – characterizing the H–O isotopic signature of French rainwaters and drawing a contour map for δ^{18}O values that could be used as a reference for future studies dealing with δ^{18}O recharge signature in relation to the characterization of surface waters and/or groundwater bodies.

2. Rainwater samples

2.1. Sampling sites

The five monitoring stations (Brest, Dax, Orléans, Thonon and Avignon) were selected in order to have a good distribution over the national territory (Fig. 1). This enables, firstly, following the evolution of the isotopic signal over a West–East transect from Brest to Thonon via Orléans, and, secondly, to observe the influence of the Mediterranean versus Atlantic air masses.

Monthly rain water samples were collected at five locations which constitute the French monitoring network, which is part of the IAEA/IOW Global Network for Isotopes in Precipitation (GNIP, 2007) for isotopes of the water molecule. The long-term monthly monitoring consisted in sampling rainwater in Avignon (from May 1997 to December 2002, $n = 60$), Brest (from April 1996 to May 2003, $n = 83$), Dax (from October 1997 to April 2004, $n = 74$), Orléans (from March 1996 to May 2004, $n = 96$) and Thonon (from March 1995 to December 2002, $n = 89$).

Three of these sampling sites were monitored between 2003 and 2004 for B and Li isotopes. One, Brest, is located in the NW of France (N 48.24, W 04.31), less than 5 km from the Atlantic Ocean. Another, Dax, is located in the SW of France (N 43.44, W 01.03), 30 km from the Atlantic Ocean. The third, Orléans (N 47.54, E 01.52), is located 400 km from the Atlantic Ocean. A fourth B and Li isotope sampling site is located near Clermont-Ferrand (N 45.46, E 03.04), in the Massif Central, 200 km to the SSE of Orléans. Rainwater samples were monitored here between 1994 and 1995. The Mediterranean Sea is 300 km to the south and the Atlantic Ocean is 380 km to the west.

In addition, data for several lakes and groundwater were also considered in the present work for the δ^{18}O contour map, they were selected for areas which were poorly documented. Lakes have previously been demonstrated to be good natural rain gauges in France under well-defined conditions (Petelet-Giraud et al., 2005; lakes in pristine environments located in the upper parts of drainage basins to limit runoff). Lake water data were corrected for evaporation processes according to the evaporation lines defined in two contrasted locations (near the Dax and near Orléans monitoring stations). For each station the lake data was compared to the local rain weighted mean value, the evaporation lines had a slope of 4.9 and 4.8 for Dax and Orléans, respectively. All the lake data showing an evaporation signature were corrected by this factor to restore them to the global meteoric water line. Secondly, in other regions, and as demonstrated by Darling et al. (2003), recent groundwater (i.e. ^{3}H values >0 and ^{14}C activity close to 100%) was used as a reference material being reasonably representative of long-term rainfall. Finally, the signature calculated from that of a landsnail shell (Lécolle, 1985) was also used for the Northern part of the Rhone valley where no other data was available. To better determine the isotopic signature at the French border, data from the literature or long-term rain monitoring data in the GNIP database for neighbouring countries (GNIP, 2007; Plata-Bedmar, 1994; Longinelli and Selmo, 2003; Longinelli et al., 2006; Darling and Talbot, 2003; Darling et al., 2003; Schurch et al., 2003) were used.

2.2. Sampling technique

A polycarbonate funnel (details already given in Négrel et al. (1997)) was used to collect the rainfall samples in Brest, Dax and Orléans. The rainwater was stored in a polypropylene jerrycan to avoid any evaporation or modification of the sample. Collecting the accumulated precipitation for a month enabled a monthly sample of rain to be obtained. An automatic precipitation sampler was

also designed for collecting rainwater samples at the site near Clermont-Ferrand (details already given in Négrel and Roy (1998)).

After monthly sample collection, 100 mL were used for δD and $\delta^{18}O$ determination. The rest of the rainwater samples were filtered through pre-cleaned 0.45 μm acetate filters using a pre-cleaned Nalgene filter apparatus and the filtrate was separated into two aliquots. From this: (i) 100 and 1000 mL were acidified with double-distilled HNO_3 (pH = 2) and stored in pre-cleaned polyethylene bottles for major-cation analysis and Li isotope ratio and elemental Li and B determinations and (ii) 500 mL were stored unacidified in polyethylene bottles for anion analysis and B isotope ratio measurements.

2.3. Wind characterization

The origin of the air masses for the French rainwater under consideration was studied using the French Meteorological Institute database (meteofrance.com). Daily maximum wind direction (0–360°) and rainfall (mm) were considered. Average monthly wind direction data are given in Table 1 for each sampling point. These average values were calculated by weighting daily maximum wind directions by the corresponding rainfall amount and only rainy days were considered.

3. Analytical methods

3.1. Chemical parameters and stable isotopes of the water molecule

The rainwater samples were chemically analysed by ion chromatography (Ca, Na, K, Mg, Cl, SO_4 and NO_3 concentrations, accuracy 5%) and inductively coupled plasma mass spectrometry (Li and B concentrations, accuracy 5%). Accuracy and precision for major and trace elements was verified by repeated measurements of standard materials during the course of this study: namely Ion96-3 and LGC6020 for cations and anions and pure Li and B standard solutions (Merck) for Li and B determinations.

Oxygen-18 and ^2H measurements were performed by various French laboratories using a standardised method. At BRGM's laboratory, a Finnigan MAT 252 mass spectrometer was used with a precision of 0.1‰ for $\delta^{18}O$ and 0.8‰ for δD (vs. SMOW). Isotopic compositions are reported in the usual δ-scale (in ‰) according to δ_{sample} (‰) = $\{(R_{sample}/R_{standard}) - 1\} \times 10^3$, where R is either the $^2H/^1H$ or the $^{18}O/^{16}O$ atomic ratio.

In the present work, it was challenging to measure Li and B isotope compositions in rainwater samples due to their low content (a few μmol/L). Therefore, new sensitive techniques were developed (Millot et al., 2004a,b; Guerrot et al., 2010) in order to be able to accurately and precisely determine δ^7Li and $\delta^{11}B$ in rainwater samples.

3.2. Lithium isotopes

Lithium isotopic compositions were measured using a Neptune Multi Collector ICP-MS (Thermo Fischer Scientific). $^7Li/^6Li$ ratios were normalized to the L-SVEC standard solution (NIST SRM 8545, Flesch et al., 1973) following the standard-sample bracketing method (see Millot et al. (2004b) for more details). The analytical protocol involves the acquisition of 15 ratios with 16 s integration time per ratio, and yields in-run precision better than 0.2‰ ($2\sigma_m$, 2 × Standard Error). Blank values are low (i.e. 0.2%), and 5 min wash time is enough to reach a stable background value.

The samples must be prepared beforehand with chemical separation/purification by ion chromatography in order to produce a pure mono-elemental solution. Chemical separation of Li from the matrix was done prior to the mass analysis, following a procedure modified from the technique of James and Palmer (2000), using a cationic resin (a single column filled with 3 mL of BioRad AG® 50 W-X12 resin, 200–400 mesh) and HCl acid media (0.2 N) for 30 ng of Li. Blanks for the total chemical extraction were less than 30 pg of Li, which is negligible since it represents a 10^{-3} blank/sample ratio.

Successful quantitative measurement of Li isotopic compositions requires 100% Li recovery during laboratory processing. Therefore, frequent column calibration was done and repeated analyses of L-SVEC standard processed through columns shows 100% Li recovery and no induced isotope fractionation due to the purification process.

The accuracy and the reproducibility of the entire method (purification procedure + mass analysis) were tested by repeated measurements of a seawater sample (IRMM BCR-403) after separation of Li from the matrix, for which a mean value of δ^7Li = +30.9 ± 0.4‰ (2σ, 2 × Standard Deviation, n = 12) was obtained over the period of the duration of the analyses. This mean value is in good agreement with the authors' long-term measurement (δ^7Li = +31.0 ± 0.5‰, 2σ, n = 30, Millot et al., 2004a) and with other values reported in the literature (see, for example, Tomascak (2004) for a compilation). Consequently, based on long-term measurements of the seawater standard, it was estimated that the external reproducibility of the method was around ±0.5‰ (2σ).

In addition, the reproducibility of the method was also tested by repeated measurements of a rainwater standard solution (TMRAIN-95, Environment Canada, National Water Research Institute) after separation/purification by ion chromatography, for which a mean value of δ^7Li = +445.9 ± 0.6‰ (2σ, n = 10) was obtained over the period of the duration of the analyses. This mean value could not, however, be compared either to literature data or to certified values because this reference material is not certified for Li isotopes (only for Li concentration). In spite of this, it is of interest to note that this rainwater standard solution is significantly enriched in heavy Li (^7Li). This is, however, not surprising because this reference material is a synthetic rainwater solution (namely: *TMRAIN-95: a simulated rain sample for trace elements*). Consequently, it is likely that Li in this standard solution could come from a ^7Li-rich reagent, as was pointed out by Qi et al. (1997), who showed that δ^7Li values in laboratory reagents could range between −11‰ and +3013‰. Indeed, it is well known that Li can be isotopically fractionated due to the removal of ^6Li for use in hydrogen bombs. The remaining Li is therefore substantially enriched in ^7Li and some of this Li has found its way into laboratory reagents and into the environment (Coplen et al., 2002). In addition, an ICP ^7Li-rich standard solution (Spex) was also measured, having a mean value of δ^7Li = +241.4 ± 0.5‰ (2σ, n = 38, Millot et al., 2004a), which confirms the results found by Qi et al. (1997).

Finally, concerning the Li concentration of this rainwater standard solution (TMRAIN-95), good agreement was obtained between the values measured by ICP-MS (0.059 ± 0.003 μmol/L, 2σ, n = 10) and the certified value (0.056 ± 0.011 μmol/L).

3.3. Boron isotopes

Boron isotope compositions were determined following a newly-developed methodology for precise and accurate measurement using a Neptune double-focusing multi-collector sector ICP-MS (Guerrot et al., 2010).

To avoid any drift of the mass bias induced by the sample matrix, chemical purification of 100 ng B was done before the mass analysis, following a procedure described in Guerrot et al. (2010), using the specific B resin IRA743 and 0.42 N HNO_3 acid media, with a final B concentration of 50 ng/mL. $^{11}B/^{10}B$ ratios were normalized, following the standard-sample bracketing method, to the NIST SRM-951 standard solution (Catanzaro et al., 1970) after chemical

Table 1
Major cations and anions (Na, K, Mg, Ca, Cl, SO_4, NO_3, μmol/L), Li and B concentrations (μmol/L) and Li and B isotope compositions of rainwaters by location and sampling date. Rainfall amount (mm) and wind direction are also reported in this table. The prevailing wind direction data (in °) at each sample location were obtained from the Météo France database. Wind direction data reported for monthly average values in this table are weighted by the rainfall amount and only days with precipitation are considered. Sea-salt contribution for Li and B (in %) are also given is this table. For δ^7Li and δ^{11}B, arithmetic means with Standard Deviation are also given.

Location/sampling date	Reference	Rainfall amount (mm)	Main wind direction	Na (μmol/L)	K (μmol/L)	Mg (μmol/L)	Ca (μmol/L)	Cl (μmol/L)	SO_4 (μmol/L)	NO_3 (μmol/L)	Li seasalt (%)	B seasalt (%)	Li (μmol/L)	B (μmol/L)	δ^7Li (‰)	δ^{11}B (‰)	δ^7Li (‰) arithmetic mean	δ^{11}B (‰) arithmetic mean
Brest																		
July 2003	03-E-524	32	223	117.5	5.8	16.1	8.5	117.7	21.3	36.7	12.5	22.8	0.051	0.398	23.4	35.1	22.5 ± 4.3	37.4 ± 3.8
August 2003	03-E-525	6	105	235.0	31.9	62.8	65.8	228.6	113.9	172.0	9.0	4.8	0.142	3.793	19.3	27.5		
September 2003	03-E-526	73	176	74.3	2.8	10.9	7.9	75.2	22.3	68.9	7.9	21.9	0.051	0.262	15.1	38.1		
October 2003	03-E-527	62	193	208.3	5.6	23.8	11.4	218.9	32.2	58.9	21.6	48.9	0.052	0.329	22.2	39.6		
November 2003	03-E-528	155	129	142.6	4.0	17.2	6.0	150.1	23.2	16.7	14.7	53.3	0.053	0.207	17.7	40.3		
December 2003	03-E-529	109	174	292.7	7.6	33.1	6.2	322.3	31.3	32.1	26.6	75.9	0.060	0.298	27.2	40.6		
January 2004	04-E-52	174	232	231.7	5.1	25.7	7.0	243.1	25.5	6.8	25.4	83.7	0.050	0.214	28.6	40.1		
February 2004	04-E-53	44	57	393.8	10.3	47.8	15.9	450.1	46.0	36.0	36.5	85.7	0.059	0.355	26.3	37.8		
March 2004	04-E-54	83	209	346.2	11.0	40.6	12.6	390.4	42.3	47.0	45.0	59.5	0.042	0.449	25.8	39.5		
April 2004	04-E-55	66	150	227.7	4.8	27.6	10.2	236.3	39.3	57.8	37.0	49.2	0.033	0.357	22.7	37.5		
May 2004	04-E-56	37	234	323.9	10.7	39.5	12.6	366.2	42.1	80.3	39.0	41.8	0.045	0.599	19.4	35.2		
Dax																		
July 2003	03-E-164	39	256	204.3	63.6	24.4	55.2	156.6	43.9		16.0	15.6	0.069	1.013	34.1	15.9	22.8 ± 4.3	11.4 ± 6.6
August 2003	03-E-165	45.4	248	89.5	9.2	14.9	33.8	50.7	40.8	49.7	6.2	5.9	0.078	1.167	21.5	7.9		
September 2003	03-E-166	105.4	225	196.1	14.3	18.0	23.2	176.3	32.5	2.6	12.2	21.1	0.087	0.717	21.1	12.9		
October 2003	03-E-147	203.1	207	273.6	50.2	26.9	57.8	272.3	33.8	110.6	19.3	18.0	0.077	1.174	25.2	8.3		
November 2003	03-E-148	118.7	238	155.7	15.9	15.2	25.7	136.6	24.8	–	13.5	14.5	0.062	0.830	19.8	2.0		
December 2003	03-E-149	110.7	230	194.2	11.5	16.9	44.6	167.0	30.6	2.9	18.2	25.2	0.058	0.595	21.0	11.8		
January 2004	03-E-150	187.3	242	176.4	9.3	16.9	20.8	164.8	25.9		20.2	13.7	0.047	0.997	23.0	7.1		
February 2004	03-E-151	66.8	212	203.9	51.0	29.6	49.2	198.3	44.9	28.7	19.0	42.7	0.058	0.369	23.5	19.8		
March 2004	03-E-152	62.1	210	137.4	41.9	27.1	64.5	135.5	36.9	3.5	13.6	16.0	0.055	0.662	17.2	9.4		
April 2004	03-E-153	115.1	255	255.2	53.8	33.7	65.0	247.3	18.3	3.0	20.4	17.9	0.068	1.099	18.9	7.9		
May 2004	03-E-154	155.1	243	160.1	10.9	19.8	31.4	163.7	23.5		17.2	13.8	0.050	0.898	22.8	7.8		
June 2004	03-E-155	10.2	268	108.3	26.8	22.8	114.4	113.5	42.0		7.4	6.2	0.079	1.340	25.3	26.5		
Orléans																		
January 2004	04-E-46	118	221	38.7	6.9	5.8	8.9	32.7	8.4	.	5.1	.	0.041	0.029	13.0	29.8	16.1 ± 4.8	8.4 ± 11.7
March 2004	04-E-48	54	231	61.4	11.3	10.8	21.4	49.6	22.6	39.4	6.0	11.6	0.055	0.408	14.2	13.1		
May 2004	04-E-50	55	243	52.4	17.0	8.2	12.7	39.4	14.1	9.5	6.2	5.0	0.046	0.818	19.2	6.0		
July 2004	04-E-295	57	220	53.4	13.5	12.0	23.3	30.4	21.0	–	4.3	2.1	0.068	1.987	11.2	−0.3		
August 2004	04-E-296	120	267	34.5	6.6	11.6	21.0	16.6	14.0	–	3.3	1.1	0.057	2.430	9.2	−2.4		
September 2004	04-E-297	11.5	234	96.9	19.4	22.8	39.4	98.3	27.9		6.5	1.2	0.081	6.184	19.4	−3.3		
October 2004	04-E-298	80	175	59.0	14.4	8.9	12.9	41.7	16.5	12.9	8.4	3.7	0.038	1.246	14.3	0.0		
November 2004	04-E-299	23	219	92.3	60.5	13.3	17.8	66.8	39.5	59.0	9.7	25.4	0.052	0.281	22.9	22.7		
December 2004	04-E-300	54	201	51.0	17.8	6.3	9.4	50.1	13.0	19.8	7.6	18.2	0.036	0.217	21.9	9.8		
Clermont-Ferrand																		
March 31–April 22, 1994	PSM1	120	288	39.1	4.1	4.4	12.3	39.4	51.0	74.6	4.3	9.7	0.049	0.312	77.6	11.9	26.2 ± 29.7	23.2 ± 12.2
April 22–May 3, 1994	PSM2	40	173	6.1	4.1	2.1	10.5	7.0	23.4	16.7	0.8	3.0	0.041	0.156	6.7	22.9		
May 3–25, 1994	PSM3	110	239	3.9	2.6	1.7	8.0	7.0	16.1	34.1	4.8	2.6	0.004	0.116	8.7	28.7		
May 25–June 17, 1994	PSM4	37	256	9.1	7.2	0.2	14.8	16.9	19.8	–	0.7	3.7	0.075	0.191	4.9	25.0		
June 17–July 28, 1994	PSM5	95	256	20.0	23.8	4.3	79.0	31.0	47.9	42.9								
July 28–August 18, 1994	PSM6	110	243	4.8	3.3	0.9	16.0	16.9	33.3	30.2	0.8	1.5	0.033	0.248	6.7	32.8		
September19–October 5, 1994	PSM7	120	294	4.3	2.3	1.9	16.8	7.9	7.1	12.7	0.9	3.2	0.027	0.106	9.0	32.0		
October 5–27, 1994	PSM8	110	152	8.7	2.6	0.8	15.0	10.1	7.3	–	1.8	13.4	0.027	0.050	14.7	19.5		
October 27–November 17, 1994	PSM9	110	172	0.4	13.6	6.3	1.0	13.5	4.2									
November 17–December 16, 1994	PSM10	5	246	6.5	3.8	6.3	9.5	13.0	36.6	53.8								
December 16, 1994–January 17, 1995	PSM11	28	197	32.2	1.8	8.3	12.0	44.2	21.6	38.7	4.0	14.5	0.044	0.172	63.8	27.2		
January 17–30, 1995	PSM12	20	195	8.7	3.1	5.8	3.3	14.1	6.1	–	1.1	6.4	0.041	0.104	33.2	25.4		
January 30–March 6, 1995	PSM13	65	214	43.0	2.3	4.0	5.8	21.7	13.2	19.0	0.8	6.4	0.292	0.520	95.6	4.8		
March 6–April 6, 1995	PSM14	20	258	23.0	5.1	3.2	12.3	25.4	14.2	17.5								
April 6–May 12, 1995	PSM15	58	302	8.3	4.1	2.3	11.0	11.8	39.4	47.0	2.0	4.0	0.022	0.160	3.2	19.8		
May 12–June 15, 1995	PSM16	115	229	8.7	4.9	2.6	18.0			–	1.1	3.0	0.044	0.226	7.8	25.2		
June 15–July 7, 1995	PSM17	10	124	4.8	9.0	–	12.0	37.5	13.9	69.2	0.7	1.5	0.037	0.239	8.3	26.8		

purification (Guerrot et al., 2010). Analytical uncertainty for each individual determination was better than 0.1‰ at $2\sigma_m$ ($n = 20$). Accuracy and reproducibility of the whole process were determined by repeated measurements of a seawater solution (IAEA-B1) with a mean value of $\delta^{11}B = +39.36 \pm 0.43‰$ (2σ, $n = 20$). The authors' measurements using the positive-TIMS-Cs_2BO_2 technique ($\delta^{11}B = +39.24 \pm 0.36‰$ (2σ, $n = 19$), are in good agreement with this mean value as well as with the data compilation obtained for an intercomparison exercise (Gonfiantini et al., 2003) and with the worldwide accepted value for seawater.

Consequently, based on long-term measurements of seawater standards, it was estimated that the external reproducibility of the method was around ±0.4‰ (2σ).

4. Results

4.1. Stable isotopes of the water molecule: δD and $\delta^{18}O$

The equation of the Global Meteoric Water Line (GMWL) is $\delta D = 8 \times \delta^{18}O + 10$ (Craig, 1961). The arithmetic (unweighted) means of isotopic ratios in precipitation from 410 stations (IAEA network, data from 1961 to 2000) are described by the following equation: $\delta D = 8.07\ (\pm 0.02) \times \delta^{18}O + 9.9\ (\pm 0.1)$, $R^2 = 0.98$ (Gourcy et al., 2005). Long-term means weighted by the amount of precipitation were calculated only for the year for which more than 70% of the rainfall was analysed and at least 1 a of observation was available, the relationship becomes: $\delta D_{weighted} = 8.14\ (\pm 0.02) \times \delta^{18}O + 10.9\ (\pm 0.2)$, $R^2 = 0.98$ (Gourcy et al., 2005). When all the available data from the five French monitoring stations are plotted in a $\delta^{18}O$ vs. δD diagram (Fig. 2a), the following equation can be calculated: $\delta D = 7.727\ (\pm 0.066) \times \delta^{18}O + 7.033\ (\pm 0.451)$, $R^2 = 0.97$, $n = 411$. When only annual weighted mean values are used for each monitoring station (Fig. 2b), the equation becomes: $\delta D = 8.347\ (\pm 0.153) \times \delta^{18}O + 11.662\ (\pm 1.048)$, $R^2 = 0.99$, $n = 31$.

These global results are close to the Global Meteoric Water Line despite the variability that can be found at each French station. The weighted mean for each station integrates all the available data over the monitoring period (stars in Fig. 2b). The Avignon weighted mean for the period 1997–2002, $\delta^{18}O = -5.81‰$, is similar to the one calculated during the 1997–1998 period, i.e. $\delta^{18}O = -6.1‰$ (Celle et al., 2000). These weighted means are reported in Fig. 2b, in which all points plot very close to the GMWL, and highlight the continental effect (also called the distance-from-the-coast-effect) with progressive depletion in heavy isotopes from Brest (Atlantic coast) to Thonon via Orléans (Fig. 1). It is worth noting that the best fit regression lines of the annual weighted means of these three stations described a quasi-straight line very close to the GMWL (Fig. 2b), suggesting a genetic link for rainfall from the three stations.

In greater detail, the continental effect can be assessed between the Brest and Thonon samples (355 km apart) after removing the altitude effect for the Thonon station (at an altitude of 385 m). Blavoux (1978) calculated an altitudinal gradient of −0.3‰/100 m in this region (Chablais, pre-Alpes), leading to a continental effect of −3.2‰ $\delta^{18}O$/1000 km in an eastward direction from the French Atlantic Coast. This value is in good agreement with the assessment of Lécolle (1985) over the French territory. The continental effect varies considerably from place to place and from season to season (Ladouche et al., 2009), even over a low-relief profile. It is also strongly correlated with the temperature gradient and depends on both the topography and the climate regime.

Average annual $\delta^{18}O$ values vary from year to year (Fig. 2b). For the five French monitoring stations, the $\delta^{18}O$ values vary between 1‰ and 2‰ over the monitoring period, as was observed in Wallingford, UK (Darling and Talbot, 2003). This is typical of temperate climates where a large part of the spread is caused by variations in the average annual temperature (Gat et al., 2001). These variations from year to year show why it is difficult to assess the real signature of precipitation in a given place without long-term monitoring. This should be kept in mind when drawing a contour map of $\delta^{18}O$ for a vast territory for which only a few long-term monitoring data are available.

4.2. Contour map of the stable isotopic signature of oxygen ($\delta^{18}O$)

The world map developed by the IAEA from GNIP data (GNIP, 2007) is one of the few contour maps of the atmospheric signal that exist today. In France, a $\delta^{18}O$ contour map was drawn by Lécolle (1985), based on the O isotopic composition of the carbonate shell of landsnails, which have been shown to be directly linked to the annual mean $\delta^{18}O$ of rainwater. A second map, based on a few rainwater and groundwater measurements, was produced by Razafindrakoto (1988).

In the present work, the stations in Brest, Dax, Orléans, Avignon and Thonon (Fig. 1) were monitored monthly for the $\delta^{18}O$ and δD atmospheric signal. Rain samples from the BDISO databank are from studies dedicated to the knowledge and functioning of specific aquifers, often represent only a few months of monitoring, and are not for the same time periods. From all the available data, data points were selected with the following criteria: (1) there must be at least 1 a of monitoring; (2) isotopic data should be associated with the rainfall amount (if rainfall values are unavailable, data are weighted by those from the nearest meteorological station at the same altitude); (3) when two points are close, only the longest and more recent monitoring campaign is selected, as well as the lowest altitude point to minimize the altitude effect when drawing the map. Rain data from 44 points were selected (Fig. 3). Some regions are poorly documented and additional data were selected: 13 lakes, 12 groundwater bodies and one landsnail shell (see Section 2.1). In addition, and to better determine the isotopic signature at the French border, literature data or long-term rain monitoring data in the GNIP database for neighbouring countries were used (GNIP, 2007; Plata-Bedmar, 1994; Longinelli and Selmo, 2003; Longinelli et al., 2006; Darling and Talbot, 2003; Darling et al., 2003; Schurch et al., 2003).

The contour map of $\delta^{18}O$ values (Fig. 3) was drawn manually for the following reasons: (1) to take into account the altitude from the topographic digital terrain model (DTM) for a better interpolation, reflecting the altitude affect and (2) to give a greater weight to the most representative samples (length of the monitoring campaign, altitude, etc.) when large isotopic variations were observed at small scale. The attempts to automatically generate the map with dedicated software with kriging methods were rather inconclusive mainly because, as the data include the altitude effect, it was impossible to take into account the DTM in the interpolation without a risk of taking the altitude effect into account twice.

4.3. Lithium an boron concentrations in rainwaters

Major elements (cations and anions) and Li and B concentrations in rainwater samples collected in Brest, Dax, Orléans and Clermont-Ferrand are given in Table 1. When Cl concentrations are plotted as a function of Na concentrations (Fig. 4, Négrel et al., 2007), a good correlation is observed for the rainwater samples. The regression line between these two major elements is also shown in Fig. 4. A 95% confidence level is assigned to the data that falls between the two lines. The seawater dilution line is also shown in Fig. 4. Chloride concentrations show a very strong correlation with Na concentrations ($R^2 = 0.99$). All the samples lie near the seawater dilution line, indicating that both the Na and Cl in these samples come from sea salt. The Brest and the Dax rainwater

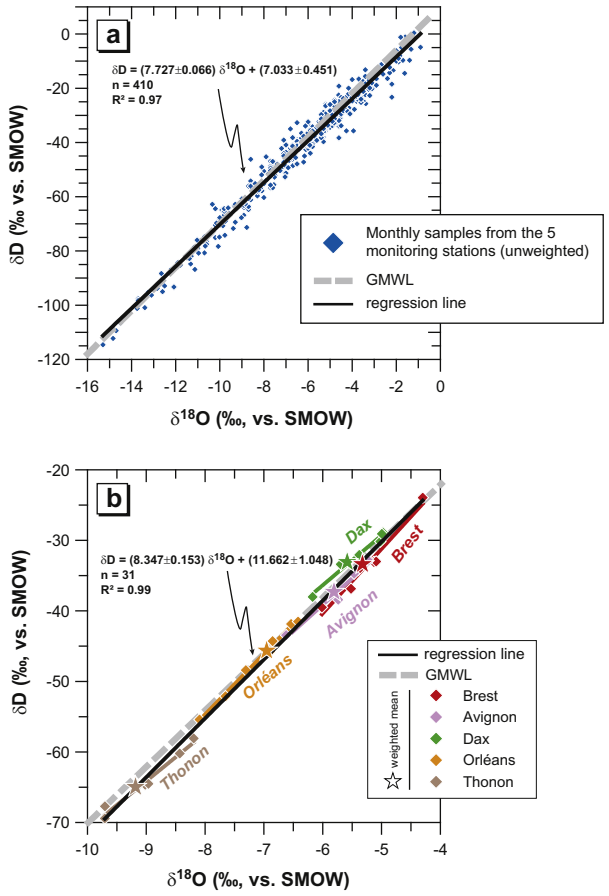

Fig. 2. (a) $\delta^{18}O$ vs. δD for all the monthly samples from the five long-term monitoring stations (Orléans, Brest, Dax, Thonon and Avignon). (b) Annual weighted means of the same five stations. The Global Meteoric Water Line is also drawn (GMWL, $\delta D = 8 \times \delta^{18}O + 10$). Stars correspond to the weight mean value at each station.

samples have the highest Na and Cl concentrations, whereas those collected near Clermont-Ferrand have the lowest concentrations in both Na and Cl.

Lithium and B concentrations in rainwater samples range from 0.004 to 0.292 μmol/L and from 0.029 to 6.184 μmol/L, respectively. This range of variation for Li concentrations is significantly lower than the only other value reported for rainwater (i.e. Li = 0.520 μmol/L, in Hawaii, Pistiner and Henderson, 2003). On the other hand, B concentrations reported here are in agreement with literature data, with some of the present values higher (Chetelat et al., 2005, 2009; Rose-Koga et al., 2006).

Lithium concentrations are more homogeneous than B concentrations from one sampling site to another (Table 1). The mean Li concentrations are quite similar, 0.058, 0.066, 0.053 and 0.057 μmol/L, for rainwaters collected at Brest, Dax, Orléans and near Clermont-Ferrand, respectively, whereas they are more heterogeneous for B, i.e. 0.66, 0.90, 1.51 and 0.20 μmol/L for rainwaters collected at Brest, Dax, Orléans and near Clermont-Ferrand, respectively.

4.4. Lithium and boron isotopes in rainwaters

Lithium and B isotope compositions are reported in Table 1 and Fig. 5. The most striking outcome of this study is that there is a very large range of variation (between +3.2‰ and +95.6‰) for δ^7Li in rainwaters. Mean δ^7Li values are +22.5‰, +22.8‰, +16.1‰ and +26.2‰ for samples collected in Brest, Dax, Orléans and near Clermont-Ferrand, respectively (Table 1). This range of variation is consistent with the only other value reported for rainwater (δ^7Li = +14.3‰, in Hawaii; Pistiner and Henderson, 2003). Furthermore, δ^7Li values in rainwaters are different from the δ^7Li signature of seawater (+31‰; Millot et al., 2004a).

$\delta^{11}B$ in rainwaters also shows a very wide range of variation, between −3.3‰ and +40.6‰. The mean $\delta^{11}B$ values are +37.4‰, +11.4‰, +8.4‰ and +23.2‰ for rainwaters collected in Brest, Dax, Orléans and near Clermont-Ferrand, respectively (Table 1). This is in agreement with literature data (Chetelat et al., 2005, 2009; Rose-Koga et al., 2006) and is different from the $\delta^{11}B$ signature of seawater (+39.5‰; see data compilation reported by Aggarwal et al. (2004)), except for Brest. Thus, the difference between rainwater values and the seawater signal for both Li and B isotopes should be highlighted.

In Fig. 5a and b, δ^7Li and $\delta^{11}B$ values are plotted as a function of Li and B concentrations, respectively. No general relationship is observed between δ^7Li and Li concentrations (Fig. 5a). Indeed, the range of δ^7Li variation is covered at both low and high Li concentrations (with the exception of the 3 ^7Li-rich samples from Clermont-Ferrand). On the other hand, there seems to be an inverse relationship between $\delta^{11}B$ and B concentrations (Fig. 5b): from high $\delta^{11}B$ values (close to the seawater signature, i.e. corresponding to rainwater samples from Brest, which is near the ocean) down to nearly −3‰ as B concentrations increase. This also means that high B concentrations in rainwaters are associated with low $\delta^{11}B$ values, especially for Orléans rainwater samples.

5. Discussion

5.1. Contour map of the stable isotopic signature of oxygen

The map of the meteoric $\delta^{18}O$ signal (Fig. 3) clearly shows the main causes of the variation in the isotopic signature of rainwater. The continental and altitude effects are clearly visible. It is also in good agreement with the map drawn by Lécolle (1985), with a high degree of precision, especially in the North. The new contour map still remains quite schematic because of the limited number of available data points and the complexity of the French topography. This is especially true in mountainous regions, where the density of data is too low and the relief too uneven to be able to draw reliable lines. $\delta^{18}O$ iso-value lines are, therefore, represented by dotted lines in the Pyrénées and the Alps.

The map also shows that the signature along the Atlantic coast is relatively homogeneous with a $\delta^{18}O$ value of around −5‰, despite the difference in latitude and the known climatic differences. The same phenomenon is observed on the Mediterranean coast of Italy (Longinelli and Selmo, 2003) and can be at least partially related to the contribution of seawater vapour to the coastal precipitation, with values characteristic of a first condensate of water vapour (Gat et al., 2001). While the isotopic signal on the Mediterranean coast is not significantly different from that on the Atlantic coast, the Mediterranean signature is more rapidly depleted in heavy isotopes on moving inland from the coast. This could be due to the presence of mountains close to the coast, which generate rainfall. Rainwater in and around Paris is less depleted in heavy isotopes than available data indicates for the surrounding area. This might be explained by a slightly higher temperature induced by the high population density and intensive industrial activity. Such a phenomenon has been described for Rome (Italy, Longinelli and Selmo, 2003). The Northern coast has a $\delta^{18}O$ signal, depleted in heavy isotopes compared to the Atlantic coast (−6.5‰ vs. −5.3‰ in Brest and −5.6‰ in Dax), which suggests that clouds that produce rainfall are already depleted in heavy isotopes. This phenom-

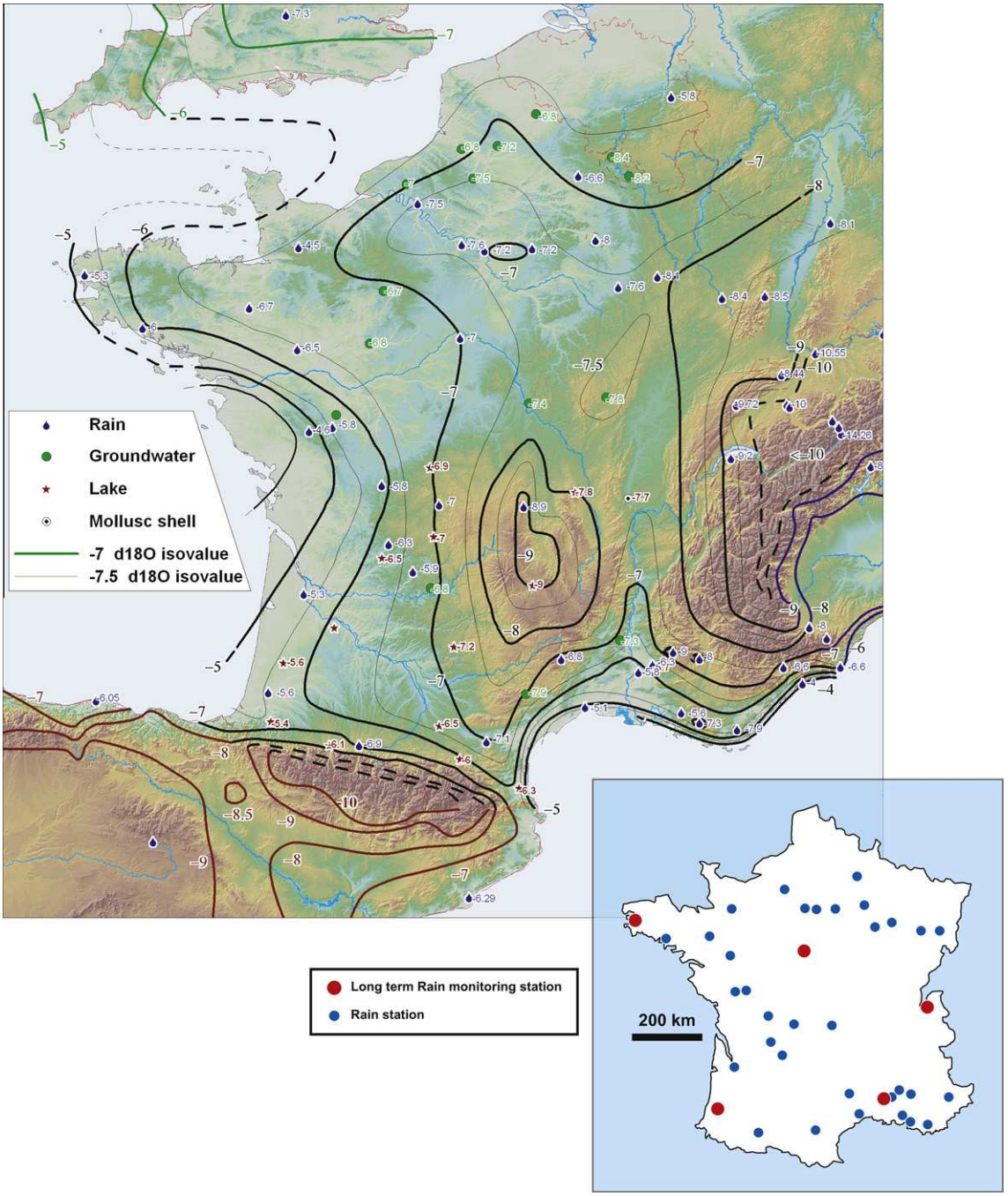

Fig. 3. Isovalue contour lines of the mean annual O isotopic composition ($\delta^{18}O$) of rainwater in France. This map is based on rainwater, groundwater, lake (corrected for evaporation) and landsnail shell data. Contour lines from Spain (Plata-Bedmar, 1994), Italy (Longinelli and Selmo, 2003; Longinelli et al., 2006) and United Kingdom (Darling and Talbot, 2003; Darling et al., 2003), together with Swiss data (Schurch et al., 2003) were also used to constrain lines at the French borders. The location of rainwater sampling stations for $\delta^{18}O$ vs. δD is also shown on this map (blue: short-term monitoring; red: long-term monitoring). (For interpretation of the references to colour in this figure legend, the reader is referred to the web version of this article.)

enon has been observed over the British Isles. The $\delta^{18}O$ contour lines are parallel on each side of the Chanel.

This map is the first one produced at the national scale based on most of the isotopic data available in France, and which takes into account data for neighbouring countries in order to better constrain the contour lines along the borders. It is, therefore, a unique tool for assessing the stable isotopic signature of aquifer recharge for O isotopes. Nevertheless, it is worth noting that the rainwater data used often integrate only 1 a of rainfall and it has been shown that the mean annual weighted $\delta^{18}O$ values vary from 1‰ to 2‰ due to variations in the average annual temperature typical of temperate climates. This map can, therefore, be a valuable addition to local rain monitoring when a specific aquifer is being studied.

In this paper, only the $\delta^{18}O$ signature for France is reported. However, δD can be determined using the global correlation between δD and $\delta^{18}O$ from the Global Meteoric Water Line since all the data considered plot, for the most part, along this line.

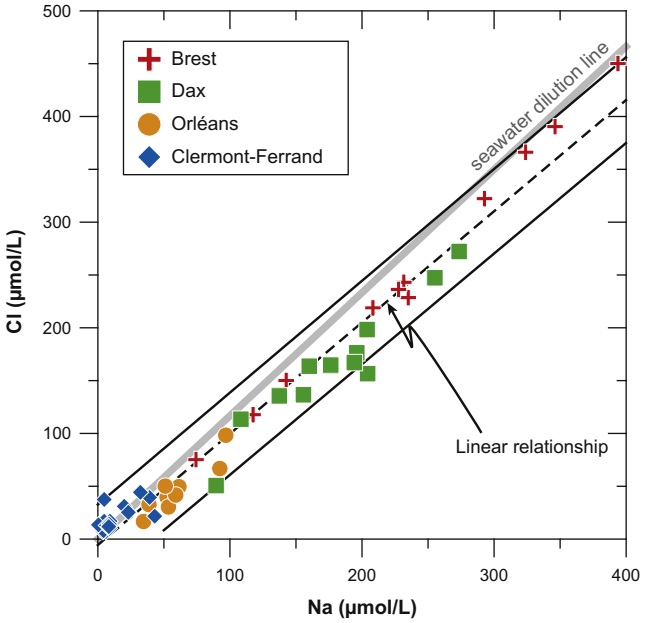

Fig. 4. Cl concentrations in rainwaters (µmol/L) plotted as a function of the Na concentrations in rainwaters (µmol/L). The seawater dilution line and the linear relationship between Cl and Na are shown. A 95% confidence level is assigned to the data that falls between the two lines (modified from Négrel et al. (2007)).

5.2. Lithium and boron isotopes variations

5.2.1. Seasonal and spatio-temporal variations

Monitoring rainwater samples over a period of 1 a at different locations allows studying seasonal effects on the range of variation for both Li and B isotopes.

On the one hand, the rainfall amount seems to have no effect on δ^7Li variations (Table 1). The total range of variation for δ^7Li values seems to be independent of the rainfall amount, and this is especially true for Orléans, Brest and Dax. In contrast, for Brest and Dax samples (sampling points on or near the coast), the rainfall amount does seem to control δ^{11}B variations to some extent. When the rainfall amount increases, the δ^{11}B values increase for the Brest samples but decrease for the Dax samples. It is very likely that when the rainfall amount is high, there is a large contribution of salts derived from seawater. This is especially true for the Brest rainwater samples (sampling point less than 5 km from the Atlantic Ocean). However, the distribution of δ^{11}B in rainwater samples from Dax (30 km inland) is more complex and will be discussed in the next section. In contrast, rainwater samples from inland sampling points (Orléans and Clermont-Ferrand) do not show any correlation of δ^{11}B values with the rainfall amount.

On the other hand, the month does not appear to have any direct effect on δ^7Li values (Table 1). However, ^{7}Li-rich values for Clermont-Ferrand rainwater are observed during the winter and spring seasons (December, February and April). Also, there appears to be no correlation between δ^{11}B values and the month. The range of variation for δ^{11}B is controlled, mainly, by the location (inland vs. coastal) of the sampling point.

5.2.2. Wind direction and air mass origin

Lithium concentrations and δ^7Li values were plotted as a function of the wind direction (Fig. 6). The wind direction does not control Li content in Brest and Clermont-Ferrand rainwater samples (Fig. 6b and h). For Dax and Orléans sampling sites, however, there is a relationship between Li concentration and wind direction (Fig. 6d and f). The Li concentration is controlled by the origin of the air masses for these rainwater samples, with higher Li concentrations in rainwater coming from the ocean (wind direction around 270°, i.e. W). With regard to δ^7Li values, no effect is observed, here again, for Brest rainwaters (Fig. 6a), which means that most of the rainwater at this site is homogeneous for both Li and its isotopes, even though the wind direction can range significantly (from 50° to 240°, i.e., NE to WSW). For Dax and Orléans samples, the opposite phenomena are observed concerning Li isotopes. When the air masses have a Western origin (oceanic input), δ^7Li values tend to increase slightly for Dax rainwaters but decrease slightly for Orléans rainwaters (Fig. 6c and e). The most striking observation concerns Clermont-Ferrand rainwaters, for which δ^7Li values display two interesting trends as a function of the wind direction (Fig. 6g). In winter and spring samples, there is a general positive trend between δ^7Li and wind direction. However, autumn and summer samples show no change in the δ^7Li signature when the wind direction is between 120° and 300° (SE–NW). This means that the ^{7}Li-rich rainwaters are characterized by air masses coming from the SSW of the sampling site during the winter and spring.

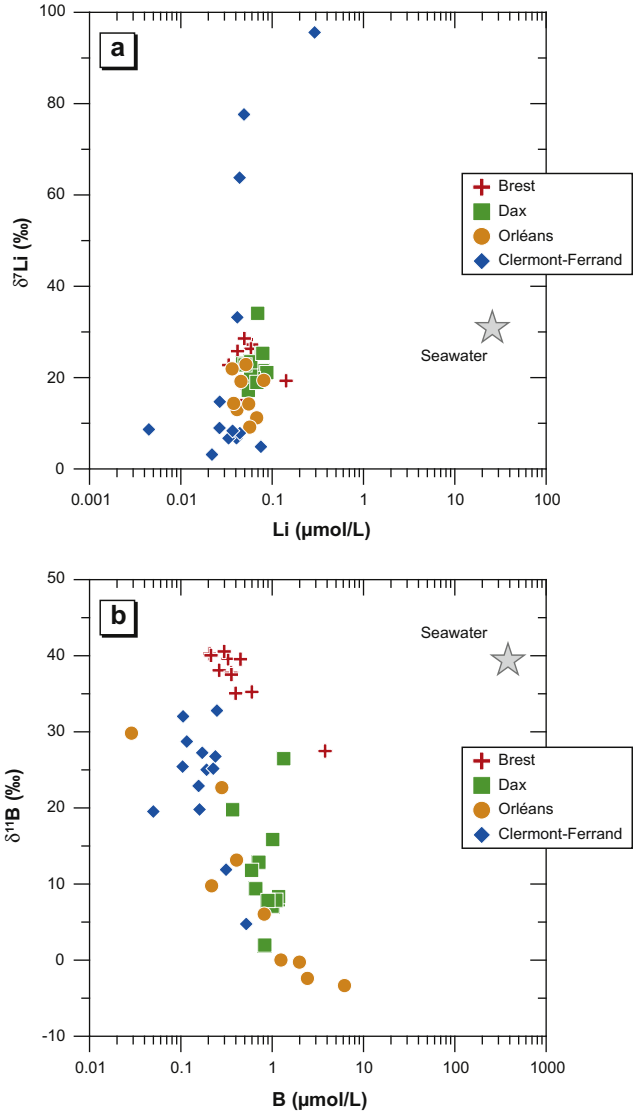

Fig. 5. (a and b) δ^7Li and δ^{11}B (‰) values plotted as a function of Li and B concentrations (µmol/L, log scale), respectively, in rainwaters and seawater.

Boron concentrations and δ^{11}B values were plotted as a function of the wind direction (Fig. 7). Boron concentrations in Brest and Clermont-Ferrand rainwaters are not controlled primarily by the

wind direction (Fig. 7b and h, respectively). However, for Dax and Orléans rainwaters, B concentrations increase when the wind comes from West of the sampling site (marine origin, Fig. 7d and f). $\delta^{11}B$ values in rainwater in Orléans decrease slightly when the wind direction ranges from 180° (S) to 270° (W) (Fig. 7e).

There is no evidence that $\delta^{11}B$ values in Brest and Clermont-Ferrand rainwaters are controlled by the wind direction (Fig. 7a and g), whereas $\delta^{11}B$ values in Dax rainwaters increase when the wind direction ranges from 210° (SW) to 270° (W) (Fig. 7c). It is known that, in this area, rainfall comes not only from the Atlantic Ocean to the West, but also from the Pyrénées Mountains to the South. Therefore, it can be assumed that for the Dax rainwater samples: (i) during the summer and winter (low rainfall), $\delta^{11}B$ is controlled mainly by the sea salt contribution coming from the Atlantic Ocean, whereas (ii) during spring and autumn when rainfall is heavier, $\delta^{11}B$ might also be controlled by rain coming from the mountains that has been in contact with local dust (i.e. silicate, carbonate and/or evaporite particulates from the Pyrénées), lowering $\delta^{11}B$ values. In addition, as Négrel et al. (2007) have observed for Sr isotopes at the same sampling site, biogenic sources might also contribute to the $\delta^{11}B$ signature of the Dax samples, also lowering the $\delta^{11}B$ values. Indeed, Dax is located in a huge maritime pine forest (*Pinus pinaster*) that covers 860,000 ha, the trees growing in sand containing chlorite, micas, feldspars and quartz (Righi and De Connick, 1977).

The origin of the air masses is, therefore, an important factor that can control the dissolved concentration of Li and B for the Dax and Orléans sampling sites, but seems to have no effect on Clermont-Ferrand and Brest rainwaters. This is probably due to the homogeneity of the rainfall for the Brest sampling site. On the other hand, for Dax, rainwater could have two main origins – the SSW (with lower $\delta^{7}Li$ and $\delta^{11}B$ values) or the W (with higher $\delta^{7}Li$ and $\delta^{11}B$ values), which reflects the contribution of marine sea salts. For Clermont-Ferrand, the wind direction has no significant effect on either Li or B concentrations, whereas it has been seen that the ^{7}Li-rich rainwaters are characterized by air masses coming from the SSW of the sampling site during the winter and spring.

The spatial range of variation for Li and B isotopes could then be studied because rainwater samples have been monitored at different locations in France (coastal and inland). The rainwaters sampled at Brest, near the sea, have both $\delta^{7}Li$ and $\delta^{11}B$ values close to the seawater signature (Figs. 5 and 8), whereas those sampled at Dax, Orléans and Clermont-Ferrand have a very broad range of variation for both $\delta^{7}Li$ and $\delta^{11}B$ values – from crustal values (i.e. from −2‰ to +2‰ and from −5‰ to +10‰, respectively, for $\delta^{7}Li$ and $\delta^{11}B$, Teng et al., 2004; Tomascak, 2004; Barth, 1993, 2000; Millot et al., 2007) up to the $\delta^{7}Li$ and $\delta^{11}B$ signatures of seawater (+31.0‰ and +39.5‰, respectively, for $\delta^{7}Li$ and $\delta^{11}B$). However, higher $\delta^{7}Li$ values were measured in some rainwater samples collected near Clermont-Ferrand. Therefore, the origins of Li and B in rainwaters, and the associated isotope signatures, that might explain the observed range of variation for both Li and B isotope systematics are discussed below.

5.3. Origin of lithium and boron in rainwaters

Seawater (by contributing sea salts) might be one of the major suppliers of atmospheric Li and B, but other sources must also to be taken into account. Therefore, the contribution of sea salts to Li and B in rainwater samples were determined.

Sodium concentrations in rainwater samples can be used to estimate the sea salt contribution of other ions because Na is the best tracer of sea salt input in rainwater (Keene et al., 1986; Négrel and Roy, 1998; Basak and Alagha, 2004; Rastogi and Sarin, 2005). Distinguishing between the sea salt (ss) and non-sea salt (nss) component contributions in rainwater (rw) is essential if it is wished to characterize the chemistry of precipitation (Négrel and Roy, 1998; Schmitt and Stille, 2005; Al-Khashman, 2005; Rastogi and Sarin, 2005; Négrel et al., 2007).

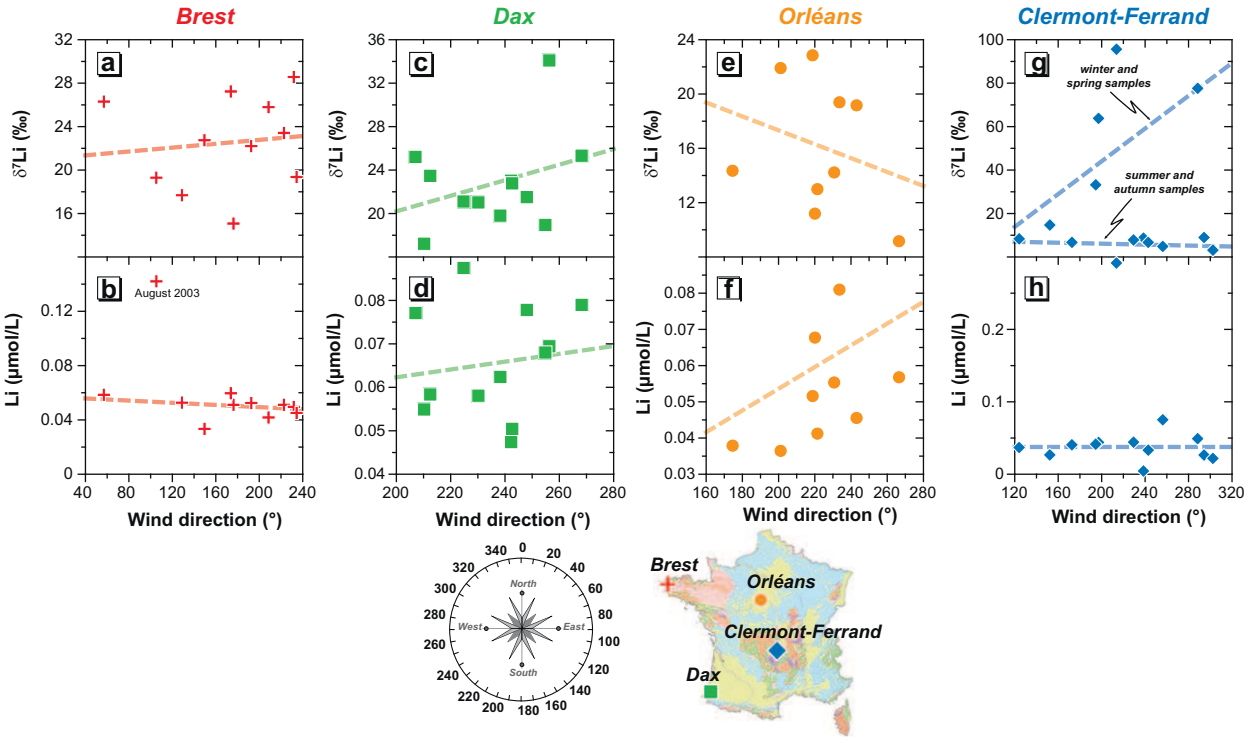

Fig. 6. $\delta^{7}Li$ (‰) values and Li concentrations (µmol/L) plotted as a function of wind direction for each sampling site. Bold and dashed lines represent parameter trends as a function of wind direction. These lines correspond to general trends observed rather than calculated regression.

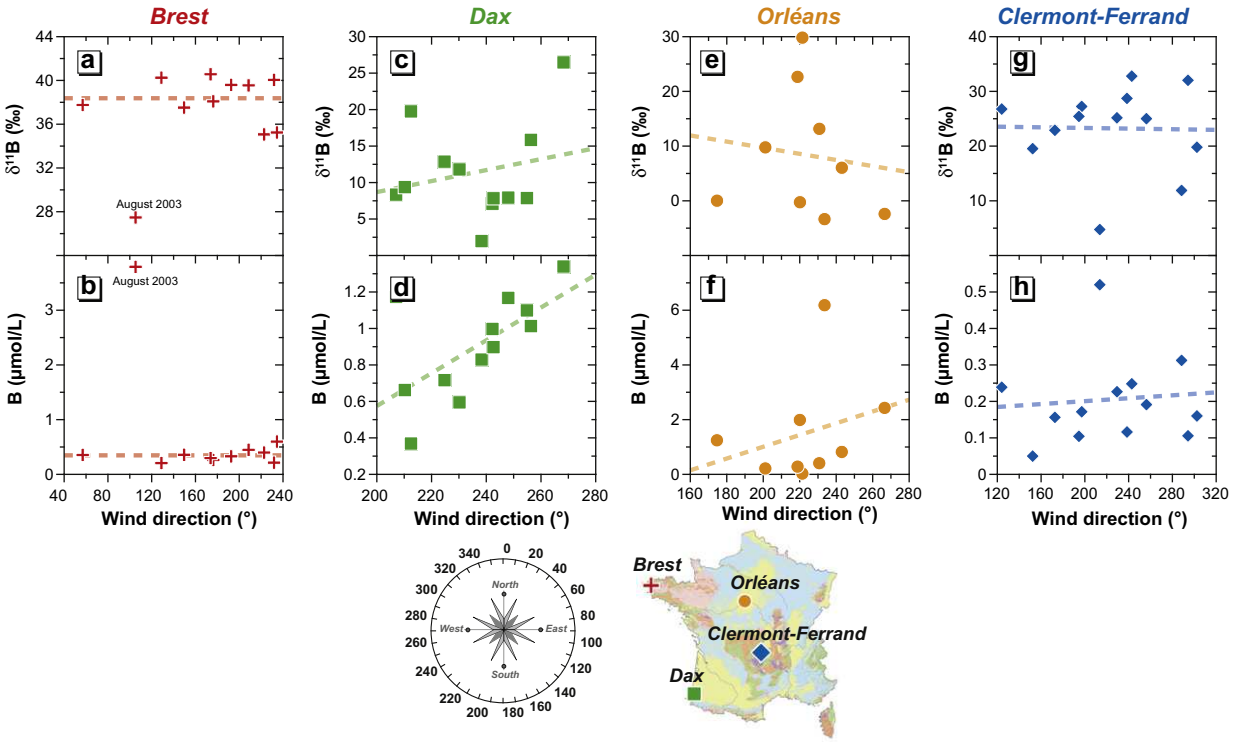

Fig. 7. $\delta^{11}B$ (‰) values and B concentrations (µmol/L) plotted as a function of wind direction for each sampling site. Bold and dashed lines represent parameter trends as a function of wind direction. These lines correspond to general trends observed rather than calculated regression.

To calculate the contribution of Li and B (X in Eq. (1)) in the sea salt component (ss) with seawater (sw) characteristics, the following equation is used:

$$X_{ss} = Na_{rw} \times \left(\frac{X}{Na}\right)_{sw} \quad (1)$$

Sodium is used as a marine tracer in rainwater (see Négrel and Roy (1998) and references therein). The contribution of the non-sea salt component (nss) is the difference between the total composition of rainwater (rw) and the sea salt (ss) contribution:

$$X_{nss} = X_{rw} - X_{ss} \quad (2)$$

This equation enables the determination of the contribution of sea salts to Li and B in rainwaters (Table 1 and Fig. 9). Results show that the contribution of sea salt for B in rainwaters is greater than that for Li. Indeed, considering average values for the four different sampling sites, it can be seen that the marine contribution (sea salt) to B in rainwaters is twice that to Li (22.3% and 12.0%, respectively, Fig. 9). The distance-from-the-coast-effect (inland vs. coastal location) is the key parameter controlling the marine contribution of both Li and B to rainwater concentrations. Samples collected inland (Orléans and Clermont-Ferrand) show the lowest sea salt contributions. Rainwaters from Dax have intermediate values (Fig. 9), whereas rainwaters collected at Brest have the highest contributions of marine sea salt to Li and B concentrations (25% and 49.8% on average, respectively, for Li and B).

Although these results are not surprising, they show that although seawater does, indeed, supply dissolved atmospheric Li and B, non-sea-salt sources represent the major source of Li and B in rainwaters.

5.4. Lithium isotopes in rainwaters

The fact that most dissolved Li in rainwaters does not have a marine origin is in agreement with the range observed in δ^7Li in the samples (+3.2‰ and +95.6‰) compared to the marine signature of Li isotopes (~+31‰).

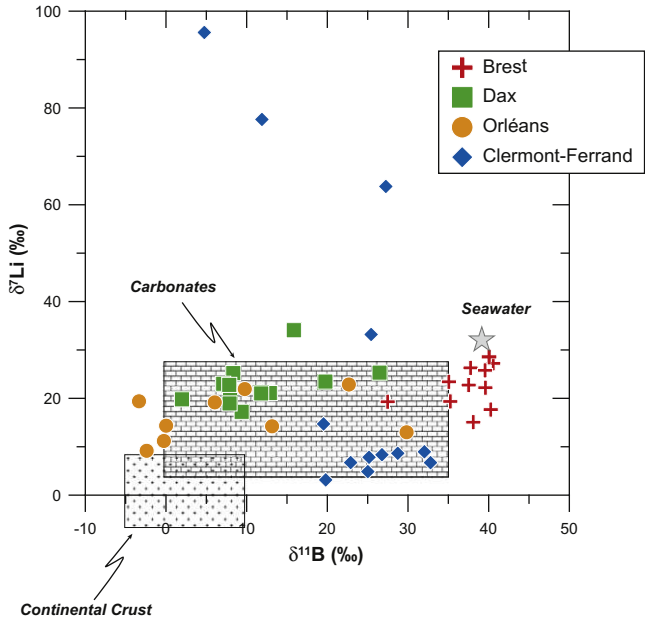

Fig. 8. δ^7Li (‰) plotted as a function of δ^{11}B (‰) in rainwater samples. See text for comments.

δ^7Li values in rainwater samples were plotted as a function of Li derived from sea salt (Fig. 9a) in an attempt to identify the different sources contributing to the rainwater Li isotope signature. For rainwater sampled at a coastal location (Brest), the marine contribution is relatively great (9–45%), but another source or other sources is/are needed in order to explain the range of variation in

these δ^7Li values (+15.1‰ to +28.6‰). The same is observed for rainwaters collected at Dax and Orléans, but at these locations the non-sea-salt contribution should be even greater since these sites are located inland (especially Orléans) and show lower marine contributions (Table 1). The dissolution of either Li-bearing minerals or anthropogenic inputs might explain lower δ^7Li values compared to the seawater signature (~+31‰).

Continental rocks have δ^7Li values ranging from −4‰ to +8‰ (Teng et al. (2004), Millot et al. (2010) and references therein) and might contribute to rainwater signatures by interaction in the atmosphere between continental particles and water molecules. In addition, most carbonates analysed to date show δ^7Li values between +6‰ and >25‰ (e.g. Hoefs and Sywall, 1997; Hall et al., 2005; Hathorne and James, 2006; Vigier et al., 2007) and could also be cited as sources. It is, however, more likely that multiple sources exist for the crustal component on the scale of France.

The three rainwater samples from Clermont-Ferrand having a ^{7}Li-rich signature (δ^7Li values of +63.8‰, +77.6‰ and +95.6‰) are, however, notable because they have significantly heavier Li isotopic compositions than seawater. Négrel and Roy (1998) and Roy and Négrel (2001) have shown that rainwater in this area is likely to record an anthropogenic input due to agricultural activities (e.g. fertilizer application). These high δ^7Li values might, therefore, be explained by the contribution of a local input derived from fertilizers and/or soil amendments used by farmers in this area. This is also in good agreement with recent results of Négrel et al. (2009, 2010) regarding the Li isotopic characterization of a peat bog located near the sampling site. In that study, the ^{7}Li-rich contribution to surface waters is explained by the dissolution of fertilizers and soil amendments having δ^7Li values higher than +215‰ (Négrel et al., 2009, 2010). This heavy Li component is attributed to synthetic Li added to fertilizers and soil amendments, derived from a ^{7}Li-rich reagent, as was reported by Qi et al. (1997). In addition, it has been shown (Section 5.2.2) that these ^{7}Li-rich rainwaters are characterized by air masses coming from the SSW of the sampling site during the winter and spring, which is when soils are fertilized and amended.

When Li isotopes are plotted as a function of the Na/Li molar ratio (Fig. 10), it is observed that samples from Clermont-Ferrand seem to indicate a mixing of a crustal component (granite and/or carbonate) and an anthropogenic component (^{7}Li-rich end-member), whereas samples from Brest, Dax and Orléans seem to indicate a mixing of a crustal component (complex due to the relative contribution of different particles derived from carbonate or granite) and a marine end-member.

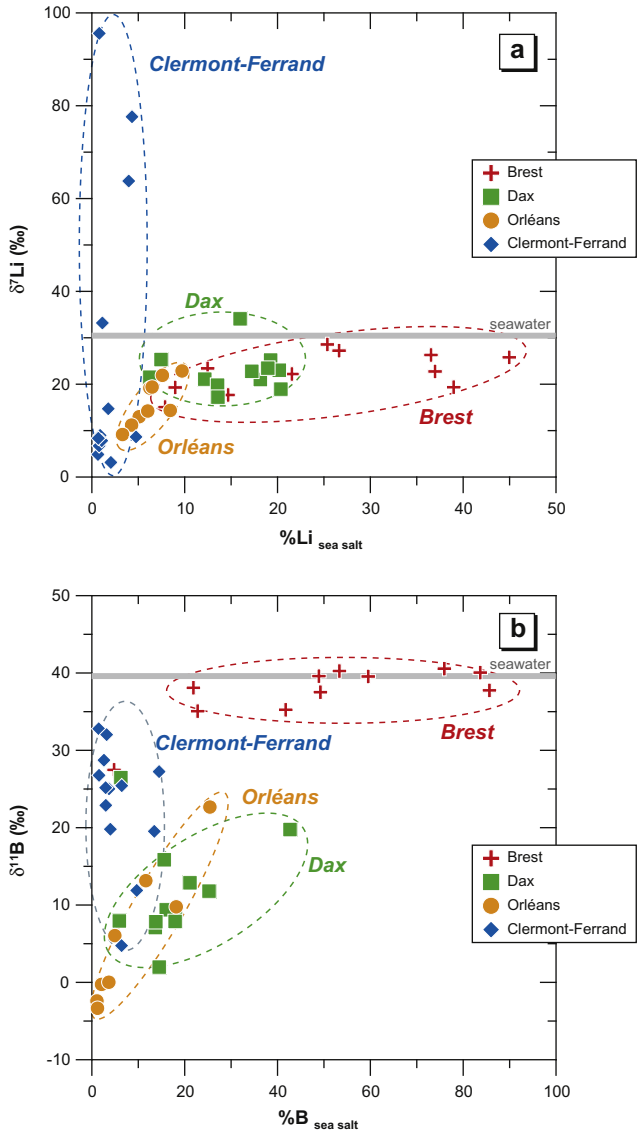

Fig. 9. (a and b) Li and B isotopic compositions plotted as a function of Li and B contribution of marine sea salts in rainwater samples, respectively.

5.5. Boron isotopes in rainwaters

As stated above, most of the dissolved B in rainwater is not of marine origin (for rainwater samples collected at inland locations in Orléans and Clermont-Ferrand, in particular). This is in agreement with the range observed in δ^{11}B values in the samples (−3.3‰ to +40.6‰) compared to the marine signature of B isotopes (+39.5‰, Aggarwal et al. (2004) and data therein).

The δ^{11}B values in rainwater samples have been plotted as a function of B derived from sea salt (Fig. 9b). Seawater seems, nevertheless, to be a major supplier of rainwater B in Brest, near the ocean. However, the rainwater sample collected at Brest in August 2003 is notable (the lowest δ^{11}B value: +27.5‰). It was collected at a time when France and Western Europe were having an exceptionally severe heat wave with record temperatures and little rainfall (Luterbacher et al., 2004; Chase et al., 2006), and it is very likely that this sample is not representative.

With reference to the Dax, Orléans and Clermont-Ferrand rainwater samples, another source/other sources is/are needed in order to explain the range of variation in δ^{11}B values. As for Li, the dissolution of either B-bearing minerals or anthropogenic inputs might explain δ^{11}B values lower than the seawater signature (+39.5‰). A crustal component probably contributes to rainwater signatures by the interaction in the atmosphere of continental particles and water molecules. Boron isotopic compositions for the main crustal lithologies have been well identified, with δ^{11}B values ranging from −5‰ to +10‰, +15‰ to +30‰ and 0‰ to +35‰, for granite/gneiss, marine evaporite and carbonate, respectively (Barth, 1993, 2000). This crustal component is expected to contribute to the B isotopic rainwater signature, although the crustal component is probably made up of a combination of several sources (different particles coming from different lithologies).

Plotting B isotopic compositions as a function of NO_3/B molar ratios (NO_3 being a good tracer of fertilizer) provides additional and important information (Fig. 11). Samples from Dax, for which a possible biogenic input has already been suggested, are in agreement with field data reported by Chetelat et al. (2005) for the biomass-derived end-member (this is also true for most samples from Orléans, located near a large forested area, "La Sologne", an area covering 500,000 ha). In addition, the B values in rainwaters from this study are little affected by anthropogenic emissions

compared to those of rainwater sampled in Paris that have an urban aerosol component (Chetelat et al., 2009). Most rainwater samples from Clermont-Ferrand (for which a possible fertilizer input has been cited, based on Li isotope data) also reveal a mixing trend toward a fertilizer end-member (Fig. 11) based on B isotope tracing.

6. Conclusions and perspectives

In the present work, the first results have been reported for both Li and B isotope ratios in rainwater samples collected over a long time period (i.e. monthly rainfall events over 1 a) at a national scale (from coastal and inland locations). In addition, the stable isotopes of the water molecule (δD and $\delta^{18}O$) have also been reported here for the same locations. This work has made it possible to better characterize Li, B, H and O isotopes in rainwaters. The main results of this study are:

- A contour map of France for $\delta^{18}O$ was drawn after compiling data that included more than 400 values from all of France. This map could be used as a reference for future studies concerning the recharge $\delta^{18}O$ signature in surface water and groundwater body characterization. It represents a unique tool for assessing the stable isotopic signature of the recharge of aquifers for O isotopes.
- Li and B concentrations and $\delta^{7}Li$ and $\delta^{11}B$ signatures in rainwater samples collected over 1 a at four stations (Brest, Dax, Orléans and Clermont-Ferrand) varied greatly over the sampling period. Lithium and B concentrations are low and comprised between 0.004 and 0.292 μmol/L and 0.029 and 6.184 μmol/L, respectively. $\delta^{7}Li$ and $\delta^{11}B$ values in rainwaters also vary greatly between +3.2‰ and +95.6‰ and −3.3‰ and +40.6‰ over a period of 1 a, respectively.
- The seasonal effect (i.e. the month or rainfall amount) is not the main controlling factor for the Li and B isotopic variations. However, the continental effect (distance from the coast) is a key parameter, determining the origin of both Li and B derived from marine sea salts. In addition, the origin of air masses (wind direction) is also a key parameter that controls the contribution of sea salts derived from the Ocean.
- The most striking outcome of this study is that most Li and B in rainwaters does not have a marine origin. Seawater is not the major supplier of atmospheric Li and B and a non-sea-salt source, such as a crustal component and/or an anthropogenic contribution, should also be taken into account when Li and B isotopes are studied in hydrogeochemistry as an input to surface waters and a recharge to groundwater bodies. This may be important in the understanding of dissolved Li and B distributions in ground- and formation waters, and should be taken into account in future studies.
- The fact that most of dissolved Li and B in rainwaters does not have a marine origin could be of importance in hydrogeochemical studies of surface water and groundwater bodies because rainwater is an input for the former and a recharge for the latter. The non-sea-salt signature for Li and B isotopes should, therefore, be taken into consideration for future studies in the investigation of their isotope systematics in surface and groundwater.

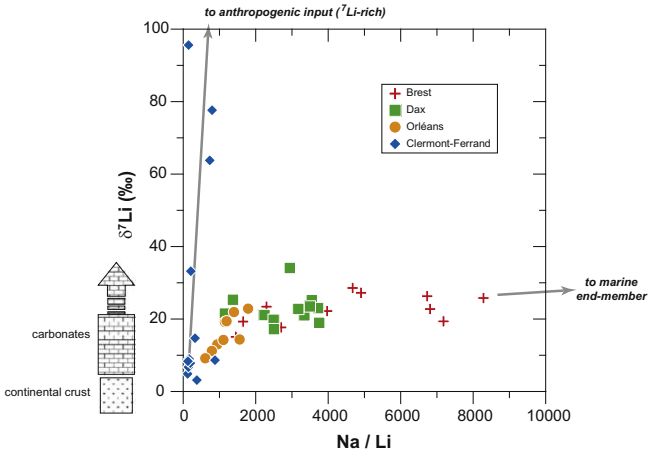

Fig. 10. $\delta^{7}Li$ (‰) plotted as a function of the Na/Li molar ratio. See text for comments.

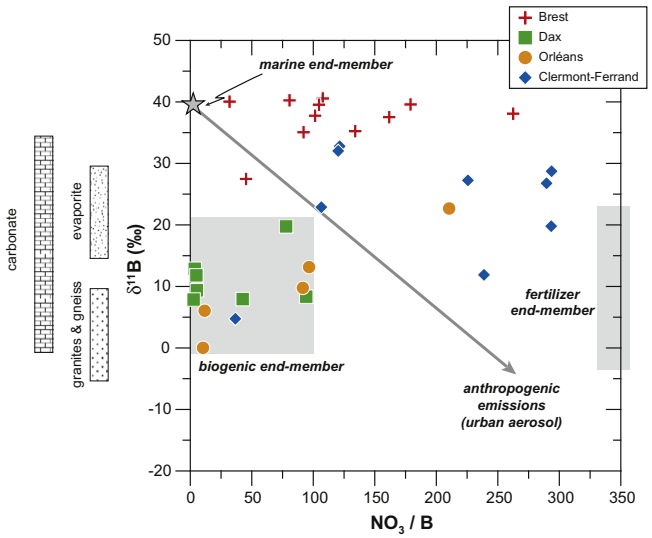

Fig. 11. $\delta^{11}B$ (‰) plotted as a function of NO_3/B molar ratios. The anthropogenic end-member (urban aerosols) is from Chetelat et al. (2009), the biomass-derived end-member is from Chetelat et al. (2005) and the fertilizer end-member is from Widory (pers. comm.).

To summarize, this study provides a framework for isotopic investigations of surface and groundwaters and is the first comprehensive study of Li and B isotopes in rainwaters. This framework could be used in future studies to illustrate how these data for rainwaters samples can add to the global understanding of geochemical processes in hydrology.

Finally, this work also adds to the potential for use of Li and B isotopes as environmental tracers.

Acknowledgements

This work was funded by the Research Division of the BRGM. The authors thank all the people who have contributed to the French Isotopic Data Base (BDISO) through their technical assistance, sampling and isotopic measurements: University of Paris-Sud (Orsay), University of Avignon, Centre de Recherches Géodynamiques (Thonon-les-Bains), CEA (Saclay) and BRGM in Orléans. BDISO aims at gathering isotopic data (mainly $\delta^{18}O$, δD, ^{3}H, ^{14}C, $\delta^{13}C$, $^{87}Sr/^{86}Sr$, $\delta^{11}B$ and $\delta^{15}N$) on French groundwater, surface water and rainwater. We thank J. Garnier for compiling most of the $\delta^{18}O$ and δD data and drawing the first version of the $\delta^{18}O$ contour map presented here. We thank Météo France (Direction de la Production) for providing the wind direction and rainfall data. This work benefited from the collaboration of BRGM's chemistry laboratories for major and trace element analyses: J.P. Ghestem, T. Conte

and C. Crouzet are thanked for their help, as well as C. Fléhoc for stable isotope measurements (δD and $\delta^{18}O$). We also would like to thank M. Robert for her help in the Neptune laboratory. We thank three anonymous reviewers for providing critical comments that improved this manuscript. L. Aquilina is also thanked for editorial handling and constructive comments. This is BRGM Contribution No. 6712.

References

Aggarwal, J.K., Mezger, K., Pernicka, E., Meixner, A., 2004. The effect of instrumental mass bias on $\delta^{11}B$ measurements: a comparison between thermal ionisation mass spectrometry and multiple-collector ICP-MS. Int. J. Mass Spectrom. 232, 259–263.

Al-Khashman, O.A., 2005. Ionic composition of wet precipitation in the Petra Region, Jordan. Atmos. Res. 78, 1–12.

Barth, S.R., 1993. Boron isotope variations in nature: a synthesis. Geol. Rundsch 82, 640–641.

Barth, S.R., 2000. Geochemical and boron, oxygen and hydrogen isotopic constraints on the origin of salinity in groundwaters from the crystalline basement of the Alpine Foreland. Appl. Geochem. 15, 937–952.

Basak, B., Alagha, O., 2004. The chemical composition of rainwater over Büyükçekmece Lake, Istanbul. Atmos. Res. 71, 275–288.

BDISO, 2007. French Isotopic Data Base on groundwater, surface water and rainwater. <http://infoterre.brgm.fr/eSIG/index.jsp>.

Berner, E.K., Berner, R.A., 1987. The Global Water Cycle. Geochemistry and Environment. Prentice Hall.

Blavoux, B., 1978. Etude du cycle de l'eau au moyen de l'oxygène 18 et du Tritium. Possibilités et limites de la méthode des isotopes en milieu en hydrologie de la zone tempérée. Thèse d'Etat, Univ. Paris VI, France.

Catanzaro, E.J., Champion, C.E., Garner, E.L., Marinenko, G., Sappenfield, K.M., Shields, W.R., 1970. Standard Reference Materials: Boric Acid; Isotopic and Assay Standard Reference Materials. US National Bureau of Standards, Special Publication 260-17.

Celle, H., Daniel, M., Mudry, J., Blavoux, B., 2000. Signal pluie et traçage par les isotopes stables en Méditerranée occidentale. Exemple de la région avignonnaise (Sud-Est de la France). C.R. Acad. Sci. Paris 331, 647–650.

Celle-Jeanton, H., Travi, Y., Blavoux, B., 2001. Isotopic typology of the precipitation in the Western Mediterranean region at three different time scales. Geophys. Res. Lett. 28, 1215–1218.

Chase, T.N., Wolter, K., Pielke, R.A., Rasool, I., 2006. Was the 2003 summer European heat wave unusual in a global context? Geophys. Res. Lett. 33, L23709.

Chetelat, B., Gaillardet, J., Freydier, R., Négrel, Ph., 2005. Boron isotopes in precipitation: experimental constraints and field evidence from French Guiana. Earth Planet. Sci. Lett. 235, 16–30.

Chetelat, B., Gaillardet, J., Freydier, R., 2009. Use of B isotopes as a tracer of anthropogenic emissions in the atmosphere of Paris, France. Appl. Geochem. 24, 810–820.

Coplen, T.B., Hopple, J.A., Böhlke, J.K., Peiser, H.S., Rieder, S.E., Krouse, H.R., Rosman, K.J.R., Ding, T., Vocke Jr., R.D., Révész, K.M., Lamberty, A., Taylor, P., De Bièvre, P., 2002. Compilation of minimum and maximum isotope ratios of selected elements in naturally occurring terrestrial materials and reagents. US Geol. Surv. Water-Resour. Invest. Rep. 01-4222.

Craig, H., 1961. Isotopic variations in meteoric waters. Science 133, 1702–1703.

Darling, W.G., Talbot, J.C., 2003. The O and H stable isotopic composition of fresh waters in the British Isles. 1. Rainfall. Hydrol. Earth Syst. Sci. 7, 163–181.

Darling, W.G., Bath, A.H., Talbot, J.C., 2003. The O and H stable isotopic composition of fresh waters in the British Isles. 2. Surface waters and groundwater. Hydrol. Earth Syst. Sci. 7, 183–195.

Flesch, G.D., Anderson, A.R., Svec, H.J., 1973. A secondary isotopic standard for $^6Li/^7Li$ determinations. Int. J. Mass Spectrom. Ion Phys. 12, 265–272.

Gat, J.R., Mook, W.G., Meijer, H.A.J., 2001. Volume II: atmospheric water. In: Mook, W.G. (Ed.), Environmental Isotopes in the Hydrological Cycle. Principles and Applications. IHP-V Technical Documents in Hydrology, No. 39. UNESCO-IAEA.

GNIP, 2007. Global Network of Isotopes in Precipitation. <http://isohis.iaea.org/>.

Gonfiantini, R., Tonarini, S., Gröning, M., Adorni-Braccesi, A., Al-Ammar, A.S., Astner, M., Bächler, S., Barnes, R.M., Bassett, R.L., Cocherie, A., Deyhle, A., Dini, A., Ferrara, G., Gaillardet, J., Grimm, J., Guerrot, C., Krähenbühl, U., Layne, G., Lemarchand, D., Meixner, A., Northington, D.J., Pennisi, M., Reitznerová, E., Rodushkin, I., Sugiura, N., Surberg, R., Tonn, S., Wiedenbeck, M., Wunderli, S., Xiao, Y., Zack, T., 2003. Intercomparison of boron isotope and concentration measurements. Part II: evaluation of results. Geostand. News: J. Geostand. Geoanal. 27, 41–57.

Gourcy, L., Groening, M., Aggarwal, P.K., 2005. Stable oxygen and hydrogen isotopes in precipitation. In: Aggarwal, P.K., Gat, J.R., Froehlich, K.F.O. (Eds.), Isotopes in the Water Cycle: Past, Present and Future of the Developing Science, pp. 39–51.

Guerrot, C., Millot, R., Robert, M., Négrel, Ph., 2010. Accurate and high-precision determination of boron isotopic ratio by MC-ICP-MS Neptune. Geostand. Geoanal. Res. 34, 1–10.

Hall, J.M., Chan, L.H., McDonough, W.F., Turekian, K.K., 2005. Determination of the lithium isotopic composition of planktic foraminifera and its application as a paleo-seawater proxy. Marine Geol. 217, 255–265.

Hathorne, E.C., James, R.H., 2006. Temporal record of lithium in seawater: a tracer for silicate weathering? Earth Planet. Sci. Lett. 246, 393–406.

Hoefs, J., Sywall, M., 1997. Lithium isotope composition of quaternary biogene carbonates and a global lithium isotope balance. Geochim. Cosmochim. Acta 61, 2679–2690.

James, R.H., Palmer, M.R., 2000. The lithium isotope composition of international rock standards. Chem. Geol. 166, 319–326.

Junge, C.E., 1963. Air Chemistry and Radioactivity. Academic Press, New York.

Keene, W.C., Pszenny, A.A.P., Galloway, J., Hawley, M.E., 1986. Sea-salt corrections and interpretation of constituent ratios in marine precipitation. J. Geophys. Res. 91, 6647–6658.

Ladouche, B., Aquilina, L., Dörfliger, N., 2009. Chemical and isotopic investigation of rainwater in Southern France (1996–2002): potential use as input signal for karst functioning investigation. J. Hydrol. 367, 150–164.

Lécolle, P., 1985. The oxygen isotope composition of landsnail shells as a climatic indicator: applications to hydrogeology and paleoclimatology. Chem. Geol. 58, 157–181.

Longinelli, A., Selmo, E., 2003. Isotopic composition of precipitation in Italy: a first overall map. J. Hydrol. 270, 75–88.

Longinelli, A., Anglesio, E., Flora, O., Iacumin, P., Selmo, E., 2006. Isotopic composition of precipitation in Northern Italy: reverse effect of anomalous climatic events. J. Hydrol. 329, 471–476.

Luterbacher, J., Dietrich, D., Xoplaki, E., Grosjean, M., Wanner, H., 2004. European seasonal and annual temperature variability, trends, and extremes since 1500. Science 303, 1499–1503.

Millot, R., Guerrot, C., Bullen, T.D., 2004a. Precise measurement of Li isotopes by MC-ICP-MS and comparison with TIMS analyses. In: Winter Conference on Plasma Spectrochemistry, January 5–10, Fort Lauderdale, USA.

Millot, R., Guerrot, C., Vigier, N., 2004b. Accurate and high precision measurement of lithium isotopes in two reference materials by MC-ICP-MS. Geostand. Geoanal. Res. 28, 53–159.

Millot, R., Négrel, Ph., Petelet-Giraud, E., 2007. Multi-isotopic (Li, B, Sr, Nd) approach for geothermal reservoir characterization in the Limagne Basin (Massif Central, France). Appl. Geochem. 22, 2307–2325.

Millot, R., Vigier, N., Gaillardet, J., 2010. Behaviour of lithium and its isotopes during weathering in the Mackenzie Basin, Canada. Geochim. Cosmochim. Acta 74, 3897–3912.

Miyata, Y., Tokieda, T., Amakawa, H., Uematsu, M., Nozaki, Y., 2000. Boron isotope variations in the atmosphere. Tellus 52B, 1057–1065.

Négrel, Ph., Roy, S., 1998. Chemistry of rainwater in the Massif Central (France): a strontium isotope and major element study. Appl. Geochem. 13, 941–952.

Négrel, Ph., Lachassagne, P., Laporte, P., 1997. Caractérisation chimique et isotopique des pluies de Cayenne (Guyane Francaise). C.R. Acad. Sci. Paris 324, 379–386.

Négrel, Ph., Guerrot, C., Millot, R., 2007. Chemical and strontium isotope characterization of rainwater in France: influence of sources and hydrogeochemical implications. Isotopes Environ. Health Studies 43, 179–196.

Négrel, Ph., Millot, R., Brenot, A., 2009. Lithium isotopes as a probe of groundwater circulation in a peat land. In: 8th International Symposium on Applied Isotope Geochemistry, La Malbaie, Canada.

Négrel, Ph., Millot, R., Brenot, A., Bertin, C., 2010. Lithium isotopes as tracers of groundwater circulation in a peatland. Chem. Geol., in press. doi:10.1016/j.chemgeo.2010.06.008.

Petelet-Giraud, E., Casanova, J., Chery, L., Négrel, Ph., Bushaert, S., 2005. Attempt of isotopic characterisation (delta O-18 and delta H-2) of present rainwater signature using lakes and reservoirs: application to south-western France. Houille Blanche 2, 57–62.

Pistiner, J.S., Henderson, G.M., 2003. Lithium isotope fractionation during continental weathering processes. Earth Planet. Sci. Lett. 214, 327–339.

Plata-Bedmar, A., 1994. Isotopic composition of precipitation and groundwater of the Iberian Peninsula. Centro des Estudios de tecnicas Aplicadas, Madrid (Spain) (in Spanish).

Pogge von Strandmann, P.A.E., Burton, K.W., James, R.H., van Calsteren, P., Gislason, S.R., Mokadem, F., 2006. Riverine behaviour of uranium and lithium isotopes in an actively glaciated basaltic terrain. Earth Planet. Sci. Lett. 251, 134–147.

Qi, H.P., Coplen, T.B., Wang, Q.Z., Wang, Y.H., 1997. Unnatural isotopic composition of lithium reagents. Anal. Chem. 69, 4076–4078.

Rastogi, N., Sarin, M.M., 2005. Chemical characteristics of individual rain events from a semi-arid region in India: three-year study. Atmos. Environ. 39, 3313–3323.

Razafindrakoto, S., 1988. Teneurs en isotopes stables des précipitations et des eaux souterraines et leurs variations en France. PhD thesis, Univ. d'Avignon et des Pays de Vaucluse.

Righi, D., De Connick, F., 1977. Mineralogic evolution in hydromorphic sandy soils and podzols in "Landes du médoc", France. Geoderma 19, 339–359.

Rose-Koga, E.F., Sheppard, S.M.F., Chaussidon, M., Carignan, J., 2006. Boron isotopic composition of atmospheric precipitations and liquid–vapor fractionations. Geochim. Cosmochim. Acta 70, 1603–1615.

Roy, S., Négrel, Ph., 2001. A Pb isotope and trace element study of rainwater from the Massif Central (France). Sci. Total Environ. 277, 225–239.

Rozanski, K., Araguas-Araguas, L., Gonfiantini, R., 1993. Isotopic patterns in modern global precipitation. In: Climate Change in Continental Isotopic Records. Geophysical Monograph 78. American Geophysical Union.

Schmitt, A.D., Stille, P., 2005. The source of calcium in wet anthropogenic deposit: Ca–Sr isotope evidence. Geochim. Cosmochim. Acta 69, 3463–3468.

Schurch, M., Kozel, R., Schotterer, U., Tripet, J.P., 2003. Observation of isotopes in the water cycle – the Swiss National Network (NISOT). Environ. Geol. 45, 1–11.
Teng, F.Z., McDonough, W.F., Rudnick, R.L., Dalpé, C., Tomascak, P.B., Chappell, B.W., Gao, S., 2004. Lithium isotopic composition and concentration of the upper continental crust. Geochim. Cosmochim. Acta 68, 4167–4178.
Tomascak, P.B., 2004. Developments in the understanding and application of lithium isotopes in the earth and planetary sciences. Rev. Mineral. Geochem. 55, 153–195.
Vigier, N., Rollion-Bard, C., Spezzaferri, S., Brunet, F., 2007. In-situ measurements of Li isotopes in foraminifera. Geochem. Geophys. Geosyst., Q01003.
Widory, D., Petelet-Giraud, E., Négrel, Ph., Ladouche, B., 2005. Tracking the sources of nitrate in groundwater using coupled nitrogen and boron isotopes: a synthesis. Environ. Sci. Technol. 39, 539–548.

Available online at www.sciencedirect.com
ScienceDirect
Geochimica et Cosmochimica Acta 74 (2010) 3897–3912
Geochimica et Cosmochimica Acta
www.elsevier.com/locate/gca

Behaviour of lithium and its isotopes during weathering in the Mackenzie Basin, Canada

Romain Millot [a,*], Nathalie Vigier [b], Jérôme Gaillardet [c]

[a] BRGM, Metrology Monitoring Analysis Department, Orléans, France
[b] CRPG, CNRS, Nancy-Université, Vandœuvre-lès-Nancy, France
[c] Institut de Physique du Globe de Paris, Sorbonne-Paris-Cité University and CNRS, Paris, France

Received 22 September 2009; accepted in revised form 22 April 2010; available online 27 April 2010

Abstract

We report Li isotopic compositions, for river waters and suspended sediments, of about 40 rivers sampled within the Mackenzie River Basin in northwestern Canada. The aim of this study is to characterize the behaviour of Li and its isotopes during weathering at the scale of a large mixed lithology basin. The Mackenzie River waters display systematically heavier Li isotopic compositions relative to source rocks and suspended sediments. The range in δ^7Li is larger in dissolved load (from +9.3‰ to +29.0‰) compared to suspended sediments (from −1.7‰ to +3.2‰), which are not significantly different from δ^7Li values in bedrocks. Our study shows that dissolved Li is essentially derived from the weathering of silicates and that its isotopic composition in the dissolved load is inversely correlated with its relative mobility when compared to Na. The highest enrichment of ^{7}Li in the dissolved load is reported when Li is not or poorly incorporated in secondary phases after its release into solution by mineral dissolution. This counterintuitive observation is interpreted by the mixing of water types derived from two different weathering regimes producing different Li isotopic compositions within the Mackenzie River Basin. The incipient weathering regime characterizing the Rocky Mountains and the Shield areas produces ^{7}Li enrichment in the fluid phase that is most simply explained by the precipitation of oxyhydroxide phases fractionating Li isotopes. The second weathering regime is found in the lowland area and produces the lower δ^7Li waters (but still enriched in ^{7}Li compared to bedrocks) and the most Li-depleted waters (compared to Na). Fractionation factors suggest that the incorporation of Li in clay minerals is the mechanism that explains the isotopic composition of the lowland rivers. The correlation of boron and lithium concentrations found in the dissolved load of the Mackenzie Rivers suggests that precipitation of clay minerals is favoured by the relatively high residence time of water in groundwater. In the Shield and Rocky Mountains, Li isotopes suggest that clay minerals are not forming and that secondary minerals with stronger affinity for ^{7}Li appear.

Although the weathering mechanisms operating in the Mackenzie Basin need to be characterized more precisely, the Li isotope data reported here clearly show the control of Li isotopes by the weathering intensity. The spatial diversity of weathering regimes, resulting from a complex combination of factors such as topography, geology, climate and hydrology explains, in fine, the spatial distribution of Li isotopic ratios in the large drainage basin of the Mackenzie River. There is no simple relationship between Li isotopic composition and chemical denudation fluxes in the Mackenzie River Basin.

1. INTRODUCTION

Assessing the behaviour of lithium and the distribution of Li isotopes during weathering is of major importance for studying water/rock interactions at the surface of the Earth. This is because lithium (^{6}Li ~7.5% and ^{7}Li ~92.5%) is a fluid-mobile element and, due to the large relative mass difference between its two stable isotopes, it is subject to significant low temperature mass fractionation which provides key information on the nature of weathering processes.

* Corresponding author. Tel.: +33 2 38 64 48 32.
E-mail address: r.millot@brgm.fr (R. Millot).

0016-7037/$ - see front matter © 2010 Elsevier Ltd. All rights reserved.
doi:10.1016/j.gca.2010.04.025

Recent studies have shown that the range of δ^7Li values spans more than 40‰ at the Earth surface ($\delta^7Li = (^7Li/^6Li_{sample}/^7Li/^6Li_{L\text{-}SVEC} - 1) \times 10^3$), (e.g. Pistiner and Henderson, 2003; Huh et al., 2004; Kisakürek et al., 2004, 2005; Rudnick et al., 2004; Hathorne and James, 2006; Pogge von Strandmann et al., 2006; Vigier et al., 2009). Furthermore, the world-wide range of δ^7Li in river waters is between +6‰ and +33‰ (Huh et al., 1998, 2001). There are as yet few studies concerning mixed lithology basins, but these suggest that river water δ^7Li is not affected by differences in catchment lithology (Huh et al., 1998; Kisakürek et al., 2005). Rather, lithium isotopes are thought to be strongly affected by isotope fractionation during secondary mineral formation and the degree and type of silicate weathering (Huh et al., 2004; Kisakürek et al., 2004, 2005; Hathorne and James, 2006; Pogge von Strandmann et al., 2006; Vigier et al., 2009).

To date, both the magnitude of the Li isotopic fractionation associated with water–rock interaction processes, and the factors controlling these fractionations, are poorly understood. However, both field and experimental studies have shown that ^6Li is preferentially retained by secondary minerals during silicate weathering (Pistiner and Henderson, 2003; Kisakürek et al., 2004; Pogge von Strandmann et al., 2006; Vigier et al., 2009). Accordingly, the fractionation of Li isotopes is dependent upon the extent of chemical weathering. Large fractionation seems to occur during superficial weathering while little fractionation is observed during more intense or prolonged weathering in stable environments (Huh et al., 1998, 2001; Pogge von Strandmann et al., 2006).

Lithium isotopic fractionation has been documented in numerous natural environments, with experimental and natural data (Huh et al., 2001; Pistiner and Henderson, 2003; Tomascak, 2004). It has been shown that partial dissolution of basalts does not result in fractionation of lithium isotopes, but that dissolution of granitic rock can cause fractionation (Pistiner and Henderson, 2003). In addition, adsorption onto mineral surfaces can also be a mechanism of Li isotopic fractionation in the hydrosphere. Sorption of Li from aqueous solutions by mineral phases at the temperature of the Earth's surface has been highlighted by Taylor and Urey (1938), as well as by Anderson et al. (1989). Li sorption experiments utilizing several minerals (Pistiner and Henderson, 2003) have revealed that Li isotopic fractionation does not occur when this element is not incorporated into the structure of the solid (physical sorption). When Li is incorporated by stronger bonds (chemical sorption), an isotopic fractionation is observed that is dependent on the chemical structure of the minerals (Anghel et al., 2002). The most significant Li isotopic fractionation factor ($\Delta_{solution\text{–}solid}$) $\sim +14‰$ has been measured for gibbsite. For Li sorption processes between solution and different solids (clay minerals such as kaolinite and vermiculite, and freshwater sediments), Zhang et al. (1998) have observed even higher Li isotopic fractionation factors ($\Delta_{solution\text{–}solid} \sim +22‰$).

In the present paper, we have undertaken a systematic study of the weathering products (both dissolved load and suspended sediments) of the Mackenzie River Basin, one of the major high latitude river basins of North America. This area is of particular interest because it has previously been extensively studied and is well characterized from a lithology and weathering mass budget point of view (Vigier et al., 2001; Millot et al., 2002; Gaillardet et al., 2003; Millot et al., 2003). Also, there is a clear contrast between mountains and plains, with a fourfold increase of silicate chemical weathering rates in the plains (Millot et al., 2003). A direct comparison of silicate weathering rates and river Li isotope compositions can be performed. In this paper, we evaluate the potential of Li isotopes as a tracer of silicate weathering processes in large mixed lithology basins at the scale of a large river basin.

2. GEOLOGICAL SETTING AND SAMPLE LOCATIONS

This study focuses on the Mackenzie River Basin and adjacent river basins (Stikine, Nass, Skeena, Fraser, and Yukon rivers). Most of the river waters and sediments are from the Mackenzie River Basin itself (Fig. 1), which is located in northwestern Canada under arctic and subarctic climate. The mainstream of the Mackenzie River was sampled at two locations (samples CAN96-6 at the river mouth and CAN96-25 upstream). The main tributaries of the Mackenzie River are the Red Arctic River (CAN96-7), the Liard River (CAN96-26), the Peel River (CAN96-5), the Peace River (CAN96-15 and CAN96-37), the Slave River (CAN96-38) and the Athabasca River (CAN96-42).

The Mackenzie River Basin is composed of three main structural units, corresponding to different geomorphological zones: namely, the Rocky and the Mackenzie Mountains in the western part, the Interior Platform (lowlands), and the Canadian Shield (in the eastern part), (Fig. 1). Rivers belonging to a transition zone correspond to basins draining the foothills located between the Rockies and the low-lying plains. From a mass budget point of view, the mainstream of the Mackenzie is mostly fed by tributaries draining the Interior Plain. River samples from the adjacent basins of the Yukon and Fraser Rivers are also considered here because their geological contexts are similar to those of the Upper Liard and Athabasca sub-basins, both located in the Rocky Mountains. Finally, the main rivers draining the Western Canadian orogenic belt were also analysed (Nass, Skeena, and Stikine River).

Sampled rivers therefore drain a large range of lithologies: volcanics and immature volcano-clastic sediments in the Western Canadian orogenic belt (Stikine terrane), carbonates and slates in the Mackenzie Mountains, marine and non-marine sedimentary rocks (Cambrian to Cretaceous limestones, shales and sandstones) in the Interior Plains of the basin, and old silicate rocks (Archean granites and gneisses) in the Slave Province of the Canadian Shield.

The chemical weathering conditions and physical erosion rates differ greatly depending on the runoff and basin lithology. Chemical denudation rates in this arctic zone are rather low compared to other major river basins, as determined by Millot et al. (2003) and Gaillardet et al. (2003). Full details concerning river samples (geological

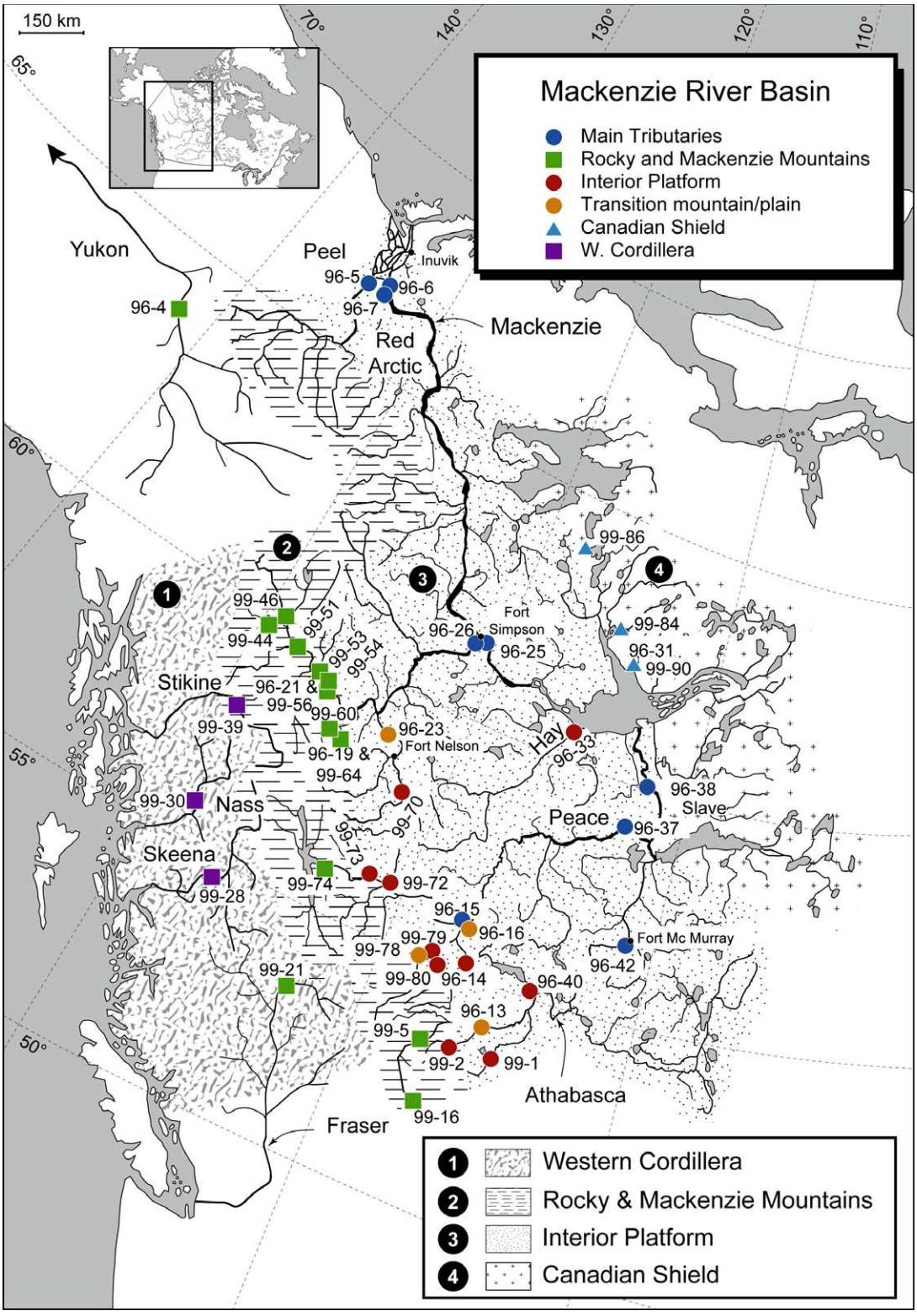

Fig. 1. Map showing the sample locations within the Mackenzie River Basin and adjacent basins (Yukon, Stikine, Nass, Skeena and Fraser Basin).

and hydrological contexts) have been published in Millot et al. (2003) for the Mackenzie River Basin, in Millot et al. (2002) for the rivers of the Canadian Shield and in Gaillardet et al. (2003) for rivers of the Western Cordillera.

3. ANALYTICAL METHODS

3.1. Sampling methodology, major and trace element concentration measurements

River waters were sampled twice during the high flow stage of the summer season (August 1996 and June 1999). In the field, 10–15 L of river water was collected in acid-washed containers for major and trace elements, and isotopic measurements (Millot et al., 2003). Samples were filtered a few hours later, using a Sartorius frontal filtration unit (0.2 μm cellulose acetate filter, 142 mm diameter). After filtration, samples were stored in acid-washed polypropylene bottles. The river sediments were collected after drying and centrifugation of the retentate of river water filtration. The samples for cations and trace element concentrations and Li isotope analyses were acidified to pH 2 with ultrapure HNO_3. Bottles for anion analyses were not acidified.

Lithium concentrations (for river waters and suspended sediment samples) were determined by ICP-MS (VG PlasmaQuad II+) with indium as an internal standard, with a precision of ±5%.

Major and trace elements are reported in Millot et al. (2003) for the Mackenzie River Basin, in Millot et al. (2002) for the rivers of the Canadian Shield, and in Gaillardet et al. (2003) for rivers of the Western Cordillera, respectively.

3.2. Lithium isotope measurements

Lithium isotopic compositions were measured using a Neptune Multi-Collector ICP-MS (Millot et al., 2004). $^7Li/^6Li$ ratios were normalized to the L-SVEC standard solution (NIST SRM 8545, Flesch et al., 1973) following the standard-sample bracketing method. Typical in-run precision on the determination of δ^7Li is about 0.1–0.2‰ ($2\sigma_m$, standard error of the mean).

Chemical separation of Li from the matrix was achieved before isotope analyses, following a procedure modified from the technique of James and Palmer (2000) that uses a cationic exchange resin (a single column filled with 3 mL of Bio-Rad AG® 50W-X12 resin, 200–400 mesh) and HCl media (0.2 N) for 30 ng of Li. Blanks for the total chemical extraction were less than 30 pg of Li, which is negligible since this represents a blank/sample ratio of $<10^{-3}$.

Successful quantitative measurement of Li isotopic compositions requires 100% Li recovery during laboratory processing. Therefore, frequent column calibrations were performed and repeated analysis of L-SVEC standard processed through the columns shows that no isotope fractionation occurred as a result of the purification process.

Accuracy and reproducibility of the isotopic measurements were tested by repeated analyses of three Li standard solutions (namely ^6Li–N, LiCl–N and ^7Li–N, Carignan et al., 2007). Mean values of $\delta^7Li = -8.0‰ \pm 0.3$ (2σ, $n = 38$), $\delta^7Li = +10.1‰ \pm 0.2$ (2σ, $n = 46$) and $\delta^7Li = +30.2‰ \pm 0.3$ (2σ, $n = 89$), were obtained for ^6Li–N, LiCl–N and ^7Li–N, respectively, over a period of 10 months. Thus, long-term reproducibility of the Li mass analysis is better than 0.3‰ at the two sigma level for standard solutions (σ: standard deviation).

The accuracy and reproducibility of the entire method (purification procedure + mass analysis) were tested by repeated measurement of a seawater standard solution (IRMM BCR-403) after separation of Li from the matrix, for which we obtained a mean value of $\delta^7Li = +30.8‰ \pm 0.4$ (2σ, $n = 15$) over the period of the duration of the analyses. This mean value is in a good agreement with our long-term measurements ($\delta^7Li = +31.0‰ \pm 0.5$, 2σ, $n = 30$, Millot et al., 2004) and with other values reported in the literature (see, for example Carignan et al., 2004; Tomascak, 2004, for a compilation).

For suspended sediments, as well as for sands and rocks, a total digestion of 50 mg of crushed sample was performed over 4 days at 100 °C in a closed beaker with a mixture of three ultrapure acids: 4 mL of HF (23 N), 1 mL of HNO_3 (14 N) and 0.1 mL of $HClO_4$ (12 N). The solution was subsequently evaporated to dryness and 4 mL of HCl (6 N) was added and left for a further 4 days at 100 °C. Sample aliquots (30 ng of Li) of the residue of the acid dissolution were then dissolved in 0.5 mL of HCl (0.2 N), before being placed on cation exchange columns for Li separation. Accuracy and reproducibility of the procedure for solid samples (dissolution + purification procedure + mass analysis) were tested by repeated measurement of the JB-2 basalt standard (Geological Survey of Japan) which gave a mean value of $\delta^7Li = +4.9‰ \pm 0.6$ (2σ, $n = 17$), in good agreement with published values (see Jeffcoate et al., 2004; Tomascak, 2004; Carignan et al., 2007, for data compilation).

4. RESULTS

4.1. Dissolved phase

Lithium concentrations (Table 1) in the Mackenzie Basin river waters display a wide range of values, from 0.05 μmol/L (for the Skeena River in the Western Cordillera) to 1.29 μmol/L (for the Hay River located in the lowlands). The Mackenzie River at the river mouth (CAN96-6) has a Li concentration of 0.57 μmol/L. The main tributaries, which are mainly located in the low-lying plains, show a mean value of Li of 0.63 μmol/L, ($n = 11$). The group of rivers draining the Interior Platform display the highest Li contents (mean value of 0.85 μmol/L, $n = 9$). In contrast, rivers of the Shield and the Western Cordillera areas display the lowest Li levels (~0.16 μmol/L, $n = 4$ and ~0.08 μmol/L, $n = 3$, respectively). Also, rivers draining the Rocky Mountains have low Li contents (mean value of 0.30 μmol/L, $n = 11$). Finally, Li contents for rivers located in the transition zone are intermediate between those from the Rockies and those from the low-lying plains (mean Li = 0.54 μmol/L, $n = 4$).

Compared to the concentrations of dissolved Li reported in the pioneering work of Reeder et al. (1972) for the Mackenzie River system (Li ranging from <0.7 to 4.5 μmol/L), our values are clearly lower in the present case (from 0.05 to 1.29 μmol/L). This difference is likely to be related to the method used for the Li determination in waters. Indeed, Reeder et al. (1972) reported a detection limit of

Table 1
Lithium isotopic composition δ^7Li (‰) and concentrations (μmol/L) for rivers waters of the Mackenzie Basin and the Western Cordillera. Analytical precision for each δ^7Li measurement is reported in this table and range from 0.1‰ to 0.3‰ ($2\sigma_m$). As mentioned in the analytical section, the total reproducibility is ±0.5‰ (2σ) and has been determined by long-term repeated measurements of a seawater sample (Millot et al., 2004). Surface area (km^2), river discharge (km^2/year), runoff (mm/year) and silicate weathering rates (tons/km^2/year and mg/L) have also been added in this table (from Millot et al., 2003).

Tributaries	Sample number	River name	δ^7Li (‰)	$2\sigma_m$	Li (μmol/L)	Area (km^2)	Discharge (km^3/year)	Runoff (mm/year)	Silicate weathering rate	
									(tons/km^2/year)	(mg/L)
Main tributaries	CAN96-5	Peel (Fort McPherson)	+13.3	0.1	0.71	70,600	21.65	307	1.73	5.63
	CAN96-6	Mackenzie (Tsiigehtchic)	+15.0	0.2	0.57	16,80,000	283.70	169	1.03	6.12
	CAN96-7	Red Arctic (Tsiigehtchic)	+13.8	0.1	0.89	18,600	5.02	270	1.37	5.08
	CAN96-15	Peace (Peace River)	+15.2	0.2	0.23	186,000	57.75	310	0.92	2.96
	CAN96-25	Mackenzie (Fort Simpson)	+16.5	0.3	0.53	12,70,000	137.90	139	1.05	7.57
	CAN96-26	Liard (Fort Simpson)	+14.3	0.1	0.63	275,000	77.32	281	1.19	4.24
	CAN96-37	Peace (Peace Point)	+15.4	0.1	0.52	305,500	67.01	219	1.30	5.92
	CAN96-38	Slave (Fort Smith)	+15.5	0.2	0.60	616,400	100.98	164	1.14	6.94
	CAN96-42	Athabasca (Fort McMurray)	+12.7	0.2	0.86	131,000	20.86	159	1.94	12.19
Rocky and Mackenzie Mountains	CAN96-4	Yukon (Dawson)	+17.9	0.2	0.32	—	—	—	—	—
	CAN96-19	Racing	+12.2	0.1	0.43	1900	2.30	1209	0.65	0.53
	CAN99-5	Athabasca (Hinton)	+15.4	0.2	0.45	9780	5.46	558	0.49	0.88
	CAN96-21	Liard (Liard River)	+12.9	0.1	0.36	33,400	11.71	351	0.79	2.24
	CAN99-21	Fraser	+17.5	0.1	0.11	—	—	—	—	—
	CAN99-46	Liard (Upper Liard)	+20.5	0.1	0.19	33,400	11.71	351	0.64	1.83
	CAN99-54	Smith	+12.6	0.1	0.19	3740	0.77	207	0.13	0.62
	CAN99-56	Liard (Liard River)	+18.3	0.2	0.19	—	—	—	—	—
	CAN99-60	Toad	+15.8	0.1	0.50	2570	1.37	532	0.55	1.04
	CAN99-64	Racing	+13.0	0.1	0.36	1900	2.30	1209	0.65	0.54
	CAN99-74	Peace (Hudson's Hope)	+17.0	0.2	0.18	69,900	34.71	497	0.89	1.79
Interior Platform	CAN96-14	Little Smoky	+11.8	0.2	0.69	3010	0.77	257	2.42	9.43
	CAN96-33	Hay (mouth)	+16.3	0.1	1.29	47,900	3.60	75	1.34	17.84
	CAN96-40	Lesser Slave	+10.1	0.1	1.21	13,600	1.32	97	1.28	13.21
	CAN99-1	Pembina (Evansburg)	+16.8	0.1	0.53	2900	1.12	386	4.33	11.21
	CAN99-2	McLeod	+15.4	0.1	0.85	9100	2.11	232	2.71	11.68
	CAN99-71	Doig	+13.3	0.1	1.02	—	—	—	—	—
	CAN99-72	Beatton	+11.4	0.1	0.51	—	—	—	—	—
	CAN99-79	Simonette	+11.4	0.1	1.02	5050	1.16	229	3.94	17.17
	CAN99-80	Little Smoky	+12.9	0.1	0.58	3010	0.77	257	2.38	9.26
Transition mountain/plain	CAN96-13	Athabasca	+14.8	0.2	0.29	—	—	—	—	—
	CAN96-16/1	Smoky	+12.1	0.1	0.56	51,300	11.83	231	1.90	8.22
	CAN96-23	Fort Nelson	+11.8	0.1	0.89	—	—	—	—	5.98
	CAN99-78	Smoky	+9.3	0.1	0.41	51,300	11.83	231	0.80	3.48
Canadian Shield	CAN96-31	Yellowknife	+26.9	0.1	0.17	16,300	1.16	71	0.27	3.80
	CAN99-84	Wecho	+26.0	0.2	0.20	3400	0.31	90	0.39	4.28
	CAN99-86	Wopmay	+25.2	0.1	0.07	—	—	—	0.33	2.83
	CAN99-90	Yellowknife	+29.0	0.1	0.19	16,300	1.16	71	0.28	3.87
Western Cordillera	CAN99-28	Skeena	+24.9	0.2	0.05	42,200	30.36	719	4.20	5.84
	CAN99-30	Nass	+21.6	0.1	0.09	19,200	24.68	1285	5.00	3.89
	CAN99-39	Stikine	+21.7	0.1	0.10	29,300	23.83	811	4.10	5.06

0.70 μmol/L (~5 μg/L) by atomic adsorption in the early 1970s, whereas it is now ~0.01 μmol/L using modern ICP-MS techniques. Consequently, it is obvious that Reeder et al. (1972) were not able to measure low lithium concentrations in some of the rivers of the Mackenzie Basin (indeed Li was not detected in 49 samples of their suite of 101 river samples).

Lithium isotopic compositions in the Mackenzie River waters (Table 1) range from δ^7Li = +9.3 (for the Smoky River located in the transition zone) to +29.0‰ (for the Yellowknife River located in the Slave Province). Rivers from the lowland regions vary from +10.1‰ to +16.8‰ with an average of +13.2‰. Rivers from the Rockies display higher δ^7Li values (from +12.2‰ to +20.5‰, with an average of +15.7‰), when compared to rivers draining the plains. Rivers draining the Western Cordillera and the Canadian Shield show the heaviest isotope compositions, with δ^7Li ranging between +25.2‰ and +29.0‰ for the Shield rivers and between +21.6‰ and +24.9‰ for the western orogenic belt (Stikine terrane).

An inverse relationship of Li isotopic composition with Li concentrations is observed for the Mackenzie River system (Fig. 2). It is clear from this figure that the different physiographic provinces in the basin are characterized by

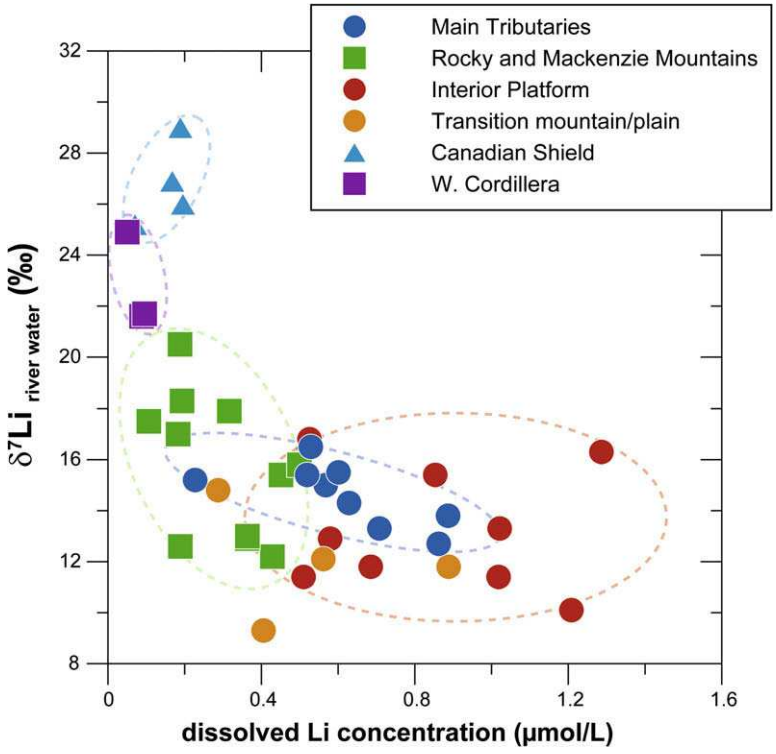

Fig. 2. Inverse correlation of Li isotopic composition and Li concentration in the dissolved load. In this diagram, the geomorphorphic provinces of the Mackenzie River Basin are well distinguished.

different domains. The large tributaries display δ^7Li values that essentially reflect the mixture of waters from the mountains and waters from the lowlands, in the range +12.7‰ to +16.5‰ (with an average of +14.6‰). The Mackenzie River at river mouth (CAN96-6) shows a δ^7Li value of +15.0‰, close to both values reported by Huh et al. (1998) for the Mackenzie River mainstream (+17.9‰ and +15.7‰, respectively).

4.2. River sediments and bedrocks

Lithium concentrations in suspended sediments of the Mackenzie Basin rivers (Table 2) range between 17.8 µg/g (for the Mackenzie River at river mouth) and 57.8 µg/g (for the Trout River in the Rockies). Lithium contents of the Mackenzie suspended sediments show almost the same range as that determined for the suspended sediments of the Orinoco Basin (from 5.2 to 71.3 µg/g, see Huh et al., 2001) and are close to the mean value of 35 ± 11 µg/g reported for the Upper Continental Crust (UCC) by Teng et al. (2004).

The isotopic composition of the suspended sediments range from −1.7‰ to +3.2‰, with a mean value of +0.4‰ ($n = 20$, Table 2), identical, within uncertainties, to the estimate of the UCC (δ^7Li from −2‰ to +2‰, Teng et al., 2004). Suspended sediments from the main tributaries of the Mackenzie Basin display slightly negative δ^7Li values (from −1.6‰ to −0.2‰) whereas δ^7Li of suspended sediments of rivers located in the Rocky Mountains are slightly positive (from +0.3‰ to +3.2‰). The suspended sediments of the Nass and Stikine Rivers (Western Cordillera) exhibit positive and similar isotope signatures (δ^7Li = +1.0‰ and +1.2‰, respectively). As for Li content, the range of δ^7Li for suspended sediments of the Mackenzie Basin is comparable with the values obtained by Huh et al. (2001) for silicate regions of the Orinoco Basin. δ^7Li values measured in suspended sediments are also in good agreement with the range reported by Kisakürek et al. (2005) for the Himalayan rivers (−3.9‰ to +3.0‰).

The sand sample collected at the mouth of the Mackenzie River (CAN96-6) has a Li concentration of 47.4 µg/g, which is lower than the Li content of the corresponding suspended material (57.8 µg/g) and a Li isotopic composition of −0.5‰, not significantly different from that of the corresponding suspended sediments (−0.9‰).

Bedrocks (carbonates and black shales) sampled in the basin, and assumed to be representative of the main type of rocks exposures, display Li contents ranging between 1.5 and 64.4 µg/g (Table 3). The carbonate samples from the Rocky Mountains (CAN99-65) display the lowest concentration (1.5 µg/g), in agreement with literature data reported for other carbonates (e.g. Huh et al., 2001; Hathorne and James, 2006). In contrast, Li contents in black shales from the Interior Platform are high (29.1 and 64.4 µg/g). Two glacial tills sampled within the Slave Province (Yellowknife and Prosperous Lake) display different Li concentrations of 16.2 and 54.6 µg/g, respectively.

The carbonate sample (CAN99-65, Rocky Mountains) has the highest δ^7Li value (+7.2‰), in agreement with other values reported for continental carbonates by Huh et al.

Table 2
Lithium isotopic composition δ^7Li (‰) and concentrations (μg/g) in suspended sediments for rivers from the Mackenzie Basin and adjacent basins draining the Canadian orogenic belt (Western Cordillera). Na and Al concentrations are also given in μg/g.

Tributaries	Sample number	River name	δ^7Li (‰)	$2\sigma_m$	Li (μg/g)	Na (μg/g)	Al (μg/g)
Main tributaries	CAN96-6	Mackenzie (Tsiigehtchic)	−0.9	0.2	57.8	3710	70,200
	CAN96-7	Red Arctic (Tsiigehtchic)	−1.6	0.1	56.8	2819	73,535
	CAN96-26	Liard (Fort Simpson)	−1.3	0.2	46.1	3339	71,206
	CAN96-38	Slave (Fort Smith)	−0.2	0.1	41.2	5268	67,447
Rocky and Mackenzie Mountains	CAN99-5	Athabasca (Hinton)	+2.6	0.2	28.9	—	—
	CAN99-16	Athabasca (Falls)	+3.2	0.1	19.4	—	—
	CAN99-21	Fraser	+1.4	0.1	48.3	10,387	92,276
	CAN99-44	French	+1.7	0.2	17.9	4377	46,059
	CAN99-46	Liard (Upper Liard)	+0.9	0.2	35.1	8235	65,224
	CAN99-51	Hyland	+0.3	0.1	44.3	8458	71,206
	CAN99-53	Coal	+0.3	0.1	46.2	7939	70,306
	CAN99-57	Trout	+2.8	0.2	17.8	3042	32,082
Interior Platform	CAN96-14	Little Smoky	−0.5	0.1	37.8	5713	79,888
	CAN99-72	Beatton	−1.7	0.2	51.4	2968	77,294
	CAN99-73	Halfway	+0.6	0.1	30.5	2968	50,029
Transition mountain/plain	CAN96-16	Smoky	−0.4	0.1	38.9	5565	76,024
	CAN99-78	Smoky	−0.1	0.1	35.3	4674	64,376
	CAN96-23	Fort Nelson	−1.2	0.2	56.1	3190	74,965
Western Cordillera	CAN99-30	Nass	+1.0	0.2	37.6	14,690	73,376
	CAN99-39	Stikine	+1.2	0.1	24.5	15,358	75,071

Table 3
δ^7Li (‰) and Li concentrations (μg/g) in sand samples from the Mackenzie River at the river mouth (CAN96-6), as well as in carbonate, black shales, and two glacial tills sampled on the Canadian Shield.

Tributaries	Sample type	Sample number	Sample name/location	δ^7Li (‰)	$2\sigma_m$	Li (μg/g)
Main tributaries	Sand	CAN96-6	Mackenzie at Tsiigehtchic	−0.5	0.1	47.4
Rocky and Mackenzie Mountains	Black shale	CAN99-5	Athabasca at Hinton	−1.0	0.2	29.1
	Carbonate	CAN99-65	McDonald	+7.2	0.1	1.5
Transition mountain/plain	Black shale	CAN99-70	Sikanni Chief	−1.1	0.1	64.4
Canadian Shield	Glacial till	CAN96-31	Yellowknife	+4.8	0.2	16.2
	Glacial till		Prosperous Lake	+5.2	0.2	54.6

(2001). This value is likely to reflect a mixing between pure marine carbonate (δ^7Li > +25‰, Tomascak, 2004; Hall et al., 2005; Hathorne and James, 2006; Vigier et al., 2007) and detrital phases with much lower δ^7Li values and higher Li contents. δ^7Li for the black shales are negative (−1.0‰ and −1.1‰ for the Interior Plains and for the transition zone samples, respectively), but remain close to the estimate of the UCC. Finally, the two glacial till samples display relatively similar δ^7Li values of +4.8‰ and +5.2‰, respectively.

5. DISCUSSION

5.1. Sources of dissolved lithium

The sources of dissolved lithium in the river waters of the Mackenzie Basin can be assumed to be either released by rock weathering (including solubilisation of the bedrock, and destabilisation or desorption from secondary minerals), derived from the atmosphere (via precipitation or wet deposition), or derived from groundwater input. First of all, atmospheric input can be evaluated using chloride concentrations if no evaporite is present within the drainage basin. This is the case for most of the rivers of the Mackenzie Basin, as shown by Millot et al. (2002, 2003) and Gaillardet et al. (2003). In particular, rivers draining the Shield area, characterized by low chemical weathering rates, are good candidates for estimating the atmospheric input of Li. Rivers draining the Canadian Shield have low dissolved Li contents (from 0.07 to 0.2 μmol/L) and display the highest δ^7Li values, close to that of the ocean (δ^7Li = +31.0‰), a priori suggesting a marine origin for Li via seasalt input through precipitation. Then, if we assume that all chloride in the Shield rivers (with Li/Cl = 5×10^{-3} and δ^7Li = +25.2‰ on average) is of atmospheric origin and that marine salts have seawater Li/Cl molar ratios of 5×10^{-5} and δ^7Li = +31.0‰, it can be calculated that only a small fraction of riverine Li (<1%) in these rivers originates from seasalt input through precipitation. The same calculation for rivers draining the Western Cordillera (i.e. the rainy region:

1500–1750 mm/year compared to 350 mm/year in the Shield area) indicates that a maximum of only ~0.4% riverine Li could have been supplied by precipitation.

We provided evidence in a previous paper (Millot et al., 2002), that the rivers of the Shield area (Slave Province) are characterized by a chloride excess compared to a pure marine input, and we attributed their relatively high Cl concentrations to the dissolution of evaporite-type aerosols derived from the dry area located south of the Great Slave Lake. Cambrian evaporites occur at the base of the sedimentary basin of the lowlands, and these have contributed to redeposited salt in modern lakes. The Salt River is one of the rivers that is highly influenced by the dissolution of these formations. Although this river was not analysed in the present work, Li and Na concentrations of the Salt River (Li = 4.5 μmol/L and Na = 276.45 mmol/L) have been reported by Reeder et al. (1972). The typical Li/Na ratio of this river is 1.6×10^{-5} mol/mol. Considering this ratio along with the highest Cl concentration found in rivers draining the Slave Province (80 μmol/L), we estimate there is a negligible Li input from evaporites in the Shield rivers (less than 0.4% of lithium derived from evaporite).

In summary, our calculations indicate that the contribution of Li coming from precipitation and wet deposition is negligible, and that dissolved Li in all sampled rivers is mainly derived from weathering of silicate and carbonate rocks. Although carbonates have relatively low Li concentrations (<1 μg/g) compared to silicates (higher than 50 μg/g), their higher dissolution rates may make them a significant source of Li in carbonate rich-regions. Millot et al. (2002) showed that the areas of the Mackenzie Basin which are most influenced by carbonate dissolution are the Rocky and Mackenzie Mountains. In contrast, the lowlands are less influenced by this lithology and the Shield area displays no input from carbonate weathering.

The proportions of lithium derived from silicate and carbonate weathering can be calculated from the results of the inversion model (Millot et al., 2003) which allowed us to determine, for each major element present in the dissolved phase, the proportion derived from the weathering of silicate and carbonate end-members within the Mackenzie River Basin. We use a mean Li/Ca molar ratio of 15×10^{-6} for carbonates, in agreement with Li/Ca molar ratios ranging from 10×10^{-6} to about 20×10^{-6} reported in carbonates elsewhere (Hall and Chan, 2004; Lear and Rosenthal, 2006; Hathorne et al., 2009), and determine that the carbonate end-member contribution is very low for lithium. Between 90.5% and 99.4% of dissolved lithium is thus derived from silicate weathering in the Mackenzie River Basin (Fig. 3).

These estimates agree well with previous studies that have inferred that most riverine Li derives from silicate lithologies (Huh et al., 1998; Kisakürek et al., 2005). In addition, the absence of a correlation between Li and Sr isotopic ratios (from Millot et al., 2003) argues against a carbonate weathering control on riverine Li isotopic composition. We therefore conclude that Li concentrations in the dissolved load of rivers in the Mackenzie Basin are essentially controlled by silicate weathering. Dissolved Li isotopic compositions are however highly variable within the Mackenzie River Basin (from +9.3‰ to +29.0‰), suggesting variable fractionation of Li isotopes during silicate weathering.

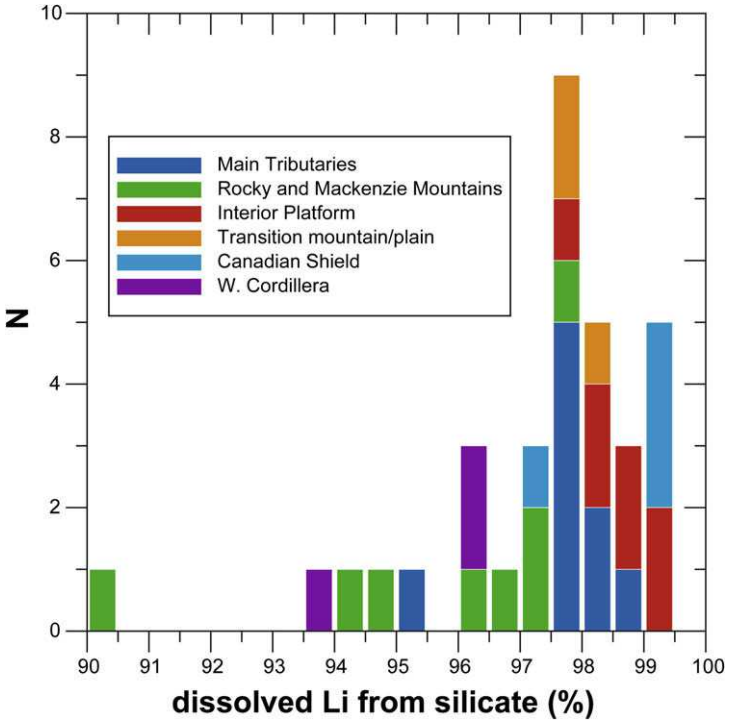

Fig. 3. Histogram for Li contribution coming from silicate weathering (%) in Mackenzie River water samples.

5.2. Li isotopes and silicate weathering regimes

5.2.1. Evidence for isotope fractionation during chemical weathering

River dissolved loads are systematically enriched in ^{7}Li relative to bedrocks and suspended particles (Fig. 4). In this regard, lithium is similar to boron (Lemarchand and Gaillardet, 2006). However, the dissolved loads exhibit a large range of δ^7Li values across the sampled rivers. A part of this variability may derive from the δ^7Li of bedrocks, which might differ between the main provinces of the Mackenzie Basin. Literature data indicate that the Li isotopic composition of continental granites (−2‰ to +3‰, Teng et al., 2004, 2006, 2008, 2009) is slightly different from the shales and loesses from which they were derived (−3‰ to +5‰). The Li isotopic composition of the Canadian Shield bedrock (mainly consisting of granites and associated crystalline rocks, Millot et al., 2002) is averaged in the glacial till samples reported in Table 3. In concordance with literature data, the δ^7Li values measured in till samples are higher than those measured in the bedrocks from the lowlands and the Rocky Mountains (which are mainly recycled materials such as shales, black shales, slates and a few low grade metamorphic rocks). In Fig. 4, we report δ^7Li values in silicate bedrocks compiled from the literature together with the results from this study. Suspended sediment and sand samples from the Mackenzie Rivers fall within the range of bedrocks defined by our bedrock samples and by literature data (Fig. 4). However, a positive trend between δ^7Li and Na/Al is observed (Fig. 5). Due to the high solubility of Na during chemical weathering compared to Al which is immobile, the Na/Al ratio can be regarded as "a weathering index". The low Na/Al ratios associated with low δ^7Li values suggests that lithium isotopes are fractionated by chemical weathering processes. The direction of the fractionation in the suspended sediments is consistent with the enrichment of ^{7}Li in the dissolved load since the lowest Na/Al are associated with the lowest δ^7Li. Because the suspended sediments of the Mackenzie Rivers are essentially derived from sedimentary rocks (the Shield area does not contribute significant sediment), it is difficult to conclude whether the Na loss recorded in the Na/Al ratio is due to present day weathering conditions, or whether the low Na/Al ratios are inherited from previous cycles of erosion and sedimentation. Examples of shale composites reported in the literature, such as the PAAS or NASC (Post Archean Australian Shale and North American Shale Composite: Holland, 1978; Taylor and MacLennan, 1985) do indeed show Na depletion compared to granodioritic Upper Continental Crust (Taylor and MacLennan, 1985; Gaillardet et al., 1999). Given the low grade silicate weathering in the Mackenzie River Basin (Millot et al., 2003), and the overlap of bedrock and suspended sediment Li isotopic compositions (Fig. 4), we favour the hypothesis that Na/Al in the suspended sediments essentially records bedrock geochemistry rather than present day weathering products. Therefore the trend of increasing Li isotopic composition with Na/Al ratio (Fig. 5) is likely inherited from the

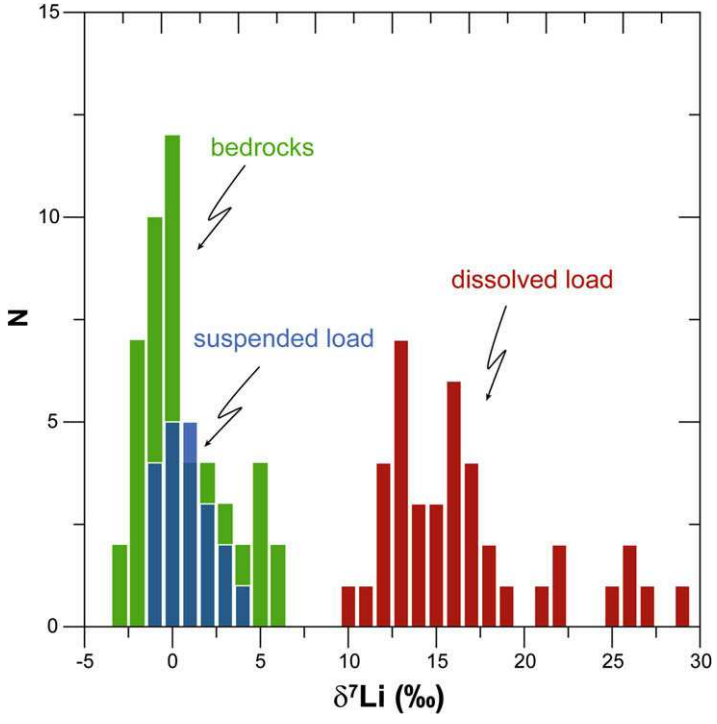

Fig. 4. Histogram of Li isotopic composition in the dissolved and suspended loads of the Mackenzie Rivers. Bedrock values from this study (four values) and from a compilation of literature data on shale, granite and loess (Teng et al., 2004) are added for comparison. This figure clearly shows the ^{7}Li enrichment of the dissolved phase compared to bedrocks, while suspended sediments and bedrocks are essentially similar.

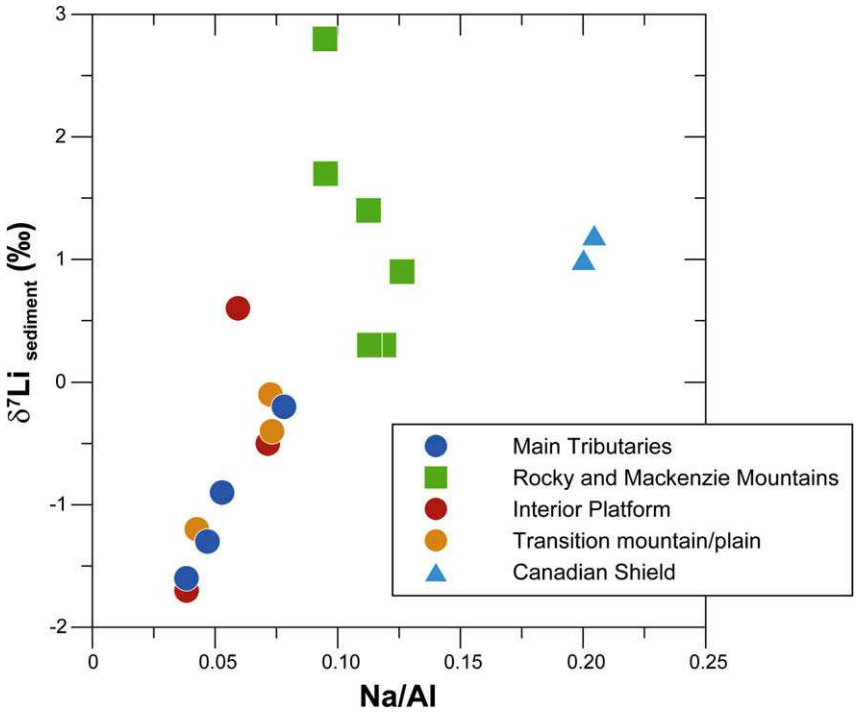

Fig. 5. Lithium isotopic composition in the suspended sediments of the Mackenzie Rivers (main tributaries, Rocky and Mackenzie Mountains, Interior Platform and transition mountain/plain) and glacial till sample (Canadian Shield) as a function of Na/Al ratio. This ratio can be seen as a proxy for Na loss compared to Al, and is therefore a weathering intensity proxy. Na loss can be attributed either to present day weathering processes or to previous episodes of weathering that would have occurred during the geological history of the sedimentary bedrocks.

bedrock history. From a mass budget perspective, it is not easy to estimate the partitioning of Li transported in the dissolved and particulate load because chemical weathering does not proceed at steady state (Vigier et al., 2001). However, the above considerations suggest that the dissolved load clearly reflects the fractionation of Li isotopes during chemical weathering (with the enrichment of ^{7}Li in the fluid), while the suspended phase is not significantly different from the bedrock. In other words, the dissolved load is sensitive to water–rock interactions, but solids are not, because chemical weathering is too weak. Investigating in more detail the isotopic composition of Li in river suspended sediments as a function of weathering rate is beyond the scope of the present paper, but would be interesting to do at large scale. The next section focuses on the dissolved load.

5.2.2. Influence of the weathering regime

We show in the following that the range of Li isotopic composition measured in the rivers of the Mackenzie Basin is related to the weathering regime.

The Li/Na* ratio in the dissolved load, when compared to that in the bedrock can be used as an index of Li mobility compared to Na. Both elements are alkali metals, thus mobile during water–rock interactions. As shown by a number of previous studies, in contrast to Na, Li is likely to be incorporated into secondary minerals, such as clays. By analogy with the study of Georg et al. (2007) concerning the mobility of Si isotopes during chemical weathering in Iceland, we can define f_{Li}, the fraction of Li remaining in solution relative to Na, as:

$$f_{Li} = \frac{(Li/Na^{*})_{dissolved}}{(Li/Na)_{bedrock}} \quad (1)$$

where Na* is the Na concentration corrected for atmospheric input and for evaporite dissolution using the results of Millot et al. (2003). Correction for evaporite dissolution only significantly affects a few samples. A value of 1 for f_{Li} means that chemical weathering is congruent. While dissolution is usually thought to be incongruent, precipitation of secondary phases is the most probable process that will fractionate Li and Na, Li being known to have affinity for clay minerals, while Na is much more mobile and hardly reincorporated into clay minerals.

We used the suspended sediment compositions, where available, to estimate the bedrock Li/Na ratio. In the Canadian Shield province, because rivers at the time of sampling contained very low levels of suspended sediment, we used two glacial till samples (Table 3) which display contrasting Li/Na ratios. The calculated f_{Li} in the rivers of the Mackenzie Basin range between 0.1 (in the lowlands and main tributaries) and 0.8 in the rivers of the Shield area. Intermediate values are found in the Rocky Mountains and in the Western Cordillera. This indicates that the reincorporation of Li into secondary phases is more important in the lowlands and main tributaries than in the Cordillera and Rocky Mountain samples. In Fig. 6, the dissolved Li/Na in the Shield rivers were normalized to the Prosperous Lake till

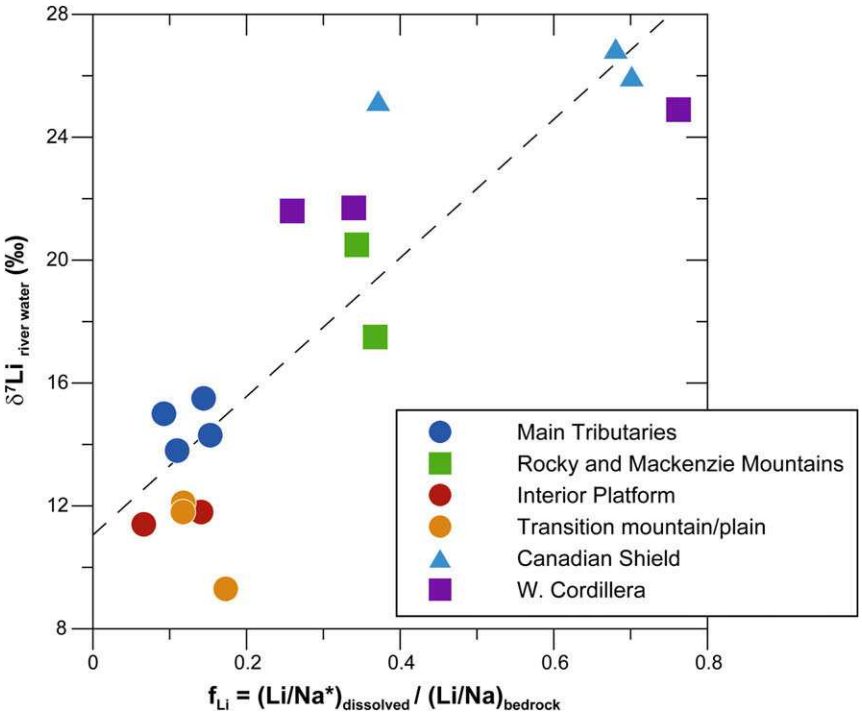

Fig. 6. Lithium isotopic composition in the dissolved load as a function of f_{Li}. f_{Li} represents the relative mobility of Li with respect to Na, an element not generally known to be reincorporated into secondary phases. This parameter is defined as the ratio of Li/Na in the dissolved load to that in the suspended sediments or, in the case of the Shield province, to the Prosperous Lake moraine. Na^* denotes here that the Na concentrations are corrected for atmospheric input and, for a couple of rivers, are corrected for evaporite dissolution according to the results of Millot et al. (2003). Ratios in suspended sediments are considered to represent bedrock ratios. For the Shield rivers, if the glacial till (sample CAN96-31) is used for normalizing the Li/Na data from the Shield rivers then f_{Li} values higher that 1 would be obtained for these rivers (not shown in the figure), but lithium isotopic composition and f_{Li} are still correlated.

sample. If the till sample CAN96-31 (Yellowknife) is used as a reference for the parent bedrock in the Slave Province, then f_{Li} values higher than 1 are found. Values of f_{Li} higher than 1 would mean a preferential leaching of Li compared to Na. Although Prosperous Lake till sample is our preferred bedrock estimate here, we nevertheless consider f_{Li} higher than 1 (and CAN96-31 as a source rock) as a possible scenario. Despite these uncertainties on the bedrock in the Shield province, f_{Li} provides a relative indication of Li mobility during weathering.

When the isotopic composition of dissolved lithium is plotted as a function of f_{Li}, a correlation appears (Fig. 6). This correlation can be explained by a binary mixing between waters draining areas characterized by two markedly different weathering regimes.

The first end-member needed to account for the correlation between f_{Li} and δ^7Li of the dissolved load corresponds to a weathering regime where Li is significantly precipitated in the solids compared to Na, most probably incorporated into Li-rich secondary minerals (clays). The lowlands and the transition zone areas best characterize this weathering regime since they display the lowest f_{Li} values. Numerous studies have shown that Li isotopes are fractionated during the formation of secondary minerals. The ~13‰ isotopic shift between the composition of the dissolved load and the bedrock in the lowlands is, to a first order, compatible with the estimated clay-solution isotopic fractionation at equilibrium (Taylor and Urey, 1938; Chan et al., 1992; Zhang et al., 1998; Pistiner and Henderson, 2003; Vigier et al., 2008). The formation of secondary solids, being kinetically limited, requires a favourable environment. Using boron isotopes, Lemarchand and Gaillardet (2006) have suggested that most of the dissolved boron in rivers is derived from the shallow groundwater system (drift aquifers). As shown by Lemay (2002), high lithium concentrations (3–15 μmol/L) are also measured in these groundwaters. The correlation between boron and lithium concentrations that links both rivers and groundwaters (Fig. 7) strongly argues for a significant input of Li to the lowland rivers from groundwaters. Because groundwaters have long residence times relative to surface waters, chemical weathering reactions can proceed further than in the Shield or Rocky Mountains areas where the residence time of water is not sufficiently long (Lemarchand and Gaillardet, 2006). We therefore suggest that the residence time of water in groundwater counteracts the effect of low temperature and favours the formation of secondary minerals that fractionate Li isotopes (Fig. 6) at equilibrium.

The second end-member in Fig. 6 corresponds to the Shield and Rocky Mountains areas, and displays the highest δ^7Li and f_{Li} values. This situation may appear as a paradox because f_{Li} indicates no or low Li incorporation in secondary products of weathering, while the isotopic shift between Li in the bedrock and dissolved Li is at its

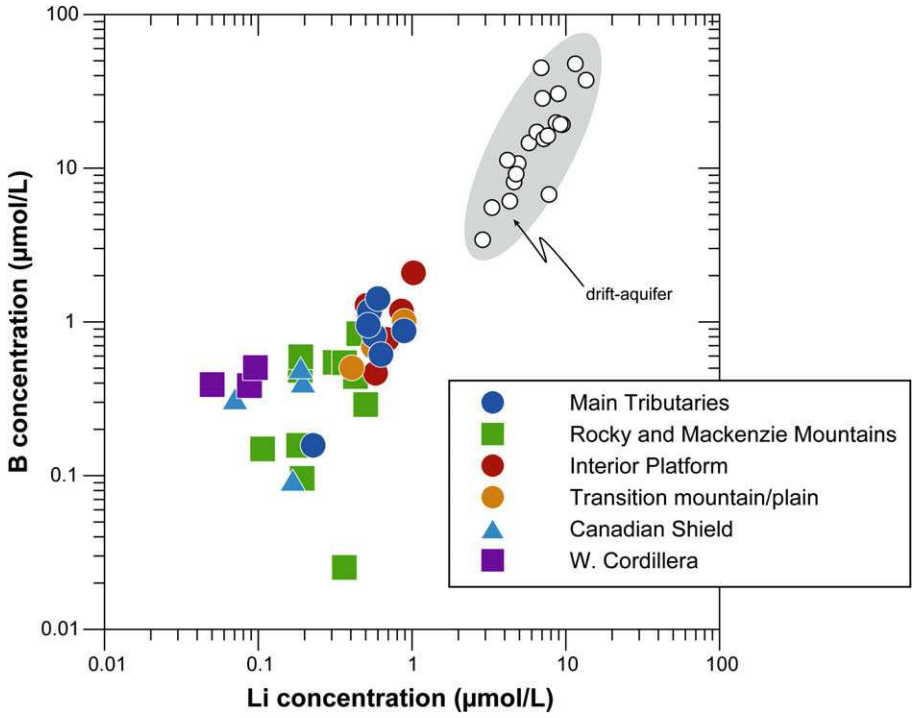

Fig. 7. Relationship between boron and lithium concentrations in the dissolved load of the rivers sampled in this study. Data from drift aquifers reported by Lemay (2002) have been added to show that the contribution from a groundwater input is likely. Boron data are from Lemarchand and Gaillardet (2006). Boron isotopic data strongly suggest that boron isotopic composition was acquired during reactive transport of boron in shallow groundwaters of relatively high water residence time, and that, boron is therefore a good tracer of the groundwater contribution.

maximum (from +16‰ to +22‰). The Rocky Mountains and the Shield province are areas characterized by particularly low chemical weathering rates (Millot et al., 2003), in contrast to the lowlands. These regions have been deglaciated relatively recently and are characterized by abundant bare rocks and poorly developed soils. The Rocky and Mackenzie Mountains areas have relatively high river sediment yields with sediments mostly derived from glacial erosion (Millot et al., 2003) and not from soils. The Shield area is characterized by important glacial till deposits. Several hypotheses can be invoked to explain the enrichment of ^{7}Li in the waters of the Rocky Mountains and of the Shield area. The most evident possibility is that the formation of some secondary mineral could fractionate Li isotopes. As indicated by the f_{Li} values close to 1, the incorporation of Li into secondary phases should not be quantitatively important in these regions but should however be visible in terms of isotope fractionation. A good candidate is Mn and Fe-oxyhydroxide minerals. Adsorption of Li onto Fe- and Mn-oxyhydroxide surfaces have been reported by Chan and Hein (2007) with preferential enrichment of ^{6}Li in the deposit, thus consistent with the observed heavy isotope enrichment in the fluids. A recent study reports the enrichment of the heavy isotope of Li in the dissolved load of glacial and non-glacial rivers from Greenland and attributes it to the preferential uptake of ^{6}Li during inner sphere sorption of Li^{+} on the Fe-oxyhydroxide surfaces (Wimpenny et al., 2010). The same mechanism can be invoked here. The difference between the study of Wimpenny et al. (2010) and our study is that the Shield rivers, that have ^{7}Li-enriched waters, are not sulphate-rich and therefore that sulphide oxidation, a mechanism proposed by the authors to explain the abundance of Fe-oxides in Greenland, is not applicable to the Shield rivers. The presence of Fe-oxyhydroxides minerals in the Shield rivers could be tested by analysing Mn and Fe river deposits often found in river bedloads, at the surface of blocks and boulders for example. In addition, saturation state calculations (using PHREEQC modelling) indicate that the waters are supersaturated with respect to goethite in this area.

A second possibility to explain the enrichment of ^{7}Li in the dissolved load of the Shield and Mackenzie Mountain rivers could be a fractionation of Li isotopes during mineral dissolution. Experimental work on basalt dissolution does not show evidence of Li isotope fractionation during dissolution (Pistiner and Henderson, 2003), but we can imagine a number of natural processes potentially able to fractionate Li isotopes during mineral dissolution. The preferential release of ^{7}Li could be possible either by the preferential dissolution of ^{7}Li-enriched phases, or as a transient effect of the leaching process with formation of unstable secondary phases such as Si-gel layers around minerals. So far, Li isotope heterogeneity at the mineral scale has not been observed within a single bedrock, but we cannot exclude the existence of low temperature minerals that would show ^{7}Li enrichments. What is interesting here is that the ^{7}Li enrichment in waters is observed in the geological context of glacial erosion (still active in the Rockies and in the form

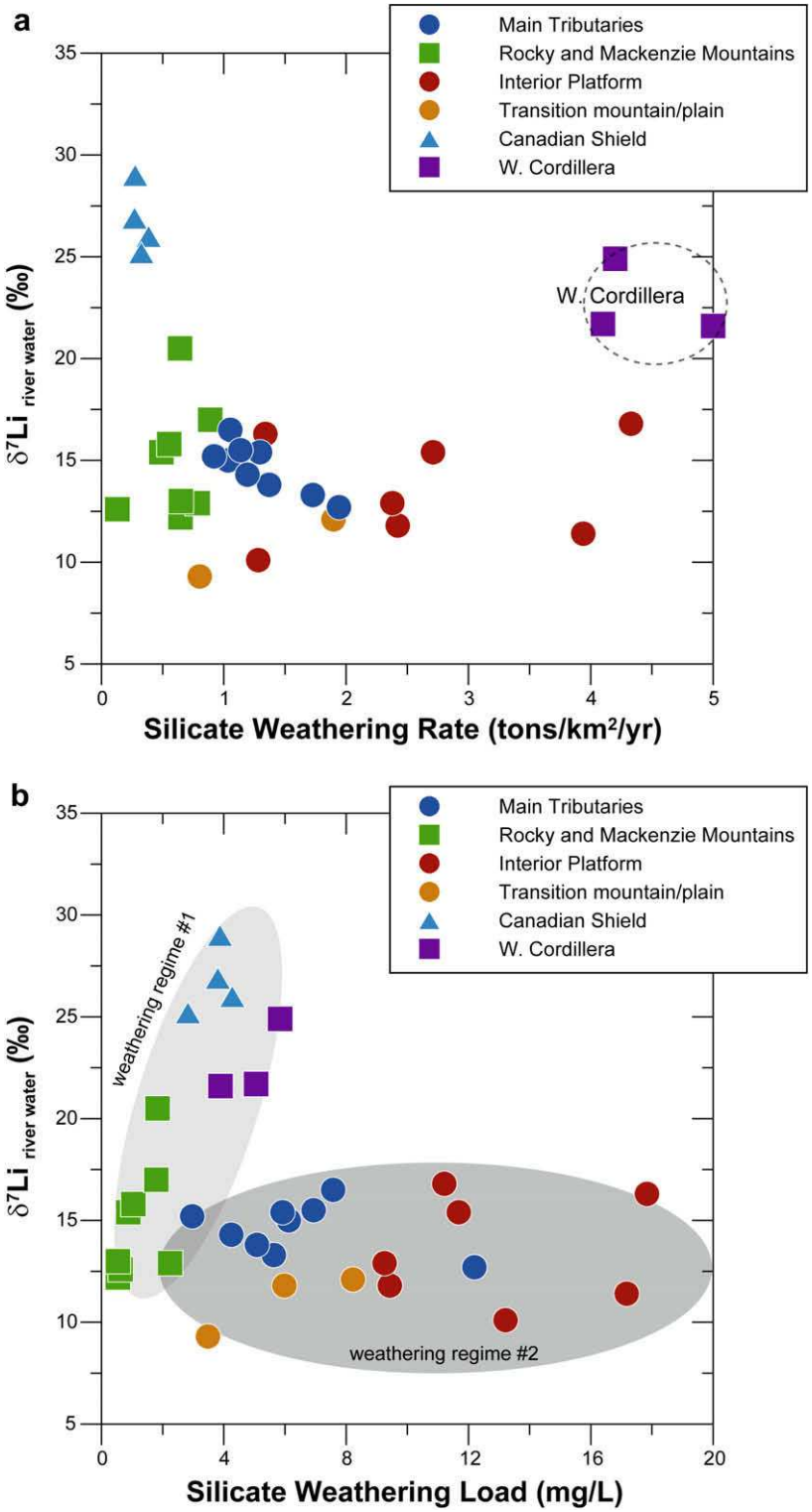

Fig. 8. Li isotopic composition as a function of silicate weathering rate (a) and silicate weathering load (b) for the river samples. Silicate weathering rates were calculated in Millot et al. (2003) based on the inversion of major element concentration and Sr isotope data in the dissolved load, and by Gaillardet et al. (2003) for the Stikine province. In (b), the observed feature is consistent with the idea developed here that the Li isotopic composition of water in the Mackenzie Basin rivers reflects mixing between waters modified by weak (incipient or surficial) weathering (weathering regime #1) and waters dominated by more intense water–rock interactions with the formation of secondary phases in the lowlands of the Mackenzie River Basin (weathering regime #2).

of glacial deposits in the Shield area). The abundance of fine glacial flour allows specific weathering reactions to occur, that have been observed experimentally (in columns of grind granitic material, White et al., 1998) or in nature (Anderson et al., 1989). In particular fast dissolving accessory phases like carbonates and sulphides have been shown to contribute significantly to solute export in the early stages of weathering.

Whatever the reason for Li isotope fractionation, our data do show that incipient weathering of rocks can produce ^{7}Li-enriched fluids. The similar enrichments found in Greenland (Wimpenny et al., 2010) or in very recently deglaciated moraine in the granitic Swiss Alps (Lemarchand et al., 2009) shows that Li isotopes are very sensitive to the early stages of chemical weathering. Future studies will be necessary to investigate Li isotope fractionation in incipient weathering conditions and the isotopic heterogeneity of bedrocks to precisely determine the mechanisms that result in the preferential release of heavy Li isotopes in solution.

According to the above discussion, all sampled rivers in the Mackenzie Basin have an isotopic composition reflecting a mixture of water masses that have interacted with bedrock minerals according to two contrasting weathering regimes. On one hand, oxyhydroxide formation and/or leaching of comminuted bedrock produces ^{7}Li-enriched waters, similarly to that occurring in glacial and non-glacial rivers from Greenland. On the other hand, the more optimum weathering conditions of the low-lying plain aquifers will produce waters with Li isotopic compositions lower by about 20‰. As indicated by the previous studies of our group, the weathering rates of silicates in these two contrasted environments differ by a factor of 3–4, probably accelerated in the lowlands by the contribution of groundwaters (Lemarchand and Gaillardet, 2006) and the chelating effects of organic matter (Millot et al., 2003). The Li isotopic data presented here show that the Li isotopic signature of waters is more influenced by the precipitation of specific secondary phases than weathering rates. The relationship between chemical weathering rates of silicates (calculated from the inversion of major element concentrations and Sr isotopic ratios by Millot et al., 2003), and δ^7Li measured in the dissolved loads is shown in Fig. 8a. There is no clear relationship at the scale of the Mackenzie River Basin between the Li isotopic composition and the specific flux of chemical denudation, showing that secondary mineral formation is not necessarily related to denudation fluxes. In particular, the high fluxes observed for the Western Cordillera and visible in Fig. 8 are due to the combined effects of runoff and the volcanic nature of bedrocks (Gaillardet et al., 2003). The absence of a relationship between chemical denudation rate and water lithium isotopic composition is in contrast with the relationship observed on small monolithologic rivers in Iceland (Vigier et al., 2009).

Two trends of δ^7Li with total dissolved load derived from silicate weathering in mg/L are observed (Fig. 8b), corresponding to the two weathering regimes described above. The first trend of increasing ^{7}Li enrichment with dissolved solutes only contains samples from the Shield and Rocky–Mackenzie Mountains from the first weathering regime described above. By contrast, the waters most influenced by the second weathering regime show constant Li isotopic composition with total dissolved load concentration derived from silicate weathering. Fig. 8b confirms the broad idea that Li isotopes are indicative of the regime weathering. Regimes characterized by secondary clay formation have Li isotopic composition between 10‰ and 15‰ and show no relationship with silicate weathering rates, while weathering regimes characterized by incipient weathering, or weathering of comminuted bedrocks, are characterized by higher Li isotopic composition.

6. CONCLUSIONS

The Li isotopic composition measured in the rivers of the Mackenzie Basin shows that ^{7}Li is enriched in the dissolved load and that δ^7Li can vary by 20‰ within a large river basin. The δ^7Li of the particulate load reflects that of the bedrock and ranges between −2‰ and +3‰. Our study shows that dissolved Li in river waters is essentially derived from the weathering of silicates and that Li isotopic ratios of the dissolved load depends on the weathering regime of silicates.

If Na is considered as a soluble element not incorporated in secondary phases, river waters showing Li/Na ratios much lower than the bedrock ratio have the lowest isotopic compositions. Although the fractionation coefficients between solution and newly formed solids remain poorly known and need to be better constrained by experimental work, our isotopic data are consistent with the incorporation of Li into clay minerals at equilibrium. Groundwaters, in particular shallow aquifers in the low-lying plains of the basin, seem to play an important role in the acquisition of the dissolved Li isotope composition, probably because high residence times favour the formation of clay mineral. The most ^{7}Li-enriched waters are observed in the Rocky Mountains and in the Shield areas of the basin. In these areas, by analogy to previous work in Greenland (Wimpenny et al., 2010), we suggest that high δ^7Li values in rivers result from the fractionation associated with Li sorption onto Mn- and Fe-oxyhydroxide surfaces. However, another mechanism could be that leaching is likely to be a non-negligible process of water–rock interaction due to surficial or incipient weathering, being able to produce ^{7}Li-enriched waters. Experimental work will be necessary for better understanding the behaviour of Li isotopes in incipient weathering regimes.

To summarize, this large scale study shows that dissolved Li is essentially derived from silicate weathering but shows that silicate weathering does not have a unique isotopic signature. A very large variability of Li isotopic ratios exists within the Mackenzie Basin and is strongly spatialized. This is an important result if Li isotopes in the ocean are to be used as a proxy for the secular evolution of the Earth's surface. This study suggests that, rather than weathering fluxes, the weathering regime controls the Li isotopic signature of silicate weathering. Future work will have to address the role of the different parameters that define the weathering regime: time, climate, hydrological setting, residence time of water, biological parameters.

ACKNOWLEDGMENTS

This work was supported by the French program funded by the INSU-CNRS (PNSE contribution 322). We would like to express special thanks to B. Dupré for measurements of trace elements in Toulouse University. We also would like to acknowledge B. Dupré, C. Gariépy and D. Lemarchand for their help in collecting river samples. We thank E. Lemarchand and E.T. Tipper for fruitful discussions. R.M. would like to thank Ph. Négrel and T.D. Bullen for comments in an earlier version of the manuscript and the Research Division of BRGM is also acknowledged for funding. We thank R. James, P. Pogge van Strandmann and B. Reynolds for providing critical comments that improved this manuscript. D. Vance is also thanked for editorial handling and constructive comments. Finally, we also would like to thank P. Burnard and R.H. Hilton for comments and English corrections. This is IPGP contribution no. 2581 and BRGM contribution no. 6327.

REFERENCES

Anderson M. A., Bertsch P. M. and Miller W. P. (1989) Exchange and apparent fixation of lithium in selected soils and clay minerals. *Soil Sci.* **148**, 46–52.

Anghel I., Turin H. J. and Reimus P. W. (2002) Lithium sorption to Yucca mountain tuffs. *Appl. Geochem.* **17**, 819–824.

Carignan J., Cardinal D., Eisenhauer A., Galy A., Rehkämper M., Wombacher F. and Vigier N. (2004) A reflection on Mg, Ca, Cd, Li and Si isotopic measurements and related reference materials. *Geostand. Geoanal. Res.* **28**, 139–148.

Carignan J., Vigier N. and Millot R. (2007) Three secondary reference materials for Li isotopic measurements: ^{7}Li–N, ^{6}Li–N and LiCl–N. *Geostand. Geoanal. Res.* **31**, 7–12.

Chan L. H. and Hein J. R. (2007) Lithium contents and isotopic compositions of ferromanganese deposits from the global ocean. *Deep-Sea Res. II: Top. Stud. Oceanogr.* **54**, 1147–1162.

Chan L. H., Edmond J. M., Thompson G. and Gillis K. (1992) Lithium isotopic composition of submarine basalts: implications for the lithium cycle to the ocean. *Earth Planet. Sci. Lett.* **108**, 151–160.

Flesch G. D., Anderson A. R. and Svec H. J. (1973) A secondary isotopic standard for ^{6}Li/^{7}Li determinations. *Int. J. Mass Spectrom. Ion Phys.* **12**, 265–272.

Gaillardet J., Dupré B., Louvat P. and Allègre C. J. (1999) Global silicate weathering and CO_2 consumption rates deduced from the chemistry of large rivers. *Chem. Geol.* **159**, 3–30.

Gaillardet J., Millot R. and Dupré B. (2003) Chemical denudation rates of the western Canadian orogenic belt: the Stikine terrane. *Chem. Geol.* **201**, 257–279.

Georg R. B., Reynolds B. C., West A. J., Burton K. W. and Halliday A. N. (2007) Silicon isotope variations accompanying basalt weathering in Iceland. *Earth Planet. Sci. Lett.* **261**, 476–490.

Hall J. M. and Chan L. H. (2004) Li/Ca in multiple species of benthic and planktonic foraminifera: thermocline, latitudinal, and glacial–interglacial variation. *Geochim. Cosmochim. Acta* **68**, 529–545.

Hall J. M., Chan L. H., McDonough W. F. and Turekian K. K. (2005) Determination of the lithium isotopic composition of planktic foraminifera and its application as a paleo-seawater proxy. *Mar. Geol.* **217**, 255–265.

Hathorne E. C. and James R. H. (2006) Temporal record of lithium in seawater: a tracer for silicate weathering? *Earth Planet. Sci. Lett.* **246**, 393–406.

Hathorne E. C., James R. H. and Lampitt R. S. (2009) Environmental versus biomineralization controls on the intratest variation in the trace element composition of the planktonic foraminifera *G. inflata* and *G. scitula*. *Paleoceanography* **24**, PA4204.

Holland H. D. (1978) *The Chemistry of Oceans and Atmosphere*. Wiley and Sons, New York.

Huh Y., Chan L. C., Zhang L. and Edmond J. M. (1998) Lithium and its isotopes in major world rivers: implications for weathering and the oceanic budget. *Geochim. Cosmochim. Acta* **62**, 2039–2051.

Huh Y., Chan L. C. and Edmond J. M. (2001) Lithium isotopes as a probe of weathering processes: Orinoco River. *Earth Planet. Sci. Lett.* **194**, 189–199.

Huh Y., Chan L. C. and Chadwick O. A. (2004) Behavior of lithium and its isotopes during weathering of Hawaiian basalt. *Geochem. Geophys. Geosyst.* **5**, 1–22.

James R. H. and Palmer M. R. (2000) The lithium isotope composition of international rock standards. *Chem. Geol.* **166**, 319–326.

Jeffcoate A. B., Elliott T., Thomas A. and Bouman C. (2004) Precise, small sample size determinations of lithium isotopic compositions of geological reference materials and modern seawater by MC-ICP-MS. *Geostand. Geoanal. Res.* **28**, 161–172.

Kisakürek B., Widdowson M. and James R. H. (2004) Behaviour of Li isotopes during continental weathering: the Bidar laterite profile, India. *Chem. Geol.* **212**, 27–44.

Kisakürek B., James R. H. and Harris N. B. W. (2005) Li and δ^{7}Li in Himalayan rivers: proxies for silicate weathering? *Earth Planet. Sci. Lett.* **237**, 387–401.

Lear C. H. and Rosenthal Y. (2006) Benthic foraminiferal Li/Ca: insights into Cenozoic seawater carbonate saturation state. *Geology* **34**, 985–988.

Lemarchand D. and Gaillardet J. (2006) Transient features of the erosion of shales in the Mackenzie basin (Canada), evidences from boron isotopes. *Earth Planet. Sci. Lett.* **245**, 174–189.

Lemarchand E., Tipper E. T., Hindshaw R., Wiederhold J. G., Reynolds B. C., Bourdon B. and Kretzchmar R. (2009) Li isotope fractionation in surface waters of an alpine granitic catchment. In *Goldschmidt Conference*, #A742 (abstr.).

Lemay T. G. (2002) Geochemical and isotope data for formation water from selected wells, cretaceous to quaternary succession, Athabasca oil sand (in situ) area, Alberta, EUB/AGS Geo-Note 2002-02, pp. 1–30.

Millot R., Gaillardet J., Dupré B. and Allègre C. J. (2002) The global control of silicate weathering rates and the coupling with physical erosion: new insights from the Canadian Shield. *Earth Planet. Sci. Lett.* **196**, 83–98.

Millot R., Gaillardet J., Dupré B. and Allègre C. J. (2003) Northern latitude chemical weathering rates: clues from the Mackenzie River Basin, Canada. *Geochim. Cosmochim. Acta* **67**, 1305–1329.

Millot R., Guerrot C. and Vigier N. (2004) Accurate and high-precision measurement of lithium isotopes in two reference materials by MC-ICP-MS. *Geostand. Geoanal. Res.* **28**, 153–159.

Pistiner J. S. and Henderson G. M. (2003) Lithium isotope fractionation during continental weathering processes. *Earth Planet. Sci. Lett.* **214**, 327–339.

Pogge von Strandmann P. A. E., Burton K. W., James R. H., van Calsteren P., Gislason S. R. and Mokadem F. (2006) Riverine behaviour of uranium and lithium isotopes in an actively glaciated basaltic terrain. *Earth Planet. Sci. Lett.* **251**, 134–147.

Reeder S. W., Hitchon B. and Levinson A. A. (1972) Hydrogeochemistry of the surface waters of the Mackenzie River drainage basin, Canada: I. Factors controlling inorganic composition. *Geochim. Cosmochim. Acta* **36**, 825–865.

Rudnick R. L., Tomascak P. B., Njo H. B. and Robert Gardner L. (2004) Extreme lithium isotopic fractionation during continental weathering revealed in saprolites from South Carolina. *Chem. Geol.* **212**, 45–57.

Taylor S. R. and MacLennan S. M. (1985) *The Continental Crust: Its Composition and Evolution*. Blackwell Scientific Publications, 312p.

Taylor S. R. and Urey H. C. (1938) Fractionation of the lithium and potassium isotopes by chemical exchange with zeolites. *J. Chem. Phys.* **6**, 429–438.

Teng F. Z., McDonough W. F., Rudnick R. L., Dalpé C., Tomascak P. B., Chappell B. W. and Gao S. (2004) Lithium isotopic composition and concentration of the upper continental crust. *Geochim. Cosmochim. Acta* **68**, 4167–4178.

Teng F. Z., McDonough W. F., Rudnick R. L. and Walker R. J. (2006) Diffusion-driven extreme lithium isotopic fractionation in country rocks of the Tin Mountain pegmatite. *Earth Planet. Sci. Lett.* **243**, 701–710.

Teng F. Z., Rudnick R. L., McDonough W. F., Gao S., Tomascak P. B. and Liu Y. (2008) Lithium isotopic composition and concentration of the deep continental crust. *Chem. Geol.* **255**, 47–59.

Teng F. Z., Rudnick R. L., McDonough W. F. and Wu F. Y. (2009) Lithium isotopic systematics of A-type granites and their mafic enclaves: further constraints on the Li isotopic composition of the continental crust. *Chem. Geol.* **262**, 370–379.

Tomascak P. B. (2004) Developments in the understanding and application of lithium isotopes in the Earth and Planetary Sciences. *Rev. Mineral. Geochem.* **55**, 153–195.

Vigier N., Bourdon B., Turner S. and Allègre C. J. (2001) Erosion timescales derived from U-decay series measurements in rivers. *Earth Planet. Sci. Lett.* **193**, 549–563.

Vigier N., Rollion-Bard C., Spezzaferri S. and Brunet F. (2007) In-situ measurements of Li isotopes in foraminifera. *Geochem. Geophys. Geosyst.*, Q01003.

Vigier N., Decarreau A., Millot R., Carignan J., Petit S. and France-Lanord C. (2008) Quantifying Li isotope fractionation during smectite formation and implications for the Li cycle. *Geochim. Cosmochim. Acta* **72**, 780–792.

Vigier N., Gislason S. R., Burton K. W., Millot R. and Mokadem F. (2009) The relationship between riverine lithium isotope composition and silicate weathering rates in Iceland. *Earth Planet. Sci. Lett.* **287**, 434–441.

White A. F., Blum A. E., Schulz M. S., Vivit D. V., Larsen M. and Murphy S. F. (1998) Chemical weathering in a tropical watershed, Luquillo Mountains, Puerto Rico: I. Long-term versus short-term chemical fluxes. *Geochim. Cosmochim. Acta* **62**, 209–226.

Wimpenny J., James R. H., Burton K. W., Gannoun A., Mokadem F. and Gíslason S. R. (2010) Glacial effects on weathering processes: new insights from the elemental and lithium isotopic composition of West Greenland rivers. *Earth Planet. Sci. Lett.* **290**, 427–437.

Zhang L., Chan L. H. and Gieskes J. M. (1998) Lithium isotope geochemistry of pore waters from Ocean Drilling Program Sites 918 and 919, Irminger Basin. *Geochim. Cosmochim. Acta* **62**, 2437–2450.

Associate editor: Derek Vance

Available online at www.sciencedirect.com
ScienceDirect
Geochimica et Cosmochimica Acta 74 (2010) 4612–4628
Geochimica et Cosmochimica Acta
www.elsevier.com/locate/gca

Lithium isotope systematics in a forested granitic catchment (Strengbach, Vosges Mountains, France)

Emmanuel Lemarchand [a,*], François Chabaux [a], Nathalie Vigier [b], Romain Millot [c], Marie-Claire Pierret [a]

[a] CGS-EOST, Université de Strasbourg et CNRS, 1 rue Blessig, F-67084 Strasbourg Cedex, France
[b] CRPG, CNRS, Nancy-Université, 15 rue Notre-Dame des Pauvres, BP 20, F-54501 Vandoeuvre-les-Nancy, France
[c] BRGM, Metrology Monitoring Analysis Department, Orléans, France

Received 4 December 2009; accepted in revised form 23 April 2010; available online 6 May 2010

Abstract

Over the last decade it has become apparent that Li isotopes may be a good proxy to trace silicate weathering. However, the exact mechanisms which drive the behaviour of Li isotopes in surface environments are not totally understood and there is a need to better calibrate and characterize this proxy. In this study, we analysed the Li concentrations and isotopic compositions in the various surface reservoirs (soils, rocks, waters and plants) of a small forested granitic catchment located in the Vosges Mountains (Strengbach catchment, France, OHGE http://ohge.u-strasbg.fr). Li fluxes were calculated in both soil profiles and at the basin scale and it was found that even in this forested basin, atmospheric inputs and litter fall represented a minor flux compared to input derived from the weathering of rocks and soil minerals (which together represent a minimum of 70% of dissolved Li). Li isotope ratios in soil pore waters show large depth dependent variations. Average dissolved δ^7Li decreases from −1.1‰ to −14.4‰ between 0 and −30 cm, but is +30.7‰ at −60 cm. This range of Li isotopic compositions is very large and it encompasses almost the entire range of terrestrial Li isotope compositions that have been previously reported. We interpret these variations to result from both the dissolution and precipitation of secondary phases. Large isotopic variations were also measured in the springs and stream waters, with δ^7Li varying from +5.3‰ to +19.6‰. δ^7Li increases from the top to the bottom of the basin and also covaries with discharge at the outlet. These variations are interpreted to reflect isotopic fractionations occurring during secondary phase precipitation along the water pathway through the rocks. We suggest that the dissolved δ^7Li increases with increasing residence time of waters through the rocks, and so with increasing time of interaction between waters and solids. A dissolution precipitation model was used to fit the dissolved Li isotopic compositions. It was found that the isotopic compositions of springs and stream waters are explicable by an isotopic fractionation of −5‰ to −14‰ (best fit −10.8‰), in agreement with Li incorporation into clay. In soil solutions, it was found that isotopic fractionation during secondary precipitation is larger (at least −23‰), suggesting a major role for different secondary phases, such as iron oxides that maybe incorporate Li with a higher isotope fractionation.

1. INTRODUCTION

Studies of silicate rock weathering have mobilized great energy in the geochemistry community because it is a key parameter in many surface earth science domains such as long term climate modelling (Berner, 1995; Walker, 1981), quantifying element fluxes from continents to oceans (Dupré et al., 2003), or understanding soil formation (Anderson et al., 2007). Improvements in mass spectrometry techniques, particularly since the recent advent of MC-ICP-MS, allowed the development of new isotopic proxies for silicate weathering, thus broadening the scope of investigations in this area. Lithium is one proxy that has been considerably developed during the last decade.

* Corresponding author. Address: IBP and IGMR, ETH Zurich, CHN, F 75, Universitätstrasse 16, 8092 Zurich, Switzerland. Tel.: +41 0 44 632 57 73; fax: +41 0 44 633 11 18.
E-mail addresses: lemarchand@env.ethz.ch (E. Lemarchand), Chabaux@illite.u-strasbg.fr (F. Chabaux).

0016-7037/$ - see front matter © 2010 Elsevier Ltd. All rights reserved.
doi:10.1016/j.gca.2010.04.057

Because Li is concentrated in silicates and because its isotopes fractionate during solid/solution interactions, lithium appears to be an ideal proxy for silicate weathering. Lithium has only two stable isotopes, ^{6}Li and ^{7}Li, with natural $^{7}Li/^{6}Li \sim 12$. The large relative mass difference between its two isotopes induces important isotopic fractionations during geochemical reactions, leading to a large range of isotopic compositions (noted $\delta^{7}Li$, see Tomascak, 2004 for a review) among various earth materials ($\delta^{7}Li$ ranges from $-15‰$ (relative to standard LSVEC) in peridotite and pyroxenite–xenoliths to $>+30‰$ in marine biogenic carbonates, Tomascak, 2004).

On the Earth's surface, large isotopic fractionations have been observed between solids and solutions. For instance, $\delta^{7}Li$ of the dissolved load in large rivers is systematically higher than that of the corresponding sediments, with values ranging from $+6‰$ to $+36‰$ in the dissolved load and from $-4‰$ to $+5‰$ for suspended sediments (Huh et al., 2001, 1998; Kisakurek et al., 2005). This difference was attributed to isotopic fractionation occurring during weathering processes, ^{6}Li being preferentially incorporated into secondary minerals (Huh et al., 2001, 1998; Vigier et al., 2008). Recent studies also suggest that $\delta^{7}Li$ of the river dissolved load is not directly related to lithology, but rather to the intensity and regime of silicate weathering at the scale of the basin (Vigier et al., 2009; Millot et al., 2010). In rivers draining an actively glaciated basaltic terrain, it has also been shown that the dissolved $\delta^{7}Li$ decreases with increasing weathering intensity (Pogge von Strandmann et al., 2006). Studies of lithium isotopes in soils and weathering profiles showed that ^{7}Li is preferentially leached from solids, decreasing the $\delta^{7}Li$ of the weathered horizons compared to the bedrock (Huh, 2004; Kisakurek et al., 2004; Rudnick et al., 2004). Pistiner and Henderson (2003) experimentally investigated Li adsorption at the surface of various minerals, and they showed that the isotopic fractionation is strongly dependant on the mineral on which Li is adsorbed and on the nature of the Li surface complexes. They found almost no isotopic fractionation during Li adsorption at the surface of illite (where Li is considered to be adsorbed as an outer sphere $Li^{+}(H_2O)_4$ complex) whereas strong isotope fractionation ($-13‰$) was observed during Li sorption at the surface of gibbsite (where Li would be adsorbed as an inner sphere complex with covalent bonds to the gibbsite surface). In contrast, Zhang et al. (1998) measured strong Li isotopic

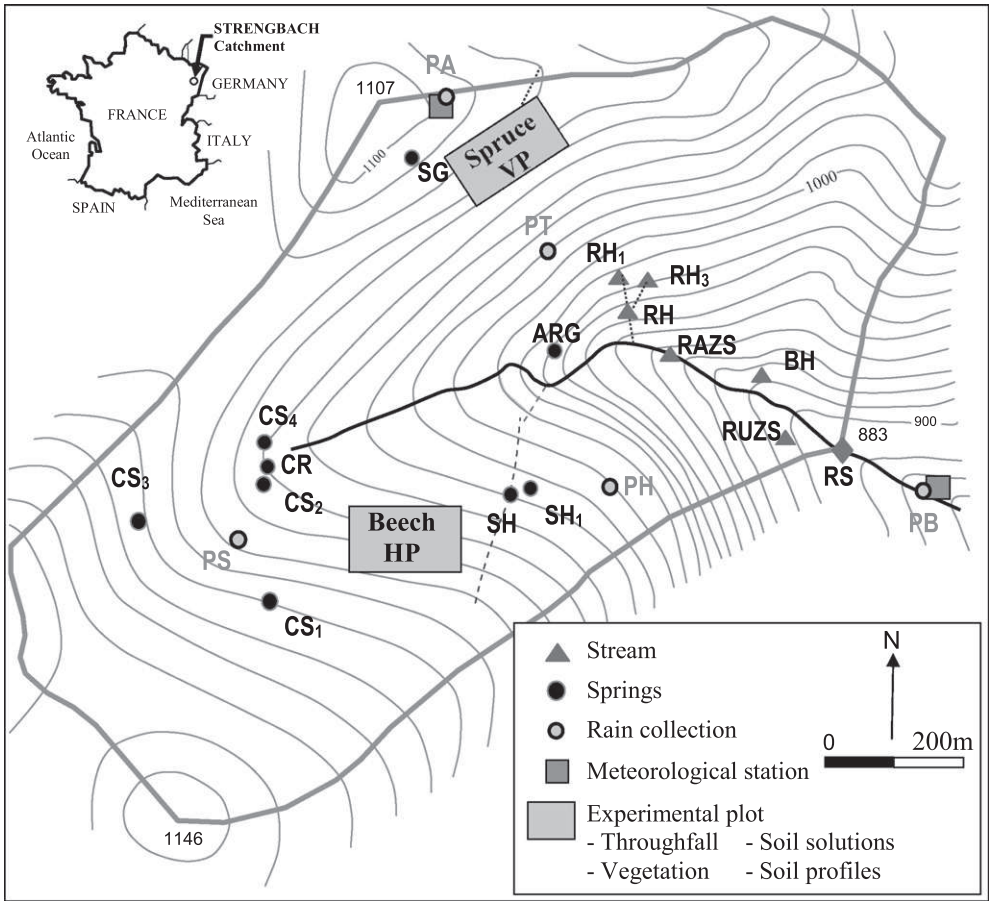

Fig. 1. The Strengbach catchment. RS is the catchment outlet; RAZS corresponds to the main stream upstream of the saturated zone area; RUZS, BH, RH, RH_1 and RH_3 are small tributaries; SG, ARG, CR, CS_1, CS_2, CS_3, CS_4, SH and SH_1 are springs; rain water was collected at PA, PB, PH, PS and PT; Two sites were studied in more detail: one under spruce (VP) and the other one under beeches (HP). On those two sites, throughfall samples were collected, as well as soil solutions, soils and vegetation.

fractionation during sorption to the surface of kaolinite (−21‰), vermiculite (−29‰) and Mississippi sediments (−21 to −24‰). Recently, it was found experimentally that the substitution of Li for Mg in smectite induces an isotopic fractionation of −10‰ at 25 °C (Vigier et al., 2008).

In parallel, the role of the biosphere has been little studied, and the implications of isotopic fractionation occurring in soils and saprolites on δ^7Li in rivers has not been investigated in detail. Our approach was to explore the behaviour of Li isotopes in the Strengbach catchment. This site is a small forested granitic catchment which offers the advantage that it has been intensively studied and monitored since 1986. Many studies have already provided constraints on hydrogeochemical fluxes and weathering processes in this catchment, using major and trace element concentrations, and isotope systematics (Sr, U-Th, Ca, B). In this study, we present the analyses of Li concentrations and isotopic compositions in the various compartments (i.e. rocks, soils, vegetation, soil waters, rainfall, springs and stream waters) of this catchment in order to better understand the behaviour of lithium isotopes during weathering processes.

2. SITE DESCRIPTION

The Strengbach forested catchment is located on the eastern part of the Vosges Mountains (NE of France) (Fig. 1). Its elevation ranges from 883 to 1146 m over an area of 80 ha. The bedrock is "The Brezouard granite", a leucogranite which has undergone hydrothermal alteration, particularly on the northern side of the catchment (El Gh'mari, 1995). In addition, a band of gneiss is in contact with the granite at the top on the north. A saprolite layer of locally up to 10 m thickness covers the bedrock. The soils that lie on the saprolite are acidic, rather deep (80 cm on average), coarse and contain 60% of sands on average (Fichter et al., 1998a, b). The soils composition differ from the north-facing (podzolic soils) to the south-facing slopes (brown acidic soils) of the catchment. 90% of the catchment area is covered by forests consisting of 80% of Norwegian spruce and 20% of mixed beech and silver fir.

The Strengbach zone has a temperate oceanic mountainous climate. Mean annual precipitation is about 1400 mm, and average monthly temperatures range from −2 to +14 °C (Probst et al., 1990; Probst, 1997). The snowfall period lasts from December to April. The snow cover is characterized by an important interannual variability and is often not continuous through the winter. The mean annual runoff is 850 mm, consisting of high flow from autumn to spring, and lowest water levels at the end of summer. A permanent water saturated zone (5% of the total study area), located at the outlet of the catchment, plays a significant role in the outlet flow, unusually during storm events (the saturated area can represent 30 to 39% of the total runoff during the first stage of a storm event. Ladouche et al., 2001).

The Strengbach catchment has been studied since 1986, originally to assess the effects of acid rain on a forested ecosystem (Dambrine et al., 1998b; El Gh'mari, 1995; Probst et al., 1990, 2000, 1995, 1992). It has now become an experimental basin (Hydro Geochemical Observatory of the Environment, http://ohge.u-strabg.fr) used to study and characterize hydrogeochemical mechanisms in forested ecosystems, using the geochemistry of major and trace elements, as well as various isotopic systems such as B, Ca, Sr, U-Th (Aubert et al., 2002b, 2004; Cividini et al., 2010; Dambrine et al., 1998b; El Gh'mari, 1995; Probst et al., 1990, 2000, 1995, 1992; Fichter et al., 1998b; Riotte and Chabaux, 1999). On two experimental plots (VP under spruce and HP under beeches on Fig. 1), polyethylene gutters and lysimetric plates installed at various soil depths allow the collection of throughfall samples and gravitational soil waters.

3. SAMPLING AND PROCESSING

For this study, 30 water samples were collected at regular intervals over 2 years (Fig. 1, Table 1). Fourteen correspond to various springs, one to the outlet, one to the mainstream before the saturated area, 5 are rain waters collected at various points in the catchment, 6 are gravitational soil solutions and 3 are throughfall (rain and throughfall samples were collected at 1 m up to the soil, avoiding interaction with soils). Waters were stored in polypropylene bottles previously washed with 1 M HCl, and were filtered at 0.45 μm at the laboratory. One aliquot (250 mL) was used for measurements of pH, alkalinity, dissolved organic carbon (DOC), and concentrations of major ions. Another aliquot (2 L when available) was acidified with 2% HNO_3 and was used for isotopic analyses.

Lithium concentrations were analysed in most of these samples and Li isotopic compositions were measured on 19 selected samples (see Fig. 1 for localities): springs (CR, SH, SG), small tributaries (RH, BH and RUZS), soil solutions (under spruce) (F-5, F-10, F-30, F-60), and stream waters above the saturated zone area (RAZS). All those samples were analysed for three contrasting hydrological events. We also analysed six samples of outlet water (RS) corresponding to various water discharges. Lithium concentration and isotopic composition were also analysed in granite, soils, and vegetation. As the saprolite layer is too thick, there is no outcrop of in situ fresh granite in the catchment area. Thus, we analysed a minimally weathered autochthonous rock. For soil and vegetation analyses, we chose to focus our study on site VP (under spruce).

Soils were dried in an oven (60 °C) until no significant mass change could be measured (several hours), and were then sieved at 2 mm. Soils and granite were crushed with an agate mortar and sieved to <100 μm. About 100 mg of the resultant powder was introduced into a 15 mL Teflon beaker and digested with a HF/HNO_3 mixture. Remaining organic matter was digested with 1 mL of $HClO_4$ for 1 day at 150 °C. The solution was then evaporated to dryness and dissolved again in HNO_3. The last step was repeated three times, and finally the sample was dissolved in 10 mL of 7 N HNO_3. After drying in a 60 °C oven, vegetation samples (needles, small roots, small branches and trunk wood) were reduced to a powder as fine as possible in an agate mortar. About 2 g were then introduced into a 120 mL Teflon beaker and were digested with 25 mL of concentrated HNO_3

Table 1
Lithium concentrations measured into rocks, soils, vegetation and waters of the Strengbach catchment.

Bulk soil																		Vegetation													
Soil depth (cm)	0–4		4–20		20–42		42–55		55–63		63–75		> 75		Parent granite			Tree section (spruce)			Small roots		Small branches			Needles		Young needles		Trunk		
[Li] (μmol/kg)	7470		14,780		18,559		17,637		17,641		17,399		18,422		19,341			[Li] (μmol/kg)			154		56			30		7.3		154		
Solutions (nmol/L)																															
		Springs and stream waters																Throughfall samples			Rain waters					Soil solutions					
Date	Outlet discharge (L/s)	CR1	CR2	CR3	CR4	CR	SG	SH1	SH	ARG	RH1	RH3	RH	RAZS	BH	RUZS	RS	PLH4	PLHx	PL5	PA	PB	PT	PH	PS	F-5	F-10	F-30	F-60	E4	E5	
05/07/04	4.8																94															
19/07/04	5.1																80															
26/07/04	3.8																76															
02/08/04	3.2																80															
06/09/04	8.9																85															
28/09/04	5.56	99	113			98	395			108			113	85	109	64	76	7.6	7.1							339	925	894		268			
02/11/04	59.3					89						117					80	5.2		14	1.4			1.2		478	816	639	398	281	80	
13/12/04	21.9	106	105	68	85	94	368			110		116			127	86	85			54	2.0					423	756	498	153	224			
24/01/05	42.6					89			126			104					93	6.9		13	4.6	2.4	2.3	3.2		385	569	599	322	149	53	
07/03/05	8.37											92			100			5.0			4.6	7.9	12			226	543	751	43	112	67	
29/03/05	48.7	89		59		75			120	90		99			141	91	87	13								176	236	362	268	86	60	
03/05/05	22.7	82	77	54	58	89	265	130	115	99		85		70	102	66	81		7.8	14	6.1			35	4.9	165	299	344		157	66	
31/05/05	11.7	103	98	62	75	90	328	147	173	97		95			110	71			12		3.9	3.0	2.9	4.5		140	297	349		125			
11/07/05	3.85	107	96	64	86	90	336			98	73	132	105		107	56	83		6.1	32	2.3	1.9	1.7		2.0	112	180	490		184		
25/07/05	13.2																92															
08/08/05	5.6																85															
22/08/05	6.9	107	101	61	87	100	356	157	172	103	65	123	101		112	102	89		8.5		2.7	2.9		3.2	5.9	259	443	622		211	80	
05/09/05	5.3																81															
19/09/05	14.9																84															
03/10/05	14	96		61		97	307		155						107		84		5.8		2.4	2.2			2.9	254	435	618	268	198	92	
09/11/05	5.34				86	105				101		115	110	79	111	64	78			58	2.3	2.3		2.9		364	377		251			
07/02/06	8.2	95	98	58	78	90			151			103						13			10	4.5		10	5.2	395	167	472	183	179	29	
03/04/06	120	84	76	58	55	81	293	113	128	81	163	88	91	93	133	110	105	3.3			1.7	1.6	1.6	2.4	2.0	348	309	550	198	165	79	
22/05/06	10.7	86	84	55	67		314	134		81	68	88	82	71	107		89		5.8	26		3.3		5.2	5.8		359	342		107	49	
10/07/06	3.6	107	123	69	132					106	70	126	101		121	51	79	11		40	8.6	4.1	3.8	5.1	5.6	222	461	479	346	157	89	
24/07/06	3.6																83															
07/08/06	4.1																77															
21/08/06	22.4	84	88	55	66	70	319		148	85		91	88	74	116	83	97		8.6	15	1.5				0.8	224	109	475	251	141	71	
04/09/06	18.2																81															
02/10/06	35	98	99	63	77	82	343		168	97	89	105	94	85	122	102	96	7.3	6.5	15	16	6.2	4.9	28	2.8	247	197	550	278	227	82	
Mean	20.6	96	97	60	79	89	330	136	146	97	88	105	98	80	115	79	85	8.0	7.6	28	4.7	3.5	4.2	9.1	3.8	280	415	531	247	175	69	

and some drops of H_2O_2. After 5 days, the solution was evaporated to dryness and the resultant solid was dissolved again in ~10 mL of HNO_3 and transferred to a 15 mL Teflon beaker. The sample was then evaporated, and remaining organic matter was digested with 1 mL of $HClO_4$ for 1 day at 150 °C. $HClO_4$ was evaporated and the sample was dissolved again in HNO_3 and evaporated three times. Finally, the sample was dissolved in 10 mL of 7 N HNO_3.

4. ANALYTICAL METHODS

4.1. Li concentrations

Li concentrations were determined both by ion chromatography and Quad-ICP-MS. More than 200 samples were analysed using each method, resulting in 374 Li concentrations and the inter-comparison of 45 samples.

Ion chromatographic measurements were performed using a Dionex ICS-3000 ion chromatography system, with a CS16 (5*250 mm) column. To obtain a good signal/noise ratio, the injection loop volume was chosen equal to 400 µL. A calibration curve was determined using homemade standards (14.4, 28.8, 72.0, 144.1 and 360.2 nmol/L Li) and normalised to CGLi1-1 (Inorganic Ventures) certified standard. Blanks are lower than 3 nmol/L (~2.4 10^{-4} µS min), the detection limit is 2.2 nmol/L, and the external reproducibility varies from 13% at 15 nmol/L to 2% at 150 nmol/L and higher concentrations (2σ, $n = 28$).

ICP-MS measurements were performed using a Thermoelectron X series II. Standard solutions (2.9, 28.8 and 288 nmol/L) were prepared from CGLi1-1 standard and Be was used as an internal standard. Blanks are lower than 1.4 nmol/L, the detection limit is 0.4 nmol/L and external reproducibility varies from 8% at 3 nmol/L to less than 1.5% at 300 nmol/L (2σ, $n = 10$).

For Li concentrations higher than 60 nmol/L, both methods are in good agreement ($R^2 = 0.9993$ $Y = 0.992X + 10.057$, Fig. 2A), whereas for concentrations lower than 15 nmol/L (i.e. rain water and throughfall) there is an important discrepancy between values obtained by Quad-ICP-MS and ionic chromatography. Due to the lower detection limit and better external reproducibility obtained by Quad-ICP-MS (than by ionic chromatography) we used only Quad-ICP-MS values for rain waters and throughfall samples.

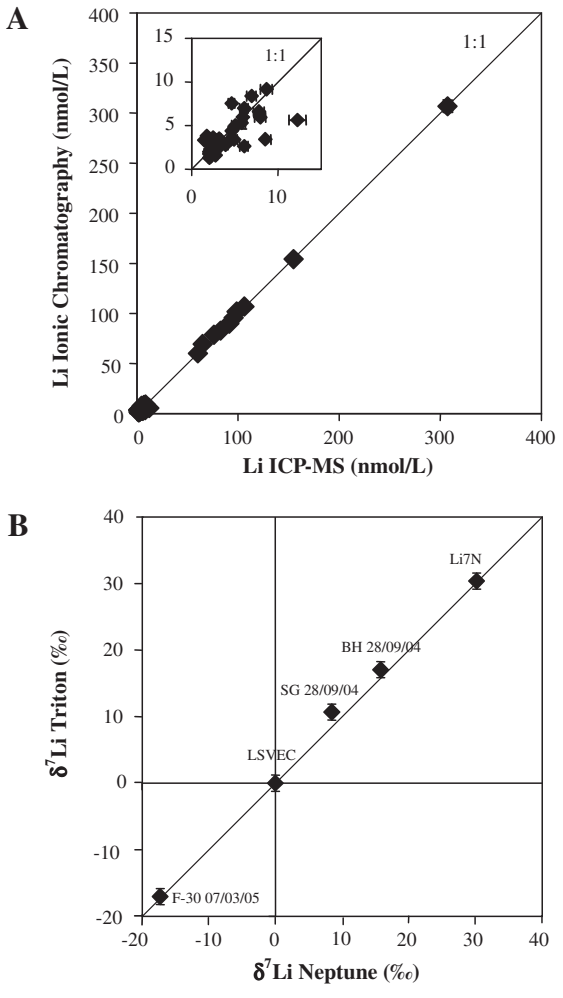

Fig. 2. (A) omparison between Ionic Chromatography and quadrupolar ICP-MS measurements of Li concentrations in water samples. (B) Comparison between Triton TIMS (CGS Strasbourg) and Neptune MC-ICP-MS (BRGM- Orléans) measurements of Li isotopic compositions in natural waters and standards.

4.2. Li isotopic ratios

Lithium was first separated from the matrix using a cation exchange column. After purification, some isotope analyses were performed on a Neptune MC-ICP-MS at BRGM Orléans, whereas others were performed on Triton P-TIMS at CGS (now the LHyGeS)-Strasbourg. All results were normalized to the international standard LSVEC (Flesh et al., 1973) according to the following equation:

$$\delta^7\mathrm{Li} = 1000 * \left(\frac{(^7\mathrm{Li}/^6\mathrm{Li})_{\mathrm{sample}}}{(^7\mathrm{Li}/^6\mathrm{Li})_{\mathrm{LSVEC}}} - 1 \right) \quad (1)$$

4.2.1. Li purification

The entire procedure for chemical purification was described in details by Vigier et al. (2008) and Millot et al. (2004). Briefly, a required volume of solution (corresponding to 30 and 100 ng Li for analyses with Neptune and Triton, respectively) was evaporated to dryness on a hot-plate at 120 °C, dissolved in HCl 1M and passed through a cation exchange column (50W-X12, 200–400 mesh) to separate Li. Because of the partial overlap between Na and Li elution peaks, this procedure was performed twice to fully eliminate sodium. Finally, the sample was evaporated to dryness.

4.2.2. δ^7Li measurements with Neptune MC-ICP-MS

Most of the δ^7Li measurements in waters were performed on the Neptune MC-ICP-MS at BRGM's Isotopic Geochemistry Laboratory. The measurement procedure was described in detail by Millot et al. (2004). Briefly, after lithium purification, the dried sample was dissolved in 3% v/v HNO_3. The volume of HNO_3 solution was chosen to

obtain a Li concentration of 30 ng ml^{-1}. The analytical protocol involved the acquisition of 15 ratios with 16 s integration time per ratio, and yielded in-run precisions 0.2‰ ($2\sigma_m$). The sample introduction rate was about 80-100 µl min^{-1} and the total volume of sample used for each measurement was less than 500–600 µl, corresponding to about 15–20 ng of Li (for a sample solution at 30 ng ml^{-1}).

Instrumental mass bias was corrected for by reference sample bracketing. The measured ^{7}Li/^{6}Li ratio of a sample was normalized to the mean ^{7}Li/^{6}Li ratio of the two LSVEC reference samples run immediately before and after the sample. Blank values were low, typically 3–4 mV for ^{7}Li (i.e. 0.2%), and 5 min wash time was enough to reach a stable background value. Repeated analyses of seawater demonstrate that the external reproducibility is 0.5‰ (2σ, $n = 31$) (Millot et al., 2004)), with a δ^7Li value of 31.0‰, in good agreement with literature values (James and Palmer, 2000; Nishio and Nakai, 2002).

4.2.3. δ^7Li measurements with Triton P-TIMS

Li isotope analyses of waters from 22/05/2006, rock, soils and vegetation were performed on a Triton TIMS at CGS in Strasbourg, using a double filament method, modified from James and Palmer (2000). First, the dried sample (100 ng of Li) was dissolved in 1 µL of 0.1 M H_3PO_4 and 4 µL of H_2O, loaded onto a Re filament, evaporated with a current of 1 A and heated slowly to 2 A until fumes were no longer observed. In the Triton source, the current of the ionisation filament was increased until the temperature measured by the optical pyrometer was 1050 °C. Then, the evaporation filament was heated slowly until the ^{7}Li signal was 30 V. For the Triton, the distance between the two extreme Faraday cups is large enough to analyse ^{6}Li and ^{7}Li simultaneously, and our measurements were performed in static mode. We observed that the beam focus could change the value of ^{7}Li/^{6}Li. Moreover, the ^{7}Li/^{6}Li varied during the first cycles. However, after $\sim$ 500 cycles (4 s per cycle), ^{7}Li/^{6}Li stabilised and remained constant through time. When this plateau was reached, we focused the signal and recorded the following 500 cycles. With this method the obtained in-run precision was typically ±0.2‰, and it was always better than ±0.45‰ ($2\sigma_m$). Repeated measurements of isotopic standards LSVEC and Li7-N (Carignan et al., 2007) performed during different analyses sessions provided an external reproducibility better than ±1.3‰ (2σ, $n = 13$). The average value obtained for Li7N was equal to 30.4 ± 0.6‰ ($n = 5$), in very good agreement with the value reported by Carignan et al. (2007) (30.2 ± 0.3 ‰, $n = 89$). The comparison of analyses of standards and natural samples performed on both Neptune and Triton instruments showed a good agreement between these two methods (Fig. 2B), enabling us to precisely and accurately determine Li isotopic ratios in our samples.

5. RESULTS

5.1. Li concentrations

The lowest dissolved concentrations are observed in rain waters (mean [Li] = 5 nmol/L) whereas the highest are measured in soil solutions (mean [Li] = 299 nmol/L) (Table 1). In springs and stream waters, Li concentrations are intermediate and vary between 60 nmol/L in spring CS3 and 330 nmol/L in spring SG. The mean concentration at the outlet (RS) is 85 nmol/L (ranging from 76 to 105 nmol/L). Li concentrations in vegetation are extremely low compared to soils and rocks, with values 3–4 orders of magnitude lower. Li is slightly less concentrated in soils than in bedrock, but the range for the bedrock might be larger than exhibited by our sample. Moreover, it is clear that Li concentrations in soils, normalized to an element known to be immobile during weathering such as Zr, are low relative to the bedrock and decrease in surface horizons (Fig. 3A). In contrast, Li concentrations normalized to a mobile element such as Na increase from bedrock to the deepest soils (Fig. 3B).

In order to correctly compare the Li concentration of the various water samples without the effect of dilution, it is useful to normalize it to the concentration of another dissolved element. Normalised to soluble elements such as Na or Ca, Li concentrations in waters (soil solutions, springs, stream and rain waters) are also quite variable. Those variations depend on both the date and the location of the sampling, as can be seen in Li/Ca versus Li/Na elemental ratio diagrams (Fig. 4). Rain and throughfall values overlap the entire range of springs and stream waters values, whereas the soil solutions are characterized by higher Li/Ca ratios.

In detail, Li concentrations can be used to define three groups of springs: The north springs (SG, RH1, RH3, RH, ARG, BH), the south west springs (CS1, CS2, CS3,

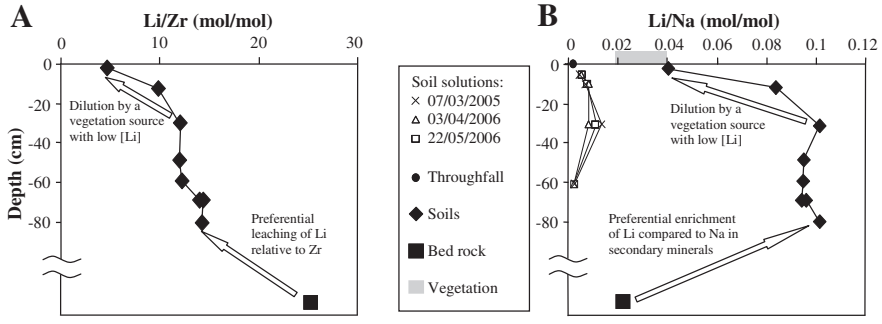

Fig. 3. Li evolution in the soils under spruce as a function of depth. (A) Li/Zr ratio in soils and bedrock. B: Li/Na in soils, bedrock, vegetation, throughfall and soil solutions.

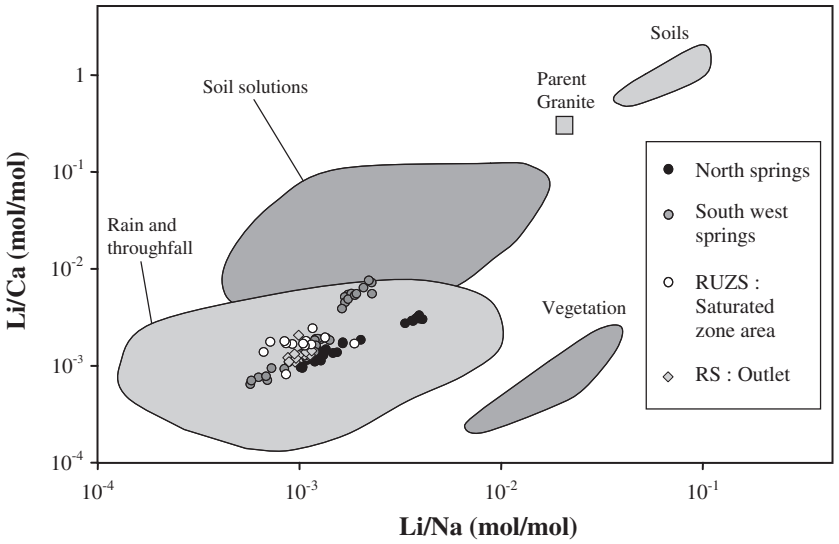

Fig. 4. Li/Ca versus Li/Na concentrations measured in waters, soils, granite and vegetation of the Strengbach catchment. For better visibility, only one point out of three corresponding to springs and stream waters is represented.

CS4, CR, SH, SH1) and the saturated zone area (RUZS) (Fig. 4). The same patterns are observed for other elements such as Na, Ca, and Mg (Prunier, 2008). Each one of those groups defines distinctive co-variation trends in the Li/Ca versus Li/Na diagram. It appears that these ratios for soils are higher than for parent granite whereas they are the lowest for waters (springs and stream). If we consider that the main source of Li into soils and waters is the parent granite, the observed alignments could then be explained by a chemical fractionation during weathering, with Li being released into waters at a different rate than Na and Ca. However, it is known that the bed rock of this catchment is not totally homogeneous. The northern side granite has undergone hydrothermal alteration and banded gneiss is located at the top of this side (El Gh'mari, 1995). Thus, the slight difference observed on Fig. 4 between the alignment of north and south west springs can be also attributed to the two different lithologies: non-hydrothermalized granite for south west springs and hydrothermally altered granite for north springs.

Rain and throughfall samples have a much larger range of values than the spring and stream waters in the Li/Ca versus Li/Na diagram (Fig. 4). Our data allow us to evaluate the cause of this dispersion in elemental ratios. Dissolved elements in rain waters can originate from three distinct sources: the ocean, the interaction of rain water

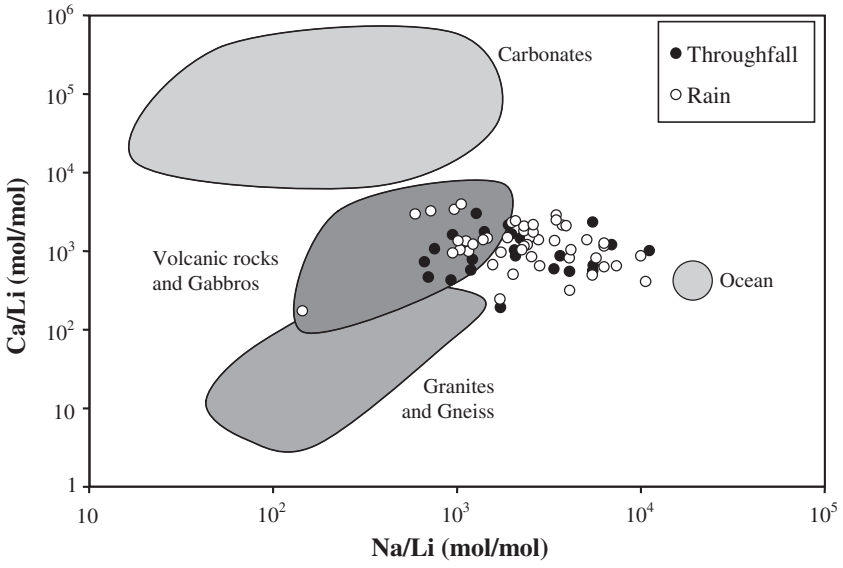

Fig. 5. Ca/Li versus Na/Li measured in rain and throughfall. Grey areas represent ocean, silicate, and carbonate end members. To determine silicate and carbonate end members, we compiled standard values extracted from the GeoRem database (Jochum et al., 2005 and see http://georem.mpch-mainz.gwdg.de).

Table 2
Na, Ca, CI and Li concentrations, and Li isotopic compositions ($\delta^7Li = 1000*(({}^7Li/{}^6Li)_{sample}/({}^7Li/{}^6Li)_{LSVEC}-1)$) of rock, soils, vegetation and waters selected for the isotopic study.

	Date	RS discharge	Na (μmol/L)	Ca (μmol/L)	Cl (μmol/L)	Li (nmol/L)	δ^7Li (‰)
Springs and stream waters							
CR	28/09/04	5.56	96	74	53	97	+6.6
	03/04/06	120	75	71	49	81	+10.3
	22/05/06	10.7	83	66	47	79	+8.2
SG	28/09/04	5.56	103	125	50	395	+8.5
	03/04/06	120	72	91	34	293	+6.2
	22/05/06	10.7	90	111	40	314	+7.4
SH	28/09/04	5.56	84	23	49	187	+5.3
	03/04/06	120	68	24	44	128	+8.7
	22/05/06	10.7	76	24	43	153	+7.4
RH	28/09/04	5.56	97	106	61	113	+9.6
	03/04/06	120	81	85	54	91	+8.1
	22/05/06	10.7	84	83	48	82	+8.8
RAZS	28/09/04	5.56	90	77	54	85	+15.1
	03/04/06	120	76	67	52	93	+11.5
	22/05/06	10.7	84	68	51	71	+14.0
BH	28/09/04	5.56	100	95	66	109	+15.8
	03/04/06	120	81	76	48	133	+10.9
	22/05/06	10.7	84	75	39	107	+13.9
RUZS	28/09/04	5.56	89	36	20	64	+19.6
	03/04/06	120	82	56	53	110	+9.1
	22/05/06	10.7	63	41	10	67	+16.6
RS	28/09/04	5.56	90	70	53	76	+16.9
	02/11/04	59.3	84	73	57	80	+13.2
	29/03/05	48.7	79	68	56	87	+13.8
	03/05/05	22.7	76	63	44	81	+14.8
	11/07/05	3.85	80	63	41	83	+16.8
	03/04/06	120	76	64	52	105	+12.4
	22/05/06	10.7	82	64	45	89	+16.8
Throughfall							
PL5	02/11/04		13	6	16	14	−1.1
Soil solutions							
F-5	07/03/05		55	17	66	226	−10.7
	07/02/06		87	33	135	395	−4.6
	03/04/06		71	21	68	348	−6.0
	22/05/06		46	17	33	233	−7.9
F-10	07/03/05		82	18	111	543	−16.6
	07/02/06		40	10	54	167	−9.7
	03/04/06		39	12	40	309	−10.7
	22/05/06		49	15	33	359	−7.4
	07/03/05		57	15	84	751	−17.3
	07/02/06		70	14	112	472	−14.5
	03/04/06		69	15	79	550	−14
	22/05/06		31	8	29	342	−11.9
	07/03/05		19	2	10	398	+33.1
	03/04/06		100	12	79	198	+28.0
	22/05/06		117	7	61	218	+31.0

Soil depth (cm)	Na (mmol/kg)	Ca (mmol/kg)	Li (mmol/kg)	δ^7Li (‰)
Bulk soil				
0–4	185	12	7.5	+0.4
4–20	176	13	15	+3.2
20–42	183	11	19	−1.1
42–55	185	13	18	+0.8

Table 2 (*continued*)

Soil depth (cm)	Na (mmol/kg)	Ca (mmol/kg)	Li (mmol/kg)	δ^7Li (‰)
55–63	186	13	18	+3.3
63–75	185	13	17	+0.9
>75	182	15	18	+0.7
Parent granite	888	59	19	+0.3

Tree section	Na (mmol/kg)	Ca (mmol/kg)	Li (μmol/kg)	δ^7Li (‰)
Vegetation (spruce)				
Small roots	4.1	66	154	−4.3
Small branches	2.8	54	56	−7.4
Needles	30	30	30	−4.3
Young needles	7.0	7.1	7.3	−6.0

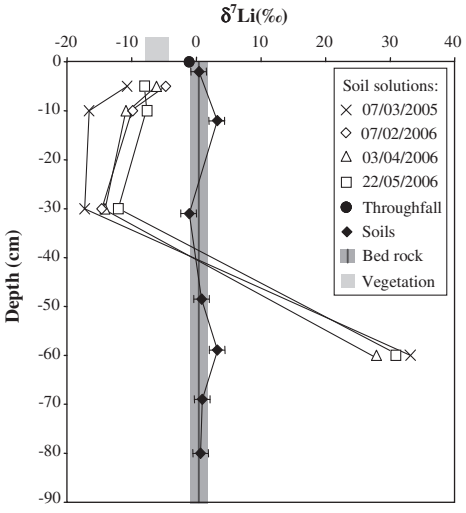

Fig. 6. Lithium isotopic compositions measured within the VP (under spruce) experimental site. ($\delta^7Li = 1000^*((^7Li/^6Li)_{sample}/(^7Li/^6Li)_{LSVEC}-1)$.

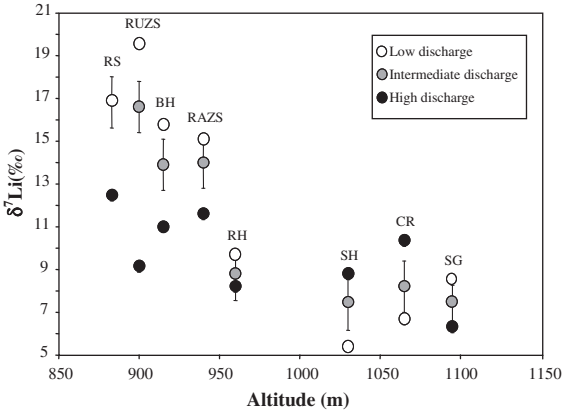

Fig. 7. Lithium isotopic compositions in springs and stream water samples as a function of altitude for the three different sampling discharges.

with atmospheric dust (silicates and carbonates), and finally from vegetation exudates (in throughfall). This last source

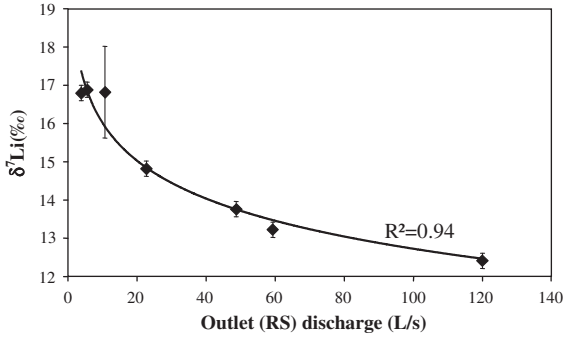

Fig. 8. Dissolved Li isotopic compositions measured at the outlet as a function of water discharge.

can affect fluxes of Ca and K for instance, but in contrast is not significant for Na (Cenki-Tok et al., 2009; Chabaux et al., 2005; Dambrine et al., 1998a; Schmitt and Stille, 2005). Because the Li/Na ratio in vegetation is clearly higher than that of the rain waters (Fig. 4), a Li flux from vegetation would be characterized by a higher Li/Na ratio in throughfall compared to rain samples, which is not the case (Fig. 5). In contrast, in the Ca/Li versus Na/Li diagram, rain water and throughfall seem to define the same dispersion area, without any apparent influence of the vegetation endmember, indicating that vegetation weakly (or does not) affects the Li concentration of rain water. In other words, Li in throughfall principally comes from atmospheric input without any significant influence from vegetation, despite the dense forest cover. Thus, the highest Li concentrations measured in throughfall compared to rain waters (Table 1) can be explained by the leaching of atmospheric aerosols deposited onto the leaves and the needles. As a consequence, rain and throughfall chemistry should define a mixture between an oceanic endmember and a dust endmember. The dispersion of the points representing rain water and throughfall must be explained by a mixture between at least three endmembers (Fig. 5). We propose that one is the ocean, and the two others come from rain interactions with at least two different lithogenic dusts, likely two different silicates but a carbonate contribution can not be excluded. As can be seen on Fig. 5, the mixture between these three endmembers can explain the compositions of all the rain water and throughfall samples.

5.2. Li isotopic compositions

Li isotopic compositions of solids show little variation from sample to sample. The δ^7Li values of soils are close to those of the parent granite (+0.3‰) within error (in good agreement with published values in granites (+0.4‰ to +1.2‰, James and Palmer, 2000; −2.5‰ to +2.7‰, Teng et al., 2004), and no clear relationship with depth is observed (Table 2, Fig. 6). The δ^7Li signature of different parts of trees from the same plot (roots, branches, needles), from −4.3 to −7.4‰, are in the same range as those of shallow soil solutions (Table 2). We therefore propose that the Li uptake by vegetation comes from soil solutions. The results obtained here do not allow interpretation of possible Li isotopic fractionation inside the tree. However, biological uptake and vegetation recycling do not seem to affect Li isotopes in the first layer of the soil. The lack of resolvable influence from litter degradation on Li isotope composition in soils is not surprising, since the Li concentration in vegetation is three orders of magnitude lower than in soils (Table 1). Thus, the first layer of the soil appears to be a mixture between mineral soil and organic litter, with soil–Li being diluted by litter, explaining its low Li/Na (Fig. 3B).

In contrast, the dissolved Li isotopic compositions are very variable, ranging from +5.3‰ to +19.6‰ in springs and stream waters, and from −17.3‰ to +33.1‰ in soil solutions. This range of isotopic composition is extreme, and it is remarkable that at the scale of such a small basin, we observe a range in Li isotope compositions similar to the entire terrestrial range (−15‰ to >30‰, Tomascak, 2004). In the upper layers of the soils, dissolved δ^7Li decreases from −1‰ at 0cm (throughfall) to −17‰ at −30 cm, and then strongly increases up to +33‰ at −60 cm. These huge variations are reproducible over time and do not seem to be affected significantly by water fluxes and seasonal changes (Table 2, Fig. 6).

It is also remarkable that at low and intermediate discharge, the dissolved Li isotope composition in springs and stream waters is strongly influenced by altitude: δ^7Li of springs located at the top of the catchment (CR, SG, SH, RH, elevation > 950 m) range from +5.3‰ to +10.3‰, whereas in waters sampled at the bottom of the basin (RAZS, BH, RUZS, elevation<950m) δ^7Li varies from +9.1‰ to +19.6‰ (Table 2, Fig. 7). The relationship between δ^7Li and water discharge is not simple at the top of the catchment (δ^7Li increases with increasing discharge for CR and SH, whereas it decreases for SG and RH). In contrast, for the samples located below 950 m, δ^7Li systematically decreases with increasing discharge (Fig. 7), and a clear relationship between δ^7Li and water discharge is observed at the outlet of the basin (Fig. 8).

6. DISCUSSION AND MODELLING

6.1. Determining Li atmospheric and biologic contribution

6.1.1. For the stream

Taking into account the mean annual runoff (810 mm/year during the sampling period, OHGE data), the total surface area of the basin (80 ha) and the mean Li concentration at the outlet of the basin (85 nmol/L), it is possible to determine the amount of lithium exported from the catchment each year (55.2 mol/year). Atmospheric inputs can also be calculated, using the mean annual precipitation (1515 mm/year during the sampling period, OHGE data), and the mean Li concentration in rain waters (5 nmol/L). Thus, rain waters provide 6.1 mol/year of lithium to the catchment, which represents 11% of lithium exported at the outlet. However, rain waters collected outside the vegetal cover probably do not represent all the atmospheric lithium flux to the catchment. As 90% of the basin surface is covered by forest, and as a large part (not to say the main part) of Li in throughfall certainly comes from leaching of atmospheric aerosols deposited onto the leaves and the needles (cf. §5.1.), the estimate of atmospheric Li input must be calculated with Li concentrations measured in throughfall and not only in rain water collected outside the vegetal cover. During our sampling period, the mean annual throughfall precipitation was 820 mm, and the mean Li concentration was 21.6 nmol/L. Over 90% of the basin area, this corresponds to 12.8 mol Li/year. Adding the rainfall flux over the 10% of the basin not covered by trees, the total atmospheric Li input is 13.4 mol Li/year, which represents 24.2% of lithium exported to the outlet. An alternative method for calculating the atmospheric contribution on the Li budget is to use the mean annual Li/Cl ratio in rain ($8.12\ 10^{-4}$ mol/mol) and throughfall ($5.87\ 10^{-4}$ mol/mol) and the mean annual Cl concentrations in the stream ($4.95\ 10^{-2}$ mmol/L). The implicit assumption for such a calculation are that Cl behaviour is conservative in the basin, and that Cl in the stream only originates from atmospheric inputs. A simple calculation based on the mean annual precipitation and runoff shows that the second hypothesis is not verified in the Strengbach catchment: atmospheric Cl represents only 70% of the Cl exported at the outlet, which means that 30% comes from a local source which is not identified. Considering that only 70% of the Cl concentration measured at the outlet originates from atmospheric inputs, we calculated that atmospheric Li input represents 25.8% of the dissolved Li in the stream at the outlet, in very good agreement with the calculation based on water fluxes.

Table 3
Li annual fluxes along the soil profile, calculated using Cl as a conservative element or using a hydrological model (from Cenki-Tok et al., 2009).

		Li Flux (kmol/m^2/s)	
	Depth (cm)	Calculation with Cl fluxes	Calculation with hydrological model
Soil solutions under spruces	0	29	29
	−5	160	287
	−10	267	401
	−30	283	480
	−60	87	221
Soil solutions under beeches	0	9.5	9.5
	−10	122	220
	−70	40	80

However, this does not mean that ~25% of the lithium exported at the outlet comes directly from precipitation, because most of it would interact with soil and rock before being released to the stream water. This would imply, however, that at least 75% of lithium exported from the basin comes from soils and rocks weathering.

Another factor likely to impact Li behaviour is its recycling by vegetation. Assuming that the biomass is at steady state, uptake of Li by vegetation should be equal to the litter fall Li flux. Li concentration was not measured in litter, but we can consider that the average Li concentration in needles and small branches is a good approximation. Taking 300 g m^{-2} $year^{-1}$ for litter fall (a common value for temperate forests, Bray and Gorham, 1964), we calculated that this Li input into the soil is equal to 13 μmol m^{-2} $year^{-1}$. This represents 10 mol/year at the basin scale, i.e. 18% of Li exported at the outlet, but most of this Li is probably stored in the soils as adsorbed and coprecipitated Li. This calculated flux is a maximum, but it is known that in this basin the biomass is increasing, and the litterfall is clearly overestimated in our calculation. Thus, the impact of vegetation on Li behaviour at the basin scale appears very limited compared to weathering reactions.

In summary, these mass budgets confirm that most of the Li flux in springs and stream waters originates from weathering reactions, and that the observed variations in concentration as well as concentration ratio observed in springs and stream waters at the basin scale cannot be explained by variable contributions from the atmospheric or biologic pools. This is also supported by the linear trends defined by springs and stream waters in Fig. 4, between two end members which are neither vegetation, nor rainfall or throughfall. Thus, weathering reactions clearly appear to be the major controlling factor for Li concentrations in surface waters at the basin scale.

6.1.2. For soil solutions

Li fluxes in soil solutions across the different sampling depths can be calculated in two different ways. The first method is based on Cl concentrations, considering that all dissolved Cl comes from atmospheric inputs and that its behaviour is conservative during water transfer into the soils (neither adsorbed by plants or minerals, nor released by the soils).

In these conditions, the Li annual input flux (F_{Li}) at each depth is calculated through the following equation:

$$F_{Li} = \frac{C_{Li}}{C_{Cl}} * F_{Cl}^{0} \quad (2)$$

where C_{Li} and C_{Cl} are the respective concentrations of Li and Cl at the given depth and $F_{Cl}{}^{0}$ is the Cl flux from throughfall. Results of this calculation for the sampling period (09/2004–10/2006) are given in Table 3. In both plots (under spruce (VP) and under beeches (HP)), they show a strong Li input in the top layers of the soil, and a Li sink in the deepest horizons. Those results also show that throughfall represent only 8% and 11% of the Li flux measured at −10 cm for the HP and VP, respectively. However, such an assumption of conservative behaviour of Cl in soil waters, and hence such a calculation approach, has been questioned by recent works which have shown that dissolved Cl in soils can be complexed by organic matter or taken up by vegetation (Bastviken et al., 2007; Rodstedth et al., 2003). However, from these recent works, the extent of these processes remains quite limited and could affect about 25% of dissolved chloride. If such processes occur in the Strengbach soils, calculated Li fluxes in soil solutions would be modified. However, this would not change our major conclusions. The proportion of atmospheric Li in the top soil horizons would be relatively low compared to the total Li flux.

The second method used to calculate fluxes in soil solutions consists of using a hydro geological model to determine the water flow at each considered depth. This was the approach used by Goddéris et al. (2006) in their modelling of weathering fluxes, and in recent studies of Ca and B isotope behaviours in this catchment (Cenki-Tok et al., 2009, Cividini et al., 2010). The results obtained with those models are presented in Table 3. They differ from the results obtained using Cl fluxes but give the same kind of variations, with a systematic flux increase in the upper soil layers implying that the proportion of atmospheric Li rapidly becomes low. Thus, whatever the calculation method used, the results show that even in surface horizons, the contribution of atmospheric Li is not dominant in soil solutions and remains lower than 11% of the total Li flux below −10 cm.

Another Li input into the soil is the litter fall. We calculated that this Li input into the soil VP (under spruce) is equal to 13 μmol m^{-2} $year^{-1}$ (cf. § 6.1.1.), which represents only 10% of dissolved Li at -5cm and less than 6% at −30 cm (with the hypothesis that all Li contained in the litter is dissolved, which is probably not the case). Overall these results mean that most of the dissolved Li in soil solutions comes from water/mineral reactions (at least 72% at −5 cm and 84% at −30 cm), and are only slightly affected by atmospheric input and biological processes. This certainly explains why in soil solutions Li concentrations are positively correlated with chemical elements brought into soil solution by water/rock interactions, such as Si, Na and Al, and are not correlated with elements known to be affected by biological cycles in this basin, such as K, Ca and DOC (not shown). Consequently, as for Li concentration in spring and stream waters, variations of Li concentrations in soil solutions and their isotopic variations are explained by mineralogical reactions.

6.2. Reactive transport models

6.2.1. Modelling soil solution δ^7Li

From the previous discussions, and regardless of the estimation method used, the Li flux in soil solutions strongly increases from the surface to −30 cm, and then decreases until −60 cm. Those variations cannot be linked to plant cycling in the upper part of the profile; thus, they must be explained by water–rock interactions. For all sampling periods, and also on average, soil solution δ^7Li is systematically low when Li input flux is high, and vice-versa at depth. Goddéris et al. (2006) simulated the concentration of major species within the same soil profile using a numerical model of chemical weathering in soil horizons and underly-

ing bedrock (WITCH) coupled to a numerical model of water and carbon cycles in forest ecosystems (ASPECTS). They proposed that secondary minerals dissolve at the top of the profile, and others precipitate in the deepest soil layers. The variations of the soil Li/Zr ratio with depth in the first meter of the soil (Fig. 3A) indicate that Li is leached during granite weathering in agreement with the behaviour of this element; however, the higher Li/Na and Li/Ca ratio in soils than in the parent granite, and the lower Li/Na and Li/Ca values in surface waters, indicate that Li is less mobile than cations such as Na or Ca. This chemical fractionation between Li and other cations can be attributed to Li preferential uptake in precipitated secondary minerals such as clays or oxides which are known to incorporate Li during precipitation (Pistiner and Henderson, 2003; Vigier et al., 2008). These minerals are present in soils, the saprolite and rocks of the catchment (clays, mainly smectite and illite, could comprise up to 30% and Fe-oxides up to 5% in rocks and soils (El Gh'mari, 1995; Fichter et al., 1998b). Goddéris et al. (2006, 2009) show the key role played by smectite and illite in understanding cation concentrations (Mg, K, Ca) in the stream and along the soil solution profiles. Thus, a scenario like the one proposed by Goddéris et al. (2006, 2009) could reconcile, in a simple manner, the variations of the Li fluxes observed in the soil solutions. The Li isotopic data in the present study bring an additional constraint to the discussion below.

Isotopic measurements and calculations were performed only on the spruce plot, which is the site where the soil solutions were analysed along the profile at four different depths. Within uncertainties, Li depletion in soils compared to granite does not seem to significantly induce isotopic variation (Fig. 6). This is in agreement with dissolution of primary minerals without any Li isotopic fractionation (Pistiner and Henderson, 2003). In soil solutions, the isotopic variations are large, with negative values in all layers of the soil (−5‰ to −17‰), except very positive values at −60 cm (+28‰ to +33‰). Related to the Li fluxes calculated previously (§6.1.2, Table 3), these isotopic variations have to be explained by a preferential input of ^{6}Li to the soil solutions within the upper 30 cm of the soil, compared to a loss of ^{6}Li between −30 and −60 cm.

Considering secondary phase dissolution in the upper soil, the isotopic composition of Li flux added to the soil solutions between 0 and −30 cm depth can be calculated by the following mass budget:

$$\delta_{sp} = \frac{F_{-30}\delta_{-30} - F_{th}\delta_{th} + F_{veg}\delta_{veg}}{F_{-30} - F_{th} + F_{veg}} \quad (3)$$

where are the isotopic composition δ_{sp} (to be calculated), δ_{-30} (average = −14.4‰), δ_{veg} (average = −5.5‰) and δ_{th} (=−1.1‰) are the isotopic composition (‰) of secondary phases (assumed to be equal to the isotopic composition of Li flux added to the soil solutions between 0 and −30 cm depth), soil solution at −30 cm, vegetation uptake and throughfall respectively, and F_{-30} (284 or 479 μmol m^{-2} $year^{-1}$ calculated from the Cl budget or hydrological budget respectively), F_{veg} (13 μmol m^{-2} $year^{-1}$) and F_{th} (29 μmol m^{-2} $year^{-1}$) are the gross Li flux corresponding to the soil solution at −30 cm, vegetation and throughfall, respectively. The model yields identical results for the isotopic composition within uncertainty using fluxes derived from either the hydrological budget or the Cl^- budget (−15.2‰ and −15.3‰, respectively). Considering that this input is related to clay dissolution as already proposed by Goddéris et al. (2006), and considering that those clay minerals were directly formed from the congruent dissolution of granite (δ^7Li = 0.3‰), this means that the Li isotopic fractionation occurring during secondary phase precipitation is equal to −15.5‰, in good agreement with the estimated values of Vigier et al. (2008) and Chan et al. (1992) for Li incorporation into octahedral sites (−10‰ to −17‰). However, in this calculation we only took into account dissolution of secondary phases, but primary phases are also probably dissolving, and the isotopic composition results, in fact, from a mixture between dissolution of secondary and primary phases. Thus, the isotopic fractionation calculated here is a minimum and the isotopic composition of secondary phases which are dissolved in the first layer of the soil is probably lighter than −15.3‰.

In their modelling of weathering fluxes in this soil, Goddéris et al. (2006) found that below −30 cm, secondary phases precipitate, but some primary phases dissolve. Moreover, the recent study of calcium isotopes in the same soil profile showed that a Ca flux from the soil to the solution is required to equilibrate the Ca isotopes budget in the soil solutions (Cenki-Tok et al., 2009). To model the Li isotopic composition of soil solutions, we used a reactive model in which the Li concentration and isotopic composition of the water evolves with dissolution and precipitation fluxes. This model is described in the appendix. Briefly, this model is based on classical reactive transport equations, with the two main assumptions of negligible diffusion of chemical species and steady state conditions. In those conditions, the Li isotopic fractionation δ_{prec} occurring during secondary phase precipitation between −30 and −60 cm can be expressed as:

$$\delta_{prec} = \frac{\delta_{-60} - \delta_{diss} + (\delta_{diss} - \delta_{-30}) \cdot \left(\frac{C_{-30}}{C_{-60}}\right)^{\frac{1}{1-a}}}{a \cdot \left(\left(\frac{C_{-30}}{C_{-60}}\right)^{\frac{1}{1-a}} - 1\right)} \quad (4)$$

in which δ_{diss}, δ_{-30}, δ_{-60}, are the Li isotopic compositions of dissolution flux and soil solutions at −30 and −60 cm, respectively, C_{-30} and C_{-60} are the Li concentrations in the soil solution at −30 and −60 cm, respectively and $a = J_{prec}/J_{diss}$ is the ratio between the precipitation and the dissolution flux. On Fig. 9, we have plotted δ_{prec} versus J_{prec}/J_{diss} using the Li fluxes calculated previously (Table 3), and using the isotopic composition of granite (+0.3‰) for δ_{diss}. It is found that the isotopic fractionation must be at least −23.4‰ with the Li fluxes calculated using the conservative behaviour of Cl or −26.1‰ using the hydrological model. This isotopic fractionation is higher than published estimates for Li incorporation into smectites (−10 to −17‰) (Vigier et al., 2008; Chan et al., 1992), but is compatible with values reported by Zhang et al. (1998) for Li adsorption onto kaolinite and vermiculite (−21‰ and −29‰, respectively). However, the relatively good reproducibility of the isotopic profile over different sampling periods (Fig. 6) makes it unlikely that the adsorption–

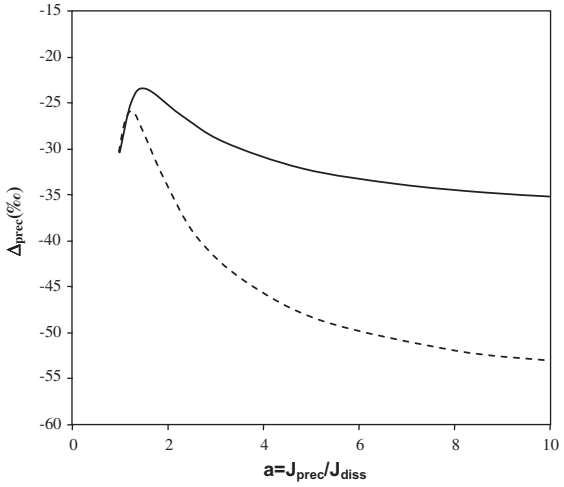

Fig. 9. Calculated Li isotopic fractionation during secondary phase precipitation from −30 to −60 cm in the soil VP as a function of the ratio between precipitation and dissolution fluxes. Solid line: Li fluxes calculated by considering the conservative behaviour of Cl. Dotted line: Li fluxes calculated using a hydrological model.

desorption process or cationic exchange of exchangeable complexes (CEC) are significant in the soil profile in the present study. Both processes depend of several parameters with a seasonal cycle like water fluxes, proton production by vegetation, dissolved organic carbon, or major chemical composition. It is also possible that another secondary phase with still undetermined isotopic fractionation, such as iron oxides, precipitates. This last hypothesis would be in agreement with the Li isotopic fractionation (∼−25‰) calculated by Kisakurek et al. (2004) between an iron oxide rich horizon and a paleowatertable. This isotopic fractionation is also higher than the one calculated in the 0 to −30 cm layer. This can be because dissolution of primary minerals was not taken into account in the top layer of the soil.

To summarize, the observed variations of Li isotopic composition in soil solutions are best explained by a dissolution-precipitation model. Li bearing primary silicate minerals are likely dissolve without any significant isotopic fractionation. In the deepest horizons (30–60 cm), secondary minerals, including clay minerals and oxides, could precipitate, preferentially incorporating light Li isotopes and increasing the Li isotopic composition in soil solutions from −30 to −60 cm. In the soil horizons above −30 cm, our data would indicate that those secondary minerals with low isotopic composition are now dissolving, thus decreasing the isotopic composition of soil solutions from 0 to −30 cm. This hypothesis is in good agreement with the modelling proposed by Goddéris et al. (2006, 2009), in which the dissolution/precipitation rate of smectite in the soil profile under spruce varied strongly between 40 and 60 cm depth.

6.2.2. Modelling springs and stream waters δ^7Li

We showed in section 6.1 that Li concentration variations in springs and stream waters are principally controlled by water–rock interactions with little contribution from biological cycling and atmospheric inputs. Li isotope behaviour in spring and stream waters vary as a function of their altitude: the high altitude springs are characterized by low and relatively stable δ^7Li, whereas for spring and stream waters sampled below 950 m, δ^7Li is systematically higher than at the top of the basin and decreases with increasing discharge (Fig. 7). Those spatiotemporal variations can be explained by mixing between different hydrogeochemical reservoirs in the watershed, marked by different water/rock interactions and/or by spatial and temporal variations of the pathways of waters through the watershed horizons, each water pathway being characterized by specific water–rock interactions and hence different geochemical signatures. Indeed, long water pathway in deep rocks are in good agreement with isotope hydrological studies of this catchment (Viville et al., 2006) that showed that the mean water transit time is 38.5 months, implying that water is partly stored in fractured rocks as deep as 45 m (Viville et al., 2006). Consequently, it can be envisioned that when contact time is increased, more Li coprecipitates in secondary minerals, and thus, dissolved δ^7Li increases, as well as Li/X (X = Na, Ca, Cl…) ratios.

Such a scenario easily explains the observed trends in the Li/Ca versus Li/Na diagram (Fig. 4), and that the Li isotope composition of spring and stream waters can vary with altitude and water discharge (Figs. 7 and 8). Such a scenario is also entirely consistent with the interpretations given for explaining the variations of Sr, U and Ca isotope ratios in the water samples from the Strengbach Catchment (Aubert et al., 2002a; Riotte and Chabaux, 1999; Prunier, 2008; Cenki-Tok et al., 2009). Aubert et al. (2002a) explained the variation of the Sr isotope ratios of the stream waters (RS) with the discharge by the contribution of waters from deep soil profile during the recession stage and also by various contributions of waters from distinct areas such as the opposite slopes and the saturated area (RUZS). Similarly, Riotte and Chabaux (1999) interpreted the variations of the decrease of the (^{234}U/^{238}U) activity ratios of the stream waters at the outlet of the catchment when the discharge increases by a mixing scenario between a “deep” water enriched in ^{234}U which weathered the bedrock and a shallower water with U activity ratios below unity representing a mobilization of U from material already weathered, i.e. from soil horizons and/or weathering profile. More recently the Ca isotope variations in source and stream waters of the Strengbach watershed (Cenki-Tok et al., 2009) have also been interpreted in terms of water mixing between deep waters, marked by alteration of primary minerals of the bedrock and more surficial waters significantly influenced by the Ca cycling by vegetation.

This scenario was tested by the model used previously to explain the isotopic variations measured in soil solutions (see appendix and §6.2). To avoid dilution effects, we used the Li concentrations normalised to Cl, with the hypothesis that Cl is not involved in dissolution-precipitation processes. The dissolved Li isotopic composition δ can be expressed as:

$$\delta = \delta_{diss} - a\Delta_{prec} + (\delta_0 + a\Delta_{prec} - \delta_{diss}) \cdot \left(\frac{(Li/Cl)_0}{(Li/Cl)}\right)^{\frac{1}{1-a}} \quad (5)$$

in which δ_{diss} and δ_0 are the Li isotopic compositions of dissolution flux and initial solution respectively, $(Li/Cl)_0$ is the Li/Cl ratio of initial solution, δ_{prec} is the isotopic fractionation occurring during secondary phase precipitation, and $a = J_{prec}/J_{diss}$ is the ratio between the precipitation and the dissolution flux. We consider that the main Li source in springs and stream waters is the dissolution of granite without isotopic fractionation, and that the Li isotopic variations result from preferential ^{6}Li uptake during secondary precipitation. Therefore, in equation 6 the value of δ_0 and δ_{diss} was assumed to be equal to +0.3‰ (the isotopic composition of the granite), and we fitted δ_{prec}, $a = J_{prec}/J_{diss}$, and $(Li/Cl)_0$. On Fig. 10, it can be seen that most of the points can be explained by this model, with $(Li/Cl)_0 = 0.0048$, $-14‰ < \delta_{prec} < -5‰$ (best fit: $\delta_{prec} = -10.7‰$), and $a = 1.57$. A few points are characterized by higher Li/Cl ratio (RUZS at low and intermediate discharge and SG). Those points can be fitted with $(Li/Cl)_0 = 0.0092$, $\delta_{prec} = -15.9‰$, and $a = 1.26$. Again, the calculated δ_{prec} are in good agreement with published values (Chan et al., 1992; Vigier et al., 2008).

The difference with the isotopic fractionation calculated between soil solutions and secondary phase precipitation deeper than 30 cm (<−23.4‰) suggests that the precipitated phases are not the same in both cases. For the soil solutions, the secondary phase which precipitates and induces the isotopic fractionation is unknown. In springs and stream waters, the good agreement between the isotopic fractionation calculated in the present work and the one determined by Vigier et al. (2008) strongly suggests that clay precipitation is the main process which leads to the dissolved Li isotopic variations. Another question is the relationship between the soil solutions and the springs and stream waters. The springs and stream data are not correctly fitted with a higher δ_0 (for instance, with $\delta_0 = +30.7‰$, the isotopic composition of the soil solutions at −60 cm), indicating that deep soil solutions and springs and stream waters are disconnected from a Li point of view. If we consider that the springs and stream waters flowed through the soils before their pathway into the saprolite and the rock porosity, this means that the deep soil water Li was entirely lost before its interaction with deeper saprolite and/or bedrock. In other words, the source of Li present in springs and stream comes from the bedrock dissolution without or with a very poor influence of deep soil solutions.

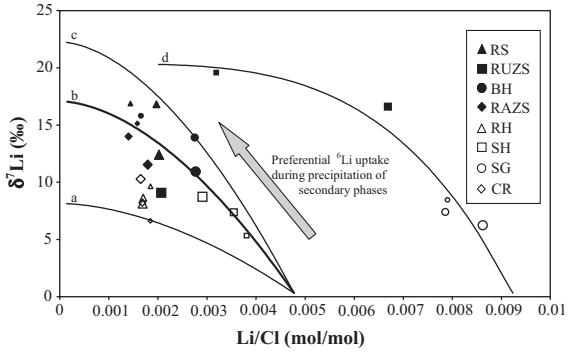

Fig. 10. Dissolved Li isotopic compositions in springs and stream waters as a function of Li/Cl. For each sample, the smaller point corresponds to the lowest water discharge, the bigger point corresponds to the highest discharge. Curves represent the modelling results. a, b, c: $(Li/Cl)_0 = 0.0048$ and $J_{prec}/J_{diss} = 1.57$, d: $(Li/Cl)_0 = 0.0092$ and $J_{prec}/J_{diss} = 1.26$; a: $\delta_{prec} = -5‰$, b (best fit): $\delta_{prec} = -10.7‰$, c: $\delta_{prec} = -14‰$, d: $\delta_{prec} = -15.9‰$.

The geochemical cycle of Li in the first meter of soil presents, then, a dynamic, completely independent and different from weathering dynamic in the deep horizons, but both of them emphasize the key role played by secondary phases.

7. CONCLUSION

This study shows that dissolved lithium isotopic composition can strongly vary at the scale of a small catchment. Those isotopic variations are only weakly influenced by atmospheric inputs and vegetation cycling, but depend mainly on weathering reactions. They could be related to solid/solution interactions during weathering. At the scale of the catchment, Li concentrations and isotopic compositions in springs and stream waters are controlled by contact time between water and rocks, which allows more or less lithium uptake by precipitation of secondary minerals. This observation suggests that lithium isotopes are a good tracer of water/rock interactions, and potentially of water pathways. The modelling shows that the data are in agreement with a dissolution-precipitation process. The calculated isotopic fractionation during precipitation indicates that clay precipitation is probably the main process which leads to the observed isotopic variations. Huge isotope variations were observed in soil waters (from −17.3 to +33.1‰). They were explained by dissolution-precipitation processes. Primary phases are dissolved all along the profile, but secondary phases are dissolved in the top layers, whereas they precipitate deeper than −30 cm. However, the calculated isotopic fractionation for the precipitation of secondary phases between −30 and −60 cm is higher than those known for isotopic fractionation during clay precipitation based on experimental studies. It is thus possible that another phase precipitates with a higher isotope fractionation. Oxides could be a good candidate but this process has never been investigated experimentally to our knowledge. These results confirm that the soil is a strongly reactive compartment, which must be integrated in studies at catchment scale to understand the processes at the biosphere interface and the biological signature. Moreover, the results obtained on several tree parts (roots to leaves) show that their Li signatures could be explained by an uptake from the shallow soil solutions.

Even if more experimental and natural data are needed to calibrate this tool, this study shows that Li isotopes are already able to give some important constraints on weathering mechanisms and hydro chemical fluxes in a small catchment.

ACKNOWLEDGMENTS

This study has been financially supported by REALISE (Reseau Alsace de Laboratoires en Ingénierie et Sciences pour l'Environnement), the region of the Alsace, and the French CNRS program 'EC2CO-Cytrix'. E. Lemarchand acknowledges the fund-

ing of a post-doctoral grant by "la Fondation Simone et Cino del Duca de L'Institut de France".

Sylvain Benarioumlil is thanked for his assistance in field work and sample processing. Quadrupolar ICP-MS measurements were performed by René Boutin and major elements concentrations were measured by Daniel Millon and Sophie Gangloff. Daniel Millon and Sophie Gangloff are also thanked for their assistance in Li concentration measurements with ionic chromatography. Bernard Kiefel is acknowledged for his help in TIMS measurements and Thierry Perrone for help in clean lab using. We acknowledge Damien Lemarchand and Peter Stille for fruitful discussions. Ruth Hindshaw and Edward Tipper are thanked for scientific comments and English corrections. We are grateful to Derek Vance, Heather Buss, and two anonymous reviewers whose comments helped us to greatly improve this manuscript.

APPENDIX A. MODELLING OF DISSOLVED LI ISOTOPE COMPOSITION DURING DISSOLUTION-PRECIPITATION PROCESSES

To model the effect of dissolution-precipitation on the dissolved Li isotopic compositions, we were inspired by the work of Johnson and DePaolo (1994), in which they used reactive transport equations to model isotopic data in groundwater–rocks systems.

In our modelling, we considered that the diffusion of chemical species is negligible and that the system is in a steady-state condition (dC/dt=0, dr/dt=0). With those assumptions, the evolution of the dissolved Li concentration C and Li isotopic ratio r along the water path can be written as:

$$v\frac{dC}{dx} = J_{\text{diss}} - J_{\text{prec}} \tag{6}$$

$$V\frac{dr}{dx} = \frac{\mathrm{J}_{\text{diss}}}{C}(r_{\text{diss}} - r) - \frac{\mathrm{J}_{\text{prec}}}{C}(r_{\text{prec}} - r) \tag{7}$$

with v being the fluid velocity, J_{diss} and J_{prec} being the lithium dissolution and precipitation fluxes, and r_{diss} and r_{prec} being the isotopic ratios of dissolved and precipitated Li.

Eqs. (1) and (2) can be combined as:

$$dr = \frac{r_{\text{diss}} - r - \frac{J_{\text{prec}}}{J_{\text{diss}}}(r_{prec} - r)}{1 - \frac{J_{\text{prec}}}{J_{\text{diss}}}} \times \frac{dC}{C} \tag{8}$$

Using the δ notation $\delta = 1000 \times (\frac{r}{r_{\text{standard}}} - 1)$ and $\Delta_{\text{prec}} = \delta_{\text{prec}} - \delta$, we can then write:

$$\dot{\delta} = \frac{\delta_{\text{diss}} - \delta - \frac{\mathrm{J}_{\text{prec}}}{\mathrm{J}_{\text{diss}}}\Delta\text{prec}}{1 - \frac{\mathrm{J}_{\text{prec}}}{\mathrm{J}_{\text{diss}}}} \times \frac{dC}{C} \tag{9}$$

The integration of the Eq. (4) along a water pathway gives:

$$\begin{aligned}
&\left[-\text{Log}(\delta_{\text{diss}} - \delta - \frac{\mathrm{J}_{\text{prec}}}{\mathrm{J}_{\text{diss}}}\Delta\text{prec})\right]_0^x \\
&= \frac{1}{1 - \frac{\mathrm{J}_{\text{prec}}}{\mathrm{J}_{\text{diss}}}} \times \left[\text{Log}((1 - \frac{\mathrm{J}_{\text{prec}}}{J_{\text{diss}}}))\right]_0^x \\
&\quad - \text{Log}\frac{\delta_{\text{diss}} - \delta_x - \frac{\mathrm{J}_{\text{prec}}}{\mathrm{J}_{\text{diss}}}\Delta\text{prec}}{\delta_{\text{diss}} - \delta_0 - \frac{\mathrm{J}_{\text{prec}}}{\mathrm{J}_{\text{diss}}}\Delta\text{prec}} \\
&= \text{Log}\left(\frac{C_x}{C_0}\right)^{\frac{1}{1 - \frac{\mathrm{J}_{\text{prec}}}{\mathrm{J}_{\text{diss}}}}}
\end{aligned} \tag{10}$$

For each sample, we can then write:

$$\delta = \delta_{\text{diss}} - a\Delta_{\text{prec}} + (\delta_0 + a\Delta_{\text{prec}} - \delta_{\text{diss}}) \cdot \left(\frac{C_0}{C}\right)^{\frac{1}{1-a}}; \quad \text{with a} = \frac{\mathrm{J}_{\text{prec}}}{\mathrm{J}_{\text{diss}}} \tag{11}$$

It can also be useful to express the precipitation isotopic fractionation:

$$\Delta_{\text{prec}} = \frac{\delta - \delta_{\text{diss}} + (\delta_{\text{diss}} - \delta_0) \cdot (\frac{C_0}{C})^{\frac{1}{1-a}}}{a \cdot ((\frac{C_0}{C})^{\frac{1}{1-a}} - 1)} \tag{12}$$

REFERENCES

Anderson S. P., von Blanckenburg F. and White A. F. (2007) Physical and chemical controls on the critical zone. *Elements* **3**(5), 315–319.

Aubert D., Probst A. and Stille P. (2004) Distribution and origin of major and trace elements (particularly REE, U and Th) into labile and residual phases in an acid soil profile (Vosges Mountains, France). *Appl. Geochem.* **19**(6), 899–916.

Aubert D., Probst A., Stille P. and Viville D. (2002a) Evidence of hydrological control of Sr behavior in stream water (Strengbach catchment, Vosges mountains, France). *Appl. Geochem.* **17**(3), 285–300.

Aubert D., Stille P., Probst A., Gauthier-lafaye F., Pourcelot L. and Del nero M. (2002b) Characterization and migration of atmospheric REE in soils and surface waters. *Geochim. Cosmochim. Acta* **66**(19), 3339–3350.

Bastviken D., Thomsen F., Svensson T., Karlsson S., Sandén P., Shaw G., Mathucha M. and Öberg G. (2007) Chloride retention in forest soil by microbial uptake and by natural chlorination of organic matter. *Geochim. Cosmochim. Acta* **71**(13), 3182–3192.

Berner R. A. (1995) Chemical weathering and its effect on atmospheric CO_2 and climate in chemical weathering rates of silicate minerals. *Rev. Miner. Geochem.* **31**, 565–583.

Bray R. and Gorham E. (1964) Litter production in forests of the world. *Adv. Ecol. Res.* **2**, 101–157.

Carignan J., Vigier N. and Millot R. (2007) Three secondary reference materials for lithium isotope measurements: Li7–N, Li6–N and LiCl–N solutions. *Geostand. Geoanal. Res.* **31**(1), 7–12.

Cenki-Tok B., Chabaux F., Lemarchand D., Schmitt A. D., Pierret M. C., Viville D., Bagard M. L. and Stille P. (2009) The impact of water–rock interaction and vegetation on calcium isotope fractionation in soil- and stream waters of a small, forested catchment (the Strengbach case). *Geochim. Cosmochim. Acta* **73**(8), 2215–2228.

Chabaux F., Riotte J., Schmitt A.-D., Carignan J., Herckes P., Pierret M.-C. and Wortham H. (2005) Variations of U and Sr isotope ratios in Alsace and Luxembourg rain waters: origin and hydrogeochemical implications. *Comptes Rendus Geosci.* **337**(16), 1447–1456.

Chan L. H., Edmond J. M., Thompson G. and Gillis K. (1992) Lithium isotopic composition of submarine basalts: implications for the lithium cycle in the oceans. *Earth Planet. Sci. Lett.* **108**(1–3), 151–160.

Cividini D., Lemarchand D., Chabaux F., Boutin R. and Pierret M.-C. (2010) From biological to lithological control of the B geochemical cycle in a forest watershed (Strengbach, Vosges). *Geochim. Cosmochim. Acta* **74**(16), 3143–3163.

Dambrine E., Pollier B., Bonneau M. and Ignatova N. (1998a) Use of artificial trees to assess dry deposition in spruce stands. *Atmos. Environ.* **32**(10), 1817–1824.

Dambrine E., Pollier B., Poszwa A., Ranger J., Probst A., Viville D., Biron P. and Granier A. (1998b) Evidence of current soil acidification in spruce stands in the Vosges Mountains, North-Eastern France. *Water Air Soil Pollut.* **105**(1), 43–52.

Dupré B., Dessert C., Oliva P., Goddéris Y., Viers J., François L., Millot R. and Gaillardet J. (2003) Rivers, chemical weathering and Earth's climate. *C.R. Geosci.* **335**(16), 1141–1160.

El Gh'mari (1995) Etude pétrographique, minéralogique et géochimique de la dynamique d'altération d'un granite soumis aux dépôts atmosphériques acides (bassin versant du Strengbach, Vosges, France): Mécanismes, bilans et modélisations, Université Louis Pasteur, PhD thesis.

Fichter J., Turpault M.-P., Dambrine E. and Jacques R. (1998a) Localization of base cations in particle size fractions of acid forest soils (Vosges Mountains, N-E France). *Geoderma* **82**(4), 295–314.

Fichter J., Turpault M.-P., Dambrine E. and Ranger J. (1998b) Mineral evolution of acid forest soils in the Strengbach catchment (Vosges mountains, N-E France). *Geoderma* **82**(4), 315–340.

Flesh G. D., Anderson A. R. and Svec H. J. (1973) A secondary isotopic standard for 6Li/7Li determinations. *Int. J. Mass Spectrom. Ion Phys.* **12**, 265–272.

Goddéris Y., C. R., Schott J., Pierret M. C. and François L. (2009) Towards an integrated model of weathering, climate and biospheric processes. *Rev. Mineral. Geochem.* **70**, 411–434.

Goddéris Y., Francois L. M., Probst A., Schott J., Moncoulon D., Labat D. and Viville D. (2006) Modelling weathering processes at the catchment scale: The WITCH numerical model. *Geochim. Cosmochim. Acta* **70**(5), 1128–1147.

Huh Y., Chan L. H. and Chadwick O. A. (2004) Behavior of lithium and its isotopes during weathering of Hawaiian basalt. *Geochem. Geophys. Geosyst.* **5.**

Huh Y., Chan L. H. and Edmond J. M. (2001) Lithium isotopes as a probe of weathering processes: Orinoco River. *Earth Planet. Sci. Lett.* **194**(1–2), 189–199.

Huh Y., Chan L. H., Zhang L. and Edmond J. M. (1998) Lithium and its isotopes in major world rivers: Implications for weathering and the oceanic budget. *Geochim. Cosmochim. Acta* **62**(12), 2039–2051.

James R. H. and Palmer M. R. (2000) The lithium isotope composition of international rock standards. *Chem. Geol.* **166**(3–4), 319–326.

Jochum K. P., Nohl U., Herwig K., Lammel E., Stoll B. and Hofmann A. W. (2005) GeoReM: A new geochemical database for reference materials and isotopic standards. *Geostand Geoanal. Res.* **29**(3), 333–338.

Johnson T. and DePaolo D. J. (1994) Interpretation of isotopic data in groundwater-rock systems: Model development and application to Sr isotope data from Yucca Mountain. *Water Resource Res.* **30**(5), 1571–1587.

Kisakurek B., James R. H. and Harris N. B. W. (2005) Li and delta Li-7 in Himalayan rivers: proxies for silicate weathering? *Earth Planet Sci. Lett.* **237**(3–4), 387–401.

Kisakurek B., Widdowson M. and James R. H. (2004) Behaviour of Li isotopes during continental weathering: the Bidar laterite profile, India. *Chem. Geol.* **212**(1–2), 27–44.

Ladouche B., Probst A., Viville D., Idir S., Baqué D., Loubet M., Probst J. L. and Bariac T. (2001) Hydrograph separation using isotopic, chemical and hydrological approaches (Strengbach catchment, France). *J. Hydrol.* **242**(3–4), 255–274.

Millot R., Guerrot C. and Vigier N. (2004) Accurate and high-precision measurement of lithium isotopes in two reference materials by MC-ICP-MS. *Geostand. Geoanal. Res.* **28**(1), 153–159.

Millot R., Vigier N., and Gaillardet J. (2010) Behaviour of lithium and its isotopes during weathering in the Mackenzie Basin, Canada. *Geochim. Cosmochim. Acta* In Press. doi:10.1016/j.gca.2010.04.025.

Nishio Y. and Nakai S. (2002) Accurate and precise lithium isotopic determinations of igneous rock samples using multi-collector inductively coupled plasma mass spectrometry. *Anal. Chim. Acta* **456**(2), 271–281.

Pistiner J. S. and Henderson G. M. (2003) Lithium-isotope fractionation during continental weathering processes. *Earth Planet Sci. Lett.* **214**(1–2), 327–339.

Pogge von Strandmann P. A. E., Burton K. W., James R. H., van Calsteren P., Gislason S. R. and Mokadem F. (2006) Riverine behaviour of uranium and lithium isotopes in an actively glaciated basaltic terrain. *Earth Planet Sci. Lett.* **251**(1–2), 134–147.

Probst A., Dambrine E., Viville D. and Fritz B. (1990) Influence of acid atmospheric inputs on surface water chemistry and mineral fluxes in a declining spruce stand within a small granitic catchment (Vosges Massif, France). *J. Hydrol.* **116**(1–4), 101–124.

Probst A., El Gh'mari A., Aubert D., Fritz B. and McNutt R. (2000) Strontium as a tracer of weathering processes in a silicate catchment polluted by acid atmospheric inputs, Strengbach, France. *Chem. Geol.* **170**(1–4), 203–219.

Probst A., Fritz B. and Viville D. (1995) Mid-term trends in acid precipitation, streamwater chemistry and element budgets in the strengbach catchment (Vosges Mountains, France). *Water Air Soil Pollut.* **79**(1), 39–59.

Probst and Viville (1997) Bilan hydrogéochimique d'un petit bassin versant forestier des Vosges granitiques en Alsace: Le bassin amont du Strengbach a Aubure (Haut-Rhin). In *Rapport d'activité scientifique ZAFA 1.3 de l'IFARE (Institut Franco-Allemand de Recherche sur l'Environnement), Conseil de l'Europe*, pp. 59–66.

Probst A., Viville D., Fritz B., Ambroise B. and Dambrine E. (1992) Hydrochemical budgets of a small forested granitic catchment exposed to acid deposition: The strengbach catchment case study (Vosges massif, France). *Water Air Soil Pollut.* **62**(3), 337–347.

Prunier, J. (2008) Etude du fonctionnement d'un écosystème forestier en climat tempéré, par l'apport de la géochimie élémentaire et isotopique (Sr, U-Th-Ra). Cas du bassin versant du Strengbach. *PhD Thesis,* University Louis Pasteur, Strasbourg, France.

Riotte J. and Chabaux F. (1999) 234U/238U) activity ratios in freshwaters as tracers of hydrological processes: the Strengbach watershed (Vosges, France. *Geochim. Cosmochim. Acta* **63**(9), 1263–1275.

Rodstedth M., Stahlberg C., Sandén P. and Öberg G. (2003) Chloride imbalances in soil lysimeters. *Chemosphere* **52**(2), 381–389.

Rudnick R. L., Tomascak P. B., Njo H. B. and Gardner L. R. (2004) Extreme lithium isotopic fractionation during continental weathering revealed in saprolites from South Carolina. *Chem. Geol.* **212**(1–2), 45–57.

Schmitt A.-D. and Stille P. (2005) The source of calcium in wet atmospheric deposits: Ca-Sr isotope evidence. *Geochim. Cosmochim. Acta* **69**(14), 3463–3468.

Teng F.-Z., McDonough W. F., Rudnick R. L., Dalpé C., Tomascak P. B., Chappell B. W. and Gao S. (2004) Lithium isotopic composition and concentration of the upper continental crust. *Chem.Geol.* **68**(20), 4167–4178.

Tomascak P. B. (2004) Developments in the understanding and application of lithium isotopes in the earth and planetary sciences in geochemistry of non-traditional stable isotopes. *Rev. Miner. Geochem.* **55**, 153–195.

Vigier N., Decarreau A., Millot R., Carignan J., Petit S. and France-Lanord C. (2008) Quantifying Li isotope fractionation during smectite formation and implications for the Li cycle. *Geochim. Cosmochim. Acta* **72**(3), 780–792.

Vigier N., Gislason S. R., Burton K. W., Millot R. and Mokadem F. (2009) The relationship between riverine lithium isotope composition and silicate weathering rates in Iceland. *Earth Planet. Sci. Lett.* **287**, 434–441.

Viville D., Ladouche B. and Bariac T. (2006) Isotope hydrological study of mean transit time in the granitic Strengbach catchment (Vosges massif, France): application of the flowPC model with modified input function. *Hydrol. Proc.s* **20**, 1737–1751.

Walker J.C.G., Hays P.B. and Kasting J.F. (1981) A negative feedback mechanism for the long-term stabilisation of Earth's surface temperature. *J. Geophys. Res.* **86** (NC10) 9776–9782.

Zhang L. B., Chan L. H. and Gieskes J. M. (1998) Lithium isotope geochemistry of pore waters from Ocean Drilling Program Sites 918 and 919, Irminger Basin. *Geochim. Cosmochim. Acta* **62**(14), 2437–2450.

Associate editor: Derek Vance

Available online at www.sciencedirect.com
ScienceDirect
Applied Geochemistry 22 (2007) 2307–2325
Applied Geochemistry
www.elsevier.com/locate/apgeochem

Multi-isotopic (Li, B, Sr, Nd) approach for geothermal reservoir characterization in the Limagne Basin (Massif Central, France)

R. Millot *, Ph. Négrel, E. Petelet-Giraud

BRGM, 3, Avenue Claude Guillemin, BP 36009, 45060 Orléans Cedex 2, France

Received 25 July 2006; accepted 27 April 2007
Editorial handling by H. Armannsson
Available online 8 June 2007

Abstract

A multi-isotopic study of thermo-mineral waters from the Limagne Basin (French Massif Central) is reported. Lithium, B, Sr and Nd isotopic signatures in thermo-mineral waters and bedrocks were combined in order to determine the origin of these fluids from a reservoir point of view. Strontium and Nd isotopic systems showed that the thermo-mineral waters are mostly derived from a granitic reservoir type, with the exception of a few water samples having Sr and Nd isotopic signatures also reflecting a volcanic contribution (basalts). In a second step, Li and B isotopes were investigated, given that Li and B isotopic systematics are potentially affected by mass dependent fractionation during water/rock interaction and could provide some information on what takes place during this process. A great diversity of thermo-mineral waters within the Aigueperse area was clearly observed, which is directly related to the origin of these thermal waters in terms of reservoirs. These different geothermal reservoirs are characterized by different geological settings and intensity of water/rock interaction (i.e. depth and temperature).

The combination of Li, B, Sr and Nd isotopic systems highlight the complexity of the study of these geothermal reservoirs and that the use of only one isotopic tool could lead to an incomplete interpretation of the origin of water. The new approach using Li isotopes shows a very interesting potential with additional information on the intensity of water/rock interaction.

1. Introduction

Within the framework of the development of renewable energy in France, a research project involving an inventory of geothermal resources has been carried out jointly by the French agency for environment and energy management (ADEME) and the French Geosurvey (BRGM). The compilation of the national geothermic potential research project (COPGEN) is focused on the Allier Limagne Basin in France, which geologically belongs to Tertiary basins located on the northern edge of the Massif Central (Fig. 1). This area exhibits a number of geological, thermal and hydrogeological characteristics (e.g. high temperature of waters, porosity and

* Corresponding author.
E-mail address: r.millot@brgm.fr (R. Millot).

0883-2927/$ - see front matter © 2007 Elsevier Ltd. All rights reserved.
doi:10.1016/j.apgeochem.2007.04.022

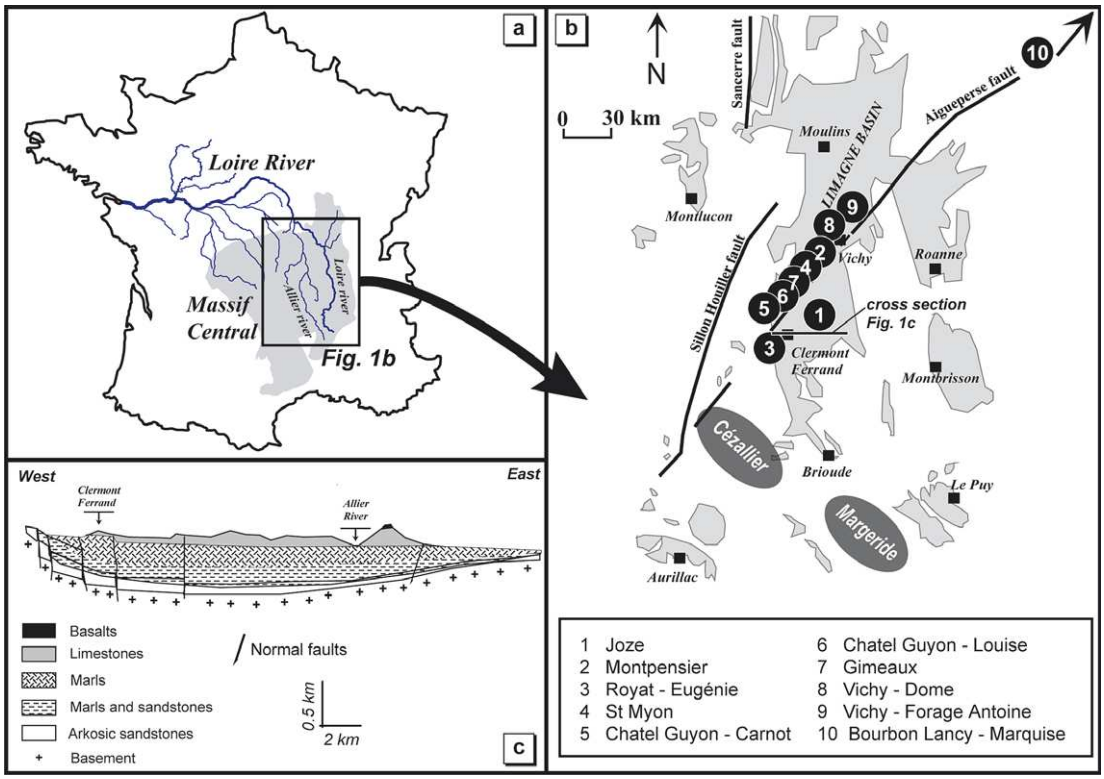

Fig. 1. (a) General map of the French Massif Central, (b) the Allier Limagne Basin and the sampling location sites for the 10 thermo-mineral waters from the Aigueperse fault, (c) synthetic geological section and lithostratigraphic sequence.

permeability of the reservoir rocks) that are interesting from a geothermal point of view.

The present study deals with the geochemistry of thermo-mineral waters from the Aigueperse fault zone. These waters and reservoir rocks are characterized by studying Li, B, Sr and Nd isotopes.

Major elements were used to determine the chemical signature of the thermal waters. Indeed, it is well known that the concentrations of most dissolved elements in thermo-mineral waters are functions of the aquifer temperature and the weathered mineralogical assemblage. However, it is likely that re-equilibration or change in composition could occur at lower temperatures as the water flows from the reservoir to the surface. For this reason, the use of a multi-isotopic approach is relevant and could give additional information for the characterization of thermal waters in relation to their source. Thus, Sr and Nd isotopes are investigated in order to better define the signature of the reservoir from which the geothermal waters are derived, given that Sr and Nd isotopes in geothermal waters reflect the origin of water/rock interaction (Goldstein and Jacobsen, 1987; Négrel et al., 1997, 2000; Négrel, 1999). Boron isotopic compositions were determined in an attempt to elucidate the source of B in these waters with reference to recent studies dealing with B isotopes in geothermal waters (Aggarwal et al., 2000, 2003; Kasemann et al., 2004). The use of Li isotopic systematics is explored, following recent papers indicating that Li isotopes seem to be an effective tracer of water/rock interaction (Huh et al., 1998, 2001). Indeed, it has been shown that Li isotopic signatures in waters are not related to lithology, but rather indicate Li isotope fractionation related to the intensity of water/rock interaction. However, the extent of Li isotopic fractionation and the parameters that control it remain poorly constrained.

2. Geological setting

The first results of the COPGEN project (Genter et al., 2003, 2005) have shown that the main geothermal reservoirs are likely located in arkosic formations at the edge of the basin, where a large

fault system (the Aigueperse fault in particular) allows the thermal waters to circulate (Fig. 1). The clastic formations of the deeper part of the Limagne Basin systems represent potential geothermal reservoirs with favourable petrophysical properties (porosity, permeability).

The geological synthesis is based on Genter et al. (2003). The Tertiary basins of the Massif Central belong to the Western European Rift initiated in the Eocene and set up in the Oligocene during the phase of extension, which affected the Western European Platform in front of the Alpine chain. The grabens of Limagne, mainly located north of the Massif Central (Fig. 1), are characterized by a typical evolution of a passive rift and show (1) a strong subsidence with important sedimentation (>3000 m); (2) active sedimentation at sea level, as shown by numerous marine incursions, between the Upper Eocene and the Oligocene; (3) important crustal thinning, and finally (4) scattered volcanism (basalts) mostly located in the west, which is not initiated until the end of the phase of sedimentation and then increases during the Lower Miocene.

The Allier Limagne area is a graben, separated by normal faults (Fig. 1b). The area under consideration covers approximately 22,600 km^2 with an important network of faults, the directions of which are mainly NS, NNE–SSW and NE–SW. To the south of the city of Clermont Ferrand, many volcanic reliefs are observed. They are primarily post-rifting.

In the Limagne Tertiary basin, sedimentary formations occur with ages varying from the Oligocene to the Pliocene as well as from the Pleistocene. Basaltic rocks of Oligocene and Miocene age are found on top of these sedimentary sequences. The horst structures on the border of the basin are made up of (1) metamorphic, magmatic, volcanogenic and sedimentary formations (Variscan basement of the Massif Central of Hercynian age), and of (2) Tertiary to Quaternary basalts. The Variscan basement constitutes the substratum of the Limagne Basin. The arkosic formations, representing potential geothermal reservoirs, are positioned at the bottom of the basin and are covered by sedimentary sequences comprising marls, argillaceous formations, evaporites and limestones (Fig. 1c).

The geothermal potential of the Limagne Basin area was recently investigated by Serra et al. (2007) using several geothermometers (i.e. Na–K, Na–K–Ca, Na/Li, Mg/Li, Sr/K^2, Ca/K^2 and F*K) yielding deep reservoir temperatures of about 180–230 °C in the western part of the Limagne Basin (Châtel-Guyon, Gimeaux, Joze, Bourbon Lancy, Montpensier, Royat and St Myon), whereas the geothermometer temperatures were lower (about 150–160 °C) in the Vichy area.

3. Sampling strategy and analytical methods

Serra et al. (2003), in a compilation of 285 samples from the French Massif Central, for which major and some trace element data were reported, defined 14 different groups of thermo-mineral waters based on the chemistry of cations and anions. Considering the main groups of waters proposed by Serra et al. (2003), 10 thermo-mineral waters (Fig. 1b) were sampled in spring 2003 within the Allier Limagne area (Aigueperse fault zone) for major and trace element analysis as well as for isotopic measurements (δ^7Li, $\delta^{11}B$, $^{87}Sr/^{86}Sr$, $^{143}Nd/^{144}Nd$).

The waters from Montpensier [2], Royat–Eugénie [3], Châtel-Guyon (Carnot [5] and Louise [6]), Vichy (Dôme [8] and Forage Antoine [9]), and Bourbon Lancy (Marquise) [10] were sampled from drill holes. Water samples from Joze [1], St Myon [4] and Gimeaux [7] were collected from sources or from natural rising springs. These 10 thermo-mineral waters correspond to the sample group hereafter named ''Aigueperse'' (Fig. 1b).

In the field, water samples were collected in acid-washed polyethylene bottles after filtration through 0.2 μm Sartorius® cellulose acetate filters. Alkalinity was determined in the field by Gran's method. Water samples were then acidified to pH < 2, by adding ultra-pure HNO_3, except those intended for anion and B isotope determination, which were kept unacidified. The pH was measured on site using an Ingold electrode and an Orion 250 pH-meter. The electrical conductivity was measured with a microprocessor conductivity-meter WTW LF96 calibrated at 25 °C.

The major cations were analyzed by atomic absorption spectrometry (Ca^{2+}, Na^+, K^+, Mg^{2+}, precision ±5–10%), the anions by ion chromatography (Cl^-, SO_4^{2-}, NO_3^-, precision ±5–10%), and the trace elements by inductively coupled plasma mass spectrometry (ICP-MS), Li, B, Sm, Nd, Sr, precision ±5%).

Lithium isotopic ratios were determined using a Neptune MC-ICP-MS (Millot et al., 2004). $^7Li/^6Li$ ratios were normalized to the L-SVEC standard solution (NIST SRM8545, Flesch et al., 1973) following

the standard sample bracketing method. Typical in-run precision for the determination of δ^7Li is about 0.1–0.2‰ ($2\sigma_m$). Chemical separation of Li from the matrix was achieved by following a procedure adapted from the technique of James and Palmer (2000), using a cationic resin (Bio Rad AG® 50W-X12, 200–400 mesh) and HCl acid media (0.2 N) for 30 ng of Li. Blanks for the total chemical extraction were less than 20–30 pg of Li, which is negligible since it represents a 10^{-3} blank/sample ratio. The reproducibility of the total method (purification procedure + mass analysis) was tested by repeated measurements of a seawater standard (IRMM BCR-403) after separation of Li from the matrix, for which a mean value of $\delta^7Li = +30.8‰ \pm 0.4$ (2σ, $n = 15$) was obtained, for the duration of the analysis. This mean value is in good agreement with the values from long term measurements ($\delta^7Li = +31.0‰ \pm 0.5$, 2σ, $n = 30$, Millot et al., 2004) and other values reported in the literature (Tomascak, 2004).

Strontium and Nd isotopic determinations were carried out using a Finnigan MAT 262 multi-collector mass spectrometer according to the technique given by Négrel et al. (2000). Boron isotopic ratios were determined on a Finnigan MAT 261 solid source mass spectrometer following the methods described by Casanova et al. (2001) and Kloppmann et al. (2001).

4. Results and comments

The results for the Aigueperse water samples are presented in Tables 1 and 2. These 10 thermo-mineral samples are compared to other samples from the French Massif Central, from the Margeride and the Cézallier areas for which major, trace element and isotopic data have been previously published by Négrel et al. (1997, 2000), Mossadik (1997) and Négrel (1999). Lithium isotope measurements for waters from the Cézallier and the Margeride area are a part of the present work (Table 3).

4.1. Major elements

The results of the 10 water samples from Aigueperse are in good agreement with those of the entire database of thermo-mineral waters from the Massif Central area (Serra et al., 2003). Basically, most of the waters are of the Na–HCO_3 type. In particular, this is the case for Vichy Dôme [8], Forage Antoine [9], Montpensier [2], St Myon [4], Joze [1] and Royat Eugénie [3]. By contrast, thermo-mineral waters

Table 1
pH, temperature, conductivity and major cation and anion concentrations for the 10 thermo-mineral waters sampled in 2003 within the Aigueperse fault zone

Sampling date	#	Name	pH	Temperature (°C)	Conductivity (μS/cm)	Na (μmol/L)	K (μmol/L)	Ca (μmol/L)	Mg (μmol/L)	HCO_3 (μmol/L)	Cl (μmol/L)	SO_4 (μmol/L)
6/4/2003	[1]	Joze	6.3	13.5	5130	32,739	4169	9077	3918	48,780	11,819	1250
6/4/2003	[2]	Montpensier	6.9	41.8	5400	55,652	1944	2369	2062	60,620	6375	2698
6/4/2003	[3]	Royat–Eugénie	6.5	34.2	5790	40,565	2448	5960	4897	39,980	28,773	1073
6/4/2003	[4]	St. Myon	6.1	12.1	3400	30,913	1345	4514	2362	39,670	5952	2115
6/5/2003	[5]	Châtel-Guyon–Carnot	6.4	36	8730	36,696	2189	14,963	15,432	42,870	60,000	3344
6/5/2003	[6]	Châtel-Guyon–Louise	6.4	34.5	8450	36,043	2031	13,616	15,144	42,000	58,787	3104
6/3/2003	[7]	Gimeaux	6.2	25.3	4050	21,087	1130	6658	6173	30,280	17,348	2115
6/5/2003	[8]	Vichy–Dôme	7.0	62.2	7400	74,348	2384	990	329	75,730	10,014	1885
6/5/2003	[9]	Vichy–Forage Antoine	7.1	72.6	5740	64,348	1854	676	288	66,790	7729	1542
6/12/2003	[10]	Bourbon Lancy–Marquise	6.6	56.5	3000	20,609	921	1643	107	4920	21,410	778

Table 2
Li, B, Sr, Nd concentrations and isotopic compositions of thermo-mineral waters from Aigueperse

Sampling date	#	Name	Li (μmol/L)	B (μmol/L)	Sr (μmol/L)	Nd (nmol/L)	δ^7Li (‰)	δ^{11}B (‰)	$^{87}Sr/^{86}Sr$	$^{143}Nd/^{144}Nd$
6/4/2003	[1]	Joze	630	126.7	32.5	0.312	5.2	1.9	0.713687	0.512221
6/4/2003	[2]	Montpensier	1020	108.2	39.4	0.180	6.9	0.3	0.713186	0.512123
6/4/2003	[3]	Royat–Eugénie	955	642.0	67.5	0.104	2.4	−6.3	0.712181	0.512377
6/4/2003	[4]	St Myon	621	59.9	35.2	0.589	5.0	0.2	0.713456	0.512274
6/5/2003	[5]	Châtel-Guyon–Carnot	707	120.3	99.7	0.305	3.3	12.6	0.710581	0.512492
6/5/2003	[6]	Châtel-Guyon–Louise	679	111.0	95.8	0.430	3.4	11.3	0.710518	0.512469
6/3/2003	[7]	Gimeaux	416	58.2	44.6	0.409	2.5	7.7	0.712503	0.512193
6/5/2003	[8]	Vichy–Dôme	749	165.6	16.5	0.104	6.2	0.9	0.714393	0.512252
6/5/2003	[9]	Vichy–Forage Antoine	674	142.5	18.1	0.104	6.6	0.7	0.714056	0.512101
6/12/2003	[10]	Bourbon Lancy–Marquise	723	162.8	11.0	0.069	5.2	−2.8	0.710940	0.512136

Table 3
Li concentrations and δ^7Li values (‰) for thermal waters originating from the Cézallier and the Margeride area

	Sample number	Sampling date	Name	Li (μmol/L)	δ^7Li (‰)
Cézallier	CZ006	03/95	Le Bard Maçonnerie	729.4	4.4
	CZ005	07/95	StHérent Rivière	707.6	4.3
	–	07/95	Zagat max	991.4	3.0
	CZ018	03/95	Chassole Ste Marguerite	771.3	2.9
	CZ195	03/95	Zagat max	835.9	2.9
	CZ030	07/95	Vèze Supérieure	471.8	2.8
	CZ026	03/95	Chantejail	762.7	2.9
	CZ021	07/95	Le Moulin	716.7	3.2
	CZ042	03/95	Conche Tuyau	252.2	4.8
	CZ043	07/95	Pyronnée Captage	253.6	5.5
Margeride	–	5/11/1995	Fontaine Haut MAZEL	298.5	5.0
	–	–	Fontaines basses n°1	551.2	4.9
	–	5/11/1995	Ranc 1	158.0	3.8
	–	5/11/1995	Ranc 2	396.6	2.6

Sample locations and data for major elements are from Négrel et al. (1997, 2000) and Négrel (1999).

from Châtel-Guyon [5–6] are closer to the Ca–SO_4 type, water from Bourbon Lancy [10] is of the Na–Cl type, whereas the water sample from Gimeaux [7] is intermediate between a Ca–HCO_3 and a Na–HCO_3 type. In addition, the Cl^- contents vary between 10 and 80% of the total anions. Sodium concentrations vary between 40 and 100% of the total cation concentrations (after Na, Ca and Mg are the other major cations with equal share). From the examination of the major cations and anions, it clearly appears that the thermo-mineral waters present very different chemical signatures, whereas they are quite close geographically and located in the same regime of water/rock interaction.

Because Na and Cl are the most abundant cation and anion, respectively, it is interesting to investigate the relationship between these two elements in a wider context by comparing the Aigueperse samples with the Cézallier and Margeride thermo-mineral waters. Such a comparison is presented in Fig. 2a and allows Cl (considered as a conservative element) to be compared with Na concentrations, which are mostly controlled by the intensity of water/rock interaction. Sodium concentrations will also be used in the following section in order to comment on the origin of the elements with respect to water/rock interaction. For every group of thermo-mineral waters, different linear relationships can be observed between Na and Cl concentrations (Fig. 2a). In general, the 10 water samples from Aigueperse are in good agreement with the previous compilation of Serra et al. (2003) (Fig. 2a). It is observed that most

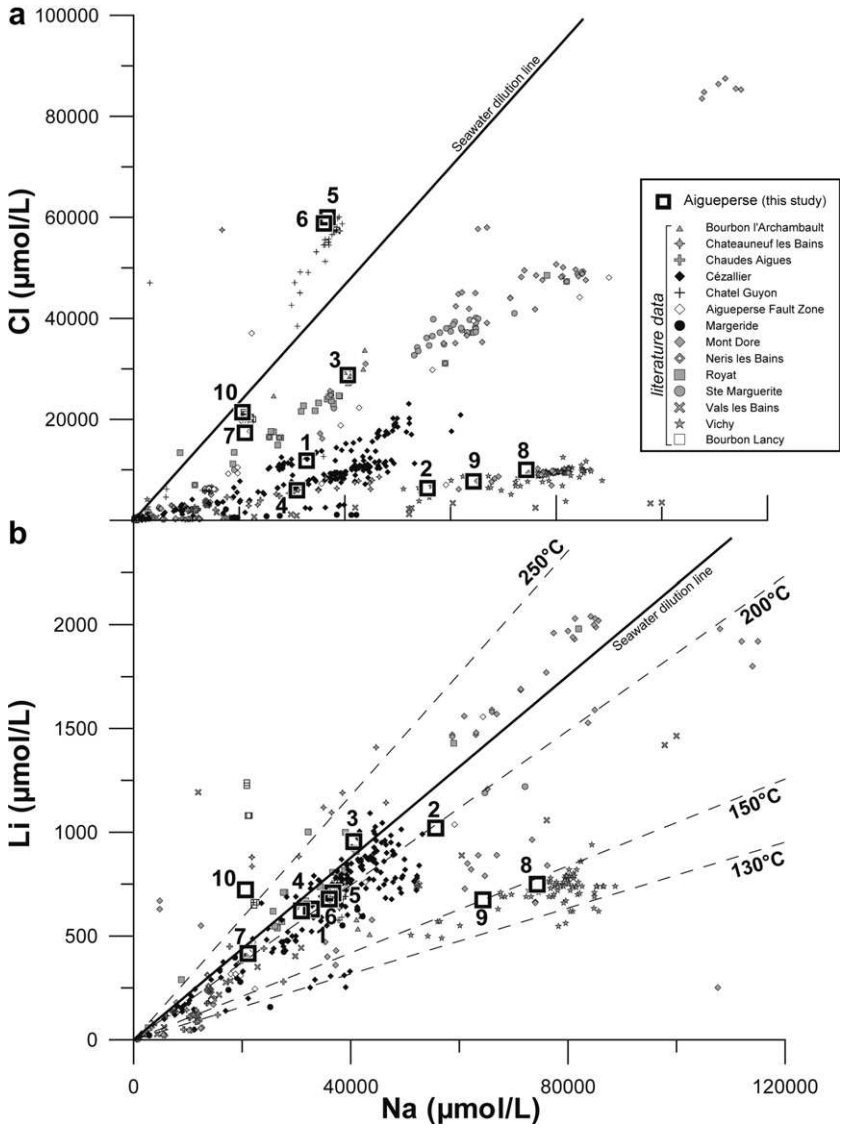

Fig. 2. (a) Cl vs. Na (µmol/L) diagram for thermal waters from Aigueperse, Cézallier and Margeride in the global context of the French Massif Central (see text for references and comments). (b) Li vs. Na (µmol/L) diagram and geothermometric relations (Fouillac and Michard, 1981) in thermal waters of the Limagne Basin (Aigueperse, Cézallier and Margeride) compared to the entire French Massif Central area. Data from the literature were compiled by Serra et al. (2003). Numbers correspond to samples: [1] Joze, [2] Montpensier, [3] Royat–Eugénie, [4] St Myon, [5] Châtel-Guyon–Carnot, [6] Châtel-Guyon–Louise, [7] Gimeaux, [8] Vichy–Dôme, [9] Vichy–forage Antoine and [10] Bourbon Lancy–Marquise.

of the thermo-mineral waters plot below the seawater line, meaning that they are enriched in Na with respect to Cl. The exceptions are waters from Châtel-Guyon (Carnot [5] and Louise [6]), plotting above the seawater line and consequently being enriched in Cl with respect to Na. Most of the thermo-mineral waters cover a wide range of Cl and Na concentrations, those from Vichy [8–9] show smaller variations. This result agrees with the previous study by Michard et al. (1976) on the same area. For the St Myon sample [4], it is observed that also Na and Cl concentrations are consistent with the first trend obtained for thermo-mineral waters in the Cézallier area (see Michard et al., 1987), whereas the Joze sample [1] is closer to the second trend described for the Cézallier waters by Michard et al. (1987). Finally, the Gimeaux sample [7] is close to the seawater line with a slight enrichment in Na with respect to Cl, and the

Bourbon Lancy sample (Marquise) [10] is located on the seawater line in this diagram.

4.2. Lithium isotopes

Lithium concentrations range from 158 to 1020 μmol/L in waters from Aigueperse, Cézallier and Margeride (Tables 2 and 3). When Li concentrations are plotted vs. Na concentrations (Fig. 2b), different groups of waters that as a function of their Li/Na molar ratio correspond to different geographical zones are clearly observed. Most of the water samples show a Li/Na molar ratio close or slightly lower than that of seawater. Consequently, thermo-mineral waters are depleted in Li to some extent with respect to Na by comparison to seawater. In Fig. 2b, the dashed lines corresponding to temperatures of water/rock interaction are shown calculated with the equation for the Na/Li geothermometer of Fouillac and Michard (1981). Based on Fig. 2b, the temperature of water/rock interaction ranges from approximately 130 to 230 °C. Low temperature waters (130–150 °C) correspond to thermal waters from Vichy [8–9], whereas high temperature waters (200–230 °C) occur in Royat [3], Joze [1] and Gimeaux [7].

Waters from Aigueperse have δ^7Li values ranging from +2.4 to +6.9‰, in Royat–Eugénie [3] and Montpensier [2] (Fig. 3). The range of variation is similar for waters from the Cézallier and the Margeride areas (from +2.6 to +5.5‰). The δ^7Li values for these waters are consistent with values compiled by Coplen et al. (2002) for surface waters and are intermediate between the Li isotopic ratios of the Upper Continental Crust (UCC: from −2 to +2‰, Teng et al., 2004) and global river waters (from +6 to +33‰, Huh et al., 1998, 2001).

No simple relationship is observed when δ^7Li values are plotted vs. the Li concentration in the waters. The range of δ^7Li values covers both low and high Li concentrations. However, a trend seems to appear when δ^7Li values are reported as a function of the Li/Na molar ratio (Fig. 3), especially for the Cézallier and the Margeride waters, suggesting that when Li/Na ratios increase, δ^7Li values decrease. Such a relationship is however not observed for some Aigueperse samples.

4.3. Boron isotopes

It is well known that B is a mobile element during water/rock interaction and it is derived either from

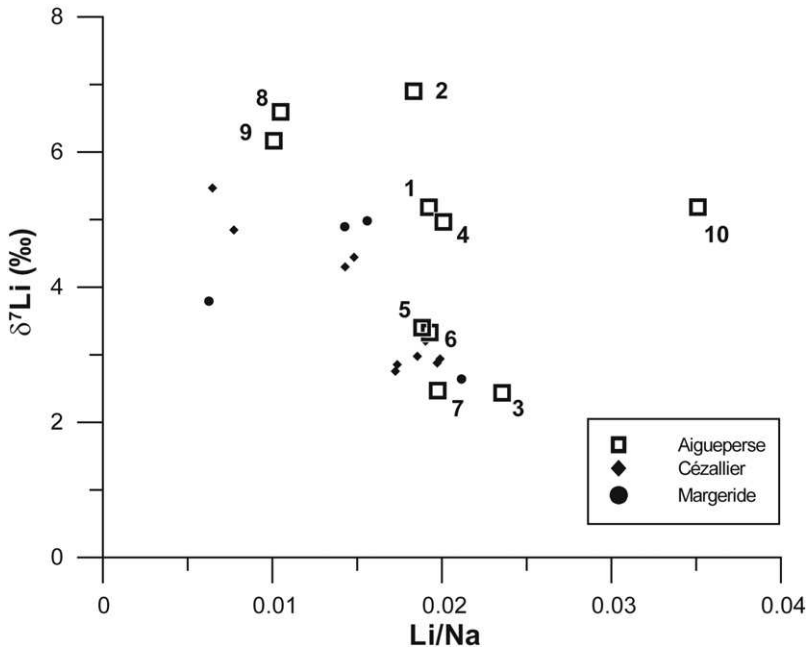

Fig. 3. Lithium isotopic ratios (δ^7Li, ‰) against the Li/Na molar ratio for waters originating in the Aigueperse, Cézallier and Margeride areas. Numbers correspond to samples: [1] Joze, [2] Montpensier, [3] Royat–Eugénie, [4] St Myon, [5] Châtel-Guyon–Carnot, [6] Châtel-Guyon–Louise, [7] Gimeaux, [8] Vichy–Dôme, [9] Vichy–forage Antoine and [10] Bourbon Lancy–Marquise.

weathering of rocks or from atmospheric inputs (Barth, 1993, 2000). In general, thermo-mineral waters from the French Massif Central (Mossadik, 1997; Serra et al., 2003) display a large range of B concentrations. Specifically, B concentrations in Aigueperse waters lie between 58 and 642 μmol/L and are characterized by light B isotopic compositions ranging from −6.3 to +12.6‰, in agreement with the mean value of the UCC (Barth, 1993).

In Fig. 4, B isotopic compositions are reported as a function of the Cl/B molar ratio for samples from the Limagne Basin (Aigueperse, Cézallier and Margeride). Thermo-mineral waters from Cézallier and Aigueperse seem to define a general trend of increasing $\delta^{11}B$ with increasing Cl/B ratio. By contrast, data from the Margeride are individual and do not appear to follow this relationship, with heavy $\delta^{11}B$ associated with low Cl/B ratios. In this diagram, data from deep saline waters of the Paris basin (Mossadik, 1997) were also added in order to put the samples from the Massif Central in a more general context of B isotopic signatures.

4.4. Strontium isotopes

Strontium concentrations range from 11 to 100 μmol/L in thermo-mineral waters from Aigueperse. In the Sr vs. Na plot (Fig. 5a) there is a wide scatter for waters from the Massif Central. However, it seems that there is an overall correlation between Sr and Na concentrations.

Strontium isotopic ratios in Aigueperse thermal waters (Table 2) lie between 0.71052 and 0.71439. In the diagram showing $^{87}Sr/^{86}Sr$ vs. 1/Sr (Fig. 6) for all the waters of the Massif Central, no linear trend appears, meaning that simple mixing between two components is not the main process that controls the Sr isotopic composition of the waters. Indeed, the range of Sr concentrations is covered by $^{87}Sr/^{86}Sr$ isotopic ratios in the range 0.704–0.705 (typical signature of waters derived from water/basalt interaction) as well as $^{87}Sr/^{86}Sr$ about 0.714–0.716, characteristic of the signature of waters in a granitic environment (Goldstein and Jacobsen, 1987; Négrel, 1999; Négrel et al., 2000).

4.5. Neodymium isotopes

Thermo-mineral waters from Aigueperse display a large range of Nd concentrations (from 0.069 to 0.589 nmol/L). No relationship is observed between Nd and Na (Fig. 5b) for Aigueperse, Cézallier and Margeride thermal waters. Basically, Nd concentrations are not related to Na concentrations. Sodium

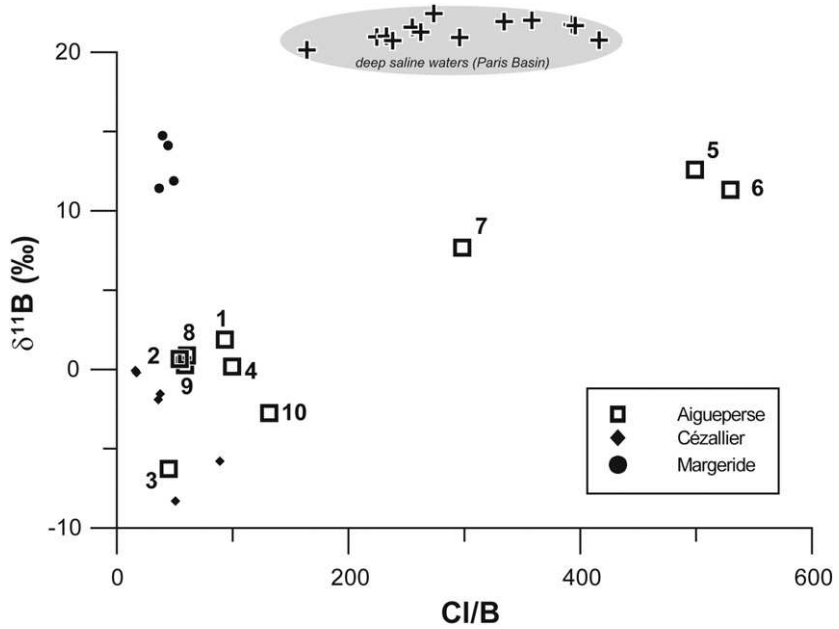

Fig. 4. Boron isotopic ratios ($\delta^{11}B$, ‰) against the Cl/B molar ratio in thermal waters from the Aigueperse, Cézallier and Margeride area. Data for brackish waters from the Paris Basin (Mossadik, 1997) have also been added for comparison. Numbers correspond to samples: [1] Joze, [2] Montpensier, [3] Royat–Eugénie, [4] St Myon, [5] Châtel- Guyon–Carnot, [6] Châtel-Guyon–Louise, [7] Gimeaux, [8] Vichy–Dôme, [9] Vichy–forage Antoine and [10] Bourbon Lancy–Marquise.

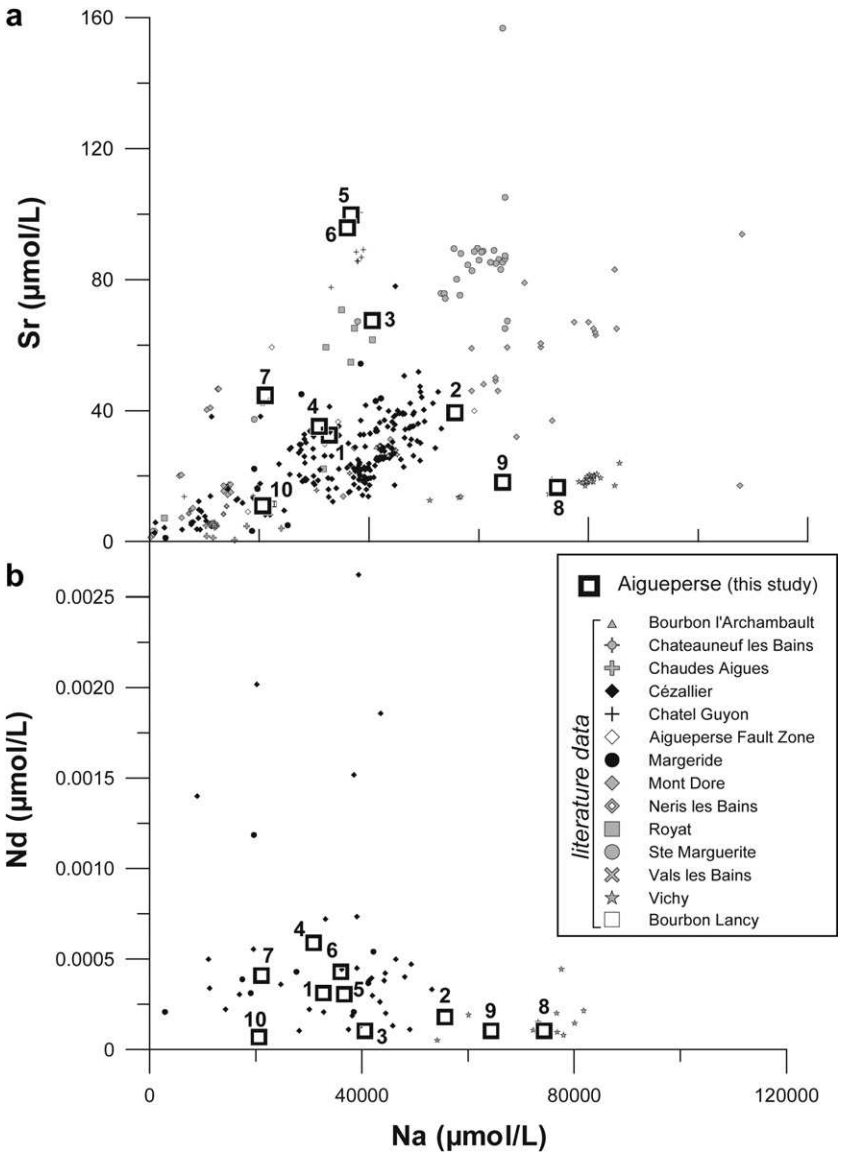

Fig. 5. Strontium and Nd concentrations against Na concentration in thermal waters from the Limagne Basin. Data from the literature were compiled by Serra et al. (2003). Numbers correspond to samples: [1] Joze, [2] Montpensier, [3] Royat–Eugénie, [4] St Myon, [5] Châtel-Guyon–Carnot, [6] Châtel-Guyon–Louise, [7] Gimeaux, [8] Vichy–Dôme, [9] Vichy–forage Antoine and [10] Bourbon Lancy–Marquise.

concentrations vary widely (from 10,000 to 80,000 µmol/L), whereas Nd concentrations are lower than 1 nmol/L, with a few exceptions in the range of 1–2.5 µmol/L.

As already reported for Sr isotopes, no simple relationship is observed when $^{143}Nd/^{144}Nd$ isotopic ratios are plotted against the inverse of the Nd concentration (Fig. 7), even though $^{143}Nd/^{144}Nd$ ratios vary between 0.51205 and 0.51270. Thermo-mineral waters from Châtel-Guyon [5–6] exhibit higher Nd isotopic ratios, but those from Montpensier [2] and Vichy-Antoine [9] lower $^{143}Nd/^{144}Nd$ values. In this context, high Nd isotopic ratios may be explained by water/rock interaction of volcanics (basalts, Négrel et al., 2000), e.g. in the case of Cézallier waters. Such an explanation may also be invoked for the Châtel-Guyon samples [5–6], although a sedimentary origin is also possible.

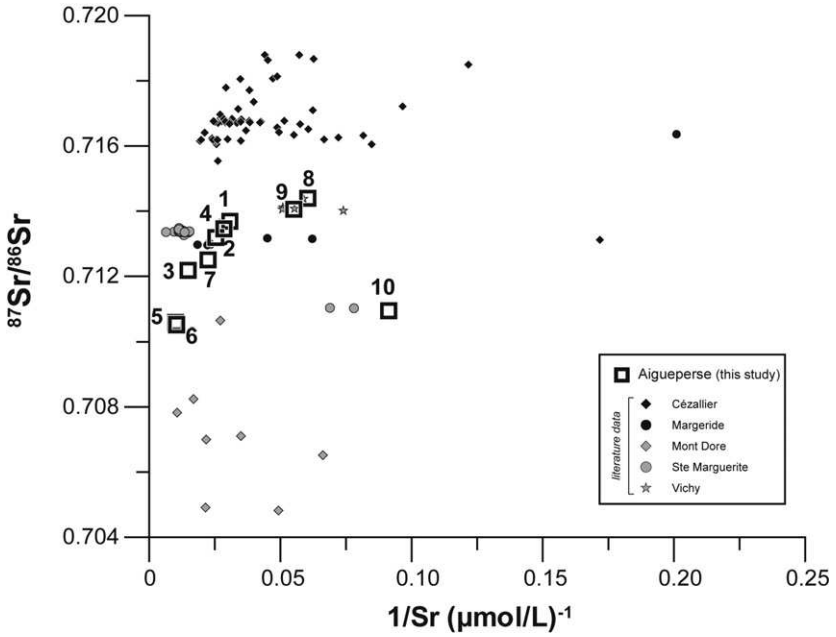

Fig. 6. Strontium isotopic ratios plotted vs. the inverse of Sr concentration for waters originating from the Aigueperse, Cézallier and Margeride area. Numbers correspond to samples: [1] Joze, [2] Montpensier, [3] Royat–Eugénie, [4] St Myon, [5] Châtel-Guyon–Carnot, [6] Châtel-Guyon–Louise, [7] Gimeaux, [8] Vichy–Dôme, [9] Vichy–forage Antoine and [10] Bourbon Lancy–Marquise.

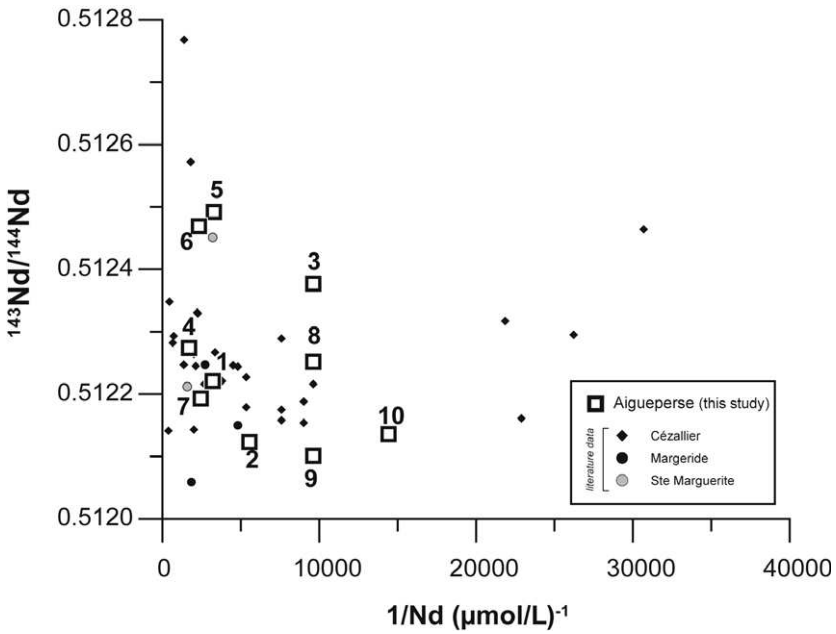

Fig. 7. Neodymium isotopic ratios plotted against the inverse of Nd concentration for waters from the Limagne Basin (Aigueperse, Cézallier and Margeride area). Data from the literature were compiled by Serra et al. (2003). Numbers correspond to samples: [1] Joze, [2] Montpensier, [3] Royat–Eugénie, [4] St. Myon, [5] Châtel-Guyon–Carnot, [6] Châtel-Guyon–Louise, [7] Gimeaux, [8] Vichy–Dôme, [9] Vichy–forage Antoine and [10] Bourbon Lancy–Marquise.

At this stage, it clearly appears that a combination of the different isotopic systems would be necessary in order to characterize further the origin of thermo-mineral waters. Such an approach is the basis of the discussion of this paper.

5. Discussion

5.1. Reservoir rocks

The different types of rocks in the Aigueperse area, assumed to correspond to the potential reservoir from which the thermo-mineral waters are derived (Genter et al., 2003, 2005), are discussed in this section.

In the literature, only few isotope data are reported and those which are reported are on Sr and Nd isotopes. In order to characterize the rocks within the Allier Limagne Basin, isotopes were determined for all major rock types sampled by Dagallier (2004) following the geological characterization reported by Genter et al. (2003). The different categories of rocks are compiled in Table 4, together with Sr, Nd and Li concentrations and isotopic ratios. In addition, the analysis of a sample of a halite deposit is also reported for Li and B isotopes, whereas Sr isotope data are taken from Briot et al. (2001).

The study of the Allier Limagne Basin showed that the succession of the facies consists of five main lithostratigraphic units (from the base to the top): a detritic unit, a sandy unit, a sandy-argillaceous unit, then a mixed sandy-argillaceous and calcareous unit, then finally a calcareous summit unit (sometimes evaporitic, halite).

The Sr isotopic ratios of arkosic deposits (Table 4) range from 0.71641 to 0.72799 and Nd isotopic ratios range between 0.512146 and 0.512184. Marls and carbonates (Table 4) have $^{87}Sr/^{86}Sr$ ratios in the range of 0.71319–0.71375, whereas their $^{143}Nd/^{144}Nd$ ratios lie between 0.512216 and 0.512178. The Sr and Nd isotopic ratios of the limestone sample are 0.71543 and 0.512167, respectively.

A granite ($^{87}Sr/^{86}Sr = 0.718936$, $^{143}Nd/^{144}Nd = 0.512252$), a marl ($^{87}Sr/^{86}Sr = 0.728377$, $^{143}Nd/^{144}Nd = 0.512147$) and a sandstone sample ($^{87}Sr/^{86}Sr = 0.717494$, $^{143}Nd/^{144}Nd = 0.51218$) from a drill core at Aigueperse were analyzed (AP 101, Genter et al., 2003; Dagallier, 2004).

Granites and gneisses from the French Massif Central are well characterized by Sr and Nd isotope ratios (Pin and Duthou, 1990; Williamson et al., 1996; Downes and Duthou, 1988; Duthou et al., 1984, 1998; Briand et al., 2002). In addition, the range of variation in $\delta^{11}B$ for granites has been compiled in the studies of Smith and Yardley (1996) and Barth (2000). The volcanic rocks have also been analyzed for Sr and Nd isotopes by Chauvel (1982), Chauvel and Jahn (1984), Downes (1984), Briot (1990), Briot et al. (1991) and by Pin and Paquette (2002). The range of variation for B isotopes in volcanics (basalts) is compiled in the studies of Ishikawa and Nakamura (1992), Gurenko and Chaussidon (1997) and Tonarini et al. (2001, 2004).

By contrast, the Sr and Nd isotopic compositions of the sedimentary rocks from the Allier Limagne

Table 4
Li, B, Sr, Nd concentrations and isotopic compositions of different rock types sampled by Dagallier (2004) following the geological characterization reported in Genter et al. (2003) from drillings

Number	Sample name	Rock type	Li (mg/Kg)	Sr (mg/Kg)	Nd (mg/Kg)	δ^7Li (‰)	$\delta^{11}B$ (‰)	$^{87}Sr/^{86}Sr$	$^{143}Nd/^{144}Nd$
# 1	Royat	Arkosic	78	489	53.5	1.9	–	0.716408	0.512184
# 4	Cournon	Marl/limestone	224	2442	14.8	−7.0	–	0.713187	0.512216
# 6	Ste Marguerite	Marl/limestone	120	1012	18.8	−5.4	–	0.713748	0.512178
# 8	Longues	Arkosic	75	359	10	9.8	–	0.718187	0.512171
# 9	Billom	Arkosic	78	146	22.8	5.9	–	0.725368	0.512157
# 10	Château de Ravel	Arkosic	91	83	6.6	9.0	–	0.727985	0.512146
# 12	Couzes, St Floret	Limestone	20	584	2.8	−2.1	–	0.715426	0.512167
#13	St Floret	Granite	64	324	53.3	−2.0	–	–	–
Ap 101 K29	Aigueperse	Granite	50	322	38	−2.3	–	0.718936	0.512252
Ap 101 CR20	Aigueperse	Marl	226	121	46.6	−6.5	–	0.728377	0.512147
Ap 101 CR21	Aigueperse	Sandstone	117	700	36.4	−4.0	–	0.717494	0.51218
–	Halite	Saline deposit	–	–	–	9.6	21.8	0.71321–0.71442	–

$^{87}Sr/^{86}Sr$ for the halite sample is from Briot et al. (2001).

Basin have not been investigated in detail. Carbonate layers only from the Clermont Basin have been studied by Briot and Poidevin (1998) and Briot et al. (2001), showing a decrease of the $^{87}Sr/^{86}Sr$ ratios, from 0.7147 down to 0.7115 with time. However, Hercynian metasediments have been analyzed by Pin (1989), and show a range of variation between 0.718–0.732 and 0.51180–0.51221 for $^{87}Sr/^{86}Sr$ and $^{143}Nd/^{144}Nd$ isotopic ratios, respectively. In addition, saline deposits (anhydrite and gypsum) have been characterized by $^{87}Sr/^{86}Sr$ ratios ranging between 0.71321 and 0.71442 (Briot et al., 2001; Poidevin, personal communication).

There is unfortunately very little data in the literature on the Li isotopic composition of the Earth's crust. Very recently, Teng et al. (2004) reported the concentrations and isotopic ratios of various types of rocks (shales, loess and granites) in order to estimate the Li isotopic ratio of the UCC. According to this study, the δ^7Li of granites ranges between −2 and +2‰ and the δ^7Li of basalts (MORB, OIB and arc basalts) varies from +2 to +6‰. In order to be able to discuss the Li analyses of thermo-mineral waters of the Limagne Basin, the Li content and isotopic composition of 12 rocks that are representative of the potential reservoir sources were measured. The samples listed in Table 4 include sedimentary rocks of arkosic type, marls, sandstones and limestones, and also two granites (St Floret and Aigueperse) as well as a halite sample. The Li concentrations of these rocks vary over an order of magnitude (from 20 to 225 μg/g) and the δ^7Li lies between −7.0 and +9.8‰.

If the Li isotopic signatures of thermo-mineral waters are compared with those of rocks, it is observed that δ^7Li values for the waters are more consistent and always positive (from +2.5 to +6.9‰), whereas the δ^7Li values for the rocks are variable (−7.0– +9.8‰). With the exception of the arkosic deposits, the δ^7Li values for the rocks are systematically lower than those for the waters. Such a result is in a good agreement with the idea that the process of isotopic fractionation occurs during water/rock interaction, during which the heavy isotope (^7Li) is preferentially released into solution compared to the bedrock (Huh et al., 1998, 2001; Tomascak, 2004).

However at this point, it seems difficult to clearly identify the reservoir rocks by the Li isotopic composition of the thermo-mineral waters. Considering the isotopic fractionation during water/rock interaction, it can however be assumed that arkosic rocks certainly do not represent the main reservoir for Li. Indeed, the isotopic composition of these rocks covers the same range as the waters, while ^7Li is preferentially released into solution during water/rock interaction. Granites, sandstone, marls and limestones could however be considered as potential sources for Li in thermo-mineral waters. In order to be able to further identify the reservoir rocks and to define more clearly the mechanisms of fractionation that affect the Li isotopes, a multi-isotopic approach is used in this discussion.

5.2. Multi-isotopic characterization of thermal waters

5.2.1. Origin of thermal waters

Basically, Sr and Nd isotopes are good tracers of the origin of the source of solute during water/rock interaction. More specifically, $^{87}Sr/^{86}Sr$ and $^{143}Nd/^{144}Nd$ isotopic ratios in river waters are directly related to the type of lithology drained by the rivers (Goldstein and Jacobsen, 1987) because Sr and Nd isotopes are not subjected to mass dependent fractionation during weathering processes.

In Fig. 8, the data from Serra et al. (2003) and from this study are reported for Sr and Nd isotopes in thermal waters as well as in potential reservoir rocks. Three main lithologies are shown in Fig. 8 with their range of Sr and Nd isotopic signature in granites, basalts and sedimentary rocks.

As already mentioned, it has been shown by Goldstein and Jacobsen (1987) that an inverse relationship exists between Sr and Nd isotopic systems for large river basins on a global scale. Such a general inverse relationship is also observed between Sr and Nd isotopes in the thermo-mineral waters of the French Massif Central. However, the most important information is that the majority of the thermal waters are consistent with the range defined for Sr and Nd isotope ratios in granites with the exception of waters from Châtel-Guyon (Carnot [5] and Louise [6]) and Royat [3], which seem to define a trend toward a volcanic end member.

In more detail, thermal waters from the Aigueperse fault zone can be separated into three groups according to their Sr and Nd isotopic compositions. First of all, for Montpensier [2] and Gimeaux [7] waters, the Sr and Nd isotopic signatures are in a good agreement with a signature derived mainly from deep parent rocks belonging to the basement of the sedimentary sequence. For Montpensier [2] however, the Sr and Nd isotopic ratios of the waters are slightly lower than those of the parent rocks.

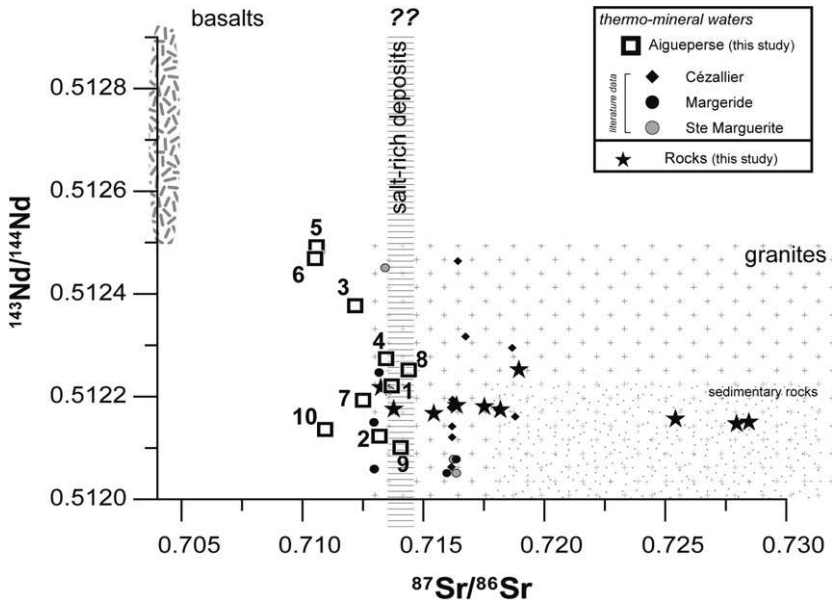

Fig. 8. Comparison of Nd and Sr isotopic ratios in geothermal waters and rocks from the Aigueperse, Cézallier and Margeride area. Numbers correspond to samples: [1] Joze, [2] Montpensier, [3] Royat–Eugénie, [4] St. Myon, [5] Châtel-Guyon–Carnot, [6] Châtel-Guyon–Louise, [7] Gimeaux, [8] Vichy–Dôme, [9] Vichy–forage Antoine and [10] Bourbon Lancy–Marquise.

For Gimeaux [7], there is a good agreement with a signature of the water essentially derived from deep water/granite interactions. Secondly, the Sr and Nd isotopic signatures of thermal waters from Joze [1], Saint-Myon [4] and Vichy [8–9] thermo-mineral waters seem to reflect a typical signature derived from sedimentary rocks (marls, sandstones and limestones). Finally, the Sr and Nd isotopic ratios of the thermal waters from Châtel-Guyon [5–6], Royat [3] and Bourbon Lancy [10] are compatible with both types of lithologies (basement rocks and sediments). Because of their low $^{87}Sr/^{86}Sr$ and high $^{143}Nd/^{144}Nd$ ratios, these thermal waters could also have a volcanic origin. Thus, to summarize, it is worth noting that the thermal waters are mostly derived from three main reservoirs: granites, sedimentary rocks and volcanic rocks.

Strontium and Nd isotopes are now compared to B isotopes. On the one hand, comparison of Sr to B isotopic ratios (Fig. 9a) clearly confirms that thermal waters from Saint Myon [4], Montpensier [2], Joze [1] and Vichy [8-9] are mainly derived from a granitic reservoir. It also shows that the contribution of a volcanic reservoir (basalt) is minor for those samples having $^{87}Sr/^{86}Sr$ isotopic ratios about 0.713–0.715. However, thermal waters from Bourbon Lancy [10] and Royat [3] have $^{87}Sr/^{86}Sr$ isotopic ratios (0.711–0.712) that are slightly lower than those of granites, whereas their $\delta^{11}B$ values are in agreement with a granitic signature ($\delta^{11}B$ from -10 to 0‰).

Furthermore, the B isotopic signature of thermal waters from Gimeaux [7] and Châtel-Guyon [5–6] is above the range defined for granites and volcanic rocks, suggesting that another contribution is likely and that this contribution has a $\delta^{11}B$ value higher than +13‰.

On the other hand, the combined use of Nd and B isotopes (Fig. 9b), also confirms that the volcanic reservoir does not contribute significantly to the signature of the thermal waters from Saint Myon [4], Montpensier [2], Vichy [8–9] and Bourbon Lancy [10]. Moreover, the thermal water from Royat [3] has Nd and B isotopic signatures that are intermediate between a granitic and a volcanic signature. As already mentioned the Sr and B isotope values for the thermal waters from Gimeaux [7] and Châtel-Guyon [5–6] are above the range defined for a granitic reservoir. Thus, a source rock with high $\delta^{11}B$ values (higher than +13‰) is needed to explain the B isotopic composition of these thermal waters.

5.2.2. Water/rock interaction

In Fig. 10, the isotopic ratios of Sr and Nd are shown as a function of the Li isotope ratios for thermo-mineral waters as well as for the main

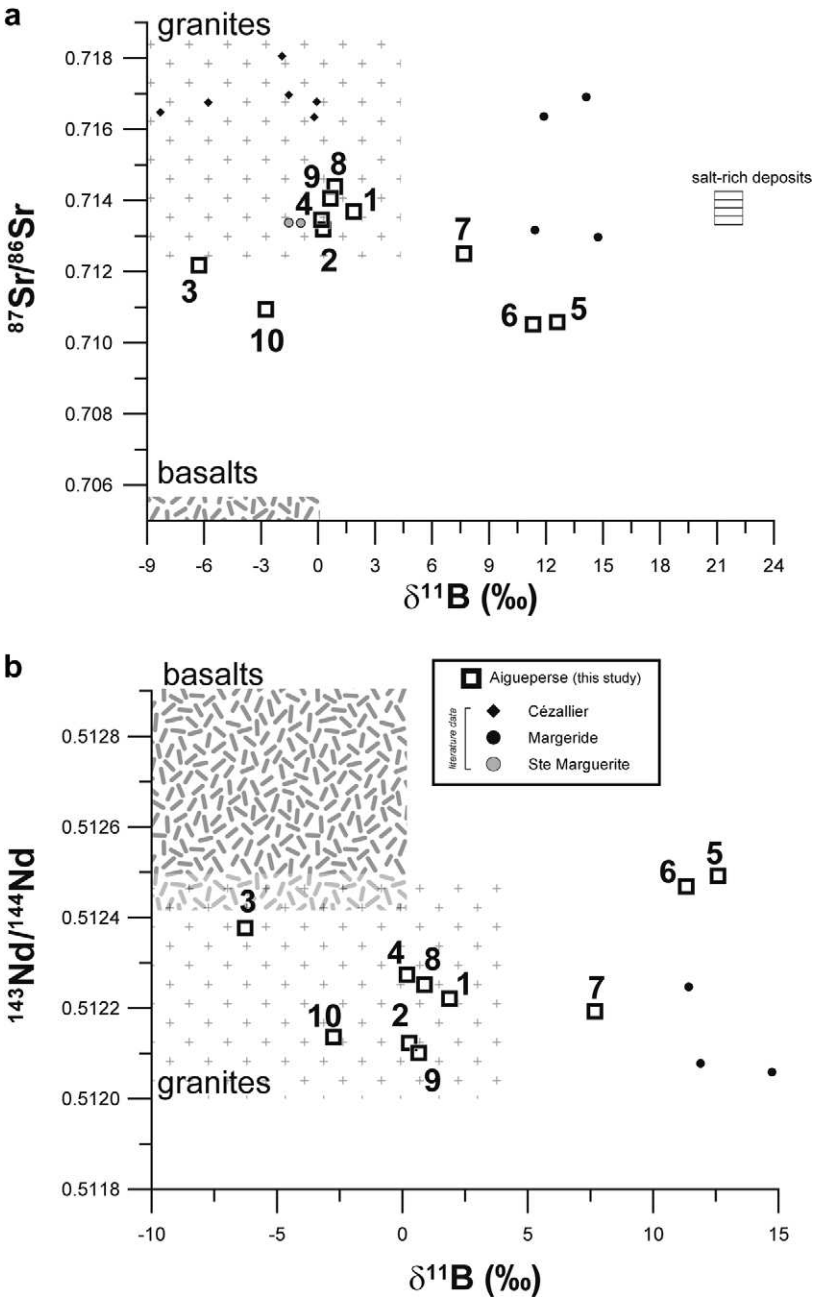

Fig. 9. Sr and Nd isotopic ratios against B isotopic signatures in geothermal waters from the Limagne Basin. Numbers correspond to samples: [1] Joze, [2] Montpensier, [3] Royat–Eugénie, [4] St. Myon, [5] Châtel-Guyon–Carnot, [6] Châtel-Guyon–Louise, [7] Gimeaux, [8] Vichy–Dôme, [9] Vichy–forage Antoine and [10] Bourbon Lancy–Marquise.

reservoir rocks. Such a presentation makes it possible to compare isotopic tracers, which are not subjected to fractionation during water/rock interaction (Sr and Nd isotopes) and Li isotopes which are affected. The various ranges for the granites, basalts and salt-rich deposits have been described previously for the $^{87}Sr/^{86}Sr$ and $^{143}Nd/^{144}Nd$ ratios. The Li values for the granites and basalts are those from Teng et al. (2004).

It is well established that the Sr and Nd isotopic ratios of waters are good tracers of the reservoir source, because the Nd and Sr isotopic composition of thermo-mineral water is the fingerprint of the isotopic composition of the bedrock with which it has

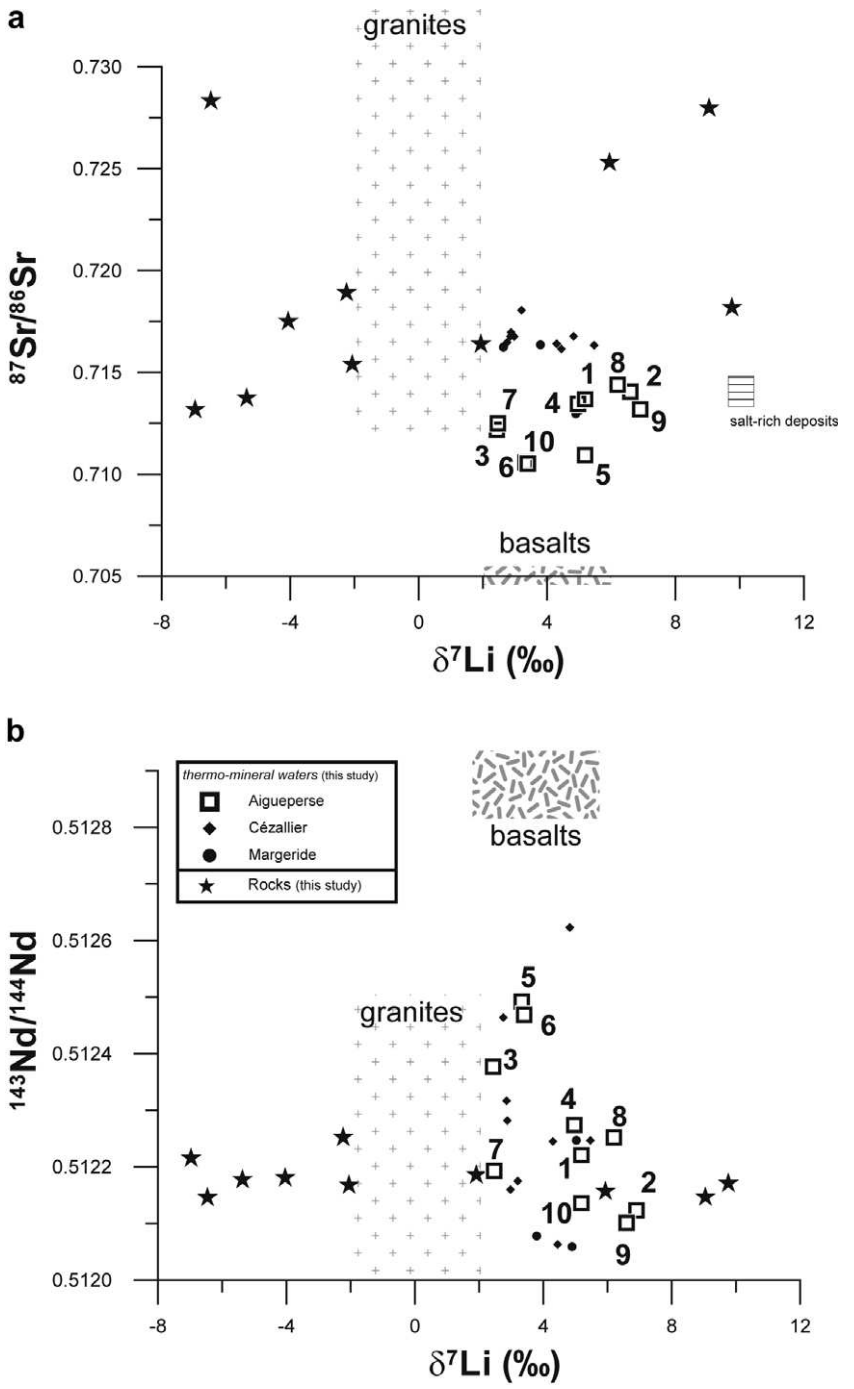

Fig. 10. Sr and Nd isotopic ratios plotted vs. Li isotopes in geothermal waters and rocks from the Limagne Basin. Numbers correspond to samples: [1] Joze, [2] Montpensier, [3] Royat–Eugénie, [4] St. Myon, [5] Châtel-Guyon–Carnot, [6] Châtel-Guyon–Louise, [7] Gimeaux, [8] Vichy–Dôme, [9] Vichy–forage Antoine and [10] Bourbon Lancy–Marquise.

interacted. By contrast, the Li isotopic signature in the water integrates two different components. The first component is directly related to the signature of the bedrock, whereas the second component integrates the fractionation that occurs during the process of water/rock interaction. These two effects are combined in the isotopic signature of a water sample and it is difficult to distinguish the

contribution of one compared to the other. However, during water/rock interaction, it is well established that the ^{7}Li isotope is preferentially released into solution, whereas ^{6}Li is mostly retained in the solid products of weathering (Huh et al., 1998, 2001; Tomascak, 2004). Consequently, the $\delta^{7}Li$ of the water should be higher than that of the rock with which it has interacted.

On the other hand, the Li isotopic ratio of the potential reservoir rocks is known, because it was determined in the present study. Consequently, Fig. 10 should be interpreted by taking into account the fact that the Sr and Nd isotopic signatures of the waters are identical to those of the rocks, whereas for Li isotopes, the $\delta^{7}Li$ value of the waters is higher than the $\delta^{7}Li$ value of the reservoir rock because of fractionation of Li isotopes.

Thus, by comparing Sr/Nd with Li isotopes, it can be observed that: 1/thermal waters from Cézallier reflect an interaction with a granitic reservoir, 2/ waters from Aigueperse also integrate a component resulting from the water/rock interaction of volcanics (basalts), and 3/it is unlikely that the arkosic rocks and the salt-rich deposits contribute significantly to the Li isotopic signature of the waters, since their $\delta^{7}Li$ values are higher than the signature in the geothermal waters. Unfortunately, the contribution of the other sedimentary rocks such as the marls, the sandstones or limestones cannot be discussed further in connection with the Limagne Basin.

As B and Li isotopic systems are potentially subjected to isotopic fractionation during water/rock interaction, it is interesting to couple these two isotopic systematics. In Fig. 11, the B isotopic ratios are compared to Li isotope ratios in thermo-mineral waters from the Cézallier, the Margeride and the Aigueperse areas. The various ranges for granites and basalts are also shown in this graph.

Two groups of points can be distinguished within Fig. 11. It is worth noting that the difference between these two groups is essentially based on the variations of B isotopic ratios. Indeed, the $\delta^{11}B$ isotopic signatures of thermal waters from Gimeaux [7], Châtel-Guyon (Carnot [5] and Louise [6]) and from the Margeride are systematically higher than those of the other groups of thermo-mineral waters. As already observed by comparing B–Sr–Nd isotopes, Gimeaux [7] and Châtel-Guyon waters [5–6] on the one hand and waters from the Margeride on the other hand have a different origin. By contrast, if Li and B isotope ratios are now

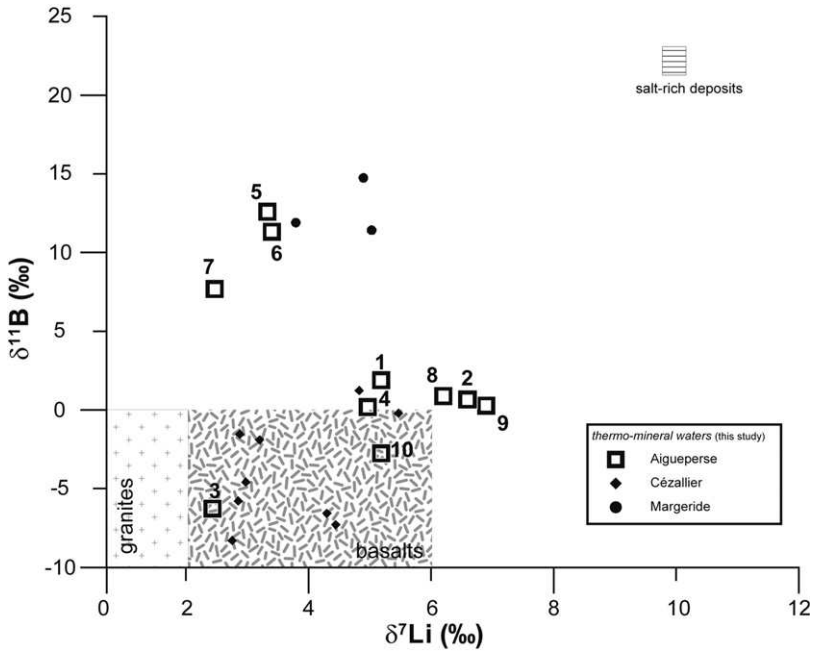

Fig. 11. Comparison of Li and B isotopes in thermo-mineral waters from Aigueperse, Cézallier and Margeride (Limagne Basin). Numbers correspond to samples: [1] Joze, [2] Montpensier, [3] Royat–Eugénie, [4] St. Myon, [5] Châtel-Guyon–Carnot, [6] Châtel-Guyon–Louise, [7] Gimeaux, [8] Vichy–Dôme, [9] Vichy–forage Antoine and [10] Bourbon Lancy–Marquise.

compared (Fig. 11), it can be seen that these geothermal waters seem to be similar. However, they are very different from the other thermo-mineral waters with respect to their Li and B isotopic signatures. The second group of samples (which represents the majority of samples) plots relatively close to the range defined for granitic and basaltic signatures, although some waters plot at slightly higher B–Li isotopic ratios. This observation is in agreement with the fact that ^{7}Li is preferentially released into solution during water/rock interaction and that the δ^{7}Li signature of the water is thus always higher than the δ^{7}Li value of the reservoir rock. In the second group of samples, it is interesting to note that for the entire set of geothermal waters, the B and Li isotopic values are correlated overall. Indeed, the highest values of δ^{7}Li correspond to the highest values of δ^{11}B and vice versa. This observation remains true for the first group of points.

This approach with Li isotopes is original and shows that the δ^{7}Li signature in thermal waters can reveal that Li isotopic systematics could be a very relevant tool for the characterization of water/rock interaction at high temperature. However, the nature and extent of Li isotope fractionation in relation to the intensity of water/rock interaction (i.e. depth and temperature and probably residence time) must be more precisely constrained in future studies that will enable improvement of our understanding of Li behaviour in geothermal systems.

6. Conclusions and perspectives

The multi-isotopic characterization of geothermal waters from the Aigueperse fault zone has made it possible to better define the origin of these waters from a reservoir point of view. The results for Sr and Nd isotopes show that the Aigueperse thermal waters are mostly derived from a granitic reservoir, with the exception of waters from Châtel-Guyon [5–6] and Royat [3] that gave Sr and Nd isotopic signatures reflecting a volcanic contribution (basalts). The examination of B isotopes confirm these results but also suggests that another component is needed in order to explain the origin and history of the waters with the highest δ^{11}B ratios. The information obtained through Li isotopes also proves that the geothermal reservoir is mainly of granitic and volcanic types. In addition Li isotopic signatures suggest that Li in geothermal waters is not derived from arkosic deposits. To summarize, a great diversity of thermo-mineral waters can be clearly observed within the Aigueperse area. Large differences in terms of major cation composition, salinity, and isotopic signatures are present, which are directly related to the origin of these thermal waters in terms of reservoirs. These different geothermal reservoirs are characterized by different geological settings and intensity of water/rock interaction (i.e. depth and temperature).

The combination of Li, B, Sr and Nd isotopic systems highlights the complexity of the study of these geothermal reservoirs, and the use of only one isotopic tool could lead to an incomplete interpretation of the origin of water. The new approach with Li isotopes shows a very interesting potential related to the intensity of water/rock interaction. In future, it could be interesting, to reduce the area of study in order to better constrain the reservoir from a lithological point of view, and thus further characterize the nature and extent of Li isotopic fractionation in geothermal waters with respect to the deep geothermal reservoir.

The deep temperatures of the reservoirs, between 150 and 230 °C estimated by chemical geothermometers (Serra et al., 2007), as well as the presence of a fractured basement and the evidence of water circulation given by the multi-isotope tracing, encourage wider investigations to be carried out within the framework of geothermal development for electricity and heat production in this area.

Acknowledgments

This work was financially supported within the scope of the research partnership between BRGM and ADEME and, more specifically, through the project compilation of the national geothermic potential (COPGEN). Financial support from the *Région Centre* is also acknowledged for the acquisition of the Neptune MC-ICP-MS. We would like to acknowledge A. Genter, C. Guerrot and H. Serra for fruitful discussions. P. Möller and an anonymous reviewer are acknowledged for providing helpful reviews of this manuscript. H. Ármannsson is thanked for editorial handling and constructive comments. This is BRGM contribution n° 4633.

References

Aggarwal, J.K., Palmer, M.R., Bullen, T.D., Arnórsson, S., Ragnarsdóttir, K.V., 2000. The boron isotope systematics of

Icelandic geothermal waters: 1. meteoric water charged systems. Geochim. Cosmochim. Acta 64, 579–585.

Aggarwal, J.K., Sheppard, D., Mezger, K., Pernicka, E., 2003. Precise and accurate determination of boron isotope ratios by multiple collector ICP–MS: origin of boron in the Ngawha geothermal system, New Zealand. Chem. Geol 199, 331–342.

Barth, S.R., 1993. Boron isotope variations in nature: a synthesis. Geol. Rundsch 82, 640–641.

Barth, S.R., 2000. Geochemical and boron, oxygen and hydrogen isotopic constraints on the origin of salinity in groundwaters from the crystalline basement of the Alpine Foreland. Appl. Geochem. 15, 937–952.

Briand, B., Duthou, J.L., Guerrot, C., Chenevoy, M., 2002. Les " granites à tablettes d'orthose " du Vivarais, témoins d'un magmatisme post-épaississement d'âge Dinantien inférieur; identification d'une unité géologique Nord-Ouest-Vivarais. C. R. Geosci. 334, 741–747.

Briot, D., 1990. Magma mixing versus xenocryst assimilation: the genesis of trachyandesites in Sancy volcano, Massif Central, France. Lithos 25, 227–241.

Briot, D., Poidevin, J.L., 1998. Sr isotope stratigraphy of some Rupelian carbonated laminites from the Limagne Basin: influence of seawater in the rift of the French Massif central? C. R. Acad. Sci. 326, 479–483.

Briot, D., Cantagrel, J.M., Dupuy, C., Harmon, R.S., 1991. Geochemical evolution in crustal magma reservoirs: trace-element and Sr–Nd–O isotopic variations in two continental intraplate series at Monts Dore, Massif Central, France. Chem. Geol. 89, 281–303.

Briot, D., Poidevin, J.L., Hugueney, M., 2001. Apports de l'étude isotopique Sr et Nd des sédiments cénozoïques de Limagne à la compréhension du fonctionnement du rift du Massif Central Français. Bull. Soc. Géol. Fr. 172, 17–24.

Casanova, J., Négrel, Ph., Kloppmann, W., Aranyossy, J.F., 2001. Origin of deep saline groundwaters in the Vienne granitoids (France). Constraints inferred from Boron and Strontium isotopes. Geofluids 1, 91–102.

Chauvel, C., 1982. Géochimie isotopique (Nd, Sr) et géochimie des éléments traces des basaltes alcalins du Massif Central français : contraintes pétrogénétiques et arguments en faveur du métasomatisme mantellique. Thesis, Univ. Rennes, France.

Chauvel, C., Jahn, B.M., 1984. Nd–Sr isotope and REE geochemistry of alkali basalts from the Massif Central, France. Geochim. Cosmochim. Acta. 48, 93–110.

Coplen, T.B., Hopple, J.A., Böhlke, J.K., Peiser, H.S., Rieder, S.E., Krouse, H.R., Rosman, K.J.R., Ding, T., Vocke, Jr. R.D., Révész, K.M., Lamberty, A., Taylor, P., De Bièvre P., 2002. Compilation of minimum and maximum isotope ratios of selected elements in naturally occurring terrestrial materials and reagents. US Geol. Surv. Water-Resour. Investig. Rep. 01–4222.

Dagallier, A., 2004. Assessment of geothermal energy potential of the tertiary Limagne Basin (France). MSc. in Environmental Engineering, Environment and Resources DTU, Technical Univ. Denmark.

Downes, H., 1984. Sr and Nd isotope geochemistry of coexisting alkaline magma series, Cantal, Massif Central, France. Earth Planet. Sci. Lett. 69, 321–334.

Downes, H., Duthou, J.L., 1988. Isotopic and trace element arguments for the lower crustal origin of Hercynian granitoids and Pre-Hercynian orthogneiss, massif Central, France. Chem. Geol. 68, 291–308.

Duthou, J.L., Cantagrel, J.M., Didier, J., Vialette, Y., 1984. Palaeozoic granitoids from the French Massif Central: age and origin studied by ^{87}Rb–^{87}Sr system. Phys. Earth Planet. In. 35, 131–144.

Duthou, J.L., Chenevoy, M., Gay, M., 1998. Evidence for, and consequences of, Middle Visean magmatism on the south side of the Pilat Massif, eastern French Massif Central. C. R. Acad. Sci. 327, 749–754.

Flesch, G.D., Anderson, A.R., Svec, H.J., 1973. A secondary isotopic standard for $^{6}Li/^{7}Li$ determinations. Int. J. Mass Spec. Ion Phys. 12, 265–272.

Fouillac, C., Michard, G., 1981. Sodium/lithium ratio in water applied to geothermometry of geothermal reservoirs. Geothermics 10, 55–70.

Genter, A., Giot, D., Lieutenant, N., Nehlig, P., Rocher, Ph., Roig, J.Y., Chevremont, Ph., Guillou-Frottier, L., Martelet, G., Bitri, A., Perrin, J., Serrano, O., Courtois, N., Vigouroux, P., Négrel, P., Serra, H., Petelet-Giraud, E., 2003. Méthodologie de l'inventaire géothermique des Limagnes : Projet COPGEN, Compilation des données, Rapport BRGM RP-52644-FR.

Genter, A., Giot, D., Guillou-Frottier, L., Calcagno, P., Courtois, N., Courrioux, G., Dagallier, A., Giraud-Petelet, E., Goyeneche, O., Lieutenant, N., Martelet, G., Negrel, P., Rocher, P., Serra, H., Serrano, O., Laplaige, P., 2005. Low to medium temperature geothermal resources in the Limagne Basin (France). In: Horne, R., Okandan, E. (Eds). Proceedings of World Geothermal Congress 2005, Antalya, Turkey, 24–29 April 2005.

Goldstein, S.J., Jacobsen, S.B., 1987. The Nd and Sr Isotopic systematics of river water dissolved material: implications for the sources of Nd and Sr in seawater. Chem. Geol. 66, 245–272.

Gurenko, A.A., Chaussidon, M., 1997. Boron concentrations and isotopic composition of the Icelandic mantle: evidence from glass inclusions in olivine. Chem. Geol. 135, 21–34.

Huh, Y., Chan, L.H., Zhang, L., Edmond, J.M., 1998. Lithium and its isotopes in major world rivers: implications for weathering and the oceanic budget. Geochim. Cosmochim. Acta 62, 2039–2051.

Huh, Y., Chan, L.H., Edmond, J.M., 2001. Lithium isotopes as a probe of weathering processes: Orinoco river. Earth Planet Sci. Lett. 194, 189–199.

Ishikawa, T., Nakamura, E., 1992. Boron isotope geochemistry of the oceanic crust from DSDP/ODP Hole 504B. Geochim. Cosmochim. Acta 56, 1633–1639.

James, R.H., Palmer, M.R., 2000. The lithium isotope composition of international rock standards. Chem. Geol. 166, 319–326.

Kasemann, S.A., Meixner, A., Erzinger, J., Viramonte, J.G., Alonso, R.N., Franz, G., 2004. Boron isotope composition of geothermal fluids and borate minerals from salar deposits (central Andes/NW Argentina). J. South Am. Earth Sci. 16, 685–697.

Kloppmann, W., Négrel, Ph., Casanova, J., Klinge, H., Schelkes, K., Guerrot, C., 2001. Halite dissolution derived brines in the vicinity of a Permian salt dome (N German Basin). Evidence from boron, strontium, oxygen and hydrogen isotopes. Geochim. Cosmochim. Acta. 65, 4087–4101.

Michard, G., Stettler, A., Fouillac, C., Ouzounian, G., Mandeville, D., 1976. Subsuperficial changes in chemical composition of the thermomineral waters of Vichy basin: geothermal implications. Geochem. J. 10, 155–161.

Michard, G., Fouillac, C., Vuataz, F.D., Criaud, A., 1987. Etude chimique et modèle d'évolution des eaux minérales du Cézallier. Géologie de la France, n°4, mémoire GPF, tome 2, 133–144.

Millot, R., Guerrot, C., Vigier, N., 2004. Accurate and high-precision measurement of lithium isotopes in two reference materials by MC-ICP-MS. Geostand. Geoanal. Res. 28, 153–159.

Mossadik, H., 1997. Les isotopes du bore, traceurs naturels dans les eaux: Mise au point de l'analyse en spectrométrie de masse à source solide et applications à différents environnements. Thèse, Univ. Orléans, France.

Négrel, Ph., 1999. Geochemical study in a granitic area, the Margeride, France: chemical element behavior and $^{87}Sr/^{86}Sr$ constraints. Aquat. Geochem. 5, 125–165.

Négrel, Ph., Fouillac, C., Brach, M., 1997. Occurrence of mineral water springs in the stream channel of the Allier River (Massif Central, France): chemical and Sr isotope constraints. J. Hydrol. 203, 143–153.

Négrel, Ph., Guerrot, C., Cocherie, A., Azaroual, M., Brach, M., Fouillac, C., 2000. Rare earth elements, neodymium and strontium isotopic systematics in mineral waters: evidence from the Massif Central, France. Appl. Geochem. 15, 1345–1367.

Pin, C., 1989. Essai sur la chronologie et l'évolution géodynamique de la chaîne hercynienne d'Europe (thèse de sciences naturelles), Thèse d'état, Univ. Clermont-Ferrand, France.

Pin, C., Duthou, J.L., 1990. Sources of Hercynian granitoids from the French Massif Central: inferences from Nd isotopes and consequences for crustal evolution. Chem. Geol. 83, 281–296.

Pin, C., Paquette, J.L., 2002. Le magmatisme basique calcoalcalin d'âge dévono-dinantien du nord du Massif Central, témoin d'une marge active hercynienne: arguments géochimiques et isotopiques Sr/Nd: Sr-Nd isotope and trace element evidence for a Late Devonian active margin in northern Massif-Central (France). Geodinamica Acta 15, 63–77.

Serra, H., Petelet-Giraud, E., Négrel, Ph., 2003. Inventaire du potentiel géothermique de la Limagne (COPGEN). Synthèse bibliographique de la géochimie des eaux thermales. Rap. BRGM/RP-52587-FR.

Serra, H., Négrel, Ph., Petelet-Giraud, E., 2007. Geochemical modelling approaches for investigating geothermal reservoir temperatures: application to the Limagne Basin (Massif Central, France). J. Volc. Geotherm. Res., submitted for publication.

Smith, M.P., Yardley, B.W.D., 1996. The boron isotopic composition of tourmaline as a guide to fluid processes in the southwestern England orefield: an ion microprobe study. Geochim. Cosmochim. Acta. 60, 1415–1427.

Teng, F.Z., McDonough, W.F., Rudnick, R.L., Dalpé, C., Tomascak, P.B., Chappell, B.W., Gao, S., 2004. Lithium isotopic composition and concentration of the upper continental crust. Geochim. Cosmochim. Acta. 68, 4167–4178.

Tomascak, P.B., 2004. Developments in the understanding and application of lithium isotopes in the earth and planetary sciences. Rev. Mineral. Geochem. 55, 153–195.

Tonarini, S., Armienti, P., D'Orazio, M., Innocenti, F., 2001. Subduction-like fluids in the genesis of Mt. Etna magmas: evidence from boron isotopes and fluid mobile elements. Earth Planet. Sci. Lett. 192, 471–483.

Tonarini, S., Leeman, W.P., Civetta, L., D'Antonio, M., Ferrara, G., Necco, A., 2004. B/Nb and ^{11}B systematics in the Phlegrean Volcanic District, Italy. J. Volc. Geotherm. Res. 133, 123–139.

Williamson, B.J., Shaw, A., Downes, H., Thirlwall, M.F., 1996. Geochemical constraints on the genesis of Hercynian two-micas leucogranites from the Massif Central, France. Chem. Geol. 127, 25–42.

ELSEVIER

Chemical Geology 244 (2007) 664–678

CHEMICAL GEOLOGY
INCLUDING
ISOTOPE GEOSCIENCE

www.elsevier.com/locate/chemgeo

Multi-isotopic tracing (δ^7Li, δ^{11}B, ^{87}Sr/^{86}Sr) and chemical geothermometry: evidence from hydro-geothermal systems in France

Romain Millot *, Philippe Négrel

BRGM, Metrology Monitoring Analysis Department, Orléans, France

Received 9 January 2007; received in revised form 6 July 2007; accepted 16 July 2007

Editor: D. Rickard

Abstract

In the present work, we report the results of a multi-isotopic study (δ^7Li, δ^{11}B and ^{87}Sr/^{86}Sr) on waters collected from different hydro-and geothermal sites in France. The aim of this study was to characterize hydro-and geothermal reservoirs by coupling a multi-isotopic approach with in-depth temperature of the reservoir calculated using chemical geothermometers. A database constituted by 36 water samples (thermal, thermo-mineral and geothermal waters) was selected in order to cover a wide range of temperatures and to be representative of water/rock interactions with various types of lithologies. We clearly observed that the wide range of ^{87}Sr/^{86}Sr isotopic ratios in the waters (0.70755-0.72187) appear to be largely controlled by the dominant host lithologies with Sr isotopic signatures ranging from high values (resulting from interaction from granite and/or gneiss type >0.714) to lower ^{87}Sr/^{86}Sr ratios (closer to Sr isotopic ratios observed in the sedimentary zones <0.712). Boron isotopic ratios lay between -8.3 and +21.6‰, also reflecting a lithological control over δ^{11}B signatures. In addition, no simple or direct relationship was observed for either boron or strontium isotopic signatures with the temperature of the reservoir. In contrast, temperature plays an important role in controlling the lithium isotope composition of the hydro-and geothermal fluids. δ^7Li signatures are comprised between -0.1 and +10.0‰ for temperatures ranging from 60 to 230 °C. This result seems to prove that lithium isotopic systematics represents a useful tool suitable for the characterization of hydrothermal and geothermal waters and suggests that the δ^7Li composition of geothermal waters may be utilised as a geothermometer (δ^7Li=-0.043±0.003 T+11.9±0.5).

Keywords: lithium; boron; strontium isotopes; hydrothermal waters; geothermal waters; chemical geothermometry

1. Introduction

The present study deals with the isotope geochemistry of different types of mineralized waters (thermo-mineral, thermal and geothermal waters), collected from different sites in France in order to cover a wide range of water/rock interaction settings.

The approach in this work deals with the isotopic compositions of hydro-geothermal waters in relation to a physical parameter of crucial importance in the characterization of the hydro-geothermal fluids: the temperature of the deep reservoir. For lithium, this approach is particularly relevant considering that Li is a soluble element during water/rock interaction and that the Na/Li chemical geothermometer is a useful tool in the determination of the temperature of hydro-geothermal waters (Fouillac and Michard, 1981). The main objective of the present work is to establish the nature and extent of

* Corresponding author.
E-mail address: r.millot@brgm.fr (R. Millot).

0009-2541/$ - see front matter © 2007 Elsevier B.V. All rights reserved.
doi:10.1016/j.chemgeo.2007.07.015

Li isotope fractionation during water/rock interaction in the range of temperature from 60 to 230 °C.

Lithium has two stable isotopes of mass 6 and 7, with natural abundances of 7.5% and 92.5% respectively. Lithium is a mobile element that tends to preferentially go into the fluid phase during water/rock interactions. The relative mass difference between the two isotopes is considerable (17%) and it is capable of producing significant mass dependant fractionation during geochemical processes. The range of variation in lithium isotopic compositions is more than 50‰ in geological materials (Coplen et al., 2002; Tomascak, 2004). Li isotopic systematics is a relatively new isotopic tracer for which all the processes that could induce isotopic fractionation are not yet well constrained. However in the context of water/rock interactions, numerous studies (Huh et al., 1998; 2001; Pistiner and Henderson, 2003; Kisakürek et al., 2004, 2005; Pogge von Strandmann et al., 2006; Millot et al., in preparation) have clearly shown that isotopic fractionation supports the enrichment of the heavy isotope (^{7}Li) in solution, the light isotope (^{6}Li) being preferentially retained in secondary weathering minerals. On the other hand, lithium isotopic fractionation is also temperature dependant (Chan and Edmond, 1988; Chan et al., 1992, 1993, 1994; James et al., 1999), and may induce measurable variations (in the range of several ‰), even at high temperature (Wunder et al., 2006; Millot et al., submitted for publication).

Boron has two isotopes of mass 10 and 11, with natural abundances of 19.9% and 80.1% respectively. It is well known that boron is also a mobile element during water/rock interactions and is essentially derived either from rock weathering or from atmospheric inputs (Barth, 1993, 2000). Boron isotopic signatures (δ^{11}B) range from-30 to +60‰ in natural environments, thus boron isotopes show considerable potential for characterising mixing phenomena and tracing specific processes. More specifically, boron isotopic systematics may be used as a potential tracer of groundwater evolution (i.e. aquifers, deep crustal fluids, Barth, 2000; Pennisi et al., 2000; Négrel et al., 2002; Casanova et al., 2001, 2002, 2005). In several studies, boron isotope compositions were also used in an attempt to elucidate the source of B in hydrothermal and geothermal waters (Musashi et al. 1988; Palmer and Sturchio 1990; Palmer 1991; Aggarwal et al., 2000, 2003; Kasemann et al., 2004).

Sr isotopes are known to be good tracers of water/rock interactions. More specifically, ^{87}Sr/^{86}Sr isotopic ratios in river water are directly controlled by the dominant host lithologies (Goldstein and Jacobsen, 1987). The variations in the Sr isotopic ratios of hydro-systems could also provide information on the origin and the mixing proportions of the various fluid components (Banner et al. 1989; Négrel et al. 2001; Négrel and Petelet-Giraud 2005), and on the nature and the intensity of the water/rock interaction process in relation to weathering source tracing (Négrel et al., 1993; Millot et al., 2002, 2003).

A multi-isotopic approach is applied in the present work for the characterization of hydro-geothermal waters in relation to their source (lithology and temperature) in order to evaluate the control of these parameters on the δ^7Li- δ^{11}B-^{87}Sr/^{86}Sr signature of these waters. From a general point of view, and particularly in geothermal exploration, the geochemical characterization of geothermal waters is necessary to control the quality of these waters, to determine their origin and to constrain the mechanisms of water/rock interaction at high temperature with a view to resource development.

2. The study sites: general setting

2.1. The Massif Central

Within the Massif Central (Fig. 1a), 5 different sites were studied: Aigueperse, Cézallier, Sail-sous-Couzan, Margeride and Cantal areas.

2.1.1. Aigueperse

The studied area in the Allier Limagne is a graben of 22,600 km^2 area with up to 3,000 m of sediments (Genter et al., 2003, 2005). The Limagne Tertiary basin (Fig. 1b) is made of formations dating from the Oligocene to the Pliocene and also contains Pleistocene sedimentary formations. The arkosic sandstone formations of the deeper part of the Limagne Basin systems represent potential geothermal reservoirs with favourable petrophysical properties (porosity, permeability).

Ten sites were sampled along the study zone (Fig. 1b). Waters from Joze, St Myon and Gimeaux were obtained from sources or samples taken from natural rising springs. The fluids of Montpensier, Royat (Eugénie), Châtel-Guyon (Carnot and Louise), Vichy (Dôme and Forage Antoine) and Bourbon Lancy (Marquise) were collected by drilling. Some of the waters are cold at shallow depth (Joze and St Myon), while others are warm with temperatures ranging from 25 °C (Gimeaux) to 73 °C (Vichy – Forage Antoine). Additional details concerning geological and the hydrological settings has already been reported by Millot et al. (in press) and Serra et al. (2007).

2.1.2. Cézallier

In the Cézallier area, several springs emerge with a low flow rate (i.e. a few litres/min) from the intensively

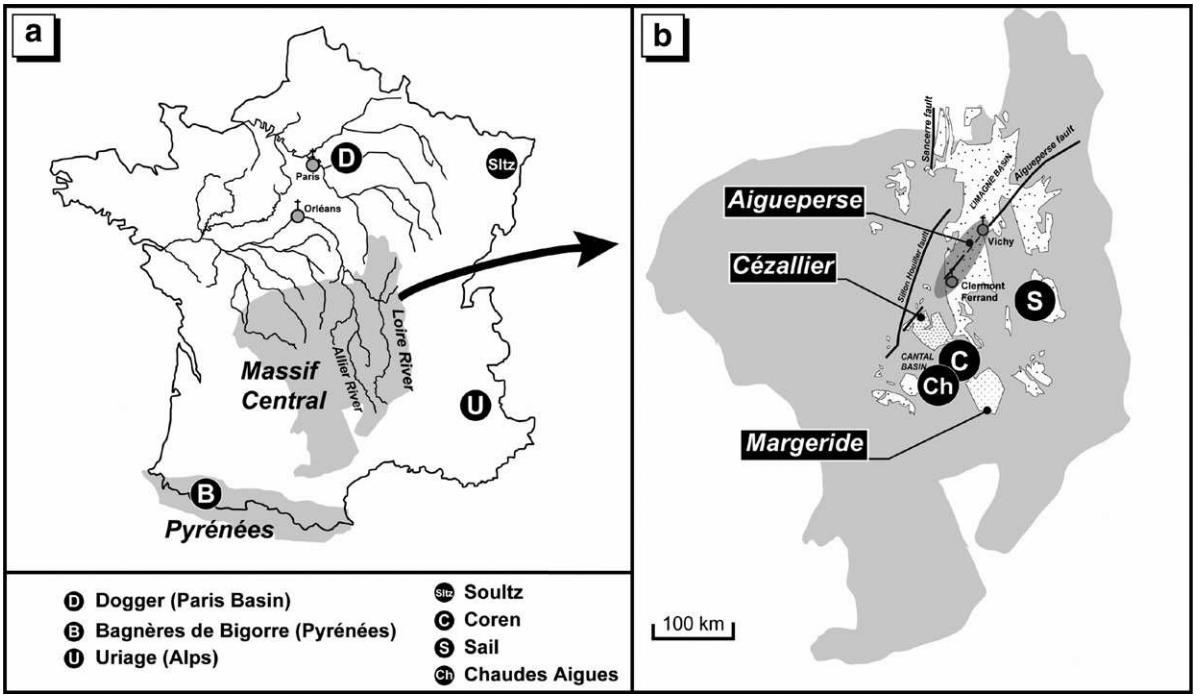

Fig. 1. (a) Map showing the sample location of French geothermal and thermo-mineral waters. (b) The detailed map of the French Massif Central is given on the right hand side of the figure for the location of Aigueperse, Cézallier, Margeride, Coren, Chaudes Aigues and Sail-sous-Couzan samples.

fractured basement (Michard et al., 1987; Criaud and Fouillac, 1986a,b; Beaucaire et al., 1987). The Cézallier area is made up primarily of a metamorphic Variscan basement. The two main bedrock types are gneiss and volcanic deposits of the lava plateau (Feuga, 1987). Ten sites were sampled along the study zone of the Cézallier (Négrel et al., 2000).

2.1.3. Sail-sous-Couzan

The studied mineral water (Casanova et al., 2004) is located in the village of Sail-sous-Couzan (east Massif Central, Fig. 1b), emerging from granite-migmatite series (Gagny et al., 1989). The water is characterized by slightly acidic pH (6.2), high CO_2 concentrations and high dissolved concentrations leading to a Na-Cl-HCO_3 type. The water is K-rich, since the granite contains a large amount of K-bearing phases. The water sample was collected in a borehole, regularly pumped at 100 m depth in the granite.

2.1.4. The Margeride and the Cantal (Chaudes Aigues and Coren)

In the Margeride Massif (located south of the Massif Central, Fig. 1b), Na-HCO_3 springs emerge in the granite with a low flow rate (Négrel et al., 2000). Further to the west, the Chaudes Aigues and Coren springs emerge (de Goër de Herve et al., 1988,1991). This hydrothermal activity is related to a mantle upwelling, which resulted in important alkaline volcanic activity during the Neogene. The waters emerge from the biotite-sillimanite gneiss of the para-autochthonous series (de Goër de Herve et al., 1991). The salinities of the waters are close to 940 mg/L with pH=6.3.

Just north of the Chaudes Aigues location (Fig. 1b), the cold spring of Coren emerges. The spring is located in the gneiss series (de Goër de Herve et al., 1988), in close relation with the Margeride Massif, and is characterized by a very high lithium content (~ 27 mg/L) in the thermo-mineral water.

2.2. Soultz

The Soultz site is located on the west side of the Oligocene Rhine Graben, on a thermal anomaly that has long been recognized. The Graben structure is filled by Tertiary deposits attaining a thickness of 1.5 km in the west and 6 km in the east.

Soultz-sous-Forêts is the French site of the European Hot Dry Rocks (HDR) program. Two boreholes were drilled at this site between 1992 and 1994 in the granitic basement to a depth of 3,600 and 3,800 m (GPK-1 and GPK-2, respectively, Aquilina et al., 1997). In 1997, a

Table 1
Synthesis of temperatures obtained by geothermometry for Aigueperse thermal waters

AIGUEPERSE sample name	Geothermometers	estimated T°C
Joze	Na-K-Ca, Ca/K^2, Na/Li	≈220 °C
Montpensier	Na/K, Na-K-Ca, Ca/K^2, F*K, Sr/K^2	≈175 °C
Royat – Eugénie	Na/K, Na-K-Ca, Na/Li, Sr/K^{22}	≈230 °C
St Myon	Na/K, Na/Li, Ca/K	≈190 °C
Châtel-Guyon - Carnot, Louise	Na/K, Na/Li	≈200 - 220 °C
Gimeaux	Na/K, Na/Li	≈200 - 230 °C
Vichy - Dôme, Forage Antoine	Na/Li	≈150 - 160 °C
Bourbon-Lancy – Marquise	Na/K, Na-K-Ca, Ca/K^2, Mg/Li, F*K	≈170 - 190 °C

From Serra et al. (2003, 2007).

circulation test showed that it was possible to circulate fluid at 25 L/s between two deep wells, 450 m apart, in the depth range of 3,500–3,800 m (Baria et al., 1999). Following this successful 4-month circulation test, GPK2 was deepened from 3,876 to 5,000 m and the bottom-hole temperature increased from 165 to 200 °C (Rabemanana et al., 2003). The sample GPK2 under consideration in the present work originates from 5,000 m.

2.3. The Paris Basin

The Paris Basin is an intracratonic basin of some 6,000 km^2 and with up to 3,000 m of sedimentary infill deposited on top of Hercynian basement. Sediments range in age from Permian to Quaternary. There are two main permeable petroleum reservoir units in the central part of the Mesozoic of the Paris Basin: the Late Triassic fluvial sandstones (Chaunoy Formation) and the Middle Jurassic marine carbonates (Dogger Formation). The Dogger aquifer is predominantly a limestone assemblage, 200-300 m thick, confined between the Liassic and Upper Callovian marls. The Dogger aquifer has a maximum depth of 1,900 m below sea level with temperatures reaching 85 °C at Meaux (Matray et al., 1994). The chemical composition shows that the waters from the Dogger aquifer are essentially Na-Ca-Cl type waters with salinities ranging from 8 to 35 g/L and generally increase with increasing depth (Matray et al., 1994). The geothermal waters under consideration in the present study (Fig. 1) originate from the Dogger formation (Meaux Hopital and Beauval).

2.4. The Pyrénées

The thermal waters are located in the Bagnères-de-Bigorre thermal district (Levet et al., 2002) with springs at Reine and Regina discharging from drill holes that are about 150 m deep. On the other hand, La Tour is a natural spring. Regina and Reine are used for their therapeutic properties in a thermal spa, whereas other springs are not in use. It has been shown by Levet et al. (2002) that the chemical characteristics of these thermal waters suggest interactions with Mesozoic evaporite and carbonate.

2.5. The Alps

Uriage is characterised by groundwater systems related to thermo-mineral springs (Razack and Dazy, 1990). The geological formations consist of a Hercynian basement and a continuous sedimentary cover from Carboniferous to Middle Jurassic age. The basement is composed mainly of mica schists. The sedimentary cover begins with clastic deposits of Paleozoic age (Carboniferous and Permian). The Triassic formations are composed of evaporites (anhydrite and gypsum), dolomites and limestones. The lower Jurassic units (Lias) comprise marly limestones (calcareous Lias), calcareous marls and shales.

The geochemistry of the Uriage spring (Sarrot-Reynauld, 1987) is typical of faulting tectonic control of groundwater occurrence in a multi-reservoir system, e.g. precipitation percolates down the system from the exposures of Triassic evaporites (gypsum and anhydrite) and basement mica schists with a deep system estimated at 4,000 m depth.

3. Methods

3.1. Sampling

Water samples for isotopic determination were collected in acid-washed polyethylene bottles and then filtered through pre-washed 0.2 μm Sartorius cellulose filters using a cleaned polycarbonate Sartorius apparatus under nitrogen. Samples were acidified with ultra pure nitric acid down to pH<2 for Sr and Li isotope determination and stored in non-acidified bottles for B isotope determination.

Table 2
Chemical and isotopic characteristics of geothermal, thermo-mineral, and thermal waters of various sites in France

Location	Sample name	water type	T (°C) emergence	T (°C) geothermometry	Na mg/L
AIGUEPERSE	Joze	Thermo-mineral water	13.5	220	753
	Montpensier	Thermo-mineral water	41.8	175	1280
	Royat - Eugénie	Thermal water	34.2	230	933
	St Myon	Thermo-mineral water	12.1	190	711
	Chatel Guyon - Carnot	Thermal water	36	210	844
	Chatel Guyon - Louise	Thermal water	34.5	210	829
	Gimeaux	Thermo-mineral water	25.3	215	485
	Vichy - Dôme	Thermal water	62.2	155	1710
	Vichy - Forage Antoine	Thermal water	72.6	155	1480
	Bourbon Lancy - Marquise	Thermal water	56.5	180	474
CEZALLIER	Le Bard Maçonnerie	Thermo-mineral water	11	200	1127
	St Hérent Rivière	Thermo-mineral water	14.6	205	1134
	Zagat max	Thermo-mineral water	13.6	210	1224
	Chassole Ste Marguerite	Thermo-mineral water	7.9	210	1017
	Zagat max	Thermo-mineral water	3.8	200	962
	Vèze Supérieure	Thermo-mineral water	15.1	205	626
	Chantejail	Thermo-mineral water	8.6	210	886
	Le Moulin	Thermo-mineral water	12.1	200	862
	Conche Tuyau	Thermo-mineral water	11.4	135	748
	Pyronnée Captage	Thermo-mineral water	16.7	125	899
FOREZ	Sail sous Couzan	Thermo-mineral water	13	200	610
MARGERIDE	Fontaine Haute Mazel	Thermo-mineral water	9.5	190	452
	Fontaine basse 1	Thermo-mineral water	9.8	185	948
	Ranc1	Thermo-mineral water	8.6	120	579
	Ranc2	Thermo-mineral water	8.4	215	429
CHAUDES AIGUES	Vialard	Thermal water	68.6	190	252
	Hospice	Thermal water	67.1	195	236
	Montchasson	Thermal water	12	210	407
	Coren	Thermo-mineral water	9.5	220	2610
SOULTZ	GPK2 5000m	geothermal water	30	230	27400
DOGGER	Meaux Hopital	geothermal water	77.6	100	9884
	Meaux Beauval 1	geothermal water	76.5	100	9147
PYRENEES	Reine	Thermal water	44.7	60	69
	La Tour	Thermal water	43.1	60	61
	Regina	Thermal water	49.9	60	70
ALPS	Uriage	Thermal water	25.2	110	2787

The typology listed in Table 2 is based on the use of the waters under consideration: 1-'geothermal waters' correspond to water samples for which a geothermal exploitation is known (Soultz, Dogger), 2-'thermo-mineral waters' correspond to saline waters that are relatively cold at the surface but are linked to a deep hot reservoir (Chaudes Aigues, Cézallier, Aigueperse, Margeride, and Sail), and 3-'thermal waters' correspond to waters used for their therapeutic properties (Pyrénées, Uriage). Lithium, boron and strontium isotopic data for Aigueperse water samples, and lithium isotopic data for Cézallier and Margeride waters are from Millot et al. (in press). Strontium isotopic data for Margeride samples are from Négrel (1999).

3.2. Major elements, Li-B-Sr concentrations and isotopic measurements

The water samples were analyzed by ion chromatography for major cations and anions (accuracy 5-10%), and by inductively coupled plasma mass spectrometry (ICP-MS) for lithium, boron and strontium concentrations (accuracy 5%).

Lithium isotopic compositions were measured using a Neptune Multi-Collector ICP-MS (Thermo Fischer Scientific) in operation at the BRGM Isotopic Geochemistry Laboratory (see Millot et al., 2004 for more details). $^{7}Li/^{6}Li$ ratios were normalized to the L-SVEC standard solution (NIST SRM 8545, Flesch et al., 1973) following the standard-sample bracketing method. Typical in-run precision on the determination of $\delta^{7}Li$ is about 0.1-0.2‰ ($2\sigma_m$). Chemical separation of lithium from the matrix was achieved before the mass analysis following a procedure modified from the technique of James and Palmer (2000) and using cationic resin (BioRad AG® 50W-X12, 200-400 mesh) and HCl acid media (0.2N) for 30 ng of lithium. Blanks for the total chemical extraction were less than 20-30 pg of Li, which is negligible since it represents a 10^{-3} blank/sample ratio. Accuracy and reproducibility of the total method (purification procedure + mass analysis) were tested by repeated

Cl mg/L	Li µg/L	B µg/L	Sr µg/L	δ^7Li (‰)	δ^{11}B (‰)	$^{87}Sr/^{86}Sr$
420	4371	1369	2850	5.2	1.9	0.713687
226	7081	1169	3450	6.9	0.3	0.713186
1021	6631	6934	5910	2.4	-6.3	0.712181
211	4311	646	3080	5.0	0.2	0.713456
2130	4911	1299	8740	3.3	12.6	0.710581
2087	4711	1199	8390	3.4	11.3	0.710518
616	2890	628	3910	2.5	7.7	0.712503
356	5201	1788	1450	6.2	0.9	0.714393
274	4681	1539	1590	6.6	0.7	0.714056
760	5021	1758	960	5.2	-2.8	0.710940
630	5062	8370	4539	4.4	-7.3	0.716155
673	4911	6897	4147	4.3	-6.6	0.716409
400	6880	nd	nd	3.0	nd	0.716756
489	5353	6740	3204	2.9	-5.8	0.716769
419	5801	1899	3571	2.9	-4.6	0.716756
228	3274	1370	2376	2.8	-8.3	0.716476
338	5293	2745	3240	2.9	-1.5	0.716965
289	4974	2457	2522	3.2	-1.9	0.718055
88	1750	1665	1702	4.8	1.2	0.716773
109	1760	1944	1589	5.5	-0.2	0.716338
66	3108	565	1762	4.4	1.1	0.714410
19	1940	169	1946	5.0	11.4	0.713167
38	4353	329	4759	4.9	14.7	0.712968
29	1097	180	436	3.8	11.9	0.716360
19	2753	1540	283	2.6	nd	0.716241
75	833	1625	450	3.1	-4.0	0.717456
75	773	1558	430	4.3	-3.4	0.721874
165	3094	3411	410	3.0	-4.1	0.717456
1830	26931	29900	943	1.5	-2.7	0.718026
59000	153000	34400	406000	-0.1	4.9	0.711319
17600	2898	21600	65300	10.0	21.6	0.707880
18400	2717	13500	64400	9.9	20.8	0.708010
110	61	97	10310	7.9	3.1	0.707642
92	52	95	9786	8.1	3.0	0.707581
111	59	86	10434	8.0	3.9	0.707550
3635	2800	1494	8920	6.9	-1.2	0.713497

measurement of a seawater sample (IRMM BCR-403) after separation of lithium from the matrix, for which we obtained a mean value of δ^7Li=+30.8‰±0.4 (2σ, n=15) over the period of the duration of the analyses. This mean value is in good agreement with our long-term measurement (δ^7Li=+31.0‰±0.5, 2σ, n=30, Millot et al., 2004) and with other values reported in the literature (see for example Tomascak 2004 for a compilation).

Boron isotopic compositions were determined on a Finnigan MAT 261 solid source mass spectrometer. For these samples, water volumes corresponding to a boron quantity about 10 µg underwent a two step chemical purification using Amberlite IRA-743 selective resin according to a method adapted from Gaillardet and Allègre (1995). The boron aliquot sample (2 µg) was then loaded onto a Ta single filament with graphite, mannitol and Cs, and the B isotopes were determined by measuring the $Cs_2BO_2^+$ ion (Spivack and Edmond, 1986; Spivack et al., 1987). Total boron blank is less than 10 ng. The values are given using the δ-notation (expressed in ‰) relative to the NBS951 boric acid standard. The $^{11}B/^{10}B$ of replicates analysis of the NBS951 boric acid standard after oxygen correction was 4.04845±0.00104 (2σ, n=19) during this period. The reproducibility of the δ^{11}B determination is then ±0.3‰ (2σ) and the internal error is better than 0.3‰ (2 σ_m).

Chemical purification of Sr (~3 μg) was performed using an ion-exchange column (Sr-Spec) before mass analysis according to a method adapted from Pin and Bassin (1992), with total blank <1 ng for the entire chemical procedure. After chemical separation, around 150 ng of Sr was loaded onto a tungsten filament with tantalum activator and analyzed with a Finnigan MAT 262 multi-collector mass spectrometer. The $^{87}Sr/^{86}Sr$ ratios were normalized to an $^{86}Sr/^{88}Sr$ ratio of 0.1194. An average internal precision of ±10 ppm (2 σ_m) was obtained and reproducibility of the $^{87}Sr/^{86}Sr$ ratio measurements was tested through repeated analyses of the NBS987 standard, for which we obtained a mean value of $0.710243 \pm 22 \times 10^{-6}$ (2σ, n=13) during the period of analysis.

3.3. Chemical geothermometry

The concentrations of most dissolved elements in thermo-mineral and/or geothermal waters are functions of the water aquifer temperature and the weathered mineralogical assemblage (White, 1965; Ellis, 1970; Truesdell, 1976; Arnórsson et al., 1983; Fouillac, 1983). Thus, as concentrations can be controlled by temperature-dependent reactions, they could theoretically be used as geothermometers to estimate the deep temperature of the water. However, to be used in this way, further conditions must be fulfilled as summarised by Fournier and Truesdell (1974), Michard (1979) and Giggenbach (1981): 1-temperature-dependent reactions occur at depth; 2-the constituents involved are sufficiently abundant (i.e. supply is not a limiting factor); 3-water/rock equilibration occurs at the reservoir temperature; 4-little or no re-equilibration or change in composition occurs at lower temperatures as the water flows from the reservoir to the surface; 5-the hot water coming from deep does not mix with cooler shallow ground water; 6-no exchange reactions with argillaceous minerals for Na and K in particular occur (Weissberg and Wilson, 1977).

Traditional geothermometer equations (White, 1965; Fournier and Rowe, 1966; Ellis, 1970; Fournier, 1973, 1977, 1979; Fournier and Truesdell, 1973; Fournier and Potter, 1979; Truesdell, 1976; Giggenbach et al., 1983; Giggenbach, 1988) include a silica geothermometer (based on quartz, chalcedony, α or β cristobalite and amorphous silica solubility), a Na/K geothermometer (controlled by plagioclase and K-feldspar equilibrium) and a Na-K-Ca geothermometer (in the case of rich-Ca waters and that can include the Mg correction).

Other chemical geothermometers have been developed, in particular those using lithium (Fouillac and Michard, 1981; Kharaka et al., 1982; Michard, 1990). Unlike Na/K geothermometers, thermometric relationships dealing with this chemical element are not linked with mineralogical equilibrium between water and Li-bearing mineral. Kharaka et al., (1982, 1985) and Kharaka and Mariner (1989) have fitted these geothermometers for water samples coming from petroleum wells. Modified versions of these Na/Li chemical geothermometers and an Mg/Li geothermometer have been developed for the estimation of sedimentary basin subsurface temperatures (from 30 to 200 °C).

Other geothermometers have been proposed. The Sr/K^2 geothermometer defined by Michard (1990) follows from a statistical analysis of granitic deep waters coming from Europe. Giggenbach et al. (1983) have also proposed an Mg/K^2 geothermometer that can be used when dissolved sodium and calcium are not at equilibrium with minerals. Other geothermometers include Ca/K^2 (Fournier and Truesdell, 1973; Michard, 1990), Cs/Na, Fe/K^2, Rb/Na, F*K and Mn/K^2 geothermometers (Michard, 1990).

The method of chemical geothermometry having been discussed, we can now focus on the water samples under consideration in the present study and more especially on the thermo-mineral waters from the Massif Central in the Aigueperse area. In the Massif Central area, it has been shown that numerous thermo-mineral waters have lost part of their initial amount of silica (Fouillac, 1983; Michard et al., 1981; 1987), which could explain the low temperatures of these waters (e.g. in the range 100-150 °C) obtained with silica geothermometers. Using the geothermometers based on cationic ratios, most of the temperatures of the reservoirs in the Massif Central at depth range between 175 and 230 °C as previously demonstrated (Michard et al., 1976, 1981, 1987; Baubron et al., 1979; Fouillac, 1983; Fouillac and Michard, 1979, 1981) with the exception of Vichy (around 130°C). The mean temperature for each site in the Aigueperse zone is given in Table 1 (Serra et al., 2003, 2007) by using the following set of geothermometers (i.e. Si, Na-K, Na-K-Ca, Na/Li, Mg/Li, Sr/K^2, Mg/K^2, Ca/K^2, Cs/Na, Fe/K^2, Rb/Na, F∗K and Mn/K^2) and applying those that are converging to the same temperature estimation (Table 1). The convergence of the geothermometers and the whole method of calculation are discussed in details by Serra et al. (2007) for the Aigueperse samples.

Similarly to the Aigueperse area, the temperatures of the reservoir(s) in the other sites (Chaudes-Aigues, Cézallier, Soultz, Pyrénées, Margeride, Sail and Dogger) were defined using several geothermometers and agree with previous studies (Fouillac and Michard, 1981; Rojas et al., 1990; Aquilina et al., 1997; Levet et al., 2002; Rabemanana et al., 2003). The results are reported in Table 2.

4. Results

4.1. Major and trace elements

A useful first step is to examine the behavior of the major cations. In this context, Fig. 2 illustrates the relationship between Cl (considered as a conservative element) and Na, which is largely controlled by the intensity of water/rock interaction.

Comparison between the Na and Cl concentrations indicates that the high salinity samples have Na/Cl ratios that are similar to those of seawater (consistent with a high formation water component of the fluids), whereas the lower salinity fluids show clear evidence of Na enrichment resulting from water-rock interaction.

Lithium concentrations range widely between 52 μg/L (La Tour, Pyrénées) and 153,000 μg/L for the GPK2 well in Soultz, but in general the Li contents are greater than 1,000 μg/L. Compared to river waters, the hydrothermal and geothermal waters are markedly enriched in lithium, with average river water concentrations (1.5 μg/L; Huh et al. 1998) being ~1,000 times lower than the waters studied here.

Boron concentrations are also very variable and range from 86 to 34,400 μg/L, respectively for Regina (Pyrénées) and Soultz. As already observed for Li concentrations, waters from the Pyrénées have the lowest concentrations for boron (from 86 to 97 μg/L).

Strontium concentrations range from 283 to 406,000 μg/L, respectively for Ranc2 (Margeride) and Soultz. Basically, low Sr concentrations are measured in the Margeride waters (283 to 436 μg/L, Ranc2 and Ranc1) as well as in Chaudes Aigues waters (from 410 to 943 μg/L), whereas the highest concentrations are found in the Soultz (406,000 μg/L, GKP2) and in the Dogger geothermal waters within the Paris Basin (~65,000 μg/L).

4.2. Lithium, boron and strontium isotopes

The δ^7Li values of the hydrothermal and geothermal waters range from-0.1 to +10.0‰, and are generally lower than the range observed in global rivers (+6.0 to +37.5‰; Huh et al., 1998). Although the relationship between δ^7Li values and Li concentrations is not simple, there is a tendency for the samples with the lowest concentrations to have the highest δ^7Li values, and visa versa (Fig. 3).

Boron isotopic compositions range from -8.3 to +21.6 ‰, with no apparent relationship between the δ^{11}B values and boron concentrations (Fig. 3).

The $^{87}Sr/^{86}Sr$ ratios of the waters range between 0.70755 and 0.72187, with a tendency for samples with the highest Sr concentrations to have the lowest isotope

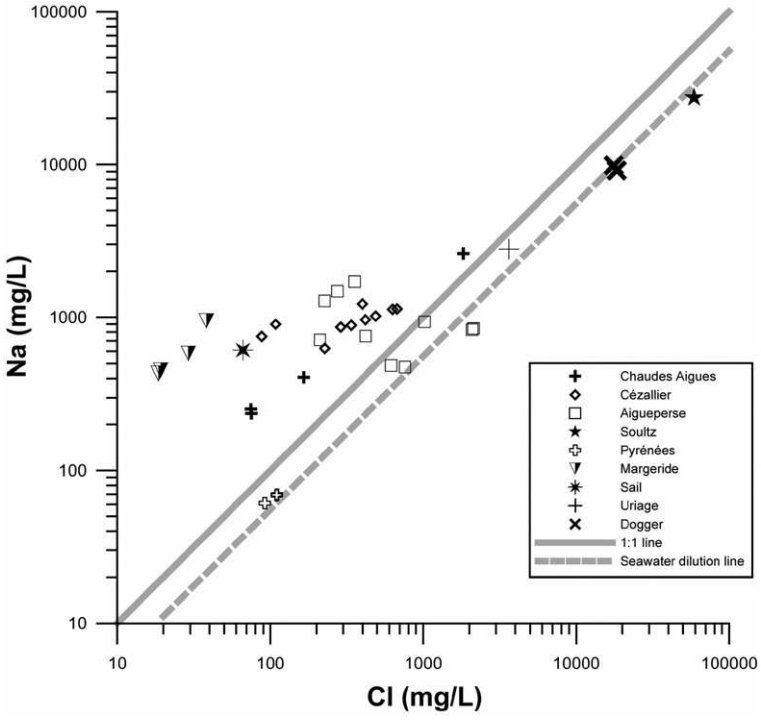

Fig. 2. Sodium concentrations (mg/L) reported as a function of chloride concentrations (mg/L) in thermal, geothermal and thermo-mineral waters. The straight line of 1:1 slope and seawater dilution line have been added in this figure for comparison.

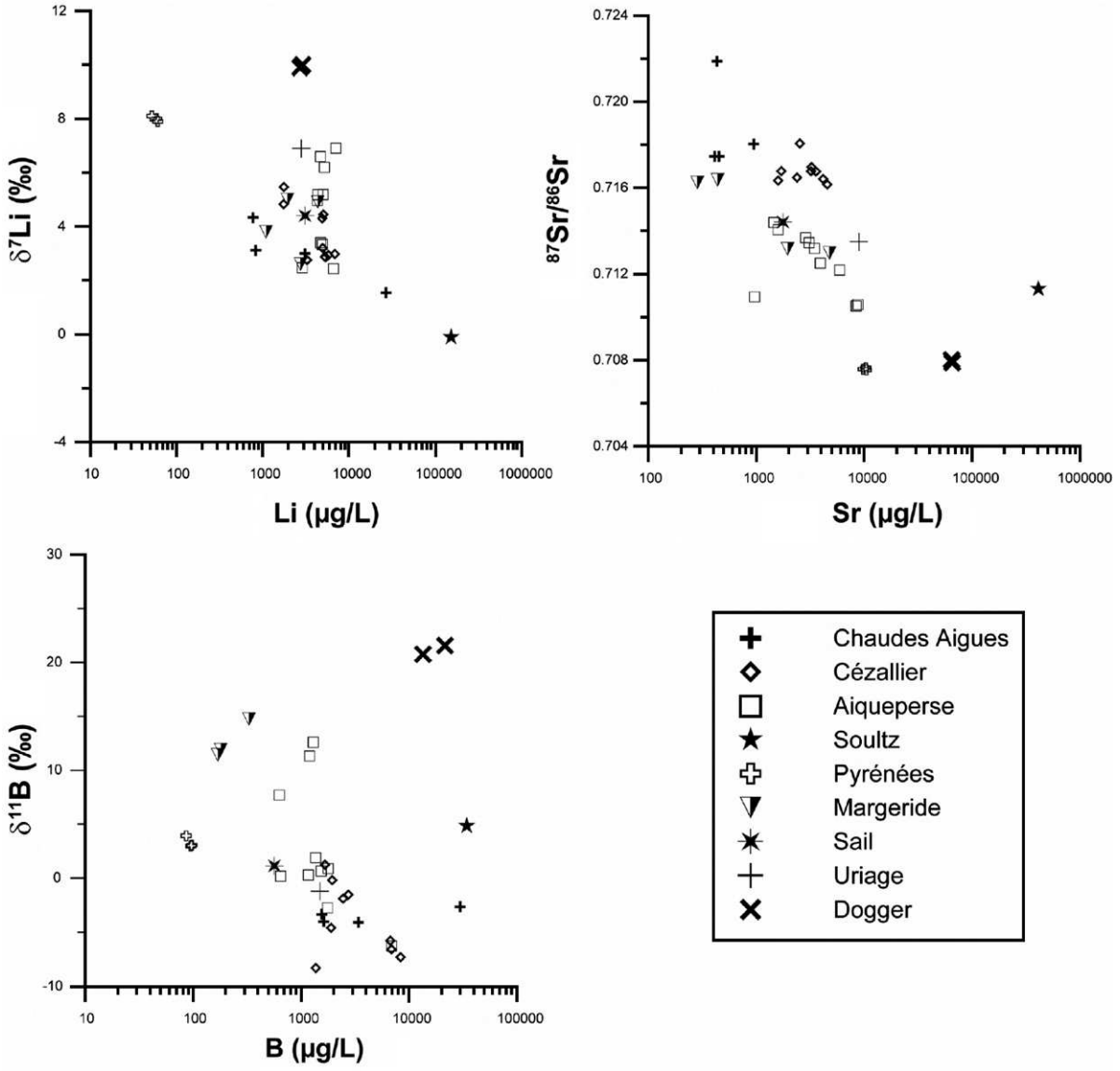

Fig. 3. Lithium, boron and strontium isotopic systematics represented as a function of their Li, B and Sr concentrations for the different thermal, geothermal and thermo-mineral waters.

ratios, and visa versa (Fig. 3). Overall, the highest $^{87}Sr/^{86}Sr$ ratios are observed in the granite-hosted systems and are consistent with previous measurements of granite-hosted fluids (Goldstein and Jacobsen, 1987; Négrel, 1999; Négrel et al., 2000).

5. Discussion

5.1. Sr- B isotopic systematics and temperature of the reservoir

The temperatures of the waters derived from the hydro-geothermal reservoirs were calculated using chemical geothermometers and show a wide range of variation between 60 and 230 °C (cf. 3.3.). The strontium and boron isotopic systematics of these waters are represented in Fig. 4 as a function of temperature.

First of all, by comparing these two types of data, it is obvious that the temperature parameter is much less constrained compared to the precision of the isotopic analyses. Indeed, we can estimate a global uncertainty about ±15% (15×10^{-2}) for temperature calculation by geothermometry. This uncertainty is based on the convergence of several geothermometers applied for the calculation. This uncertainty is significantly higher

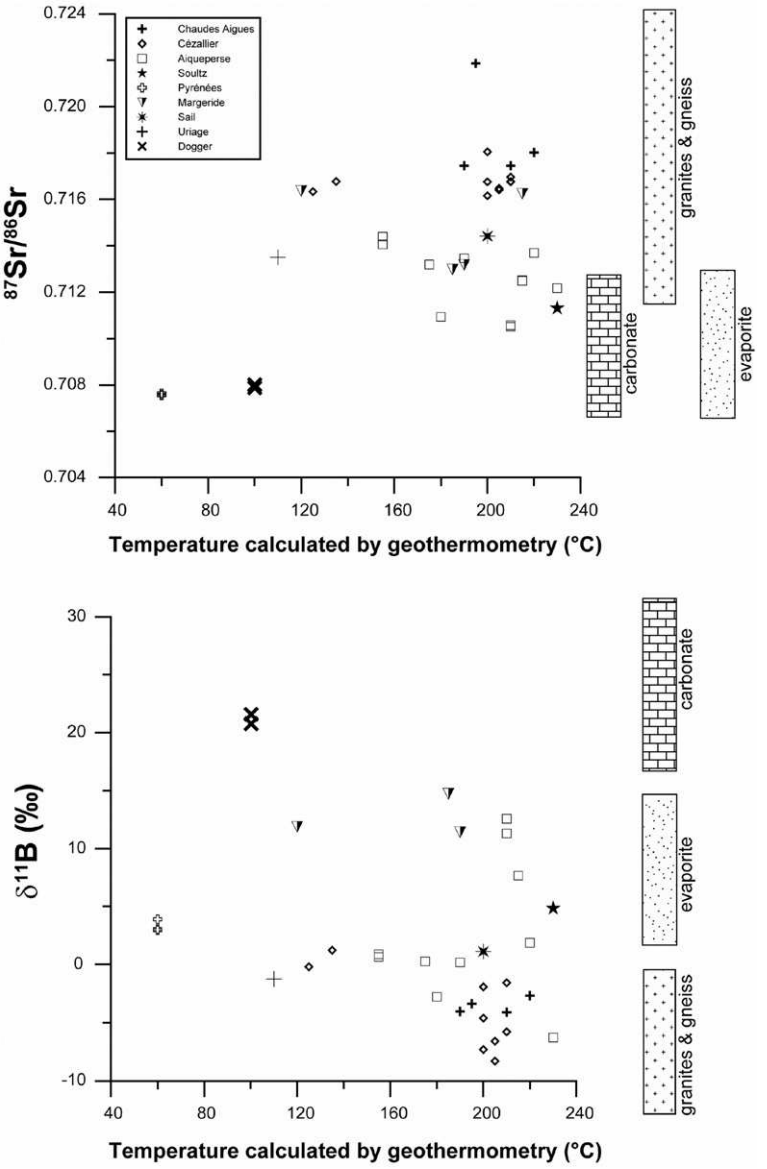

Fig. 4. Strontium isotopic ratios ($^{87}Sr/^{86}Sr$) and boron isotopic compositions ($\delta^{11}B$, ‰) plotted as a function of the temperature of the reservoir calculated by using chemical geothermometers. The ranges of variation in $^{87}Sr/^{86}Sr$ and $\delta^{11}B$ for main lithologies (granite and gneiss, carbonate and evaporite) have been added for comparison from a compilation of $^{87}Sr/^{86}Sr$ and $\delta^{11}B$ values published by Goldstein and Jacobsen (1987), Barth (1993), Négrel (1999) Négrel et al. (2000) and Barth (2000). We can remark that variations in B and Sr isotope tracers appear to be largely controlled at the first order by the dominant host lithologies. However, it is also likely that some lithologies could also present locally some variation range due to the presence of peculiar mineral phases.

compared to the level of precision for B or Sr isotopic measurements, ±0.3‰ (0.3×10^{-3}) and ±10 ppm (10×10^{-6}) respectively for $\delta^{11}B$ and $^{87}Sr/^{86}Sr$ isotopic ratios, cf. paragraph 3.2.

In Fig. 4, we observe no apparent relationship between the $\delta^{11}B$ values and $^{87}Sr/^{86}Sr$ ratios with temperature. Rather variations in both isotope tracers appear to be largely controlled by the dominant host lithologies, with samples from the granite-hosted systems (Cézallier, Margeride) having $\delta^{11}B$ values and $^{87}Sr/^{86}Sr$ ratios similar to characteristic isotope signatures of these sources. Whereas the carbonate and evaporite-hosted systems (Dogger, Pyrénées) display Sr and B isotope signatures that are similar to these source rocks. The other waters have intermediate $\delta^{11}B$-$^{87}Sr/^{86}Sr$ isotope signatures.

5.2. Lithium isotopes and temperature of the reservoir

In Fig. 5, lithium isotopic compositions of thermal, thermo-mineral and geothermal waters are represented according to the temperature of the deep reservoir. It is important to note that the temperatures reported for the deep reservoirs illustrated in Fig. 5 are the mean values calculated from several geothermometers (cf. paragraph 3.3) and do not correspond to the temperature obtained with the only Na/Li geothermometer. Again, it is important to underline the fact that we compare Li isotopic measurements (relative precision of ±0.5‰) with temperature (uncertainty about ±15%).

The Fig. 5 indicates that (in contrast to boron and strontium) temperature seems to play an important role in controlling the lithium isotope composition of the fluids analysed in this study. A corollary of this observation is that the δ^7Li values are less dependent on the nature of the host lithology. In part, this could be due to the fact that the range of δ^7Li values in the host lithologies of the systems studies here is much narrower than is the case for the δ^{11}B values and $^{87}Sr/^{86}Sr$ ratios (Goldstein and Jacobsen, 1987; Barth, 1993; Négrel, 1999; Négrel et al., 2000; Barth, 2000).

When the lithium isotopic composition (δ^7Li, ‰) of the water is reported as a function of the temperature of the reservoir (T, °C), we observe a negative linear relationship (Fig. 5) whose equation is $\delta^7Li = -0.043 \pm 0.003\ T + 11.9 \pm 0.5$ determined using the FREML method (Functional Relationship Estimation by Maximum Likelihood; AMC 2002), with correlation coefficients of-0.83 and-0.86 for Pearson's and Spearman's R respectively.

The range of variation in δ^7Li signatures of hydrothermal waters is about 10‰ for temperatures lying between 60 and 230 °C.

It is likely that most of the waters had undergone considerable cooling from their reservoir temperatures prior to sampling, either through conductive cooling or dilution by groundwaters during shallow circulation. However, the fact that the δ^7Li-reservoir temperature persists, suggests that Li isotope systematics in the reservoir has not been reset to a significant extent. In part, this could reflect the relatively low contribution of surface waters due to their low Li concentrations (Huh

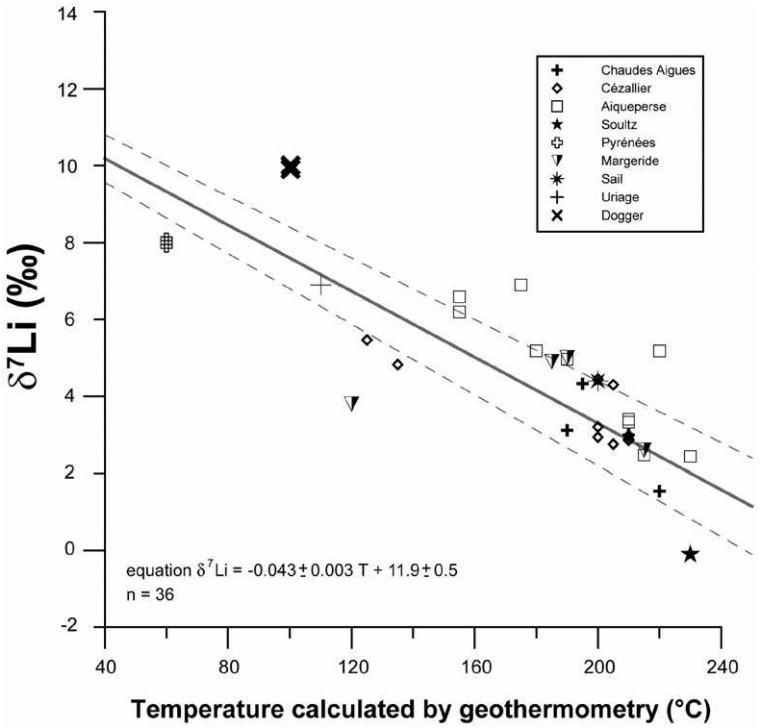

Fig. 5. Lithium isotopic composition (δ^7Li, ‰) represented as a function of the temperature of the hydro-geothermal reservoir calculated by chemical geothermometry. The regression line equation is $\delta^7Li = -0.043 \pm 0.003\ T + 11.9 \pm 0.5$ with values of-0.83 and-0.86 for Pearson's and Spearman's R coefficients respectively. We used the FREML method (Functional Relationship Estimation by Maximum Likelihood; AMC, 2002) that allows the calculation the regression equation by taking into account of the uncertainties of the data. The dashed lines represent the uncertainty on this linear correlation based on the FREML method estimation taken into account the uncertainties of each data on both X and Y axis.

et al., 1998), but it also could suggest that the kinetics of isotope re-equilibration is relatively slow.

Several studies have shown that lithium isotopes are fractionated during water-rock reactions, with the heavy isotope (^{7}Li) being preferentially released into solution, and the light isotope (^{6}Li) retained in the solid phase (Huh et al., 1998; 2001; Pistiner and Henderson, 2003; Teng et al., 2004; Kisakürek et al., 2005; Pogge von Strandmann et al., 2006; Millot et al., in preparation). As with most stable isotope systems, the extent of this isotope system is expected to be temperature dependent, with more extensive fractionation at lower temperatures. Hence, the relationship observed in Fig. 5 is most simply interpreted in terms of a greater degree of Li isotope fractionation between water and rock at lower temperatures, whereas the δ^7Li values of the higher temperature solutions are more similar to those of the host lithology. The scatter observed in the trend presumably also reflects some (relatively small) differences in the δ^7Li value of the host rocks, together with small amounts of Li derived from mixing of the spring waters with surface waters.

The observations in this study suggest that the δ^7Li composition of geothermal waters may be utilised as a geothermometer, particularly where the Li isotope composition of the host rocks are well characterised. However, further work is required to more accurately constrain the temperature dependence of Li isotope fractionation in this environment.

6. Conclusions and perspectives

The purpose of the present work was to characterize hydro-geothermal reservoirs in France by the use of a multi-isotopic study (Li, B and Sr) by coupling this approach with a more classical characterization of deep reservoirs using chemical geothermometry.

The main results of this study are:

- There is no apparent relationship between the δ^{11}B values and ^{87}Sr/^{86}Sr ratios with temperature in hydro-geothermal waters. Variations in B and Sr isotope tracers appear to be largely controlled by the dominant host lithologies.
- In contrast to boron and strontium, temperature plays an important role in controlling the lithium isotope composition of the fluids analysed in this study. When the lithium isotopic composition (δ^7Li, ‰) of the water is reported as a function of the temperature of the reservoir (T, °C), we observe a negative linear relationship whose equation is $\delta^7\text{Li} = -0.043 \pm 0.003\,T + 11.9 \pm 0.5$. This result suggests that the δ^7Li composition of geothermal waters may be utilised as a geothermometer.

However, further work is required to more accurately constrain the temperature dependence of Li isotope fractionation in hydro-geothermal systems.

It is likely that one of the best approaches would be to consider a geothermal field at a smaller scale with a more or less constant lithology and with known variations in temperature inside the geothermal system. Consequently, it should be possible to compare lithium isotopic signatures with temperature variation at the scale of a single geothermal field.

Acknowledgements

This work was financially supported within the scope of the research partnership between BRGM and ADEME and, more specifically, through the COPGEN project (Compilation of the National Geothermic Potential). Financial support from the Région Centre is also acknowledged for the acquisition of the Neptune MC-ICP-MS. We would like to acknowledge B. Sanjuan and A. Genter for fruitful discussions. This work benefited from the collaboration of C. Guerrot (BRGM, Isotope Geochemistry Unit), who provided the boron and strontium isotopic measurements. We are particularly grateful to C. Fouillac, who initiated the research program on the geochemistry of (geo)thermal waters at BRGM and helped us to work on this subject. Two anonymous reviewers are acknowledged for providing helpful reviews of this manuscript. D. Rickard is thanked for editorial handling and constructive comments. This is BRGM contribution n° 4750.

References

Aggarwal, J.K., Palmer, M.R., Bullen, T.D., Arnórsson, S., Ragnarsdóttir, K.V., 2000. The boron isotope systematics of Icelandic geothermal waters: 1. Meteoric water charged systems. Geochimica et Cosmochimica Acta 64, 579–585.

Aggarwal, J.K., Sheppard, D., Mezger, K., Pernicka, E., 2003. Precise and accurate determination of boron isotope ratios by multiple collector ICP-MS: origin of boron in the Ngawha geothermal system, New Zealand. Chemical Geology 199, 331–342.

AMC, 2002. Analytical Methods Committee. Technical brief No. 10. “Fitting a linear functional relationship to data with error on both variables”, Royal Society of Chemistry.

Aquilina, L., Pauwels, H., Genter, A., Fouillac, C., 1997. Water-rock interaction processes in the Triassic sandstone and the granitic basement of the Rhine Graben: Geochemical investigation of a geothermal reservoir. Geochimica et Cosmochimica Acta 61, 4281–4295.

Arnórsson, S., Gunnlaugsson, E., Svavarsson, H., 1983. The geochemistry of geothermal waters in Iceland. III. Chemical geothermometry in geothermal investigations. Geochimica et Cosmochimica Acta 47, 567–577.

Banner, J.L., Wasserburg, G.J., Dobson, P.F., Carpenter, A.B., Moore, C.H., 1989. Isotopic and trace element constraints on the origin and evolution of saline groundwaters from Central Missouri. Geochimica et Cosmochimica Acta 53, 383–398.

Baria, R., Baumgärtner, J., Gérard, A., Jung, R., Garnish, J., 1999. European HDR research programme at Soultz-sous-Forêts (France) 1987–1996. Geothermics 28, 655–669.

Barth, S.R., 1993. Boron isotope variations in nature: a synthesis. Geologische Rundschua 82, 640–641.

Barth, S.R., 2000. Geochemical and boron, oxygen and hydrogen isotopic constraints on the origin of salinity in groundwaters from the crystalline basement of the Alpine Foreland. Applied Geochemistry 15, 937–952.

Baubron, J.C., Bosch, B., Degranges, P., Leleu, M., Marce, A., Rissler, J.J., Sarcia, C., 1979. Geochemical studies on the thermal waters of the west border of the French Limagne. Bulletin De Mineralogie 102, 676–683.

Beaucaire, C., Criaud, A., Michard, G., 1987. Contrôle des concentrations de certains éléments trace (As, Sb, Ge, U, Ra, Ba) dans les eaux du Cézallier (Massif Central, France). Chemical Geology 63, 85–99.

Casanova, J., Négrel, Ph., Kloppmann, W., Aranyossy, J.F., 2001. Origin of deep saline groundwaters in the Vienne granitoids (France). Constrains inferred from boron and strontium isotopes. Geofluids 1, 91–102.

Casanova, J., Négrel, Ph., Petelet-Giraud, E., Kloppmann, W., 2002. The evolution of boron isotopic signature of groundwaters through silicate weathering. In 6th International Symposium on the Geochemistry of the Earth's Surface, Hawaii, vol. 6, pp. 7–12.

Casanova, J., Négrel, Ph., Brach, M., Millot, R., 2004. Temporal variations of multi-element geochemistry and isotopes tracing in mineralized waters from the Massif Central. International Workshop on the Application of Isotope Techniques in Hydrological and Environmental Studies UNESCO, Paris, France, September 6-8.

Casanova, J., Négrel, Ph., Blomqvist, R., 2005. Boron isotope fractionation in groundwaters as an indicator of permafrost past conditions in the fractured crystalline bedrock of the Fennoscandian Shield. Water Research 39, 362–370.

Chan, L.H., Edmond, J.M., 1988. Variation of lithium isotope composition in the marine environment: A preliminary report. Geochimica et Cosmochimica Acta 52, 1711–1717.

Chan, L.H., Edmond, J.M., Thompson, G., Gillis, K., 1992. Lithium isotopic composition of submarine basalts: implications for the lithium cycle in the oceans. Earth and Planetary Science Letters 108, 151–160.

Chan, L.H., Edmond, J.M., Thompson, G., 1993. A lithium isotope study of hot springs and metabasalts from mid-ocean ridge hydrothermal systems. Journal of Geophysical Research 98, 9653–9659.

Chan, L.H., Gieskes, J.M., You, C.F., Edmond, J.M., 1994. Lithium isotope geochemistry of sediments and hydrothermal fluids of the Guaymas Basin, Gulf of California. Geochimica et Cosmochimica Acta 58, 4443–4454.

Criaud, A., Fouillac, C., 1986a. Etude des eaux thermominérales carbogazeuses du Massif Central Français. I. Potentiel d'oxydo-réduction et comportement du fer. Geochimica et Cosmochimica Acta 50, 525–533.

Criaud, A., Fouillac, C., 1986b. Etude des eaux thermominérales carbogazeuses du Massif Central Français. II. Comportement de quelques métaux en trace, de l'arsenic, de l'antimoine et du germanium. Geochimica et Cosmochimica Acta 50, 1573–1582.

Coplen, T.B., Hopple, J.A., Böhlke, J.K., Peiser, H.S., Rieder, S.E., Krouse, H.R., Rosman, K.J.R., Ding, T., Vocke Jr., R.D., Révész, K.M., Lamberty, A., Taylor, P., De Bièvre, P., 2002. Compilation of minimum and maximum isotope ratios of selected elements in naturally occurring terrestrial materials and reagents. U.S. Geological Survey, Water-Resources Investigations, Report 01-4222.

Ellis, A.J., 1970. Quantitative interpretations of chemical characteristics of hydrothermal systems. Geothermics Special Issue 2, 516–528.

Flesch, G.D., Anderson, A.R., Svec, H.J., 1973. A secondary isotopic standard for $^{6}Li/^{7}Li$ determinations. International Journal of Mass Spectrometry and Ion Physics 12, 265–272.

Feuga, B., 1987. Le système geothermal du Cézallier: cadre géologique général et reconnaissance par sondages. Géologie de la France, n°4, mémoire GPF, tome, vol. 2, pp. 3–16.

Fouillac, C., 1983. Chemical geothermometry in CO2-rich thermal waters. Example of the French Massif central. Geothermics, 12, 149–160.

Fouillac, C., Michard, G., 1979. Estimation des températures des réservoirs alimentant les sources thermales de la Limagne. Comptes rendus de l'Academie des sciences 289, 289–292.

Fouillac, C., Michard, G., 1981. Sodium/Lithium ratio in water applied to geothermometry of geothermal reservoirs. Geothermics 10, 55–70.

Fournier, R.O., 1973. Silica in thermal water: Laboratory and field investigations. Proceedings of the International Symposium on Hydrogeochemistry and Biogeochemistry, Japan, 1970, Vol. 1. The Clark Company, Washington, DC, pp. 122–139.

Fournier, R.O., 1977. Chemical geothermometers and mixing models for geothermal systems. Geothermics 5, 41–50.

Fournier, R.O., 1979. A revised equation for the Na/K geothermometer. Geothermal Resources Council Transactions 3, 221–224.

Fournier, R.O., Potter 2nd, R.W., 1979. A magnesium correction to the Na-K-Ca chemical geothermometer. Geochim. Cosmochim. Acta, 43, 1543–1550.

Fournier, R.O., Rowe, J.J., 1966. Estimation of underground temperatures from the silica content of water from hot springs and wet-steam wells. American Journal of Science 264, 685–697.

Fournier, R.O., Truesdell, A.H., 1973. An empirical Na-K-Ca geothermometer for natural waters. Geochimica et Cosmochimica Acta 37, 1255–1275.

Fournier, R.O., Truesdell, A.H., 1974. Geochemical indicators of subsurface temperature– Part 2, Estimation of temperature and fraction of hot water mixed with cold water. Jour. Research U.S. Geol. Survey, 2, 263–270.

Gagny, C., Leistel, J.M., Bouiller, R., Kerrien, Y., 1989. Carte géologique de la France au 1/50.000, Feurs quadrangle and Explanatory Notes. BRGM Editions.

Gaillardet, J., Allègre, C.J., 1995. Boron isotopic compositions of corals: Seawater or diagenesis record? Earth and Planetary Science Letters, 136, 665–676.

Genter, A., Giot, D., Lieutenant, N., Nehlig, P., Rocher, Ph., Roig, J.Y., Chevremont, Ph., Guillou-Frottier, L., Martelet, G., Bitri, A., Perrin, J., Serrano, O., Courtois, N., Vigouroux, P., Négrel, P., Serra, H., Petelet-Giraud, E., 2003. Méthodologie de l'inventaire géothermique des Limagnes : Projet COPGEN, Compilation des données, Rapport BRGM RP-52644-FR. 115pp.

Genter, A., Giot, D., Guillou-Frottier, L., Calcagno, P., Courtois, N., Courrioux, G., Dagallier, A., Giraud-Petelet, E., Goyeneche, O.,

Lieutenant, N., Martelet, G., Négrel, Ph., Rocher, P., Serra, H., Serrano, O., Laplaige, P., 2005. Low to medium temperature geothermal resources in the Limagne Basin (France). Proceedings World Geothermal Congress 2005, Antalya, Turkey, 24-29 April 2005.

Giggenbach, W.F., 1981. Geothermal mineral equilibria. Geochimica et Cosmochimica Acta 45, 393–410.

Giggenbach, W.F., 1988. Geothermal solute equilibria. Derivation of Na-K-Mg-Ca geoindicators. Geochimica et Cosmochimica Acta 52, 2749–2765.

Giggenbach, W.F., Gonfiantini, R., Jangi, B.L., Truesdell, A.H., 1983. Isotopic and chemical compositions of Parbati Valley geothermal discharges, Northwest Himalaya, India. Geothermics 12, 199–222.

Goldstein, S.J., Jacobsen, S.B., 1987. The Nd and Sr Isotopic systematics of river-water dissolved material: implications for the sources of Nd and Sr in seawater. Chemical Geology 66, 245–272.

de Goër de Herve, A., Tempier, P., Simon-Coinçon, R., 1988. Carte géologique de la France au 1/50.000, Saint Flour quadrangle and Explanatory Notes. BRGM Editions.

de Goër de Herve, A., Burg, J.P., Couturie, J.P., Delpuech, A., Duthou, J.L., Etienne, R., Mercier-Batard, F., Périchaud, J.J., Pin, C., Tort, M., Turland, M., 1991. Carte géologique de la France au 1/50.000, Chaudes Aigues quadrangle and Explanatory Notes. BRGM Editions.

Kasemann, S.A., Meixner, A., Erzinger, J., Viramonte, J.G., Alonso, R.N., Franz, G., 2004. Boron isotope composition of geothermal fluids and borate minerals from salar deposits (central Andes/NW Argentina). Journal of South American Earth Sciences 16, 685–697.

Huh, Y., Chan, L.C., Zhang, L., Edmond, J.M., 1998. Lithium and its isotopes in major world rivers: implications for weathering and the oceanic budget. Geochimica et Cosmochimica Acta 62, 2039–2051.

Huh, Y., Chan, L.C., Edmond, J.M., 2001. Lithium isotopes as a probe of weathering processes: Orinoco River. Earth and Planetary Science Letters 194, 189–199.

James, R.H., Rudnicki, M.D., Palmer, M.R., 1999. The alkali element and boron geochemistry of the Escanaba Trough sediment-hosted hydrothermal system. Earth and Planetary Science Letters 171, 157–169.

James, R.H., Palmer, M.R., 2000. The lithium isotope composition of international rock standards. Chemical Geology 166, 319–326.

Kharaka, Y.K., Lico, M.S., Law-Leroy, M., 1982. Chemical geothermometers applied to formation waters, Gulf of Mexico and California basins. AAPG Bulletin 66 (5), 588.

Kharaka, Y.K., Specht, B.J., Carothers, W.W., 1985. Low-to-intermediate subsurface temperatures calculated by chemical geothermometers. The American Association of Petroleum Geologists. Annual Convention, Book of Abstracts, New Orleans, pp. 24–27.

Kharaka, Y.K., Mariner, R.H., 1989. Chemical geothermometers and their applications to waters from sedimentary basins. Thermal History of Sedimentary basins, S.C.P.M. special volume, pp. 99–117.

Kisakürek, B., Widdowson, M., James, R.H., 2004. Behaviour of Li isotopes during continental weathering: the Bidar laterite profile, India. Chemical Geology 212, 27–44.

Kisakürek, B., James, R.H., Harris, N.B.W., 2005. Li and δ^7Li in Himalayan rivers: Proxies for silicate weathering? Earth and Planetary Science Letters 237, 387–401.

Levet, S., Toutain, J.P., Munoz, M., Berger, G., Négrel, Ph., Jendrewjevski, N., Agrinier, P., Sortino, F., 2002. Geochemistry of the Bagneres de Bigorre thermal waters from the North Pyrenean zone (France). Geofluids 2, 25–40.

Matray, J.M., Lambert, M., Fontes, J.Ch., 1994. Stable isotope conservation and origin of saline waters from the middle Jurassic aquifer of the Paris Basin, France. Applied Geochemistry 9, 297–309.

Michard, G., 1979. Géothermomètres chimiques. Bull. du BRGM (2ème série), Section III, n°2, pp. 183–189.

Michard, G., 1990. Behaviour of major elements and some trace elements (Li, Rb, Cs, Sr, Fe, Mn, W, F) in deep hot waters from granitic areas. Chem. Geol. 89, 117–134.

Michard, G., Stettler, A., Fouillac, C., Ouzounian, G., Mandeville, D., 1976. Subsuperficial changes in chemical composition of the thermomineral waters of Vichy basin: geothermal implications. Geochemical Journal 10, 155–161.

Michard, G., Fouillac, C., Grimaud, D., Denis, J., 1981. Une méthode globale d'estimation des températures des réservoirs alimentant les sources thermales. Exemple du Massif central Français. Geochim. Cosmochim. Acta, 45, 1199–1207.

Michard, G., Fouillac, C., Vuataz, F.-D., Criaud, A., 1987. Étude chimique et modèle d'évolution des eaux minérales du Cézallier. Géologie de la France 4, 133–144.

Millot, R., Gaillardet, J., Dupré, B., Allègre, C.J., 2002. The global control of silicate weathering rates and the coupling with physical erosion: new insights from the Canadian Shield. Earth and Planetary Science Letters 196, 83–98.

Millot, R., Gaillardet, J., Dupré, B., Allègre, C.J., 2003. Northern latitude chemical weathering rates: clues from the Mackenzie River Basin, Canada. Geochimica et Cosmochimica Acta 67, 1305–1329.

Millot, R., Guerrot, C., Vigier, N., 2004. Accurate and high precision measurement of lithium isotopes in two reference materials by MC-ICP-MS. Geostandards and Geoanalytical Research 28, 153–159.

Millot R., Vigier N., Gaillardet J., in preparation. Behaviour of lithium and its isotopes during river weathering in the Mackenzie Basin, Canada.

Millot R., Scaillet B., Sanjuan B., submitted for publication. Lithium isotopes in geothermal systems: Guadeloupe, Martinique islands (French west Indies) and experimental approach. Geochimica et Cosmochimica.

Millot R., Négrel Ph., Petelet-Giraud E., in press. Multi-isotopic (Li, B, Sr, Nd) approach for geothermal reservoir characterization in the Limagne Basin (Massif Central, France). Applied geochemistry.

Musashi, M., Masaaki, N., Okamoto, M., Ossaka, T., Oi, T., Kakihana, H., 1988. Regional variation in the boron isotopic composition of hot spring waters from central Japan. Geochemical Journal 22, 205–214.

Négrel, Ph., 1999. Geochemical study in a granitic area, the Margeride, France: chemical element behavior and $^{87}Sr/^{86}Sr$ constraints. Aquatic Geochemistry 5, 125–165.

Négrel, Ph., Petelet-Giraud, E., 2005. Strontium isotopes as tracers of groundwaters-induced floods: the Somme case study (France). Journal Hydrology 305, 99–119.

Négrel, Ph., Allègre, C.J., Dupré, B., Lewin, E., 1993. Erosion sources determined by inversion of major and trace element ratios and strontium isotopic ratios in river water: the Congo Basin case. Earth and Planetary Science Letters 120, 59–76.

Négrel, Ph., Guerrot, C., Cocherie, A., Azaroual, M., Brach, M., Fouillac, C., 2000. Rare Earth Elements, neodymium and strontium isotopic systematics in mineral waters: evidence from the Massif Central, France. Applied Geochemistry 15, 1345–1367.

Négrel, Ph., Casanova, J., Aranyossy, J.F., 2001. Strontium isotope systematics used to decipher the origin of groundwaters sampled

from granitoids: the Vienne Case (France). Chemical Geology 177, 287–308.

Négrel, Ph., Petelet-Giraud, E., Casanova, J., Kloppmann, W., 2002. Boron isotope signatures in the coastal groundwaters of French Guiana. Water Resources Research 38 (11), 1262.

Palmer, M.R., 1991. Boron isotope systematics of hydrothermal fluids and tourmalines; a synthesis. Chemical Geology 94, 111–121.

Palmer, M.R., Sturchio, N.C., 1990. The boron isotope systematics of the Yellowstone National Park (Wyoming) hydrothermal system: A reconnaissance. Geochimica et Cosmochimica Acta 54, 2811–2815.

Pennisi, M., Leeman, W.P., Tonarini, S., Pennisi, A., Nabelek, P., 2000. Boron, Sr, O and H isotope geochemistry of groundwaters from Mt Etna (Sicily): hydrologic implications. Geochimica et Cosmochimica Acta 64, 961–974.

Pin, C., Bassin, C., 1992. Evaluation of a strontium specific extraction chromatographic method for isotopic analysis in geological materials. Geochimica et Cosmochimica Acta 269, 249–255.

Pistiner, J.S., Henderson, G.M., 2003. Lithium isotope fractionation during continental weathering processes. Earth and Planetary Science Letters 214, 327–339.

Pogge von Strandmann, P.A.E., Burton, K.W., James, R.H., van Calsteren, P., Gislason, S.R., Mokadem, F., 2006. Riverine behaviour of uranium and lithium isotopes in an actively glaciated basaltic terrain. Earth and Planetary Science Letters 251, 134–147.

Rabemanana, V., Durst, P., Bächler, D., Vuataz, F.-D., Kohl, T., 2003. Geochemical modelling of the Soultz-sous-Forêts Hot Fractured Rock system: comparison of two reservoirs at 3.8 and 5 km depth. Geothermics 32, 645–653.

Razack, M., Dazy, J., 1990. Hydrochemical characterization of groundwater mixing in sedimentary and metamorphic reservoirs with combined use of Piper's principle and factor analysis. Journal of Hydrology 114, 371–393.

Rojas, J., Giot, D., LeNindre, Y.M., Criaud, A., Fouillac, C., Brach, M., Menjoz, A., Martin, J.C., Lambert, M., Chiles, J.P., Fouillac, A.M., Pauwels, H., 1990. Caractérisation et modélisation du réservoir géothermique du Dogger, Bassin parisien, France. Document du BRGM, n°184. 240 pp.

Sarrot-Reynauld, J., 1987. Tectonique et thermalisme. Conditions d'émergence des eaux thermominérales d'Allevard et d'Uriage (Isère) et de Challes les Eaux (Savoie. 112eme Congrès National des Sociétés Savantes, Lyon, 152/162.

Serra, H., Petelet-Giraud, E., Négrel, Ph., 2003. Inventaire du potentiel géothermique de la Limagne (COPGEN). Synthèse bibliographique de la géochimie des eaux thermales. Rap. BRGM/RP-52587-FR. 84 pp.

Serra H., Négrel Ph., Petelet-Giraud E., 2007. Geochemical modelling approaches for investigating geothermal reservoir temperatures : application to the Limagne Basin (Massif Central, France). Journal of Volcanology and Geothermal Research, in revision.

Spivack, A.J., Edmond, J.M., 1986. Determination of boron isotope ratios by thermal ionisation mass spectrometry of the dicesium metaborate cation. Analytical Chemistry 58, 31–35.

Spivack, A.J., Palmer, M.R., Edmond, J.M., 1987. The sedimentary cycle of the boron isotopes. Geochimica et Cosmochimica Acta 51, 1939–1949.

Teng, F.Z., McDonough, W.F., Rudnick, R.L., Dalpé, C., Tomascak, P.B., Chappell, B.W., Gao, S., 2004. Lithium isotopic composition and concentration of the upper continental crust. Geochimica et Cosmochimica Acta 68, 4167–4178.

Tomascak, P.B., 2004. Developments in the Understanding and Application of Lithium Isotopes in the Earth and Planetary Sciences. Reviews in Mineralogy & Geochemistry, 55, pp. 153–195.

Truesdell, A.H., 1976. Geochemical techniques in exploration, summary of section III. Proc. Sec. United Nations Symp. Develop. Use Geotherm. Res., San Francisco, pp. 53–79.

Weissberg, B.G., Wilson, P.T., 1977. Montmorillonite and the Na/K geothermometer. Geochemistry 77, vol. 218. N.Z. Dept. Sci. Indust. Res. Bull., pp. 31–35.

White, D.E., 1965. Saline waters of sedimentary rocks. Fluids in Subsurface Environments- A Symposium. American Association of Petroleum Geologist Memoir 4, 342–366.

Wunder, B., Meixner, A., Romer, R.L., Heinrich, W., 2006. Temperature-dependent isotopic fractionation of lithium between clinopyroxene and high-pressure hydrous fluids. Contributions to Mineral and Petrology 151, 112–120.

Applied Geochemistry 27 (2012) 677–688

Contents lists available at SciVerse ScienceDirect

Applied Geochemistry

journal homepage: www.elsevier.com/locate/apgeochem

Geothermal waters from the Taupo Volcanic Zone, New Zealand: Li, B and Sr isotopes characterization

Romain Millot [a,*], Aimee Hegan [a,b], Philippe Négrel [a]

[a] BRGM, Metrology Monitoring Analysis Department, Orléans, France
[b] School of Earth, Atmospheric and Environmental Sciences, The University of Manchester, Manchester, United Kingdom

ARTICLE INFO

Article history:
Received 11 April 2011
Accepted 21 December 2011
Available online 8 January 2012
Editorial handling by L. Aquilina

ABSTRACT

Chemical and isotopic data for 23 geothermal water samples collected in New Zealand within the Taupo Volcanic Zone (TVZ) are reported. Major and trace elements including Li, B and Sr and their isotopic compositions (δ^7Li, δ^{11}B, ^{87}Sr/^{86}Sr) were determined in high temperature geothermal waters collected from deep boreholes in different geothermal fields (Ohaaki, Wairakei, Mokai, Kawerau and Rotokawa geothermal systems). Lithium concentrations are high (from 4.5 to 19.9 mg/L) and Li isotopic compositions (δ^7Li) are homogeneous, ranging between −0.5‰ and +1.4‰. In particular, it is noteworthy that, except for the samples from the Kawerau geothermal field having slightly higher δ^7Li values (+1.4%), the other geothermal waters have a near constant δ^7Li signature around a mean value of 0‰ ± 0.6 (2σ, $n = 21$). Boron concentrations are also high and relatively homogeneous for the geothermal samples, falling between 17.5 and 82.1 mg/L. Boron isotopic compositions (δ^{11}B) are all negative, and display a range between −6.7‰ and −1.9‰. These B isotope compositions are in agreement with those of the Ngawha geothermal field in New Zealand. Lithium and B isotope signatures are in a good agreement with a fluid signature mainly derived from water/rock interaction involving magmatic rocks with no evidence of seawater input. On the other hand, Sr concentrations are lower and more heterogeneous and fall between 2 and 165 μg/L. The ^{87}Sr/^{86}Sr ratios range from 0.70549 to 0.70961. These Sr isotope compositions overlap those of the Rotorua geothermal field in New Zealand, confirming that some geothermal waters (with more radiogenic Sr) have interacted with bedrocks from the metasedimentary basement. Each of these isotope systems on their own reveals important information about particular aspects of either water source or water/rock interaction processes, but, considered together, provide a more integrated understanding of the geothermal systems from the TVZ in New Zealand.

1. Introduction

In the present work, chemical and isotope data for 23 geothermal water samples from the Taupo Volcanic Zone (TVZ) in New Zealand are reported. Chemical and isotopic data were determined for these deep geothermal waters in order to provide further constraints on the characterization of the associated deep geothermal reservoirs. The present study aims, therefore, to characterize the fluids from the geothermal systems for the TVZ and, more specifically, to constrain the nature and origin of these fluids: two essential parameters for the characterization of a geothermal resource.

Major and trace elements are first investigated in order to determine the chemical signature of the TVZ geothermal samples. A multi-isotopic approach is then used to provide additional information for the characterization of these waters. Strontium isotopes (^{87}Sr/^{86}Sr) are investigated in order to better constrain the signature of the reservoir that the waters come from, given that Sr isotopes are a good tracer of water origin for groundwaters and geothermal waters (Stettler and Allègre, 1978; Elderfield and Greaves, 1981; Graham, 1992; Stueber et al., 1993; Aquilina et al., 1997; Négrel et al., 1997; Négrel, 1999; Vengosh et al., 2002; Millot et al., 2007). In addition, Li and B isotopic compositions of the TVZ geothermal waters were determined with the objective of evaluating the utility of these isotopic tools to constrain the water/rock interaction. Indeed, the isotopic composition of B (δ^{11}B) is determined in an attempt to elucidate the source and processes controlling B in geothermal waters (Aggarwal et al., 2003), and the use of Li isotopic systematics (δ^7Li) is also explored, following recent papers indicating that Li isotopes seem to be an effective tracer of water/rock interaction in geothermal waters (Millot et al., 2007, 2010a; Millot and Négrel, 2007).

The present study evaluates the information that can be obtained using a multi-isotopic approach to characterize geothermal waters. More precisely, it is demonstrated how a combination of these isotopic tracers can help to decipher water–rock

* Corresponding author. Tel.: +33 2 38 64 48 32; fax: +33 2 38 64 37 11.
E-mail address: r.millot@brgm.fr (R. Millot).

0883-2927/$ - see front matter © 2012 Elsevier Ltd. All rights reserved.
doi:10.1016/j.apgeochem.2011.12.015

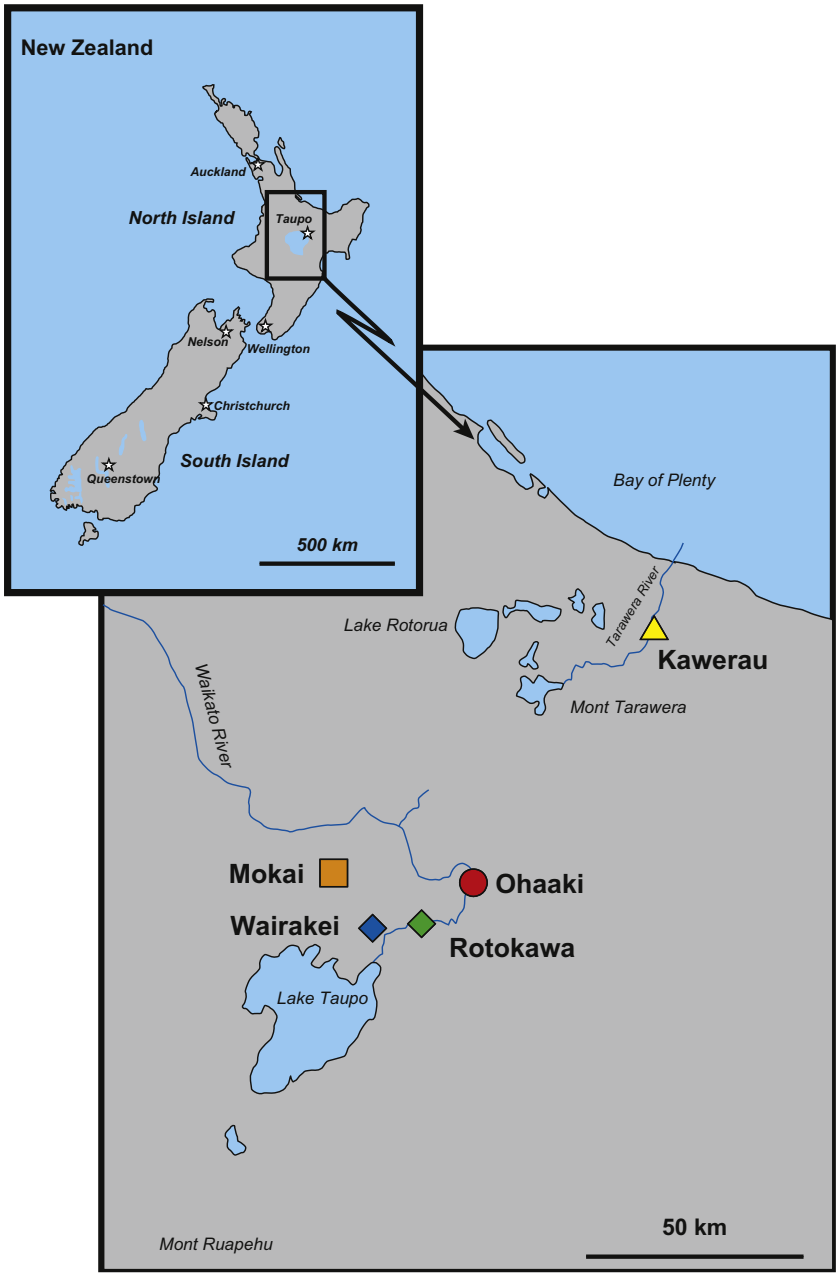

Fig. 1. Geothermal sample locations. These geothermal waters were sampled by Contact Energy Limited for the Ohaaki and Wairakei geothermal systems and by Mighty River Power Limited (MRP) for the Mokai, Kawerau and Rotokawa geothermal systems respectively.

interaction processes. However, each isotopic system can only provide information concerning the chemical behavior of the element, but considered together, this multi-isotope approach can provide a more integrated understanding of the TVZ geothermal system in New Zealand.

2. The Taupo Volcanic Zone

Situated in the middle of the North Island of New Zealand, the TVZ is an area of both volcanic and geothermal activity. Rhyolitic volcanic activity in the area is thought to have commenced 1.6 Ma ago. The enhanced activity in the region is a result of an actively extending back-arc rift, due to the subduction of the Pacific plate beneath North Island. This area is characterized by an extremely high heat flow. The average heat flux from the central zone of the TVZ, which contains most of the geothermal fields, is about 700 mW/m^2 (Bibby et al., 1995).

Geothermal systems occur in many parts of New Zealand. The conventional geothermal resources of New Zealand are currently situated at depths between 1 and 3 km, with temperatures up to 330 °C. High temperature geothermal fields ($T > 250$ °C) are principally located in the TVZ (Fig. 1), with another high temperature field at Ngawha in Northland. Moderate to low and very low temperature systems ($T < 250$ °C) are more widely scattered. Some are associated with areas of young volcanism: in Northland, Hauraki Plains, and the coastal Bay of Plenty. Many hot springs, particularly in the South Island, are associated with faults and tectonic features.

The TVZ is 20–80 km wide and extends from Mt Ruapehu in the south to the Okataina Volcanic Center (Mt Tarawera) in the north and continues 200 km offshore. The zone is flanked by thick aprons of welded pyroclastic flows that form shallow dipping plateaus.

Table 1
Sample list including geothermal site, sample i.d., latitude and longitude, depth of borehole (m), deep temperature estimates given by geothermometry (°C) and date of sampling. Major and trace elements concentrations (mg/L) in the geothermal water samples are also reported in this table and Li, B and Sr isotopic compositions. d.l. is the detection limit (5 μg/L for Mg). Individual errors ($2\sigma_m$) are also reported for isotopic data.

Geothermal system	Well ID	Coordinates		Borehole depth (m)	Deep temperature (°C)	Date	Na (mg/L)	K (mg/L)	Mg (μg/L)	Ca (mg/L)	Cl (mg/L)	SO_4 (mg/L)	Br (mg/L)	SiO_2 (mg/L)	Li (mg/L)	B (mg/L)	Sr (μg/L)	δ^7Li (‰)	$2\sigma_m$	δ^{11}B (‰)	$2\sigma_m$	$^{87}Sr/^{86}Sr$	$2\sigma_m$
		Latitude	Longitude																				
Ohaaki	BR25	S38°31′58″	E176°18′43″	680	215	10/7/2004	813	94	<d.l.	0.106	728	19	2	432	10.32	21.71	47.9	−0.01	0.12	−3.43	0.09	0.707855	0.000006
Ohaaki	BR49	S38°32′16″	E176°18′37″	1270	280	10/4/2005	1108	206.5	8.4	2.143	1475	4	3.7	967	12.74	82.13	68	0.24	0.16	−3.50	0.08	0.709612	0.000006
Ohaaki	BR9	S38°31′11″	E176°18′24″	1000	205	4/3/2006	739	72.2	8.3	1.647	666	74.8	1.9	384	7.62	17.50	99.1	−0.52	0.14	−3.93	0.06	0.706058	0.000009
Ohaaki	BR22	S38°31′10′	E176°18′34″	670	249	4/3/2006	864	137.4	5.3	1.758	1080	58.8	3.1	709	9.53	28.22	55.8	−0.30	0.24	−4.71	0.07	0.706312	0.000007
Ohaaki	BR20	S38°31′18″	E176°18′36″	1000	248	4/23/2007	825	110.2	15.4	1.859	1009	60.5	3	662	8.84	26.31	47	−0.45	0.22	−4.84	0.08	0.705900	0.000007
Ohaaki	BR54	S38°31′06″	E176°18′35″	1430	261	5/1/2007	773	121.4	<d.l.	1.624	928	43.5	2.7	792	8.27	23.06	29.7	−0.14	0.20	−4.23	0.11	0.706215	0.000007
Ohaaki	BR44	S38°31′53″	E176°19′06″	760	243	8/28/2007	839	102.2	5.1	2.146	1173	12.4	3.2	664	8.38	35.10	114.7	−0.08	0.18	−4.35	0.09	0.706837	0.000007
Ohaaki	BR14	S38°37′06″	E176°19′19″	590	226	8/31/2007	799	81.1	25.4	12.625	1308	3.9	3.7	554	6.77	36.91	165.2	−0.17	0.24	−4.30	0.07	0.705942	0.000007
Ohaaki	BR48	S38°31′06″	E176°17′53″	1360	265	9/28/2007	780	136.1	<d.l.	1.872	1017	41.3	2.8	877	8.10	25.53	26.8	−0.18	0.12	−4.39	0.07	0.706079	0.000007
Ohaaki	BR60	S38°31′10″	E176°17′54″	1800	280	7/23/2008	941	199.2	8.9	2.686	1485	10.2	4.4	984	10.10	38.40	90.4	−0.13	0.10	−6.34	0.07	0.706409	0.000008
Ohaaki	BR56	S38°31′01″	E176°18′17″	1880	297	9/3/2008	892	220.5	27.9	3.003	1508	9.5	4.3	1169	9.30	32.06	35.6	0.24	0.26	−5.45	0.08	0.706572	0.000006
Wairakei	WK245	S38°37′04″	E176°02′59″	800	251	9/7/2008	1264	217.4	<d.l.	10.923	2295	34.1	5.4	709	13.28	24.81	50.3	0.24	0.14	−2.84	0.09	0.705490	0.000009
Wairakei	WK70	S38°37′22″	E176°04′22″	600	229	10/8/2008	1080	146.1	8.6	20.434	1882	35	4.5	602	9.78	23.39	88.3	0.27	0.30	−3.23	0.08	0.705600	0.000008
Wairakei	WK247	S38°36′55″	E176°03′20″	2300	251	3/5/2007	1302	213.2	7.5	27.667	2295	34	5.8	677	12.12	25.97	101	0.23	0.12	−2.41	0.09	0.705738	0.000007
Wairakei	WK235	S38°36′53″	E176°03′23″	700	220	3/4/2008	1250	175.6	9.2	20.911	2229	33.7	5.6	477	12.58	24.06	120.9	0.31	0.18	−1.92	0.09	0.705587	0.000008
Wairakei	WK28	S38°37′32″	E176°04′09″	600	207	4/14/2008	1060	139.3	16.7	21.261	1846	44.4	4.6	455	9.48	22.44	99.4	0.11	0.18	−2.48	0.12	0.705658	0.000008
Wairakei	WK24	S38°37′21″	E176°04′18″	600	219	7/30/2008	1007	128.2	7.2	20.247	1731	34.9	4.3	521	9.03	20.75	85.9	0.69	0.18	−2.15	0.08	0.705616	0.000007
Mokai	MK3	S38°31′34″	E175°56′23″	1679	300	2/24/2009	1246	288.6	14.6	7.965	2398	11.7	5.6	799	16.88	24.79	28.5	0.02	0.16	−1.98	0.09	0.705636	0.000006
Mokai	MK7	S38°31′36″	E175°55′34″	2252	290	2/25/2009	1477	338.2	27.2	12.086	2834	6.6	5.9	777	19.94	31.10	50	0.39	0.16	−2.36	0.09	0.706789	0.000007
Kawerau	KA37	S38°03′52″	E176°43′34″	1306	270	1/29/2009	586	92.9	<d.l.	1.891	797	26.4	2	822	4.46	37.34	35.1	1.42	0.18	−2.84	0.06	0.706170	0.000009
Kawerau	KA19	S38°03′32″	E176°43′07″	1108	260	1/28/2009	665	99.4	6.9	2.468	932	14.6	2	803	4.97	42.28	55.3	1.38	0.16	−1.99	0.06	0.705919	0.000007
Rotokawa	RK14	S38°36′33″	E176°11′25″	2500	315	4/8/2009	422	126.7	<d.l.	1.632	764	2.6	1.3	1006	5.67	21.80	4.3	0.08	0.16	−6.70	0.06	0.709240	0.000007
Rotokawa	RK5	S38°36′31″	E176°11′40″	2783	320	4/7/2009	388	112.1	<d.l.	1.232	674	3.9	1.1	1027	5.18	17.90	2.1	0.06	0.20	−5.25	0.07	0.705554	0.000007

Within the TVZ, the different geothermal fields are distributed in two bands approximately 20 km apart. It was estimated by Bibby et al. (1995), that 75% of the heat flow occurs in the eastern band and 25% in the west. Samples were collected from 5 geothermal fields within the TVZ: Kawerau, Rotokawa and Ohaaki from the eastern side, and Mokai and Wairakei from the western side (Fig. 1).

Temperatures of over 300 °C are recorded for the fluids of the geothermal systems within the TVZ, generally within the eastern fields e.g. Kawerau (315 °C) and Rotokawa (330 °C) (Kissling and Weir, 2005). Maximum temperatures at Wairakei reach 265 °C (Kissling and Weir, 2005), with Mokai reaching 326 °C.

Giggenbach (1995) used the variations of H_2O, CO_2 and Cl in discharges from six geothermal systems within the TVZ to identify the existence of two distinct types of deep water supply. Falling along the eastern side of the TVZ: Kawerau, Ohaaki and Rotokawa display higher gas contents than the fields on the western side, including Mokai and Wairakei (illustrated by CO_2/Cl ratios above 3.9 ± 1.5 vs. 0.14 ± 0.1). According to Giggenbach (1995), the higher ratios are of andesitic rock origin, with the lower ratios originating from rhyolitic material. The excess volatiles present in fluid discharges from geothermal and volcanic systems along convergent plate boundaries are likely to be derived preferentially from the marine sedimentary fraction of subducted material (Giggenbach, 1995).

The Mokai geothermal system lies 25 km NW of Lake Taupo, and is thought to be 10 km^2, based on resistivity measurements (Kissling and Weir, 2005).

The Rotokawa geothermal system lies 10 km NE of Lake Taupo and has an area of 25 km^2, based on resistivity measurements (Hunt and Bowyer, 2007; Heise et al., 2008). A mix of Paleozoic and Mesozoic greywackes form the basement of the system, with a mix of ignimbrites and rhyolite lavas forming overlying layers, which are in turn covered by Holocene tuff (Krupp et al., 1986; Wilson et al., 2007).

Hydrothermally altered greywacke sandstones dominate the basements in both the Kawerau and Ohaaki geothermal fields, however, characterization by Wood et al. (2001) has shown that, despite similar lithologies, there are very different petrological characteristics between the two. As a result, the Ohaaki greywackes are analogous, in terms of bulk compositions, to granite, and the Kawerau greywackes to quartz diorite. The basement at Ohaaki also differs from those of the other fields due to the occurrence of (approx. 3%) argillite in fine partings (Wood et al., 2001).

In Table 1, the geothermal samples are listed with their origin (geothermal system), the borehole depth (m) and deep temperature (°C) estimated by chemical geothermometry (described below).

3. Analytical methods

3.1. Major and trace elements

The samples were collected, after filtration and acidification on site, by MRP and Contact Energy, from the production pipeline using a fluid sampling separator. These geothermal sites are managed by Contact Energy Limited, the Tuaropaki Power Company, the Rotokawa Joint Venture and Mighty River Power Limited. All chemical analyses were performed in the BRGM laboratories using standard water analysis techniques such as Ion Chromatography (Cl), Inductively Coupled Plasma-Atomic Emission Spectroscopy (Li, B and Sr), Inductively Coupled Plasma-Mass Spectrometry (Ca and Mg), and Flame Emission Spectrometry (Na, K, Ca and SiO_2). Major species and trace elements were determined on conditioned samples, i.e., after filtration at 0.2 μm for the major anions, and after filtration at 0.2 μm and acidification with Suprapur HNO_3 acid (down to pH = 2) for the major cations and trace elements.

Accuracy and precision for major and trace elements was verified by repeated measurements of standard materials during the course of this study: namely Ion96-3 and LGC6020 for cations and anions and pure Li, B and Sr standard solutions (Merck). The accuracy of the major and trace element data is approx. ±10%.

3.2. Lithium isotopes

Lithium isotopic compositions were measured using a Neptune Multi Collector ICP-MS (Thermo Fischer Scientific). The $^7Li/^6Li$ ratios were normalized to the L-SVEC standard solution (NIST SRM 8545, Flesch et al., 1973) following the standard-sample bracketing method (see Millot et al. (2004) for more details). The analytical protocol involves the acquisition of 15 ratios with 16 s integration time per ratio, and yields in-run precision better than 0.2‰ ($2\sigma_m$). Blank values are low, (i.e. 0.2%), and 5 min wash time is enough to reach a stable background value.

The samples were prepared beforehand by chemical separation/purification with ion chromatography in order to produce a pure mono-elemental solution. Chemical separation of Li from the matrix was achieved before the mass analysis using a cationic resin (a single column filled with 3 mL of BioRad AG® 50W-X12 resin, 200–400 mesh) and HCl acid media (0.2 N) for 30 ng of Li. Blanks for the total chemical extraction were less than 30 pg of Li, which is negligible, since it represents a 10^{-3} blank/sample ratio.

Successful quantitative measurement of Li isotopic compositions requires 100% Li recovery. The column was, therefore, frequently calibrated and repeated analysis of the L-SVEC standard processed through columns shows 100% Li recovery and no induced isotope fractionation due to the purification process.

The accuracy and reproducibility of the entire method (purification procedure + mass analysis) were tested by repeated measurement of a seawater sample (IRMM BCR-403) after separation of Li from the matrix, for which a mean value of δ^7Li = +30.9‰ ± 0.3 (2σ, n = 7) was obtained over the analysis period. This mean value is in good agreement with the authors' long-term measurement (δ^7Li = +31.0‰ ± 0.5, 2σ, n = 30, Millot et al., 2004) and with other values reported in the literature (see, for example, Millot et al., 2004 for a compilation with δ^7Li values for seawater ranging from +28.9‰ to +33.9‰). Consequently, based on long-term measurements of a seawater standard, the external reproducibility of the method was estimated to be around ±0.5‰ (2σ).

3.3. Boron isotopes

Boron isotopic compositions were determined on a Finnigan MAT 261 solid source mass spectrometer in dynamic mode. Boron isotope compositions were determined on conditioned samples (after filtration at 0.2 μm). For these samples, water volumes corresponding to a mass of 4 μg of B were processed using a two-step chemical purification through Amberlite IRA-743 selective resin. The B aliquot sample (2 μg) was then loaded onto a Ta single filament with graphite, mannitol and Cs, and the B isotopes were determined by measuring the $Cs_2BO_2^+$ ion. The total B blank is less than 10 ng. The values are given using the δ-notation (expressed in ‰) relative to the NBS951 boric acid standard. The $^{11}B/^{10}B$ of replicate analyses of the NBS951 boric acid standard after O correction was 4.05122 ± 0.00122 (2σ, n = 27) during this period. The reproducibility of the $\delta^{11}B$ determination is ±0.3‰ (2σ) and the internal uncertainty is better than 0.3‰ ($2\sigma_m$).

The accuracy and reproducibility of the whole procedure were verified by the repeated measurements of the IAEA-B1 seawater standard (Gonfiantini et al., 2003) for which the mean $\delta^{11}B$ value obtained is +39.22‰ ± 0.32 (2σ, n = 33), in agreement with the accepted value for seawater ($\delta^{11}B$ = +39.5‰, see data compilation reported by Aggarwal et al., 2004).

3.4. Strontium isotopes

Chemical purification of Sr (~3 μg) was performed using an ion-exchange column (Sr-Spec) before mass analysis according to a method adapted from Pin and Bassin (1992), with total blank <1 ng for the entire chemical procedure. After chemical separation, around 150 ng of Sr was loaded onto a W filament with Ta activator and analyzed with a Finnigan MAT 262 multi-collector mass spectrometer. The $^{87}Sr/^{86}Sr$ ratios were normalized to a $^{86}Sr/^{88}Sr$ ratio of 0.1194. An average internal precision of $\pm 10^{-5}$ ($2\sigma_m$) was obtained and the reproducibility of the $^{87}Sr/^{86}Sr$ ratio measurements was tested by repeated analyses of the NBS987 standard, for which a mean value of 0.710243 ± 0.000010 (2σ, $n = 9$) was obtained during the period of analysis.

3.5. Chemical geothermometry

The concentrations of most dissolved elements in geothermal waters depend on the groundwater temperature and the weathered mineralogical assemblage (White, 1965; Ellis, 1970; Truesdell, 1976; Arnórsson et al., 1983; Fouillac, 1983). Since concentrations can be controlled by temperature-dependent reactions, they could theoretically be used as geothermometers to estimate the deep temperature of the water. In the present study, deep temperature estimates were calculated based on SiO_2 concentrations following silica geothermometry based on quartz, chalcedony, α or β cristobalite and amorphous silica solubility (Fournier and Rowe, 1966; Helgeson et al., 1978; Arnórsson et al., 1983). These temperature estimates agree well with downhole measurements and with previous data reported in the literature (Hedenquist, 1990; Christenson et al., 2002).

4. Results and comments

4.1. Major and trace elements

Geothermal waters are commonly characterized by examining the behavior of the major elements (Table 1). In this context, Fig. 2 illustrates the relationship between Cl, considered as a conservative element, and Na, which is largely controlled by water/rock interaction. Whereas Cl concentrations range between 666 and 2834 mg/L, Na concentrations range between 388 and 1477 mg/L. A good relationship is observed between Na and Cl (Fig. 2), indicating that the geothermal waters display a large range of salinity, with Na and Cl concentrations increasing from Rotokawa, Kawerau, Ohaaki and Wairakei up to the samples from Mokai.

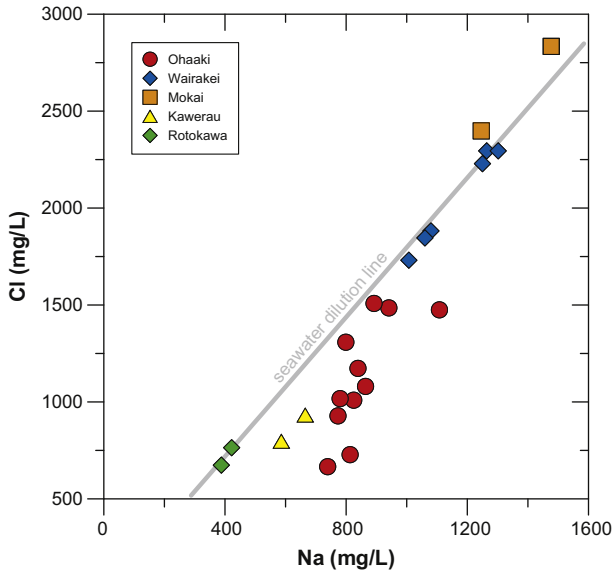

Fig. 2. Cl concentrations (mg/L) plotted as a function of Na concentrations (mg/L).

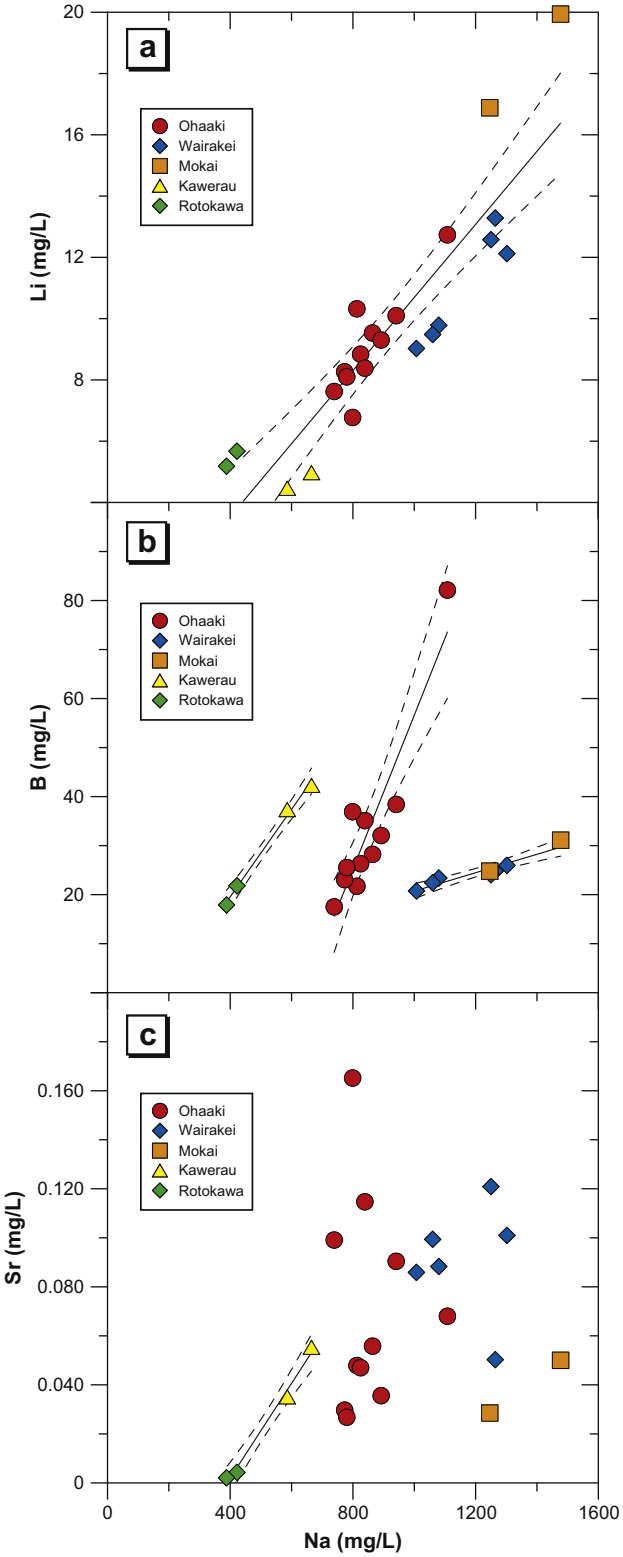

Fig. 3. Li, B and Sr concentrations (mg/L) plotted as a function of Na concentrations (mg/L). The dashed lines represent the 2σ uncertainty on the linear correlations.

Other major elements range from 72 to 338 mg/L for K, from 0.005 to 0.028 mg/L for Mg, and from 0.1 to 27.7 mg/L for Ca. Anion concentrations range between 2.6 and 74.8 mg/L for SO_4 and between 1.1 and 5.9 mg/L for Br. Silica concentrations are high, ranging from 384 to 1169 mg/L.

Concerning trace elements, and those of interest for the present work: Li concentrations are high, ranging from 4.5 to 19.9 mg/L. Boron concentrations are also high, ranging between 17.5 and 82.1 mg/L (BR49, Ohaaki). If the sample with the highest concentration is excluded, B contents are homogeneous, falling between 17.5 and 42.3 mg/L. Finally, Sr concentrations are clearly lower, ranging from 0.002 to 0.165 mg/L. The Li, B and Sr concentrations are similar to those reported in the literature for worldwide geothermal waters (Mossadik, 1997; Williams et al., 2001; Aggarwal et al., 2003; Millot and Négrel, 2007; Millot et al., 2007, 2009, 2010a).

Because Na is mainly controlled by water/rock interaction, it is interesting to also investigate the relationships between Na and Li, B and Sr (Fig. 3). Firstly, it can be observed (Fig. 3a), that all the geothermal waters define a general positive relationship between Na and Li, which suggests that, like Na, Li is mainly controlled by water/rock interaction. Secondly, and by contrast, when B concentrations are plotted against Na (Fig. 3b), different trends emerge. Indeed, different positive correlations between B and Na are observed, meaning that B is also controlled by water/rock interaction, but there is not a single general trend at the scale of the whole TVZ as observed for Li. From that graph (Fig. 3b) geothermal samples can be divided into different groups of samples: thus, the geothermal waters from Kawerau and Rotokawa seem to define a single trend, those from Ohaaki are different, and finally, those from Mokai and Wairakei seem to also plot on a single trend. These trends correlate with the spatial distribution of geothermal fields within the TVZ. The geothermal systems from Mokai and Wairakei are located on the western side of the TVZ, and those form Kawerau, Rotokawa and Ohaaki are located on the eastern side of the TVZ. Finally, when Sr concentrations are plotted as a function of Na (Fig. 3c), it seems that there is no global link between these two elements, except that the geothermal waters from Kawerau and Rotokawa show a positive relationship.

Additional information can also be obtained when the concentrations of trace elements are plotted as a function of the deep temperature of the water calculated by chemical geothermometry (Fig. 4). Both Li and B concentrations appear to be relatively constant and independent of the temperature of the fluid. On the other hand, Sr concentrations appear to be negatively correlated with the temperature of the fluid (Fig. 4b). Such a feature strongly suggests that dilution is occurring in the system by mixing of shallower and colder waters. However, it is also likely that the lower Sr contents can also be controlled by calcite precipitation. Finally, in Fig. 4d, SiO_2 concentrations and deep temperature show a strong correla-

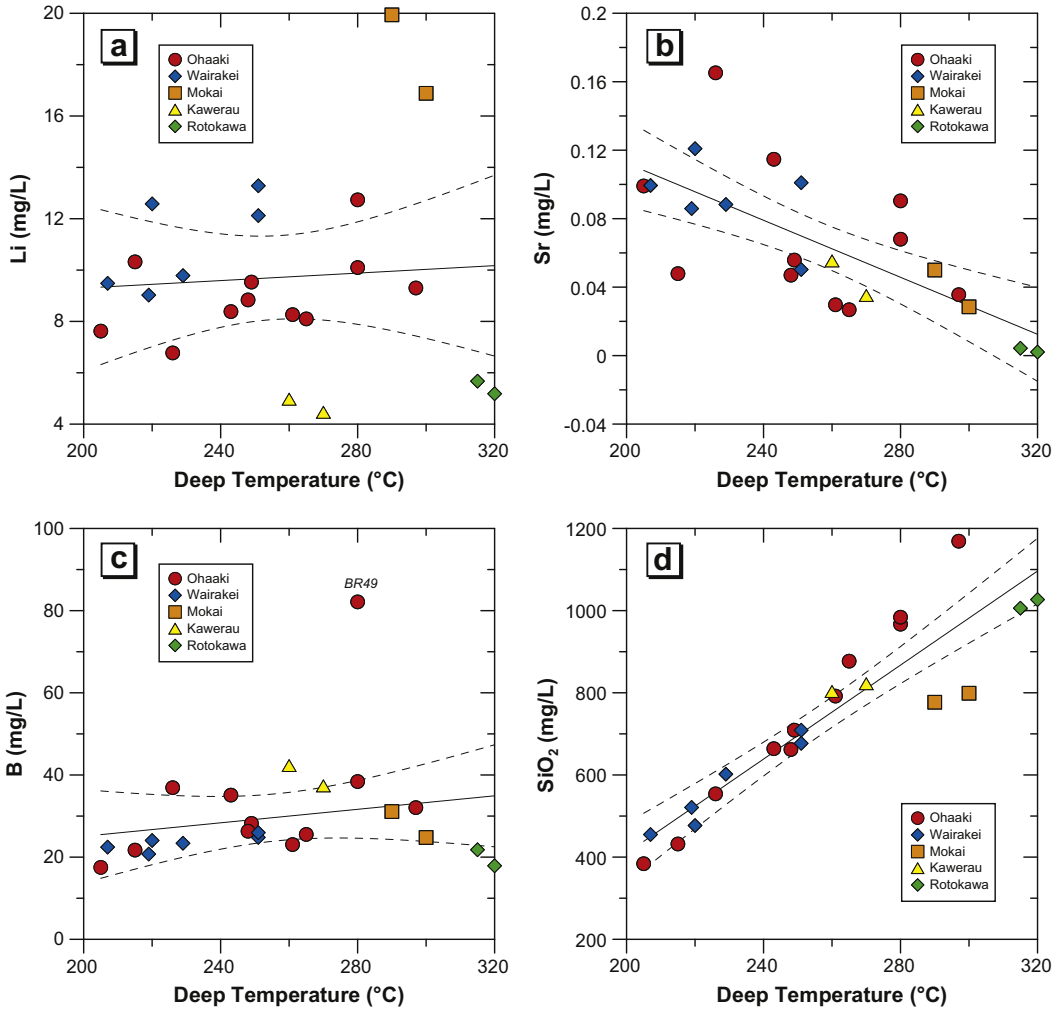

Fig. 4. Li, Sr, B and SiO_2 concentrations (mg/L) plotted as a function of the deep temperature (°C) estimated by SiO_2 geothermometry. Correlations have been added as well as a 2σ interval of confidence.

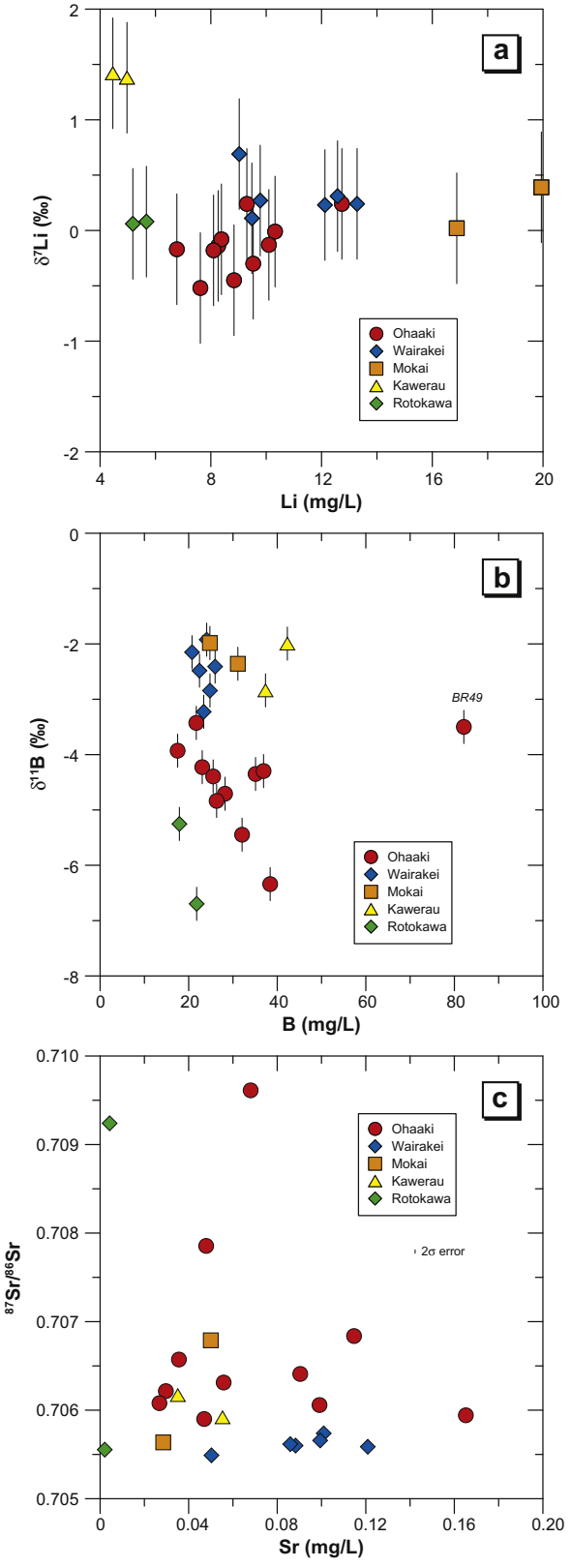

Fig. 5. (a) Li isotopes plotted as a function of Li concentrations (mg/L). The errors bars correspond to the external reproducibility of the method for Li isotope analysis ±0.5‰, 2σ. (b) B isotopes plotted as a function of B concentrations (mg/L). The errors bars correspond to the external reproducibility of the method for B isotope analysis ±0.3‰, 2σ. (c) Sr isotopes plotted as a function of Sr concentrations (mg/L). The errors bars are included within the sample symbol and correspond to the external reproducibility of the method for Sr isotopes analysis ±0.000020, 2σ.

tion (R^2 = 0.84) but this is an induced correlation, due to the fact that, deep temperature estimates were calculated based on SiO_2 concentrations using silica geothermometers.

4.2. Li–B–Sr isotopes

Lithium isotopes are reported in Table 1. Lithium isotopic compositions (δ^7Li, ‰) are homogeneous. For all the samples, the range of variation for δ^7Li values is small (1.9‰ in total) ranging between −0.52‰ and +1.42‰, respectively, for sample BR9 (Ohaaki) and KA37 (Kawerau). Omitting the two samples from Kawerau, which have slightly higher δ^7Li values (+1.42 and +1.38%), the other geothermal waters have a very constant δ^7Li signature around a mean value of 0‰ ± 0.6 (2σ, n = 21). This small range of variation (±0.6‰) is almost the same as the external reproducibility of the method for Li isotope analysis (±0.5‰, 2σ, Section 3.2). This result means either that Li has the same origin in these fluids and/or the process(es) that control Li isotope fractionation is (are) the same for all the geothermal water samples under consideration. Compared to scarce literature data for geothermal waters (Millot and Négrel, 2007; Millot et al., 2007, 2009, 2010a), those from the TVZ display low δ^7Li values.

Boron isotopes are also reported in Table 1. The range of δ^{11}B values is 4.8‰ in total, from −6.70‰ (RK14, Rotokawa) to −1.92‰ (WK235, Wairakei). A plot of B isotopes (δ^{11}B, ‰) as a function of B concentrations (Fig. 5b) shows that, with the exception of sample BR49 (Ohaaki) having the highest B concentrations, there is no large variation of both B isotopes and concentrations. However, Rotokawa and Ohaaki geothermal waters have the lowest δ^{11}B values, and, by contrast, geothermal waters from Wairakei, Mokai and Kawerau have the highest δ^{11}B values. Geothermal samples from this study can be compared with literature data from the Ngawha geothermal field (Aggarwal et al., 2003) for B isotopes. The Ngawha geothermal field is the only high temperature geothermal field in New Zealand that is located outside the TVZ. It is located on the central axis of the Northland peninsula in a Quaternary–Holocene basaltic field (Kaikohe volcanic field). Measurements of water samples from the Ngawha geothermal system fall within a limited range of δ^{11}B values between −3.9‰ and −3.1‰, overlapping the TVZ data.

Strontium isotopes are also reported in Table 1. $^{87}Sr/^{86}Sr$ ratios range from 0.70549 (WK245, Wairakei) to 0.70961 (BR49, Ohaaki). Strontium isotopes are plotted as a function of Sr concentrations in Fig. 5c and show no general trend or any relationship with the spatial distribution of the samples (eastern vs. western location). However, it is noteworthy that geothermal waters from the Wairakei field display the most constant $^{87}Sr/^{86}Sr$ ratios, between 0.70549 and 0.70574. The Sr isotope data reported here are in agreement with those of Graham (1992) for the Rotorua geothermal waters (0.70514–0.70791) and for the Ohaaki geothermal field site (0.70746, Grimes et al., 2000) also located in New Zealand.

5. Discussion

Collectively, Li, B and Sr isotopes can be used to identify the different sources contributing to the Li–B–Sr isotopic signature and to determine the main processes controlling these elements and their isotopic compositions in the geothermal waters of the TVZ.

First, Sr isotopes are investigated in the present work in order to better define the signature of the reservoir from which the geothermal waters came, given that Sr isotopes are a good tracer of water origin for groundwaters and geothermal waters (Goldstein and Jacobsen, 1987; Négrel et al., 1997, 2000; Négrel, 1999). Second, Li and B isotopic compositions (δ^7Li and δ^{11}B) are also

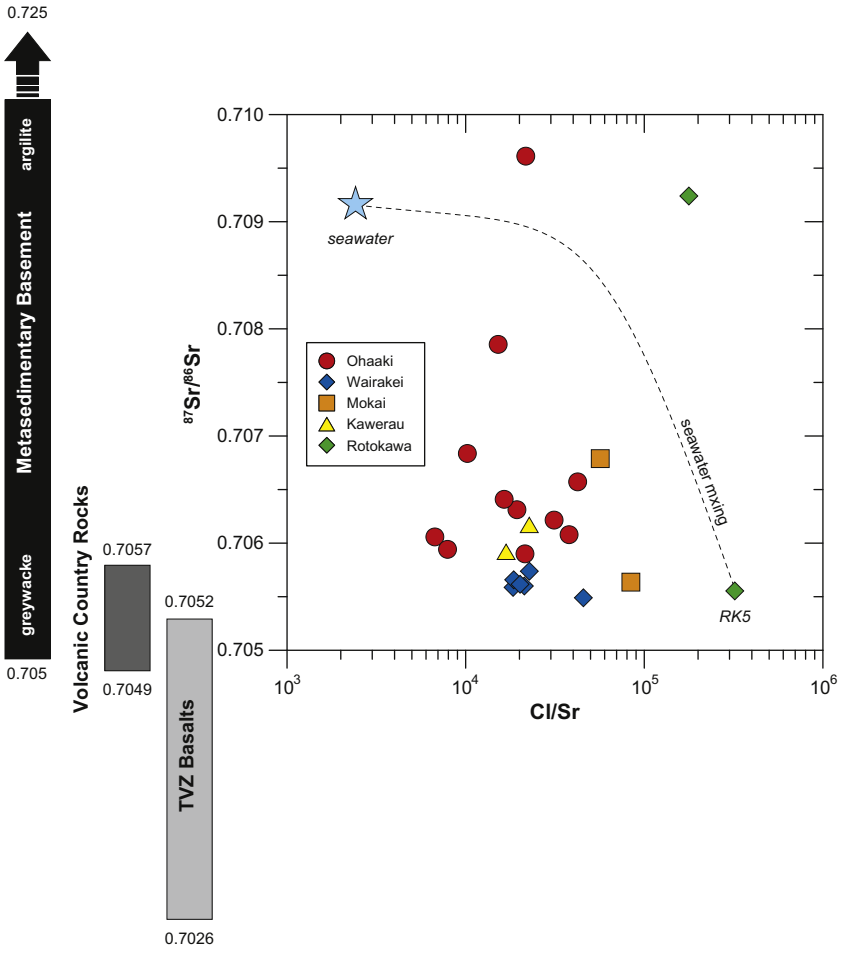

Fig. 6. Sr isotopes plotted as a function of the Cl/Sr mass ratio. Fields for volcanic country rocks, TVZ basalts and metasedimentary basement rocks have also been added, see text for comments.

considered in order to provide further constraints on the origin of Li and B in these geothermal waters.

As already mentioned, Sr isotopes display a large range in the geothermal waters of the TVZ (from 0.70549 to 0.70961). In addition, it was also observed in the previous section that if dilution processes occur in the system (by shallow, colder waters), it could probably explain the distribution of Sr concentrations. On the other hand, the higher $^{87}Sr/^{86}Sr$ ratios in geothermal waters are close to the value of modern seawater ($^{87}Sr/^{86}Sr$ = 0.70917, Dia et al., 1992). Collectively, these observations could result from dilution of geothermal waters having relatively low Sr isotope ratios by cold seawater, having a relatively high Sr isotope ratio, at shallow depth. A seawater mixing calculation is displayed in Fig. 6, in which $^{87}Sr/^{86}Sr$ ratios are plotted vs. Cl/Sr ratios. The geothermal end member is chosen to be sample RK5 (Rotokawa), which has both the lowest $^{87}Sr/^{86}Sr$ and the highest Cl/Sr ratios, and is, thus, representative of geothermal waters being least affected by a potential seawater contribution. No significant contribution of seawater for Sr is observed in the geothermal systems of the TVZ, it means that Sr and its isotopes are mainly controlled by the signature of the bedrocks themselves (by the dissolution from the different minerals).

As already mentioned in Section 2, the TVZ is an area of rhyolitic volcanic activity and hydrothermal altered sediments (greywackes) form the basement of the system. On the left side of Fig. 6, the ranges of $^{87}Sr/^{86}Sr$ ratios for the bedrocks of the system are shown: volcanic country rocks (rhyolite, ignimbrite and breccia, 0.7049–0.7057) reported by Graham (1992), basalts for the TVZ (0.7026–0.7052, Gamble et al., 1993) and metasedimentary basement rocks that have $^{87}Sr/^{86}Sr$ values between 0.705 for greywackes up to 0.725 for argillites (Graham, 1992). Therefore, it is likely that the most radiogenic Sr isotope ratios are the result of a significant contribution of waters having interacted with bedrocks having more radiogenic Sr like metasedimentary basement rocks.

Finally, when $^{87}Sr/^{86}Sr$ ratios of the TVZ fluids are compared to literature data for other geothermal fluids (Fig. 7a), the geothermal waters from the TVZ are similar to those of Graham (1992) for the Rotorua geothermal waters in New Zealand (0.70514–0.70791), but are significantly different from those of Iceland, which have $^{87}Sr/^{86}Sr$ ratios ranging between 0.7032 and 0.7042 (Millot et al., 2009). However, all of the geothermal waters display a similar range for Cl/Sr ratios, except for those of the Rotokawa geothermal field, which have higher Cl/Sr ratios. It is very likely that the significant difference in the Sr isotopes signature between the geothermal systems from New Zealand and those from Iceland is related to the signature of the volcanic basement rocks. New Zealand volcanic activity commenced 1.6 Ma ago, allowing in-growth of radiogenic Sr from Rb, whereas the geothermal systems in Iceland are located in the central volcanic area, which is only <0.8 Ma old.

Boron isotopes ($\delta^{11}B$) range from −6.70‰ to −1.92‰ in the geothermal waters from the TVZ, these values are in a good agreement with a volcanic origin for the waters (<0‰: Barth, 1993, 2000). In addition, according to Aggarwal et al. (2003) for the Ngawha geothermal field, the relatively low $\delta^{11}B$ values for the fluids implies

no significant marine input into the geothermal reservoir and this is also in accord with other geochemical data, e.g. average Cl/B = 53 compared to seawater Cl/B = 4839. In Fig. 7b, it is important to note that the worldwide geothermal waters have a $\delta^{11}B$ signature almost entirely comprised between −10‰ and 0‰, with the exception of the samples from the Reykjanes and Svartsengi geothermal fields in Iceland, for which the contribution of seawater is significant (Millot et al., 2009). In addition, as with the Na concentration (Fig. 3), the Cl/B varies according to the location of the geothermal field.

Lithium isotopic compositions (δ^7Li, ‰) are homogeneous for the geothermal waters of the TVZ. In Fig. 7c, Li isotope data for TVZ geothermal waters are compared with geothermal waters from Iceland (Millot et al., 2009) and with geothermal systems from the Guadeloupe and Martinique islands (volcanic islands belonging to the Lesser Antilles arc, French West Indies, Millot et al., 2010a). The geothermal waters from the TVZ are distinct from those of other geothermal systems. Indeed, the geothermal waters from the TVZ display the lowest δ^7Li yet reported for geothermal waters, but they also have the lowest Cl/Li ratios. In addition, whereas the geothermal fields from Iceland and the French West Indies may have a significant contribution of Li from seawater (Millot et al., 2009, 2010b), it is obvious that seawater has no influence on the composition of the geothermal waters from New-Zealand.

Several studies of Li-isotope behavior in near-surface environments have shown that δ^7Li values do not directly reflect the signature of the bedrock, but instead are controlled by fractionation during water/rock interaction by the formation of secondary minerals (Huh et al., 1998, 2001, 2004; Pistiner and Henderson, 2003; Rudnick et al., 2004; Kisakürek et al., 2004, 2005; Pogge von Strandmann et al., 2006; Vigier et al., 2009; Teng et al., 2010; Lemarchand et al., 2010; Millot et al., 2010b). It has been suggested that the δ^7Li signature in the liquid might be controlled by the preferential retention of the light Li isotope (^6Li) into secondary mineral phases during weathering. It has also been shown that the fractionation of Li isotopes during water/rock interaction also depends on temperature because different secondary minerals might control the release or uptake of Li in secondary minerals depending on the temperature of interaction and the associated dissolution/precipitation reaction (Chan and Edmond, 1988; Chan et al., 1992, 1993, 1994, 2002). All geothermal fluids from the TVZ have homogeneous and low δ^7Li values, indicating that temperature is probably not the main factor responsible for the Li isotopic composition of the geothermal fluids. Rather, it is more likely that the consistent low δ^7Li values in these geothermal fluids is due to leaching of Li from the same source rock.

When plotted on isotope vs. isotope diagrams (Fig. 8), the following conclusions can be reached: (i) Li isotope signatures are relatively homogeneous and do not allow the discrimination of any geothermal field, suggesting that the fluids are well-mixed for Li and water/rock interaction at high temperature is the main factor that determines both Li and its isotopic distribution in geothermal waters of the TVZ; (ii) B isotopes are less homogeneous, and some differences exist between the geothermal fields; although B and its isotopes are also mainly controlled by water/rock interaction processes, there is a small difference for $\delta^{11}B$ values between geothermal waters from Rotokawa and Ohaaki on the one hand and those from Mokai, Wairakei and Kawerau on the other hand; (iii) the Sr isotopes signatures vary widely and confirm a distinction between waters from different locations. The geographical distribution of the samples within the TVZ (eastern vs. western location) may affect B and Sr but not Li isotopes, meaning that it is likely that the fluids are well-mixed for Li and less so for B and Sr. In addition, for Sr isotopes, the isotopic signal also depends on the type of basement rocks.

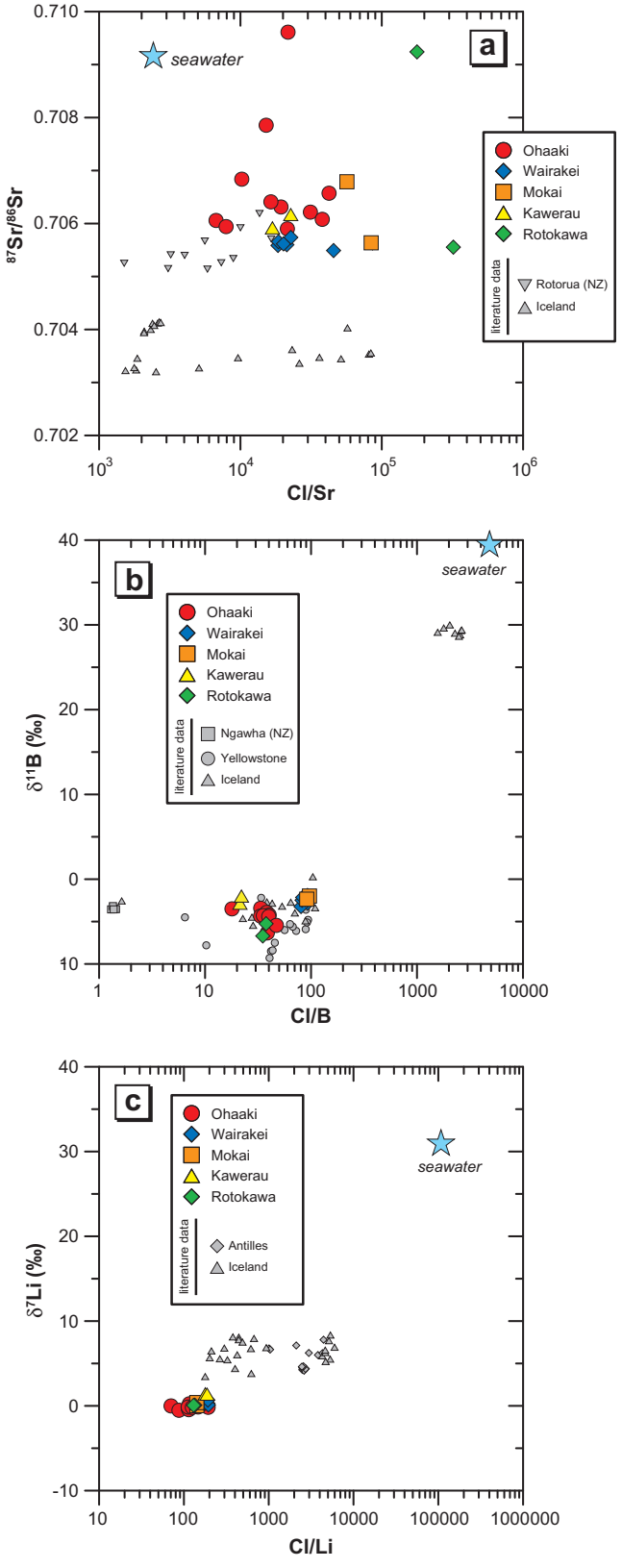

Fig. 7. (a) Sr isotopes plotted as a function of the Cl/Sr mass ratio. Comparison with geothermal waters from Rotorua geothermal system (Graham, 1992) and geothermal systems from Iceland (Millot et al., 2009). (b) B isotopes plotted as a function of Cl/B mass ratio. Comparison with geothermal waters from Ngawha geothermal system (Graham, 1992), Yellowstone (Palmer and Sturchio, 1990) and geothermal systems from Iceland (Millot et al., 2009). (c) Li isotopes plotted as a function of the Cl/Li mass ratio. Comparison with geothermal waters from Iceland (Millot et al., 2009) and from the Antilles (French West Indies, Millot et al., 2010a).

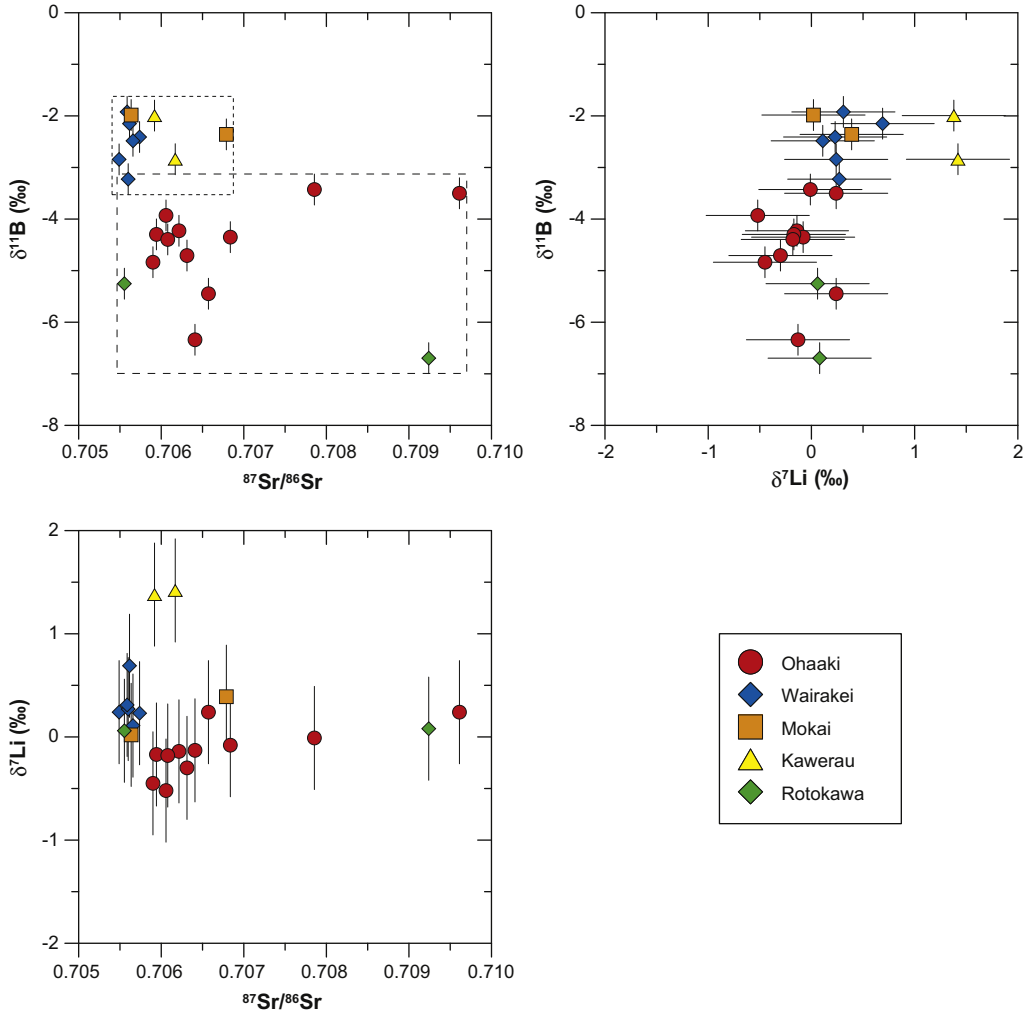

Fig. 8. Multi-isotopic (Li–B–Sr) characterization of geothermal waters from the Taupo Volcanic Zone.

6. Conclusions

The main conclusions of the Li–B–Sr isotopes characterization of the geothermal waters from the Taupo Volcanic Zone are:

- Lithium concentrations are high (ranging from 4.5 to 19.9 mg/L) and Li isotopic compositions (δ^7Li) are relatively homogeneous ranging between −0.5‰ and +1.4‰. Lithium isotope tracing shows that the input of seawater is negligible in these geothermal waters and that Li and its isotopes are mainly controlled by equilibrium exchange with magmatic rocks at high temperature.
- Boron concentrations are also high (17.5 and 82.1 mg/L) and relatively homogeneous and B isotopic compositions (δ^{11}B) are all negative, ranging from −6.7‰ to −1.9‰. This B isotope signature is in good agreement with a fluid signature derived mainly from water/rock interaction involving magmatic rocks and no seawater input.
- Strontium concentrations (0.02–0.165 mg/L) are lower and more heterogeneous and ^{87}Sr/^{86}Sr ratios range between 0.70549 and 0.70961. These Sr isotope compositions are similar to those of local magmatic bedrocks and the highest Sr isotope ratios are the result of a significant contribution of waters having interacted with bedrocks having more radiogenic Sr such as metasedimentary basement rocks.

Each of these isotope systems on their own reveals important information about particular aspects of either water source or water/rock interaction processes, but, considered together, they provide a more integrated understanding of the geothermal systems from the TVZ in New Zealand. However, the combination of Li, B and Sr isotopic systems highlights the complexity of these geothermal waters, and the use of only one isotopic tool could lead to an incomplete characterization of the geothermal waters.

Acknowledgements

This work was funded by the Research Division of the BRGM. This work benefited from the collaboration of BRGM Chemistry Laboratories for the major and trace elemental analyses: J.P. Ghestem, T. Conte and C. Crouzet are thanked for their help, as well as M. Robert for her help in the Neptune laboratory. C. Guerrot (TIMS analytic sector, BRGM) is acknowledged for B and Sr isotope data. We cordially thank Contact Energy Limited, the Tuaropaki Power Company, the Rotokawa Joint Venture and Mighty River Power Limited for providing the samples. Ed Mroczek (GNS Science) and Tom Powell (Mighty River Power Limited) are acknowledged for critical comments. E. Petelet-Giraud is also thanked for fruitful discussions. A. Hegan was supported by a fellowship from AquaTRAIN MRTN (Contract No. MRTN-CT-2006-035420) funded by the European Commission FP6 Marie Curie Actions – Human Re-

sources and Mobility Activity Area, Research Training Networks. We also would like to thank T.D. Bullen for English corrections and RM is particularly grateful to C. Fouillac for the opportunity to work on this subject. R. Rudnick and an anonymous reviewer are acknowledged for providing helpful reviews of this manuscript. L. Aquilina is also thanked for editorial handling and constructive comments. This is BRGM Contribution No. 653418.

References

Aggarwal, J.K., Sheppard, D., Mezger, K., Pernicka, E., 2003. Precise and accurate determination of boron isotope ratios by multiple collector ICP-MS: origin of boron in the Ngawha geothermal system, New Zealand. Chem. Geol. 199, 331–342.

Aggarwal, J.K., Mezger, K., Pernicka, E., Meixner, A., 2004. The effect of instrumental mass bias on $\delta^{11}B$ measurements: a comparison between thermal ionisation mass spectrometry and multiple-collector ICP-MS. Int. J. Mass Spectrom. 232, 259–263.

Aquilina, L., Pauwels, H., Genter, A., Fouillac, C., 1997. Water–rock interaction processes in the Triassic sandstone and the granitic basement of the Rhine Graben: geochemical investigation of a geothermal reservoir. Geochim. Cosmochim. Acta 61, 4281–4295.

Arnórsson, S., Gunnlaugsson, E., Svavarsson, H., 1983. The geochemistry of geothermal waters in Iceland. III. Chemical geothermometry in geothermal investigations. Geochim. Cosmochim. Acta 47, 567–577.

Barth, S.R., 1993. Boron isotope variations in nature: a synthesis. Geol. Rundsch. 82, 640–641.

Barth, S.R., 2000. Geochemical and boron, oxygen and hydrogen isotopic constraints on the origin of salinity in groundwaters from the crystalline basement of the Alpine Foreland. Appl. Geochem. 15, 937–952.

Bibby, H.M., Caldwell, T.G., Davey, F.J., Webb, T.H., 1995. Geophysical evidence on the structure of the Taupo Volcanic Zone and its hydrothermal circulation. J. Volcanol. Geotherm. Res. 68, 29–58.

Chan, L.H., Edmond, J.M., 1988. Variation of lithium isotope composition in the marine environment: a preliminary report. Geochim. Cosmochim. Acta 52, 1711–1717.

Chan, L.H., Edmond, J.M., Thompson, G., Gillis, K., 1992. Lithium isotopic composition of submarine basalts: implications for the lithium cycle in the oceans. Earth Planet. Sci. Lett. 108, 151–160.

Chan, L.H., Edmond, J.M., Thompson, G., 1993. A lithium isotope study of hot springs and metabasalts from mid-ocean ridge hydrothermal systems. J. Geophys. Res. 98, 9653–9659.

Chan, L.H., Gieskes, J.M., You, C.F., Edmond, J.M., 1994. Lithium isotope geochemistry of sediments and hydrothermal fluids of the Guaymas Basin, Gulf of California. Geochim. Cosmochim. Acta 58, 4443–4454.

Chan, L.H., Alt, J.C., Teagle, D.A.H., 2002. Lithium and lithium isotope profiles through the upper oceanic crust: a study of seawater-basalt exchange at ODP Sites 504B and 896A. Earth Planet. Sci. Lett. 201, 187–201.

Christenson, B.W., Mroczek, E.K., Kennedy, B.M., van Soest, M.C., Stewart, M.K., Lyon, G., 2002. Ohaaki reservoir chemistry: characteristics of an arc-type hydrothermal system in the Taupo Volcanic Zone, New Zealand. J. Volcanol. Geotherm. Res. 115, 53–82.

Dia, A.N., Cohen, A.S., O'Nions, R.K., Shackleton, N.J., 1992. Seawater Sr isotope variation over the past 300 kyr and influence of global climate cycles. Nature 356, 786–788.

Elderfield, H., Greaves, M.J., 1981. Strontium isotope geochemistry of Icelandic geothermal systems and implications for sea water chemistry. Geochim. Cosmochim. Acta 45, 2201–2212.

Ellis, A.J., 1970. Quantitative interpretations of chemical characteristics of hydrothermal systems. Geothermics Spec. Iss. 2, 516–528.

Flesch, G.D., Anderson, A.R., Svec, H.J., 1973. A secondary isotopic standard for $^6Li/^7Li$ determinations. Int. J. Mass Spectrom. Ion Phys. 12, 265–272.

Fouillac, C., 1983. Chemical geothermometry in CO_2-rich thermal waters. Example of the French Massif central. Geothermics 12, 149–160.

Fournier, R.O., Rowe, J.J., 1966. Estimation of underground temperatures from the silica content of water from hot springs and wet-steam wells. Am. J. Sci. 264, 685–697.

Gamble, J.A., Smith, I.E.M., McCulloch, M.T., Graham, I.J., Kokelaar, B.P., 1993. The geochemistry and petrogenesis of basalts from the Taupo Volcanic Zone and Kermadec Island Arc, S.W. Pacific. J. Volcanol. Geotherm. Res. 54, 265–290.

Giggenbach, W.F., 1995. Variations in the chemical and isotopic composition of fluids discharged from the Taupo Volcanic Zone, New Zealand. J. Volcanol. Geotherm. Res. 68, 89–116.

Goldstein, S.J., Jacobsen, S.B., 1987. The Nd and Sr isotopic systematics of river-water dissolved material: implications for the sources of Nd and Sr in seawater. Chem. Geol. 66, 245–272.

Gonfiantini, R., Tonarini, S., Gröning, M., Adorni-Braccesi, A., Al-Ammar, A.S., Astner, M., Bächler, S., Barnes, R.M., Bassett, R.L., Cocherie, A., Deyhle, A., Dini, A., Ferrara, G., Gaillardet, J., Grimm, J., Guerrot, C., Krähenbühl, U., Layne, G., Lemarchand, D., Meixner, A., Northington, D.J., Pennisi, M., Reitznerová, E., Rodushkin, I., Sugiura, N., Surberg, R., Tonn, S., Wiedenbeck, M., Wunderli, S., Xiao, Y., Zack, T., 2003. Intercomparison of boron isotope and concentration measurements. Part II: Evaluation of results. Geostand. Newslett. 27, 41–57.

Graham, I.J., 1992. Strontium isotope compositions of Rotorua geothermal waters. Geothermics 21, 165–180.

Grimes, S., Rickard, D., Hawkesworth, C., van Calsteren, P., Browne, R., 2000. The Broadlands–Ohaaki geothermal system, New Zealand Part 1. Strontium isotope distribution in well BrO-29. Chem. Geol. 163, 247–265.

Hedenquist, J.W., 1990. The thermal and geochemical structure of the Broadlands-Ohaaki geothermal system, New Zealand. Geothermics 19, 151–185.

Heise, W., Caldwell, T.G., Bibby, H.M., Bannister, S.C., 2008. Three-dimensional modelling of magnetotelluric data from the Rotokawa geothermal field, Taupo Volcanic Zone, New Zealand. Geophys. J. Int. 173, 740–750.

Helgeson, H.C., Delany, J.M., Nesbitt, H.W., Bird, D.K., 1978. Summary and critique of the thermodynamic properties of rock-forming minerals. Am. J. Sci. 278A.

Huh, Y., Chan, L.C., Zhang, L., Edmond, J.M., 1998. Lithium and its isotopes in major world rivers: implications for weathering and the oceanic budget. Geochim. Cosmochim. Acta 62, 2039–2051.

Huh, Y., Chan, L.C., Edmond, J.M., 2001. Lithium isotopes as a probe of weathering processes: Orinoco River. Earth Planet. Sci. Lett. 194, 189–199.

Huh, Y., Chan, L.C., Chadwick, O.A., 2004. Behavior of lithium and its isotopes during weathering of Hawaiian basalt. Geochem. Geophys. Geosyst. 5, 1–22.

Hunt, T., Bowyer, D., 2007. Reinjection and gravity changes at Rotokawa geothermal field, New Zealand. Geothermics 36, 421–435.

Kisakürek, B., Widdowson, M., James, R.H., 2004. Behaviour of Li isotopes during continental weathering: the Bidar laterite profile, India. Chem. Geol. 212, 27–44.

Kisakürek, B., James, R.H., Harris, N.B.W., 2005. Li and δ^7Li in Himalayan rivers: proxies for silicate weathering? Earth Planet. Sci. Lett. 237, 387–401.

Kissling, W.M., Weir, G.J., 2005. The spatial distribution of the geothermal fields in the Taupo Volcanic Zone, New Zealand. J. Volcanol. Geotherm. Res. 145, 136–150.

Krupp, E., Browne, P.R.L., Henley, R.W., Seward, T.M., 1986. Rotokawa geothermal field. In: Henley, R.W., Hedenquist, J.W., Roberts, P.J. (Eds.), Guide to the Active Epithermal (Geothermal) Systems and Precious Metal Deposits of New Zealand. Gebruder Borntraeger, Berlin, Stuttgart, pp. 47–55.

Lemarchand, E., Chabaux, F., Vigier, N., Millot, R., Pierret, M.C., 2010. Lithium isotope systematics in a forested granitic catchment (Strengbach, Vosges Mountains, France). Geochim. Cosmochim. Acta 74, 4612–4628.

Millot, R., Négrel, Ph., 2007. Multi-isotopic tracing (δ^7Li, $\delta^{11}B$, $^{87}Sr/^{86}Sr$) and chemical geothermometry: evidence from hydro-geothermal systems in France. Chem. Geol. 244, 664–678.

Millot, R., Guerrot, C., Vigier, N., 2004. Accurate and high precision measurement of lithium isotopes in two reference materials by MC-ICP-MS. Geostand. Geoanal. Res. 28, 53–159.

Millot, R., Négrel, Ph., Petelet-Giraud, E., 2007. Multi-isotopic (Li, B, Sr, Nd) approach for geothermal reservoir characterization in the Limagne Basin (Massif Central, France). Appl. Geochem. 22, 2307–2325.

Millot, R., Asmundsson, R., Négrel, Ph., Sanjuan, B., Bullen, T.D., 2009. Multi-isotopic (H, O, C, S, Li, B, Si, Sr, Nd) approach for geothermal fluid characterization in Iceland. In: Goldschmidt Conf. 2009, Davos, Switzerland.

Millot, R., Scaillet, B., Sanjuan, B., 2010a. Lithium isotopes in island arc geothermal systems: Guadeloupe, Martinique (French West Indies) and experimental approach. Geochim. Cosmochim. Acta 74, 1852–1871.

Millot, R., Vigier, N., Gaillardet, J., 2010b. Behaviour of lithium and its isotopes during weathering in the Mackenzie Basin, Canada. Geochim. Cosmochim. Acta 74, 3897–3912.

Mossadik, H., 1997. Les isotopes du bore, traceurs naturels dans les eaux. Mise au point de l'analyse en spectrométrie de masse à source solide et application à différents environnements. PhD Thesis, Université d'Orléans.

Négrel, Ph., 1999. Geochemical study in a granitic area, the Margeride, France: chemical element behavior and $^{87}Sr/^{86}Sr$ constraints. Aquat. Geochem. 5, 125–165.

Négrel, Ph., Fouillac, C., Brach, M., 1997. Occurrence of mineral water springs in the stream channel of the Allier River (Massif Central, France): chemical and Sr isotope constraints. J. Hydrol. 203, 143–153.

Négrel, Ph., Guerrot, C., Cocherie, A., Azaroual, M., Brach, M., Fouillac, C., 2000. Rare Earth Elements, neodymium and strontium isotopic systematics in mineral waters: evidence from the Massif Central, France. Appl. Geochem. 15, 1345–1367.

Palmer, M.R., Sturchio, N.C., 1990. The boron isotope systematics of the Yellowstone National Park (Wyoming) hydrothermal system: a reconnaissance. Geochim. Cosmochim. Acta 54, 2811–2815.

Pin, C., Bassin, C., 1992. Evaluation of a strontium specific extraction chromatographic method for isotopic analysis in geological materials. Anal. Chim. Acta 269, 249–255.

Pistiner, J.S., Henderson, G.M., 2003. Lithium isotope fractionation during continental weathering processes. Earth Planet. Sci. Lett. 214, 327–339.

Pogge von Strandmann, P.A.E., Burton, K.W., James, R.H., van Calsteren, P., Gislason, S.R., Mokadem, F., 2006. Riverine behaviour of uranium and lithium isotopes in an actively glaciated basaltic terrain. Earth Planet. Sci. Lett. 251, 134–147.

Rudnick, R.L., Tomascak, P.B., Njo, H.B., Gardner, L.R., 2004. Extreme lithium isotopic fractionation during continental weathering revealed in saprolites from South Carolina. Chem. Geol. 212, 45–57.

Stettler, A., Allègre, C.J., 1978. $^{87}Rb–^{87}Sr$ studies of waters in a geothermal area: the Cantal, France. Earth Planet. Sci. Lett. 38, 364–372.

Stueber, A.M., Walter, L.M., Huston, T.J., Pushkar, P., 1993. Formation waters from Mississippian–Pennsylvanian reservoirs, Illinois basin, USA: chemical and isotopic constraints on evolution and migration. Geochim. Cosmochim. Acta 57, 763–784.

Teng, F.Z., Li, W.Y., Rudnick, R.L., Gardner, L.R., 2010. Contrasting lithium and magnesium isotope fractionation during continental weathering. Earth Planet. Sci. Lett. 300, 63–71.
Truesdell, A.H., 1976. Geochemical techniques in exploration, summary of section III. In: Proc. 2nd United Nations Symp. Development and Use of Geothermermal Research, San Francisco, pp. 53–79.
Vengosh, A., Helvaci, C., Karamanderesi, I.H., 2002. Geochemical constraints for the origin of thermal waters from western Turkey. Appl. Geochem. 17, 163–183.
Vigier, N., Gislason, S.R., Burton, K.W., Millot, R., Mokadem, F., 2009. The relationship between riverine lithium isotope composition and silicate weathering rates in Iceland. Earth Planet. Sci. Lett. 287, 434–441.
White, D.E., 1965. Saline waters of sedimentary rocks. Fluids in subsurface environments – a symposium. Am. Assoc. Petrol. Geol. Mem. 4, 342–366.
Williams, L.B., Hervig, R.L., Hutcheon, I., 2001. Boron isotope geochemistry during diagenesis Part II. Application to organic-rich sediments. Geochim. Cosmochim. Acta 65, 1783–1794.
Wilson, N., Webster-Brown, J., Brown, K., 2007. Controls on stibnite precipitation at two New Zealand geothermal power stations. Geothermics 36, 330–347.
Wood, C.P., Brathwaite, R.L., Rosenberg, M.D., 2001. Basement structure, lithology and permeability at Kawerau and Ohaaki geothermal fields, New Zealand. Geothermics 30, 461–481.

Available online at www.sciencedirect.com
ScienceDirect
Geochimica et Cosmochimica Acta 74 (2010) 1852–1871
Geochimica et Cosmochimica Acta
www.elsevier.com/locate/gca

Lithium isotopes in island arc geothermal systems: Guadeloupe, Martinique (French West Indies) and experimental approach

Romain Millot [a,*], Bruno Scaillet [b], Bernard Sanjuan [c]

[a] BRGM, Metrology Monitoring Analysis Department, Orléans, France
[b] CNRS/INSU-Université d'Orléans-Université François Rabelais Tours, UMR 6113, Institut des Sciences de la Terre d'Orléans, Orléans, France
[c] BRGM, Department of Geothermal Energy, Orléans, France

Received 20 July 2009; accepted in revised form 1 December 2009; available online 4 January 2010

Abstract

We report lithium (Li) isotopic measurements in seawater-derived waters that were discharged from geothermal wells, thermal springs, and sub-marine springs located in volcanic island arc areas in Guadeloupe (the Bouillante geothermal field) and Martinique (Lamentin plain and the Diamant areas). While Li isotopic signatures of the geothermal fluids collected from deep reservoirs were found to be homogeneous for a given site, the δ^7Li signatures for each of these reservoirs were significantly different. The first low temperature (25–250 °C) experiments of Li isotope exchange during seawater/basalt interaction confirmed that Li isotopic exchange is strongly temperature dependent, as previously inferred from natural studies. Li isotopic fractionation ranged from +19.4‰ ($\Delta_{solution-solid}$) at 25 °C to +6.7‰ at 250 °C. These experiments demonstrated the importance of Li isotopic fractionation during the formation of Li-bearing secondary minerals and allowed us to determine the following empirical relationship between isotopic fractionation and temperature: $\Delta_{solution-solid} = 7847/T - 8.093$. Application of experimental results and literature data to the Bouillante area suggested that geothermal water was in equilibrium at 250–260 °C. It likely has a deep and large reservoir located in the upper sheeted dike complex of the oceanic crust, just below the transition zone between andesite volcanic flows and the basaltic dikes. The upper dike section, from which Li is extracted by hydrothermal fluids, was characterized by light Li isotopic values in the rocks, indicating retention of ^{6}Li by the altered rocks. For the Lamentin and Diamant areas, the geothermal fluids appeared to be in equilibrium with reservoir volcano-sedimentary rocks at 90–120 °C and 180 °C, respectively. Further evidence for this argument is provided by the fact that only the Na/Li thermometric relationship determined for sedimentary basins yielded temperature values in agreement with those measured or estimated for the reservoir fluids. This suggests the importance of a sedimentary signature in these reservoir rocks. Altogether, this study highlights that the use of Li isotopic systematics is a powerful tool for characterizing the origin of geothermal waters as well as the nature of their reservoir rocks.

1. INTRODUCTION

The increasing demand for energy and a desire to increase energy autonomy in the Lesser Antilles (French West Indies) have resulted in a number of BRGM (French Geological Survey) geothermal research projects focused on the islands of Guadeloupe (Traineau et al., 1997; Correia et al., 2000; Sanjuan et al., 2001; Fabriol et al., 2005; Mas et al., 2006) and Martinique (Genter et al., 2002; Sanjuan et al., 2002a, 2002b, 2005) over the past decade.

Previous surveys have led to a better understanding of geothermal systems associated with deep boreholes and thermal springs in these areas (Sanjuan, 2001; Sanjuan et al., 2002a, 2002b). The chemical characterization of

* Corresponding author. Tel.: +33 2 38 64 48 32.
E-mail address: r.millot@brgm.fr (R. Millot).

0016-7037/$ - see front matter © 2009 Elsevier Ltd. All rights reserved.
doi:10.1016/j.gca.2009.12.007

thermal water is generally very useful for geothermal exploration. It is also essential if we wish to control water quality, determine its origin and understand the mechanisms of water/rock interactions at high temperature for the purpose of developing geothermal resources.

The chemical composition of geothermal water in terms of reactive major and trace elements is related to the intensity of water/rock interactions and the mineralogical assemblage of the surrounding rocks. Classical geothermometers, such as dissolved silica, Na–K, Na–K–Ca or K–Mg, applied to geothermal waters (Fournier and Rowe, 1966; Fournier and Truesdell, 1973; Fournier, 1979; Michard, 1979, 1990; Giggenbach, 1988) enable the temperature estimation of deep reservoirs that feed geothermal fields. However, the values estimated for such temperatures are not always consistent with each other. The three Na/Li thermometric relationships (Fouillac and Michard, 1981; Kharaka et al., 1982; Kharaka and Mariner, 1989) differ from classical geothermometers in that they associate a major (sodium) and a trace element (lithium), the latter of which gives an additional temperature constraint. Owing to the relatively low reactivity of Li during ascent to the surface, these thermometric relationships appear to be very reliable. They also act as useful tools for characterizing the source (i.e., deep conditions) of geothermal waters.

The aim of this study was to improve geothermal reservoir exploration and its associated characterization methods. As such, the main objective of the present work was to better understand the behavior of Li within an island arc geothermal environment through the use of its isotope systematics. One particularly important aspect of this work was to establish the nature, extent and mechanism of Li isotope fractionation as a function of temperature during water/rock interaction.

Lithium is a chemical element with two isotopes at masses of 6 and 7, which have natural abundances of 7.5% and 92.5%, respectively. Li is a fluid-mobile element that tends to preferentially partition into the fluid phase during water/rock interaction. The relative mass difference between the two isotopes is considerable (17%) and is likely to generate large mass dependent fractionation during geochemical processes, even at high temperature. The range of variation in Li isotopic compositions is more than 50‰ in geological materials (Coplen et al., 2002; Tomascak, 2004). Li concentrations in natural waters are essentially controlled by water–rock interaction processes, which depend on a number of factors. These include, for example: the mineral assemblage in contact with water, the chemical composition of this water, dissolution–precipitation or exchange reactions, temperature and water–rock ratio. To date, both the magnitude of the Li isotopic fractionation associated with water–rock interaction processes and the factors controlling these fractionations are still poorly understood. However, water–rock interaction studies carried out with altered rocks at low to moderate temperatures indicate that the associated Li isotopic fractionation is characterized by the enrichment of the solution in the heavy isotope ^{7}Li. On the other hand, the light isotope (^{6}Li) is preferentially retained by secondary alteration minerals.

Lithium isotopic fractionation has been documented in numerous natural environments, with experimental and natural data (Huh et al., 2001; Pistiner and Henderson, 2003; Tomascak, 2004). Both types of data suggest that the processes of mineral dissolution are not characterized by significant Li isotopic fractionation. In contrast, adsorption onto mineral surfaces is a major mechanism of Li isotopic fractionation in the hydrosphere. Sorption of Li from aqueous solutions by mineral phases at the temperature of the Earth's surface has been highlighted by Taylor and Urey (1938), as well as by Anderson et al. (1989). Previous Li sorption experiments utilizing several minerals (Pistiner and Henderson, 2003) have revealed that Li isotopic fractionation does not occur when this element is not incorporated into the structure of the solid (physical sorption). When Li is incorporated by stronger bonds (chemical sorption), an isotopic fractionation is observed that is dependent on the chemical structure of the minerals (Anghel et al., 2002). The most significant Li isotopic fractionation factor ($\Delta_{\text{solution–solid}}$) $\sim +14‰$ has been measured for gibbsite. For Li sorption processes between seawater and different solids (clay minerals such as kaolinite and vermiculite, and freshwater sediments), Zhang et al. (1998) have observed a still higher Li isotopic fractionation factor ($\Delta_{\text{solution-solid}} \sim +22‰$).

Laboratory experiments carried out to gain insight into Li isotope behavior during interactions of high-temperature fluids with various materials all show the extraction of Li from basalt, altered basalt and sediments, even at temperatures <100 °C. Li is incorporated into clays (e.g., smectites and illites) at temperatures up to 150 °C during basalt alteration (Seyfried et al., 1998; James et al., 2003). In this case, the affinity is proportional to the fluid/rock ratio, such that Li is simultaneously added to and removed from fluids. Under high temperature, solid-dominated hydrothermal conditions (350 °C), Li is largely removed from solids and kept in solution, rather than in the alteration products.

Most of the Li isotopic fractionation values reported in the literature come from studies of the interaction between seawater and altered basalts. The isotopic fractionation factors inferred from these studies give $\Delta_{\text{solution–altered rock}}$ values of 4‰ at 350 °C, 9‰ at 160 °C and 19‰ at 2 °C (Chan and Edmond, 1988; Chan et al., 1992, 1993, 1994; James et al., 1999). Wunder et al. (2006) have also recently reported a temperature-dependent relationship of Li isotopic fractionation. This was determined from experiments between Li-bearing clinopyroxene and aqueous fluids, albeit at P–T (pressure–temperature) conditions largely outside those explored here (500–900 °C at 20,000 bar).

In this study, we measured the Li isotopic composition of various water samples (i.e., geothermal waters, thermal springs and sub-marine thermal springs). As mentioned above, the Li concentration and isotope composition of geothermal fluids are a function of many parameters, including water and rock compositions, water/rock ratio, mineral–fluid partition and mineral–fluid isotopic fractionation, with the last two being temperature dependent. To disentangle the relative importance of each of these parameters, we performed laboratory simulations of Li isotopic behavior during water/rock interaction across a wide temperature range (25–250 °C). These experimental results were then applied to natural systems to infer water origins and reservoir rock compositions.

2. GEOTHERMAL SETTING

Guadeloupe and Martinique are volcanic islands belonging to the Lesser Antilles arc (Fig. 1). Samples of geothermal waters were collected at three different sites: (1) the Bouillante area (Guadeloupe), (2) the Lamentin area (Martinique) and (3) the Diamant area (Martinique).

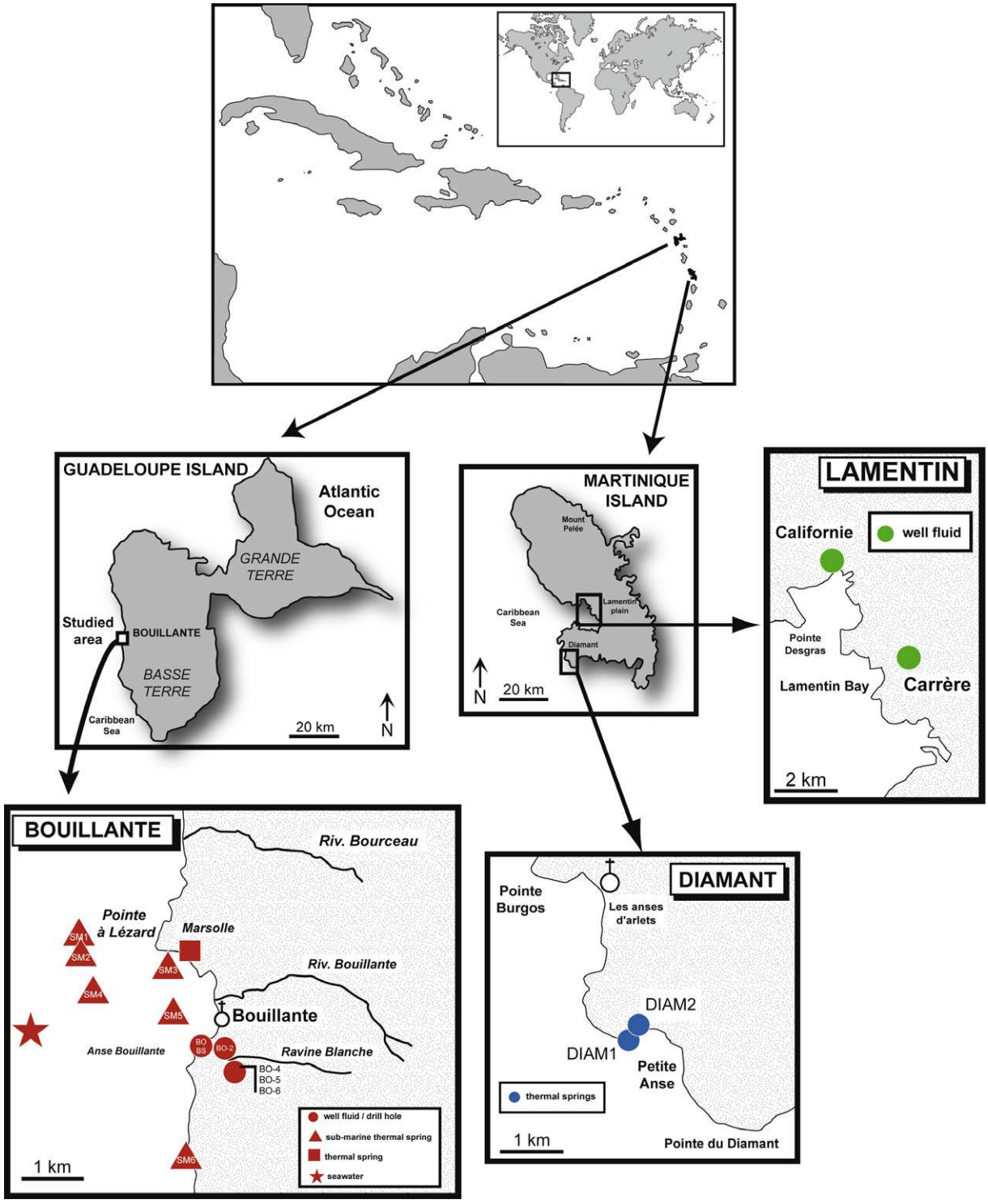

Fig. 1. Map of sampling sites in the Bouillante area (Guadeloupe), Lamentin and Diamant areas (Martinique). Detailed information concerning the location of sampling sites can be found in Traineau et al. (1997), Sanjuan and Brach (1997) and Sanjuan et al. (2001) for the Bouillante area, and in Sanjuan et al. (2002a, 2002b, 2003, 2005) for Martinique (Lamentin plain and Diamant areas).

2.1. Bouillante area

The Bouillante geothermal area is located on the west coast of Basse-Terre (Guadeloupe, Fig. 1). This area developed near the seaside and around the town of Bouillante, where there are numerous hydrothermal vents, including hot springs, mud pools, steaming grounds and fumaroles (in French, 'bouillante' means 'boiling'; Traineau et al., 1997).

Most of the active geothermal manifestations are located south of Bouillante Bay, around the geothermal power plant, where deep wells (BO-2, BO-4, BO-5 and BO-6) are located. Between 1996 and 2002, only BO-2 was productive (150 tons/h of fluid, including 30 tons/h of steam). Since 2005, the new geothermal power plant has been fed by wells BO-4, BO-5 and BO-6 (a maximum production of about 570 tons/h of fluid, including 115 tons/h of steam). There are also numerous sub-marine hot springs, especially north of Bouillante Bay (Traineau et al., 1997; Sanjuan, 2001) and an interesting terrestrial thermal spring for geothermal exploration (Marsolle spring; Sanjuan and Brach, 1997; Mas et al., 2006).

Geochemical characterization has provided the following information about the Bouillante geothermal field. The water flowing through the geothermal reservoir, whether sampled in wells or hot springs, has a homogeneous composition over the scale of the Bouillante region (Traineau et al., 1997; Sanjuan et al., 2001). Geothermal NaCl fluid (total dissolved solids TDS $\approx$ 20 g/L, pH = 5.3) is the result of the mixing of about 58% seawater and 42% fresh water. The fresh surface water is likely fed by rainfall on the western side of the island (Pitons de Bouillante). The amount of associated incondensable gases, made up predominantly (90–95%) of CO_2, is low (<0.1% in mass).

The homogeneity of chemical and isotopic compositions of the geothermal fluids and the convergence of chemical geothermometers, such as Silica–Quartz, Na/K and K/Mg (Fournier and Rowe, 1966; Fournier, 1979; Michard, 1979; Giggenbach, 1988), toward a maximum temperature value of around 250–260 °C, all suggest the existence of a common large deep reservoir. The volume of this reservoir was estimated to be higher than 30 million m^3, using tracer test results. The Na/Li geothermometer determined by Fouillac and Michard (1981) for saline geothermal waters in volcanic and granitic environments gives a temperature value of 224 °C, similar to that obtained using the Na/K/Ca geothermometer (226 °C; Fournier and Truesdell, 1973). However, this is slightly lower than those either measured inside the geothermal wells or estimated using classical geothermometers. Geochemical modeling has shown that the reservoir fluid is in chemical equilibrium with a mineralogical assemblage made up of albite, K-feldspar, quartz, calcite, disordered dolomite, anhydrite, illite, smectite and zeolites at 250–260 °C (Sanjuan et al., 2001).

2.2. Lamentin plain

The Lamentin plain, on the western coast of Martinique (Fig. 1), south of Fort de France, is an alluvial plain with a surface area of approximately 100 km^2. The Lamentin area corresponds to a major graben zone limited by NW–SE faults and intersected by NE–SW faults. There are numerous thermal springs aligned along an axis oriented NNW–SSE to NW–SE in the area. Their flow rate is generally low and they are characterized by the presence of CO_2-rich NaCl fluids (Sanjuan et al., 2002a, 2002b), with exit temperatures ranging from 37 to 58 °C.

Three boreholes were drilled at a depth of 1000 m in this area in 2001. Only the borehole Californie, located farther north, indicated the presence of hot fluid close to 90 °C at a depth of 400 m. A fluid with a similar chemical composition but with a lower temperature (50 °C) was also found at a depth of about 400 m in the borehole Carrère, which is near thermal springs.

The geochemical study of fluids collected from these exploration boreholes and thermal springs suggests that the current hydrothermal system is concentrated northward, in relation to a general outflow coming from the NW, and is at relatively deep depths. The geothermal NaCl fluid, made up of about 30% seawater and 70% freshwater (TDS $\approx$ 10–11 g/L; pH = 6.2) and accompanied mainly by magmatic CO_2 gas, probably comes from a reservoir located close to seawater. Chemical geothermometers, such as Silica–Chalcedony, Na/K/Ca/Mg and K/Mg (Fournier and Potter, 1979; Arnorsson and Gunnlaugsson, 1983; Giggenbach, 1988), suggest reaction with volcano-sedimentary rocks at temperatures ranging from 90 to 120 °C, which are identical to the maximum values (90–100 °C) measured in the boreholes (Sanjuan et al., 2002a, 2002b). The Na/K and Na/K/Ca geothermometers (Fournier and Truesdell, 1973; Fournier, 1979; Michard, 1979) yield higher temperatures.

With regards to the Na/Li geothermometer, only the relationship determined by Kharaka et al. (1982), for waters from world geothermal and US oil sedimentary basins, yields temperatures close to that measured in the boreholes (Sanjuan et al., 2002a, 2002b). This result thus strongly suggests the importance of a sedimentary signature in the reservoir rocks.

2.3. Diamant area

The Diamant area is located in southern Martinique (Fig. 1). An extensive survey of gas and water geochemistry (Sanjuan et al., 2003, 2005) confirmed the presence of high-temperature zones of geothermal interest. In this area, the only thermal spring (Petite Anse) has several discharge points near the seaside, from which two water samples were collected (DIAM1 and DIAM2). The main emergence (DIAM1) has a temperature close to 35 °C at the surface. The deep geothermal NaCl fluid, discharged from this emergence, has a high salinity (TDS $\approx$ 20 g/L) and a pH value close to 5.3. Abundant magmatic CO_2 gas emanations are associated with this fluid (Sanjuan et al., 2003, 2005). The location of the thermal spring, the nature of this fluid and its high salinity all suggest a marine origin. Its exceedingly low δD value (−22‰), compared to other values observed in the fluids of Martinique and the Lesser Antilles, also points out a magmatic contribution.

The geochemical characteristics of this fluid and especially the use of chemical geothermometers, such as Sil-

ica–Quartz, Na/K, Na/K/Ca, or isotopic geothermometers, such as $\delta^{18}O(H_2O–SO_4)$ (Fournier and Rowe, 1966; Mizutani and Rafter, 1969; Fournier and Truesdell, 1973; Fournier, 1979), enabled the identification of a geothermal reservoir at about 180 °C (Sanjuan et al., 2003, 2005). As for the Lamentin geothermal fluid, only the Na/Li relationship determined by Kharaka et al. (1982) gives temperature values in agreement with that estimated for the reservoir fluid, again suggesting the importance of a sedimentary signature in the reservoir rocks.

3. ANALYTICAL METHODS

3.1. Major and trace elements

All chemical analyses were carried out in the BRGM laboratories using standard water analysis techniques, such as ion chromatography, atomic absorption spectrophotometry, inductively coupled plasma mass spectrometry (ICP-MS), colorimetry, ion electrode and titration. The accuracy of the determination of major species was better than ±5%. Alkalinity was determined in the field following HCl titration and Gran's method. Ion balance values lower than 7% suggested a good quality for analyses of major species (Table 2). Li concentrations in geothermal waters were determined by ICP-MS (accuracy ±5%).

Chemical analyses of the major species and trace elements were carried out on conditioned samples: after filtration at 0.2 μm for the major anions, and after filtration at 0.2 μm and acidification with Suprapur HNO_3 acid (down to pH = 2) for the major cations and trace elements. Bottles for anion analyses were kept non-acidified. Water samples for Li isotopic determination were collected in acid-washed polyethylene bottles and then filtered through pre-washed 0.2 μm Sartorius cellulose filters using a cleaned polycarbonate Sartorius apparatus under nitrogen. Samples were acidified with ultra pure nitric acid down to pH ~ 2.

Accuracy and precision for major and trace elements was verified by repeated measurements of standard materials during the course of this study: namely Ion96-3 and LGC6020 for cations and anions, and a pure Li standard solution (Merck 1-70223.05) for Li determination. All samples were analyzed after dilution to minimize matrix effects during measurement and also to match the matrix of the standard materials. In addition, the calibration curve of the measurement was performed following the "standard addition" technique for saline samples.

Table 1
Seawater/basalt interaction at different temperatures. Lithium concentration (μg/L) and isotopic composition (δ^7Li, ‰) values in the solution are grouped according to the experimental method used and run duration for each experiment carried out at 25, 75, 200 and 250 °C. The initial solution was a seawater solution diluted to 60% (with ultrapure H_2O Milli-Q). It had a Li concentration of Li = 100 μg/L and a Li isotopic composition of $\delta^7Li = +31.0‰$. Sample aliquots (300 μl) were filtered and weighed. We did not rinse the solids before digestion; it is likely that Li from the solution might be adsorbed or precipitated on the solids after the experiment, even after filtration. However, this certainly had no effect due to the low contents of Li in the remaining solution compared to Li contents in the solids. During mass spectrometry analysis, the ^{7}Li beam intensity of the sample was compared to that of the L-SVEC standards (standard bracketing measurement), enabling determination of the Li concentration of the solution. We estimated a typical error of ±10% for this determination based on replicate measurements of seawater samples. Replicate analyses were performed for experiments carried out at 250 °C and were in good agreement, within a range of ±0.5‰ (2σ). To repeatedly sample the gold capsules using the autoclave furnace systems, we initially prepared several gold capsules within the autoclave. These were removed one by one at each sampling time for analysis.

Temperature (°C)	Experimental device	Run duration (days)	Li (μg/L)	δ^7Li (‰)	$2\sigma_m$ (‰)
25	PFA beaker in oven	2	114	26.4	0.3
	Solid: 500 mg	7	103	26.7	0.1
	Liquid: 5 mL	35	123	24.8	0.1
		70	97	24.8	0.1
		245	121	23.5	0.1
75	PFA beaker in oven	2	116	22.6	0.1
	Solid: 500 mg	7	150	20.9	0.1
	Liquid: 5 mL	35	166	17.8	0.1
		70	158	17.9	0.1
		245	220	16.5	0.1
200	PTFE bomb in oven	3	–	14.5	0.1
	Solid: 1000 mg	7	–	14.5	0.1
	Liquid: 10 mL				
200	Gold capsule in autoclave furnace system	1	212	14.2	0.1
	Solid: 30 mg	2	233	14.7	0.1
	Liquid: 300 μL	12	214	15.2	0.1
250	Gold capsule in autoclave furnace system	1	284	13.1	0.3
	Solid: 30 mg	2	316	11.7	0.1
	Liquid: 300 uL	7	352	11.6	0.1

Liquid: seawater IRMM BCR-403 ($\delta^7Li = +31.0‰ \pm 0.5$, Li = 0.18 mg/L) solution diluted to 60% solid: JB-2 tholeiitic basalt ($\delta^7Li = +4.9‰ \pm 0.6$, Li = 7.78 μg/g).

Table 2
Major cations and anions, Li concentrations and Li isotopic compositions of water samples from the Bouillante, Lamentin and Diamant geothermal fields. The temperatures given are those measured during sampling, whereas the temperatures within the geothermal reservoirs were around 250–260 °C, 90–120 °C and 180 °C, respectively, for Bouillante, Lamentin and Diamant. Sample BO-4-00-220A was collected in the weir box, BO-4-00-222B after the phase separator, and BO-4-00-222C is a sample of condensate after steam separation. The uncertainty in δ^7Li values is reported in this table (ranging between 0.1‰ and 0.4‰, $2\sigma_m$). However, based on long-term measurements of both seawater and JB-2 basalt standards, we estimate the external reproducibility of our method as being around ±0.5‰ (2σ).

Sample type	Sample name	Sampling date	Sampling temperature	pH	Conductivity at 25 °C (mS/cm)	Na (mg/L)	K (mg/L)	Mg (mg/L)	Ca (mg/L)	SiO_2 (mg/L)	HCO_3 (mg/L)	CI (mg/L)	SO_4 (mg/L)	Σ+ (meq/L)	Σ− (meq/L)	Ionic Balance (%)	Li (mg/L)	δ^7Li (‰)	$2\sigma_m$ (‰)
Bouillante																			
Well fluid	BO-4-99F640	03/07/1999	255	5.54	27.6	5050	743	30	1700	275	154	11,650	40	326	332	−2	4.28	4.4	0.2
Well fluid	BO-2-99F320	07/07/1999	242	5.61	27.7	5000	805	14	1700	537	78.1	11,880	14.3	324	337	−4	4.35	4.4	0.1
Well fluid	BO-4-222A	16/05/2000	95	7.51	42.5	7806	1195	2.9	2427	721	21.4	16,134	33	492	456	7	6.48	4.3	0.3
Well fluid	BO-5-02-MEHP	23/07/2002	32.1	7.07	37.4	6420	971	2.4	2300	174	31.7	14,645	22.1	419	414	1	5.60	4.1	0.2
Well fluid	BO-2-TDP	16/05/2000	68	7.30	43.3	7405	1117	1.4	2468	710	20.7	16,317	21.8	474	461	3	6.00	4.4	0.2
Well fluid	BO-4-00-220A	13/05/2000	95	7.25	42.8	7752	1166	3	2466	735	23.8	16,080	31.8	491	455	7	6.5	4.5	0.1
Well fluid	BO-4-00-222B	16/05/2000	95	6.53	35.4	6412	931	2.5	2017	573	23.2	13,568	29.7	404	384	5	5.28	4.7	0.2
Well fluid	BO-4-00-222C	16/05/2000	95	5.34	0.08	–	–	–	–	1.5	15.9	1.7	1.5	–	–	–	0.0005	4.8	0.2
Well fluid	BO-6-04-P12	05/04/2001	–	7.54	41.8	7100	1025	3.3	2450	685	25.3	16,500	30.8	458	467	−2	6.7	4.6	0.2
Drill hole	BO-BS	31/01/2001	93	6.16	36.9	7707	778	6.8	2750	168	1.22	17,250	45	493	488	1	6.6	3.8	0.3
Drill hole	BO-BS	24/07/2002	90.6	7.25	42.5	7365	793	7.4	2400	174	–	16,290	41.8	461	460	0	6.1	4.2	0.2
Sub-marine spring	SM1	28/10/1998	96	5.51	39.7	8500	545	815	1039	156	127.5	16,766	1714	503	511	−2	1.92	6.0	0.2
Sub-marine spring	SM2	29/10/1998	72	6.21	43.7	10,000	473	1076	847	102	178.1	18,806	2362	578	583	−1	1.10	7.6	0.3
Sub-marine spring	BO-98 SM3	29/10/1998	94	6.27	36.2	7500	619	533	1358	201	5.3	15,543	1149	454	462	−2	3.02	4.8	0.2
Sub-marine spring	SM4	30/10/1998	62	6.35	45.0	10,500	440	1248	616	36	169	19,498	2700	602	609	−1	0.55	10.8	0.3
Sub-marine spring	SM5	30/10/1998	60	6.97	46.6	11,000	399	1377	470	2.1	147.6	20,235	2900	626	634	−1	0.186	26.1	0.3
Sub-marine spring	SM6	30/10/1998	54	6.78	17.5	3200	204	166	843	142	68.9	7105	326	200	208	−4	1.65	5.4	0.2
Sub-marine spring	BO-9628	27/05/1996	92	6.05	40.2	8073	587	1014	1014	131	162.3	17,053	1662	501	518	−4	2.60	5.8	0.4
Sub-marine spring	BO-9629	27/05/1996	52	6.81	43.7	9886	469	11,308	834	0.71	142	19,499	2602	592	607	−3	0.53	8.3	0.2
Thermal spring	Marsolle	26/05/1996	44.3	7.18	2.3	171	16	13	44	87	167	277	29	11	11	−1	0.046	5.8	0.3
Seawater	Eau de Mer	30/10/1998	29	8.23	46.6	11,000	401	1346	467	0.43	169	20,181	3000	623	635	−2	0.25	29.3	0.4
Lamentin																			
Well fluid	Californie	26/03/2002	73.6	6.04	20.6	3790	124	130	725	69	982	7050	316	215	222	−3	1.59	7.8	0.3
Well fluid	Carrère	05/12/2001	40.1	6.12	19.6	3280	122	183	778	90	1622.6	6358	127	200	209	−4	1.67	6.0	0.1
Well fluid	Carrère	21/11/2001	41	6.08	19.7	3310	125	187	830	91	1592.7	6335	333	204	212	−4	1.47	6.2	0.2
Seawater	MER	09/12/2001	29	–	–	11,400	309	1200	390	–	143	20,200	2626	622	627	−1	0.23	30.1	0.4
Diamant																			
Thermal spring	DIAM1	06/12/2001	35.3	5.99	28.4	6050	295	300	1100	131	1679	10,200	500	351	326	7	10.10	6.8	0.1
Thermal spring	DIAM1	25/03/2001	34	6.15	23.8	5396	474	263	991	154	930	9730	493	318	300	6	9.95	7.1	0.1
Thermal spring	DIAM2	25/03/2001	30.4	7.10	14.7	3253	322	175	594	151	1300	5070	760	194	180	7	5.89	6.3	0.1
Thermal spring	DIAM2	06/12/2001	31.3	6.53	17.6	3340	178	174	565	137	1290	5200	817	192	185	4	5.52	6.6	0.1
Seawater	Mer	09/12/2001	28.5	8.19	53.5	11,400	309	1200	390	0.19	152	20,200	2626	622	627	−1	0.226	30.5	0.2

3.2. Lithium isotopes

Lithium isotopic compositions were measured using a Neptune Multi Collector ICP-MS (Thermo Fischer Scientific). $^7Li/^6Li$ ratios were normalized to the L-SVEC standard solution (NIST SRM 8545, Flesch et al., 1973) following the standard-sample bracketing method (see Millot et al., 2004 for more details). The analytical protocol involved the acquisition of 15 ratios with 16 s integration time per ratio, and yielded in-run precision better than 0.4‰ ($2\sigma_m$). Blank values were low (i.e., 0.2%), and the 5-min wash time was enough to reach a stable background value.

The samples were prepared beforehand with chemical separation/purification by ion chromatography, as required to produce a pure mono-elemental solution. Chemical separation of Li from the matrix was achieved before the mass analysis following a procedure modified from the technique of James and Palmer (2000). This method required the use of cationic resin (a single column filled with 3 mL of Bio-Rad AG® 50W-X12 resin, 200–400 mesh) and HCl acid media (0.2 N) for 30 ng of Li. Blanks for the total chemical extraction were less than 30 pg of Li, which is negligible as it represents a 10^{-3} blank/sample ratio.

Successful quantitative measurement of Li isotopic compositions requires 100% Li recovery during laboratory processing. Therefore, frequent column calibrations were performed. Repeated analyses of the L-SVEC standard processed through columns showed 100% Li recovery and no induced isotope fractionation due to the purification process.

Accuracy and reproducibility of the entire method (purification procedure + mass analysis) were tested by repeated measurement of a seawater sample (IRMM BCR-403) after separation of Li from the matrix. For this we obtained a mean value of $\delta^7Li = +30.8‰ \pm 0.4$ (2σ, $n = 15$) over the duration of the analyses. This average is in good agreement with our long-term measurement ($\delta^7Li = +31.0‰ \pm 0.5$, 2σ, $n = 30$, Millot et al., 2004) and with other values reported in the literature (see, for example, Tomascak, 2004 for a compilation). For rocks, a total digestion of the sample was necessary before separation of Li from the matrix. About 50 mg of crushed sample was dissolved in a closed beaker with an ultrapure mixture of three acids for 4 days at 100 °C: 4 ml of HF (23 N), 1 ml of HNO_3 (14 N) and 0.1 ml of $HClO_4$ (12 N). Four days later, once the acid mixture had evaporated, 4 ml of HCl acid (6 N) was added for 4 days at 100 °C. A sample aliquot (30 ng of Li) of the acid dissolution residue was then dissolved in 0.5 ml of HCl (0.2 N) before being placed in a column containing cationic resin for Li separation. Blanks for the total digestion of the solid samples by acids (HF, HNO_3, $HClO_4$ and HCl) were less than 300 pg of Li. Considering the Li concentration in the solid samples (from 5 to 50 μg/g) and the sample quantity taken for acid digestion (50 mg), it appeared that the quantity of Li ranged from 250 to 2500 ng. Consequently the blank accounted for only 0.01–0.1% of the sample, which is negligible.

Accuracy and reproducibility of the procedure for solid samples (dissolution + purification procedure + mass analysis) was tested by repeated measurement of the JB-2 basalt standard (Geological Survey of Japan). This yielded a mean value of $\delta^7Li = +4.9‰ \pm 0.6$ (2σ, $n = 17$), which is in good agreement with published values (see Carignan et al., 2007 and Tomascak, 2004 for data compilation).

Therefore, based on long-term measurements of both seawater and JB-2 basalt standards, we estimate the external reproducibility of our method to be around ±0.5‰ (2σ).

3.3. Experimental techniques for seawater/basalt interaction

To determine the extent of Li isotope fractionation during water/rock interaction as a function of temperature, we performed a series of laboratory experiments. These experiments consisted of determining Li isotopic fractionation during the interaction of basalt with seawater at different temperatures (25, 75, 200 and 250 °C) and various pressures. This was the first study involving Li isotope exchange experiments for low temperature water/rock interaction (below 100 °C).

The basalt chosen for the experiments was the JB-2 tholeiitic basalt (Japan Geological Survey), which is a well characterized secondary reference material for Li isotopes and Li concentration ($\delta^7Li = +4.9‰ \pm 0.6$, Li = 7.78 μg/g). Seawater chosen for the experiments was the reference material IRMM BCR-403 ($\delta^7Li = +31.0‰ \pm 0.5$, Li = 0.18 mg/L, Millot et al., 2004).

Experiments were carried out with a seawater/basalt mass ratio of 10 and a seawater solution diluted to 60% (with ultrapure H_2O Milli-Q), to reproduce the natural conditions (water/rock ratio and seawater dilution) found in the Bouillante geothermal site.

Experimental run durations varied from days to weeks, depending on the applied temperature (Table 1). Li concentration and Li isotope composition (δ^7Li) were measured through time in sampled aliquots of the solution that had interacted with the basalt at various temperatures (25, 75, 200 and 250 °C).

Two different experimental devices were used. For experiments carried out at 25, 75 and 200 °C, large volumes (5–10 ml) of solution were put into closed beakers and then placed in an oven. For experiments carried out at 200 and 250 °C, small volumes of solution (300 μl) were loaded in gold capsules and then placed in an autoclave. We were therefore able to compare the results obtained from the two devices at 200 °C (oven and autoclave furnace system).

For experiments at 25 and 75 °C, 5 ml of diluted seawater was initially placed with 500 mg of powdered JB-2 basalt in a closed Teflon PFA (perfluoroalkoxy plastic) beaker and then placed in a temperature-controlled oven, with temperatures set at 25 or 75 °C. The temperature inside the oven varied less than 5% over the total duration of the experiments. The solution was sampled after 2 days and then after 1, 5, 10 and 35 weeks (Table 1). The samples (300 μl) were filtered using 0.20 μm filter prior to Li isotopic measurement, to ensure that only dissolved Li was sampled, without any contribution from powdered basalt.

At 200 °C, 10 ml of diluted seawater with 1 g of powdered JB-2 basalt was put in a Teflon PTFE bomb within

a screw-top stainless-steel container and then placed in an oven at 200 °C. Solution aliquots (300 µl filtered) were sampled after 3 and 7 days.

Experiments were also carried out at 200 and 250 °C in an autoclave furnace system under high pressure at the Institut des Sciences de la Terre d'Orléans (ISTO). Diluted seawater (300 µl) and powdered basalt (30 mg) were loaded in gold capsules (4 cm long, 5 mm in diameter) that were previously cleaned by boiling in diluted HCl solution and then in distilled water. The powdered basalt was placed at the bottom of the gold capsule before the diluted seawater was added. Once filled with diluted seawater, the capsules were welded shut using a graphite arc welder. The weight of the capsules was used to monitor loss during welding. The capsules were then placed in an internally heated pressure vessel, which was pressurized with Argon (Ar; Scaillet et al., 1992), at either 200 or 250 °C ($P = 150$ bar). Run durations varied between 1 and 12 days (Table 1), during which the temperature remained within 1 °C of the target value. Pressure fluctuations related to changes in room temperature were less than 5 bar. Overall, the uncertainties in temperature and pressure values reported here were estimated to be ±5 °C and ±5 bar. Upon completion of the run, capsules were removed from the vessel, weighed to check for leaks and opened. The sampled solution was then filtered at 0.2 µm. No experiments showed weight changes in excess of 0.2 mg, which is within the analytical uncertainty of the balance.

Possible contaminants for experiments using Teflon PFA beakers (25 and 75 °C), a Teflon PTFE bomb (200 °C) and gold capsules (200 and 250 °C) were tested for by running diluted seawater without powdered basalt for several days and by comparing Li concentration and δ^7Li values before and after run completion. This clearly showed that there was no variation in either the Li concentration (0.1 mg/L, 60% diluted) or δ^7Li values (^{7}Li = +31.0‰). Thus, there was no Li contamination from containers or handling.

At the end of each experiment (25, 75, 200 and 250 °C), Li isotope compositions (δ^7Li) were measured in the solid products, to determine the Li isotope fractionation between the liquid and solid phases.

3.4. Mineral characterization

The residual solids (powdered basalt after interaction) were analyzed at the end of each experiment (25, 75, 200 and 250 °C). Transmission electron microscopy (TEM) was performed at the University of Orléans to determine the bulk mineralogical composition of the residual solid after interaction. In addition, infrared spectra were obtained on a BRUKER Equinox IFS55 Fourier transform infrared (FTIR) spectrometer by transmission through a pellet of a mixture of 150 mg KBr with less than 1 mg of sample. The spectrometer was equipped with a high energy source, separating KBr and a DTGS (deuterated triglycine sulfate) detector, making it possible to explore the IR average ranging classically from 4000 to 350 cm^{-1}. The spectral resolution was 4 cm^{-1}, with 32 scans used for both the background and the samples.

4. RESULTS

4.1. Bouillante, Lamentin and Diamant areas

Lithium concentrations spanned more than two orders of magnitude in the water samples collected from the Bouillante area, ranging from 0.046 mg/L for the terrestrial thermal spring Marsolle and 0.19 mg/L for the sub-marine spring SM5 (for the lowest concentrations) up to 6.7 mg/L for the deep geothermal water (well BO-6). The low Li concentration observed in the water sample collected from the thermal spring Marsolle can be explained by its low TDS (close to 0.8 g/L; Mas et al., 2006), due to a predominant contribution of fresh water that was estimated at about 98% (Sanjuan and Brach, 1997). Fluids from the wells had the highest Li concentrations, ranging from 4.3 to 6.7 mg/L, depending on the sampling conditions (i.e., down-hole sampling, sampling after phase separator, sampling in the weir box; see Table 2). Generally, the down-hole water sample was representative of the deep fluid. The increasing concentrations observed for most of the chemical species (including Li) in the samples of residual fluid collected at the surface (after separator or in the weir box) were the result of the formation and loss of steam, the amount of which depended on the temperature and pressure conditions of the phase separation.

Lithium isotopic compositions (δ^7Li) were also quite variable and ranged from +3.8 for the BO-BS water sample to +29.3‰ for the seawater sample. However, it is important to note that all the well fluids in the Bouillante geothermal field (BO-2, BO-4, BO-5 and BO-6 samples) had similar δ^7Li values. These geothermal water samples were collected from the various wells intersecting the deep reservoir and under different sampling conditions (from 1999 to 2002). They presented δ^7Li signatures between +4.2 and +4.8‰, with an average value of $\delta^7\text{Li} = +4.4‰ \pm 0.4$ (2σ, $n = 8$). This constancy in δ^7Li values (±0.4‰, close to the reproducibility of the analytical determination of δ^7Li, ±0.5‰ 2σ), clearly shows that geothermal fluids discharged from the wells were homogeneous from a Li isotope point of view. Consequently, this demonstrates that all of the geothermal wells are probably fed by a common reservoir.

These conclusions are in agreement with the homogeneity observed from chemical and other isotopic analyses (δD and δ^{18}O values, boron and strontium isotopes; Sanjuan et al., 2001; Mas et al., 2006). Our results show that no Li isotopic fractionation occurs (or is negligible) during the phase separation between liquid and steam, under different temperature and pressure conditions (after separator: 160 °C and 6–8 bar; in weir box: 100 °C and 1 bar, see Table 2). For instance, the δ^7Li value determined in a sample of separated steam was $\delta^7\text{Li} = +4.8‰$, (sample BO-4-00-222C, Table 2), which is identical to the δ^7Li value prior to phase separation. In addition to that, the BO-BS water samples that were collected from a shallow borehole also yielded δ^7Li values (+3.8‰ and +4.2‰) similar to those measured in the fluids discharged from geothermal wells.

The fluids discharged from sub-marine thermal springs had δ^7Li signatures ranging from +4.8‰ to +26.1‰ (sample SM5 having the highest δ^7Li value). The value for sea-

water sampled offshore in the Bouillante bay ($\delta^7Li = +29.3‰$) was at the lower end of the range of variation observed for oceans worldwide (from +29‰ to +34‰, Millot et al., 2004).

For the Lamentin plain (Martinique), Li concentrations in the water samples ranged from 0.23 mg/L (seawater) to 1.67 mg/L (borehole Carrère, Table 2). The geothermal water samples collected from the two boreholes were different, with $\delta^7Li = +7.8‰$ for the borehole Californie and +6.0‰ and +6.2‰ for the borehole Carrère. The seawater sampled near the Lamentin area had a Li isotopic composition of $\delta^7Li = +30.1‰$, which is in good agreement with the average value of seawater.

In the Diamant area, Li concentrations ranged from 0.226 mg/L (seawater) to 10.1 mg/L (thermal water sample DIAM1). The Li isotopic range was very large with δ^7Li values between +6.3‰ and +30.5‰ for the DIAM1 and seawater samples, respectively.

Water samples collected from the two discharge points of the thermal spring Petite Anse (DIAM1 and DIAM2; Fig. 1) presented a Li isotopic composition in the range of +6.3‰ to +7.1‰.

4.2. Seawater/basalt interaction experiments

The Li concentration and isotopic composition of the solutions were determined after various reaction times during seawater/basalt interaction at 25, 75, 200 and 250 °C. Results are given as a function of reaction time and interaction temperature (Table 1). For the liquid phase, Li concentrations and δ^7Li variation with time are plotted against temperature, including the initial seawater (diluted to 60%) having a Li concentration of 100 μg/L and a δ^7Li value of +31.0‰ (Fig. 2).

At 25 °C, the seawater/basalt interaction was measured in liquid samples that were collected after 2, 7, 35, 70 and 245 days. Starting from an initial value of 100 μg/L, the Li concentration varied little throughout the experiment, with values between 97 and 123 μg/L. According to the uncertainty of the method used to measure Li concentration after run completion, there was little Li concentration variability in solution during the interaction of basalt with seawater at 25 °C. On the other hand, starting from an initial value of $\delta^7Li = +31.0‰$, the Li isotopic composition of the solution decreased rapidly and significantly to reach a δ^7Li value of +23.5‰ after 245 days.

At 75 °C, sample aliquots were collected after 2, 7, 35, 70 and 245 days. The Li concentration increased steadily with time up to 220 μg/L (twice the initial value). With increasing Li in solution, δ^7Li values in the solution decreased. The δ^7Li signature dropped from +31.0‰ to +16.5‰ after 245 days.

At 200 °C, the Li concentration significantly increased in solution during seawater/basalt interaction, both in experiments carried out with the PTFE bomb and in those completed with gold capsules in an autoclave. This increase was observed after 1 day of interaction (212 μg/L), after which the Li concentration did not vary appreciably (Fig. 2). The Li isotopic composition of the solution decreased rapidly and significantly down to a minimum δ^7Li value of around +14.5‰. Values were identical for both the PTFE-bomb and gold-capsule methods (+14.2‰ to +14.7‰). The fact that the same δ^7Li values were obtained with both methods and that the δ^7Li signature was constant with time shows that steady state was probably reached for Li isotope exchange. The Li isotopic signature was $\delta^7Li = +15.2‰$ after 12 days, which is identical to +14.5‰ considering the external reproducibility of the method: ±0.5‰ (2σ).

At 250 °C, the Li concentration rapidly increased in solution and tended to a maximum of 352 μg/L after 7 days (more than three times the initial value of 100 μg/L). Li isotope variation at 250 °C showed a strong decrease from +31.0‰ down to +13.1‰ after 1 day, after which the values were constant at +11.7‰ and +11.6‰ after 2 and 7 days, respectively.

In addition to the fluid, the Li isotopic composition of the residual solid (powdered basalt after interaction) was analyzed at the end of each experiment (25, 75, 200 and 250 °C). These δ^7Li values (Table 3) were identical to the initial value measured for the JB-2 basalt, showing that there was no measurable variation in the Li isotopic composition of bulk solid phase during these experiments. This reflects the order of magnitude difference in Li concentrations between the starting solid and fluid phases.

5. DISCUSSION

5.1. Li isotopic systematics in geothermal systems

A graph of the Li isotopic composition (δ^7Li) for various waters from the Bouillante geothermal area plotted against the Li/Cl ratio is shown in Fig. 3a. This figure reveals the mixing process (shown by a hyperbolic curve on the graph) and highlights samples having the highest Li/Cl ratios (i.e., those enriched in Li), which are the samples of interest for the study of geothermal systems.

As previously stressed, the critical finding from our field measurements was that all of the deep geothermal fluids from the Bouillante area (BO-2, BO-4, BO-5, BO-6 and BO-BS) had very homogeneous Li isotopic signatures, with an average value of $\delta^7Li = +4.4‰ \pm 0.5$ (Fig. 3b). These well fluids also correspond to the samples with the highest Li/Cl ratios (from 3.7×10^{-4} to 4.1×10^{-4}) and belong to the Bouillante geothermal reservoir, for which a deep temperature was estimated at 250–260 °C.

On the other hand, it is apparent that fluid samples collected from the sub-marine thermal springs define a good mixing trend between geothermal reservoir fluid and seawater, the latter having a high Li isotopic signature of $\delta^7Li = +29.3‰$ and a low Li/Cl ratio of 0.1×10^{-4}. This mixing process has already been reported, on the basis of major element concentrations, by Traineau et al. (1997), Sanjuan and Brach (1997) and Sanjuan et al. (2001), and is confirmed here using Li isotope tracing. Our inferred mixing range (%) is in agreement with previous estimates (Fig. 3a). Another very interesting result for geothermal exploration is that the water sample collected from the terrestrial thermal spring Marsolle, which is comprised of about 98% freshwater, is also located on the hyperbolic

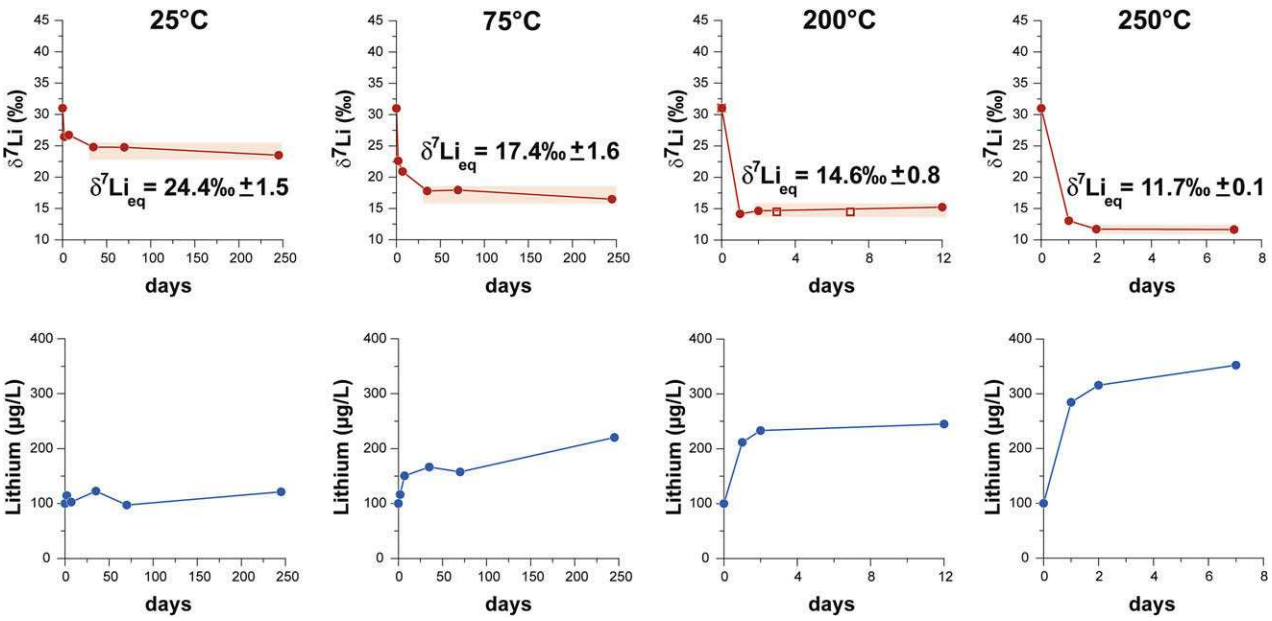

Fig. 2. Graphs showing the evolution over time of the solution for lithium isotopic composition in red (δ^7Li, ‰) and Li concentration in blue (Li, µg/L) during experiments at 25, 75, 200 and 250 °C. Lithium isotopic composition determined at steady state (δ^7Li $_{equ}$, i.e., equilibrium: equ) in the solution corresponds to the average value reached at isotopic steady state and is calculated by averaging the constant values at the end of each run. At 200 °C, red circles and red squares correspond, respectively, to experiments carried out with gold capsules in an autoclave and with a Teflon PTFE bomb placed in a screw-top stainless-steel container in an oven.

curve of mixing between seawater and geothermal fluid (Fig. 3a). This suggests that this thermal spring is supplied by water from the Bouillante geothermal reservoir. Due to the low TDS of this water and to the presence of seawater, Fig. 3a and the $^{87}Sr/^{86}Sr$ versus Sr/Cl diagram (Sanjuan and Brach, 1997) are the only methods that reveal the contribution of geothermal water toward the composition of this thermal spring.

The geothermal waters of the Lamentin area, which are initially made up of a mixture of seawater and fresh surface water, differ significantly from Bouillante samples with respect to their Li isotope signature, with $\delta^7Li = +7.8‰$ for the borehole Californie and +6.0‰ and +6.2‰ for the two Carrère boreholes. These fluids correspond to the Lamentin geothermal reservoir with an average value of $\delta^7Li = +6.7‰$ ($n = 3$), the deep temperature of which was estimated to be between 90 and 120 °C. The Li isotopic signature of the Lamentin geothermal reservoir is, therefore, very different from that of Bouillante (Fig. 3b).

Table 3
Li isotopic composition determined at steady state in the solution (δ^7Li $_{solution}$) and solid phases (δ^7Li $_{basalt}$) for seawater/basalt interaction experiments carried out at 25, 75, 200 and 250 °C. The uncertainty is the standard deviation (2σ of the δ^7Li values at run completion for each experiment. The fractionation ($\Delta_{solution-solid}$) is the difference in Li isotopic composition between the solution and the basalt for each experiment at steady state.

Temperature (°C)	$\delta^7Li_{solution}$ (‰)	δ^7Li_{basalt} (‰)	$\Delta_{solution-solid}$ (‰)
25	24.4 ± 1.5	5.0	19.4
75	17.4 ± 1.6	4.9	12.5
200	14.6 ± 0.8	5.1	9.5
250	11.7 ± 0.1	5.0	6.7

Fig. 3a shows the waters collected from wells and submarine thermal springs in both the Bouillante and Lamentin geothermal sites, for comparison. The hyperbolic curves for mixing of deep reservoir fluids and seawater are also shown for each geothermal system. These illustrate that the Bouillante and Lamentin geothermal reservoirs are very different in terms of both their Li isotopic signature and their Li/Cl ratios. This probably results from the difference in temperatures of their respective reservoir sources (90–120 °C for Lamentin and 250–260 °C for Bouillante). Indeed, at higher temperature, it is likely that more Li is released to the geothermal water, thus lowering the δ^7Li signature of the water, which would trend toward that of the interacting reservoir rocks. The extent of Li isotope fractionation as a function of temperature during water/rock interaction will be discussed in Section 5.2. Alternatively, these Li isotopic signatures might also result from differences in the lithology and nature of the reservoir rocks at the two sites.

In the Diamant area, a comparison of chemical compositions for samples DIAM1 and DIAM2 indicated a dilution by fresh surface water. The origin of these saline thermal waters seems to be relatively complex (Sanjuan et al., 2003, 2005). Their δ^7Li signatures, however, were similar at the 2σ level (+6.8‰ and +6.2‰ for DIAM1, +7.1‰ and +6.6‰ for DIAM2, respectively). This suggests that they came from the same geothermal reservoir at 180 °C. Binary diagrams, such as δD–$\delta^{18}O$, δD–Cl, $\delta^{18}O$–Cl and Br–Cl (Sanjuan et al., 2002a, 2002b, 2003, 2005), clearly indicate that the geothermal waters collected from

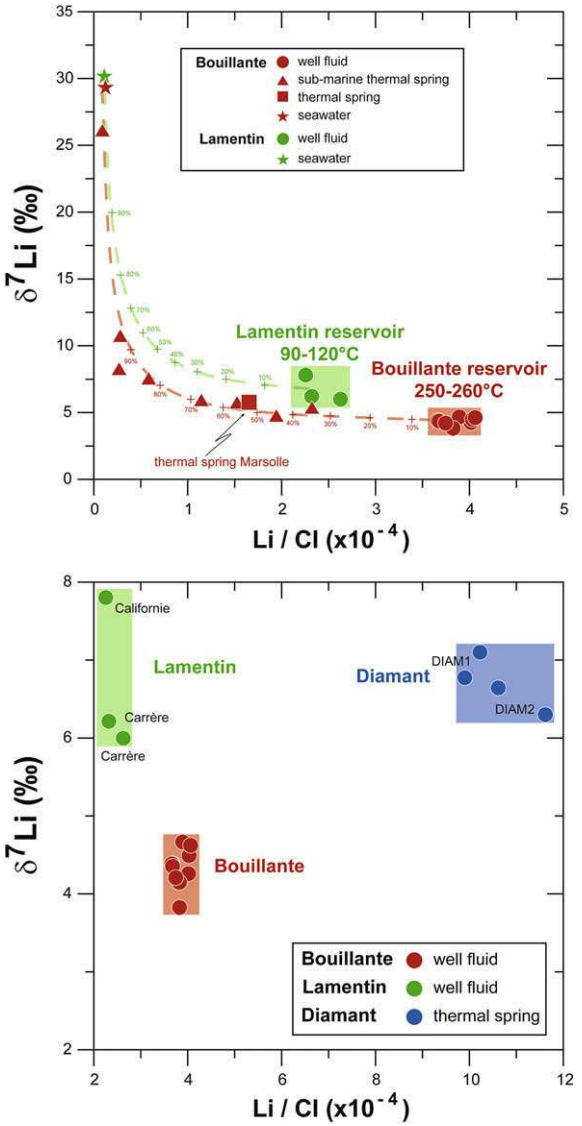

Fig. 3. Lithium isotopic compositions (δ^7Li, ‰) in waters from the Bouillante (red), Lamentin (green) and Diamant (blue) geothermal fields plotted as a function of the Li/Cl ratio. The temperature of the deep geothermal reservoir was estimated by geothermometry to be about 90–120 °C, 180 °C and 250–260 °C for the Lamentin, Diamant and Bouillante areas, respectively. In 3a, the mixing proportions have been added for each mixing corresponding to the proportion of seawater in %. (For interpretation of the references in color in this figure legend, the reader is referred to the web version of this article.)

the Lamentin area could not have resulted from a mixing between geothermal waters from the Diamant area, seawater and freshwater. This is also confirmed in Fig. 3b.

5.2. Lithium isotopic fractionation and temperature dependence

5.2.1. Lithium isotope exchange experiments

Experiments were carried out at different temperatures to investigate Li isotope exchange between a diluted seawater solution and a powdered basalt. The evolution over time of Li concentrations in solution clearly indicates a temperature dependence of Li and its isotopes (Fig. 2 and Section 4.2). Indeed, the release of Li into solution for each experiment increased with temperature. In addition, we observed (Fig. 4) that, during our experiments, Li and δ^7Li data agreed well with a simple mixing process between the initial basalt and seawater. This confirms that Li is a fluid-mobile element that tends to preferentially pass into the fluid phase during water/rock interaction.

To help in the characterization of processes controlling Li and its isotopes in our experiments, the mineralogy of the residual solids was investigated after run completion. Transmission electron micrographs (Fig. 5) clearly show that alteration minerals were observed for experiments carried out at 25 and 75 °C (alteration rings can be seen in Fig. 5b and c; these are highlighted by black arrows). These show that the formation of secondary minerals was much more important for experiments carried at higher temperature (200 and 250 °C in Fig. 5d and e).

Moreover, IR spectra were obtained by FTIR spectrometry for the same residual solids after run completion (at 25, 75, 200 and 250 °C, Fig 6a) and for the starting unaltered basalt (Fig 6a). IR spectra obtained in transmission show the lines characteristic of salts contained in sea water and basalt, for the solids having interacted at 25 and 75 °C (Fig. 6b). On the other hand, for solids having interacted at higher temperatures (200 and 250 °C, Fig. 6b), we noticed the presence of lines that are characteristic of clay minerals. The lines fell close to that of a nontronite (smectite), for the sample having interacted at 200 °C (line around 3565 cm^{-1} in the field containing OH bond elongations), and between a nontronite and a beidellite (line centered around 3605 cm^{-1} in the field containing OH bond elongations), for the sample having interacted at 250 °C. In addition, X-ray diffraction spectra confirmed the pres-

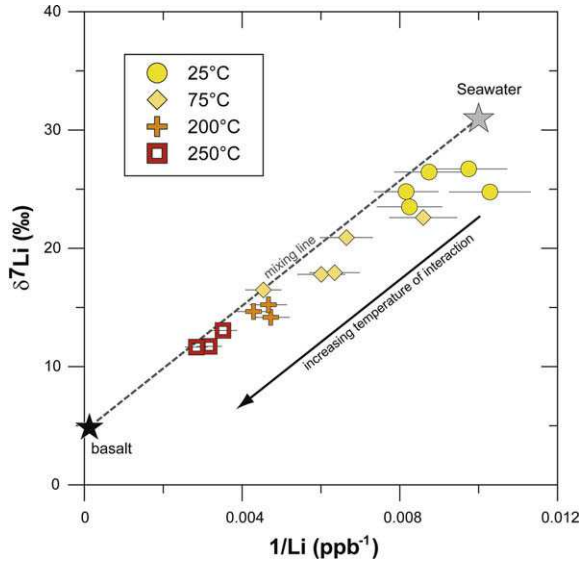

Fig. 4. Graphs showing the lithium isotopic composition (δ^7Li, ‰) as a function of 1/Li (ppb^{-1}) in the liquid fraction during experiments at 25, 75, 200 and 250 °C.

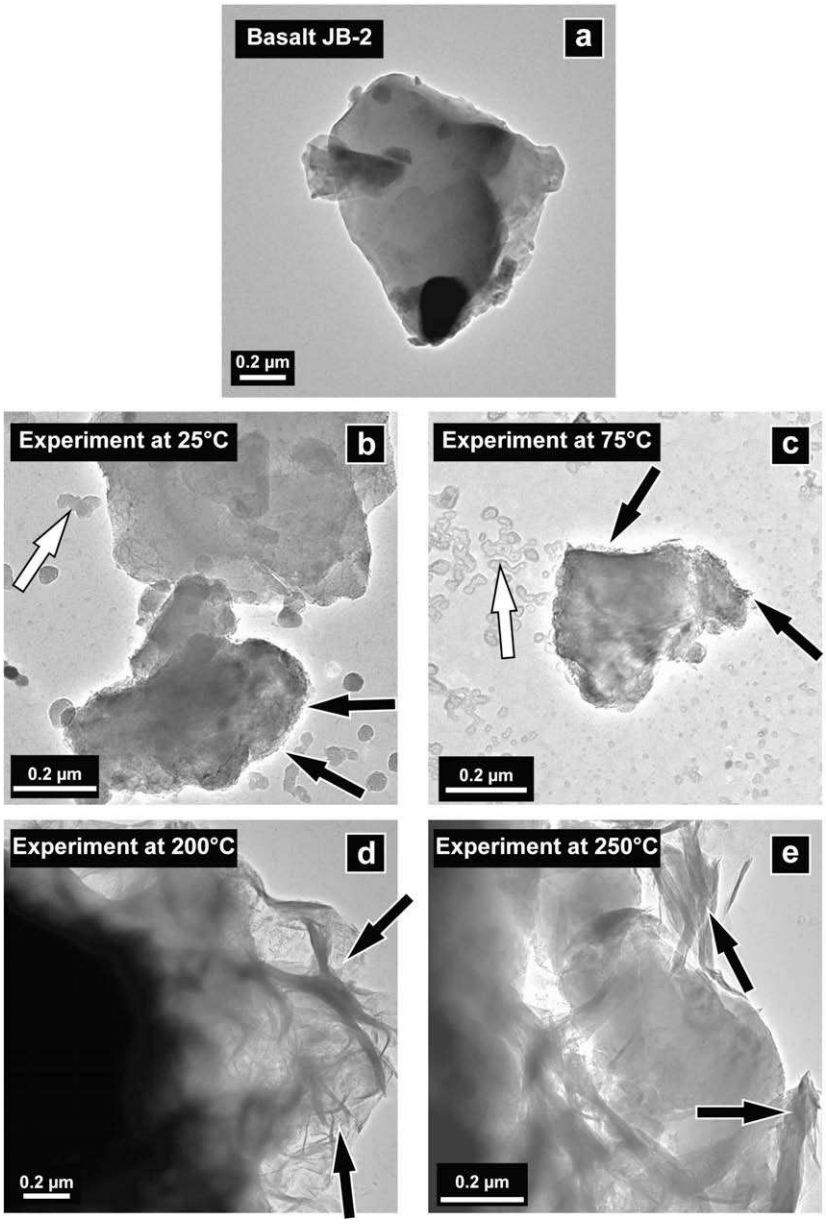

Fig. 5. Transmission electron micrographs of the starting solid material (basalt JB-2) and the different solid run products (powdered basalt after interaction) at the end of each experiment (25, 75, 200 and 250 °C). The black arrows show the formation of clay minerals. The white arrows show the presence of residual salts after the evaporation of remaining seawater.

ence of smectite minerals in the solids having interacted at 200 and 250 °C.

However, experiments carried out by James et al. (2003) have shown that Li is taken up by basalt alteration phases at 150 °C and then released at higher temperature. Uptake of Li by alteration minerals is not a one-way process. The fact that such a behavior was not observed in our experiments is possibly related to the different experimental conditions explored in our study relative to those of James et al. (e.g., water/rock ratio, initial Li concentration in the solution). In particular, in our experiments there was a large initial Li concentration gradient between the starting solution ($5\ mL \times 100\ ng/g = 500\ ng$ Li) and the basalt ($0.5\ g \times 7.78\ \mu g/g = 3.9\ \mu g$ Li).

In spite of this, during our experiments it was quite obvious that secondary minerals (clays) were formed during water/rock interaction, and that this may have played a key role in the Li isotopic trends documented here. The importance of Li isotopic fractionation during formation of Li-bearing secondary minerals has already been addressed in previous works (Chan and Edmond, 1988; Chan et al., 1992, 1993, 1994; James et al., 1999). These reports have shown that fractionation occurs when ^{6}Li is removed from the solution when clay minerals precipitate. In contrast, according to these works, the heavy Li isotope (^{7}Li) is not preferentially released into solution, as there is no reason to expect Li isotope fractionation during dissolution of a fresh basalt (Pistiner and Henderson, 2003).

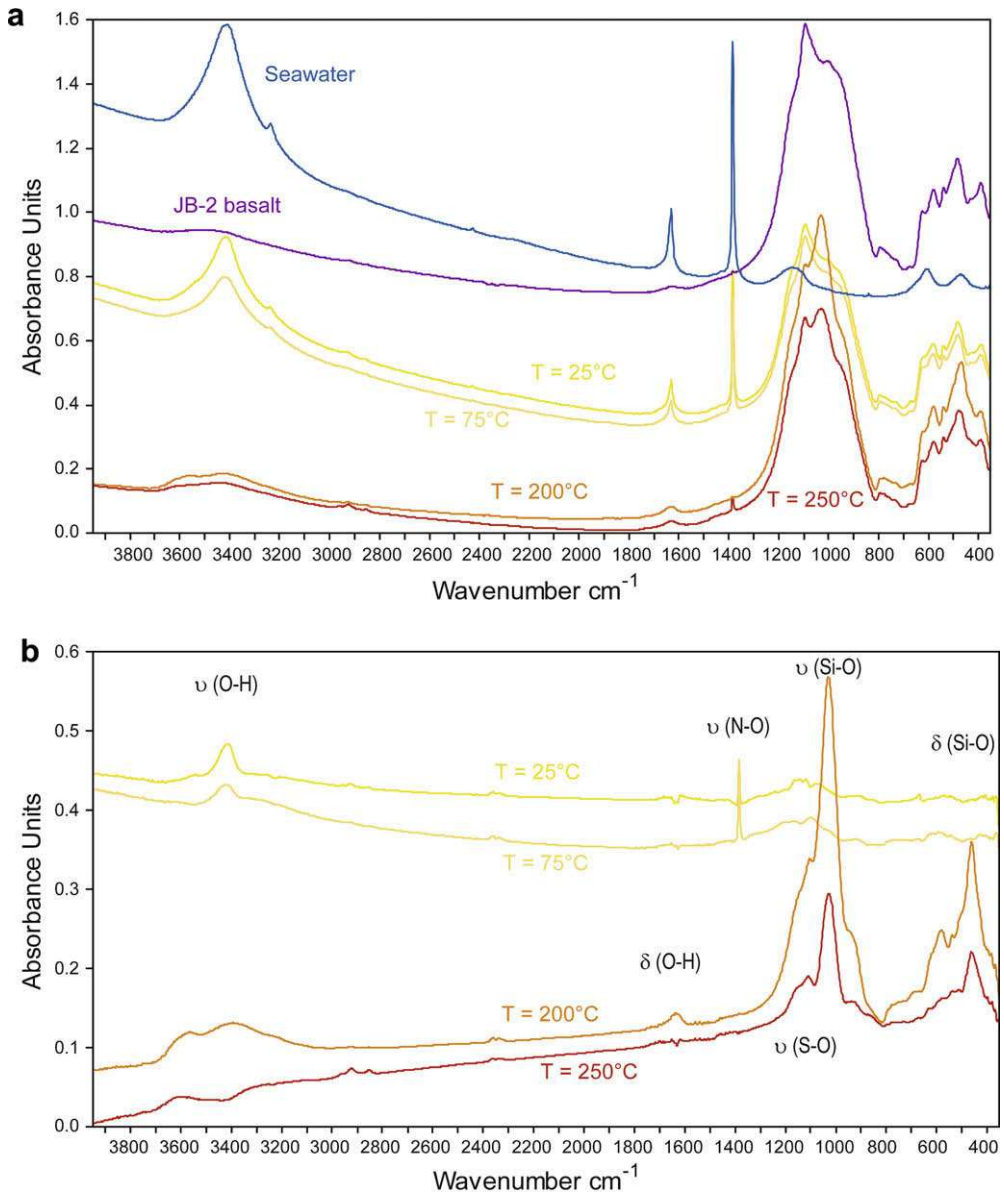

Fig. 6. (a) Infrared spectra obtained by FTIR spectrometry for residual solids after run completion (at 25, 75, 200 and 250 °C) and the initial materials (seawater and basalt). (b) Infrared spectra for experiments after correction for the remaining seawater and initial basalt.

In light of the above evidence, we suggest that the behavior of Li (concentration and isotopic ratio) in our experiments was essentially controlled by two complementary processes: (1) mixing between Li in the initial solution (seawater, $\delta^7Li = +31‰$) and Li release into the solution from the basalt (Figs. 2 and 4) and (2) uptake of lithium into secondary minerals, which is a temperature-dependent process.

Considering the water/rock ratio and the Li concentrations in seawater and basalt, we estimate that the maximum Li concentration in the solution was about 880 μg/L. Upon inspection of Fig. 2, it is obvious, however, that this maximum value was not reached in any case, implying that another process (not simple dissolution) was controlling the release of Li into the solution. We propose the following scenario for the observed trends in Li and its isotopes in our experiments: as reaction time proceeds, the Li concentration in the solution increases and the δ^7Li values flatten out. For any given temperature, two successive processes control Li and its isotopes, as is schematically illustrated in Fig. 7. First, dissolution processes are predominant and release Li into solution (consequently δ^7Li sharply decreases, whereas Li concentrations increase). This step is short, as observed in Fig. 2. Then, during the second step, a steady state is reached between dissolution of basalt, on the one hand, and precipitation of alteration minerals, on the other hand. The competition between dissolution and precipitation processes is likely to be the key factor controlling Li and its isotopes in these experiments.

In addition to the different processes controlling Li, the question of steady state is thus crucial for a correct application of the experimental results. The fact that δ^7Li values

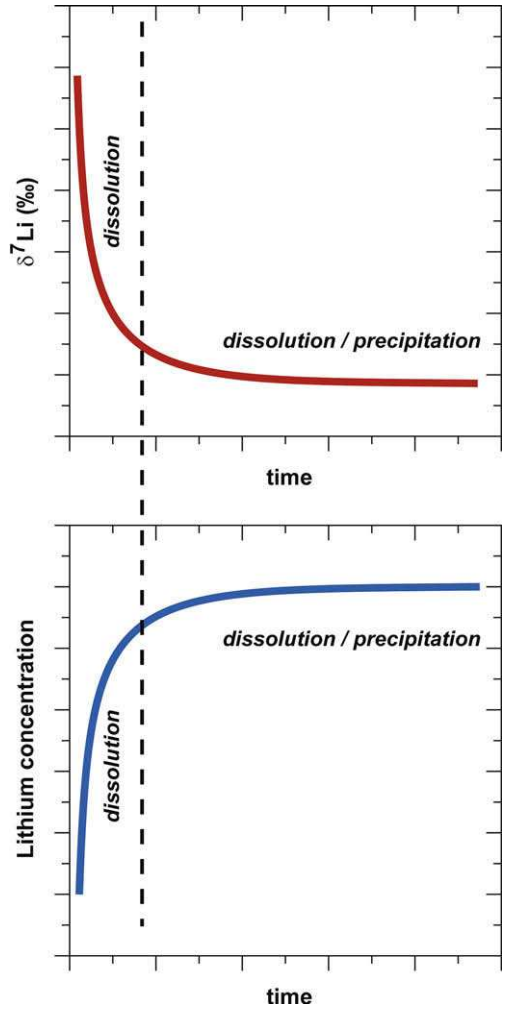

Fig. 7. Schematic graph showing the evolution of δ^7Li values and lithium concentrations in liquid as a function of time.

were constant and reached a plateau at the end of each experiment is a good indication of having attained an isotopic steady state. We can, therefore, determine the δ^7Li signature of the solution at steady state by averaging the constant values measured after run completion for each experiment (Fig. 2). These δ^7Li signatures in solution determined at steady state ($\delta^7Li_{solution}$) are given in Table 3.

Isotopic fractionation ($\Delta_{solution-solid}$) between the solution and the solid can then be calculated after run completion (when isotopic steady state was reached, Table 3). Fractionation factors ranged from +6.7‰ to +19.4‰ for experiments carried at 250 and 25 °C, respectively. At low temperature (25 °C), Li isotopic fractionation was much more important ($\Delta_{solution-solid}$ = +19.4‰). The fractionation factor decreased from +12.5‰ at 75 °C and +9.5‰ at 200 °C to a value of +6.7‰ at 250 °C. Altogether, these experiments confirm the strong temperature dependence of Li isotope exchange during water/rock interaction (Fig. 8a).

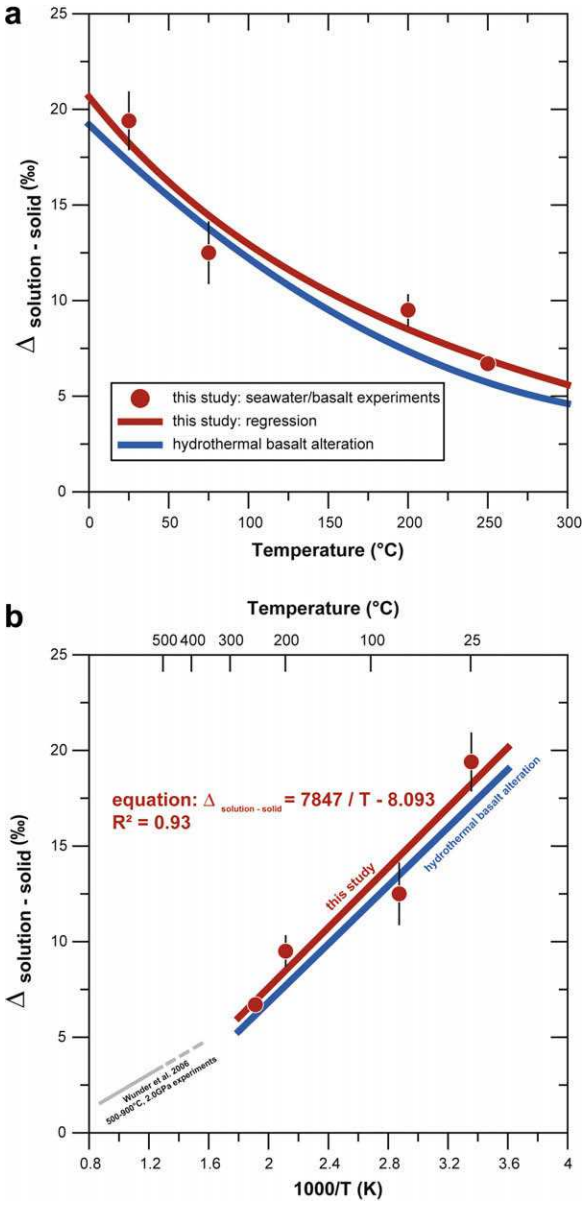

Fig. 8. (a) Lithium isotopic fractionation between solution and solid ($\Delta_{solution-solid}$) determined in our experiments versus the interaction temperature (red circles and red curve). The blue curve corresponds to isotopic fractionation factors inferred from studies of altered basalt and hydrothermal solutions that give Δ values of +4‰ at 350 °C, +9‰ at 160 °C and +19‰ at 2 °C (Chan and Edmond, 1988; Chan et al., 1992, 1993, 1994; James et al., 1999). (b) Lithium isotopic fractionation between solution and solid ($\Delta_{solution-solid}$) calculated in our experiments (red circles) versus the inverse of the temperature of interaction (1000/T, K^{-1}). The red line represents the correlation obtained in our experiments. The blue line corresponds to isotopic fractionation inferred from hydrothermal basalt interaction. The grey line represents the experimental relationship determined by Wunder et al. (2006), between 500 and 900 °C, and the dashed grey line is an extrapolation below 500 °C. (For interpretation of the references in color in this figure legend, the reader is referred to the web version of this article.)

In addition to this experimental approach, the water/rock interaction process may also be investigated using the modeling method reported by Magenheim et al. (1995). In this model, the initial rock is incrementally destroyed, and Li is partitioned into the fluid and alteration phases. The relationship of the integrated concentration of the two isotopes ^{6}Li and ^{7}Li in solution with the rock/water ratio (r/w) is described by the following two equations:

$$r/w = -\frac{1}{K} \times \ln\left(\frac{^6\mathrm{Li}_r - K \times {}^6\mathrm{Li}_w}{^6\mathrm{Li}_r - K \times {}^6\mathrm{Li}_0}\right) \quad (1)$$

$$r/w = -\frac{1}{\alpha K} \times \ln\left(\frac{^7Li_r - \alpha K \times {}^7Li_w}{^7Li_r - \alpha K \times {}^7Li_0}\right) \quad (2)$$

where $^6\mathrm{Li}_0$ and $^7\mathrm{Li}_0$ are the initial concentrations of the two isotopes in the starting solution (seawater diluted, Li = 0.1 mg/L and δ^7Li = +31‰), $^6\mathrm{Li}_r$ and $^7\mathrm{Li}_r$ are the concentrations of the two isotopes in the initial rock (basalt JB-2, Li = 7.78 μg/g and δ^7Li = +4.9‰), K is the distribution coefficient of an isotope between the solution (Li_w) and altered phase (Li_{alt}), and α is the associated isotopic fractionation ($\alpha = (^7\mathrm{Li}/^6\mathrm{Li})_{liquid}/(^7\mathrm{Li}/^6\mathrm{Li})_{solid}$). Thus:

$$^6\mathrm{Li}_{alt} = K\,^6\mathrm{Li}_w \quad (3)$$

and

$$^7\mathrm{Li}_{alt} = \alpha K\,^7\mathrm{Li}_w \quad (4)$$

Because K and α are temperature dependent, different values are used for the calculations, with data as compiled by Magenheim et al. (1995) and Chan et al. (2002). The empirical values for the parameters used are as follows: for 260 °C, $K = 0.35$ and $\alpha = 0.994$; for 300 °C, $K = 0.32$ and $\alpha = 0.995$; for 350 °C, $K = 0.27$; $\alpha = 0.996$; and for 400 °C, $K = 0.23$ and $\alpha = 0.997$.

The δ^7Li values calculated for liquid and solid phases following Magenheim's model are reported as a function of the water/rock ratio (w/r) in Fig. 9. We note that this model is in good agreement with our experimental results. Indeed, this model takes into account a fractionation of 6‰ at 260 °C between liquid and solid phases, which is similar to the value obtained in our experiments (i.e., 6.7‰ at 250 °C). It is important to highlight that this isotopic fractionation value was not a function of the water/rock ratio (w/r). The difference between δ^7Li in liquid and solid phases was independent of the water/rock ratio (see Fig. 9).

This feature can be investigated further by comparing our experimental constraints with Li isotopic fractionation and values determined either in natural environments or in other experimental studies. Most Li fractionation values reported so far in the literature come from studies of interaction between seawater and more or less weathered basalt. The isotopic fractionation factors inferred from these studies give Δ values of +4‰ at 350 °C, +9‰ at 160 °C and +19‰ at 2 °C (Chan and Edmond, 1988; Chan et al., 1992, 1993, 1994; James et al., 1999). These Δ values are shown in Fig. 8a as 'hydrothermal basalt alteration', for which an empirical equation was reported by James et al. (1999). Chan et al. (1994) have also shown that the isotopic composition of fluids decreases with increasing temperature. Their results clearly demonstrate that Li mobilization is a temperature-dependent process. Li release can begin at relatively low temperatures and increases with heating. Our experimental data are in good agreement with the relation-

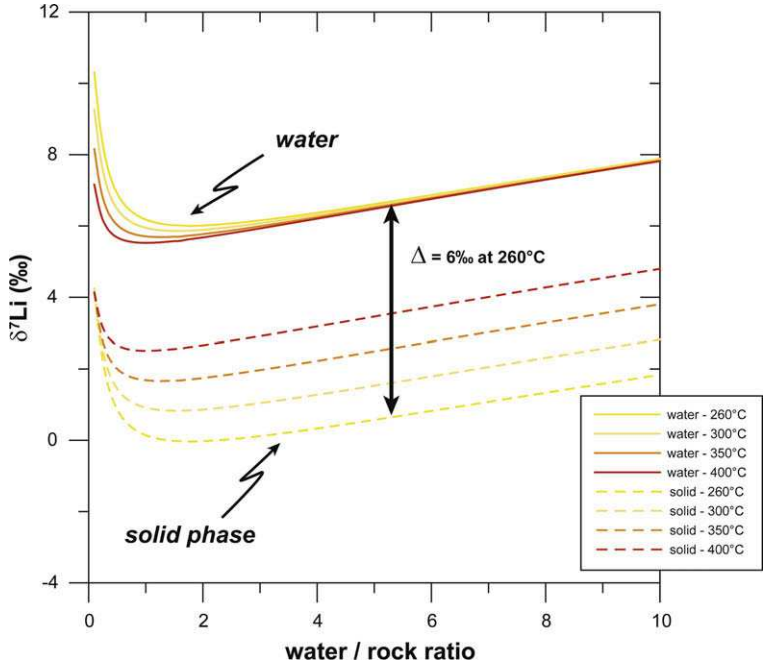

Fig. 9. Lithium isotopic composition (δ^7Li, ‰) for water and solid (alteration products) phases as a function of water/rock ratio (w/r) following Magenheim's model (Magenheim et al., 1995) for temperatures of interaction ranging between 260 and 400 °C. The empirical values for the parameters used are as follows: for 260 °C, $K = 0.35$ and $\alpha = 0.994$; for 300 °C, $K = 0.32$ and $\alpha = 0.995$; for 350 °C, $K = 0.27$ and $\alpha = 0.996$; and for 400 °C, $K = 0.23$ and $\alpha = 0.997$.

ship inferred from natural systems, namely 'hydrothermal basalt alteration' (Fig. 8a).

In Fig. 8b, isotopic fractionation determined using our experiments ($\Delta_{solution-solid}$) is plotted as a function of $1000/T$ (temperature in Kelvin, K). This graph enabled determination of the empirical relationship (Eq. (5)) between the isotopic fractionation and the reciprocal temperature ($R^2 = 0.93$):

$$\Delta_{solution-solid} = \frac{7847}{T} - 8.093 \quad (5)$$

Fig. 8 also displays the data of Wunder et al. (2006) who experimentally worked out the Li isotopic fractionation between clinopyroxene and aqueous fluids at temperatures between 500 and 900 °C at 2.0 GPa. According to these authors, there is significant fractionation (about +1‰) even at high temperatures (900 °C). Their relationship is shown in Fig. 8b, where the dashed-line corresponds to an extrapolation to temperatures below 500 °C. Although the relationships derived by Wunder et al. (2006) are not strictly comparable to ours, owing to the widely different experimental conditions explored and solid composition used, the two data sets agree remarkably with each other. This considerably strengthens the use of Li isotopes as tracers of fluid–mineral interaction processes over a large range of P–T conditions.

5.2.2. Application to deep saline geothermal waters in volcanic island arc areas

The Li isotopic compositions of deep saline geothermal waters are plotted as a function of reservoir temperatures, as determined either by direct measurements or via chemical geothermometers (Fig. 10). The obtained relationship supports a temperature dependence of the Li isotopic signature in the geothermal reservoir. This figure shows, as a general rule, that the higher the reservoir temperature, the lower the Li isotopic signature of the geothermal waters. However, it is important to point out that the δ^7Li signatures in the Lamentin and Diamant geothermal waters were very similar, despite having significantly different reservoir temperatures.

Using the experimental data ($\Delta_{solution-solid}$) obtained during this study (Table 1), as well as assuming consistent Li behavior between the water/rock interaction processes occurring during the experiments and within the geothermal reservoirs of Bouillante, Lamentin and Diamant, the δ^7Li signatures of the reservoir rocks were estimated from the δ^7Li values determined in the geothermal waters (see in Fig. 10).

The δ^7Li value found for the rocks of the Bouillante deep reservoir was close to $-2.4‰ \pm 0.6$ (see Fig. 10). It is obvious that this value is very different from the positive Li isotopic signature of volcanic island arc lavas (Tomascak, 2004). The presence of sediments could explain this

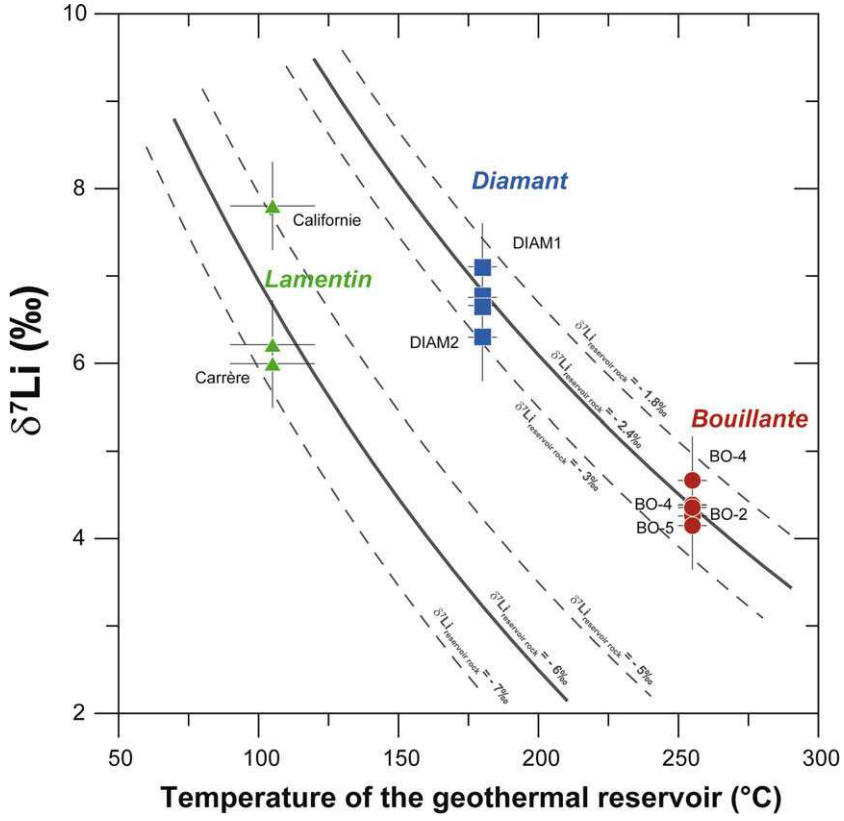

Fig. 10. Lithium isotopic compositions (δ^7Li, ‰) in well fluids from the Lamentin, Diamant and Bouillante geothermal fields plotted as a function of the temperature of the reservoir determined either by direct measurements (Bouillante and Lamentin wells) or chemical geothermometers (Diamant, Bouillante and Lamentin wells). Parametric curves correspond to different values of δ^7Li in reservoir rocks (from −1.8‰ to −7‰), assuming the temperature dependence of Li isotopic fractionation obtained in the present work by experiments (Table 3). See text for comments.

light Li isotopic value. However, this contribution seems to be minor or negligible in the Bouillante geothermal reservoir, because the Na/Li geothermometer determined for oil-field and sedimentary basins by Kharaka et al. (1982) cannot be used for this reservoir. Only the Na/Li geothermometer determined by Fouillac and Michard (1981) for saline geothermal waters in volcanic (and granitic) environments provides a reliable temperature estimate. Light Li isotopic values have also been observed for mantle-derived materials, such as metasomatized xenoliths or some peridotites (James and Palmer, 2000; Decitre et al., 2002; Tomascak, 2004). However, it would be difficult to explain their presence in the context of the Bouillante geothermal area. This is especially true as the hydrothermal waters in contact with serpentinized peridotites often have chemical compositions very different (very high pH, low dissolved silica; Benton et al., 2004) from those analyzed for the Bouillante geothermal water. In this case, the light δ^7Li value would rather be associated to altered rocks located in the upper sheeted dike complex of the oceanic crust, just below the transition zone between andesite volcanic flows and the basaltic dikes. Indeed, the upper dike section, in which Li is extracted by hydrothermal fluid circulation, is characterized by light Li isotopic values in rocks (from −5‰ to 1‰; Chan et al., 1996, 2002), indicating retention of ^{6}Li by the altered rocks. According to Chan et al. (1992) who analyzed an altered metabasalt (abundance of chlorite with minor amphibole) from the ocean floor of the MAR (Mid Atlantic Ridge) median valley, with a δ^7Li value of −2.1‰: "Li is not quantitatively extracted by the circulating fluid but may be partially retained in the greenschist facies minerals during hydrothermal activity, the lighter isotope being preferentially taken up in the solid phase". This zone is a privileged region of fluid mixing.

In addition, on the basis of geological and geophysical arguments (BO-4 log data up to a depth of 2500 m in Dorel et al., 1979; Andreieff et al., 1987; Sanjuan et al., 2004), the upper basalt dike zone would be located in the Bouillante area at a depth ranging from 3 to 5 km. Li enrichment is accompanied by relatively low isotopic compositions, which indicate the influence of basalt-derived Li during mineralization and alteration. The high Li concentration analyzed for the Bouillante geothermal fluid (about 4.5 mg/L) compared to the experimental fluid at 250 °C, which was produced using a water/rock ratio of 10 (352 μg/L; i.e., the maximum Li concentrations determined in our experiments, Table 1, Fig. 2), suggests a lower water/rock ratio of about 1–5 in the Bouillante reservoir. It is important to keep in mind that the initial Li concentration in the Bouillante reservoir rocks could be very different from that of the rock used in the laboratory experiments (7.78 μg/g).

The δ^7Li value of −2.4‰ ± 0.6 determined for reservoir rocks in the Bouillante area at 260 °C can be also found using the model of Magenheim et al. (1995), considering a water/rock ratio (w/r) close to 4–5, a Li concentration of 15 μg/g and a δ^7Li value of 2.7‰ for the initial fresh rock. This Li isotopic value is commonly observed in samples of unaltered basalts and basaltic andesites or lavas from subduction zones and island arcs (δ^7Li values from 1.1‰ to 7.6‰; Moriguti and Nakamura, 1998; Magna et al., 2003).

When considering the Bouillante area, such a water/rock ratio parameter can be also estimated using the relationship reported by Edmond et al. (1979):

$$w/r = \frac{\mathrm{Li_{FR}}}{\mathrm{Li_{GF}} - \mathrm{Li_{DSW}}} \quad (6)$$

where $\mathrm{Li_{FR}}$ is the Li concentration in the fresh rock, $\mathrm{Li_{GF}}$ is the Li concentration in the geothermal fluid and $\mathrm{Li_{IF}}$ is the Li concentration in the diluted seawater (i.e., initial fluid).

For different Li concentrations in the fresh rock ($\mathrm{Li_{FR}}$ ranging from 5, 10, 15 and 25 μg/g), we obtained the following values for the water/rock ratio (w/r): 1.2, 2.4, 3.6 and 4.8, respectively. These values are in good agreement with estimates based on our experimental constraints (w/r from 1 to 5).

Lastly, the w/r at Bouillante can also be estimated using the relationship of Albarède et al. (1981) for Sr isotopes concerning hydrothermal alteration of the oceanic crust:

$$w/r = \frac{\left(\frac{^{87}\mathrm{Sr}}{^{86}\mathrm{Sr}}\right)_{\mathrm{GF}} - \left(\frac{^{87}\mathrm{Sr}}{^{86}\mathrm{Sr}}\right)_{\mathrm{FR}}}{\left(\frac{^{87}\mathrm{Sr}}{^{86}\mathrm{Sr}}\right)_{\mathrm{DSW}} - \left(\frac{^{87}\mathrm{Sr}}{^{86}\mathrm{Sr}}\right)_{\mathrm{GF}}} \times \frac{\mathrm{Sr_{FR}}}{\mathrm{Sr_{DSW}}} \quad (7)$$

where $(^{87}\mathrm{Sr}/^{86}\mathrm{Sr})_{\mathrm{GF}} = 0.70496$ (reported by Mas et al., 2006), $(^{87}\mathrm{Sr}/^{86}\mathrm{Sr})_{\mathrm{FR}} = 0.7041$ (Sanjuan and Brach, 1997) and $(^{87}\mathrm{Sr}/^{86}\mathrm{Sr})_{\mathrm{DSW}} = 0.709$ (Sanjuan and Brach, 1997) are the Sr isotopic ratios of geothermal fluid, fresh rock and seawater, respectively. $\mathrm{Sr_{FR}}$ and $\mathrm{Sr_{DSW}}$ are the Sr concentrations for fresh rock and diluted seawater, respectively (we assume here that the dilution of seawater (60%) by fresh water (40%) did not affect the Sr isotopic ratio).

After calculation, we obtained a w/r value close to 4.1 for $\mathrm{Sr_{FR}} = 100$ μg/g and $w/r = 8.2$ for $\mathrm{Sr_{FR}} = 200$ μg/g.

Thus, it appears that both Li and Sr-based estimates converge towards a w/r value around 4–5. This assumes that Li and Sr concentrations in the fresh rock were close to 15–20 and 100 μg/g, respectively, which are values commonly observed in subduction zone and island arc basalts that are enriched in Li relative to the mantle (around 3–4 μg/g in MORB; Ryan and Langmuir, 1987).

For the Diamant area, the same value of δ^7Li as that of Bouillante (close to −2.4‰ ± 0.6) was found for the reservoir rocks. Given that the Na/Li geothermometer suggests that the geothermal fluid is partially in equilibrium with sedimentary rocks, contrary to the Bouillante area and according to the literature data (Tomascak, 2004; Chan et al., 2006; Millot et al., 2007), this negative value could reflect the presence of volcano-sedimentary rocks in the deep reservoir.

In the Lamentin plain, the geothermal reservoir is relatively shallow and is comprised of volcano-sedimentary rocks. The Na/Li geothermometer, which also suggests that the geothermal fluid is partially in equilibrium with sedimentary rocks, is in a good agreement with this reservoir composition. The δ^7Li values estimated for the reservoir rocks (close to −6‰ ± 1; Fig. 10) were low compared to literature data (Tomascak, 2004). However, a δ^7Li value of −4.7‰ was found in altered white lava collected from the borehole Carrère at a depth of 414 m (Table 4). As shown by Sturchio and Chan (2003) for the Yellowstone system, hydrothermal alteration products of volcanic rocks have

Table 4
Li and Li isotopic compositions of a rock sample collected in the Lamentin area (Carrère, drilling LA02).

	Sample name	Depth (m)	δ^7Li (‰)	$2\sigma_m$ (‰)	Li (μg/g)
Lamentin	Carrère LA02 drilling	414	−4.7	0.1	74

also exhibited extremely low δ^7Li values (−4.8‰). On the other hand, it is possible that the Li isotopic fractionation equation determined for basalt in this study is less well adapted for the volcano-sedimentary rocks that constitute this reservoir, where sedimentary rocks are abundant.

Lithium concentrations and δ^7Li values are, therefore, not only a useful tool to estimate the temperature of geothermal reservoirs, but can also be used to determine the nature (and sometimes the depth) of the reservoir rocks. Additional water/rock interaction experiments (e.g., fresh water/basalt, seawater and fresh water/andesite) similar to those reported here would enable the completion of this study and add to our understanding of Li behavior in island arc geothermal systems.

6. CONCLUSIONS

The behavior of Li and its isotopes have been characterized in geothermal systems located in volcanic island arc areas, such as those in Guadeloupe and Martinique. The main results of this study are:

- Deep geothermal waters collected from wells and thermal springs indicate that Li isotopic signatures are homogeneous for a given site. The Li isotope variation at the Bouillante geothermal reservoir was the most homogeneous, with a mean value of $\delta^7\text{Li} = +4.4‰ \pm 0.4$ (2σ, $n = 8$) and without any short term temporal variation (1999–2002). This confirms the geochemical homogeneity of the studied geothermal systems and provides a strong argument for using the Li/Na geothermometer to calculate reservoir temperature.
- Li isotopic signatures of each of these geothermal systems were also very different, as a result of the highly variable temperatures of water/rock interaction (90–120 °C for the Lamentin plain, 180 °C for the Diamant area and 250–260 °C for the Bouillante geothermal fields) and the lithological differences of the reservoir rocks.
- Li isotopic tracing confirms a process of mixing between deep geothermal fluid and seawater for sub-marine thermal springs.
- Experiments of seawater/basalt interaction were carried out at different temperatures and the results confirm the temperature dependence of Li isotope fractionation, with values ranging from +19.4‰ to +6.7‰ ($\Delta_{solution-solid}$) between 25 and 250 °C, respectively, in agreement with available field and experimental data. We suggest that, in our experiments, Li and its isotopes were controlled by two complementary processes: (1) mixing between Li in seawater and Li released in solution from the basalt and (2) uptake of Li into secondary minerals.
- These experiments allow us to determine the following empirical relationship between the isotopic fractionation and the temperature: $\Delta_{solution-solid} = 7847/T - 8.093$ (temperature in Kelvin).
- These experimental results were applied to the saline geothermal waters collected from the Bouillante and Lamentin wells, as well as from the Diamant thermal spring. Results suggest that the Bouillante geothermal water is in equilibrium with a reservoir composed of rocks located in the upper sheeted dike complex of the oceanic crust. This reservoir acts as a privileged region of fluid mixing and is located just below the transition zone between andesite volcanic flows and basaltic dikes. Based on BO-4 log data, geological and geophysical arguments, this zone would be situated at a depth ranging from 3 to 5 km. In the Lamentin and Diamant areas, the Na/Li geothermometer and the Li isotopic signature suggest that the geothermal fluid is in equilibrium with volcano-sedimentary reservoir rocks. In addition, for the Lamentin and Diamant geothermal areas, we know that the Na/Li thermometric relationship determined for sedimentary basins (Kharaka et al., 1982) gives temperature values in agreement with temperatures estimated for the reservoir fluids, suggesting the importance of a sedimentary signature in the reservoir rocks.
- Therefore, we conclude that lithium isotopic systematics is a powerful tool for temperature characterization, and can also be used to infer the origin of waters and the nature of reservoir rocks.

ACKNOWLEDGMENTS

This work was funded by a BRGM-ADEME joint research partnership through the GHEDOM project (*Géothermie Haute Enthalpie dans les Départements d'Outre-Mer*). We thank M. Brach for his help collecting samples, BRGM Offices (SGR/Guadeloupe and SGR/Martinique), CFG Services and Geothermie Bouillante for their local help. This work benefited from the collaboration of BRGM laboratories (Metrology Monitoring Analysis Department) for major and trace elemental analyses: J.P. Ghestem, T. Conte and C. Crouzet are thanked for their help, and F. Delorme, V. Jean-Prost and C. Bény provided TEM, XRD and FTIR spectral analyses. We also would like to thank M. Robert for her help in the Neptune laboratory. We also acknowledge A. Genter and Ph. Négrel for fruitful discussions. R.M. is particularly grateful to C. Fouillac, A.M. Fouillac and J.P. Girard for the opportunity to work on this subject. L.H. Chan is also acknowledged for providing helpful comments in an earlier version of the manuscript. We thank P. Tomascak and an anonymous reviewer for providing critical comments that improved this manuscript. J. Ishibashi is also thanked for editorial handling and constructive comments. Finally, we also would like to thank A. Hegan for comments and English corrections. This is BRGM Contribution No. 6275.

REFERENCES

Albarède F., Michard A., Minster J. F. and Michard G. (1981) 87Sr/86Sr ratios in hydrothermal waters and deposits from the East Pacific Rise at 21N. *Earth Planet. Sci. Lett.* **55**, 229–236.

Anderson M. A., Bertsch P. M. and Miller W. P. (1989) Exchange and apparent fixation of lithium in selected soils and clay minerals. *Soil Sci.* **148**, 46–52.

Andreieff P., Bouysse Ph. and Westercamp D. (1987) Géologie de l'arc insulaire des Petites Antilles, et évolution géodynamique de l'Est-Caraïbe. *Thèse de Doctorat d'Etat ès Sciences*, vol. 1. Université de Bordeaux. 360p.

Anghel I., Turin H. J. and Reimus P. W. (2002) Lithium sorption to Yucca mountain tuffs. *Appl. Geochem.* **17**, 819–824.

Arnorsson S. and Gunnlaugsson E. (1983) The chemistry of geothermal waters in Iceland. III. Chemical geothermometry in geothermal investigations. *Geochim. Cosmochim. Acta* **47**, 567–577.

Benton L. D., Ryan J. G. and Savov I. P. (2004) Lithium abundance and isotope systematics of forearc serpentinites, Conical Seamont, Mariana forearc: insights into the mechanics of slab-mantle exchange during subduction. *Geochem. Geophys. Geosyst.* **8**. doi:10.1029/2004GC000708.

Carignan J., Vigier N. and Millot R. (2007) Three secondary reference materials for Li isotopic measurements: ^{7}Li–N, ^{6}Li–N and LiCl–N. *Geostand. Geoanal. Res.* **31**, 7–12.

Chan L. H. and Edmond J. M. (1988) Variation of lithium isotope composition in the marine environment: a preliminary report. *Geochim. Cosmochim. Acta* **52**, 1711–1717.

Chan L. H., Edmond J. M., Thompson G. and Gillis K. (1992) Lithium isotopic composition of submarine basalts: implications for the lithium cycle in the oceans. *Earth Planet. Sci. Lett.* **108**, 151–160.

Chan L. H., Edmond J. M. and Thompson G. (1993) A lithium isotope study of hot springs and metabasalts from mid-ocean ridge hydrothermal systems. *J. Geophys. Res.* **98**, 9653–9659.

Chan L. H., Gieskes J. M., You C. F. and Edmond J. M. (1994) Lithium isotope geochemistry of sediments and hydrothermal fluids of the Guaymas Basin, Gulf of California. *Geochim. Cosmochim. Acta* **58**, 4443–4454.

Chan L. H., Alt J. C. and Teagle D. A. H. (1996) Alteration of the upper 1.8 kilometers of oceanic crust: a lithium isotope record at ODP site 504B. *Trans. Am. Geophys. Union* **77**, F805.

Chan L. H., Alt J. C. and Teagle D. A. H. (2002) Lithium and lithium isotope profiles through the upper oceanic crust: a study of seawater-basalt exchange at ODP Sites 504B and 896A. *Earth Planet. Sci. Lett.* **201**, 187–201.

Coplen T. B., Hopple J. A., Böhlke J. K., Peiser H. S., Rieder S. E., Krouse H. R., Rosman K. J. R., Ding T., Vocke, Jr., R. D., Révész K. M., Lamberty A., Taylor P. and De Bièvre P. (2002) Compilation of minimum and maximum isotope ratios of selected elements in naturally occurring terrestrial materials and reagents. U.S. Geological Survey, *Water-Resources Investigations.* Report 01-4222.

Correia H., Sigurdsson O., Sanjuan B., Tulinius H. and Lasne E. (2000) Stimulation test of a high-enthalpy geothermal well by cold water injection. In *Geothermal Resources Council Transactions, Davis, CA*, vol. 24. pp. 129–136.

Decitre S., Deloule E., Reisberg L., James R., Agrinier P. and Mével C. (2002) Behavior of lithium and its isotopes during serpentinization of oceanic peridotites. *Geochem. Geophys. Geosyst.*. doi:10.1029/2001GC000178.

Dorel J., Eschenbrenner S. and Feuillard M. (1979) Coupes sismiques des structures superficielles dans les petites Antilles – I. Guadeloupe. *Pageoph* **117**, 1050–1069.

Edmond J. M., Measures C., Mc Duff R. E., Chan L. H., Collier R. and Grant B. (1979) Ridge crest hydrothermal activity and the balances of the major and minor elements in the Ocean: the Galapagos data. *Earth Planet. Sci. Lett.* **46**, 1–18.

Fabriol H., Bitri A., Bourgeois B., Debeglia N., Genter A., Guennoc P., Jousset P., Miehe J. M., Roig J. Y., Thinon I., Traineau H., Sanjuan B. and Truffert C. (2005) Geophysical methods applied to the assessment of the Bouillante geothermal field (Guadeloupe, French West Indies). In *Proceedings World Geothermal Congress 2005, Antalya, Turkey, 24–29 April 2005*.

Flesch G. D., Anderson A. R. and Svec H. J. (1973) A secondary isotopic standard for ^{6}Li/^{7}Li determinations. *Int. J. Mass Spectrom. Ion Phys.* **12**, 265–272.

Fouillac C. and Michard G. (1981) Sodium/lithium ratio in water applied to geothermometry of geothermal reservoirs. *Geothermics* **10**, 55–70.

Fournier R. O. and Rowe J. J. (1966) Estimation of underground temperatures from the silica content of water from hot springs and wet-steam wells. *Am. J. Sci.* **264**, 685–697.

Fournier R. O. and Truesdell A. H. (1973) An empirical Na–K–Ca geothermometer for natural waters. *Geochim. Cosmochim. Acta* **37**, 1255–1275.

Fournier R. O. and Potter R. W. (1979) Magnesium correction to the Na–K–Ca chemical geothermometer. *Geochim. Cosmochim. Acta* **43**, 1543–1550.

Fournier R. O. (1979) A revised equation for the Na/K geothermometer. *Geotherm. Res. Counc. Trans.* **3**, 221–224.

Genter A., Traineau H., Degouy M., Correia H., Mas A., Patrier P., Roig J. Y. and Sanjuan B. (2002) Preliminary geological results of recent exploratory drillings in a geothermal fractured reservoir at Lamentin (French West Indies, Martinique). In *Proceedings, 27th Workshop on Geothermal Reservoir Engineering, Stanford University, Stanford, CA*. pp. 241–247.

Giggenbach W. F. (1988) Geothermal solute equilibria. Derivation of Na–K–Mg–Ca geoindicators. *Geochim. Cosmochim. Acta* **52**, 2749–2765.

Huh Y., Chan L. H. and Edmond J. M. (2001) Lithium isotopes as a probe of weathering processes: Orinoco river. *Earth Planet. Sci. Lett.* **194**, 189–199.

James R. H., Rudnicki M. D. and Palmer M. R. (1999) The alkali element and boron geochemistry of the Escanaba Trough sediment-hosted hydrothermal system. *Earth Planet. Sci. Lett.* **171**, 157–169.

James R. H. and Palmer M. R. (2000) The lithium isotope composition of international rock standards. *Chem. Geol.* **166**, 319–326.

James R. H., Allen D. E. and Seyfried W. E. (2003) An experimental study of alteration of oceanic crust and terrigenous sediments at moderate temperatures (51 to 350 °C): Insights as to chemical processes in near-shore ridge-flank hydrothermal systems. *Geochim. Cosmochim. Acta* **67**, 681–691.

Kharaka Y. K., Lico M. S. and Lax L. M. (1982) Chemical geothermometers applied to formation waters, Gulf of Mexico and California basins. *Am. Assoc. Petrol. Geol. Bull.* **66**, 588.

Kharaka Y. K. and Mariner R. H. (1989) Chemical geothermometers and their application to formation waters from sedimentary basins. In *Thermal History of Sedimentary Basins: Methods and Case Histories* (eds. N. D. Naeser and T. H. McCulloch). Springer-Verlag, New York, pp. 99–117.

Magenheim A. J., Spivack A. J., Alt J. C., Bayhurst G., Chan L. H., Zuleger E. and Gieskes J. M. (1995) Borehole fluid chemistry in hole 504B, leg 137: formation water or in-situ reaction? In *Proceedings of the Ocean Drilling Program, Scientific Results*, vol. 137/140. pp. 141–152.

Magna T., Wiechert U., Grove T. L. and Halliday A. N. (2003) Lithium isotope composition of arc volcanics from the Mt Shasta region, N California. *Geochim. Cosmochim. Acta* **67**, A267.

Mas A., Guisseau D., Patrier P., Beaufort D., Genter A., Sanjuan B. and Girard J. P. (2006) Clay minerals related to the hydrothermal activity of the Bouillante geothermal field (Guadeloupe). *J. Volcanol. Geotherm. Res.* **158**, 380–400.

Michard G. (1979) Géothermomètres chimiques. *Bull. du BRGM (2ème série)*, Section III, vol. 2. BRGM, pp. 183–189.

Michard G. (1990) Behaviour of major elements and some trace elements (Li, Rb, Cs, Sr, Fe, Mn, W, F) in deep hot waters from granitic areas. *Chem. Geol.* **89**, 117–134.

Millot R., Guerrot C. and Vigier N. (2004) Accurate and high precision measurement of lithium isotopes in two reference materials by MC-ICP-MS. *Geostand. Geoanal. Res.* **28**, 53–159.

Millot R., Ph Négrel. and Petelet-Giraud E. (2007) Multi-isotopic (Li, B, Sr, Nd) approach for geothermal reservoir characterization in the Limagne Basin (Massif Central, France). *Appl. Geochem.* **22**, 2307–2325.

Mizutani Y. and Rafter T. A. (1969) Oxygen isotopic composition of sulphates. 3. Oxygen isotopic fractionation in the bisulphate ion–water system. *N. Zealand J. Sci.* **12**, 54–59.

Moriguti T. and Nakamura E. (1998) Across-arc variation of Li isotopes in lavas and implications for crust/mantle recycling at subduction zones. *Earth Planet. Sci. Lett.* **163**, 167–174.

Pistiner J. S. and Henderson G. M. (2003) Lithium isotope fractionation during continental weathering processes. *Earth Planet. Sci. Lett.* **214**, 327–339.

Ryan J. G. and Langmuir C. H. (1987) The systematics of lithium abundances in young volcanic rocks. *Geochim. Cosmochim. Acta* **51**, 1727–1741.

Sanjuan B. and Brach M. (1997) Etude hydrogéochimique du champ géothermique de Bouillante (Guadeloupe). *Report BRGM* R39880. 84p.

Sanjuan B. (2001) Champ géothermique de Bouillante (Guadeloupe): synthèse des travaux réalisés en géochimie avant 1999. *Final report BRGM*/RC-51672-FR. 54p.

Sanjuan B., Lasne E. and Brach M. (2001) Bouillante geothermal fluid: mixing and water/rock interaction processes at 250 °C. In *Proceedings, 10th Water–Rock Interaction (WRI-10), Cagliari, Italy, June 10–15*, vol. 2. pp. 911–914.

Sanjuan B., Genter A., Correia H., Girard J. P., Roig J. Y. and Brach M. (2002a) Travaux scientifiques associés à la réalisation des trois puits d'exploration géothermique dans la plaine du Lamentin (Martinique). Convention BRGM-ADEME No. 99.05.026. *Final report BRGM*-51671-FR. 253p.

Sanjuan B., Traineau H., Genter A., Correia H., Brach M. and Degouy M. (2002b) Geochemical investigations during a new geothermal exploration phase in the Lamentin plain (Martinique, French West Indies). In *Proceedings, 27th Workshop on Geothermal Reservoir Engineering, Stanford University, Stanford, CA*. pp. 198–205.

Sanjuan B., Brach M. and Foucher J. C. (2003) Réévaluation du potentiel géothermique dans les régions de Morne Rouge – Montagne Pelée et du Diamant (Martinique): étude géochimique. *Final report BRGM*/RP-52547-FR. 80p.

Sanjuan B., Le Nindre Y.-M., Menjoz A., Sbai A., Brach M. and Lasne E. (2004) Travaux de recherche liés au développement du champ géothermique de Bouillante (Guadeloupe). *Rapport BRGM/RP-53136-FR.* 166p.

Sanjuan B., Millot R., Brach M., Foucher J. C., Roig J. Y. and Baltassat J. M. (2005) Geothermal exploration in the Mount Pelée volcano-Morne Rouge and Diamant areas (Martinique, West French Indies): geochemical data. In *World Geothermal Congress 2005, Antalya, Turkey, 24–29/04/2005*.

Seyfried W. E., Chen X. and Chan L. H. (1998) Trace element mobility and Lithium isotope exchange during hydrothermal alteration of seafloor weathered basalt: an experimental study at 350 °C, 500 bars. *Geochim. Cosmochim. Acta* **62**, 949–960.

Scaillet B., Pichavant M., Roux J., Humbert G. and Lefevre A. (1992) Improvements of the Shaw membrane technique for measurement and control of fH_2 at high temperatures and pressures. *Am. Mineral.* **77**, 647–655.

Sturchio N. C. and Chan L. H. (2003) Lithium isotope geochemistry of the Yellowstone hydrothermal system, vol. 10. Society of Economic Geologists (US). pp. 171–180 (Special Publication).

Taylor T. I. and Urey H. C. (1938) Fractionation of the lithium and potassium isotopes by chemical exchange with zeolites. *J. Chem. Phys.* **6**, 429–438.

Tomascak P. B. (2004) Developments in the understanding and application of lithium isotopes in the earth and planetary sciences. In *Reviews in Mineralogy & Geochemistry*, vol. 55. Mineralogical Society of America, pp. 153–195.

Traineau H., Sanjuan B., Beaufort D., Brach M., Castaing C., Correia H., Genter A. and Herbrich B. (1997) The Bouillante geothermal field (F.W.I.) revisited: new data on the fractured geothermal reservoir in light of a future stimulation experiment in a low productive well. In *Proceedings, Twenty-second Workshop on Geothermal Reservoir Engineering, Stanford University, Stanford, California, January 27–29, 1997, SGP-TR-155.* pp. 97–104.

Wunder B., Meixner A., Romer R. L. and Heinrich W. (2006) Temperature-dependent isotopic fractionation of lithium between clinopyroxene and high-pressure hydrous fluids. *Contrib. Mineral Petrol.* **151**, 112–120.

Zhang L., Chan L. H. and Gieskes J. M. (1998) Lithium isotope geochemistry of pore waters from Ocean drilling program sites 918 and 919, Irminger basin. *Geochim. Cosmochim. Acta* **62**, 2437–2450.

Associate editor: Jun-ichiro Ishibashi

Résumé

Ce manuscrit constitue la synthèse des travaux de Recherches menés au BRGM au cours de ces 10 dernières années dans la thématique de le géochimie isotopique du lithium. Tout d'abord, nous décrivons en détails le protocole de mesure par MC-ICP-MS (Multi Collector Inductively Coupled Plasma Mass Spectrometer) des isotopes du lithium dans des matrices liquides et solides. Cette mesure requiert une bonne validation de l'ensemble de la chaine analytique. Ensuite, nous illustrons à travers différents exemples, l'application de cet outil isotopique à la compréhension des systèmes et des milieux comme les eaux de pluies et les fleuves ainsi que dans les interactions eau/roche à basse et haute température à travers l'étude des eaux thermo-minérales et des eaux géothermales et enfin des systèmes expérimentaux.

Les principales conclusions de ce travail sont les suivantes : 1/ la distribution du lithium et de ses isotopes dans les eaux de surface (pluies et rivières) est très variable. Le lithium des pluies n'est pas uniquement d'origine marine et les autres sources doivent donc être prises en compte comme les apports anthropiques. 2/ Le lithium dans les eaux de rivières provient quasi exclusivement de l'altération des roches silicatées et les compositions isotopiques du lithium dans les eaux des rivières sont donc un bon traceur du régime d'altération qui est contrôlé par la balance entre la dissolution des minéraux primaires et la précipitation des minéraux secondaires qui fractionnent les rapports isotopiques des eaux en incorporant préférentiellement du ^{6}Li. 3/ Les compositions isotopiques du lithium dans les eaux thermominérales présentent aussi de grandes variations et le δ^{7}Li d'une eau est inversement corrélé à la température profonde du réservoir. La thermo-dépendance du fractionnement isotopique du lithium est étudiée entre l'eau et la roche, à fois pour des systèmes géothermaux mais aussi par une approche expérimentale.

Le fractionnement des isotopes du lithium dans les hydrosystèmes dépend donc de l'intensité des interactions eau/roche à la fois en terme de température dans les systèmes géothermaux et du régime d'altération pour les eaux de surface. Le mécanisme commun de contrôle est l'équilibre entre dissolution de minéraux primaires et formation de minéraux secondaires.

Abstract

This manuscript is a summary of the research work carried out at BRGM over the past 10 years under my direction in the field of lithium isotope geochemistry. First, we describe in detail the protocol for measurement of lithium isotopes in liquid and solid matrices by MC-ICP-MS (Multi Collector Inductively Coupled Plasma Mass Spectrometer). This protocol requires validation of the entire analytical procedure. Then, we illustrate through various examples, the application of this isotopic tool in environmental systems such as rainwater and rivers, and during water/rock interactions at low and high temperature through the study of thermo-mineral and geothermal waters and finally in experimental systems.

The main conclusions of this work are: 1/ the distribution of lithium and its isotopes in surface water (rain and rivers) is highly variable. Lithium in rain is in part derived from the oceans but other sources such as anthropogenic inputs and dust must be taken into account. 2/ Lithium in river waters is almost exclusively derived from the alteration of silicate rocks. The isotopic composition of lithium in river waters is a good tracer of the "weathering regime" which controls the balance between the dissolution of primary minerals and the precipitation of secondary minerals that can fractionate the lithium isotopic ratios of river waters by preferentially incorporating ^{6}Li. 3/ The isotopic composition of lithium in thermo-mineral waters also shows great variation and $^{7/6}$Li of water is inversely correlated to the deep reservoir temperature. The thermo-dependence of the lithium isotopic fractionation between water and rock has been studied in both natural geothermal systems and with experimental approaches.

Fractionation of lithium isotopes in hydrologic systems depends on the intensity of water/rock interactions both in terms of temperature in geothermal systems and "weathering regime" in surface waters. The common controlling mechanism of lithium isotope compositions is the balance between dissolution of primary minerals and formation of secondary minerals.